



THE GEOLOGY OF THE GOSSE PILE ULTRAMAFIC  
INTRUSION AND OF THE SURROUNDING GRANULITES,  
TOMKINSON RANGES, CENTRAL AUSTRALIA.

by

ALAN CHARLES MOORE  
M.Sc. (Rhodes, South Africa).

Department of Geology and Mineralogy,  
The University of Adelaide,  
South Australia, 5001.

April, 1970.



## ORIGIN OF THE NAME "GOSSE PILE"

On October 10th, 1873 the explorer, Ernest Giles, while in the Cavenagh Ranges of Western Australia climbed a hill to obtain bearings. Near the summit he observed a small pile of stones which he thought had been erected by W.C. Gosse who had passed that way about one month earlier. Giles, supposing that Gosse had already named the hills, "merely called them 'Gosse's Pile' ". This name has, for no apparent reason, since been applied to another hill about 3 km north-east of Mount Davies in South Australia by Terry (1928), Sprigg and Wilson (1959) and Mirams (1964). Through usage this name has become accepted as the correct name for the lozenge-shaped hill which, with the surrounding outcrops, provides the material for the present study. An Advisory Nomenclature Committee to the South Australian Minister of Lands has recommended that the apostrophe be dropped from place names in most cases. Since the name "Gosse Pile" has been applied to a geographical feature rather than the original pile of stones built by Gosse, this recommendation has been followed throughout this thesis. The area around, and including, Gosse Pile is known to the local aborigines as Numbunja.

Frontispiece: Gosse Pile from the air, facing northeast. Mt. Davies in the foreground.

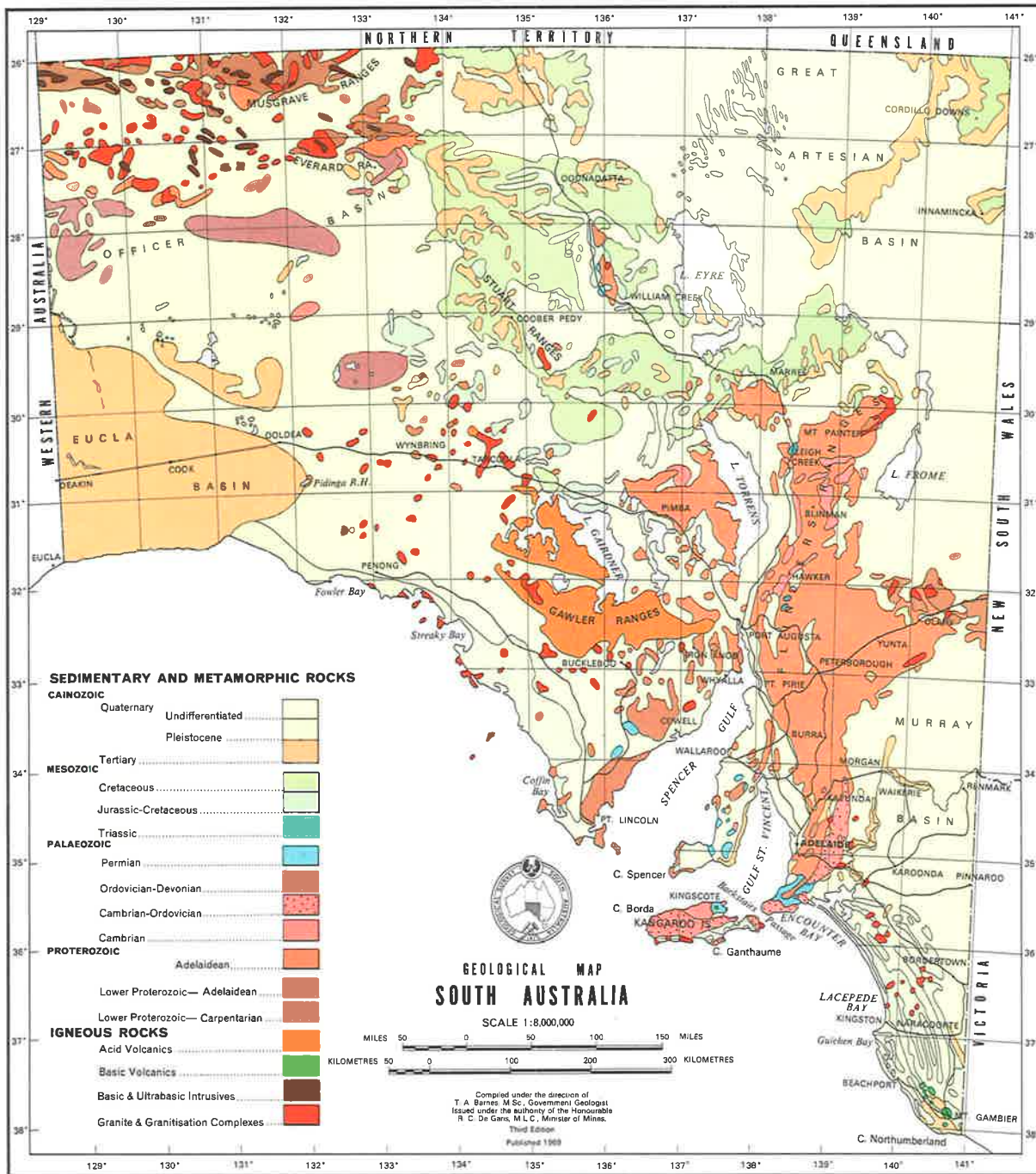




TABLE OF CONTENTS

|  | Page |
|--|------|
| SUMMARY  | i-v  |
| STATEMENT OF ORIGINALITY   | vi   |
| ACKNOWLEDGEMENTS   | vii  |
| INTRODUCTION   | 1    |
| <br><u>SECTION 1. REGIONAL GEOLOGY</u>                                 |      |
| 1.1 STRUCTURE AND METAMORPHISM   | 5    |
| 1.2 THE GILES COMPLEX  | 9    |
| 1.3 POST-GILES COMPLEX INTRUSIVES                                      | 11   |
| 1.4 YOUNGER UNITS  | 13   |
| 1.5 SUMMARY OF THE REGIONAL GEOLOGICAL HISTORY                         | 14   |
| 1.6 ECONOMIC POTENTIAL AND SILCRETE                                    | 15   |
| <br><u>SECTION 2. LOCAL GEOLOGY. THE GRANULITES</u>                    |      |
| 2.1 INTRODUCTION   | 18   |
| STRUCTURE  |      |
| 2.2 DISTRIBUTION AND S-SURFACES  | 19   |
| 2.3 FOLDS  | 22   |
| 2.4 FAULTS   | 25   |
| 2.5 CONCLUSIONS  | 32   |
| TEXTURES   |      |
| 2.6 TEXTURES OF THE GRANULITES   | 34   |
| 2.7 RELATIONSHIPS BETWEEN ROCK TYPES AND THEIR TEXTURES<br>AND FABRICS | 42   |
| 2.8 INTERPRETATION OF THE TEXTURES                                     | 45   |

---

## PETROGRAPHY AND MINERALOGY

|        |   |    |
|--------|---|----|
| 2.9    | PETROGRAPHY AND MINERALOGY OF THE GRANULITES                                    | 53 |
| 2.9.1  | The acid granulites   | 53 |
| 2.9.2  | The basic granulites  | 64 |
| 2.9.3  | The calc-silicate rocks   | 68 |
| 2.10   | DISCUSSION OF PARTICULAR MINERAL ASSEMBLAGES                                    | 75 |
| 2.10.1 | Corona-like textures involving garnet<br>and sillimanite                        | 75 |
| 2.10.2 | Corona-like textures involving garnet<br>between mafic minerals and plagioclase | 83 |
| 2.10.3 | Corundum occurrences  | 87 |

## METAMORPHISM AND ORIGIN

|      |                            |     |
|------|----------------------------|-----|
| 2.11 | CONDITIONS OF METAMORPHISM | 93  |
| 2.12 | ORIGIN OF THE GRANULITES   | 110 |
| 2.13 | CONCLUSIONS                | 122 |

SECTION 3. LOCAL GEOLOGY. THE GOSSE PILE ULTRAMAFIC BODY  
AND ASSOCIATED INTRUSIVES

|     |             |     |
|-----|-------------|-----|
| 3.1 | TERMINOLOGY | 123 |
|-----|-------------|-----|

## GEOLOGY AND PETROGRAPHY

|       |                                       |     |
|-------|---------------------------------------|-----|
| 3.2   | GEOLOGY AND PETROGRAPHY OF GOSSE PILE | 127 |
| 3.2.1 | The layered sequence                  | 128 |
| 3.2.2 | The picrite-serpentinite rocks        | 133 |
| 3.2.3 | The noritic intrusive                 | 136 |
| 3.2.4 | The dolerites                         | 139 |
| 3.2.5 | The olivine-gabbro                    | 141 |

## TEXTURES

|       |                                     |     |
|-------|-------------------------------------|-----|
| 3.3   | TEXTURES                            | 142 |
| 3.3.1 | Igneous, or primary, textures       | 142 |
| 3.3.2 | Metamorphic, or secondary, textures | 151 |

|   | Page |
|---|------|
| LAYERING  |      |
| 3.4 LAYERING  | 157  |
| 3.4.1. Primary layering (S <sub>i</sub> )   | 158  |
| 3.4.2 Tectonic layering (S <sub>t</sub> )   | 170  |
| PETROLOGY AND MINERALOGY  |      |
| 3.5 PETROLOGY   | 180  |
| 3.6 MINERALOGY  | 192  |
| 3.6.1 Plagioclase   | 192  |
| 3.6.2 The Pyroxenes   | 210  |
| 3.6.3 Other minerals (olivine, opaque minerals,<br>serpentine minerals)                         | 242  |
| 3.7 CONCLUSIONS   | 249  |
| <br><u>SECTION 4. SUMMARY OF THE GEOLOGICAL HISTORY OF THE AREA</u><br><u>AROUND GOSSE PILE</u> |      |
| 4.1 SUMMARY OF THE GEOLOGICAL HISTORY OF THE AREA AROUND<br>GOSSE PILE                          | 255  |

#### APPENDICES

##### APPENDIX 1

|   |            |
|---|------------|
| MODAL ANALYSES OF ROCKS FROM GOSSE PILE | 1(i)-1(iv) |
|---|------------|

##### APPENDIX 2

|   |                                |
|---|--------------------------------|
| A METHOD FOR DETERMINING MINERAL COMPOSITIONS BY<br>MEASUREMENT OF THE MASS ABSORPTION COEFFICIENT<br>(Reprint from Am. Miner., 54, 1180-1189). | pages<br>numbered<br>1180-1189 |
|---|--------------------------------|

##### APPENDIX 3

|                        |            |
|------------------------|------------|
| METHODS AND TECHNIQUES | 3(i)-3(ix) |
|------------------------|------------|

APPENDIX 4

SUMMARY OF THE PAPER BY NESBITT et.al. (1969),  
"The Giles Complex, Central Australia: a  
stratified sequence of basic and ultrabasic  
intrusions" (in press)

4(i)-4(iv)

APPENDIX 5

BRIEF DESCRIPTIONS OF ROCKS MENTIONED IN THE TEXT

5(i)-5(xvi)

REFERENCES

(i)-(xli)

---

## SUMMARY

An area, 5 km by 9 km, in the eastern Tomkinson Ranges, central Australia, has been mapped in detail. The hard rock geology consists of granulite facies rocks (for convenience termed "granulites") into which have been intruded various igneous rocks. The most important of these is the Gosse Pile layered intrusion, an ultramafic part of the Giles Complex.

Following a brief discussion of the regional geology of the central Musgrave Block, the local geology (i.e. the area studied in detail) is discussed in two main sections; the granulites and the rocks of Gosse Pile itself.

Studies of the structure of the granulites in the area around Gosse Pile has indicated at least two periods of folding: one prior to, and one post-dating the intrusion of the Giles Complex rocks. These deformations are recognised on the basis of fold style and overprinting relationships. Faults in the granulites are of two types, classified as mylonites and brittle faults. Some petrofabric work on one of the mylonites indicates it has a monoclinic fabric. An attempt is made to correlate the textures and fabrics of the granulites with the rock type in which they occur and, statistically, a strong relationship has been shown to exist. The textures are then interpreted in relation to the deformational history of the rocks and their mineralogy. The petrography and mineralogy of the granulites have been studied in detail, with particular attention being paid to



the existence and interpretation of unusual mineral associations. These include corona textures of garnet around sillimanite cores, garnet rims between plagioclase and mafic minerals and the occurrence of corundum, apparently exsolved from ilmenite and spinel.

The granulites, including acid rocks (quartz + feldspar + mafic minerals), basic rocks (pyroxene + amphibole + feldspar) and calc-silicate rocks (marble and diopside + scapolite rocks), are thought to represent an original sedimentary sequence which has been through several metamorphic cycles. These culminated in granulite facies metamorphism, estimated (with reservation) to have been at about  $1,000^{\circ}\text{C}$  and 10 kb, some 1,300 - 1,600 m.y. ago.

Much later, (estimated to be at least 200 m.y. after the granulite facies metamorphism) tholeiitic magma was intruded into the granulites. This underwent fractional crystallization to produce the ultramafic sequence, with cyclic units, of Gosse Pile. The crystallization is considered to have been under conditions of high pressure, probably in the lower crust and crude estimations of absolute conditions are  $1,200 - 1,300^{\circ}\text{C}$  at 10-14 kb. The evidence for high pressure crystallization is as follows:

- (i) The presence of spinel exsolution in the pyroxenes;
- (ii) The presence of rutile exsolution in the orthopyroxene;
- (iii) High  $\text{R}_2\text{O}_3$  contents of the pyroxenes;
- (iv) High values for the distribution coefficients for Mg and Fe between co-existing pyroxenes;

- (v) The dominance of orthopyroxene over olivine as an early cumulus phase.

The unexpected lack of chromite horizons may also be attributed to conditions of high pressure crystallization.

Soon after crystallization of the ultramafic sequence and prior to complete cooling, low angle thrusting separated the more felsic upper portion and produced a gneissic zone with textures and fabrics similar to those found in high-grade metamorphic rocks or "alpine-type" intrusions. The mineralogy is unchanged. Thus, within a single body there is a gradation from typical igneous to typical metamorphic textures and fabrics, and petrofabric work has been carried out on both types. The orthopyroxenites show a strong igneous lamination in the relatively undeformed area.

It has been established that, post-dating this thrusting, there have been several intrusions including dolerite, picrite and noritic rocks. It is not known for certain whether these were intruded before or after the deformation which folded the ultramafic sequence into a near-vertical position because of the lack of relevant field evidence. However, on the basis of evidence found elsewhere it seems likely that the amphibole - dolerites were intruded prior to this deformation ( $D_2$ ) and that the schistosity developed within them can be correlated with an  $S_2$  schistosity in the granulites. Since this dolerite cuts the present sill of later noritic material west of Gosse Pile it means that all of these rocks probably were intruded

before the  $D_2$  deformation.

The mineralogy of the rocks of Gosse Pile has been studied in detail. The plagioclases of the layered sequence are commonly antiperthitic, an unusual feature for feldspars from layered intrusions. A determinative curve, relating  $\Gamma$  values and An content of heated plagioclases has been established. During this study, and one involving measurement of the Sr content of the plagioclases a method for indirectly determining mineral compositions by measurement of their mass absorption coefficients was established. This is given in an appendix.

The exsolution features of the pyroxenes (spinel, rutile, pyroxene) have been studied and interpretations of their origins given. The orthopyroxenes show the development of "hour-glass" structures, a feature usually found in clinopyroxenes. The distribution of some major and some minor elements between co-existing pyroxenes has been measured, the most important of which have been Mg and Fe distribution. These indicate high values for the distribution coefficient, similar to the values obtained for pyroxenes from ultramafic nodules from basalts. Other minerals (olivine, oxide and sulphide minerals, and serpentine) are only briefly described.

The present boundaries of Gosse Pile are marked mainly by brittle faults which have produced fault breccias. Small, oxide-rich dolerites are associated with this period of brittle faulting which has also produced a series of minor faults within Gosse Pile which

strike east-west, N.W. and N.E. The most recent events have been the deep weathering of the eastern part of the picrite intrusion, to produce serpentinite with associated silcrete and magnesite deposits, and later weathering and erosion which has given Gosse Pile and the surrounding granulites their present profile.

Research, the results of which are contained in this thesis, was carried out between May 1966 and March 1970, during which time I was employed as a full-time Demonstrator in Geology at the University of Adelaide. This thesis contains no material which has been accepted for the award of any other degree or diploma in any University and it contains, to the best of my knowledge and belief, no material previously written or published by another person except where due reference and acknowledgement is made in the text.

Signed:

Alan Moore,

1 April, 1970.



ACKNOWLEDGEMENTS

No thesis of this nature is the work of a single person because the writer is dependent upon the advice, encouragement, criticism and assistance of colleagues, friends and family. This thesis is no exception and I place on record here my thanks to all those who have given so much to me in this respect. A list of all such persons would be excessively long, but some must be mentioned by name:

Dr. R.W. Nesbitt, my supervisor who also suggested the project; Professor R.W.R. Rutland; Dr. R.L. Oliver; Dr. T.P. Hopwood; Dr. A.W. Kleeman; Miss E.M. McBriar; Dr. J.B. Jones; Mr. O.R. Stanley; Mr. A.D.T. Goode; Mr. P.D. Fleming; Mr. A.R. Milnes; Dr. R. Offler; Professor J.F. Lovering; my wife and both our families.

Mrs. B. Goode, who very efficiently typed this thesis.

Mr. Max Foale and the late Mr. J. Probert, who produced most of the photographic plates.

## LIST OF ABBREVIATIONS USED IN THE TEXT

Only less common abbreviations are listed, and thus excluded are the generally accepted abbreviations such as chemical symbols, mathematical symbols and those for common measurements (e.g. min for minute, hr for hour, mm for millimetre, etc.).

### 1. In analyses

A.A.S. : atomic absorption spectrograph/spectroscopy  
n.a. : not analysed  
n.d. : analysed but not detected  
p.p.m. : parts per million  
tr : trace (amount detected too small for accurate measurement of quantity present)  
X.R.D. : X-ray diffraction  
X.R.F. : X-ray fluorescence

### 2. Minerals

|      |                 |         |                      |
|------|-----------------|---------|----------------------|
| ab   | : albite        | hc      | : hercynite          |
| al   | : almandine     | hy      | : hypersthene        |
| amph | : amphibole     | il      | : ilmenite           |
| an   | : anorthite     | K-f     | : potassium feldspar |
| bi   | : biotite       | mt      | : magnetite          |
| c    | : corundum      | ol      | : olivine            |
| cc   | : calcite       | or      | : orthoclase         |
| ch   | : chondrodite   | opx     | : orthopyroxene      |
| cord | : cordierite    | phlog   | : phlogopite         |
| cm   | : chromite      | plag    | : plagioclase        |
| cpx  | : clinopyroxene | py      | : pyrope             |
| di   | : diopside      | px      | : pyroxene           |
| en   | : enstatite     | q       | : quartz             |
| fa   | : fayalite      | s or sp | : spinel             |
| fo   | : forsterite    | sill    | : sillimanite        |
| fs   | : ferrosilite   | spess   | : spessartine        |
| ga   | : garnet        | wo      | : wollastonite       |
| hb   | : hornblende    |         |                      |

### 3. General

- AMDEL : Australian Mineral Development Laboratories.
- C.P. : crossed polars
- P.P.L. : plane polarized light
- m.y. : million years
- $P_f$  : The pressure on any fluid phase(s), f, which may or may not be pure. f may be  $\text{CO}_2$ ,  $\text{H}_2\text{O}$ , F etc. or combinations of these. The partial pressure of a fluid phase is considered to be the product of the total fluid pressure and the mole fraction of that phase in the mixture of fluids present. In most cases f is probably  $\text{H}_2\text{O}$  or  $(\text{H}_2\text{O} + \text{CO}_2)$ .
- $P_{E_i}$  : The equilibrium pressure of component i; it is the pressure on a pure fluid (i) in equilibrium with solid phases.
- ss : solid solution.

SITUATION

PREVIOUS INVESTIGATIONS

STATEMENT OF THE PROBLEM



## SITUATION

Gosse Pile, situated at the eastern end of the Tomkinson Ranges in South Australia, is about 32 km east of the Western Australia border and 21 km south of the Northern Territory border, (Fig. 1.1). The area is entirely within the North West Reserve for Aborigines. The nearest permanent settlements are the Giles Meteorological Station in Western Australia (193 km by road west) and the Amata Homestead (previously called Musgrave Park) and settlement (209 km by road east). The Tomkinson Ranges form a discontinuous mountain chain about 160 km long, most of which is in Western Australia. The highest point is Mt. Davies at 1,043 metres, while Gosse Pile stands some 945 metres above sea level. The ranges consist of large masses of mafic and ultramafic intrusives of the Giles Complex (Sprigg and Wilson, 1959), granulite facies metamorphic rocks and granites, all of which crop out as scattered hills and inselbergs of various sizes and are surrounded by wide alluvial, sandy plains. These plains, containing sand ridges fixed by sparse vegetation, are relatively elevated (450 - 670 metres above sea level) compared with the Central Australian depressed areas.

The rainfall of the region shows great seasonal variation but is probably of the order of 23 cm per annum while the annual evaporation is probably about 305 cm (Mirams, 1964). Because of these factors and the high absorbency of the plain sands there is no well developed drainage pattern. Water courses originate as torrent channels in the ranges and flow only during heavy rains. Few exist for more than a few miles from the principal ranges.



PREVIOUS INVESTIGATIONS

Gosse (1874) and Giles (1874) were the first white men to traverse this part of Australia and they named most of the topographic features. Streich (1893) and Basedow (1905) were the first to give geological accounts of the area and to collect specimens of the rocks. Robinson (1949) gave brief petrological descriptions of some of the specimens collected by Basedow including some from quite close to Gosse Pile. Between 1954 and 1957 the Southwestern Mining Company mapped the intrusive rocks of the Giles Complex, including those of Gosse Pile. This work was incorporated into the more detailed maps of the area produced by the South Australian Department of Mines (Thomson, Mirams and Johnson, 1962; Thomson, 1964). Mirams and McCarthy (Mirams, 1964) produced a geological and petrographical description of much of the area covered by the Department of Mines maps (particularly the Mann Sheet) as well as showing an annotated aerial photograph of Gosse Pile.

In their interpretation of the regional geology of the Musgrave Block, Sprigg and Wilson (1959) made only brief mention of Gosse Pile and the surrounding rocks. They considered Gosse Pile to be an integral part of "a once continuous basic and ultrabasic composite (?) lopolith", similar to the Bushveld Igneous Complex, South Africa. Since a brief report on the Mount Davies intrusion by Nesbitt and Kleeman (1964) considerable work has been done on various aspects of, and in different parts of, the Giles Complex. A number of papers have been published: Nesbitt, 1966; Nesbitt and Talbot, 1966; Compston and Nesbitt, 1967; Daniels, 1967; Facer, 1967; Goode and Krieg, 1967; Horwitz, Daniels and Kriewaldt, 1967; Kleeman and Nesbitt, 1967;

Moore, 1968; Turner, 1968; Trommsdorf and Wenk, 1968; Goode and Nesbitt, 1969; Moore, 1969; Nesbitt, Goode, Moore and Hopwood, 1969. A number of unpublished honours theses have also been produced: Yong, 1964; Goode and Krieg, 1965; Kleeman, 1965; Miller, 1966; Steele, 1966 and Gray, 1967.

#### STATEMENT OF THE PROBLEM

A University of Adelaide project, under the leadership of Dr. R.W. Nesbitt, was started in 1963 to study the rocks of the Giles Complex. Gosse Pile was one part of the complex selected for detailed study because it shows features not observed in other parts of the complex. The objective of this thesis is to attempt an explanation for some of these features.

- (i) Gosse Pile is one of the few ultramafic bodies found in the Giles Complex. The lack of feldspar-rich rocks is unusual especially considering the abundance of such rocks in other parts of the complex.
- (ii) Gosse Pile is very different from Mt. Davies, a body about which quite a lot of information is available. Yet these two very different intrusions are geographically close together, being separated only by the Numbunja Creek which has produced a rugged pass between them. The relationship between these two bodies was unknown prior to this investigation.

- (iii) To the south of Gosse Pile occurs a gabbro-gneiss which shows a mineralogical foliation and a texture indicating that the rocks have recrystallized under high grade metamorphic conditions, probably of the granulite facies. This feature was first noticed only in loose boulders on the outwash plain south of Gosse Pile but, since this study commenced, the rock type has been found in place at Gosse Pile, Kalka (also known as Walter Hill, Dulgunja Hill and Scarface) and in the Hinckley Ranges.
- (iv) On the north side of Gosse Pile is found a pyroxenite which shows a marked preferred orientation of crystals, a feature not observed in other intrusions of the Giles Complex.

When this study started very little work, apart from field mapping, had been done on the granulites around the Mt. Davies and Gosse Pile areas other than a few petrographic descriptions by McCarthy (Mirams, 1964) and by Goode and Krieg (1965). No detailed work had been done on the granulites around Gosse Pile. Thus, it was felt that at least a preliminary investigation of these rocks should be included in this thesis.

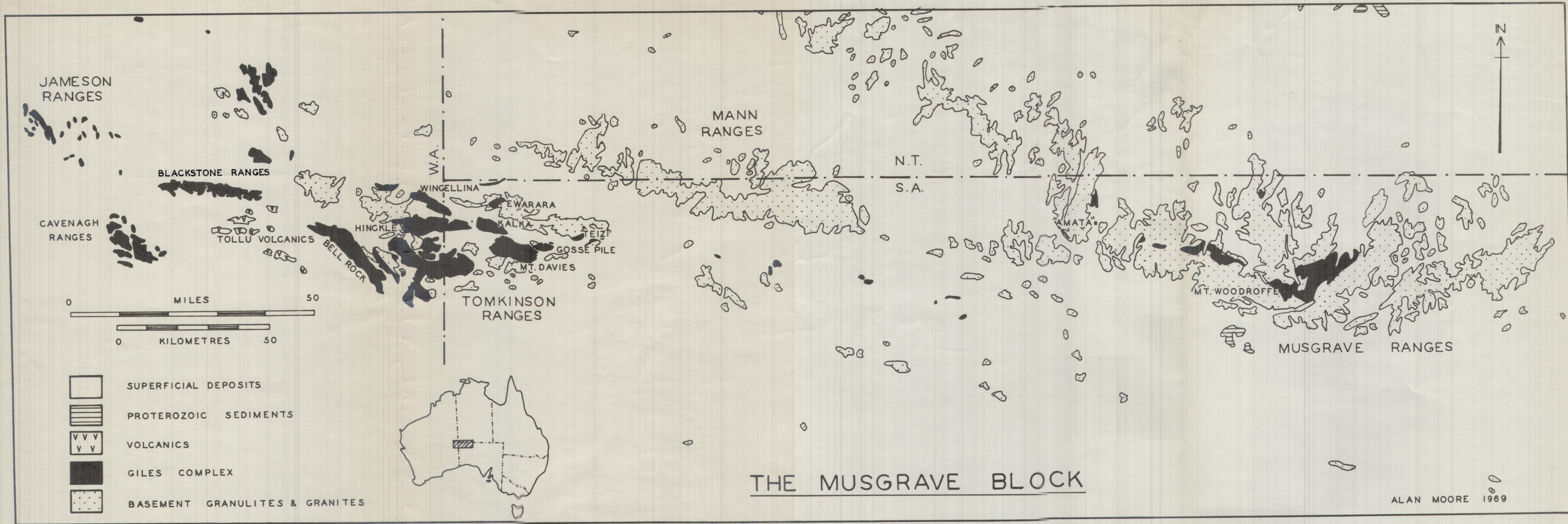
SECTION 1.

REGIONAL GEOLOGY

Fig. 1.1

Simplified map of the regional geology of the central  
Musgrave Block, Central Australia.







## 1.1 REGIONAL STRUCTURE AND METAMORPHISM

Gosse Pile and the surrounding granulites form only a very small part of the Musgrave Block (Hossfeld, 1954) which, as a structural unit extends from the Warburton Ranges in Western Australia some 640 km eastward as far as the eastern Musgrave Ranges. It is bounded by younger sediments to the north (Amadeus Basin) and to the south (Officer Basin). In South Australia it crops out as a number of sub-parallel east-west ranges, of which the Tomkinson Ranges is but one (Fig. 1.1). Wilson (1947), Robinson (1949), Wilson (1954) and Sprigg and Wilson (1959) have shown that the metamorphic rocks forming the greater part of this block are granulite facies gneisses with associated charnockites and anorthosites. In the extreme eastern part of the block the rocks are at amphibolite facies grade, changing westwards to predominantly hornblende granulite subfacies (Wilson, 1954). In the area around Gosse Pile and Mt. Davies rocks of the pyroxene granulite subfacies predominate (Nesbitt and Talbot, 1966). See Fig. 1.2.\*

In the past the Musgrave Block granulites have been generally referred to as Archaean (e.g. Glaessner and Parkin, 1958, p. 81; Mirams, 1964) because they are the oldest Precambrian rocks of the region. However, recent work has shown that the metamorphism is much younger than had been supposed. Arriens and Lambert (1969)

---

\*Fig. 1.2 and Fig. 1.3 are bound at the back of this thesis in an envelope fastened to the back cover.

have dated, by the Rb/Sr method, a number of granulite and amphibolite facies rocks from the Ernabella Mission area (east of that part of the Musgrave Block shown in Fig. 1.2). Although much scatter occurs on the resultant isochrons they conclude that granulite facies metamorphism can be dated at between 1,300 and 1,400 million years, i.e. middle Proterozoic. Horwitz, Daniels and Kriewaldt (1967) have mapped a portion of the Musgrave Block in Western Australia between latitudes  $25^{\circ}$  and  $27^{\circ}$  south. They agreed with Nesbitt and Talbot (1966) that the Giles Complex consisted of several intrusions, each with its own characteristics, rather than a single sheet disrupted by faulting as suggested by Sprigg and Wilson (1959). They have also recognised several granite generations in the area and a stratigraphic sequence in the granulites. From this they have been able to work out a folded structural layering of the rocks in that part of the Musgrave Block. Using this structural layering they constructed a tectonic interpretation of the area and concluded that there must have been two periods of regional metamorphism in the area, both prior to the intrusion of the Giles Complex. In the eastern part of the Musgrave Block other workers (Wilson, 1954; Sprigg and Wilson, 1959) have recognised only one period of metamorphism during the climax of which granitic igneous rocks (including charnockites, adamellites and granodiorites) were intruded. These rocks now form large exfoliating tors, often within the fold-axial regions of anticlines, and have outcrop patterns elongate parallel to the axial trends. Horwitz (1967), working in Western Australia

---

places this period of granitic intrusion as middle Proterozoic.

Wilson (1954), Sprigg and Wilson (1959) and Coates (1963) have shown that fold-axial trends in the eastern Musgrave Ranges are almost north-south, the folds being tight, sometimes isoclinal, and with local overfolding to the west. It is pointed out that this tight folding is characteristic only of the eastern Musgrave Ranges and can be related to shearing movements between major sub-parallel faults striking approximately west-south-west. Coates (1963) recognised a strong upper Proterozoic and pre-Ordovician folding in the eastern Musgrave Ranges where the Adelaide System (Proterozoic) occurs in open folds to the south and the folding increases in intensity northwards. Coates concluded that this folding was restricted to well-defined zones which coincide with major fault blocks in the Archaean. In view of the recent isotopic dating by Arriens and Lambert (1969) the time relationships between these periods of folding will have to be revised. In the central Musgrave Ranges there is a change in orientation of fold-axial trends and, in the Mt. Woodroffe area, open folds with fold-axial planes striking approximately east-west predominate. Sprigg and Wilson (1959) consider that this may be the influence of a later (? early Proterozoic) deformation. In the Mann and Tomkinson Ranges the fold axial planes trend approximately east-west but the fold pattern is disrupted by faulting, although the trends may still be readily observed.

As seen in Fig. 1.2 there are numerous exceptions to this general

trend. Folds which, on the basis of fold style and overprinting relationships are related to the first recognisable deformation in this area, may have their axial plane traces striking in directions other than east-west. Folds considered to be related to the second deformation appear to have consistent east-west trending axial plane traces. This is discussed in more detail in section 2.3. The Giles Complex layered bodies have been shown to truncate many folds and faults in the area (e.g. Goode and Krieg, 1965) but are themselves folded by the second deformation. Within some of the layered bodies (e.g. Kalka, Gosse Pile) a gabbro-gneiss has been developed by high temperature deformation. In Kalka (Nesbitt et. al., 1969; Goode, pers. comm.) this gabbro-gneiss contains folds related in style and orientation to those in the granulites which are designated as having been produced by the second deformation. The gabbro-gneiss is possibly an early manifestation of the tectonic activity which produced the second generation folds. Nesbitt and Talbot (1966) consider that the present attitude of the layering in the Giles Complex is the result of this second period of folding which probably took place in the middle or upper Proterozoic. This age is assigned because the Tollu volcanics, dated by Compston and Nesbitt (1967) as middle Proterozoic ( $1,060 \pm 140$  million years), are folded into a shallow syncline conformable with the folding of the surrounding gabbros (Blackstone, Bell Rock and Cavenagh Ranges). At Skirmish Hill, 32 km south of the Tollu volcanics (Fig. 1.1), the steeply dipping volcanics are adjacent to weakly deformed sediments considered to be upper Proterozoic by Johnson (1963).

In the western Tomkinson Ranges the overall structure is that of a series of relatively open folds, trending west-north-west, which become recumbent to the south-south-west in the northern part of the area (Horwitz, Daniels and Kriewaldt, 1967).

The major faults of the eastern Musgrave Ranges strike east-north-east and west-north-west (Sprigg and Wilson, 1959). In the western Musgrave, Mann and Tomkinson Ranges the major fault trend is essentially east-south-east (Thomson, Mirams and Johnson, 1962; Thomson, 1964; Major *et. al.*, 1967). Large scale fault zones (e.g. Hinckley Fault) dominate the structure of the central Musgrave Block. These fault zones, in places exceeding 1 km in width, consist of mylonite and breccia. Mirams (1964) has shown, by correlation of granitoid rocks on either side of the fault, that sinistral movement along one of these major thrust zones, on the south side of the Mann Ranges, has been of the order of 160 km.

## 1.2 THE GILES COMPLEX

The Giles Complex was originally named and defined by Sprigg (in Glaessner and Parkin, 1958), "as a layered intrusive consisting of an overlying mass of little-differentiated gabbros and norites, underlain and intruded at the base by a complex suite of ultrabasics. Earlier formed multiple intrusions of troctolitic types form well-marked banding in some cases". Nesbitt and Talbot (1966) have since shown that the rocks originally designated "Giles Complex" in fact comprise several distinct intrusions, the majority of which

are layered and characterised by the abundance of plagioclase-rich rocks, with a deficiency of ultrabasic rocks. This view is confirmed by Daniels (1967). In this work the Giles Complex is considered to define a series of layered mafic or ultramafic igneous intrusions, now occurring as distinct masses between the Jameson Ranges in Western Australia and Mt. Woodroffe in South Australia. It excludes dolerite and gabbroic dykes and sills which also occur in this area and which, when coarsely crystalline, may be difficult to distinguish in hand specimen from gabbro of the Giles Complex layered bodies. Gray (1967) has shown that picrite plugs cut dolerite dykes in the Teizi meta-anorthosite, a body which he relates to the Giles Complex. The dolerite dykes maintain an approximately north-westerly strike and are apparently not affected by the deformation which has folded the Teizi body into a plunging antiform (Gray, 1967). Similar picrites and dolerites are found transgressive to the main layered bodies.

The above definition must then exclude the dykes and picrite plugs from the term "Giles Complex" although both may be associated with, and show some petrographic features characteristic of, parts of the layered bodies. Therefore, the term "Giles Complex" is restricted to those larger, generally layered, bodies which are associated with a period of igneous activity post-dating the granulite metamorphism and folding and pre-dating the folding and faulting of these large bodies. All other igneous activity is considered to be "post-Giles".

Nesbitt and Talbot (1966) considered the intrusion of the Giles Complex (undefined) to have been completed by the upper

Proterozoic since the later folding took place at this time. Daniels (1967) has observed xenoliths of volcanic rocks in the gabbros west of Bell Rock in Western Australia (the Jameson Range Gabbro). These volcanics he correlates with the Tollu volcanics, which have been dated by Compston and Nesbitt (1967) using the Rb/Sr isochron method. The age is  $1,060 \pm 140$  million years, hence the Giles Complex in this area must be middle or upper Proterozoic, though other parts may be older. Daniels (1967) considers that the Tollu volcanics are intruded by part of the Giles Complex (undefined).

### 1.3. POST - GILES INTRUSIVES

#### Basic dykes.

Insufficient detailed work has been done on the basic dykes of the Musgrave Block to determine their relationship, if any, to the Giles Complex or when they were intruded. Some work has been carried out by Basedow (1905), Talbot and Clark (1917) and Wilson (1948) but this work, apart from that by Wilson, is mainly descriptive. Field work by Goode (pers. comm.), Gray (1967) and the author has demonstrated that there are several dyke generations, all of which are transgressive to the layering of the granulites. Some of the dykes are cut by younger dykes (each having a different petrography) and others have been cut by the picrite plugs (Gray, 1967). Gray (1967) has described basic dykes which show indications that they have crystallized under high pressure (granulite facies) and are transgressive to the dominant banding of the Teizi meta-anorthosite.

---



Large (up to 13 km in length) dykes, generally striking approximately north-west and often showing a marked preferred orientation of feldspars, are found cutting rocks of the Giles Complex and the associated granulites. These two dyke types can be distinguished on the basis of their mineralogy and texture: the former contain orthopyroxene and garnet and have a granoblastic texture (termed "gabbroic dykes" by Gray) while the latter lack orthopyroxene and garnet, contain clinopyroxene, bright green amphibole and show a strong foliation with a strong preferred orientation of plagioclase (termed "foliated dykes" by Gray). Goode (pers. comm.) has field evidence from Ewarara that the gabbroic dykes are cut by the foliated dykes, indicating definite time relationships.

A third type of dyke, apparently younger than the previous two, occurs throughout the area and has a distinctive mineralogy. It contains pigeonite, augite, plagioclase and is particularly rich in oxides. Olivine and orthopyroxene may be present in some dykes. In some areas these are porphyritic and particularly rich in olivine (Wilson, 1948; Goode, pers. comm.). This type is similar to the dolerites described by Wilson (1948) and Coates (1963). The dykes are usually found as narrow, steeply-dipping bodies associated with fault zones, although the dolerite itself is often unstressed. Coates (1963) considers that these dykes are pre-Sturtian (upper Proterozoic) since he has found boulders of this dolerite (micro-gabbro) in the Moorilyanna conglomerate which underlies the Chambers Bluff tillite. This tillite is correlated with the Sturt tillite on the basis of

---

lithological similarity in the whole stratigraphic sequence.

#### Picrite Plugs.

On the basis of the definition used in this work the picrite plugs which occur throughout this area are not considered to be part of the Giles Complex. Most commonly they are found as irregular, elongate masses associated with the layered bodies, but transgressive to the layering even though, on a broad scale, they may be elongate parallel to such layering. They are also found as almost circular masses in the granulites. The picrites have a characteristic texture: large phenocrysts of clinopyroxene, up to 3 cm, poikilitically enclose small, almost round, crystals of olivine. Plagioclase and orthopyroxene occur interstitially. They are generally undeformed (Nesbitt et. al., 1969).

#### 1.4 YOUNGER UNITS

The only units younger than the dolerites are laterites, which Mirams (1964) considers to be Tertiary by correlation with laterites in the Petermann Ranges, Northern Territory, and unconsolidated sands, which are probably Recent. Mirams (1964) recognises two Quaternary units. The alluvial plains and associated sand dunes, slope deposits marginal to the inselbergs and the material associated with the principal drainage channels he classifies as Recent. He assigns a probable Pleistocene age to the two older units. These are a rough, denuded calcrete ("kunkar") sheet elevated approximately 18 metres above the adjacent Recent deposits, and a red soil forming extensive

flats. Because the calcrete does not occur in the area around Gosse Pile and because of the similarity of the sand plains, distinguished as Pleistocene and Recent by Mirams, no effort has been made to distinguish these units on the geological map of Gosse Pile in this thesis (Fig. 1.3).

### 1.5 SUMMARY OF THE REGIONAL GEOLOGICAL HISTORY

A general summary of the regional history has been included in Table 1.1 using both published material and information supplied to the writer by Dr. R.W. Nesbitt and Mr. A.D.T. Goode. Other personal communications are noted. Some of the information tabulated has been prepared for publication (Nesbitt et. al., 1969).

Following regional granulite facies metamorphism and deformation, during which granitic rocks were intruded, intrusion of the layered mafic and ultramafic rocks of the Giles Complex took place. Local high temperature deformation of some of the layered bodies ensued, producing gabbro-gneisses. The equivalent deformation has not, so far, been recognised in the surrounding granulites. A second regional deformation took place in the Proterozoic, folding both the granulites and Giles Complex about approximately east-west trending fold axial planes. An even later, third deformation is responsible for the folding of Kalka and the apparent cross-folding of Michael Hills (Fig. 1.2). At least three periods of dolerite intrusion have occurred, the latest of which was accompanied by the production of large scale brittle faults in the Musgrave Block (e.g. the

**TABLE 1.1** Summary of the regional geological history of the Musgrave Block. The compilation of this table is the result of combined work by A.D.T. Goode, A.C. Moore and R.W. Nesbitt and incorporates published and unpublished data to which due acknowledgement is made.

| FLANKING SEDIMENTS  |               | WESTERN MUSGRAVE BLOCK |  | EASTERN MUSGRAVE BLOCK  |   |  |
|---|---------------|------------------------|--|---|---|--|
| AMADUUS BASIN   | OFFICER BASIN | W. TOMKINSON RANGES    | E. TOMKINSON RANGES  | W. MUSGRAVE RANGES  | E. MUSGRAVE RANGES                              |  |
| Folding of Palaeozoic sediments (U. Palaeozoic) <sup>1</sup>                      |               |                        |  |   |   |  |
| Palaeozoic sedimentation <sup>1</sup> (Kalyang volcanics; 480 m.y.) <sup>4</sup>  |               |                        |  |   |   |  |
| Folding of Proterozoic sediments. 1, 2, 3.  |               |                        | Major E-W mylonite zones. 5, 6. (e.g. Hinckley, Wann.)   | Major ESE-NW mylonite zones (e.g. Mann, Woodroffe, Davenport) 7       |   |  |
| Proterozoic sedimentation (Upper Bitter Springs Formation; 950 m.y.) <sup>9</sup> |               |                        |  | Proterozoic sedimentation 11, 12, 13.                                 |   |  |
| Proterozoic(?) sediments and volcanics  |               |                        | Olivine dolerite dykes   |   | Olivine dolerite dykes <sup>14</sup>            |  |
|   |               |                        | Folding (F <sub>3</sub> )  |   |   |  |
|   |               |                        | Neritic intrusions. Plagioclase plugs intruded. Basic dykes.   |   |   |  |
|   |               |                        | Folding of Tollu volcanics and of Giles Complex and granulites; F <sub>2</sub> fold styles. 6, 15, 16. |   | Folding of amphibolite facies rocks. 7, 17, 18. |  |
|   |               |                        |  | High temperature deformation of parts of Giles Complex <sup>8</sup>   |   | Dolerite dykes <sup>19</sup>                                       |
|   |               |                        | Tollu volcanics (1,050 m.y.) <sup>20, 21</sup> and layered bodies of Giles Complex.                    |   |   |  |
|   |               |                        |  | Opx adamellite intrusions   |   | Opx adamellite intrusions <sup>24</sup> (1,120 m.y.) <sup>25</sup> |
|   |               |                        | Two deformations recognised <sup>26</sup>  | One deformation recognised. F <sub>1</sub> fold styles                | One deformation recognised 7, 2, 28.            |  |
|   |               |                        | Granulite facies metamorphism(s)   | Granulite and amphibolite metamorphism (1,330 m.y.) <sup>27, 28</sup> |   |  |

**References:**

- |  |  |
|--|--|
| 1 Foran, 1966.                             | 15 Nesbitt and Talbot, 1966.             |
| 2 Costes, 1963.                            | 16 Daniels, 1967.                        |
| 3 Wells, Stewart and Skwarko, 1966.        | 17 Glaesner & Parkin, 1958.              |
| 4 Major and Teluk, 1967.                   | 18 K. Collerson, Pers. Comm.             |
| 5 Thomson, Mirams and Johnson, 1962.       | 19 G. Krieg and R. Major, Pers. Comm.    |
| 6 Goode and Nesbitt, 1969.                 | 20 Nesbitt, 1966.                        |
| 7 Major, Johnson, Leeson and Mirams, 1967. | 21 Compston and Nesbitt, 1967.           |
| 8 Forbes, 1966.                            | 22 Sprigg and Wilson, 1959.              |
| 9 Glaesner, Preiss and Walter, 1969.       | 23 Wilson, 1967.                         |
| 10 Johnson, 1963.                          | 24 Wilson, 1960.                         |
| 11 Major, 1966.                            | 25 Arriens and Lambert, 1969.            |
| 12 Sprigg, Wilson and Costes, 1959.        | 26 Herwits, Daniels and Kriewaldt, 1967. |
| 13 Wilson, 1952.                           | 27 Compston and Arriens, 1968.           |
| 14 Wilson, 1968.                           | 28 Wilson, 1956.                         |

Hinckley Fault). This period of faulting may be related to the folding of the sediments in the adjacent Officer and Amadeus Basins.

#### 1.6 ECONOMIC POTENTIAL AND THE "SILCRETE"

No economic deposits of minerals have been found in the area under discussion although there are prospects of small scale nickel and vanadium mining in the western Giles Complex, and of copper associated with the Tollu volcanics. Basedow (1905) noted the presence of chalcedonic material north of Mount Davies which, he observed, was often bright green "due to chromium staining". It is likely that he was referring to the few deposits of chrysoprase which occur within the siliceous cappings to the ultramafic parts of the complex. These siliceous horizons (termed "silcrete" by the author and "jasper" by Thomson, 1964) have been shown by Thomson (1963, 1965) to be a zone within the lateritic profiles which develop only in the ultramafic parts of the Giles Complex. These profiles are divided into three zones. At the surface is a nickeliferous ochre which is occasionally rich enough to be mined (e.g. at Wingellina, in Western Australia, where reserves are estimated to be in excess of 60 million tons, assaying 1-2% nickel.\* The Southwestern Mining Company is investigating this area and, although the ochre is rich enough by world standards to be mined, the deposits are very inconveniently situated). Underlying this ochre is the siliceous zone containing ferruginous chalcedony, white cryptocrystalline silica and occasional veins of chrysoprase. The rocks underlying the ochre zone are

---

\* Figures from the Australia and New Zealand Bank Quarterly Survey, July 1968.

probably most accurately described as chalcedonic horizons. However, for convenience the term "silcrete" is used in this work because the rock has probably formed in a manner analagous to true silcrete, namely as a result of downward leaching of silica to definite horizons within a weathering profile (Mirams, 1964; Thomson, 1965). The term was originally used by Lamplugh (1902, 1907) to describe locally indurated patches in superficial deposits when the cement is largely siliceous and since used for the silicification of subsoils by the upward migration of acidic colloidal solutions of silica derived from the leaching of underlying rocks, (e.g. Frankel and Kent, 1937). Beneath the siliceous horizon is found a serpentine zone.

In the immediate area around Gosse Pile erosion has removed almost all traces of the upper zones, leaving only an alluvium covered, highly weathered serpentine zone containing nodules of magnesite and isolated remnants of the siliceous middle zone. It should be pointed out that the siliceous capping, often up to 6 metres thick, is not restricted to the serpentine zone of Gosse Pile and is found overlying relatively fresh pyroxenite and norite, usually near fault zones, especially in the hills to the west of the main body (Fig. 1.3; AB/2).

Apart from the potential value of the nickel in the area Daniels (1967) has shown that bands of titaniferous magnetite occur in gabbros in the Western Australian section of the Giles Complex. These bands are rich in  $TiO_2$  (13% - 26%) and in  $V_2O_5$  (0.57% - 1.4%) and so may be of future economic importance. Similar bands occur over limited

---

areas near Kalka and north of Hinckley Range in South Australia but are absent in the Mount Davies and Gosse Pile areas.

Gosse Pile is considered to be the approximate site of the legendary Earls' Reef, a supposedly rich gold reef (Sprigg and Wilson, 1959). However, no gold finds in the area have ever been substantiated. Apart from the relative poverty of economic minerals in the region any development in this part of Australia would be severely hampered by the remoteness, harsh climate and lack of water.

---

SECTION 2.

LOCAL GEOLOGY

THE GRANULITES



## 2.1 INTRODUCTION

The term granulite is used here for tectonites which have mineral assemblages consistent with the granulite facies of metamorphism (Turner and Verhoogen, 1960). It includes both acid and basic rocks as well as calc-silicate rocks. The quartz-rich members of the sequence conform to the classical definition of a granulite: "quartzo-feldspathic garnet or pyroxene gneisses with little or no mica, in which quartz occurs as flattened lenticles oriented (by grain form) parallel to the foliation", (Turner and Verhoogen, 1960, p. 553).

Although many of the rocks described in the following sections could be termed "charnockitic" or "enderbitic" (Tilley, 1936) these terms have been deliberately omitted for two reasons. Firstly, the rocks can be described more precisely and simply in terms of their mineralogy and facies (e.g. q + f + px granulite) whereas terms such as "charnockite", "enderbite" and "khondalite" would require redefinition as they have been used in different senses by different authors (see Parras, 1958). Secondly, the term "charnockite" was originally used by Holland (1900) for hypersthene-bearing rocks, which he considered to be igneous, found in India. Holland specifically expressed the hope that the term would not be applied to similar rocks found elsewhere in the world. This hope has not been realised and much of the confusion surrounding the "charnockite problem" seems to have been caused by the ready application of the term to almost any hypersthene, quartz and feldspar rocks.

A wide variety of mineralogically different granulites occur in the area (Fig. 1.3) but they can be divided into three main types:

- (i) acid granulites: those rocks containing free quartz
- (ii) basic granulites: those rocks containing no free quartz
- (iii) calc-silicates: those rocks composed essentially of diopside or of calcite plus silicate minerals.

## 2.2 DISTRIBUTION AND S-SURFACES

The distribution of rock types is most readily seen by reference to the map (Fig. 1.3) and their relative abundances are shown in Table 2.1.

With respect to scale, three types of S-surface have been recognised within the granulites.

The first corresponds to a large scale compositional layering where bands and lenses of lithologically distinct units alternate. These units may be several metres thick (2 - 30m) and, in general, are large enough to be mapped on the scale of Fig. 1.3. Contacts between the acid granulites and the other two granulite types are sharp, but within each type are found two or more groups, classified on the basis of slight variations in mineralogy (Section 2.9). Contacts between these latter groups may be either sharp or transitional.

The second type of S-surface is a small-scale mineralogical banding within the above units, but measured in terms of centimetres.

Table 2.1

Relative abundances of different granulite types expressed in terms of outcrop area measured on Fig. 1.3.

| Granulite type                         | Area, in<br>km <sup>2</sup> | %      |
|--|-----------------------------|--------|
| acid granulites                        |                             |        |
| (i) q + f + px and q + f<br>granulites | 2.7602                      | 91.74  |
| (ii) q + f + ga granulites             | 0.1530                      | 5.09   |
| (iii) iron-rich granulites             | 0.0338                      | 1.12   |
| basic granulites                       | 0.0436                      | 1.45   |
| calc-silicate rocks                    | 0.0182                      | 0.60   |
| TOTAL                                  | 3.0088                      | 100.00 |

The third type of S-surface is produced by the sub-parallel alignment of elongate mineral grains, generally quartz lenses but often pyroxene or garnet grains (i.e. schistosity).

The present structural configuration of the granulites around Gosse Pile is dominated by the east-west lithological layering which, in the west, strikes north-west and is folded into an overturned, south-east plunging synform (Fig. 1.3). Since the relatively small areas of granulite around Gosse Pile are surrounded by wide alluvial plains there is no way of directly relating them to the large fold structures, with dominantly east-west axial plane traces, which lie to the north (Fig. 1.2). Because of the discontinuous nature of easily recognisable lithologies (e.g. the calc-silicate rocks or basic granulites) macroscopic\* folds are difficult to detect.

The S-surfaces made apparent by the lithological layering and mineralogical banding are termed  $S_s$ . The gross changes in lithological layering (e.g. acid granulite and marble) are considered to represent original depositional differences. However, in view of the high grade of metamorphism and the degree of deformation to which these rocks have been subjected, as well as the lens-shaped exposures of many rock types, it is thought unlikely that original bedding surfaces have been preserved, although there is no direct evidence to prove that  $S_s$  is not parallel to original bedding. Thus, it is considered that

---

\* Terminology referring to scale follows that suggested by Turner and Weiss (1963, pp. 15-16).

the gross regional distribution of rock types probably reflects an original stratigraphic distribution but that the small-scale mineralogical banding is probably the result of other processes, such as metamorphic differentiation and transposition.

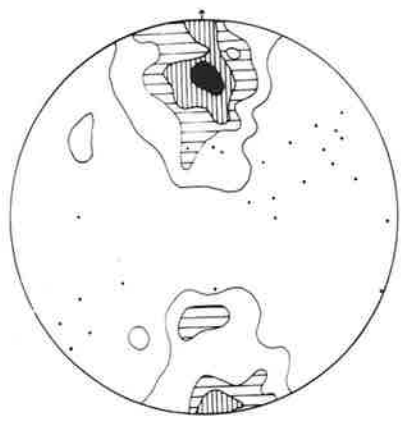
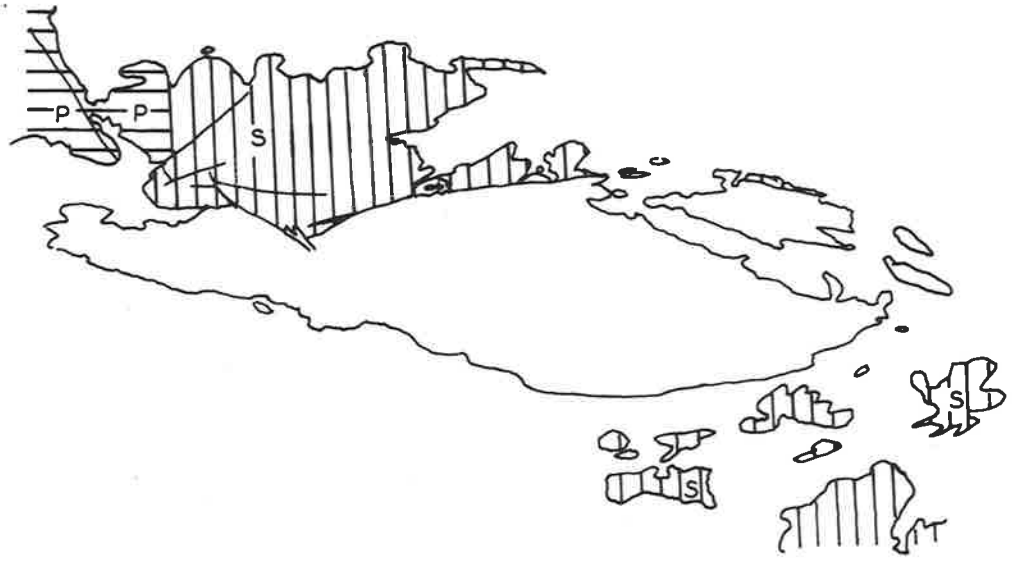
The basic granulites and calc-silicate rocks sometimes show small-scale banding but are usually rather massive and lack mesoscopic structural features such as mineral preferred orientation or folds. The acid granulites typically show a well-developed compositional layering or a schistosity or both. In those which contain only small amounts of mafic minerals (about 5 - 10%)  $S_s$  is seen as a series of aligned quartz or K-feldspar lenses as well as an arrangement of mafic minerals which form elongate clusters (Fig. 2.3). In rocks containing significant quantities of mafic minerals (about 20% or more)  $S_s$  is seen as mineralogically distinct bands within the rock (banded gneiss). Such bands are fairly continuous and can extend up to 6 m in length. Occasionally they are folded to produce appressed intrafolial folds (Figs. 2.2 and 2.8). Throughout most of the area around Gosse Pile  $S_s$  strikes approximately east-west with steep dips. However, in the western area (Fig. 1.3, AB/1) it strikes north-west. Fig. 2.1 shows the orientation of 97 poles (contoured) to the layering ( $S_s$ ) from granulites around Gosse Pile excluding the western area. The diagram also includes 25 poles to  $S_s$ , plotted as points, from the western area. The limited spread is an indication of the regularity of the orientation of  $S_s$  within fairly clearly defined areas.

Fig. 2.1

The orientation of 97 poles (contoured) and 25 poles (points) to  $S_g$  from the granulites around Gosse Pile. The shaded outline map indicates the areas in which the measurements have been made. The western section, marked P and shaded horizontally, is the area in which the 25 uncounted poles were measured. The remaining area, marked S and shaded vertically, indicates the area in which the 97 contoured poles were measured.

Contour intervals at 1%, 3%, 6% and >10% per 1% area with a maximum of 12%.

Stereographic projection on the lower hemisphere of a Schmidt equal-area net.



### 2.3 FOLDS

Fold types are distinguished essentially on the basis of fold style and the assumption is made here that the different fold styles are produced during different periods of deformation. Folds which are thought to have formed during the first recognisable deformation ( $D_1$ ) are termed  $F_1$  and are of two types.

Macroscopic  $F_1$  folds are characteristically appressed and have axial plane traces parallel to  $S_s$ , except in the hinge area. It appears that, although the majority of  $F_1$  folds have essentially east-west fold axial plane traces, there are a number of folds of different orientation, which probably formed during the same period of deformation: these are recognised on the basis of similar style. The NNW-trending synform, northwest of Gosse Pile, is an example of such a fold (Fig. 1.3 AB/1 and Fig. 2.1). Other examples can be seen west and southwest of Mt. Davies (Fig. 1.2). This variability of  $F_1$  fold axial plane traces may be due either to original inhomogeneity of the  $D_1$  deformation, either structural or stratigraphic, or due to the influence of the later ( $D_2$ ) deformation on shallow-dipping  $F_1$  fold axial planes. Until a detailed structural analysis of a large area is undertaken this problem cannot be resolved.

Intrafolial folds in the acid granulites (Fig. 2.2 and 2.8) are assumed to be the mesoscopic equivalents of the large-scale folds described above. More detailed structural analysis, comparing the orientations of the fold axes, may show this assumption to be



unjustified. These mesoscopic  $F_1$  folds are generally isoclinal with sharp hinges. They occur within  $S_s$  and their limbs are usually of unequal length. One limb often merges with another band, as shown in Fig. 2.2. These intrafolial folds commonly have developed an axial plane schistosity ( $S_1$ ) which is defined either by a shape preferred orientation of ferromagnesian mineral clusters or by shape and lattice preferred orientation of quartz and feldspar aggregates and lenses. This fabric forms a lineation (mineral rodding) which is parallel to the mesoscopic fold axes. The quartz lenticules which characterise  $S_s$  in most of the acid granulites are often folded to form hook-like features (Fig. 2.3). These are on a very small scale within the granulite fabric and are interpreted as remnant fold hinges related to  $F_1$ .

A second deformation ( $D_2$ ) has been recognised in the granulites. It produces folds ( $F_2$ ) of a different style from those described above as well as an axial plane schistosity ( $S_2$ ). This schistosity has been recognised only in the hinge zones of  $F_2$  folds where it is clearly shown by planar quartz and opaque minerals and by the formation of plate-like clusters of mafic minerals parallel to the  $F_2$  fold axial plane (Fig. 2.4). In most areas, however, the  $S_2$  schistosity is only very weakly developed.  $F_2$  folds have been recognised only in the north-western area where  $S_s$  strikes NNW. Here  $F_2$  folds have east-west trending axial plane traces which are vertical or dip steeply south, and are parallel to weakly developed  $S_2$  schistosity. These  $F_2$  folds, on a mesoscopic scale, are usually

---

Fig. 2.2

Tight intrafolial fold ( $F_1$ ) in acid granulite (q + f + ga) north of Gosse Pile; (Fig. 1.3, B/2. Near A313/423).

Photograph: T. Hopwood.

Fig. 2.3

Quartz lenses in acid granulite (q + f + px) showing remnant fold hinges ( $F_1$ ). The match is approximately parallel to  $S_S/S_1$ . From granulites north of Gosse Pile; (Fig. 1.3, B/1. Near A313/A24).

Photograph: T. Hopwood.



Fig. 2.4

$S_2$  schistosity, parallel to the match, in the hinge of a  $F_2$  fold in acid granulites (q + f + ga) north-west of Gosse Pile; (Fig. 1.3, B/2).

Photograph: T. Hopwood.

Fig. 2.5

Mesoscopic  $F_2$  folds in acid granulites (q + f + px) north-west of Gosse Pile; (Fig. 1.3, B/1. Near A313/A24).

Photograph: A. Moore.

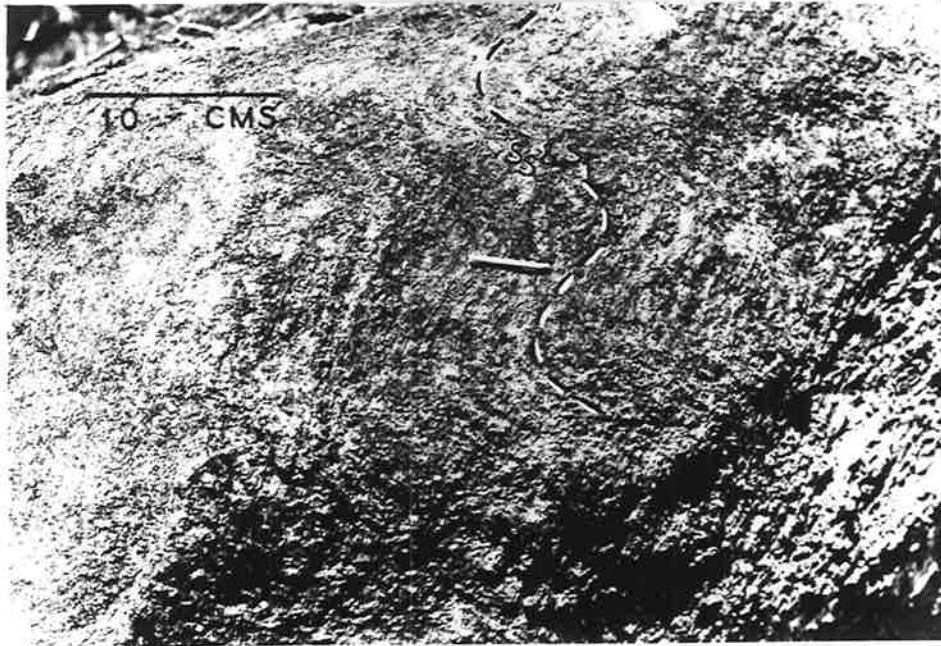
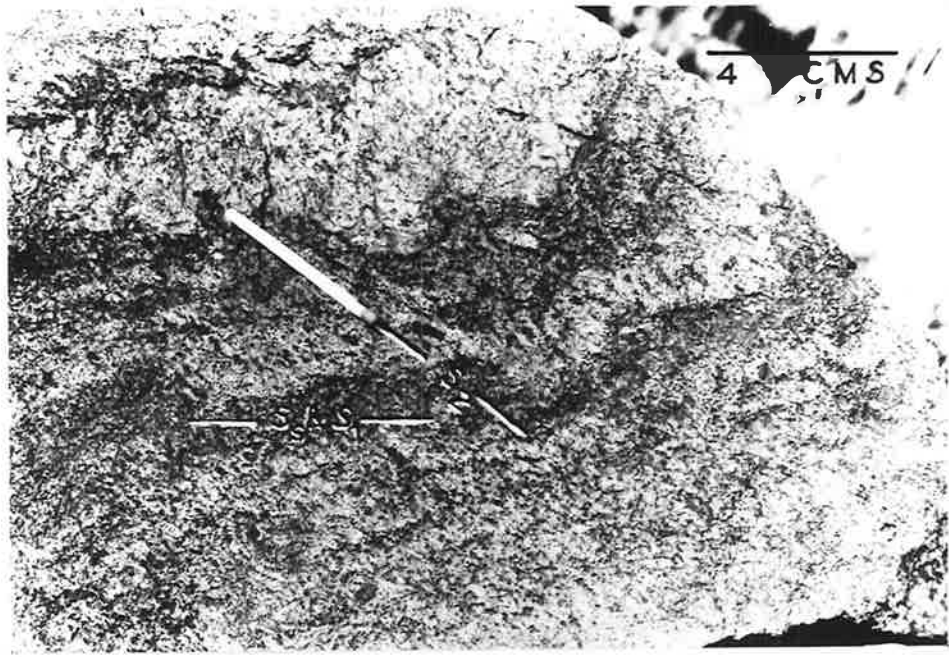


Fig. 2.6

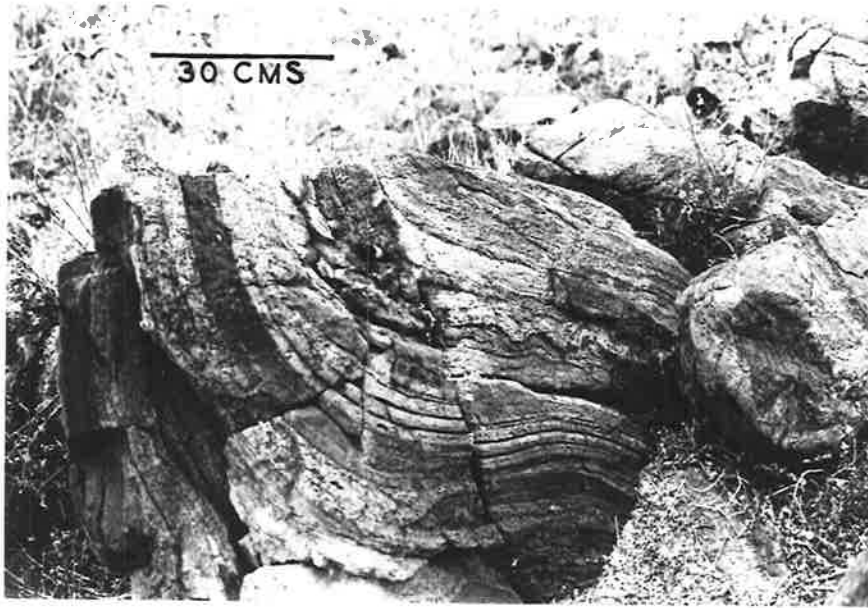
$F_2$  folds south of Mt. Davies. These have approximately east-west trending fold axial plane traces with the fold axes plunging steeply west. They occur on the east limb of a macroscopic  $F_1$  fold with a north-east trending fold axial plane trace.

Photograph: T. Hopwood.

Fig. 2.7

$F_2$  folds south of Mt. Davies (same location as those shown in Fig. 2.6). Note the refolded intrafolial  $F_1$  folds on the southern limb (left side of photograph) indicating overprinting relationships.

Photograph: T. Hopwood.



larger than  $F_1$  and generally have a broad, open structure, as illustrated in Figs. 2.5 and 2.8. The author has also observed  $F_2$  folds south of Mt. Davies where  $S_s$ , the  $S_1$  schistosity and  $F_1$  folds are all folded into broad, open  $F_2$  folds (Figs. 2.6 and 2.7). This clearly demonstrates the mesoscopic overprinting relationship. As in the Gosse Pile area, the traces of the fold axial planes trend east-west so that the trends of folds produced by the second deformation appear to be more consistent than those produced by the first. Fig. 2.8 diagrammatically represents the mesoscopic fold styles of  $F_1$  and  $F_2$  folds.

Throughout the area around Gosse Pile lineations in the granulites are only weakly developed. They are caused by intersections of  $S_s$  and  $S_1$  surfaces (seldom seen) or by a mineral rodding within the plane of the  $S_s$  surface. This is common but subtly defined. Where measured, the lineations have steep pitches, from  $80^\circ$  to vertical, and are parallel to  $F_1$  fold axes. Measurements of quartz [0001] axes in one acid granulite (A313/302) showing a strong foliation and weak lineation indicate an orthorhombic fabric with a girdle perpendicular to the lineation  $L_1$  (Fig. 2.9). Optically continuous rods of quartz occur parallel to  $L_1$  and are flattened in  $S_s$  and  $S_1$ . All of the acid granulites, except for a few garnet-bearing rocks, show some degree of preferred orientation of quartz, feldspar and, where present, sillimanite. Detailed measurements have not been made: the anisotropism was noted by inspection using a gypsum plate and rotation of the



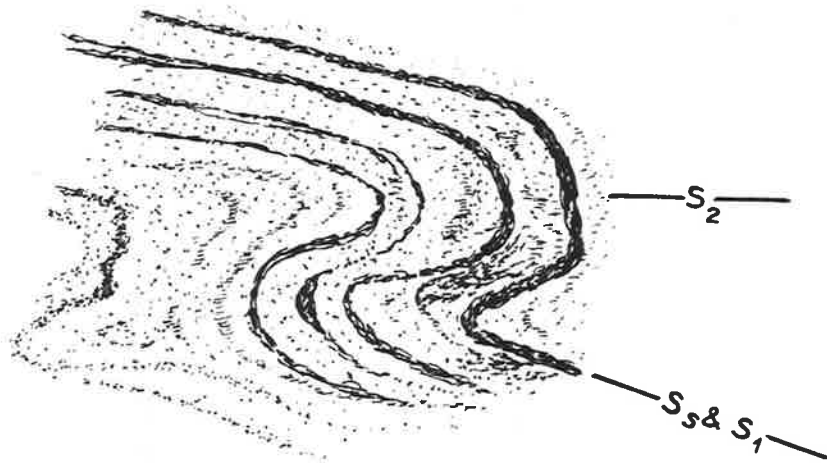
Fig. 2.8

Diagrammatic representations of the mesoscopic fold styles of  $F_1$  and  $F_2$  folds found in granulites of the Mt. Davies - Gosse Pile areas.



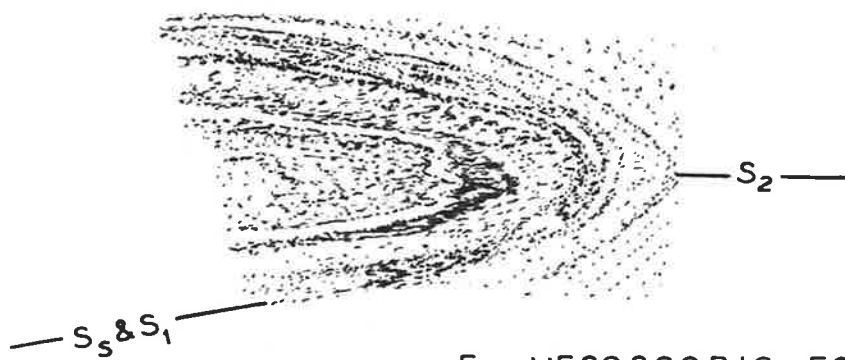
4 CM

F<sub>1</sub> INTRAFOLIAL FOLD



4 CM

F<sub>2</sub> MESOSCOPIC FOLD HINGE



30 CM

F<sub>2</sub> MESOSCOPIC FOLD HINGE

A.M. 1969.

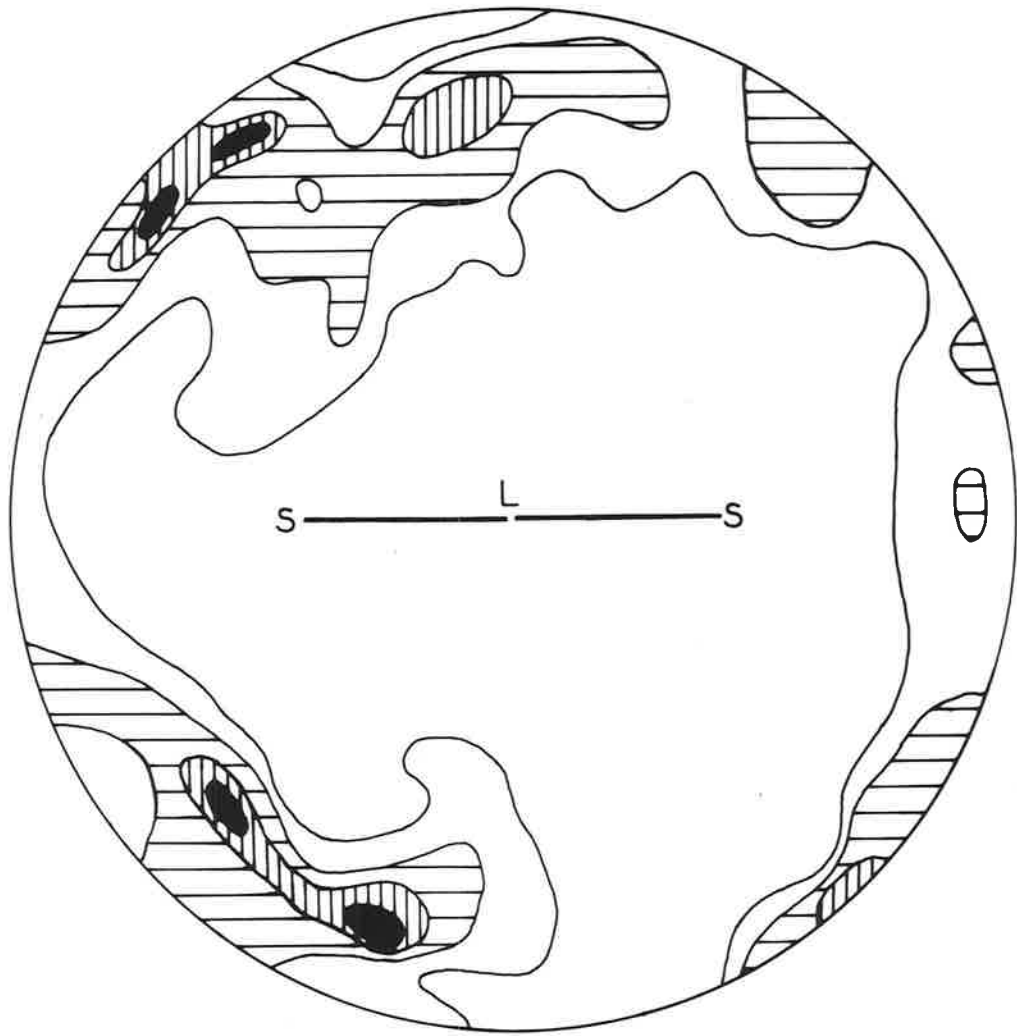
Fig. 2.9

Orientation diagram for 150 quartz [0001] axes from an acid granulite (q + f + px) from north of Gosse Pile; (Fig. 1.3, D/2. A313/302).

Contour interval: 1%, 3%, 5% and >6% per 1% area with a maximum of 7%.

S:  $S_S$  and  $S_1$  which are here parallel and marked by quartz lenticles, elongate plagioclase and lensoid pyroxene clusters.

L: Very weakly developed lineation caused by quartz rodding. Because of its weak nature the field measurement may be slightly in error.



specimen slide between crossed nicols. Rocks containing sillimanite (e.g. A313/424A) show that the sillimanite has a preferred orientation parallel to the weak lineation (Fig. 2.26).

#### 2.4 FAULTS

Faults in the granulites are common and have been classified into two types.

##### (a) Those producing fault breccias.

Generally these occur in zones varying between about 3 - 10 m in width and strike at high angles to the layering ( $S_g$ ). Some such faults are, however, roughly parallel to  $S_g$ , as for example is the fault forming the northern boundary of Gosse Pile (Fig. 1.3). These fault zones consist of disorientated angular fragments of granulite in a fine-grained matrix of finely crushed material (Fig. 2.10). These rocks are here called fault breccias although similar rocks have been termed "kakirites" (Quensel, 1916) and "trapschotten gneiss" (King and Foote, 1864).

Dark flinty veins are well developed and these occur irregularly throughout the rock. In thin section they are seen to consist of rock and mineral grains of varying size, from recognisable pieces large enough to be considered part of the fragmented granulites down to submicroscopic grains. In places there appears to have been local fusion, probably due to extra heat energy provided by friction, with the production of a brown, isotropic glass which

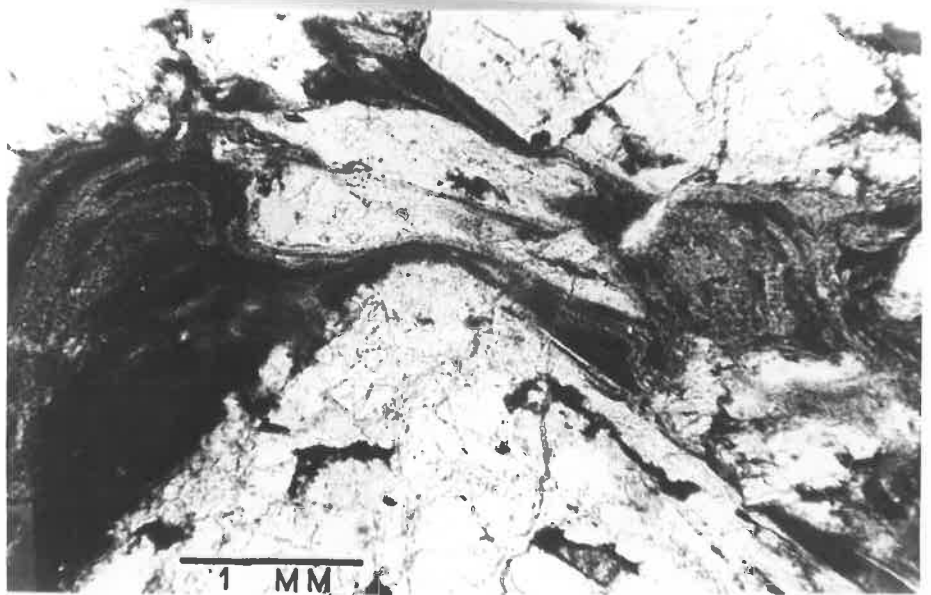
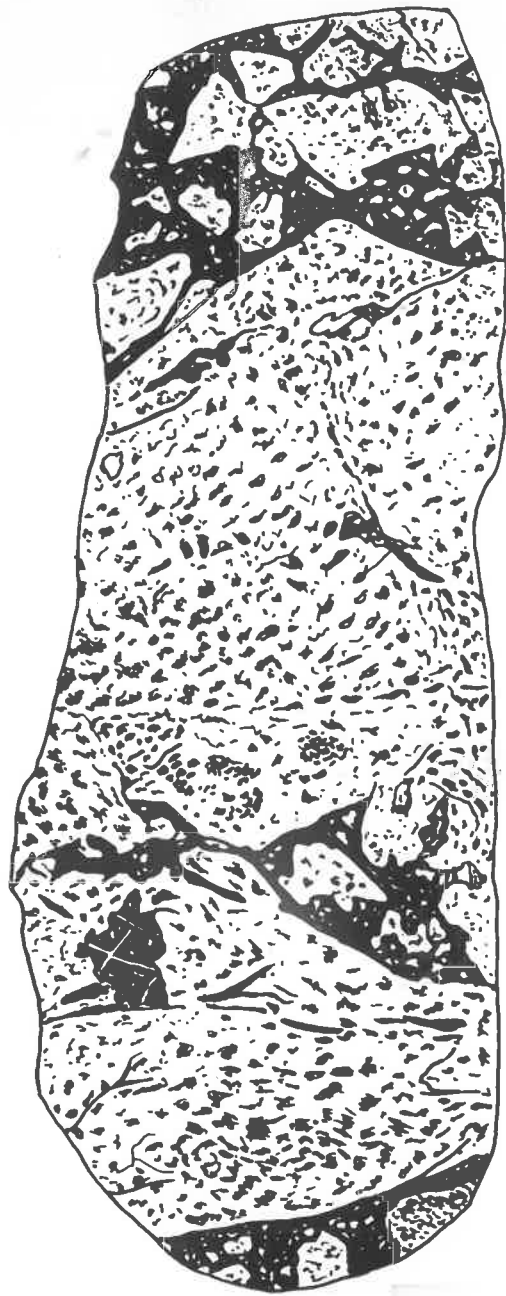
Fig. 2.10

Fault breccia in acid granulites (q + f + px) from part of the fault forming the northern boundary of Gosse Pile. Drawing is natural size; drawn from a large thin section. Note the irregular pseudotachylite veining. (A253/N21B).

Fig. 2.11

Flow structures in brown, isotropic pseudotachylite glass in a sheared acid granulite (q + f + px). P.P.L. (A313/381D).

Photograph: A. Moore.



often contains flow structures (Fig. 2.11). This vein material has probably been produced by the breakdown of rock particles by grinding with local melting. Once produced, it seems that these veins can be forced into zones of weakness in the larger rock fragments and so become locally intrusive. Their existence is directly related to the fault but measurements of the orientations of these veins gives an apparently random orientation. Veins of this type are commonly termed "pseudotachylite" (e.g. Waters and Campbell, 1935; Turner, 1948). However, this term was originally used by Shand (1916) for veins of similar appearance but not associated with shearing. Although Christie (1960) has pointed out this erroneous usage, the name conveniently describes the veins themselves, as distinct from the rock type, and has been so extensively used in the literature in this sense, that it is retained here, (e.g. see Philpotts, 1964).

It is difficult to estimate the sense or the degree of displacement along faults of this type because of the lack of marker horizons. In a few cases where the faults cut dolerite dykes, making the assumption that the dykes on either side of the fault were once continuous, estimates of the amount of lateral off-set component give values of between 10 and 50 metres.

Faults of this type probably formed as a result of brittle fracture and, for descriptive purposes, are termed "brittle faults."



(b) Those producing mylonitic rocks.

The term "mylonite" was first used by Lapworth (1885) in whose definition four conditions were implied. First, the rocks must be fine-grained; second, they must show a well-defined lamination; third, the rock must be characterised by apparent cataclastic breakdown or granulation of the component parts with only minor recrystallization (i.e. characterised by cataclastic rather than crystalloblastic textures) and fourthly, the pulverization must have taken place under conditions such that the rock retained its coherence. Of these four conditions only the first three can be observed in the field and, for the rocks classified as mylonites in this work, these were the criteria applied.

Two mylonite varieties are recognised: the initial distinction was made because of the strikingly different appearance in the field and was confirmed by their very different appearance under the microscope (compare Fig. 2.12 with Figs. 2.14 and 2.15). Both types occur in bands marked on the geological map (Fig. 1.3) as "mylonitic shear zones."

(i) Flaggy mylonite: Of this type only one example (A313/398) has been found. It crops out between the acid granulites and pyroxenites at the western end of Gosse Pile (Fig. 1.3, B/2). It forms a band, about 4 metres wide, of greenish-grey, very fine-grained and strongly laminated rock with scattered outcrops along a strike length of about 400 metres. The foliation strikes parallel

Fig. 2.12

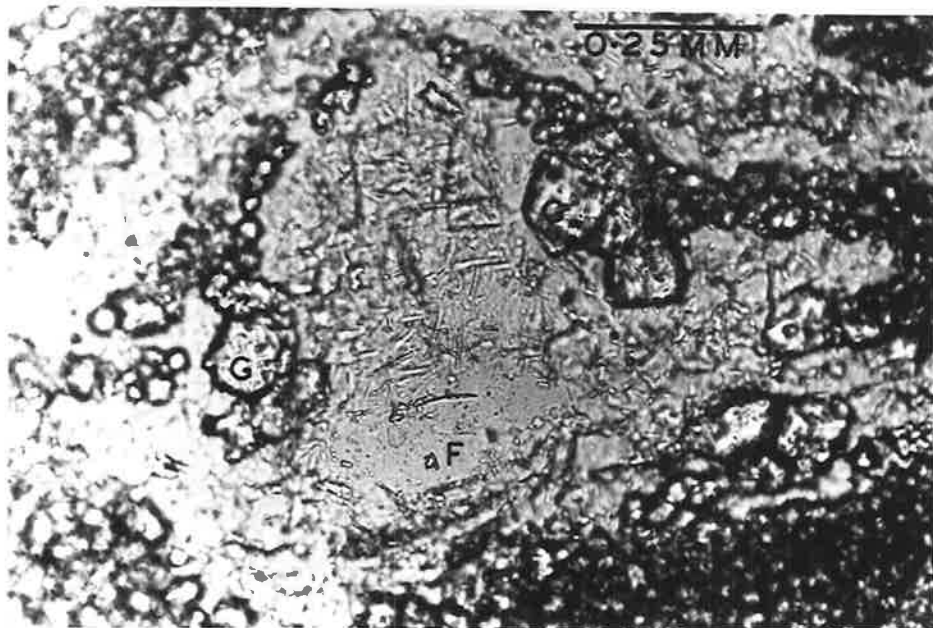
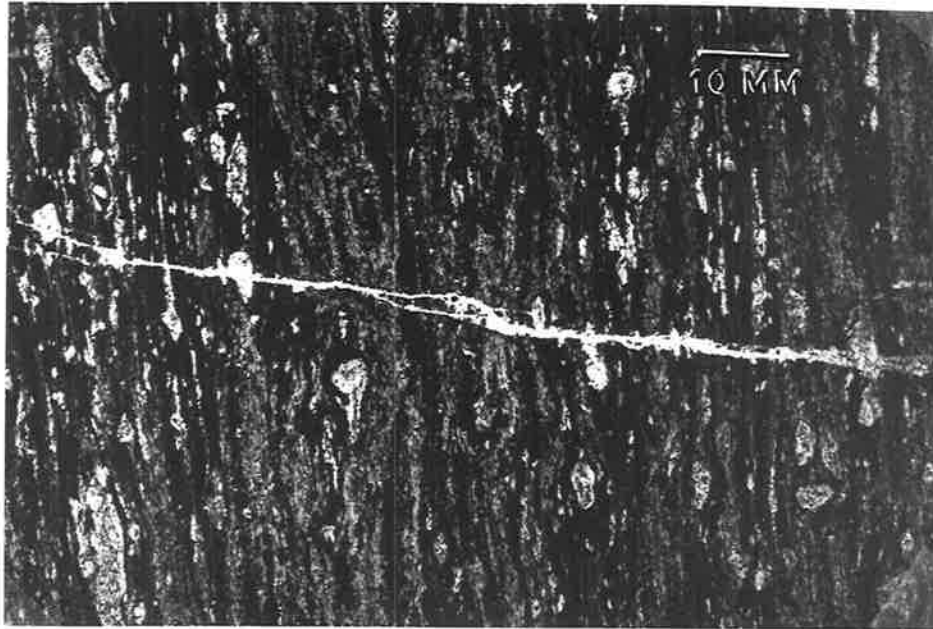
Photomicrograph of flaggy mylonite. The section is cut perpendicular to the lamination. The horizontal crack marks a joint plane. P.P.L. (A313/398).

Photograph: A. Moore.

Fig. 2.13

Augen of feldspar (F), within the flaggy mylonite, containing unidentified needles and surrounded by subhedral garnet (G). P.P.L. (A313/398).

Photograph: A. Moore.



to the contact between pyroxenite and granulites (i.e.  $300^{\circ}$ , dip vertical). It has a flaggy, or slate-like, appearance due to prominent joints, only a few centimetres apart, dipping  $15^{\circ}$  NE. It is not certain whether pyroxenite, granulite or both rock types contribute to this mylonite because it forms the contact between them.

The fine grain size and the alteration (weathering?) prevents easy identification of the minerals in thin section. Tiny, subhedral garnet crystals throughout the rock are thought to have been produced by limited neomineralization. These are especially prominent around the margins of what appear to be remnant, altered feldspar grains (Fig. 2.13). Needles of an unidentified mineral occur within the feldspar. Large areas of chlorite have been recognised as well as highly altered clinopyroxene and a few grains of strongly pleochroic biotite. An X-ray diffraction trace of the rock powder has shown a strong chlorite peak, plus peaks which can be assigned to quartz (?), clinopyroxenes, garnet and plagioclase. The quartz (?) peak is only weakly developed and, since the granulites near this mylonite are quartz-rich, it suggests that the pyroxenite is contributing the greater amount to the mylonite. A photomicrograph of this mylonite type is shown in Fig. 2.12.

(ii) Flaser mylonite: This type is found in numerous bands on the south side of Gosse Pile (Fig. 1.3, D E F/3). The bands are up to 6 metres wide and are of variable length (Fig. 1.3), and are always parallel to  $S_g$  in the granulites (compare with (i) above).

The rocks have a flinty, blue-grey appearance and are marked by a strong vertical, or near-vertical, thin lamination (S). In most, a strong vertical lineation is also developed. Flaser mylonites have been found only in quartz-rich rocks. In these, micro-augen of altered feldspar (1 mm by up to 40 mm) commonly occur, elongate parallel to the lineation.

In thin section these rocks can be seen to consist of fabric domains elongate parallel to the lamination (Fig. 2.14 and 2.15). These domains consist of: (a) numerous minute (approximately 20  $\mu$  in diameter), anhedral mineral grains and, (b) long (up to 3 mm), narrow (0.05 mm approx.) stringers of quartz. These stringers show well developed strain shadows across their lengths, and a tendency to form subgrains, each with a slightly different optic orientation. Böhm lamellae were not seen. Within these domains are occasional micro-augen of feldspar and rare mafic minerals (pyroxene and opaque minerals) which are ovoid to sigmoidal. These augen, and the quartz stringers, are elongate parallel to the strong lineation, L. In sections cut perpendicular to L and S, the quartz stringers are seen to be slightly bent about axes perpendicular to S.

Measurement of quartz c-axes show that these mylonites have an overall monoclinic fabric, with maxima inclined at about  $35^{\circ}$  to the S-surface (Fig. 2.16). If the lattice orientations of the quartz stringers were plotted separately the monoclinic symmetry appears much stronger, while the matrix material tends to produce a more orthorhombic fabric.

Fig. 2.14

Photomicrograph of a flaser mylonite from the south side of Gosse Pile; (Fig. 1.3, F/3. A313/446A).

Thin section cut perpendicular to the lamination and parallel to the lineation. C.P.

Photograph: A. Moore.

Fig. 2.15

Same as Fig. 2.14 but the thin section is cut perpendicular to both the lamination and the lineation.

C.P.

Photograph: A. Moore.

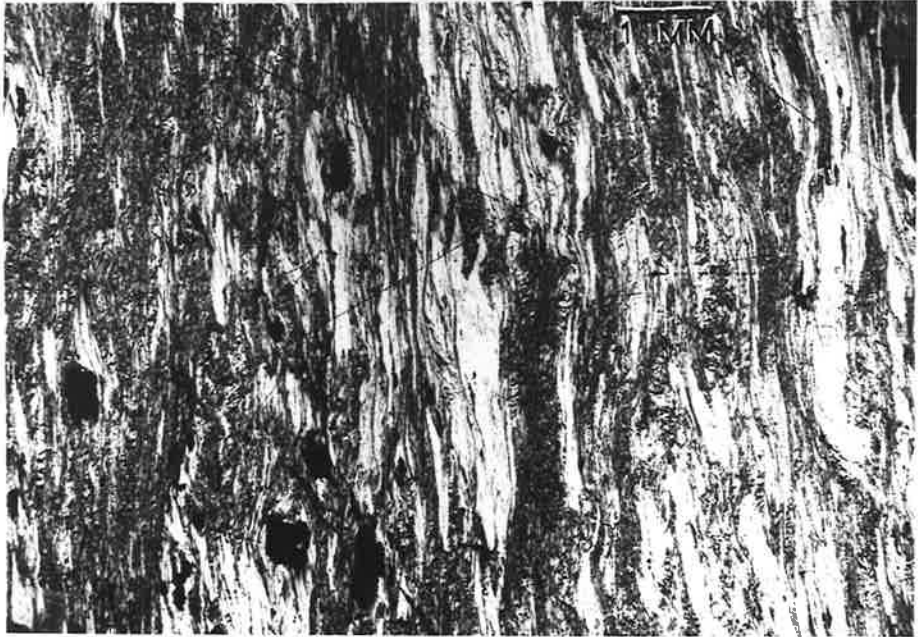
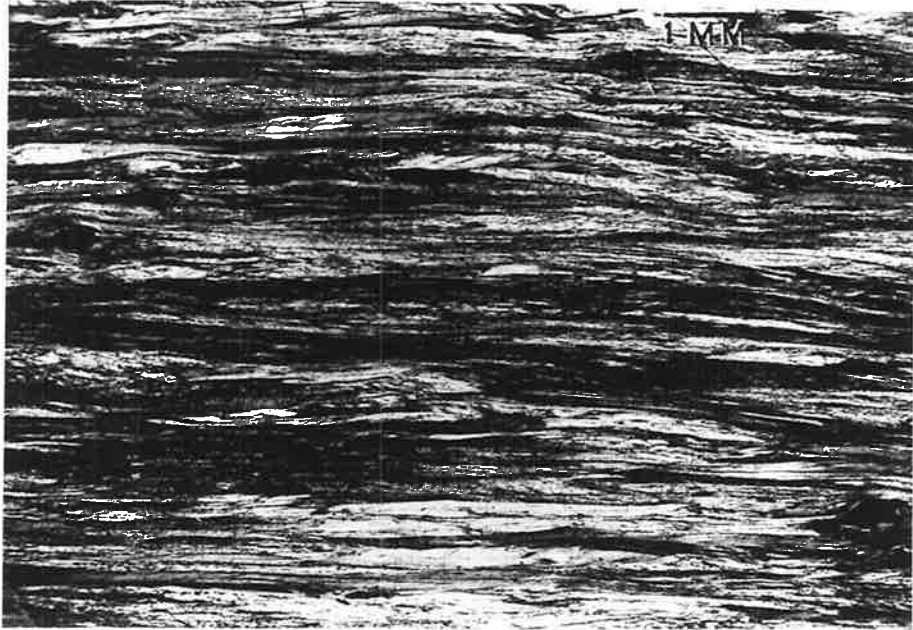


Fig. 2.16

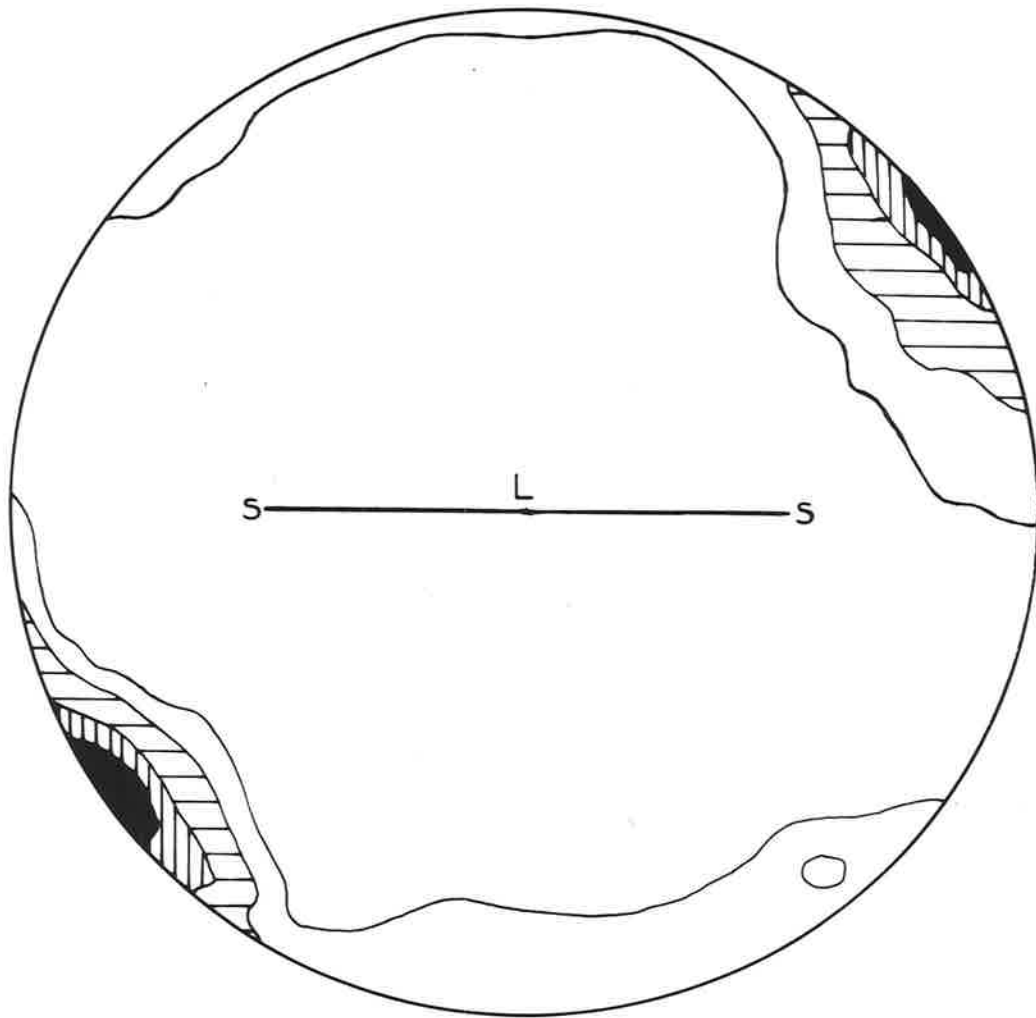
Orientation diagram of 200 quartz [0001] axes showing the fabric of a flaser mylonite (A313/446A).

Contour interval: 1%, 3%, 6%, >10% per 1% area with a maximum of 12%.

S: fine lamination, parallel to the shape orientation of quartz stringers.

L: strong lineation.





According to Sander (1930) the plane of symmetry in such a monoclinic fabric must also be a plane of symmetry in the movements which produced the fabric. Thus, according to this theory the movement direction along the mylonite must be contained in that plane and hence be at right angles to the lineation. Some of the sigmoidal feldspar micro-augen have an "S"-shape, consistent with the monoclinic symmetry. Paterson and Weiss (1961) amplified Sander's principles to show that the present symmetry of the fabric must be related to both the symmetry of the rock fabric prior to deformation (inherited fabric) and to the symmetry of the imposed fabric elements which reflect the symmetry of the forces acting during deformation. If the initial fabric was orthorhombic, since the surrounding granulites probably have orthorhombic symmetry (Fig. 2.9), this explains the orthorhombic element in the present fabric. The imposed fabric is monoclinic, indicating that the symmetry of the deformation was either monoclinic or triclinic. An interpretation of the monoclinic symmetry is to consider that the movement was at right angles to the lineation, with the southern part moving west relative to the northern part (dextral).

The apparent difference in symmetry patterns between stringers and matrix may mean that the above interpretation is open to question and that the present distribution of quartz c-axes is due

to a later, relatively minor component of deformation. This seems unlikely, but sufficient specimens from a wide enough area are not available to prove or disprove this point. If the movement along the mylonite zones is essentially strike-slip, as suggested by their present fabric, then specimens collected at different localities along the mylonite zones of this area should give a similar movement picture. In view of several objections (e.g. Anderson, 1948; Kvale, 1953) to Sander's theory, which is stated more as an axiom, it would be unwise to be too dogmatic about the interpretation of movement relative to lineation, especially in areas such as this where the principal direction of movement cannot be independently determined in the field.

Recently Johnson (1967) has suggested that there may be a close analogy between the origin of mylonite banding and that of slaty cleavage, i.e. they are both surfaces of low resolved shear stress. He concludes ~~that~~, with respect to the mylonites of the Moine Thrust zone, that these are zones of intensive flattening **and** are not necessarily related to any translative movements. Carter, Christie and Griggs (1964) have experimentally produced textures very similar to those seen in natural mylonites (see especially plate 10, Fig B) by compression (40% shortening) of quartzites under conditions of high pressure and temperature. They showed that many of the textures generally attributed to crushing and granulation can be formed by syntectonic annealing processes. If this mechanism alone was responsible for the production of the flaser mylonites

around Gosse Pile the fabric diagram would, like those of Moine Thrust mylonites, be expected to have orthorhombic symmetry (Christie, 1960). It does not and so it is concluded that there must have been some component of **dextral** translative movement which may, or may not, have been the dominant deformation in the production of the mylonites.

## 2.5 CONCLUSIONS

Within the granulites around Gosse Pile two **fold styles** have been recognised and it is assumed that these correspond to two periods of deformation. Overprinting relationships on a mesoscopic scale have been observed which tend to support this view. Throughout the greater part of the area the layering within the granulites ( $S_g$ ) is parallel, or sub-parallel, to the  $S_1$  schistosity produced by the first deformation. Second generation folds appear to have a more consistent orientation than those produced by the first deformation. Gosse Pile is separated from the granulites by fault structures so no time relationships can be deduced between the deformations and the intrusion. However, by comparison with Mt. Davies and Ewarara (Fig. 1.2), intrusion took place after  $D_1$ , since both Mt. Davies and Ewarara cut  $S_g$  and  $S_1$ . The second deformation, which is presumed responsible for folding of the Giles Complex rocks (most intrusions are now nearly vertical; eastern Kalka is overturned to the south. See Goode and Nesbitt, 1969 and Nesbitt et. al., 1969), is reflected in the granulites by broad, open folds with

consistent east-west striking axial plane traces and a generally poorly developed schistosity,  $S_2$ .  $S_2$  is generally only recognisable where there is a strong angular relationship to  $S_s/S_1$ .

The area has been extensively faulted and the faults are of two types: mylonitic (usually parallel to  $S_s/S_1$ ) and brittle (usually at an angle to  $S_s/S_1$ ). These ~~were~~ are probably formed at different times under different conditions. No direct evidence has yet been observed where the mylonite zones are cut by brittle faults, but mylonite zones are commonly cut by dolerite dykes which in other areas, are themselves cut by brittle faults. From this it is thought likely that the mylonitic zones formed during an earlier period of tectonic activity than the brittle faults.

## 2.6 TEXTURES OF THE GRANULITES

### Terminology

The terms "fabric", "texture" and "structure" have been used with different meanings by different authors. There is no apparent uniformity of usage and Turner and Verhoogen (1960, p. 62) use all three synonymously. Katz (1968) uses "fabric", "texture" and "micro-structure" in different parts of the same paper with apparently the same meaning (e.g. p. 805). In this thesis the term fabric is used to define the spatial orientation of the elements of which the rock is composed and it describes the characteristic features of the rock which arise as a result of this spatial orientation, e.g. the preferred orientation of mineral grains. This definition is in general agreement with the definition of fabric ("Gefuge", not translated as "Struktur" or "Textur") given by Sander (1930).

The term "texture" is ill-defined by geologists although it generally refers to the size, shape and arrangement of grains in the rock. To metallurgists this term refers to a preferred orientation and they use "microstructure" to refer to size, shape and arrangements of grains in polycrystalline aggregates. Some authors (e.g. Vernon, 1968) have adopted this latter metallurgical term to describe rocks. However, in geological literature "texture" is well established, even if poorly defined. For this reason it is retained in this thesis. Texture is here considered to refer to the mutual arrangement of the constituent minerals in a rock and to their relative size and shape.

Descriptive terminology, without any genetic implications, for the textures of granulites, is lacking. Buddington (1939) introduced various terms which have been adopted by Katz (1968). These terms have strong genetic connotations and imply a knowledge of the behaviour of minerals under conditions which are assumed or poorly known. Buddington (1939) defines the textures of deformed rocks from the Adirondacks in terms of the amount of cataclasis. Katz (1968) retains Buddington's terminology but uses the relative amounts of recrystallization and deformation (without microbrecciation) to define the textures of granulites (quartzo-feldspathic) from Mont Tremblant Park. This terminology has not been followed here for two reasons. Firstly, terms such as "mortar gneiss" (German: "mortel struktur") and "augen gneiss" (German: "augen struktur") have previously been used in different senses. Harker (1895), Tyrrell (1926) and Buddington (1939) use these terms with the implication that the rocks were "dynamically crushed" and the interstitial material, produced during this cataclasis, consisted of finely-crushed grains although Buddington (1939, p. 252) considered recrystallization did play a part. Katz (1968) however, applies these terms to textures which, he considers, have been produced without any recognisable stage of microbrecciation or cataclasis. Secondly, the textures described by Katz (1968) and illustrated in his paper (Figs. 6-9) are absent or uncommon in the granulites found around Gosse Pile.

Although it is very difficult to avoid genetic terms entirely when describing granulite textures it is felt that a purely

descriptive terminology is desirable. The scheme outlined below is essentially descriptive. It was originally designed for the granulites around Gosse Pile but has since been found to be applicable to granulite facies rocks from Norway and Ceylon.\*

Descriptive textural terminology.

The textures are divided into three main groups (Fig. 2.17) which are described below.

1. GRANOBLASTIC: Here the rock consists of a mosaic of xenoblastic mineral grains.

Depending on the relative sizes of these grains the group is further divided into three subgroups.

- (a) Equigranular: where the majority of constituent grains are approximately the same size.
- (b) Inequigranular: where the frequency distribution of grain sizes is distinctly bimodal such that larger grains of approximately the same size occur in a finer-grained equigranular matrix. A special case would be platy granoblastic (which is characteristic of many quartzo-feldspathic granulites) where long, plate-like crystals, generally of quartz or feldspar, occur in a finer-grained, equigranular matrix. These lenticules may be single

---

\* Specimens collected by Dr. R.L. Oliver, Department of Geology, University of Adelaide, and kindly lent by him to the author.



crystals or, more often, groups of several crystals with lattice orientations differing only slightly (i.e. separated by low angle grain boundaries).

- (c) Seriate: where the grain size frequency distribution is such that a complete gradation from the finest to the coarsest is represented.
2. FLASER: This applies to rocks in which lenses and ribbon-like crystals, usually of quartz, often showing undulose extinction, are separated by bands of finely-crystalline, usually strain-free, material. Ovoid crystals, commonly feldspar or mafic minerals, may occur within the matrix as augen-like megacrysts around which the foliation bends. Although this may be regarded as an extreme version of the platy granoblastic texture it is separated because rocks having flaser textures usually have a very strong lamination and lineation, and the length to breadth ratios of the "ribbons" are large, giving the rock a distinctive appearance.
3. MYLONITIC: Of the three terms used this has the strongest genetic implications. It is applied to rocks which, in appearance, conform as nearly as possible to mylonites as defined by Lapworth (1885) and Christie (1960). The rocks are very fine-grained and have a marked lamination ("fluxion structure"). Small megacrysts may occur within the rock and the lamination bends around these.

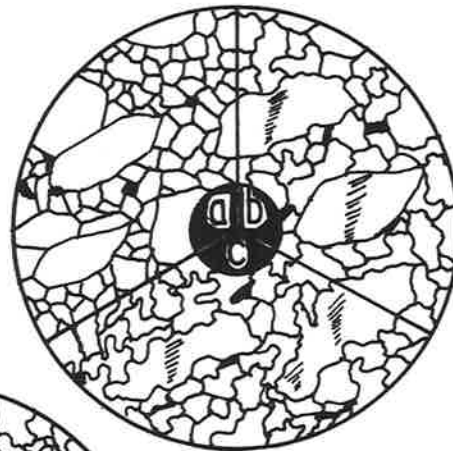
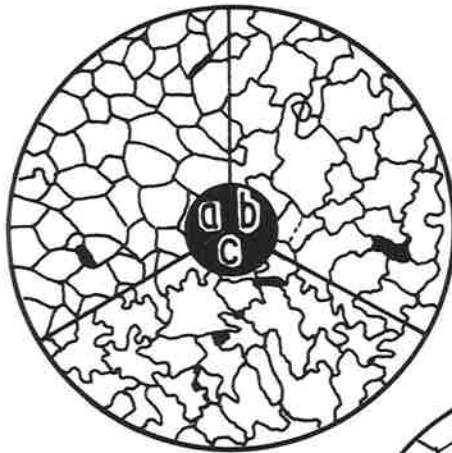
For all three texture types described above in terms of grain size and overall shape, the mutual relationship of the grain requires description. Following Berthelsen (1960) and Katz (1968) the grain boundary relationships are described as polygonal, interlobate and amoeboid. These are shown diagrammatically in Fig. 2.17. As an example of this proposed terminology a rock showing "granuloblastic" texture (Binns, 1964) would be described as having a "granoblastic equigranular polygonal" texture (Figs. 2.21 and 2.24).

This proposed textural classification does not pretend to be able to precisely describe every granulite texture in terms of only the adjectives given above and other descriptive words may be necessary. A single rock may show two textures; For example, a marble in which diopside-rich areas show equigranular polygonal textures and calcite-rich areas show inequigranular interlobate textures. In some rocks small anhedral or rounded grains occur within larger grains. In a situation such as this further qualifications may be necessary to fully describe the texture; for example: granoblastic inequigranular interlobate where larger crystals have a sieve texture. In other rocks corona textures may be found and these would require further description. However, by far the greater proportion of granulites observed by the author have textures which can be conveniently and adequately described using the terminology proposed here.

Fig. 2.17

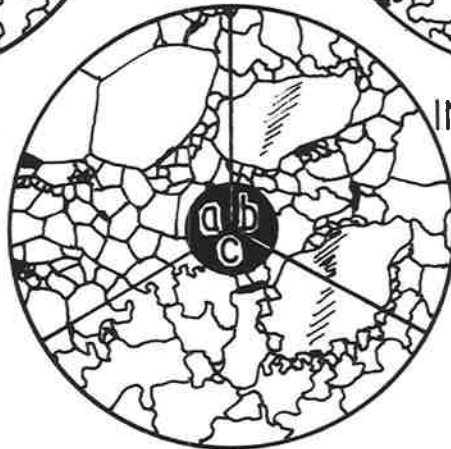
Diagrammatic representation of terminology for  
the textures of the granulites.

GRANOBLASTIC



EQUIGRANULAR

- a: polygonal
- b: interlobate
- c: amoeboid



INEQUIGRANULAR

- a: polygonal
- b: interlobate
- c: amoeboid

SERIATE

FLASER



MYLONITIC



Fig. 2.18

Inequigranular granoblastic interlobate texture of an acid granulite (q + f + px). A313/A25. C.P.

Photograph: A. Moore.

Fig. 2.19

Seriate platy granoblastic interlobate texture of an acid granulite (q + f + px). A313/302. C.P.

Photograph: A. Moore.

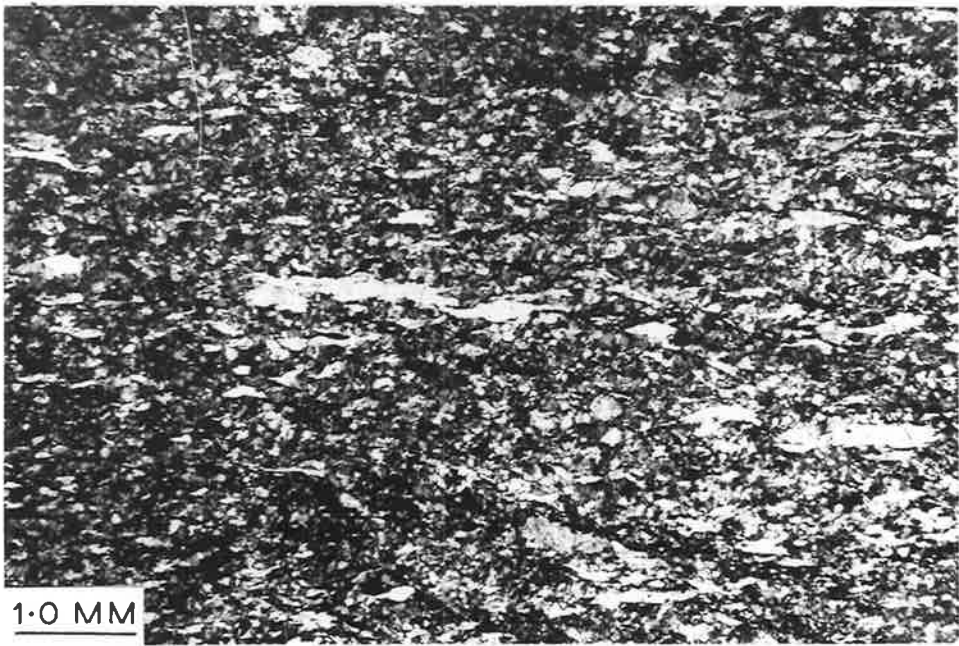
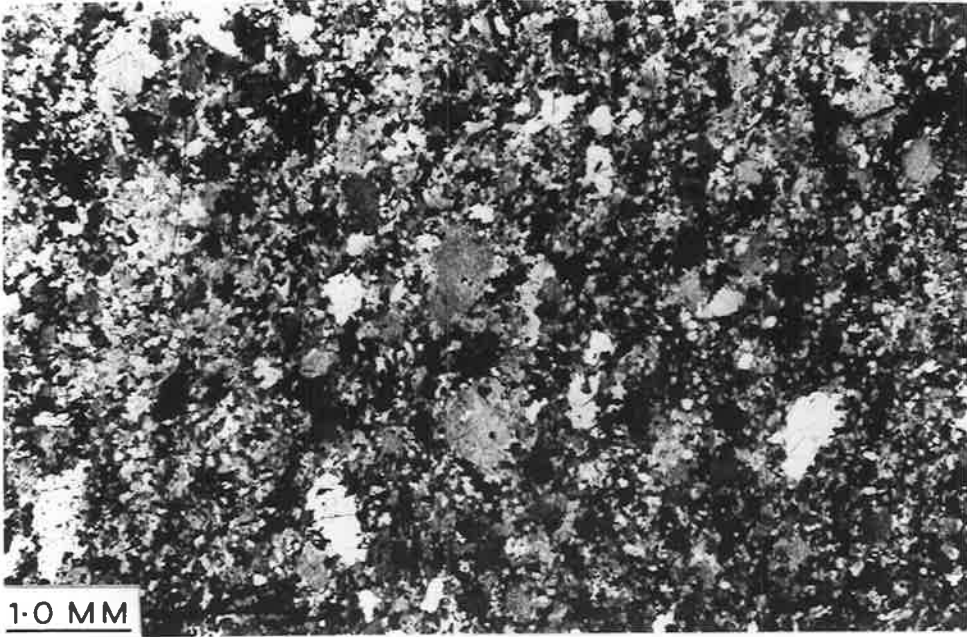


Fig. 2.20

Granoblastic equigranular polygonal texture of a layered basic granulite (hb + f + px). A253/R3. P.P.L.

Photograph: A. Moore.

Fig. 2.21

Granoblastic equigranular polygonal texture of a diopside-rich calc-silicate rock. The diopside shows alteration to granular, highly birefringent material, possibly a mixture of calcite and amphibole.

A313/297A. C.P.

Photograph: A. Moore.

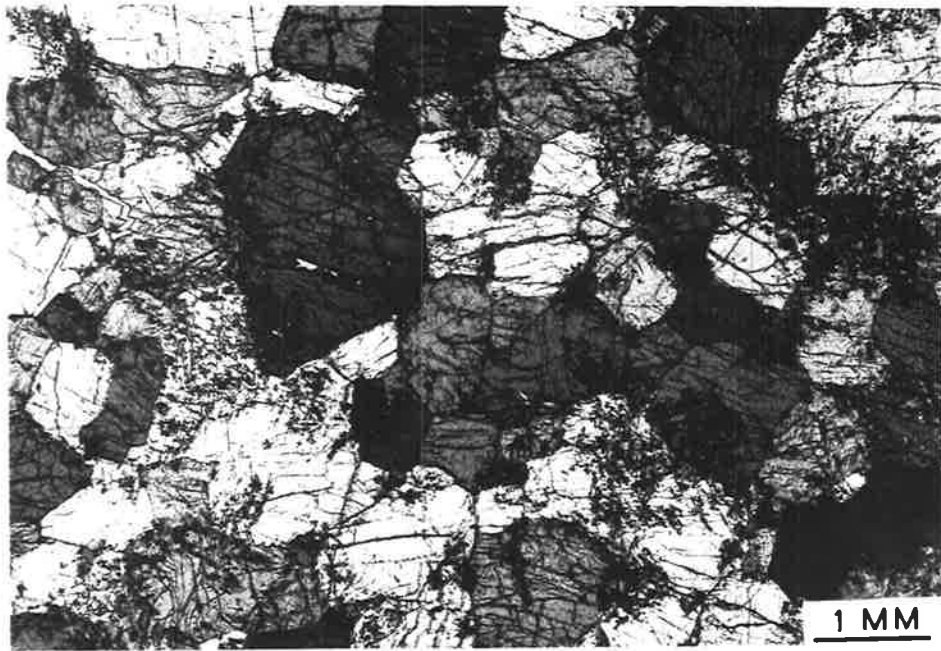
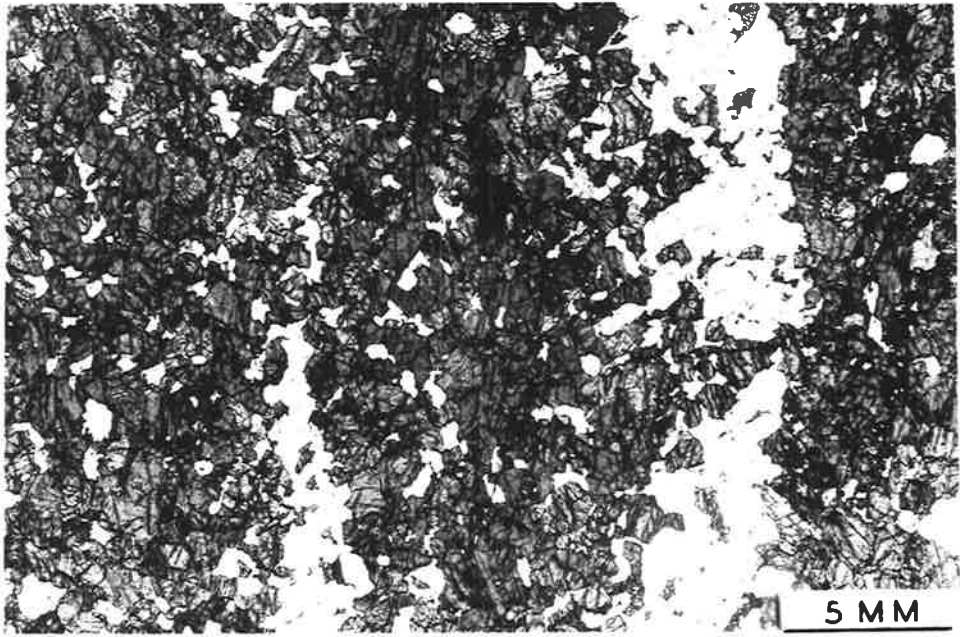




Fig. 2.22

Polygonal grain boundary relationships in a basic granulite  
(hb + f + px). A313/418. P.P.L.

Photograph: A. Moore.

Fig. 2.23

The same area as above but between crossed polars to show  
the deformation twinning in the plagioclase. A313/418. C.P.

Photograph: A. Moore.

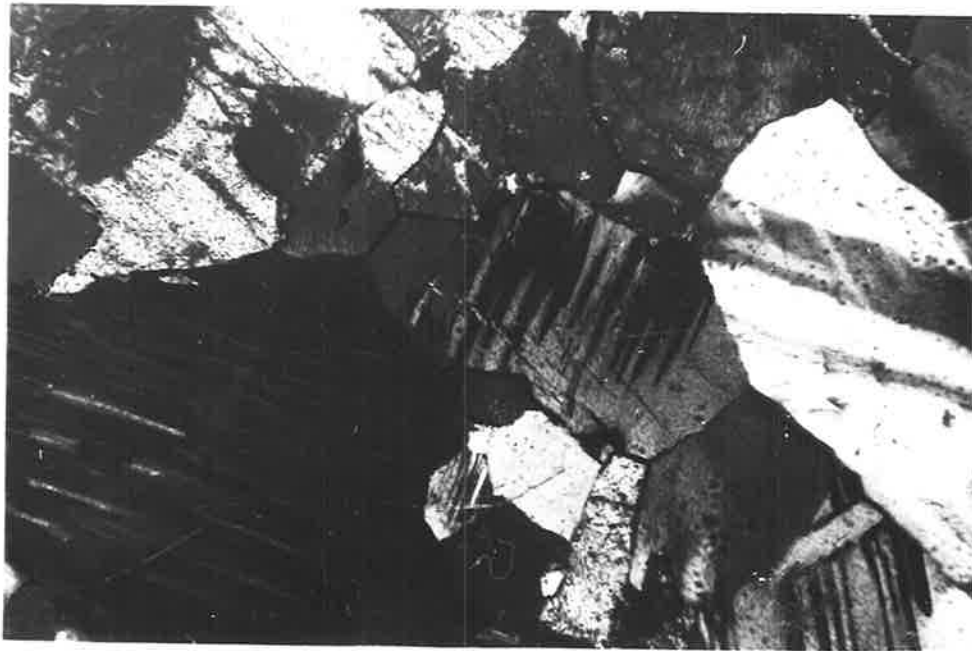
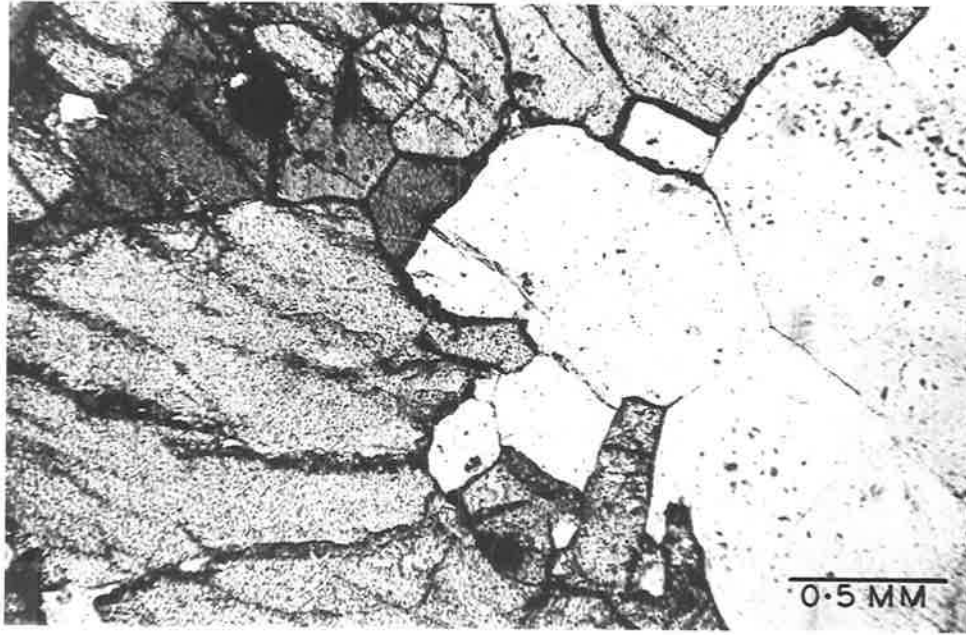


Fig. 2.24

Polygonal grain boundary relationships in a diopside-rich rock. The grain boundaries are straight or gently curved and meet in triple-point junctions at approximately  $120^\circ$ . A313/297A. C.P.

Photograph: A. Moore.

Fig. 2.25

Interlobate grain boundary relationships of an acid granulite (q + f + px). Even in these rocks there is a tendency for grain boundaries to meet in triple-point junctions. A313/413. C.P.

Photograph: A. Moore.

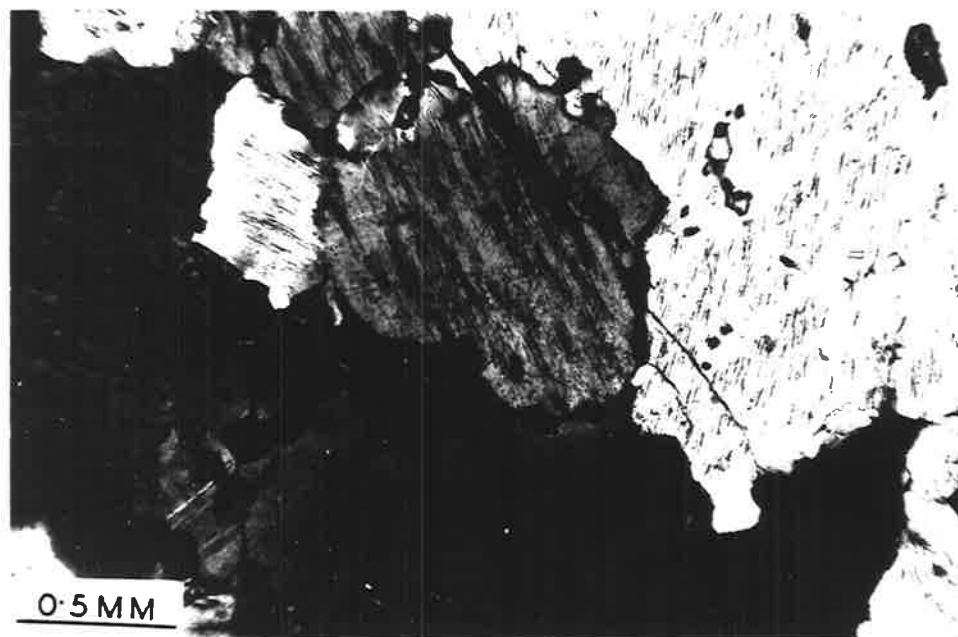
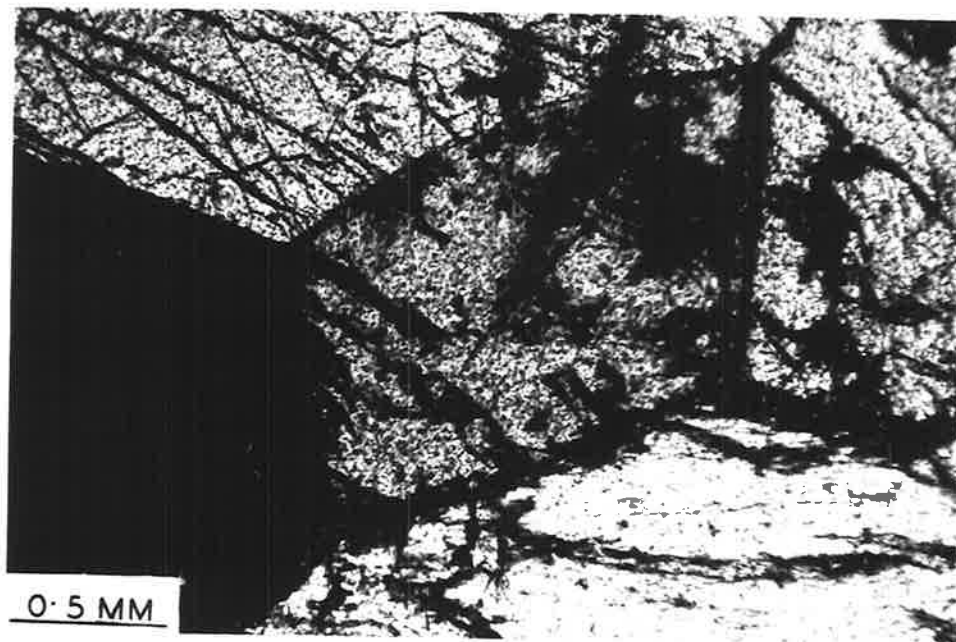


Fig. 2.26

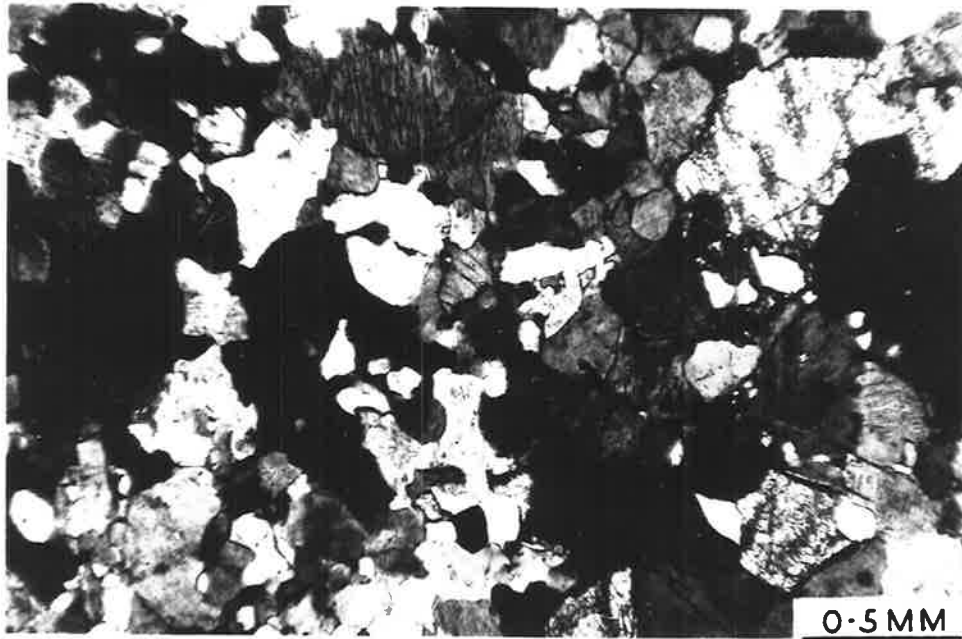
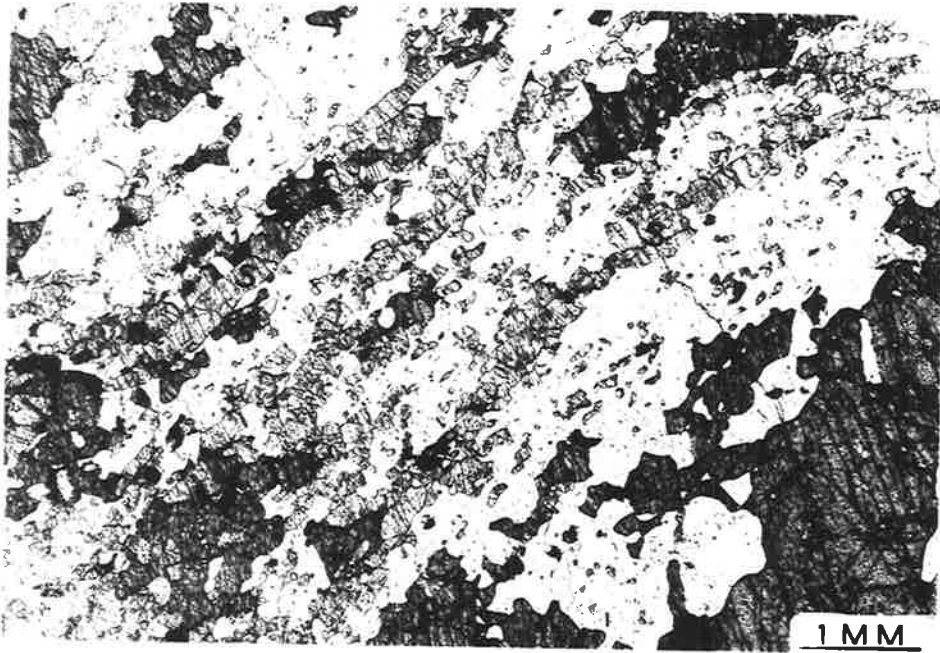
Interlobate grain boundary relationships in an acid granulite (q + f + ga + sill). Note the preferred orientation of the sillimanite (S). A313/407. P.P.L.

Photograph: A. Moore.

Fig. 2.27

Amoeboid grain boundary relationships in an acid granulite (q + f + px). A313/460. C.P.

Photograph: A. Moore.



#### Deformation and annealing.

For the granulites around Gosse Pile the hypothesis has been adopted that the textures and fabrics of the rocks have been produced as a result of deformation and recrystallization of the mineral constituents. This hypothesis has been suggested by numerous authors, from Leith (1905) to Katz (1968). The alternative is that the minerals have been progressively crushed with little or no recrystallization (see Katz, 1968, p. 810).

Thus, the textures and fabrics of the granulites are assumed to have been determined by the relative contributions of two factors: the degree of mechanical deformation (such as, movement on grain boundaries, bending and rupture of grains) and the degree of structural and/or chemical changes to produce the growth of new minerals. The first factor includes cataclasis (i.e. granulation and physical crushing of mineral grains to produce a structureless rock powder) in the extreme case, but cataclasis need not necessarily occur during mechanical deformation. The second factor is generally termed "recrystallization". This, in geological literature, usually refers to the transfer of material from stressed to unstressed regions; e.g. Barth, (1959, p. 297); Voll (1960, p. 515); Turner and Verhoogen (1960, p. 617). However, recrystallization can take place in unstressed rocks and, in geological literature, the term is often applied to cover any process of grain growth in metamorphic rocks. Rast (1965) prefers to drop the term entirely and uses

"metamorphic recrystallization" to denote the appearance of metamorphic minerals. In metallurgy "recrystallization" is not better defined and while some authors (e.g. Beck, 1954) use it in the same sense as Barth, Voll and Turner & Verhoogen, above, others (e.g. Burke and Turnbull, 1952) define it on the basis of the kinetics of the changes involved. After an extensive survey of both geological and metallurgical literature Read (1965) favours dropping the term altogether and substituting "annealing process". This suggestion is followed here.

Annealing, which may be either static or syntectonic, is defined as the process whereby a lower free energy of a polycrystalline aggregate is reached by various mechanisms of atomic readjustment. The free energy is the sum of lattice imperfections in the crystals, strain energy accumulated during plastic deformation and grain-boundary free energy associated with interfaces between component grains of the aggregate. Annealing takes place when the aggregate is subjected to temperatures high enough to activate these mechanisms: this is the annealing temperature.

Annealing takes place in five stages (Beck, 1954; Read, 1965). These stages have been deduced from experimental studies on metals but there are very strong indications that the same stages occur in the annealing of natural minerals (carbonates and silicates), e.g. Carter, Christie and Griggs, (1964); Flinn (1965); Read, (1965); Hobbs, (1968).



- (1) Recovery;
- (2) Subgrain growth or polygonization;
- (3) Primary recrystallization;
- (4) Grain growth;
- (5) Secondary recrystallization.

There is no way of quantitatively determining the former strained state of a natural tectonite, thus there is no way of recognising stage (1) above. Stage (2) is marked by the appearance of substructures, i.e. polygonization of individual grains in the rock to produce subgrains each with a slightly different lattice orientation within the parent grain. Such features may form either during static annealing following deformation (the equivalent of "cold working") or they may form during creep deformation (by comparison with experimentally deformed metals and marble).

Stage (3) is the process generally referred to as "recrystallization" by geologists and it involves the nucleation of new grains and their subsequent growth at the expense of strained matrix. This may overlap in time with stages (1) and (2) (Read, 1965) and ceases with mutual impingement of neighbouring grains (Burke & Turnbull, 1952, Fig. 3). Hence, it can be recognised in rocks only if some newly formed grains are surrounded by strained matrix, which may be either coarser- or finer-grained than the nucleating crystals, depending on the amount of nucleation. Primary recrystallization requires prior, or synchronous (during creep), deformation and is thus contrasted with stage (5).

Stages (4) and (5) involve grain boundary migration under the influence of interfacial energy in strain-free aggregates. Grain boundaries thus tend to meet three at a time, at equilibrium angles, under the influence of interfacial tension. Such angles have recently been studied in detail by Kretz (1966) and Vernon (1968) for minerals in high-grade metamorphic rocks. The period of grain growth precedes that of secondary recrystallization and is distinguished from it on the basis that it leads to a grain size frequency distribution which is unimodal whereas secondary recrystallization leads to a grain size frequency distribution which is bimodal, (Read, 1965).

Annealing processes in tectonites will be further complicated by phase changes involving chemical processes. As the physical conditions change so some minerals become unstable, and new, stable phases form from the old. This process is neo-mineralization (German: "Mineralneubildung") and is distinguished from annealing in that it involves the growth of new minerals (chemical reorganization) and not just a physical reorganization of the pre-existing mineral phases.

## 2.7 RELATIONSHIPS BETWEEN ROCK TYPES AND THEIR TEXTURES AND FABRICS

An attempt has been made to classify most of the granulite samples collected into textural types. The results are shown in Table 2.2. (The subdivision of the different granulite groups is discussed in section 2.9). Only one rock (A313/398) adequately

Table 2.2 Log likelihood ratio method for correlation between rock type and grain boundary type and between rock type and texture type.

(a)  $H_1$  : Rock textures are independent of rock type.  $H_2$  : Rock textures are dependent on rock type.

| ROCK TYPE<br>TEXTURE | ACID GRANULITES |        |        |                      | BASIC GRANULITES |              | CALC-SILICATES |        | TOTALS |
|----------------------|-----------------|--------|--------|----------------------|------------------|--------------|----------------|--------|--------|
|                      | q+f             | q+f+px | q+f+ga | iron-rich granulites | hb+f+px<br>+ ga  | anorthosites | di-rich rocks  | marble |        |
| GRANOBLASTIC         |                 |        |        |                      |                  |              |                |        |        |
| equigranular         | 0               | 1      | 1      | 3                    | 15               | 1            | 5              | 0      | 26     |
| inequigranular       | 3               | 21     | 3      | 0                    | 0                | 0            | 2              | 1      | 30     |
| seriate              | 1               | 10     | 5      | 0                    | 4                | 1            | 0              | 0      | 21     |
| FLASER               | 3               | 2      | 0      | 2                    | 0                | 0            | 0              | 0      | 7      |
| TOTALS               | 7               | 34     | 9      | 5                    | 19               | 2            | 7              | 1      | 84     |

N Log N values

|          |           |          |         |          |         |          |   |           |
|----------|-----------|----------|---------|----------|---------|----------|---|-----------|
| 0        | 0         | 0        | 3.2958  | 40.6208  | 0       | 8.0472   | 0 | -84.7105  |
| 3.2958   | 63.9350   | 3.2958   | 0       | 0        | 0       | 1.3863   | 0 | -102.0359 |
| 0        | 23.0259   | 8.0472   | 0       | 5.5452   | 0       | 0        | 0 | -63.9350  |
| 3.2958   | 1.3863    | 0        | 1.3863  | 0        | 0       | 0        | 0 | -13.6214  |
| -13.6214 | -119.8963 | -19.7750 | -8.0472 | -55.9443 | -1.3863 | -13.6214 | 0 | 372.1886  |

TOTAL : 42.16

$\chi^2_{21}$  (21 degrees of freedom) at 0.05% level = 32.67

∴ Accept  $H_2$  that rock textures are dependent on rock type.

Table 2.2 (continued)

(b)  $H_1$  : Grain boundaries are independent of rock type.  $H_2$  : Grain boundaries are dependent on rock type.

| ROCK TYPE<br>GRAIN BOUNDARY TYPE | ACID GRANULITES |        |        |                      | BASIC GRANULITES |              | CALC-SILICATES |        | TOTALS |
|----------------------------------|-----------------|--------|--------|----------------------|------------------|--------------|----------------|--------|--------|
|                                  | q+f             | q+f+px | q+f+ga | iron-rich granulites | hb+f+px ± ga     | anorthosites | di-rich rocks  | marble |        |
| Polygonal                        | 0               | 1      | 0      | 0                    | 16               | 0            | 5              | 0      | 22     |
| Interlobate                      | 3               | 7      | 1      | 3                    | 2                | 2            | 2              | 1      | 21     |
| Amoeboid                         | 4               | 26     | 8      | 2                    | 1                | 0            | 0              | 0      | 41     |
| TOTALS                           | 7               | 34     | 9      | 5                    | 19               | 2            | 7              | 1      | 84     |

N Log N Values

|          |           |          |         |          |         |          |   |           |
|----------|-----------|----------|---------|----------|---------|----------|---|-----------|
| 0        | 0         | 0        | 0       | 44.3614  | 0       | 8.0472   | 0 | -68.0029  |
| 3.2958   | 13.6214   | 0        | 3.2958  | 1.3863   | 1.3863  | 1.3863   | 0 | -63.9380  |
| 5.5452   | 84.7105   | 16.6355  | 1.3863  | 0        | 0       | 0        | 0 | -152.2565 |
| -13.6214 | -119.8963 | -19.7750 | -8.0472 | -55.9443 | -1.3863 | -13.6214 | 0 | 372.1886  |

TOTAL : 40.76

For 14 degrees of freedom  $\chi^2_{14}$  : at 0.05% level = 23.68

∴ Accept  $H_2$  that rock textures are dependent on rock type.

fits the mylonitic texture type (Fig. 2.12). It crops out between the acid granulites and the pyroxenites west of Gosse Pile and, since one or both rock types may be contributing, it has not been further considered. Statistical analysis, using the log-likelihood ratio method, which gives a close approximation to  $\chi^2$  for low expected frequency values (Kullback, 1959), shows that there is a very strong correlation between rock type and texture type. A similar statistical analysis has shown a very strong correlation between rock type and grain boundary type. In general, the acid granulites tend to have granoblastic inequigranular (including, platy granoblastic) to seriate textures (Figs. 2.18 and 2.19) while the basic granulites and calc-silicate rocks have granoblastic equigranular textures (Figs. 2.20 and 2.21). In particular, flaser textures are found only in quartz-feldspar rocks (Figs. 2.14 and 2.15) and in the iron-rich granulites. Even the two q + f + px granulites showing flaser textures contain very little pyroxene (about 8%). In general the basic granulites and diopside-rich calc-silicates have polygonal grain boundary relationships (Figs. 2.20, 2.21, 2.22, 2.23 and 2.24) while the acid granulites have amoeboid or interlobate grain boundary relationships (Figs. 2.25, 2.26 and 2.27).

Although very little detailed petrofabric work has been done on the granulites every thin section has been examined between crossed polars using a gypsum plate. This showed that, with few exceptions, the acid granulites have a strongly anisotropic

fabric. When measured on one such rock (A313/302) it showed orthorhombic fabric symmetry (Fig. 2.9). This type of fabric symmetry is common in quartzo-feldspathic granulites (Turner and Weiss, 1963) and is usually interpreted as being caused by "flattening" normal to S (e.g. Sander, 1930; Christie, 1963). The marble and diopside-rich rocks show no preferred orientation (even on sections measured using a Universal Stage) and the fabric of basic granulites, examined using the gypsum plate, similarly appeared random although detailed measurements may reveal a weak anisotropism.

Katz (1968) postulated that, for the Mont Tremblant Park granulites, grains in an unstrained state must have been recrystallised. This criterion cannot be directly applied to the rocks around Gosse Pile since nearly all the grains in the acid granulites show strain shadows, due to a later deformation after annealing. The larger quartz grains show well-developed sub-grain growth (Figs. 2.28, 2.29), both quartz and K-feldspar show strong undulose extinction and the pyroxenes show weak undulose extinction, twinning and bending. No kinking has been observed. Strain effects have not been observed in the garnet or the opaque minerals but the latter appear to have been very mobile during the "brittle" deformation and characteristically occur along fractures and grain boundaries (Fig. 2.30). Barnes (1968) made similar observations on granulites which occur **about 10km further north**. In contrast, the mafic minerals of the calc-silicate rocks and basic granulites are generally free of strain effects. An exception to this is the phlogopite in the marble which is frequently

Fig. 2.28

Well developed sub-grain growth in an originally homogeneous quartz grain. The central part shows undulose extinction which possibly indicates the initiation of very low angle\* sub-grain boundaries.

A313/A25. C.P.

Photograph: A. Moore.

---

\* low angle grain boundaries refer here to the degree of lattice disorientation between adjacent grains, and not to the angle the boundary makes with the thin section. The degree of disorientation must be less than  $10^{\circ}$  for the boundary to be termed "low angle".

---

Fig. 2.29

Sub-grain growth in an originally homogeneous elongate quartz grain. A313/404. C.P.

Photograph: A. Moore.

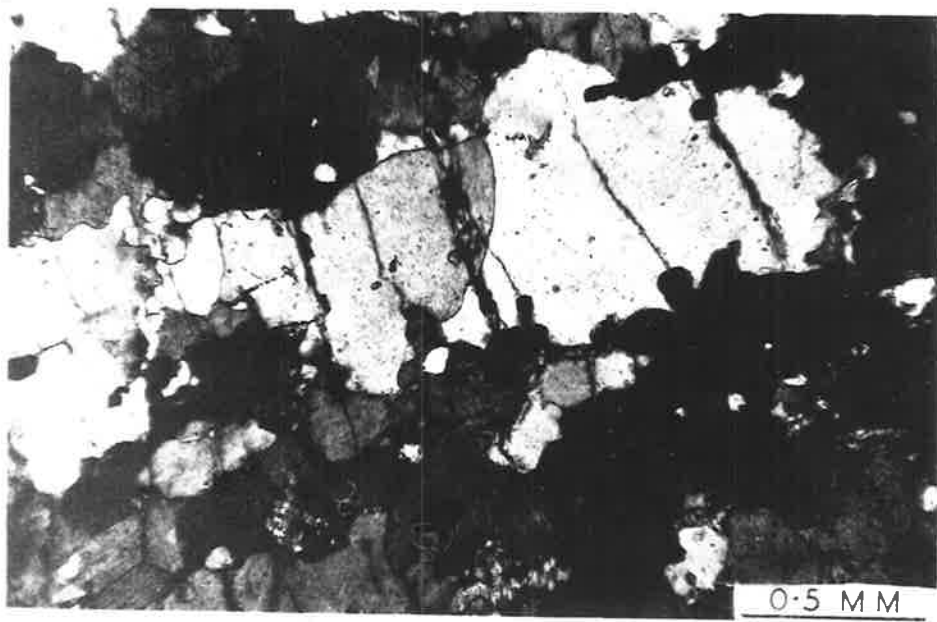
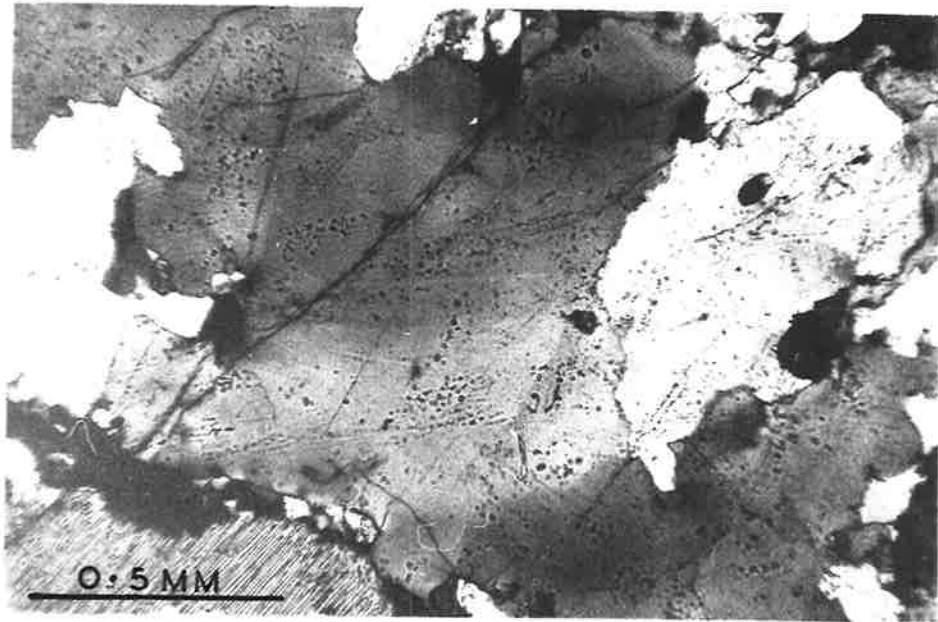




Fig. 2.30

Illustration of the apparent mobility of oxide minerals during the period of brittle deformation. Here the magnetite fills fractures in a deformed acid granulite (q + f + px).

A313/415.

P.P.L.

Photograph: A. Moore.

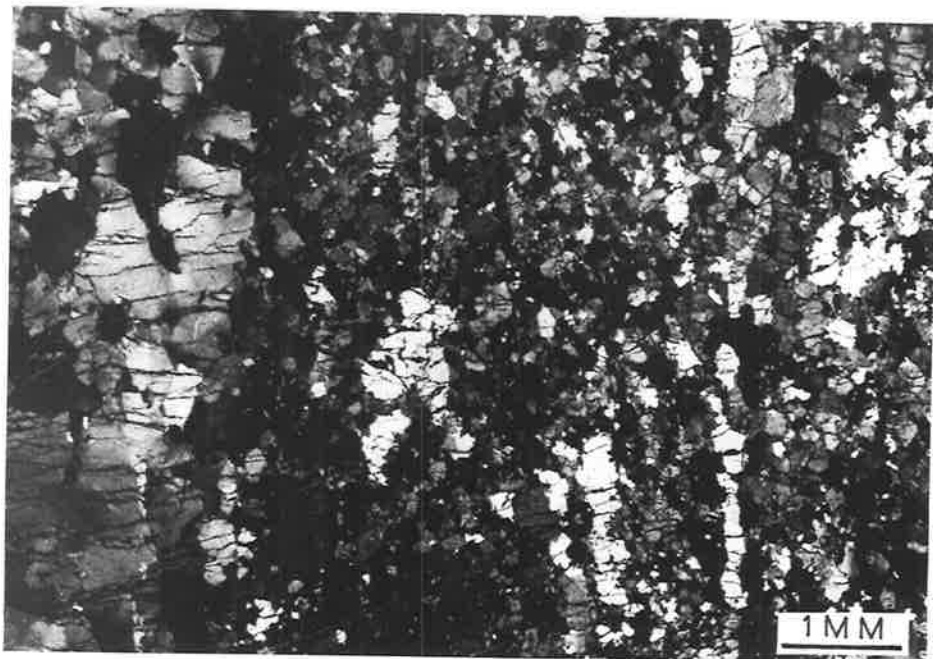
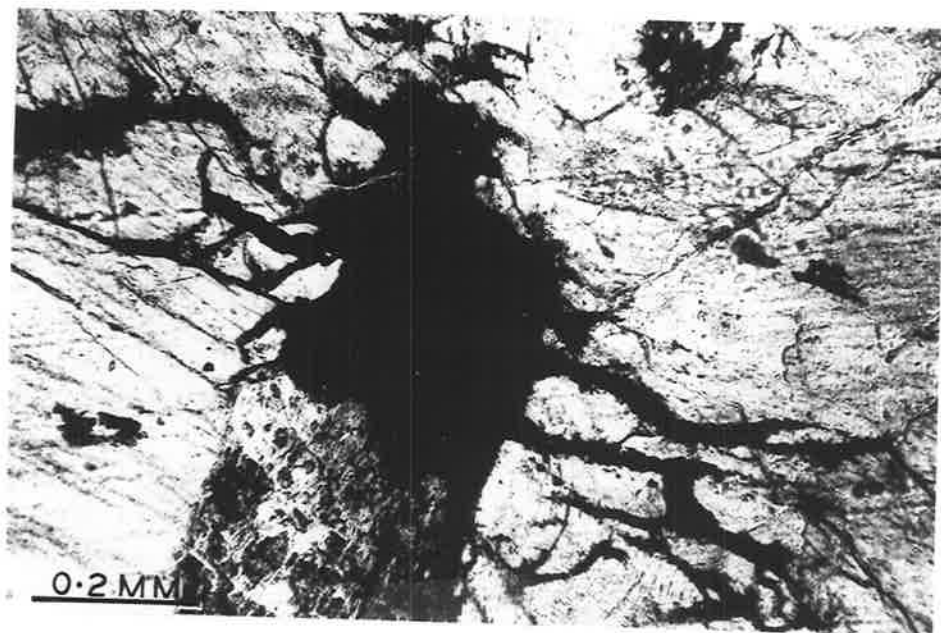
Fig. 2.31

Grain size variation in an acid granulite (q + f + px) related to the abundance of pyroxene and oxide minerals. The coarse grain-size (left) is where no minerals other than quartz occur. The fine grain-size (right) is in an area where pyroxene, feldspar and oxides are numerous.

A313/404.

C.P.

Photograph: A. Moore.



severely kinked. The plagioclase usually shows some strain shadows and deformation twinning is well developed (Fig. 2.23).

## 2.8 INTERPRETATION OF THE TEXTURES

### (1) Assumptions

In the interpretation of the granulite textures several assumptions have been made.

(a) The textures result from the effects of deformation and annealing. There is ample evidence that the rocks have been deformed both on a macroscale (e.g. folding and faulting) and on a microscale (e.g. strain shadows, deformation twinning). Evidence of annealing is derived from the presence of granoblastic polygonal textures in some rocks, the development of new phases, some of which are subhedral (e.g. sillimanite), the bimodal nature of the grain size of some acid granulites (Fig. 2.19) which cannot be related to a frequency distribution of visible inclusions\* (Fig. 2.31) and by comparison with textures of other granulites for which there is more direct evidence for annealing (e.g. Katz, 1968). The

---

\* It has been shown by experimental work in metals that the grain size in areas containing numerous inclusions is frequently smaller than in areas of the same specimen where fewer inclusions occur. This is also true of natural rock textures (Read, 1965). The inclusions are thought to inhibit grain boundary migration processes during annealing, thus preventing the growth of large grains.

alternative assumption is that the textures arose entirely as a result of deformation and the variations in grain size are due to granulation or cataclasis (e.g. Wynne-Edwards et. al., 1966). This latter hypothesis is considered less likely since textures similar to those in natural rocks have been produced experimentally in marble (Carter, Christie and Griggs, 1964) and in quartz (Hobbs, 1968) by deformation and annealing without cataclasis. Further, the natural textures in no way resemble those produced experimentally by microbrecciation (e.g. Borg and Handin, 1966) except for the local shear zones which are often associated with the pseudotachylite veins described in section 2.4. These relatively minor faults post-date the production of the gross textures of the rocks but have produced fractures, bending and undulose extinction in the minerals (Fig. 2.11).

(b) The area under discussion is very small so that it is assumed there would be no significant spatial variation in geothermal gradient over the area and there would be no, or insignificant, variation in confining pressure. However, there may have been variations in the amount and rate of strain because of the inhomogeneity of the rocks. Most of the acid granulites (making up over 97% of the area) show a well developed anisotropy (probably orthorhombic) so that it is presumed that the regional stresses by which the rocks were deformed and annealed were not hydrostatic.

---

(c) Different rocks react differently under the same regional stresses because of the different properties of their constituent minerals. Under experimental conditions it is well established that marble exhibits ductile behaviour at relatively low temperatures and pressures while quartz, at comparable strain rates and in the absence of  $(OH)^-$  in the structure, is brittle even at temperatures close to the melting point — e.g. at  $1,400^{\circ}C$  and 15kb (Hobbs, 1968). Syntectonic annealing of marble, under experimental conditions, produces strong preferred orientations. Under the natural conditions of deformation and syntectonic annealing which produce a strong anisotropy in the acid granulites one would expect a well developed mineral preferred orientation to develop in the calc-silicate rocks and the marble, and probably also the amphibole-bearing basic granulites.

The origin of the lenticular nature of the quartz in granulites has not been adequately explained apart from statements indicating that it formed as a result of flattening ("Plättung") parallel to S. This orientation is presumed to form during deformation so that the axes of maximum compressibility of quartz are parallel to the directions of maximum compressive stress (Flinn, 1965). Suggestions for the actual mechanisms involved in the flattening range from applications of Riecke's Principle to mylonitization and physical stretching.

(2) Model for the origin of the textures in the granulites.

During deformation syntectonic annealing took place which produced preferred orientations in all the rocks. Quartz, and to a lesser extent feldspar, formed elongate crystals with their direction of elongation perpendicular to the direction of greatest pressure. The dominant process was probably primary recrystallization leading to an approximately bimodal grain size frequency distribution, typified by rocks such as are illustrated in Fig. 2.18 and 2.19. The larger grains are thought to represent the parent grains and the smaller grains were formed by annealing processes. Many of the larger feldspar grains are mesoperthites and, if these had formed during annealing, then it is likely that the two phases would have crystallized separately (e.g. Hubbard, 1965; Katz, 1968). It is probable that the quartz lenticules (as in Fig. 2.18) formed from original clastic grains during syntectonic annealing by unknown mechanisms (possibly by a combination of Nabarro-Herring diffusion, or Riecke's Principle, and grain boundary migration). Flattening of highly strained quartz normal to the direction of maximum pressure has been observed experimentally (Carter, Christie and Griggs, 1964). On the other hand, Hobbs (1968) produced new grains in annealed quartz crystals which grew at high angles to the direction of maximum pressure (Plate IV D of Hobbs, 1968). Katz (1968) assumed similar, lenticular grains in Mont Tremblant Park granulites, in spite of distortion and annealing, retain the approximate original grain size of the equivalent rocks in their

pre-deformed stage. A similar assumption has not been accepted for the Gosse File granulites in view of the great changes brought about by deformation and annealing, especially over long periods of time. Present variations in grain-size can be explained in some cases in terms of differences in grain growth caused by the presence or absence of inclusions. An example of the effect of inclusions on grain-size can be seen in Fig. 2.31. The coarse-grained quartz (left) is in an area almost entirely free of "foreign" inclusions while the rest of the slide shows a much finer grain-size which can be related to the presence of pyroxene, plagioclase and opaque minerals. Differences in grain-size could also result from the presence of catalysts such as  $\text{CO}_2$  or  $(\text{OH})^-$  ions which might assist in the more rapid transfer of material and release of dislocations. Local differences in strain rate could bring about differences in grain-size and shape. A local high strain rate would cause more nuclei to form, producing an overall finer grain-size and probably a granoblastic platy rather than granoblastic inequigranular texture.

The presence of a preferred orientation in tectonites is generally considered to be due to syntectonic annealing (e.g. Turner and Weiss, 1963; de Vore, 1966) while static annealing tends to produce a random orientation, although traces of an earlier preferred orientation may remain, as has been shown by the experimental work on marble (Griggs et. al., 1960). In metals static annealing can produce a preferred orientation provided that

---

there was a pre-existing strain (Beck, 1954). Rutland (1964) has stated that, "a preferred orientation does not necessarily indicate crystallization under large stress differences, while an absence of preferred orientation does indicate crystallization in the absence of large stress differences." The lack of a strong preferred orientation in the calc-silicate rocks and basic granulites around Gosse Pile is correlated with a period of static annealing following deformation. This would involve static primary recrystallization followed by grain boundary migration under the influence of interfacial free energy. The aggregate would be relieved of strain and polygonal textures would result. Polygonal textures with grain boundaries meeting at approximately  $120^{\circ}$  are still preserved in these rocks (Figs. 2.21 and 2.22) and thus imply grain boundary migration under the influence of interfacial free energy must have taken place. The lack of megacrysts in these rocks indicates that the stage of secondary recrystallization (exaggerated grain growth) had not been reached.

Although there is insufficient experimental data available to predict the behaviour of different, but associated, deformed rocks under the influence of static annealing especially over long periods of time, it is assumed that the marble, diopside-rich rocks and amphibole-bearing basic granulites produced equigranular, strain-free, nearly polygonal aggregates more readily than the acid granulites. This may be caused by the influence of  $\text{CO}_2$  and  $(\text{OH})^-$  ions, although some doubt has been expressed as to whether these



components would significantly affect static annealing processes (Griggs, et. al., 1960). However, Heard (1963) has shown that  $\text{CO}_2$  diffusion in the calcite lattice is possibly important in governing the rate of movement of crystal imperfections and hence creep during syntectonic annealing of marble. Hobbs (1968) has shown that even traces of  $(\text{OH})^-$  ions in quartz can produce remarkable changes in its behaviour during deformation. Another factor which may have been of considerable importance is that the critical annealing temperature may have been lower for these rocks than for the acid granulites.

Voll (1960) suggested that polygonal textures indicate equilibrium textures and sutured boundaries indicate some "subsequent deformation and local recrystallization". However, similar sutured boundaries are commonly found in metals which have undergone creep deformation or strain induced grain boundary migration (Read, 1965). Similar boundaries have been experimentally produced in statically annealed calcite aggregates (Heard, 1963) and single quartz crystals (Hobbs, 1968). Thus, sutured grain boundaries (e.g. Fig. 2.25) probably were produced during the first period of deformation and annealing and do not necessarily imply a second period of deformation and annealing.

However, following the period of static annealing, deformation has occurred. It produced strain effects (undulose extinction, deformation twinning of plagioclase, kinking in mica) and fractures

---

in all the rocks. Although this deformation may have induced some grain boundary migration and possibly some polygonization (of quartz lenses) it appears to have produced features post-dating the gross textural characteristics of the rocks. Either it was not severe enough or at too low a temperature to cause much change in the rock fabrics already formed.

It is difficult to relate deformational episodes deduced purely from textural studies to those deduced from the structural data (sections 2.2, 2.3 and 2.4). However, both the first and second deformations recognised structurally involved folding of the granulites, a process which would involve considerable plastic, or creep, deformation of the rocks and hence significant changes in their fabrics and textures. Since the second deformation recognised by textural studies was considered to be relatively slight and brittle, producing little effect on the pre-existing grain boundary relationships or fabrics, it must have occurred after folding. Thus, the first deformation and annealing recognised texturally probably corresponds to the second deformation, or even both deformations, recognised structurally. The second deformation recognised texturally apparently does not correspond to any major phase of folding recognised in the granulites but is related to the period of faulting which produced the mylonite zones (e.g. Hinckley mylonite) and brittle faults.

## 2.9 PETROGRAPHY AND MINERALOGY OF THE GRANULITES.

There are three main types of granulite, each of which can be subdivided into groups on the basis of differences in mineralogy.

### 2.9.1 The Acid Granulites.

This major type is divided into four groups.

#### (i) Quartz + feldspar + pyroxene granulites.

These form the major lithological units around Gosse Pile, appearing in the field as massive, medium-grained, grey-green exfoliating rocks with a creamy-white weathering surface. They apparently maintain a similar mineralogical composition over large areas: changes are subtle and difficult to detect in the field since they are restricted essentially to variations in the proportions of plagioclase and K-feldspar. This is shown in Table 2.3 where modal analyses of seven specimens of these granulites are presented. In most rocks of this type which have been examined plagioclase is the dominant mineral and analyses 5 and 6 (Table 2.3) are probably representative of the majority of rocks in the area as a whole. However, most rocks collected from the north-western area (Fig. 1.3, AB/1,2 and in Fig. 2.1 the area marked "p") have K-feldspar as the dominant mineral (1, Table 2.3). A few rocks, found on the north side of Gosse Pile, which show a well developed preferred orientation and an inequigranular platy granoblastic texture, are unusual in that plagioclase is completely absent (2, Table 2.3). The grain-size is very variable and most rocks are inequigranular. However,

Table 2.3

Modal analyses of quartz + feldspar + pyroxene granulites.

| Spec. No.<br>A313/ | Analysis | Quartz | K-feldspar | Plagioclase | Pyroxene | Oxides | Apatite | Zircon | Others |
|--------------------|----------|--------|------------|-------------|----------|--------|---------|--------|--------|
| A25                | 1        | 22.5   | 54.0       | 16.9        | 4.5      | 1.4    | 0.6     | 0.1    | -      |
| 381A               | 2        | 50.2   | 46.0       | -           | 2.1      | 1.6    | -       | 0.1    | -      |
| 429                | 3        | 48.5   | 20.2       | 25.8*       | 4.3      | 0.9    | 0.2     | -      | hb:0.1 |
| 415                | 4        | 35.3   | 10.5       | 46.4        | 5.4      | 2.1    | 0.1     | 0.1    | hb:0.1 |
| 372                | 5        | 31.4   | 9.7        | 51.1        | 6.6      | 1.1    | 0.1     | tr     | -      |
| 368                | 6        | 34.2   | 8.1        | 48.3        | 8.1      | 1.2    | tr      | 0.1    | bi:tr  |
| 302                | 7        | 22.6   | 2.0        | 64.5        | 9.8      | 1.0    | 0.1     | -      | bi:tr  |

\* includes 0.1% myrmekite.

Notes: In all modal analyses quoted in all tables more than 2,000 points were counted unless otherwise stated. In many samples 3,000 or more points were counted.

For the samples quoted above a high degree of operator error probably exists because the smaller grains of quartz, K-feldspar and plagioclase are difficult to distinguish in thin section, even after staining. In all cases orthopyroxene is the dominant pyroxene but no distinction has been made because of the high degree of alteration which makes positive identification difficult. The amphibole is weakly pleochroic green ( $\gamma$ ) to pale yellow-green ( $\alpha$ ) and is found mainly in the more highly sheared rocks on the south side of Gosse Pile. It is found surrounding pyroxene and oxide minerals and is probably an alteration product.

as a first approximation it can be said that the rocks tend to be medium-grained with an average grain size of quartz and feldspar being about 1-2 mm and that of pyroxene about 0.5 mm.

Quartz, blue-grey or dark grey in hand specimen is an essential component of all these rocks, making up 20% - 50% of the total rock. In thin section the quartz is seen always to be seriate, often occurring as large elongate grains and as equidimensional grains of varying size in the matrix. The larger crystals always show some degree of undulose extinction as do the majority of matrix crystals. In most cases the quartz has a lattice preferred orientation. Rutile needles commonly occur as inclusions both in the quartz and in K-feldspar with apparently random orientation. Myrmekite is found in small areas in some rocks, in all cases restricted to interfaces involving perthite. This is identical to material in Nigeria, described with illustrations by Hubbard (1966). Hubbard's view that this myrmekite formed by an exsolution process from originally calcium-rich, high-temperature alkalic feldspar crystallization, has been largely substantiated by the work of Phillips and Ransom (1968).

Plagioclase is the dominant feldspar and often is present to the exclusion of a free K-feldspar phase though it is often strongly antiperthitic. The development of antiperthite may be on an extremely fine scale and not readily observed and, in many rocks, it appears to be completely absent, particularly where free K-feldspar is a major phase (e.g. 1, Table 2.3). When observable,

the K-feldspar phase of the antiperthites forms lenticular blebs close to the centre of the plagioclase grain (e.g. Fig. 2.26).

Sen (1959) determined the orthoclase contents of plagioclases from amphibolite and granulite facies rocks in samples from India, Greenland and U.S.A. He found that the bulk orthoclase contents for plagioclases from amphibolite facies rocks range from <0.6% Or to 2.3% Or and for granulite facies rocks from 2.1% Or to 7.6% Or. This implies a trend of decreasing potassium content of the plagioclase with decreasing temperature of formation. However, water pressure could be an important factor in determining the potassium content of the plagioclase since the immiscibility gap between alkali feldspars and plagioclases is smaller in rocks with an apparently lower water content ("dry" rocks), such as these acid granulites (Tuttle and Bowen, 1958). More recently Vogel *et. al.* (1968) have shown that the origin of antiperthites in charnockitic rocks of New Jersey is not related to potassium content. They offer two possible hypotheses, both involving exsolution as a mechanism, by way of explanation. The development of antiperthite is determined either by the structure of plagioclase between certain compositional limits ( $An_{33-50}$ ) or it is dependent on the feldspar phase which crystallized first. In the granulites described here antiperthite occurs even where the plagioclase is more albitic than  $An_{33}$  and appears to be more related to the amount of free K-feldspar phase present. The antiperthites in these acid granulites have probably formed as a result of exsolution of K-feldspar from high-temperature plagioclase, as has been suggested for antiperthite in other high-

grade metamorphic terrains (e.g. Sen, 1959; Carstens, 1967).

Most of the plagioclase crystals measured (optically) have compositions in the region oligoclase to andesine ( $An_{20-35}$ ), but a few rocks have a more calcic plagioclase (maximum recorded,  $An_{55}$ ). The grains always appear to be unzoned although they usually show undulose extinction. Twinning is poorly developed in most cases and is often absent in those grains showing a strong development of antiperthite. Where present twins are always secondary (glide or deformation twins with typical wedge-shape) and are developed according to the albite and pericline laws.

K-feldspar in these rocks is always strongly perthitic with the perthite component forming undulose platelets or blebs (vein perthite and bead perthite of Hubbard, 1966). In many cases the proportion of plagioclase to K-feldspar becomes almost equal to form mesoperthite, so named by Michot (1951) who considered that it formed in a high temperature environment. Thin sections cut perpendicular to each other confirm that the plagioclase phase is elongate in two dimensions in the mesoperthite. Thin sections and stained slabs have shown that in the same rock two types of perthite can co-exist. One is a mesoperthite and the other has relatively smaller amounts of the plagioclase phase, forming rounded blebs, often concentrated near the centres of the grains. These are called microperthites for convenience. They may occur throughout the matrix of the rock but are most commonly found surrounding megacrysts of mesoperthite, rather like daughter grains around a

parent (Figs. 2.32, 2.33). Both types are characteristically free of twinning. The microperthite is found only in smaller grains and the mesoperthite generally occurs in the large grains although it is occasionally found in crystals of comparable size to the microperthite.

The origin of perthite is not known with certainty and, depending on circumstance, different theories have been advanced: simultaneous growth of the two phases, unmixing of K-Na feldspars into separate phases (exsolution) or replacement of feldspar by reaction. According to Laves and Soldatos (1963) the coarse vein-type perthites, such as occur in these granulites, originate by unmixing from mixed crystals under relatively high temperatures when the ions are sufficiently mobile to produce broad exsolution domains. Mehnert (1968), referring to perthites in granitic rocks, interprets the mode of formation of perthites as being related to shearing stress acting upon the rock involved. He suggests this by showing that microperthite is rare or absent in granites where quartz shows no evidence of deformation, while it is common in deformed rocks. The shearing may simply promote coalescence of unmixed, submicroscopic albite units. Thus, the type of perthite may be related to the complex geological history of the rock and not be a simple function of temperature.

In the acid granulites under discussion there may have been two distinct periods of perthite formation. The first formed mesoperthite prior to, or during, a period of deformation and



Fig. 2.32

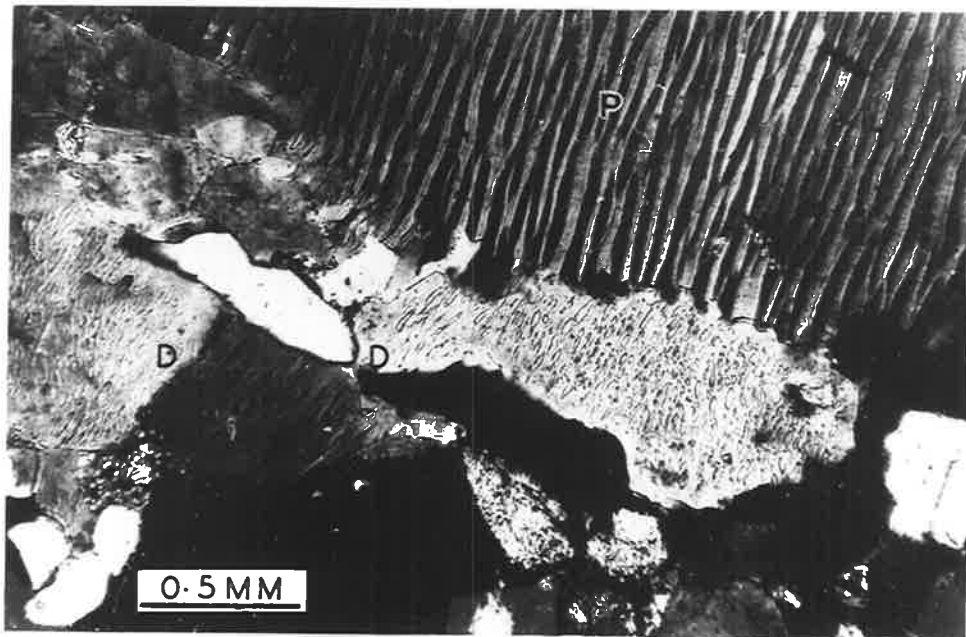
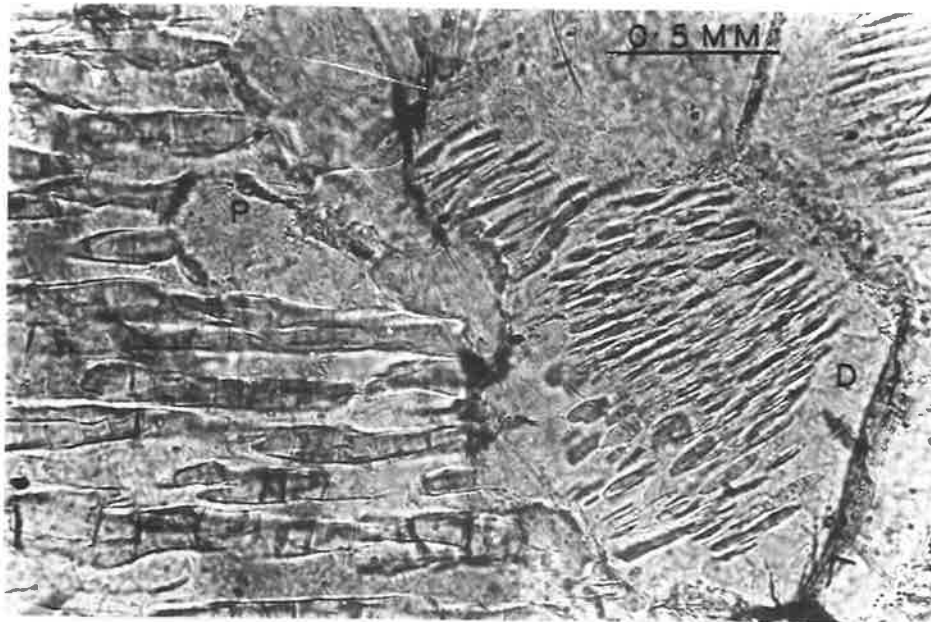
Mesoperthite (left, P) and microperthite (centre and right, D) from an acid granulite (q + f + px). A313/A25.  
P.P.L.

Photograph: A. Moore.

Fig. 2.33

Parent mesoperthite (P) and daughter microperthite (D).  
A313/437. C.P.

Photograph: A. Moore.



annealing. This deformation and annealing could also produce daughter grains around the larger K-feldspar grains by subgrain growth during which process some of the albite component could have been freed to form a part of the separate plagioclase phase. At a later stage more albite component, greatly reduced in amount relative to the K-feldspar, could unmix from the daughter grains. This type of perthite would be presumed to form at a lower temperature. To test this hypothesis samples of mesoperthite and microperthite were extracted from a stained slab of rock (A313/A25) using a dentist drill. The structural states of the K-feldspar phases and the nature of the plagioclase phases were determined from measurements of the (060) and ( $\bar{2}$ 04) reflections (Wright and Stewart, 1968; Wright, 1968). The results of this X-ray diffraction data are given in Table 2.4. The potash feldspar phases of both perthite types have broad  $131/1\bar{3}1$  peaks indicating substantial disorder and thus, generally, they would be considered as close to monoclinic. Heier (1957, 1961) has shown that the K-feldspar in rocks of the granulite facies is commonly orthoclase. Both meso- and microperthite have the same structural state, which is equivalent to that of  $P_{50-56}K-f$  (orthoclase; Fig. 2a of Wright and Stewart, 1968). Further, the K-feldspar is, in all cases, anomalous in the sense defined by Wright (1968, p. 94) in that the  $\bar{2}01$  value interpolated from the alkali exchange graph (Fig. 4 of Wright, 1968) is at least  $0.1^{\circ}2\theta$  greater than the measured value (Table 2.4). This similarity in structural state of both "parent" (mesoperthite) and "daughter" (microperthite) K-feldspar phases

Table 2.4

X-ray diffraction data of perthitic K-feldspar from A313/A25. The assistance of Mr. A.R. Milnes is gratefully acknowledged both in the separation and measurement of these samples. (CuK $\alpha$  radiation, Ni filter; Goniometer at  $\frac{1}{4}^{\circ}2\theta$ /min).

| Sample                                   | Phase | $^{\circ}2\theta$<br>$\bar{2}01_{\alpha 1}$ | $^{\circ}2\theta$<br>$131_{\alpha}$ | $^{\circ}2\theta$<br>$1\bar{3}1_{\alpha}$ | $^{\circ}2\theta$<br>$\Delta 131-1\bar{3}1$ | $^{\circ}2\theta$<br>$060_{\alpha 1}$ | $^{\circ}2\theta$<br>$\bar{2}04_{\alpha 1}$ |
|--|-------|---|-------------------------------------|---|---|---------------------------------------|---|
| Bulk perthite by heavy liquid separation | K-f   | 21.02 (21.21)                               | single 131 reflection               | n.m.                                      | -   | 41.68                                 | 50.79                                       |
|  | plag  | 22.04                                       | n.m.                                | n.m.                                      | -   | 42.29                                 | 51.43                                       |
| Mesoperthite                             | K-f   | 21.03 (21.25)                               | single 131 reflection               | n.m.                                      | -   | 41.68                                 | 50.76                                       |
|  | plag  | 22.05                                       | n.m.                                | 31.52                                     | -   | 42.29                                 | 51.36                                       |
| Microperthite 1                          | K-f   | 21.04 (21.21)                               | single 131 reflection               | n.m.                                      | -   | 41.68                                 | 50.74                                       |
|  | plag  | 22.04                                       | 31.13                               | 31.50                                     | 1.37  | n.m.                                  | 51.38                                       |
| Microperthite 2                          | K-f   | 21.05 (21.28)                               | single 131 reflection               | n.m.                                      | -   | 41.69                                 | 50.76                                       |
|  | plag  | 22.05                                       | n.m.                                | 31.50                                     | -   | n.m.                                  | n.m.  |
| Microperthite 3                          | K-f   | 21.05 (21.28)                               | single 131 reflection               | n.m.                                      | -   | 41.73                                 | 50.72                                       |
|  | plag  | 22.05                                       | n.m.                                | n.m.                                      | -   | 42.28                                 | 51.35                                       |

n.m. = not measured; reflections not adequately resolved.  $\bar{2}01$  value in parentheses is the value deduced from the alkali exchange graph of Wright (1968).

Table 2.5

(i) Partial analysis of perthite separated from A313/A25.

|                   | Wt. %     | Wt. %               | Mol%, corrected to 100% feldspar |
|-------------------|-----------|---------------------|----------------------------------|
| K <sub>2</sub> O  | 9.23      | Or <sub>54.53</sub> | Or <sub>55.0</sub>               |
| Na <sub>2</sub> O | 3.95      | Ab <sub>33.43</sub> | Ab <sub>35.8</sub>               |
| CaO               | 1.83      | An <sub>9.05</sub>  | An <sub>9.2</sub>                |
| Sr                | 700 ppm   |                     |                                  |
| Rb                | 253 ppm   |                     |                                  |
| Ba                | 4,192 ppm |                     |                                  |

(ii) X-ray diffraction data of heated perthite from A313/A25.

(Heated at 1,050°C.)

|               | 2θ(201) | 2θ(060) | 2θ(204) | Composition from (201) obs | Composition from (201) interpolated |
|---------------|---------|---------|---------|----------------------------|-------------------------------------|
| unheated      | 21.02   | 42.68   | 50.79   | Or <sub>87.5</sub>         | Or <sub>71</sub>                    |
| heated 4 days | 21.23   | 41.67   | 50.82   | Or <sub>69.5</sub>         | Or <sub>61.5</sub>                  |
| 6 days        | 21.23   | 41.63   | 50.82   | Or <sub>69.5</sub>         | Or <sub>74</sub>                    |
| 11 days       | 21.28   | 41.66   | 50.90   | Or <sub>65</sub>           | Or <sub>56</sub>                    |

suggests that either the proposed origin for the microperthite (i.e. annealing processes at lower temperatures) is incorrect or, during the formation of the "daughter" grains the parent mesoperthite changed its structural state accordingly. The X-ray diffraction data of Table 2.4 suggest that the plagioclase phase in all cases is oligoclase.

The anomalous nature of the K-feldspar precludes a direct estimation of the composition from the  $\bar{2}01$  reflection (Wright and Stewart, 1968; Jones, Nesbitt and Slade, 1969). A partial chemical analysis (Table 2.5) was done to determine the composition and, for comparison, the estimated composition from both measured and interpolated  $\bar{2}01$  values is included. These later values were measured on a bulk K-feldspar sample heated at  $1050^{\circ}\text{C}$  for 11 days. Heating for longer periods showed no evidence for further homogenisation.

The commonest mafic mineral is orthopyroxene which, in many samples, is highly altered to a reddish-brown material, the identity of which is unknown. Optical measurements of several partially separated orthopyroxenes indicate that they are bronzite-hypersthene in composition (Table 2.6). The pleochroic colours vary in intensity from very weak to strong, but are always distinct. There seems to be no obvious correlation between the Mg/Fe content and the strength of pleochroism and this is an observation in harmony with the conclusions of Burns (1966). The orthopyroxenes are always anhedral, occasionally appearing as skeletal growths,

Table 2.6

Pyroxenes from the quartz-feldspar-pyroxene granulites.

(i) Orthopyroxenes. Composition estimated from graphs of Leake (1968).

| Spec. No.<br>A313/- | Pleochroism | $2V_{\alpha}$ | $\alpha$ | $\gamma$ | $\text{mg} = \frac{100\text{Mg}}{\text{Mg}+\text{Fe}^{2+}+\text{Fe}^{3+}+\text{Mn}}$ |
|---------------------|-------------|---------------|----------|----------|--|
| 372                 | weak        | $68^{\circ}$  | 1.6831   | 1.6972   | 73   |
| 368                 | very strong | $58^{\circ}$  | 1.6925   | 1.7072   | 65   |
| A25                 | strong      | $68^{\circ}$  | 1.6860   | 1.7050   | 69   |
| 302                 | strong      | -             | -        | 1.6953   | 74   |

(ii) Clinopyroxenes. Compositions estimated from graphs of Deer, Howie and Zussman, (1965).

| Spec. No.<br>A313/- | $2V_{\gamma}$ | $c/\lambda$  | $\beta$ | Composition |   |    | $\text{Mg}$   |
|---------------------|---------------|--------------|---------|-------------|---|----|---|
|                     |               |              |         | Mg          | $\text{Fe}^{2+}+\text{Fe}^{3+}+\text{Mn}$ | Ca | $\frac{\text{Mg}}{\text{Mg}+\text{Fe}^{2+}+\text{Fe}^{3+}+\text{Mn}}$ |
| 372                 | $56^{\circ}$  | $43^{\circ}$ | 1.6902  | 38          | 15  | 47 | 0.72  |
| 368                 | $52^{\circ}$  | $45^{\circ}$ | 1.6934  | 36          | 19  | 45 | 0.66  |
| A25                 | $52^{\circ}$  | $45^{\circ}$ | 1.6873  | 38          | 18  | 44 | 0.68  |
| 302                 | $53^{\circ}$  | $46^{\circ}$ | 1.6886  | 41          | 15  | 44 | 0.73  |

often associated with or completely surrounding clinopyroxene. Clinopyroxene also appears as exsolution lamellae within the orthopyroxene.

Clinopyroxene is found in most of these acid granulites although generally subordinate in amount to orthopyroxene. Because it is often highly altered it is difficult to study and, in the modal analyses (Table 2.3) no attempt has been made to distinguish the two pyroxenes. Some clinopyroxenes have been separated from the rocks and their optical properties are given in Table 2.6. These are augite in composition, are pale green in thin section and are apparently non-pleochroic. Twinning, usually multiple, is almost invariably developed parallel to {100}. In a few rocks the clinopyroxene has been altered to green amphibole or chlorite and to an unidentified reddish-grey material. Where amphibole occurs in these rocks it is generally around remnant clinopyroxene and is thought to be an alteration product. It is typically dark green and strongly pleochroic ( $\alpha$ : yellowish-green;  $\gamma$ : very dark olive-green) compared with the dark brown primary amphibole found in the basic granulites. It is usually present in accessory amounts except for one rock (A313/447) where it is the only mafic mineral present. However, here the rock has been extensively deformed and contains numerous fractures so that the amphibole is probably the product of neo-mineralization.

Opaque minerals, which have not been studied in detail, form a common though never abundant, accessory. Ilmenite, with exsolved



rutile, and magnetite, which is usually associated with haematite, are the commonest varieties. Other accessory minerals include anhedral rutile, subhedral apatite laths and rounded zircon grains.

(ii) Quartz + feldspar + garnet granulites.

These are not always easily distinguished in the field from the quartz + feldspar + pyroxene granulites and, in most cases, boundaries between them are transitional. However, the rocks are usually characterised by a well-developed small-scale layering (e.g. Fig. 2.2). They occur as leucocratic, equigranular, generally banded units (up to 80 metres wide) within the q + f + px granulites. The banding is caused by garnet-rich layers about 1-5 cm wide, alternating with (quartz + feldspar)-rich layers which are about twice as wide. Stained rock slabs indicate that, within the (quartz + feldspar)-rich layers there is further banding caused by variations in the proportions of quartz to feldspar. Because of this mineralogical banding modal analyses of specimens of this granulite group would be meaningless unless large numbers of thin sections cut from several specimens at each outcrop locality were used. For only one rock has a modal analysis been attempted (A253/R16B) and the results are shown in Table 2.7. In this rock distinct garnet-rich bands were not observed although the feldspar-rich bands contain slightly more garnet than the quartz-rich bands. Two rocks of this granulite type have been chemically analysed (Table 2.8). However, neither rock could be regarded as typical of this granulite type as they were, in fact, analysed because of the mineralogical

Table 2.7

Modal analysis of the layered, quartz + feldspar + garnet granulite, A253/R16B.

Quartz-rich layers:

|                          |             |
|--------------------------|-------------|
| Quartz:                  | 65%         |
| Perthite:                | 6%          |
| Plagioclase:             | 18%         |
| Garnet:                  | 7%          |
| Sillimanite:             | 2%          |
| Mica:                    | 2%          |
| Opagues, rutile, spinel: | tr.         |
|                          | <u>100%</u> |

K-feldspar-rich layers:

|                          |             |
|--------------------------|-------------|
| Quartz:                  | 28%         |
| Perthite:                | 51%         |
| Plagioclase:             | 7%          |
| Garnet:                  | 9%          |
| Sillimanite:             | 3%          |
| Mica:                    | 1%          |
| Opagues, rutile, spinel: | 1%          |
|                          | <u>100%</u> |

Table 2.8

Chemical analyses of two quartz + feldspar + garnet granulites.

| Analysis:                      | 1         | 2         | C.I.P.W. norm.   |        |       |       |
|--------------------------------|-----------|-----------|------------------|--------|-------|-------|
| Rock                           | A313/370A | A253/R16B | Analysis:        | 1      | 2     |       |
| SiO <sub>2</sub>               | 62.04     | 67.43     | Q                | 12.45  | 32.84 |       |
| Al <sub>2</sub> O <sub>3</sub> | 15.37     | 15.69     | C                | 2.50   | 6.68  |       |
| Fe <sub>2</sub> O <sub>3</sub> | 3.77      | 0.21      | Or               | 35.87  | 15.54 |       |
| FeO                            | 4.73      | 6.52      | Ab               | 28.60  | 19.04 |       |
| MgO                            | 2.60      | 2.30      | An               | 2.02   | 6.71  |       |
| CaO                            | 0.46      | 1.51      | Hy {             | En     | 6.47  | 5.73  |
| Na <sub>2</sub> O              | 3.38      | 2.25      |                  | Fs     | 4.29  | 11.21 |
| K <sub>2</sub> O               | 6.07      | 2.63      | mt               | 5.47   | 0.30  |       |
| TiO <sub>2</sub>               | 0.97      | 0.58      | il               | 1.84   | 1.10  |       |
| MnO                            | 0.17      | 0.20      | ap               | 0.09   | 0.28  |       |
| P <sub>2</sub> O <sub>5</sub>  | 0.04      | 0.12      |                  | 99.60  | 99.44 |       |
| H <sub>2</sub> O <sup>+</sup>  | 0.51      | 0.50      | H <sub>2</sub> O | 0.58   | 0.54  |       |
| H <sub>2</sub> O <sup>-</sup>  | 0.07      | 0.04      |                  |        |       |       |
| CO <sub>2</sub>                | 0.00      | n.a.      |                  |        |       |       |
| TOTAL                          | 100.18    | 99.98     |                  | 100.18 | 99.98 |       |
| Density:                       | 2.753     | 2.853     |                  |        |       |       |

peculiarities they show: A313/370A is unusually rich in biotite (3%+) and opaque minerals (2%+) and contains modal corundum, while A253/R16B shows modal sillimanite surrounded by garnet coronas. These rocks are discussed later (Section 2.10).

The mineral content of these rocks is variable but all contain quartz as the dominant mineral (30 - 60%). It is always strained and shows undulose extinction and is rich in rutile-needle inclusions. Both perthite and antiperthitic plagioclase ( $An_{33-35}$ ) occur although the former usually dominates. Anhedral, pink garnet, which is often elongate parallel to  $S_g$ , is the main mafic mineral in all cases although reddish-brown ("fox-red") mica, nearly always present in accessory amounts, may be present in significant quantities (e.g. A313/370A). Both pyroxenes are typically absent from these rocks although Barnes (1968), working on granulites about 10km north of this area, has observed rocks containing both garnet and pyroxene(s). Accessory minerals include rounded zircon, opaque minerals (ilmenite and magnetite with haematite in the {111} planes of the magnetite and also as a free phase) and, in a few rocks, green spinel which is found in close association with magnetite. Sillimanite, found only in these garnet-bearing granulites, is a common though never abundant accessory and occurs either as large (1mm) subhedral crystals or, less commonly, as a fibrolite mat associated with pale brown mica and K-feldspar (Fig. 2.34). In one rock (A253/R16B) it is surrounded by garnet (Figs. 2.35 and 2.36). See Section 2.10. In only one rock (A313/370A) has corundum been

Fig. 2.34

Sillimanite (fibrolite) mat closely associated with K-feldspar (S and Kf), surrounding biotite (Bi) and garnet (Ga) in an acid granulite (q + f + ga). A313/424A, P.P.L.

Photograph: A. Moore.

Fig. 2.35

Corona texture in acid granulite (q + f + ga) with garnet (Ga) surrounding a sillimanite (S) core. A plagioclase (Pl) rim surrounds the garnet and separates it from the quartz (Q) and K-feldspar (Kf). The garnet is elongate parallel to  $S_s$ . Photomicrograph on left is in plane polarized light, that to the right is the same section between crossed polars. A253/R16B.

Photograph: A. Moore.

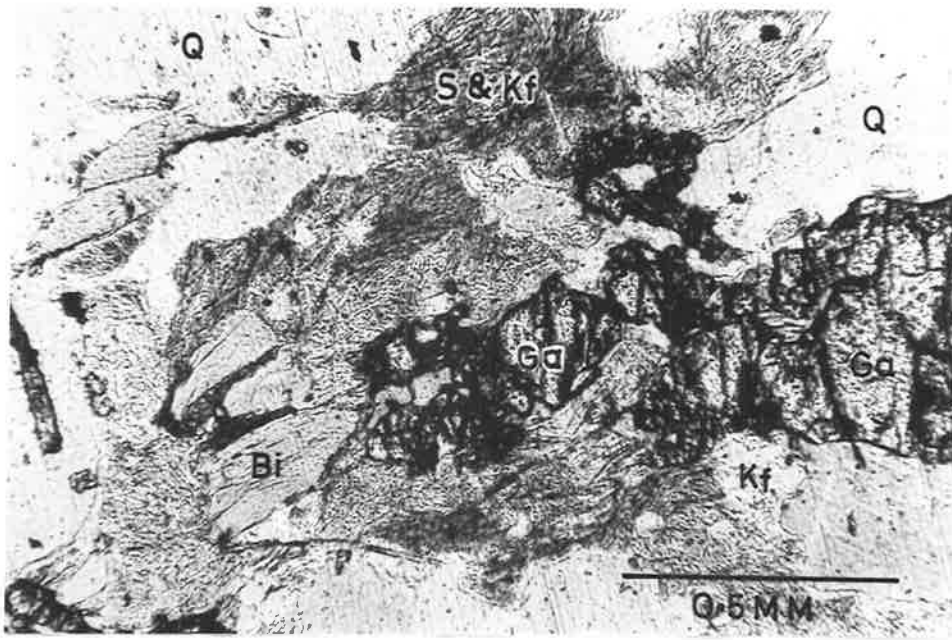


Fig. 2.36

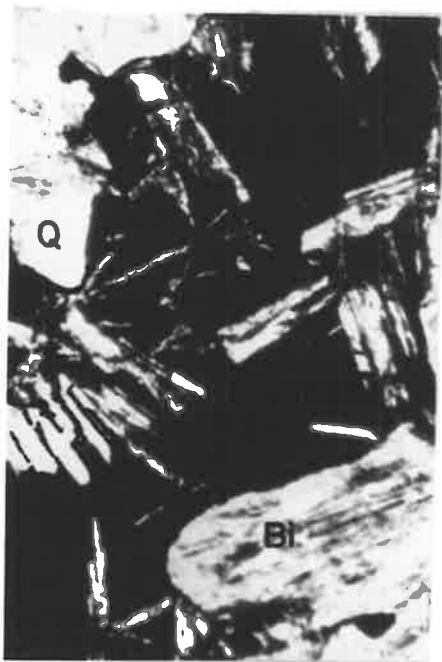
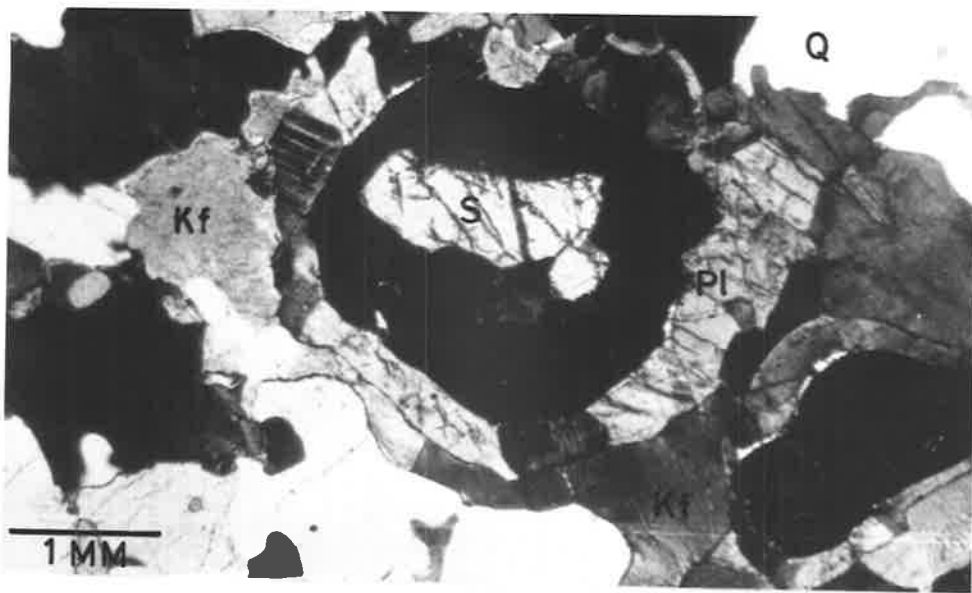
Corona texture in acid granulite (q + f + ga). This section is cut almost perpendicular to  $S_g$ , otherwise is identical to those in Fig. 2.35. A253/R16B. C.P.

Photograph: A. Moore.

Fig. 2.37

Two photomicrographs showing the inclusion (presumed exsolution) of corundum laths within ilmenite. Both are at the same scale. A313/370A. P.P.L.

Photograph: A. Moore.





found as an accessory mineral. It occurs as laths within and parallel to the  $\{111\}$  planes of ilmenite (Fig. 2.37). It is thus shielded from the surrounding quartz grains. See Section 2.10.

(iii) Quartz + feldspar granulites.

This group includes the minor occurrences of quartzite (usually mylonitic) which occur as narrow bands, up to 2 metres wide, concordant with the  $S_3/S_1$  surfaces of the surrounding granulites and forming minor ridges. Occasionally they contain "augen" of K-feldspar, some of which are up to 3 cm in length. The rocks usually show a strong preferred orientation of quartz which makes up 70 - 80% of the rock and is typically in the form of elongate stringers forming a flaser mylonite or seriate, platy granoblastic inequigranular texture. These stringers are contained within a finer-grained matrix of quartz and K-feldspar. Some of the larger K-feldspar crystals are perthitic. The only accessories are traces of opaque minerals, rounded zircon, highly altered pyroxene and very small amounts of strongly pleochroic red-brown biotite. In many rocks only some, or none, of these accessories may be observed.

(iv) Iron-rich granulites.

As do the other granulite types, these rocks occur as bands concordant with the overall granulite banding. The largest unit, some 30 metres wide, crops out as a black ridge about 1 km north of Gosse Pile (Fig. 1.3, D/1) while several smaller bands occur west and east of this. All are massive and, unless sheared, are

not internally layered. Their composition varies slightly as can be seen by the modal analyses (Table 2.9).

The dominant mineral is strained quartz which is free of inclusions. The major mafic mineral is magnetite which has been largely altered to haematite (martite) so that, in hand specimen, the rock appears as an ore of specularite even though it is strongly magnetic. Polished sections show the haematite almost completely pseudomorphing the magnetite, and that which does remain has a brownish tint in polarised light and shows weak anisotropism, indicating the presence of  $TiO_2$  in solid solution. There is no sign of ilmenite or rutile exsolution. In one rock (A313/417) secondary limonite occurs veining all the constituent minerals alike. It occurs both as transgressive veins and as micro-botryoidal colloidal deposits, often lining tiny cavities which are filled with secondary, radiating (or spherulitic) quartz. Accessory minerals include apatite and pyroxene (probably orthopyroxene because of its weak pleochroism, but not identified with certainty because it is highly altered). The iron-rich granulites are further discussed in Section 2.12.

### 2.9.2 The Basic Granulites

The basic granulites are not very numerous and occur as relatively small bands or lenses (max. 900 m by 30 m) which are concordant with and surrounded by the acid granulites. They are frequently found as relatively thin bands (2-3 metres)

Table 2.9

Modal analyses of the iron-rich granulites.

| Spec. No.<br>A313/- | Quartz | magnetite +<br>haematite | limonite | pyroxene | apatite |
|---------------------|--------|--------------------------|----------|----------|---------|
| 417                 | 35.9   | 32.7                     | 31.7     | tr       | -       |
| 455                 | 60.2   | 29.4                     | -        | 10.2     | 0.2     |
| 456                 | 69.1   | 27.4                     | -        | 3.5*     | -       |

\* This is tentatively identified as pyroxene though the identification may be incorrect. In all specimens the pyroxene(?) is extensively altered.

Table 2.10

Modal analyses of hornblende-bearing basic granulites.

| Rock      | Analysis | hb   | opx  | cpx  | plag | ga  | bi  | opaques | ap  | Grain size in<br>m.m. |      |      |
|-----------|----------|------|------|------|------|-----|-----|---------|-----|-----------------------|------|------|
|           |          |      |      |      |      |     |     |         |     | Av.                   | Max. | Min. |
| A313/418  | 1        | 5.4  | 30.1 | 11.5 | 52.5 | -   | tr  | 0.5     | -   | 2                     | 3    | 0.3  |
| A313/297  | 2        | 16.1 | 24.0 | 16.7 | 40.8 | -   | 0.1 | 2.3     | tr  | 1                     | 3    | <0.3 |
| A253/R45B | 3        | 23.8 | 24.0 | 9.1  | 42.4 | -   | -   | 0.7*    | tr  | 1                     | 5    | <0.3 |
| A253/R49A | 4        | 8.2  | 18.8 | 25.5 | 42.8 | -   | tr  | 4.7*    | tr  | 1                     | 4    | <0.3 |
| A313/428  | 5        | 21.2 | -    | 68.1 | 4.0  | -   | tr  | 6.4*    | 0.3 | 2                     | 3    | <0.3 |
| A253/R2B  | 6        | 38.2 | 13.0 | 9.6  | 34.4 | 3.6 | tr  | 1.2     | -   | 1                     | 3    | <0.3 |

\* Green spinel intergrown with the opaques and counted as opaque mineral.

Table 2.11

Optical properties and deduced compositions of the major minerals from an amphibole + pyroxene + feldspar granulite (A313/418).

| Mineral | 2V     | $\alpha/\gamma$ | $\alpha$ | $\beta$ | $\gamma$ | Composition  | $\frac{Mg}{Mg+Fe}$ |
|---------|--------|-----------------|----------|---------|----------|--|--------------------|
| opx     | 65°(-) | 0°              | 1.6838   | -       | 1.7009   | mg 71  | -                  |
| opx     | 50°(+) | 48°             | -        | 1.6833  | -        | Mg <sub>47</sub> Fe <sub>12</sub> Ca <sub>41</sub> | 0.80               |
| hb      | 67°(-) | 18°             | 1.6590   | -       | 1.6800   | mg 58  | -                  |
| plag    | - (+)  | -               | 1.5628   | -       | -        | An <sub>64</sub>                                   | -                  |

$$\Sigma Fe = Fe^{2+} + Fe^{3+} + Mn \quad (\text{after Deer, Howie and Zussman, 1965}).$$

$$mg = \frac{Mg \times 100}{Fe^{2+} + Fe^{3+} + Mn + Mg} \quad (\text{after Deer, Howie and Zussman, 1965}).$$

associated with the calc-silicate rocks and with rocks of pelitic composition, such as A313/370A. The basic granulites are commonly found as small bands within the axial planes and hinge zones of macroscopic folds ( $F_1$ ). Only the larger occurrences have been marked on the geological map (Fig. 1.3). They are divided into two groups, distinguished by the presence or absence of amphibole.

(i) Amphibole + feldspar + pyroxene  $\pm$  garnet granulite.

Melanocratic bands and lenses of amphibole-bearing basic granulites crop out as bands of varying length and ranging between 10m and 30m in width. They are readily distinguished from the surrounding acid granulites since they are much darker, with black or dark grey-green weathered surfaces and, in general, do not show layering as well developed as in the acid granulites. In some rocks small-scale banding, caused by variations in the proportions of mafic minerals to feldspar, is found and this is parallel to the  $S_S$ -surfaces of the surrounding granulites. These basic granulites are very variable in composition, as shown by the modal analyses in Table 2.10, and no single rock can be regarded as characteristic. Specimens A313/428 and A253/R2B (Table 2.10, analyses 5 & 6) are considered quite atypical since only one of each type has been found. The other analyses show similarities and are regarded as representative of the amphibole-bearing granulites.

In all these rocks "common" hornblende (Deer, Howie and Zussman, 1965) is the characteristic, though never dominant, mafic mineral. In all cases it is characterised by its pleochroism

( $\alpha$ : pale greenish-brown;  $\gamma$ : dark brown), cleavage and by the dark areas within the grains which appear to be fine "dustings" of opaque minerals. (Fig. 2.38). Both pyroxenes are usually present, except for one rare rock (A313/428) where orthopyroxene is absent. The orthopyroxenes are bronzite-hypersthene in composition and the clinopyroxenes, which invariably show multiple twinning, belong to the diopside-hedenbergite series. The green clinopyroxene shows no pleochroism, in contrast to the very strong pinkish-red ( $\alpha$ ) to grey-green ( $\gamma$ ) pleochroism of the orthopyroxene. It has a higher birefringence than the orthopyroxene and contains exsolution lamellae of this latter mineral. Both pyroxenes are commonly clouded by opaque, plate-like inclusions of haematite (?) giving a "schiller" effect. From the optically determined compositions from one basic granulite (Table 2.11) it can be seen that, in spite of the very different bulk rock composition compared with that of the acid granulites, the pyroxene compositions are not very different (Tables 2.11, 2.6), although the clinopyroxenes have somewhat different  $\text{Mg}/\text{Mg} + \text{Fe}$  ratios.

The plagioclase ( $\text{An}_{38-64}$ , from optics) of these rocks is more calcic than that of the acid granulites. It is always present and is, with one exception (A313/428), the dominant mineral phase. Unlike the plagioclase of the acid granulites it shows well developed twinning (glide twins) according to the albite and pericline laws. It is apparently free of exsolution phenomena (even at 500x magnification). This is probably a function of the initial low potassium content of the rocks as indicated by the

Fig. 2.38

Crystals of corundum within green spinel (Sp) in an amphibole-bearing basic granulite. Note the "dustings" of oxide minerals within the hornblende (Hb).

A253/R45A. P.P.L.

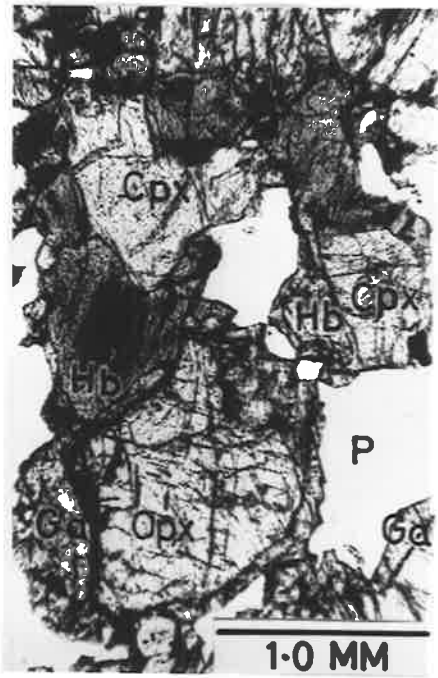
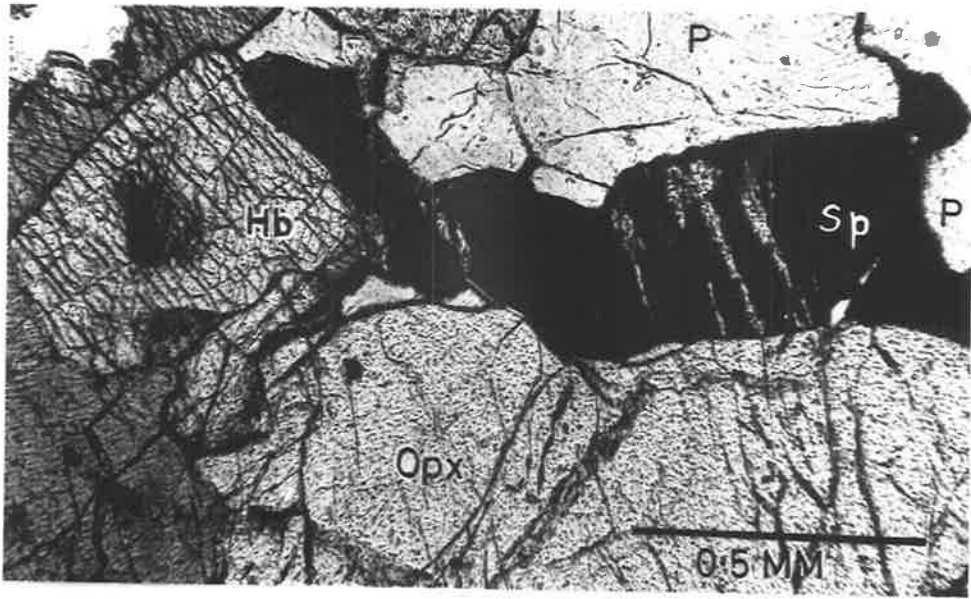
Photograph: A. Moore.

Fig. 2.39

Garnet rim (Ga) surrounding hornblende (Hb), clinopyroxene (Cpx) and orthopyroxene (Opx) and separating these minerals from plagioclase (P). The photomicrographs are the same scale: that to the left was taken with plane polarized light and that to the right between crossed polars. A253/R2B.

Photograph: A. Moore.





fact that no free K-feldspar phase is present.

Accessory minerals include ilmenite and titaniferous magnetite containing haematite exsolution, sometimes surrounding pyrite. Green spinel is a very common accessory, usually associated with magnetite either as a separate phase or intergrown. In one rock (A253/R45A), in which there is no magnetite or ilmenite, corundum occurs as lath-like crystals in the green spinel (Fig. 2.38). Very small amounts of apatite are usually found and very small amounts of red-brown biotite are occasionally observed associated with amphibole and the opaque minerals. Garnet has been observed in only one rock of this type (A253/R2B) where it occurs surrounding pyroxenes, amphibole and the opaque minerals (Fig. 2.39).

(ii) Anorthosite

Close to the northern contact between Gosse Pile and the granulites are found narrow lenses (about 2 metres wide and of variable length, the maximum being about 6 metres) of purple anorthosites which have a distinctive white weathered surface. The majority of outcrops are too small to be satisfactorily represented on Fig. 1.3. These rocks are massive, lack any distinctive foliation and are very limited in extent. They have a simple mineralogy being composed of about 98% plagioclase ( $An_{38}$  from X-ray and optical measurements). The plagioclase is strongly antiperthitic (Fig. 2.40) and shows well-developed multiple glide twins, developed according to the albite (very common) and pericline (rare) twin laws. The crystals show undulose extinction and

Fig. 2.40

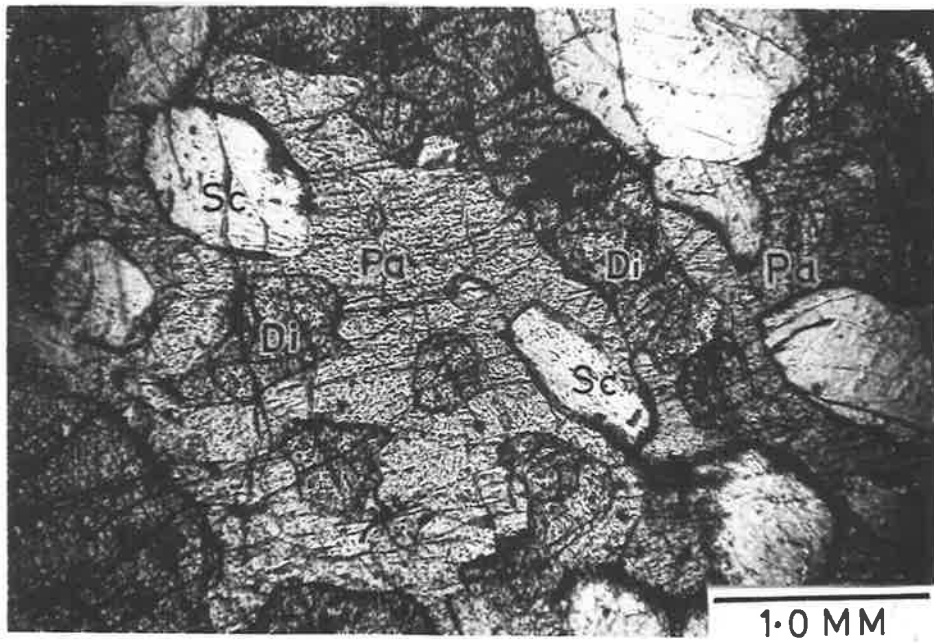
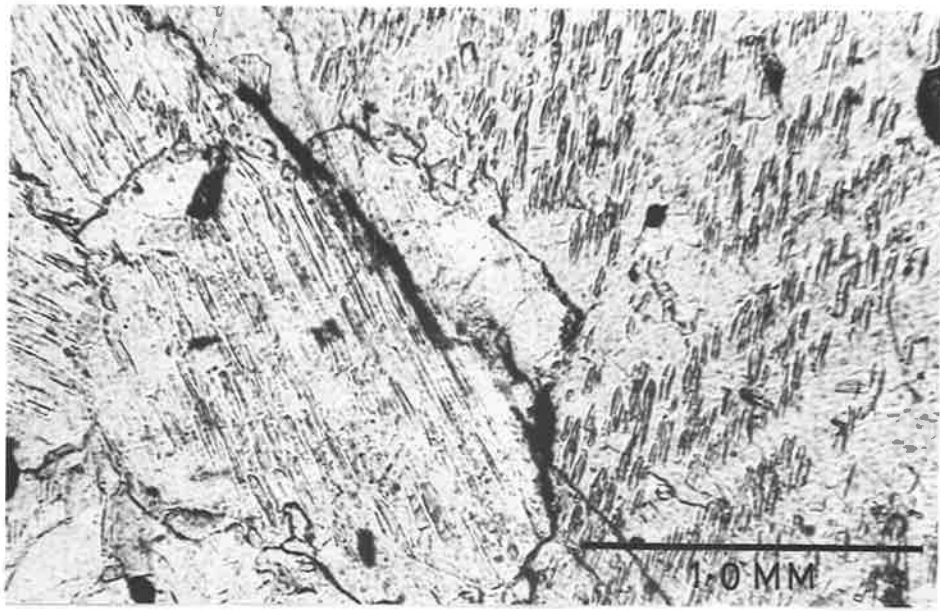
Strongly antiperthitic plagioclase in anorthosite.  
A313/264. P.P.L.

Photograph: A. Moore.

Fig. 2.41

Pargasite (Pa) poikiloblastically enclosing scapolite  
(Sc) and diopside (Di) in a diopside-rich calc-silicate  
granulite. A313/370B. P.P.L.

Photograph: A. Moore.



contain needle-like inclusions of rutile (?). The texture is typically equigranular granoblastic interlobate, and there is no lattice preferred orientation. Accessories include pale green clinopyroxene, opaque minerals which appear to have "flowed" between grain boundaries and into cracks, and some anhedral apatite laths.

### 2.9.3 The Calc-silicate Rocks

These are divided into two distinct types: diopside-rich rocks and a marble.

#### (i) Diopside-rich rocks

These apparently rare rocks in the granulites of the eastern Tomkinson Ranges have not, prior to this investigation, been described. To date they have been found only in the granulites north of Gosse Pile where they occur as numerous lenses of various dimensions: the largest recorded is 50 metres by 5 metres. Only the larger units have been shown on Fig. 1.3. They crop out as dark, grey-green rocks that weather easily producing a rubble which overlies the acid granulites. Where found in place they are seen to strike parallel to the banding of the surrounding acid granulites although they may be locally transgressive. The rocks are massive and unlayered with a coarse to medium grain-size. Although hand specimens are all very similar in appearance modal analyses (Table 2.12) show slight differences in the mineralogy of rocks from different bands and even different specimens from the same

Table 2.12

Modal analyses of diopside-rich calo-silicate rocks.

| Mineral<br>Spec. No. | di   | soap | phlog | sp  | amph             | cc | plag |
|----------------------|------|------|-------|-----|------------------|----|------|
| A313/297A            | 98.7 | 1.2  | -     | 0.1 | -                | -  | -    |
| A253/R41             | 98.6 | 1.4  | -     | -   | tr*              | tr | -    |
| A253/R16A            | 98.1 | -    | 1.9   | -   | tr*              | tr | -    |
| A253/R16C            | 91.6 | 8.3  | 0.1   | -   | tr*              | tr | -    |
| A253/R52B            | 88.2 | 9.5  | 1.5   | -   | 0.8 <sup>+</sup> | tr | -    |
| A313/370B            | 77.2 | 20.2 | 0.5   | -   | 2.1 <sup>+</sup> | -  | tr   |

\* Fine-grained grains or "feathery" grains associated with the pyroxene and probably an alteration product. The identification as amphibole is uncertain.

+ Pargasite.

Table 2.13

Chemical analyses and norms of a diopside-scapolite rock (A313/370B), using material immediately around the vug (V) and material about 1 metre from the vug (R). Analyses and structural formulae (on the basis of 6 oxygen) are given for separated diopside crystals from these rock samples.

|                                | WHOLE ROCK |       | SEPARATED DIOPSIDE         |                                   |
|--------------------------------|------------|-------|----------------------------|-----------------------------------|
|                                | R          | V     | from di + scap<br>rock (R) | euhedral crystals<br>from vug (V) |
| SiO <sub>2</sub>               | 46.25      | 47.40 | 47.19                      | 47.55                             |
| Al <sub>2</sub> O <sub>3</sub> | 11.92      | 6.14  | 9.85                       | 9.03                              |
| Fe <sub>2</sub> O <sub>3</sub> | 2.00       | 1.05  | 2.07                       | 1.06                              |
| FeO                            | 3.47       | 3.84  | 3.34                       | 3.41                              |
| MgO                            | 10.71      | 12.46 | 12.14                      | 13.41                             |
| CaO                            | 24.14      | 25.71 | 24.09                      | 24.58                             |
| Na <sub>2</sub> O              | 0.53       | 0.39  | 0.38                       | 0.28                              |
| K <sub>2</sub> O               | 0.18       | 0.24  | 0.08                       | 0.10                              |
| ThO <sub>2</sub>               | 0.58       | 0.36  | 0.63                       | 0.36                              |
| MnO                            | 0.15       | 0.17  | 0.11                       | 0.11                              |
| P <sub>2</sub> O <sub>5</sub>  | 0.00       | 0.00  | n.a.                       | n.a.                              |
| H <sub>2</sub> O <sup>+</sup>  | 0.01       | 0.05  | n.a.                       | n.a.                              |
| H <sub>2</sub> O <sup>-</sup>  | 0.00       | 0.03  | n.a.                       | n.a.                              |
| CO <sub>2</sub>                | 0.74       | 1.55  | n.a.                       | n.a.                              |
| Cr <sub>2</sub> O <sub>3</sub> | n.a.       | n.a.  | 0.02 (152ppm)              | 0.01 (82ppm)                      |
| NiO                            | n.a.       | n.a.  | 0.05 (372ppm)              | 0.05 (378ppm)                     |
| Total                          | 100.68     | 99.39 | 99.95                      | 99.95                             |

Table 2.13 (continued)

| C.I.P.W. NORMS   |        |       | STRUCTURAL FORMULAE |                  |        |        |
|------------------|--------|-------|---------------------|------------------|--------|--------|
|                  | R      | V     |                     | R                | V      |        |
| An               | 29.62  | 14.29 | Si                  | 1.7444           | 1.7565 |        |
| Lc               | 0.83   | 1.11  | Al                  | 0.2556           | 0.2435 |        |
| Ne               | 2.43   | 1.79  | Al                  | 0.1735           | 0.1494 |        |
| Di {             | Wo     | 26.76 | 34.90               | Fe <sup>3+</sup> | 0.0573 | 0.0293 |
|                  | En     | 20.73 | 26.35               | Cr <sup>3+</sup> | 0.0004 | 0.0004 |
|                  | Fs     | 3.14  | 5.02                | Fe <sup>2+</sup> | 0.1030 | 0.1052 |
| Ol {             | Fo     | 4.16  | 3.28                | Mg               | 0.6686 | 0.7380 |
|                  | Fa     | 0.69  | 0.69                | Ca               | 0.9540 | 0.9729 |
| Cs               | 6.63   | 6.15  | Na                  | 0.0271           | 0.0199 |        |
| Mt               | 2.90   | 1.52  | K                   | 0.0035           | 0.0044 |        |
| Cm               | 1.10   | 0.68  | Ti                  | 0.0173           | 0.0099 |        |
| Cc               | 1.68   | 3.52  | Mn                  | 0.0033           | 0.0033 |        |
| H <sub>2</sub> O | 0.01   | 0.08  | Ni                  | 0.0013           | 0.0013 |        |
| Total            | 100.68 | 99.39 |                     | 4.0093           | 4.0340 |        |
| D                | 3.271  | 3.239 | Fs                  | 12.8             | 10.6   |        |
|                  |        |       | En                  | 38.2             | 40.4   |        |
|                  |        |       | Wo                  | 49.0             | 49.0   |        |
|                  |        |       |                     | 100.0            | 100.0  |        |

Optical properties of diopside from diopside-scapolite rock

$\alpha$  : 1.7038 (pale green)       $\Delta$  : 0.0121  
 $\beta$  : - (yellowish-green)       $2V_{\gamma}$  :  $45^{\circ} \pm 3^{\circ}$   
 $\gamma$  : 1.7159 (green)       $c\Lambda_{\gamma}$  :  $53^{\circ}$

dispersion : strong,  $r > v$



band, e.g. A253/R16A and A253/R16C, which also have a different average grain-size.

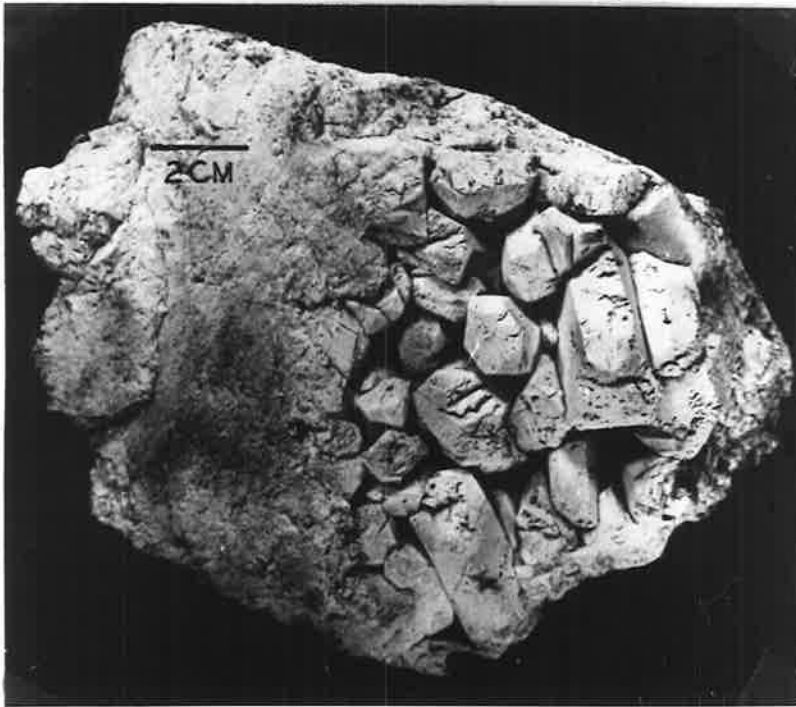
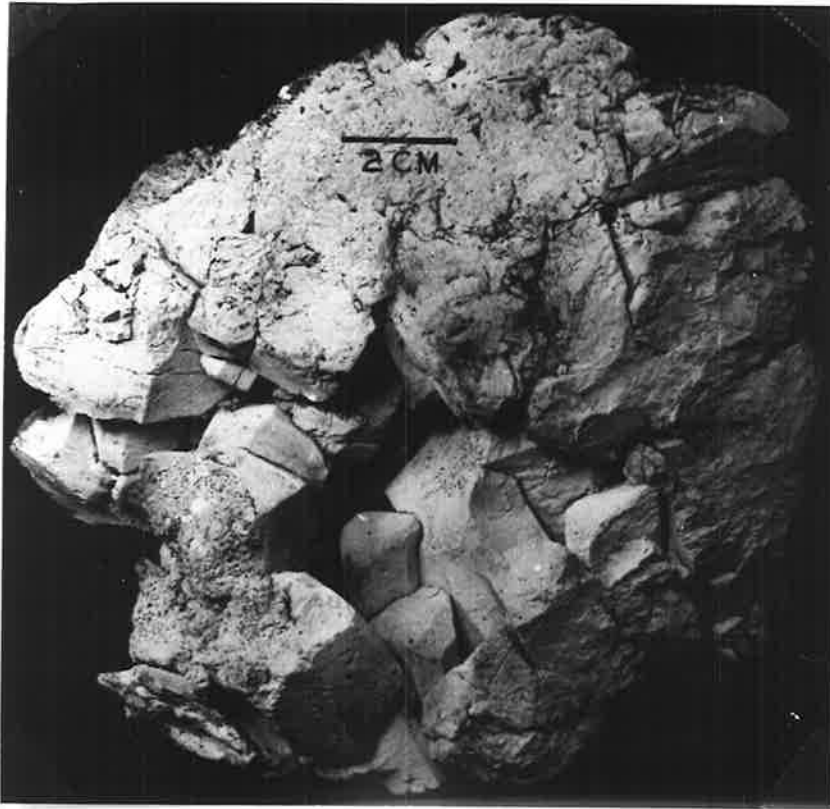
In all cases the dominant mineral is green diopside, usually making up more than 90% of the total rock. It shows well developed multiple twinning parallel to {100}. The grains are anhedral with straight, or gently curved, boundaries (Fig. 2.24). Other minerals, such as scapolite, phlogopite or calcite, which occur interstitially show a carries-type relationship towards the diopside. Where pargasite occurs it occasionally encloses rounded, apparently remnant, diopside and scapolite crystals in a poikiloblastic texture (Fig. 2.41). Extensive alteration to amphibole (?), calcite and possibly scapolite along grain boundaries, cleavages and twin planes is common. In one rock (A313/370B) a vug-like cavity, about 10cm in diameter, was found into which had grown large, euhedral diopside crystals (Fig. 2.42). Since these large crystals presumably grew under granulite facies conditions they must have grown into a space occupied either by a fluid or by a mineral, since weathered out, which offered no resistance or mutual interference to the growth of the diopside. Small quantities of pink calcite were found associated with the pyroxene in the cavity. Chemical analyses of diopside from both the cavity and from the surrounding rock as well as analyses of the unseparated rock are given in Table 2.13. There is little difference in the analyses of the material from around the vug and elsewhere in the rock, apart from  $Al_2O_3$  and  $CO_2$  contents, and there is no real difference in composition between pyroxenes from the vug and the rock. Both are unusually rich in  $Al_2O_3$ , containing over 9% compared

Fig. 2.42

Two views of the vug-like cavity within a diopside-rich calc-silicate granulite. The euhedral nature of the large diopside crystals is well shown.

The specimen has been whitened by a thin layer of ammonium chloride to increase contrast: the natural colour is dark, greyish-green.

Photograph: R. Smitt



with only 6.42% for the most aluminous diopside listed by Deer, Howie and Zussman (1963).

Scapolite is the most abundant (1-20%) accessory mineral in these rocks, although it may be absent in some (e.g. as in A253/R16A). The mean refractive index of scapolite from A313/370B is  $1.5785 \pm 0.002$  ( $\omega$  : 1.5620;  $\epsilon$  : 1.5949) indicating a composition of about 86.6% Me (Shaw, 1960). The compositions determined using the mean refractive index and the birefringence (Shaw, 1960), agree fairly closely so that the scapolite is probably not rich in sulphur (Lovering and White, 1964). An X-ray diffraction pattern (8 oscillations) shows the difference between the (400) and (112) peaks, for CuK radiation, to be  $3.626 \pm 0.005^{\circ}2\theta$ . This indicates a meionite-rich scapolite (Burley, Freeman and Shaw, 1961) in agreement with the optical determinations. Scapolite occurs as anhedral grains along diopside grain boundaries, apparently replacing the diopside (carries texture). It also occurs within diopside crystals, both as rectangular grains and as irregular, vermiform grains. In pargasite some rounded scapolite crystals occur (Fig. 2.41). Several scapolite grains within a pyroxene crystal show identical optical orientations and the appearance is similar to that of myrmekitic quartz in feldspar. In one rock (A313/370B) the scapolite is seen to be replacing plagioclase (Fig. 2.43). However, plagioclase is a very rare mineral, occurring in very small amounts interstitially and has not been observed in any other calc-silicate rock. Because of the severe alteration to scapolite and calcite, determinations of the composition were particularly

difficult. Using the well developed multiple twinning (albite - carlsbad laws) the composition was estimated as approximately  $An_{85}$  (U-stage).

Weakly pleochroic phlogopite ( $\alpha$ : colourless;  $\beta = \gamma$ : pale yellowish-brown) is a common accessory. Pink calcite is common in small amounts as an interstitial mineral and is closely associated with the scapolite and plagioclase. In the vug (A313/370B) it is abundant around diopside crystals, but whether it is a primary or secondary mineral is not certain.

The diopside is commonly altered to a "feathery" mineral (Fig. 2.21 and Fig. 2.24), especially along microfractures. This mineral is tentatively identified as amphibole. Amphibole also occurs as flake-like grains within the diopside. In two rocks fairly large crystals of amphibole occur enclosing, and possibly replacing, both diopside and scapolite (Fig. 2.41). This is identified as pargasite ( $2V_{\gamma} : 70^{\circ}$ ,  $c\wedge\gamma : 15^{\circ}$ ) by comparison with an amphibole found in the marble which has similar optical properties. Apart from a difference in refractive index (< diopside; > scapolite) it is difficult to distinguish the pargasite from the surrounding diopside as the two minerals have similar colour and interference colours.

The only other mineral identified in these rocks is a pale green spinel which occurs in trace amounts in only one specimen (A313/297A).

## (ii) Marble.

Only one, poorly exposed band of marble, 30 metres by 6 metres, has been found. It occurs about 70 metres north of Gosse Pile (Fig. 1.3, D/2) and is concordant with  $S_g$  in the enclosing acid granulites. The outcrop is very patchy and exposures fragmental because of the high susceptibility to weathering. The rock is medium-grained (average, 2mm) and fairly massive although a weak compositional banding is developed in places. These bands of pale green diopside and pink calcite are discontinuous, about 5 to 10cms wide and, where found in place, strike parallel to the length of the marble band. A partial chemical analysis of the marble is given in Table 2.14. The general variability in mineral composition is shown by the modal analyses (Table 2.15) of four specimens collected from different parts of the band.

The dominant mineral is calcite which is generally white, but pink where associated with the diopside-rich bands. X-ray powder photograph patterns of the pink and white varieties differ only slightly: that of the pink calcite indicates that the mineral has a slightly smaller cell size, suggesting substitution of calcium by a smaller cation. The pink colour of calcite is generally regarded as being caused by the entry of manganese into the calcite structure.

Within the calcite-rich parts of the marble the main silicate phase is forsterite which occurs as rounded crystals (Fig. 2.44a). The  $d_{130}$  spacing of this is  $2.766\text{\AA}$ , suggesting that the

Table 2.14

Partial chemical analysis of the marble (A313/M) excluding diopside-rich bands.

|                                |               |
|--------------------------------|---------------|
| SiO <sub>2</sub>               | 10.30         |
| Al <sub>2</sub> O <sub>3</sub> | 1.04          |
| Fe <sub>2</sub> O <sub>3</sub> | n.a.          |
| FeO                            | 0.66          |
| MgO                            | 12.99         |
| CaO                            | 43.03         |
| Na <sub>2</sub> O              | 0.01          |
| K <sub>2</sub> O               | 0.96          |
| H <sub>2</sub> O <sup>+</sup>  | 0.12          |
| H <sub>2</sub> O <sup>-</sup>  | 0.03          |
| CO <sub>2</sub>                | 31.03         |
| TOTAL                          | <u>100.17</u> |
| Density                        | 2.839         |

Table 2.15

Modal analyses of the marble north of Gosse Pile.

| Mineral<br>Spec. No.      | co   | fo   | ch   | di  | amph  | phlog | sp  |       |
|---------------------------|------|------|------|-----|-------|-------|-----|-------|
| A313/M (i)                | 68.2 | 13.5 | 10.3 | 6.7 | tr(?) | 1.0   | 0.3 |       |
| A313/M (ii)               | 72.3 | 9.1  | 5.1  | 8.2 | •     | 5.3   | -   |       |
| A253/R17                  | 76.7 | 12.1 | 0.8  | 9.3 | -     | -     | 1.1 |       |
| A313/M<br>(large section) | 72.2 | 14.2 | 6.5  | 2.8 | -     | 4.1   | 0.2 |       |
| Average of 4<br>samples   | 72.3 | 12.2 | 5.7  | 6.8 | -     | 2.6   | 0.4 |       |
|                           |      |      |      |     |       |       | D   | 2.839 |

Diopside-rich band within the marble.

|         |      |   |   |      |   |   |   |       |
|---------|------|---|---|------|---|---|---|-------|
| A313/Md | 36.8 | - | - | 73.2 | - | - | - |       |
|         |      |   |   |      |   |   | D | 3.254 |

Aluminous nodule from the diopside-rich band.

|         |     |   |   |      |      |   |     |
|---------|-----|---|---|------|------|---|-----|
| A313/Mn | 8.5 | - | - | 76.8 | 10.3 | - | 4.4 |
|---------|-----|---|---|------|------|---|-----|



Fig. 2.43

Well-twinned plagioclase showing apparent replacement  
by scapolite in a diopside-rich calc-silicate granulite.  
A313/370B. C.P.

Photograph: A. Moore.

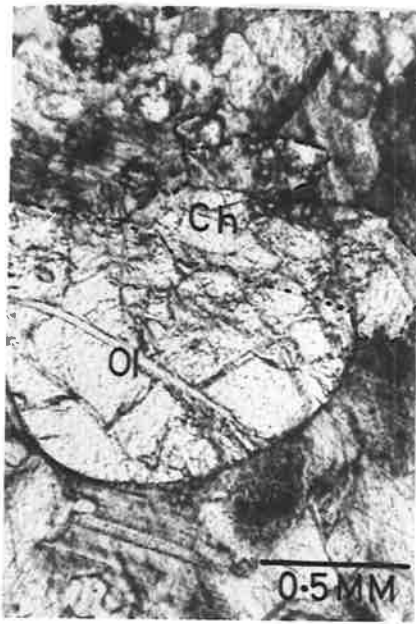
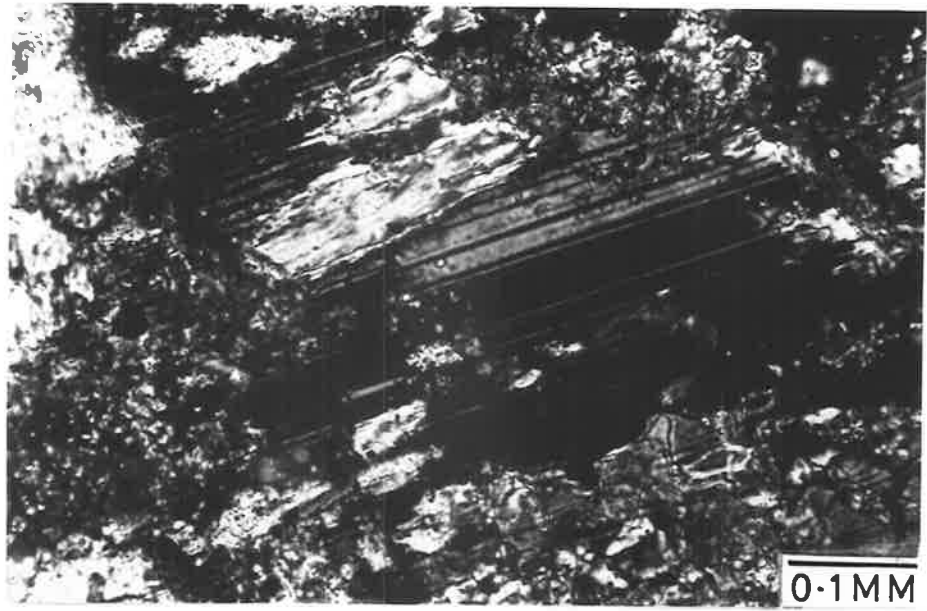
Fig. 2.44

a  
Rounded olivine (Ol) with  
associated chondrodite (Ch)  
in marble. The contact  
between the two minerals  
has been dotted in with  
ink. P.P.L.

A313/M

b  
Multiple twinning in a  
single chondrodite crystal  
in marble. C.P.

Photographs: A. Moore.



composition is very close to pure forsterite (Yoder and Sahama, 1957). The olivine is often closely associated with diopside, chondrodite, or olivine with a different optic orientation which may completely surround the first crystal and appears as an overgrowth. Many crystals are highly altered to a fibrous mineral with low interference colours, probably a serpentine. Alteration has been initiated along the irregular fractures which traverse most grains.

Closely associated with the olivine (as in Fig. 2.44a), often as rims around it or as lath-like crystals within it, is chondrodite, which also occurs as discrete, rounded crystals within the calcite. In thin sections about 0.08 mm thick it shows distinct pleochroism similar to that of staurolite ( $\alpha$ : pale yellow;  $\beta = \gamma$ : colourless). Multiple twinning is very common, the twin planes of which have been determined as  $\{001\}$  and  $\{110\}$ , Fig. 2.44b. The optical properties are:

$$\alpha : 1.5953 \pm 0.003;$$

$$\gamma : 1.6214 \pm 0.003;$$

$$2V_{\gamma} : 70^{\circ} \pm 2^{\circ}$$

$$cA_{\alpha} : 20^{\circ} \pm 2^{\circ}.$$

X-ray powder photographs give patterns which suggest that clinohumite and chondrodite may occur together, although the patterns are affected by the presence of calcite, diopside and some olivine impurities. Chondrodite is a relatively rare mineral and, as other minerals of the humite group, has a rather restricted occurrence. Recently Jones, Ribbe and Gibbs (1969) have suggested that, because of the implied special physico-chemical conditions for the formation

of humite group minerals, they may be potentially useful petrogenic indicators. Obviously an important factor will be the availability and fugacity of fluorine and water.

The other silicates are diopside and phlogopite. Pale green, non-pleochroic pyroxene showing well developed multiple twinning parallel to  $\{001\}$  and  $\{100\}$  is fairly common (Table 2.15). It occurs as rounded or irregular crystals within the calcite, sometimes entirely surrounding olivine. Phlogopite is found in most specimens in relatively small amounts as elongate crystals with rounded terminations. It is always deformed and contains numerous kink-bands. Although it usually occurs as discrete crystals it has been observed in close association with olivine in at least one slide. On the basis of the  $\beta$  index ( $\beta = \gamma : 1.5752 \pm 0.001$ ;  $2V_{\alpha} : \text{estimated as } 3^{\circ}$ ) it appears to be almost entirely free of iron (Deer, Howie and Zussman, 1963). This view is supported by the fact that, even in thick sections, no pleochroism has been observed. The only other mineral identified is pale green spinel which occurs as almost circular blebs in the calcite.

The diopside-rich bands contain only diopside and pink calcite. However, within these bands there occur almost spherical nodules, up to 5 cms in diameter, which consist of diopside, amphibole, spinel and calcite (Table 2.15). The amphibole has been identified as pargasite, essentially on the basis of optical properties as the X-ray powder photographs of tremolite, pargasite and hornblende are very similar. The pargasite ( $\alpha : 1.6152 \pm 0.003$ ;  $\gamma : 1.6368 \pm 0.003$ ;  $2V_{\gamma} : 62 \pm 2^{\circ}$ ) shows well developed, but very fine,

lamellar twinning parallel to {001}. It appears colourless in thin section though dark green in hand specimen, this colour probably being caused by the large number of rounded green spinel grains which it encloses. An X-ray powder pattern of this spinel showed it has a cell size of  $8.104\text{\AA}$ , indicating a composition very close to pure  $\text{MgAl}_2\text{O}_4$  spinel, the cell size of which is  $8.103\text{\AA}$  (Deer, Howie and Zussman, 1965).

Unlike forsterite-marbles of other granulite facies terrains this marble is free of grossular garnet.

## 2.10 DISCUSSION OF PARTICULAR MINERAL ASSOCIATIONS

### 2.10.1 Corona-like textures involving garnet, sillimanite and, in some cases, plagioclase.

In sillimanite-bearing q + f + ga granulites there has been observed a close association between sillimanite, K-feldspar and garnet (Figs. 2.34, 2.35 and 2.36), and in one rock (A253/R16B) the garnet occurs as a corona around large sillimanite crystals. This rock shows small-scale banding (Table 2.7). The type of corona found in the quartz-rich bands is illustrated diagrammatically in Fig. 2.45b while the type found in the perthite-rich band is shown in Fig. 2.45c. A similar association between garnet and sillimanite has been observed in acid granulites from near Ewarara (Fig. 1.1) collected by Mr. A.D.T. Goode. In this rock (A305/15) the sillimanite is surrounded by perthite unless separated

Fig. 2.45

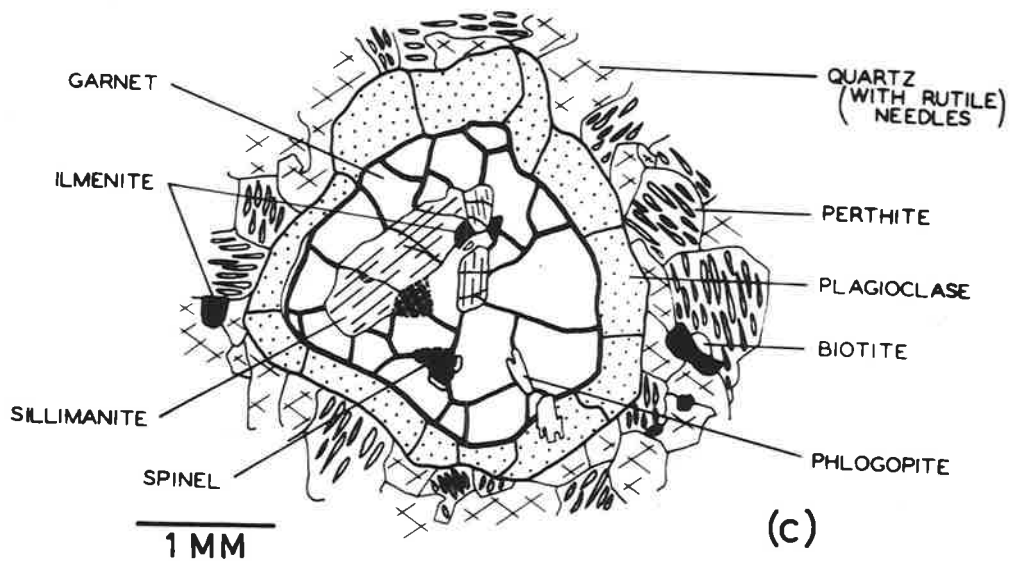
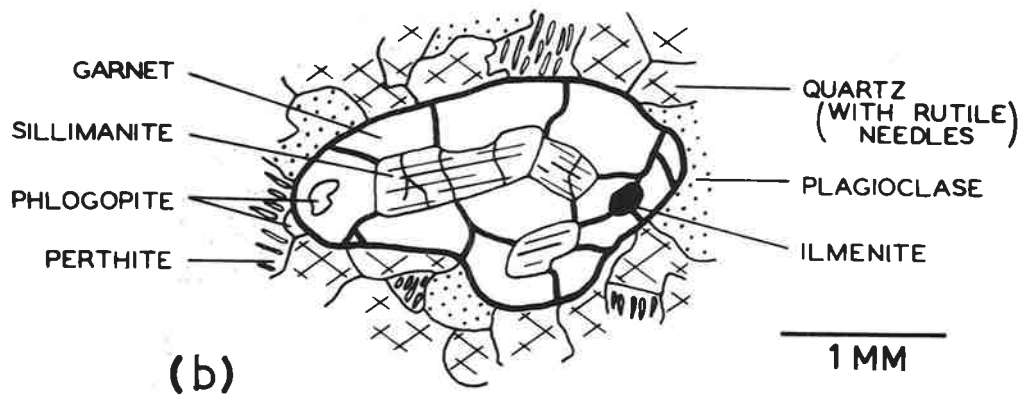
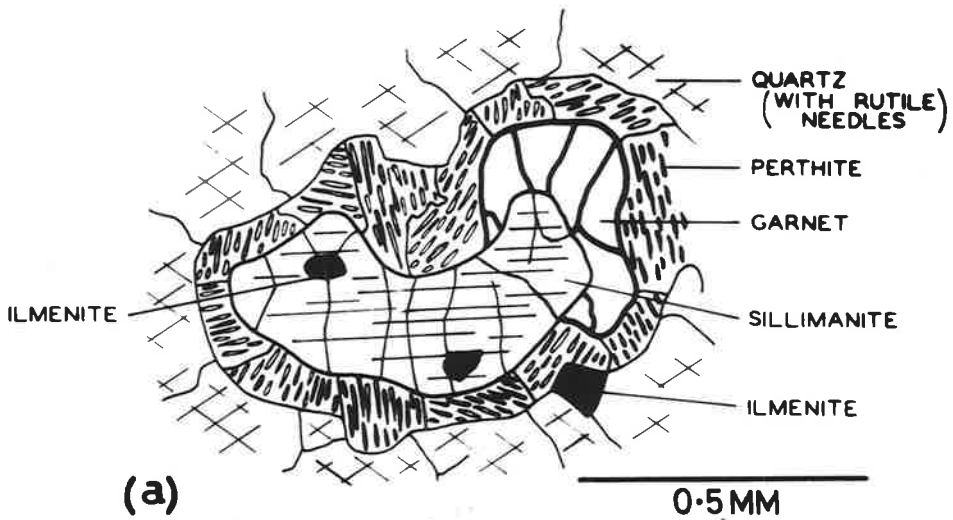
Diagrammatic illustration of the types of corona textures found within acid granulites of the eastern Tomkinson Ranges.

For interpretation see text.

Diagrams drafted by:

Miss A. Swan.

---



by a partial or complete rim of garnet (Fig. 2.45a).

#### Interpretation

Chinner (pers. comm. by letter, 1968) considers that the term "reaction rim" should be restricted to rims which separate identifiable reactants. Although the term "corona texture" is generally applied to features which are generally considered to have resulted from reaction between initially contiguous mineral grains to produce the rim between them (e.g. Shand, 1945; Mason, 1967) and is thus synonymous with "reaction rim", it can be applied to rims which have formed in different ways (A.G.I. Dictionary of Geological Terms, 1962). In this case the garnet is considered to be a corona, which is defined as a rim of one or more minerals partially or totally surrounding another. Chinner (pers. comm.), after a brief examination of these textures, concluded that the sillimanite because of its subhedral shape and apparent lack of corrosion by the garnet, was probably as much a nucleating agent as a reactant in the formation of the garnet. He feels that the garnet may have formed by diffusion of Fe and Mg from biotite elsewhere in the rock.

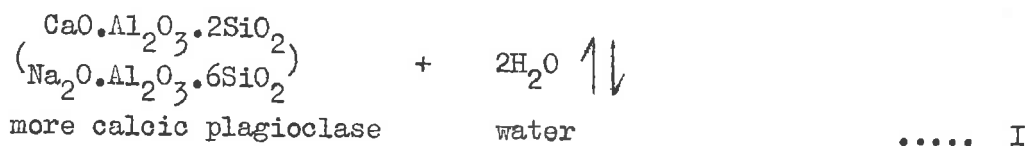
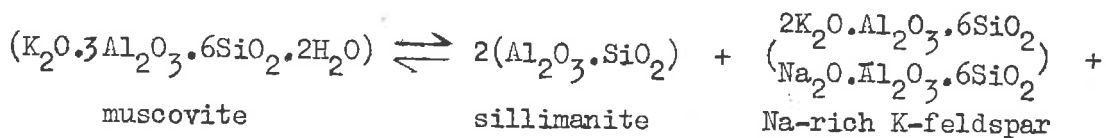
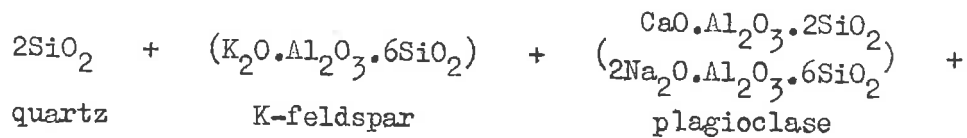
In most corona textures which have formed by reaction the reacting minerals can be easily identified and their separate contributions to the chemistry of the corona recognised. If, however, the reaction takes place by diffusion over a distance of a centimetre or so (Blackburn, 1968; Carmichael, 1968) or if one of the reactants is present in limited amounts so that it is



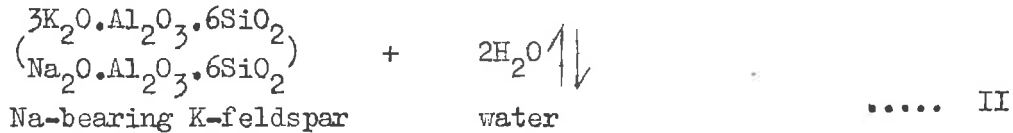
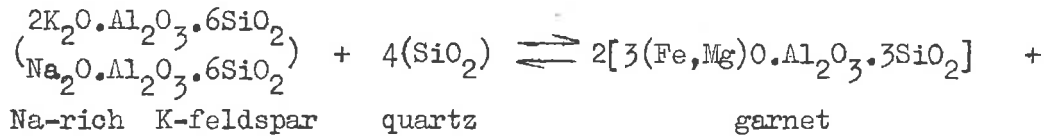
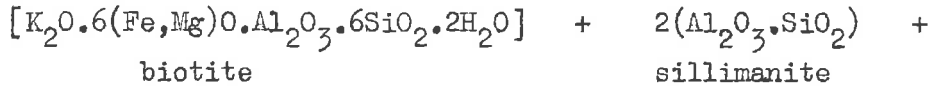
almost eliminated during the reaction, then the determination of the reactions, given the products, is difficult. The interpretation, outlined below, gives a possible mechanism for the formation of the coronas shown in Fig. 2.45b and 2.45c. The association illustrated in Fig. 2.45a is thought to arise in a similar way, where the consistent association of sillimanite and K-feldspar is regarded as significant.

It is assumed that the reactions which produced the coronas in the granulites took place between solids. Under these conditions double-decomposition type chemical equations are not strictly valid since reaction probably took place by diffusion of material across mineral interface boundaries. However, chemical equations do have value in that they show the products of the reaction to be chemically equivalent to the reactants. Blackburn (1968) has shown that diffusion, even in high-grade metamorphic rocks is probably very limited and is probably controlled by rock structures, such as banding. It is proposed that the corona-bearing granulite has acted essentially as a closed system, at least within the major lithological boundaries and probably on a much smaller scale, possibly within each band. If this is true then weight proportions of reactants, as indicated by the chemical equations, should closely match those measured within the coronas, bearing in mind that certain elements such as  $\text{SiO}_2$ ,  $\text{Na}_2\text{O}$  and  $\text{K}_2\text{O}$  are present in excess in the matrix.

Because of the very close association of K-feldspar and sillimanite in these rocks it seems reasonable to assume that the reaction which produced the sillimanite also produced the K-feldspar. Following suggestions by Guidotti (1963) the following reactions could explain the present mineral association:



If biotite were present it would remain as a stable phase during this reaction but under conditions of increasing pressure and temperature it would react with the sillimanite. If the sillimanite were present in excess then, at completion of the reaction, some would remain surrounded by the products of the reaction:



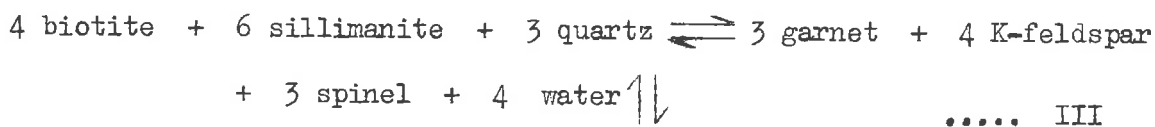
Both reactions I and II could be considered in two stages: a reaction to produce the new phase(s), followed by a feldspar equilibrium.

At lower pressures cordierite rather than garnet would be expected to form in II.

Wilson (1954) has described an acid quartz-feldspar granulite from the Musgrave Ranges, where mineral assemblages are consistent with a lower pressure of formation than those of the Tomkinson Ranges. In this rock (30228) cordierite occurs around sillimanite which encloses magnetite and green spinel.

Green spinel is commonly associated with the sillimanite in these rocks, either surrounded by sillimanite or in the garnet, most commonly along the sillimanite-garnet boundary. If the amount of silica able to diffuse to the site of reaction (II) was limited, perhaps by armoring as garnet was produced, then reaction II would

proceed as follows, (ignoring, for simplicity, the contribution by plagioclase):



The formation of the plagioclase rim around garnet in the quartz-perthite bands is problematic. Kretz (1959) showed that, under specified conditions, garnet in the presence of sillimanite contains a limited amount of grossular component. Thus, the calcium content of the garnet is, among other things, dependent on the P, T conditions. Each of these variables acts in a different way, so that the calcium content of garnet in contact with sillimanite increases with increasing pressure at constant temperature but probably decreases with increasing temperature at constant pressure. If the calcium content of the garnet, presumably derived originally from some pre-existing plagioclase, is above some critical value for the metamorphic conditions at a particular time then calcium will migrate from the garnet in order to establish equilibrium. It is impossible to fix the conditions of metamorphism based on the present calcium content of the garnet because the effects of important variables, such as  $f_{O_2}$ , Fe:Mg:Mn ratio of the garnet and the composition of the plagioclase, are unknown.

In the quartz-rich bands, where discrete plagioclase grains are common, any calcium liberated from the garnet could be taken up by this plagioclase and no rim would form around the garnet

(Fig. 2.45b). In the perthite-rich bands there is no phase which will readily accommodate the calcium so it would tend to form a rim around the garnet. Optical measurements on the rim plagioclase give a surprisingly low anorthite content of  $An_{38\pm 3}$ , which agrees well with that of the microprobe analysis (Table 2.16). Optical measurements of the plagioclase in the quartz-rich bands (where garnet is not rimmed) give values of  $An_{50\pm 5}$ . It is considered that the composition of the rim plagioclase is determined largely by the amount of calcium liberated from the garnet and the amount of sodium available, probably from the perthite. The composition of the matrix plagioclase is determined by its previous composition and by the amount of calcium added to it. Therefore, the feldspars need not have identical compositions, nor does the rim plagioclase need to be more calcic than the matrix plagioclase.

The areas of 10 coronas have been measured. Only the largest corona structures, showing the presence of all the mineral phases, were selected for measurement because, following Alling (1936), the largest grains in a thin section are the most significant in grain size studies. These give an average ratio of garnet to rim plagioclase of 1:0.54 (ranging from 1:0.89 to 1:0.23). Assuming that, in thin section, area is equivalent to volume, that the amount of CaO in the plagioclase is 7.7% (Table 2.16) and that of the garnet is 1.4% (Table 2.16), then the CaO content of the garnet prior to the formation of the plagioclase rim can be calculated. If the garnet has not changed from its present volume during the formation of the

Table 2.16

Analyses of some of the minerals occurring within the corona texture shown in Fig. 2.35.

| Analysis:                      | 1      | 2      | 3      | 4    | 5     |
|--------------------------------|--------|--------|--------|------|-------|
| SiO <sub>2</sub>               | (60.6) | (40.1) | (42.7) | n.d. | n.d.  |
| Al <sub>2</sub> O <sub>3</sub> | 24.4   | 23.4   | 56.7   | 50.8 | n.d.  |
| Fe <sub>2</sub> O <sub>3</sub> | -      | -      | 0.6    | -    | 14.0  |
| FeO                            | n.a.   | 25.6   | -      | 29.3 | 35.1  |
| MgO                            | n.a.   | 8.8    | n.d.   | 7.8  | trace |
| CaO                            | 7.7    | 1.4    | n.d.   | n.d. | n.d.  |
| Na <sub>2</sub> O              | 7.2    | n.a.   | n.a.   | n.a. | n.a.  |
| K <sub>2</sub> O               | 0.1    | n.a.   | n.d.   | n.a. | n.a.  |
| MnO                            | n.a.   | 0.7    | n.d.   | n.d. | trace |
| TiO <sub>2</sub>               | n.a.   | n.d.   | n.d.   | n.d. | 50.9  |
|                                | 100.0  | 100.0  | 100.0  | 87.9 | 100.0 |

Calculated structural formulae of the minerals.

|                  |          |            |     |      |     |
|------------------|----------|------------|-----|------|-----|
| Si               | 10.8     | 6.1        | 4.6 | -    | -   |
| Al               | 5.1      | 4.2        | 7.2 | 15.2 | -   |
| Fe <sup>3+</sup> | -        | -          | 0.1 | -    | 0.5 |
| Fe <sup>2+</sup> | -        | 3.3        | -   | 6.2  | 1.5 |
| Mg               | -        | 2.0        | -   | 3.0  | -   |
| Ca               | 1.5      | 0.2        | -   | -    | -   |
| Na               | 2.5      | -          | -   | -    | -   |
| K                | 0.0(2)   | -          | -   | -    | -   |
| Mn               | -        | 0.0(9)     | -   | -    | -   |
| Ti               | -        | -          | -   | -    | 1.9 |
|                  | Ab: 62.6 | Al: 58.5   |     |      |     |
|                  | An: 36.9 | Gross: 4.1 |     |      |     |
|                  | Or: 0.5  | Py: 35.8   |     |      |     |
|                  |          | Spess: 1.6 |     |      |     |

n.a. not analysed. n.d. not detected.

Table 2.16 (cont.)

1. Plagioclase (rim around garnet). Analyst: AMDEL.  
SiO<sub>2</sub> by difference.
2. Garnet. Analyst: AMDEL, except for FeO (titration) and Al<sub>2</sub>O<sub>3</sub> (colorimetric) by A.C. Moore on hand-picked, separated garnets. SiO<sub>2</sub> by difference.  $\underline{a} = 11.520\text{\AA}$ ,  $n = 1.783$ .
3. Sillimanite. Analyst: AMDEL. SiO<sub>2</sub> by difference.  
Total Fe quoted as Fe<sub>2</sub>O<sub>3</sub>.  $\alpha = 1.659$ ;  $\gamma = 1.676$ .
4. Green spinel. Analyst: AMDEL. Total Fe quoted as FeO.
5. Ilmenite. Analyst: AMDEL. Total Fe (Fe = 37.0%) was distributed between FeO and Fe<sub>2</sub>O<sub>3</sub> such that the sum FeO + TiO<sub>2</sub> + Fe<sub>2</sub>O<sub>3</sub> = 100.0%.

Analyses, except for elements stated, were done by Mr. P. Schultz, using electron microprobe techniques at the Australian Mineral Development Laboratories (AMDEL), Adelaide, South Australia, (Report MP1501/68). The results are judged by him to be accurate to within 10% of the values quoted. The detection limit for all elements quoted (except for Na which was 0.5%) is 0.05%.

Table 2.17

|                                | 1      | 2      |
|--------------------------------|--------|--------|
| SiO <sub>2</sub>               | 45.8   | 37.9   |
| Al <sub>2</sub> O <sub>3</sub> | 29.4   | 10.7   |
| FeO                            | 14.8   | } 37.7 |
| MgO                            | 5.0    |        |
| CaO                            | 3.0    | -      |
| Na <sub>2</sub> O              | 2.0    | -      |
| K <sub>2</sub> O               | (0.02) | 9.9    |
| H <sub>2</sub> O               | -      | 3.8    |
|                                | 100.0  | 100.0  |

1. Average composition of a corona-structure, ignoring trace amounts of MnO and TiO<sub>2</sub>, and recalculated to 100.0%. Based on analyses in Table 2.16 and the average proportions of constituent minerals measured in ten corona structures.
2. Calculated composition of a theoretical biotite which is presumed to have reacted with sillimanite to produce garnet. The FeO : MgO molecular ratio is as in the garnet (Table 2.16) and the composition is assumed as  
 $[K_2O \cdot 6(Fe, Mg)O \cdot Al_2O_3 \cdot 6SiO_2 \cdot 2H_2O]$ .



plagioclase rim it must have contained 5.5% CaO: if it has been reduced to its present size from a volume marked by the outer limit of the plagioclase rim it must have contained 3.6% CaO. These values set a maximum and minimum limit to the former CaO content of the garnet. This indicates that the garnet was calcium-rich, but the calculated values are not unreasonable considering the great variation in the CaO content of almandine garnets. For example, those from Dalradian pelitic schists range from 0.43% to 8.46% CaO (Sturt, 1962).

If it is assumed that all the (MgO + FeO) now present in the garnet of the coronas was originally in a biotite in the same molecular proportions (the theoretical composition of such a biotite is given in Table 2.17), then it is possible to determine whether the garnet could have been produced from the biotite according to reaction II by an essentially isochemical reaction, with SiO<sub>2</sub>, Na<sub>2</sub>O and K<sub>2</sub>O considered to be in excess as these are present in all of the surrounding phases. Knowing the average proportions of minerals in the coronas to be garnet:plagioclase:sillimanite:spinel:ilmenite:: 1 : 0.54 : 0.27 : 0.05 : 0.01, the average composition of a corona can be calculated from the analyses of the separate minerals (Table 2.16). If all the available FeO and MgO are held in the biotite, and if the density of biotite is assumed to be 3.0 gm/cc and that of sillimanite 3.2 gm/cc, then the weight proportions can be calculated, from the average corona composition, as biotite:sillimanite:: 157.5 : 93.4, (this ratio excludes the

$\text{Al}_2\text{O}_3$  in anorthite which contributes 3% CaO to the total corona). According to reaction II the weight ratio of biotite:sillimanite should be 3 : 1, or 157.5 : 52.5. Thus, if 100cc of material reacted there should be an excess of 41 gm sillimanite on the basis of the above calculation. In the present corona structures there is 14.4% (vol.) sillimanite so, in a hypothetical 100cc corona, 46 gm are sillimanite. This is fairly close to the calculated excess and tends to support the view that the garnet was produced by an essentially isochemical reaction, such as II above.

#### 2.10.2 Corona-like textures involving the occurrence of garnet between mafic minerals and plagioclase.

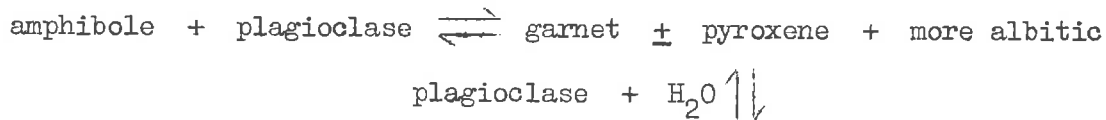
In one basic granulite (A253/R2B : see Table 2.10 and Fig. 2.39) a rim of garnet occurs surrounding many of the orthopyroxene, hornblende and oxide minerals, separating them from plagioclase. The garnet is considered to represent a reaction rim. The amphibole, pyroxenes and oxide minerals appear to be in equilibrium with each other, showing straight or gently curved boundaries and with no indications of replacement of one mineral by another. The reaction between orthopyroxene and plagioclase has been noted and described before (e.g. de Waard, 1965) and verified experimentally (Green and Ringwood, 1967). Similarly, the occurrence of a garnet reaction rim between plagioclase and amphibole has been noted by Oosterom (1963) and by Engels and Vogel (1966), and between

plagioclase and opaque minerals by Oosterom (1963)\*, by Wilcox and Poldervaart (1958) and by Gray (1967). No experimental work has so far been done on these latter reactions and they have been reported only from rocks in the upper amphibolite, granulite or eclogite facies.

The above reactions are rare in the granulites around Gosse File, though they commonly occur in the lower grade (amphibolite facies) rocks of the eastern Musgrave Ranges, near Amata, (K. Collerson, pers. comm.). Factors which probably determine whether or not reaction will occur are bulk composition,  $f_{O_2}$ ,  $P_f$  and the necessary  $P_s$ , T conditions. Ringwood and Green (1966) have shown that "rather modest changes in chemical composition can cause large changes in the pressures" under which reaction will take place. They have also demonstrated the importance of  $f_{O_2}$ : an increase raises the pressure at which garnet will be produced from plagioclase and orthopyroxene, assuming other factors are unchanged. The effect of change in  $P_f$  (particularly  $P_{H_2O}$ ) are unknown but may not be significant since water does not enter into the above reactions directly. In the case of "the reaction":

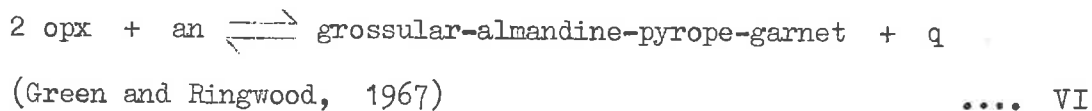
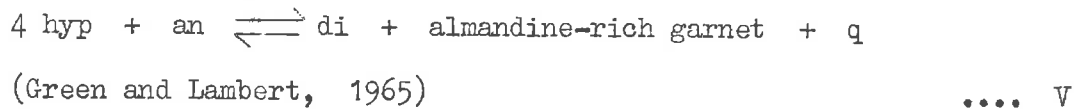
---

\* Oosterom (1963, p. 208) states, "According to Eskola (1954) such coronas are indicative of retrograde metamorphism of the rock in question." The author, after careful reading of Eskola's (1954) paper cannot find such a reference. Neither can the author find any other references in which the origin of these coronas are explained.



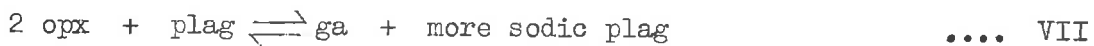
the effect of changes in  $P_{\text{H}_2\text{O}}$  may be important. In rocks of the granulite facies it is assumed that  $P_f \ll P_s$ . This assumption is discussed in more detail in Section 2.11.

Reactions proposed for the formation of garnet from orthopyroxene and plagioclase are:

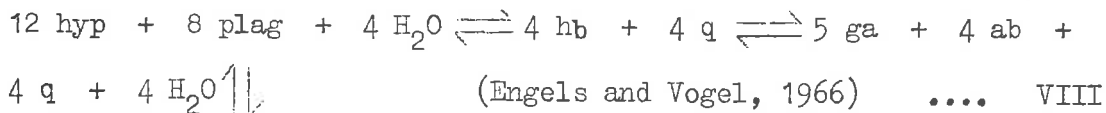


In A253/R2B there is no evidence to suggest that a separate clinopyroxene phase occurs in, or associated with, the garnet rims so reaction VI is favoured. The plagioclase involved in the actual reaction is  $\text{An}_{65}$ , while in the proposed reaction only the anorthite molecule is involved. Thus, as reaction proceeds it would be expected that the feldspar would become more albitic. This expectation appears to be realised, and where garnet rims occur the plagioclase has a parallel zone in which the extinction position differs from that in the rest of the crystal. This is thought to be dominantly compositional zoning though it may be,

in part, due to strain shadows. Albite twins extending into this zone show lower extinction angles and thus appear to be more albitic. The reaction also produces an excess of  $\text{SiO}_2$ , but quartz is not observed as a phase. However, as the proportion of  $\text{SiO}_2$  required for the more albitic plagioclase is greater than that required for calcic plagioclase the excess  $\text{SiO}_2$  produced by reaction VI might be used by the feldspar to retain the necessary Si : Al distribution in the lattice. A modified version of VI might operate:



Where a rim of garnet separating hornblende and plagioclase has been described in detail in the literature (e.g. Engels and Vogel, 1966) it occurs as part of a multiple reaction rim with an orthopyroxene core surrounded by amphibole then garnet. This is interpreted as the result of progressive metamorphism:



This argument cannot be applied in the case of A253/R2B as the orthopyroxene and hornblende are in apparent equilibrium. If the garnet is produced by a reaction between hornblende and plagioclase, analogous to reaction VI, as a result of a decrease in temperature as is suggested in Section 2.11 (a), there remains the problem of explaining how a dehydration reaction could occur during a decrease in temperature. A possible, but entirely speculative answer, is to

suggest that the hornblende lacks the required monovalent cations per formula unit. Thus, water produced by the breakdown of part of the amphibole to form garnet could be readmitted to the amphibole structure. This process could continue until such time as the stoichiometric requirements of the hornblende were met. In this respect it is worth noting that Parras (1958) found that amphiboles and biotites from granulite facies rocks of southwestern Finland were remarkably low in hydroxyl. Leake (1968) has, however, sounded a cautionary note by pointing out some of the difficulties in determining the true (OH + Cl + F) content of amphiboles and the corresponding difficulty in interpretation of their genesis. The amphibole involved in the garnet reaction may be further stabilized by the low SiO<sub>2</sub> content of the rock.

### 2.10.3 Corundum occurrences

Corundum is not an unexpected mineral in granulite facies rocks (e.g. Cooray and Kumarapeli, 1960; Foster, 1962) but, where found, it usually occurs as large crystals (up to 25 cm long) and is often mantled by K-feldspar. It is thought to form from silica-poor, pelitic sediments under conditions of high grade metamorphism. However, the corundum found in the granulites around Gosse Pile occurs as small, lath-like crystals within ilmenite or spinel (Fig. 2.37 and Fig. 2.38), a type of occurrence which has not been described before.

(a) The corundum in ilmenite has been found in only one rock (A313/370A, see Table 2.8) which is a q + f + ga granulite with an unusually high proportion of reddish-brown biotite (estimated at 3-5%). The garnet occurs as clusters of anhedral grains associated, in bands, with biotite and opaque minerals. It does not necessarily enclose the latter, although this is common. The author has identified corundum in three other rocks (A325/335N, /345, /335P) collected by Mr. K. Collerson from an area near the Amata settlement (Fig. 1.1). These are quartz + perthite + garnet rocks in which garnet, the dominant mafic phase (15-20% of the total rock), surrounds ilmenite and green spinel. The corundum laths are found within either the ilmenite or the spinel. In both cases the corundum is usually less than 0.5 mm by 0.2 mm.

The corundum was first identified on the basis of optical properties. This was confirmed by a qualitative electron microprobe analysis (done by AMDEL) on laths in A313/370A. This analysis detected only Al in the laths: other elements sought but not found were Ca, Co, Cr, Cu, Fe, K, Mg, Mn, Ni, P, S, Si and Zn. It showed also that the corundum is confined to ilmenite and is not found in the associated magnetite (Fig. 2.46). Reflected light microscopy shows that the associated magnetite contains extremely fine ( $1\mu$  by  $10\mu$ ) lamellae of either ilmenite or haematite.

The corundum laths appear to be regularly orientated within the ilmenite in three directions. This is true for both the Gosse Pile and Amata rocks. This suggests that a process of exsolution or

Fig. 2.46

Absorbed electron image.  
x150

Characteristic X-ray  
image for Al  $K_{\alpha}$   
radiation (corundum  
laths) x150.

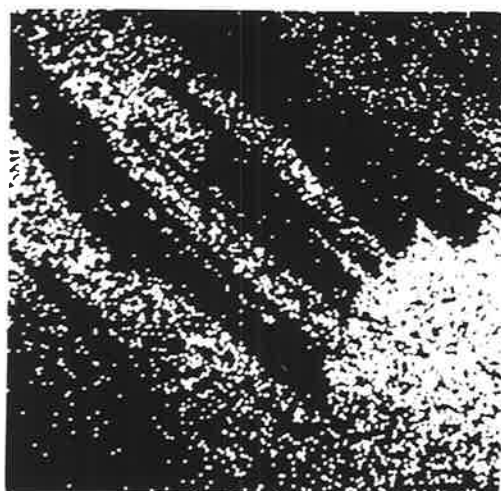
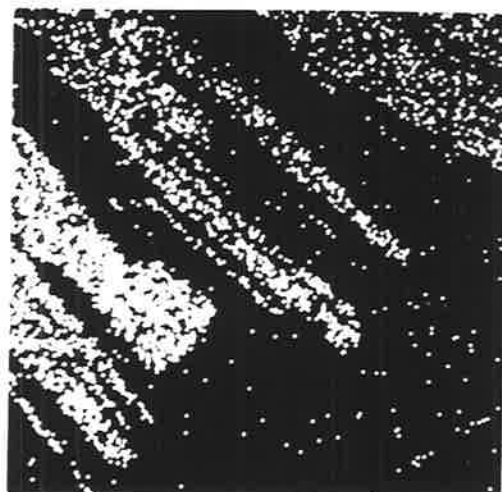
Characteristic X-ray  
image for Ti  $K_{\alpha}$  radiation  
(ilmenite host). Note  
sharp boundary against  
magnetite. x150.

Characteristic X-ray  
image Fe  $K_{\alpha}$  radiation  
(magnetite). x150

Photographs: AMDEL.

Reproduced with  
permission.





epitaxial growth has operated rather than one of accidental inclusion or reaction. Carr (1968) and others have shown that there is no stability field for co-existing quartz and corundum. Since quartz and corundum are separated by only very thin layers of ilmenite in A313/370A it is thought unlikely that the corundum grew epitaxially on crystallizing ilmenite and it is therefore considered to represent an exsolution process. Apart from a brief statement by Ramdohr (1960):

"In Ilmenit, Magnetit, wahrscheinlich auch Chromit kommt er"

[corundum] "als entmischungskörper vor",

the author is not aware of any other references dealing with the exsolution (unmixing) of corundum from an ilmenite host.

Since it has been concluded that the corundum is most likely to represent an exsolution product it can be assumed that, under some conditions of higher temperature and/or pressure, a mineral existed which contained the chemical components of both ilmenite and corundum, and possibly also spinel. Such a mineral would probably have a theoretical composition close to  $R_x^{2+} Ti_y^{4+} R_z^{3+} O_{(x+2y+1.5z)}^{2-}$ , assuming stoichiometric laws are observed and other minerals have not been directly involved in the ilmenite-corundum association. There exists a naturally occurring mineral series for which the general formula is close to that predicted above. McKie (1963) has done detailed work on the polytypes of hōgbomite, the stability ranges for which are at present unknown. This mineral, which bears some structural resemblance to both corundum and spinel, has the general formula  $R_{1-1.6}^{2+} Ti_{0.2-0.4}^{4+} R_{3.7-4.3}^{3+} O_{7.6-8.0}^{2-} (OH)_{0-0.4}^-$ , and

usually contains significant amounts of Mg. Whereas the natural Mg-högbomite remains stable or metastable in rocks now found at the earth's surface it must be assumed that the proposed "iron-högbomite" is unstable and dissociates to form corundum and ilmenite, both of which have hexagonal close packed oxygen structures. During the thermal decomposition of natural högbomite in air the first stage is the orientated exsolution of a phase that may be aluminous pseudobrookite (McKie, 1963). Under hydrothermal conditions it partially decomposes to aluminous pseudobrookite, spinel and rutile.

Minerals with structures like that of högbomite (e.g. nigerite, taaffeite) occur in regions of high grade metamorphism. Högbomite, found at Mautia Hill, Tanzania (previously Tanganyika) is considered by McKie (1959) to have formed under "significantly high pressures" and, possibly, moderate temperatures. McKie (1963) also considers that the Ti-content of a system would be a controlling factor in the stability of högbomite (in the  $\text{MgO} - \text{Al}_2\text{O}_3 - \text{SiO}_2 - \text{H}_2\text{O}$  system, so that Mg is present in excess). The author is not aware of any experimental work on the system  $\text{FeO}(\text{Fe}_2\text{O}_3) - \text{Al}_2\text{O}_3 - \text{TiO}_2$  which might provide evidence for the proposed "iron-högbomite".

(b) In the granulites around Gosse Pile only one rock (A253/R45A) has been found in which corundum, identified optically, occurs as laths within green spinel (Fig. 2.38). The rock is a basic, two pyroxene + amphibole + plagioclase granulite in which spinel (about 2%) is the only oxide phase, apart from faint "dustings" of opaque minerals within the brown hornblende (e.g. Fig. 2.38). A small

quantity of this spinel was separated and an X-ray powder pattern produced (CuK $\alpha$  radiation, Ni filter, 114mm camera). This showed very weak lines in positions corresponding to the strongest lines of corundum, confirming the optical identification. The cell size of the spinel was determined as  $a = 8.110\text{\AA}$ . If it is assumed that the spinel is a member of a solid solution series between  $\text{FeAl}_2\text{O}_4$  and  $\text{MgAl}_2\text{O}_4$ , with no other elements involved, and that  $a$  changes linearly with substitution of  $\text{Fe}^{2+}$  for  $\text{Mg}^{2+}$ , then the composition can be estimated as  $\text{Sp}_{70}\text{Hc}_{30}$ , or  $(\text{Mg}_{0.7}\text{Fe}_{0.3})\text{Al}_2\text{O}_4$ .

The author knows of no experimental work on the system  $\text{FeO} - \text{MgO} - \text{Al}_2\text{O}_3$ . The closest to this is the work of Kwestroo (1959) on the system  $\text{MgO} - \text{Fe}_2\text{O}_3 - \text{Al}_2\text{O}_3$  and that of Turnock (1959) and Turnock and Eugster (1962) on the system  $\text{FeO} - \text{Fe}_2\text{O}_3 - \text{Al}_2\text{O}_3$ . The effect of  $\text{MgO}$  on this later system is unknown. Unfortunately, Kwestroo's work has very limited application to geological materials in that mixtures were fired at only two temperatures ( $1250^\circ\text{C}$  and  $1450^\circ\text{C}$ ) under highly oxidizing conditions. However, it did show that, with decrease in temperature for aluminium-rich mixtures, the field of one spinel phase contracted in size allowing for the formation of spinel  $[(\text{Hc} + \text{Sp})_{\text{SS}}]$  and corundum. Using Turnock's work (1959, Fig. 34) it can be argued that the  $f_{\text{O}_2}$  value during the metamorphism of A253/R45A must have been very low. This is based on the absence of magnetite in the rock and noting the range over which  $\text{Hc}_{\text{SS}}$  (hercynite + magnetite only) + corundum + vapour assemblages can co-exist. As a similar example may be cited the

hercynite + corundum + ferroan cordierite assemblages described by Tilley (1924), a bulk rock analysis of which shows only a trace of  $\text{Fe}^{3+}$ , confirming the low  $f_{\text{O}_2}$  of the environment.

Further than this, no conditions of metamorphism can be deduced from the occurrence of corundum laths in spinel. An unsuccessful attempt was made to heat separated spinel samples in a hydrothermal pressure furnace to observe whether or not the corundum would be reabsorbed and under what conditions. Only about 5% of the separated and mounted unheated spinel grains showed corundum laths in thin sections, so the absence of laths in small samples could not definitely be attributed to the heating conditions. Insufficient rock was available for large quantities of spinel to be extracted. However, from petrographic evidence it is suggested that under conditions of high  $P_g$ -T (granulite facies) and low  $f_{\text{O}_2}$  there exists a field where aluminous spinel is stable and with decrease in  $P_g$  and/or T this spinel breaks down to form  $(\text{Sp} + \text{Hc})_{\text{SS}}$  + corundum.

It has been implicitly assumed in the above discussions, both (a) and (b), that a single phase has undergone unmixing to produce two phases and that no other minerals have been involved in the reactions. This assumption may be invalid because material, once part of the system, may have migrated to form another phase, or part of a phase, elsewhere. It may be necessary to consider the possible influences of all the minerals in the rock and not only the minerals of interest, i.e. spinel, corundum and ilmenite. In this regard it is noteworthy that the ilmenite - corundum

association occurs only in garnet-bearing, acid granulites. This may be a function of bulk chemistry.

## 2.11 CONDITIONS OF METAMORPHISM

### Assumptions and limitations

For different metamorphic regions there have been numerous attempts to place absolute limits on the conditions under which metamorphism has taken place. These are based on experimentally determined reactions and mineral stability fields (e.g. den Tex, 1965; Chinner, 1966; de Waard, 1967(a); Hietanen, 1967 and Turner, 1968). However, in attempting to relate a particular mineral assemblage to absolute conditions of pressure and temperature a large number of variables (e.g. bulk composition, fluid content, chemical potential or activity, vapour pressure) have to be considered as they could have marked effects on the stability ranges of many minerals generally used in petrogenic grids. For example, the pressures and temperatures at which biotite will participate in many metamorphic reactions is strongly dependent upon the  $f_{O_2}$  and  $f_{H_2O}$  conditions (Wones and Eugster, 1965). The stability curves for the iron and magnesium end members of biotite may be as much as 250°C apart (Yoder and Eugster, 1954; Eugster and Wones, 1962). In most cases the variables are quantitatively unknown and their influences can be only surmised. The temperatures at which many metamorphic reactions occur depend also on the actual process of

metamorphism and, in most cases, the processes are unknown or assumed. Wyllie (1967) concluded that, until these processes are more clearly defined, refinement of experimental techniques will not be of assistance in providing better estimates of the temperatures prevailing during metamorphism. As pointed out by Parras (1958):

"In contrast to the sterile environment of the laboratory, the natural rocks, in regard to their main and accessory components, involve us in several complications."

Bearing in mind these limitations an attempt is made here to try to set crude limits to the conditions of pressure and temperatures which prevailed during the granulite facies metamorphism of the rocks around Gosse Pile.

Before any estimates of the P,T conditions can be made an assumption concerning the rôle of water has to be accepted. There is a disturbing lack of information about the effects of water in metamorphic rocks. In the past it has generally been accepted that, even under granulite facies conditions, load pressure and water pressure (presumably not  $P_{H_2O}$ ) are approximately equal. This view is still suggested by some authors (e.g. Turner, 1968, p. 60) as an acceptable simplification. The apparent "dryness" of granulite facies assemblages is then explained by assuming that the temperatures were sufficiently high to stabilize the anhydrous minerals, even under very high water pressure (e.g. Turner and Verhoogen, 1960, p. 557). Yoder (1955) also concluded that in most regional metamorphic problems  $P_{H_2O}$  and  $P_s$  were approximately equal but if  $P_{H_2O} < P_s$  then dehydration

reactions will take place at lower temperatures, a factor which may account for the reversal of isograds occasionally observed. Yoder (1955) also emphasised that the rôle of water in metamorphism is dependent on at least four variables:  $P_s$ ,  $T$ ,  $P_{H_2O}$  and water content. Greenwood (1961) in his discussion of total pressure and water pressure in metamorphism emphasised the complexity, both mechanical and chemical, of the reactions which take place in metamorphic rocks. Since then the simplifying assumption that  $P_{H_2O} \approx P_s$  for all grades of metamorphism has been questioned by a number of authors.

Wilcox and Poldervaart (1958) considered that an "abnormal granulitic trend" of metamorphic crystallization of basaltic rocks in North Carolina, U.S.A. was due to water deficient conditions. (Yoder, 1952, defined a water deficient system as one in which there is insufficient water present to convert all the anhydrous phases present to hydrous phases that are stable at that pressure and temperature). Buddington (1963) rejected the view that load and water pressure were approximately equal for orthogneisses of the Adirondack area because successive metamorphic zones appear to vary in the reverse order to that expected if  $P_{H_2O} \approx P_s$  throughout the area. Buddington also considered that the amphibole-bearing rocks existed within this area because of their inherent inability to lose water during metamorphism. Winkler (1967, p. 131) correlates the origin of granulites with very high temperatures and the special circumstance that  $P_{H_2O}$  was much lower than  $P_s$ . Richardson, Bell and Gilbert (1968), considering an area of carbonate-free rocks in



central Connecticut, U.S.A., used the kyanite-sillimanite equilibrium curve, as determined by them, the dehydration reaction  $ms + q \rightleftharpoons Kf + sill + H_2O$  ("second sillimanite isograd") and the temperatures of these two isograds to determine the extent to which  $f_{H_2O}$  at the dehydration isograd departed from the value of  $f_{H_2O}$  in a pure water phase at the same  $P_s$  (i.e.  $PE_{H_2O}$ ) and  $T$ . They found considerable differences and it can be concluded that, in this area, the assumption  $P_s \approx P_{H_2O}$  is not valid.

For the granulites around Gosse Pile it is assumed that  $P_f \ll P_s$  during the period of granulite facies metamorphism. In most areas the major contributing phase to the fluid is likely to be water, except for the calc-silicate rocks and the marble where it is likely to be  $CO_2$ . The main reason for making this assumption is that there is no evidence of anatexis melting of the granulites, although temperatures were above at least  $650^\circ C$  since muscovite is not found in any of the rocks (Winkler, 1967, p. 74). As shown by Tuttle and Bowen (1958) a quartzo-feldspathic rock will partially melt in the presence of water as long as the water is present as a distinct phase. Melting starts at temperatures appropriate to the bulk composition of the rock and the pressure, and the amount of melt produced is dependent on the amount of water present (Kleemann, 1965; Winkler, 1967). At temperatures above  $650^\circ C$  and for quartzo-feldspathic rocks, such as occur in the acid granulites around Gosse Pile, even if the water content was very low some anatexis would be expected since, under granulite facies conditions (pressures) the

pore space of the rocks must be very small (Yoder, 1955; Greenwood, 1961; Winkler, 1967). Since no anatexis has been observed, even on a small scale, it is concluded that metamorphism took place under essentially anhydrous conditions.

For the purpose of further discussion it has been assumed that the stability ranges of critical mineral assemblages in the rocks have not been significantly affected by variations in  $f_{O_2}$ ,  $f_{H_2O}$ ,  $f_{CO_2}$  and other factors so that the estimates of their stability ranges derived from anhydrous experimental data can be directly applied. Even accepting this potentially erroneous assumption, estimates of the metamorphic conditions may be in error from another source; e.g. experimental errors which can be caused by incorrect calibration of equipment, variations in the choice of starting materials, ranges of possible error in standard thermodynamic data, production of metastable phases and variations in the stability fields caused by different preparations of the same starting materials. Bearing in mind all these limitations on the accuracy of any values estimated for the pressure and temperature conditions, an examination of the granulites around Gosse Pile can now be made.

Estimates of the pressure and temperature prevailing during the granulite facies metamorphism.

In this section the stability fields of several minerals are considered and, for clarity, these have been tabulated (Table 2.18).

Table 2.18

Summary of reaction curves used in estimating the conditions of granulite facies metamorphism for the rocks around Gosse Pile.

See Fig. 2.47.

| Reaction curves used  | P-T conditions   | Remarks  |
|---|--|--|
| Intersection of the reaction $\text{opx} + \text{plag} \rightleftharpoons \text{ga} + \text{q}$ for high alumina basalts, and the estimated feldspar solvus.      | 870°C 7kb  | Probably close to a minimum value.   |
| The aluminosilicate triple point and reaction curves.   | 600°C  | The minimum temperature possible, irrespective of pressure. All reactions must occur within the sillimanite field.   |
| Intersection of the reaction $\text{ol} + \text{plag} \rightleftharpoons \text{px} \pm \text{sp}$ for olivine normative rocks, and the estimated feldspar solvus. | 845°C $\pm$ 15°C<br>5 $\pm$ 1kb                                  | minimum values.  |
| The stability of cordierite.  | minimum values range between 910°C at 11.5kb to 1,010°C at 9.5kb |  |
| The reaction $\text{opx} + \text{plag} \rightleftharpoons \text{ga} + \text{q}$ for acid granulites (close to adamellite in bulk composition).                    | 930°C at 12.5kb  | Intersection with the estimated feldspar solvus sets a maximum pressure at a minimum temperature of 930°C. The reaction curves sets a maximum limit to P-T conditions. |

Estimated conditions of metamorphism: close to 1,000°C at 10kb (32km) with  $P_s \gg P_f$ .

(a) The presence of garnet

In section 2.10.2 a garnet corona texture between plagioclase and mafic minerals was described (Fig. 2.39). De Waard (1967a, b) used the pressure-temperature relationships of reaction IV (p. 85) and the feldspar solvus to give an estimate of the minimum absolute P-T conditions of metamorphism in the Adirondack highlands. Using the evidence of the garnet reaction (IV) as observed in specimen A253/R2B, and the evidence of the abundant development of mesoperthite in the surrounding acid granulites a similar approach can be applied here.

The position of the feldspar solvus along the Ab-Or join has been determined by Bowen and Tuttle (1950) and by Orville (1963). Although slightly different in shape the two solvi agree closely for alkali feldspar compositions around  $Or_{50-70}$  (Orville, 1963, p. 221) and for compositions near  $Or_{50}$  the composition is close to the position of the solvus crest. Thus, any movement of the crest, due to an increase in pressure, is likely to move that part of the solvus near  $Or_{55}$  by an equivalent amount. For a composition of  $Or_{55}$  (i.e. that of the K-feldspar in acid granulite A313/A25, Table 2.5) the solvus occurs at  $645^{\circ}C/2,000$  bars  $P_{H_2O}$ . The increase in temperature of the solvus crest at the Ab-Or join with increase in pressure is estimated at  $14^{\circ}C/kb$  by Yoder, Stewart and Smith (1957) and at  $10^{\circ}C/kb$  by Orville (1963). An average value of  $12^{\circ}C/kb$  has been used in Fig. 2.47, line 1. The experimental work on the alkali feldspar solvus has been done with  $P_{H_2O} = P_s$  to a maximum of 5 kb. However, changes in water

Fig. 2.47

P-T diagram illustrating the stability limits of several minerals.

1. Increase of temperature with pressure for the Or-Ab solvus crest ( $\text{Or}_{55}\text{Ab}_{45}\text{An}_0$ ). Data from Orville, 1963 ( $10^\circ\text{C}/\text{kb}$ ) and Yoder, Stewart and Smith, 1957 ( $14^\circ\text{C}/\text{kb}$ ). An average of  $12^\circ\text{C}/\text{kb}$  is marked.
  - 1a. Estimated position of the solvus crest for feldspar of composition  $\text{Or}_{55}\text{Ab}_{38}\text{An}_9$ .
  2. The reaction  $\text{opx} + \text{plag} \rightleftharpoons \text{ga} + \text{cpx} + \text{q}$  for rocks close to adamellite in composition (Green and Lambert, 1965).
  3. Above reaction for quartz tholeiite (Ringwood and Green, 1966).
  4. Above reaction for olivine tholeiite and alkali olivine basalt (Ringwood and Green, 1966).
  5. Above reaction for high alumina basalt (Green, 1967).
- The slopes for curves 2-5 taken as  $21 \text{ bar}/^\circ\text{C}$  (Ringwood and Green, 1966, p. 399).
6. The reaction  $\text{ol} + \text{plag} \rightleftharpoons \text{pyroxene} \pm \text{spinel}$  (Green and Ringwood, 1967, fig. 8).
  7. The above reaction for mineral mixtures (Kushiro and Yoder, 1966).
  - 8a. Upper limit of the reaction  $\text{ol} + \text{plag} \rightleftharpoons$  (aluminous) pyroxene for high alumina basalt (Green, 1967).

Fig. 2.47 (cont.)

8b. Lower limit of the reaction  $ol + plag \rightleftharpoons$  (aluminous) pyroxene for high alumina basalt (Green, 1967).

The slopes for 8a and 8b are taken parallel to 7.

9. Upper stability limit for cordierite (Dobretsov, 1968).

10. Upper stability limit for cordierite:

X: in artificial mixtures approaching natural rock compositions (Hensen, 1969).

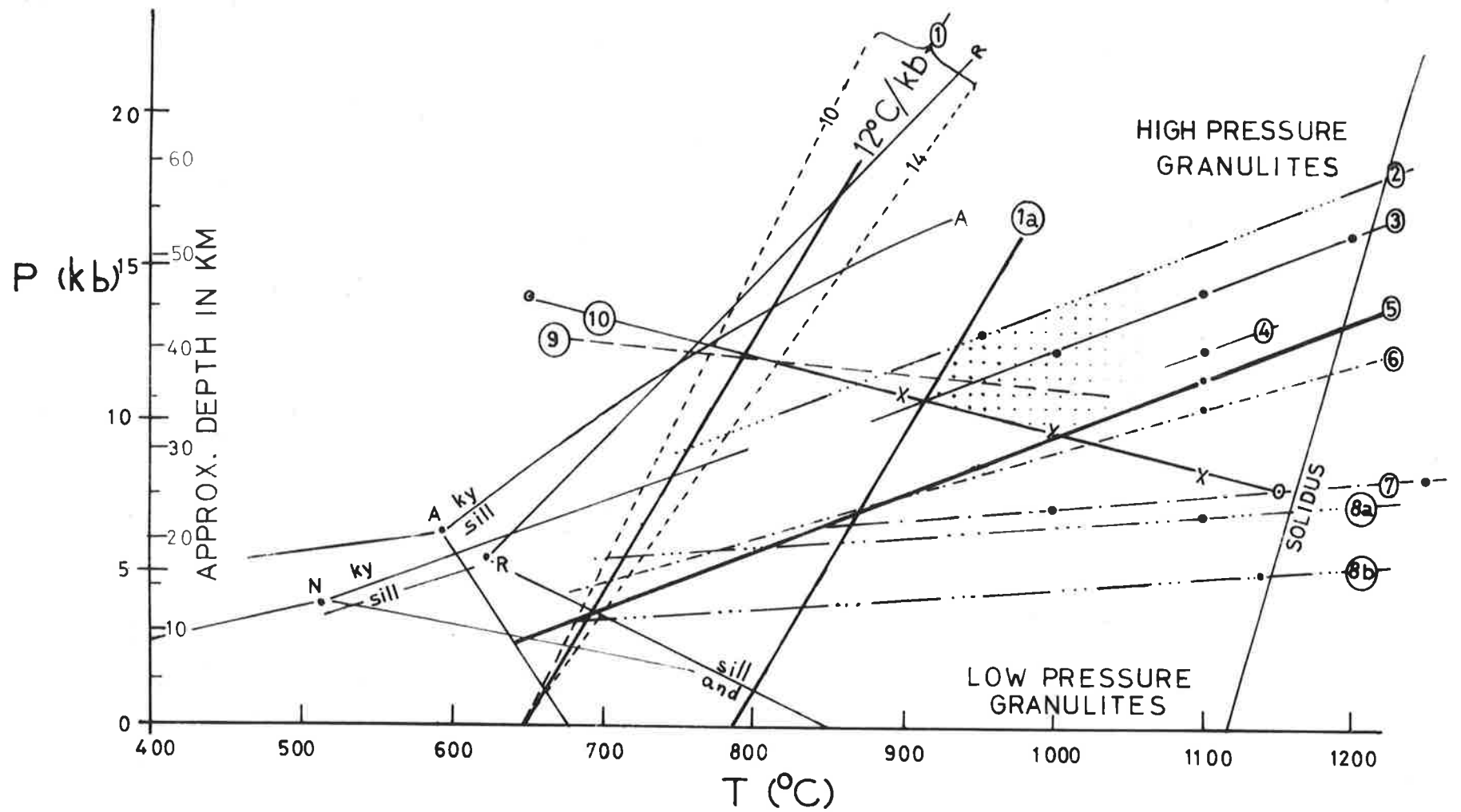
O: for Mg-cordierite (Schreyer and Yoder, 1964).

"N": The position of the  $Al_2SiO_5$  polymorph triple point with associated boundary curves as determined by Newton (1966a,b).

"A": The above, as determined by Althaus (1967).

"R": The above, as determined by Richardson, Gilbert and Bell (1969).

The stippled area indicates the conditions under which metamorphism of the rocks around Gosse Pile is presumed to have occurred.



vapour pressure are unlikely to cause measurable changes in the position of the solvus as water does not participate in equilibria involved at the solvus (Bowen and Tuttle, 1950) so that the position of the experimentally determined solvus can be used when considering granulite facies rocks where  $P_f \ll P_s$ . Diagrams of the Ab-Or-An-(H<sub>2</sub>O) system by Yoder, Stewart and Smith (1956, 1957), Carmichael (1963) and others show that the solvus "dome" rises very steeply from the Ab-Or join towards An. This means that the temperature at which exsolution will take place is rapidly increased with increase in the anorthite content of the alkali feldspar, a factor ignored by de Waard (1967a, b). The feldspar in specimen A313/A25 contains about 9.2% mol. anorthite (Table 2.5). There is insufficient experimental work available to enable an accurate section to be drawn from An through Or<sub>55</sub>Ab<sub>30</sub>An<sub>9</sub> to the Ab-Or side so that an accurate determination of the height of the solvus (in °C) for a feldspar of this composition can not be made. From the data of Yoder, Stewart and Smith (1956) and their schematic diagrams (1957) and that of Carmichael (1963) it was estimated that the solvus dome would be intersected at approximately 850°C/5kb for a feldspar of composition Or<sub>55</sub>Ab<sub>36</sub>An<sub>9</sub>. It is assumed that the rate of change of temperature with pressure remains at about 12°C/kb (1a, Fig. 2.47). Under essentially anhydrous conditions truncation of the solvus by the solidus probably takes place at much greater temperatures, thus allowing for an increased degree of solid solution between Or and An at lower temperatures (e.g. Lindsley, 1966). The approximation



involved for the above value for the above temperature of intersection (i.e.  $850^{\circ}\text{C}/5\text{kb}$ ) is emphasised by the work of Luth and Tuttle (1966) who have shown that the alkali feldspar solvus is sensitive not only to the thermal state of the feldspar (Tuttle and Bowen, 1958) but also to variations in stoichiometry (particularly the alkali :  $\text{Al}_2\text{O}_3$  molar ratio).

De Waard (1967a,b) made an erroneous assumption that changes in bulk composition make little difference to the conditions at which garnet develops at the expense of plagioclase and orthopyroxene (hereafter termed "the garnet reaction"). As can be seen from Fig. 2.47 differences in bulk composition of the rock can make differences of up to 6 kb in the pressures at which reaction will take place at the same temperature. An analysis of A253/R2B (Table 2.19) indicates that, by comparison with rocks studied experimentally, it has a composition between those of the high alumina basalt and alkali olivine basalt, perhaps nearer the latter rock type. These are represented by curves 4 and 5 of Fig. 2.47, the slopes of which are presumed to be parallel to that determined for quartz-tholeiite compositions (3, Fig. 2.47), at about  $21 \text{ bars}/^{\circ}\text{C}$  (Ringwood and Green, 1966). Curves 4 and 5 are fairly close and, as 5 marks a limiting, or extreme, composition it is considered in further discussion of the garnet reaction.

The garnet reaction curve for high alumina basalts and the estimated feldspar solvus, extrapolated as linear functions, intersect at  $870^{\circ}\text{C}$  and 7kb. According to de Waard (1967a,b) this

Table 2.19

Comparison between partial analyses of two granulites from the Gosse Pile area and some rocks which have been examined experimentally.

| Analysis:                      | 1                 | 2                | 3     | 4      | 5     |
|--------------------------------|-------------------|------------------|-------|--------|-------|
| SiO <sub>2</sub>               | 45.96             | 63.98            | 45.39 | 50.3   | 69.56 |
| Al <sub>2</sub> O <sub>3</sub> | 16.77             | 15.62            | 14.69 | 17.0   | 14.72 |
| Fe <sub>2</sub> O <sub>3</sub> | } as<br>FeO 14.88 | } as<br>FeO 5.93 | 1.87  | 1.5    | 1.73  |
| FeO                            |                   |                  | 12.42 | 7.6    | 1.73  |
| MgO                            | 9.49              | 1.56             | 10.37 | 7.8    | 1.00  |
| CaO                            | 10.84             | 3.33             | 9.14  | 11.4   | 2.46  |
| Na <sub>2</sub> O              | 1.76              | 3.51             | 2.62  | 2.8    | 3.37  |
| K <sub>2</sub> O               | 0.65              | 4.95             | 0.78  | 0.18   | 4.61  |
| MnO                            | n.a.              | n.a.             | 0.18  | 0.16   | 0.06  |
| TiO <sub>2</sub>               | 1.39              | 1.01             | 2.52  | 1.7    | 0.56  |
| loss*                          | 0.14              | -0.04            | -     | -      | -     |
| Total                          | 101.88            | 99.85            | 99.98 | 100.44 | 99.80 |

C.I.P.W. norms.

|    |       |       |      |      |      |
|----|-------|-------|------|------|------|
| q  | -     | 11.88 | -    | -    | 25.7 |
| c  | -     | -     | -    | -    | 0.2  |
| or | 3.84  | 29.25 | 4.5  | 1.1  | 27.2 |
| ab | 13.07 | 29.70 | 18.0 | 23.7 | 28.5 |
| ne | 0.99  | -     | 2.2  | -    | -    |
| an | 35.94 | 12.25 | 26.2 | 33.3 | 10.9 |
| di | 14.79 | 3.64  | 15.7 | 18.9 | -    |
| hy | -     | 11.25 | -    | 11.9 | 3.4  |
| ol | 30.47 | -     | 25.8 | 6.2  | -    |
| il | 2.66  | 1.92  | 4.8  | 3.2  | 1.1  |
| mt | **    | **    | 2.9  | 2.2  | 2.5  |

Table 2.19 (cont.)

n.a. = not analysed.

\*loss: loss, or gain, in weight after heating the rock powder at 1,000°C to constant weight.

\*\* mt: is not recorded in the norm because all Fe is calculated as FeO. If the total Fe is allotted such that in 1 90% goes to FeO and 10% to Fe<sub>2</sub>O<sub>3</sub> (i.e. FeO = 13% and Fe<sub>2</sub>O<sub>3</sub> = 0.44%) the normative magnetite is 0.64%; and in 2 the Fe is allotted such that 50% goes to FeO and 50% to Fe<sub>2</sub>O<sub>3</sub> (i.e. FeO = 2.60% and Fe<sub>2</sub>O<sub>3</sub> = 3.00%) the normative magnetite is 3.77%. Under these circumstances there are significant changes in the normative proportions of hypersthene (0.12% for 1; 3.92% for 2).

Analysis 1: A253/R2B. Basic granulite, hb + px + plag + ga  
(see Table 2.10).

2: A313/A25. Acid granulite, q + f + px (see Table 2.3).

3: Alkali olivine basalt (Green and Ringwood, 1967).

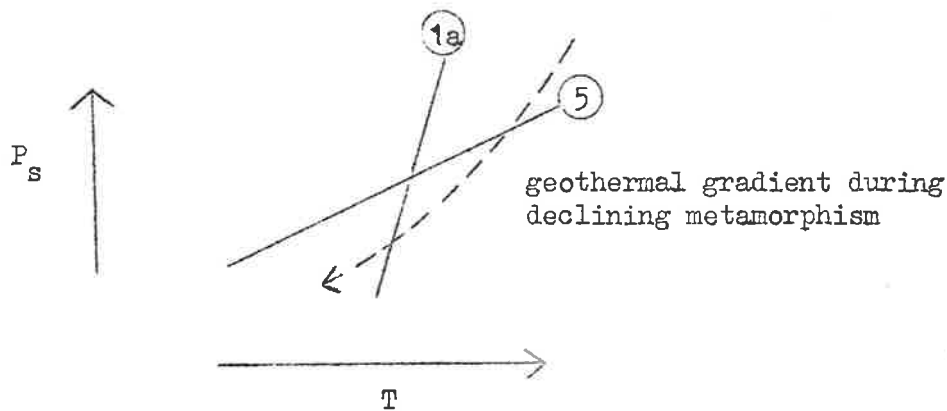
4: High alumina basalt (Green, 1967).

5: Adamellite (Green and Lambert, 1965).

Analyses 1 and 2 by A.C. Moore (MgO, alkalies and loss) and R.W. Nesbitt (all other elements).

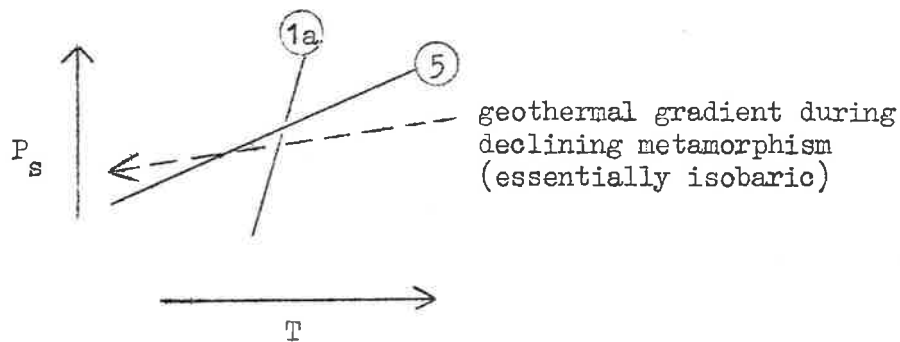
point would represent the minimum P-T conditions of metamorphism. However, if the reaction results from retrograde metamorphism (i.e. falling T with decrease in  $P_s$ ) then this point of intersection represents the minimum  $P_s$ -T conditions of metamorphism only if it is assumed that the garnet reaction occurred first, followed by feldspar exsolution to produce mesoperthites:

garnet reaction followed by exsolution



If the reactions took place in the reverse order then the point of intersection would not represent the minimum  $P_s$ -T conditions of metamorphism:

exsolution followed by garnet reaction



De Waard (1967a) has noted that the reaction between orthopyroxene and plagioclase to form garnet can be either prograde (increasing  $P_s$  and  $T$ , or increasing  $P_s$  with similar  $T$ ) or retrograde (decreasing  $T$  under similar or decreasing  $P_s$  conditions). In the granulites around Gosse Pile the reaction is very rare, being found in only one basic rock. The garnet rim is usually thin and often incomplete and, within the same thin section, may even be absent. This suggests that it probably formed during a decrease in temperature (declining metamorphism) such that the rock was in the  $ga + cpx + q$  stability field for a relatively short period of time. If not, one would expect the reaction to be more widespread and more complete, although this may be a function of rate of this reaction, and bulk compositions of the basic rocks, under the metamorphic conditions prevailing.

Thus, it is concluded that, contrary to de Waard's (1967a,b) assertion, the intersection between the feldspar solvus and the garnet reaction line does not equivocally indicate the minimum conditions of metamorphism. Moreover, the precision of this method is less than that indicated by de Waard because of the numerous assumptions which have to be adopted. The estimated minimum metamorphic conditions for the granulites around Gosse Pile are approximately  $870^{\circ}\text{C}$  and 7 kb using this method.

(b) The alumino-silicate triple point

The positions of the andalusite-sillimanite-kyanite triple point, and especially of the kyanite-sillimanite boundary curve are of the

utmost importance in metamorphic petrology because they provide a key group of phases used for interpreting P-T conditions. Because of their apparent value, both in the lower grades of metamorphism, and in the granulite facies (Green and Ringwood, 1967), the stability relations of these three alumino-silicates have been the subject of numerous investigations. Unfortunately a very large spread for the location of the triple point and for the P-T univariant curves between the various polymorphs has been obtained. Zen (1969) discussed a number of possible sources of experimental error whereby this spread might be explained and Althaus (1969) has shown experimentally that the kyanite-sillimanite reaction is at least bivariant so that some of the scatter may be due to inherent chemical differences (e.g.  $\text{Fe}_2\text{O}_3$  content) which affects the stability ranges. Chinner, Smith and Knowles (1969) considered that the influence of  $\text{Fe}^{3+}$  on the occurrence of an alumino-silicate in the stability field of another is probably overshadowed by other effects. Mr. P.D. Fleming (pers. comm.), working on andalusite-sillimanite polymorphs, has found a definite correlation between the iron content (of whole rocks and the  $\text{Al}_2\text{SiO}_5$  minerals) and the type of polymorphs produced within a very limited area. If the iron content does have an influence, the stability ranges of the sillimanite (0.45%  $\text{Fe}_2\text{O}_3$ ) used by Althaus (1967) in his experimental work are possibly comparable with those of the Gosse Pile area, (where determined it is 0.6%  $\text{Fe}_2\text{O}_3$ ; Table 2.16).

The lowest experimentally determined position for the triple point is that of Newton (1966a,b) at about  $410^\circ\text{C}/5\text{kb}$  (the centre of

a narrow rhombus extending from  $400^{\circ}\text{C}/2.5\text{kb}$  to  $630^{\circ}\text{C}/5.7\text{kb}$ ). This has been considered by a number of authors to be in a position which reasonably satisfies P-T conditions, determined by other methods, in geological occurrences. In Fig. 2.47 it is shown as the point "N". Althaus (1967) placed the triple point at about  $600^{\circ}\text{C}/6.5\text{kb}$ , the position of which, and of the reaction curves, are marked "A" in Fig. 2.47. Newton (1969) considered that the higher pressure location of the kyanite-sillimanite boundary curve of Althaus may be due to the faster rate of degradation of kyanite compared with sillimanite when the mixtures are severely ground. However, the upper limit for the triple point ( $630^{\circ}\text{C}/5.7\text{kb}$ ) as determined by Newton (1966a,b) is quite close to that of Althaus (1967). One of the most recent experimental determinations of the stability regions of the  $\text{Al}_2\text{SiO}_5$  polymorphs has been that of Richardson, Gilbert and Bell (1969) who place the triple point at  $622^{\circ}\text{C}/5.5\text{kb}$  (marked "R", Fig. 2.47) which is close to the position determined by Althaus (1967). However, the positions of the univariant (?) equilibrium boundaries are very different, particularly that for andalusite - sillimanite. Because the more recent data, both experimental and geological (see especially Rosenfeld, 1969), appear to agree fairly closely with the positions of the triple point and the reaction curves as determined by Althaus (1967) these are accepted for estimations of the P-T conditions achieved in the granulite facies metamorphism of the rocks around Gosse Pile.

---

In this area the only alumino-silicate so far observed has been sillimanite, either as large subhedral crystals, or as fibrolite. Accepting Althaus' experimental work, it can be seen that the minimum temperature at which metamorphism took place must have been at least 600°C, irrespective of pressure considerations. The boundary curves set further limitations, as can be seen in Fig. 2.47.

(c) The reaction between olivine and plagioclase

One of the commonest corona textures found in rocks, particularly igneous rocks, is the occurrence of pyroxene  $\pm$  spinel between olivine and plagioclase, e.g. Shand (1945); Oosterom (1963). This indicates that, under some conditions, olivine and plagioclase are mutually unstable. Olivine has not been found in any of the plagioclase-bearing basic granulites around Gosse Pile or surrounding areas (Barnes, 1968), even where these contain up to 24% normative olivine (Barnes, 1968). Thus, an indication of the conditions at which plagioclase and olivine are mutually exclusive might give an indication of the P-T conditions of granulite facies metamorphism. The only experimental work on the reaction  $ol + plag \rightleftharpoons$  aluminous pyroxenes  $\pm$  spinel (hereafter termed "the olivine reaction") which gives a slope to the reaction curve is that of Kushiro and Yoder (1966). They used 1:1 and 1:2 (molecular ratio) mixes of anorthite and enstatite and of anorthite and forsterite. The position and slope of the reaction curve are plotted in Fig. 2.47, curve 7. This is unlikely to be directly applicable to natural rocks where a different bulk chemistry is likely to influence the reaction.



Green (1967), in a series of experimental runs to determine the subsolidus crystallization fields of minerals in a high-alumina basalt (6.2% normative olivine) found the last traces of olivine at pressures and temperatures above 4.5kb and 1,140°C. The next run (at 6.8kb and 1,100°C) contained no olivine so that the olivine reaction must occur between these limits. These points are marked on Fig. 2.47 and lines (8a and 8b) drawn through them, assuming the slopes to be parallel to that determined by Kushiro and Yoder (1966). The zone between marks the limits between which olivine probably disappears as a result of reaction with plagioclase for high-alumina basalt compositions. For olivine tholeiites the olivine disappears at about 1,100°C/10.1kb (Green and Ringwood, 1967) and this reaction is used by them to mark the boundary between the low and intermediate pressure granulites (6, Fig. 2.47). However, the author is not certain as to how Green and Ringwood (1967) derived the slope for this reaction curve (approximately 75°C/kb), which is much steeper than that derived by Kushiro and Yoder (1966).

The intersection of 8a and 8b (Fig. 2.47) with the estimated feldspar solvus, extrapolated as linear functions, occurs at 830°C/4kb and at 860°C/6kb. This suggests that, for the granulites in the Gosse Pile area, metamorphism exceeded some temperature between 845°C ± 15°C and a pressure at 5 ± 1kb (minimum).

(d) The stability range of cordierite

The upper stability limit of Mg-cordierite under anhydrous conditions has been determined experimentally by Schreyer and Yoder (1964). More recently Hensen (1969) has used a number of synthetic compositions, simulating natural metasediments, to determine the stability of cordierite and garnet as a function of pressure, temperature and chemical composition. The curve (10, Fig. 2.47) marking the upper stability limit of cordierite for a rock with an Mg:Fe ratio of 8.7 coincides exactly with the upper stability limit of pure Mg-cordierite, as determined by Schreyer and Yoder (1964). Hensen (1969) points out that, with decreasing Mg:Fe ratio, the stability field of cordierite is decreased. Dobretsov (1968) worked out the upper stability limit of Mg-cordierite in the system MgO-Al<sub>2</sub>O<sub>3</sub>-SiO<sub>2</sub> on the basis of experimental work and thermodynamic calculations. The position of the stability curve (9, Fig. 2.47) is only slightly different from the others.

Hensen (1969) has not identified kyanite in the products of his experimental runs (cord + ga + hyp + q  $\rightleftharpoons$  ga + sill + q  $\pm$  hyp) although it should be possible to form kyanite at P-T conditions above 900°C/10.8kb if the sillimanite-kyanite reaction curve of Newton (1966a,b) is correct. The curves of Althaus (1967) and of Richardson, Bell and Gilbert (1968) indicate sillimanite would be stable to much higher pressures. The position of the triple point, determined by Hietanen (1967) on the basis of field evidence is closer to that of Althaus (1967) than that of Newton (1966a,b) and

thus supports the views expressed in (b) of this section. Hietanen (1967) also points out that cordierite is stable in many sillimanite granulites, but is absent from those that are sheared or crystallized at higher pressures.

To date cordierite has not been found in any granulites from the area around Gosse Pile (in spite of staining with trypan blue, as suggested by Boone and Wheeler, 1968), nor elsewhere in the Tomkinson Ranges (Goode and Krieg, 1965; Barnes, 1968) although it is common in chemically similar rocks from the Musgrave Ranges (Wilson, 1954). The absence of cordierite from rocks of the Tomkinson Ranges is probably a function of the higher pressures under which they crystallized.

If the upper stability limit of cordierite is as shown by the curves 9 and 10 (Fig. 2.47), then the intersection with the estimated feldspar solvus (1a) implies that temperatures must have exceeded  $910^{\circ}\text{C}$  and the minimum pressure, at this temperature, was 10.5kb. Because of the negative slope of the cordierite stability curve, higher temperatures would decrease the stability of cordierite at the same pressure. In an attempt to set the maximum P-T conditions of metamorphism the upper stability limit for co-existing orthopyroxene and plagioclase in acid rocks can be considered. This is shown by curve 2, Fig. 2.47 for rocks with compositions close to adamellite (Green and Lambert, 1965). Some acid granulites will not depart far from this composition and so the garnet reaction curve will probably not vary much from the position of curve 2 for such rocks

e.g. A313/A25, (Table 2.19). In all the acid granulites examined there is no suggestion of a reaction between plagioclase and orthopyroxene to produce garnet and clinopyroxene. It is concluded that pressures and temperatures above curve 2 could not have been involved. This line intersects the cordierite stability curve at  $870^{\circ}\text{C}/11.5\text{ kb}$  and the estimated position of the alkali feldspar solvus at  $930^{\circ}\text{C}/12.5\text{ kb}$ .

### Conclusions

Using various experimentally determined stability curves a zone of temperatures and pressures (stippled in Fig. 2.47) can be outlined at which metamorphism may have occurred. From this it is estimated that the conditions of granulite facies metamorphism for the rocks around Gosse Pile were of the order of  $1,000^{\circ}\text{C}$  at pressures of 10 kb (about 32 km depth). If the position of the cordierite stability curve were to be lower, as a result of a decrease in the Mg:Fe ratio, the estimated pressures and temperatures would be slightly less. According to the scheme of Green and Ringwood (1967) these rocks are classed as intermediate pressure granulites.

2.12 ORIGIN OF THE GRANULITES

In the area around Gosse Pile the presence of characteristic rocks such as the marble, quartzites and those rocks with pelitic compositions indicate that at least part of the granulite facies sequence is metasedimentary in origin. There is, in fact, a close similarity between these rocks and those found in the Highland Series of Ceylon (Cooray, 1962) as can be seen by the comparison presented in Table 2.20. Cooray (1962) considers that the Highland Series represents a metasedimentary sequence reconstituted under granulite facies conditions.

By far the greater proportion of rocks around Gosse Pile are the acid granulites, especially those rich in quartz and plagioclase. The mafic mineral, pyroxene or garnet, is probably determined by the bulk composition (Green and Ringwood, 1967). It is difficult to determine the origin of these rocks with certainty for, as Eskola (1952) pointed out, the same mineral assemblages could arise by primary crystallization as by metamorphic processes.

(a) The acid granulites and the evidence from zircon

Some information regarding the origin of the acid granulites may be gained by a brief examination of the zircons from these rocks. The majority show rounded or subrounded forms with no signs of overgrowths, although a very few show some subhedral shape (Fig. 2.48). Rounded zircon has been previously described from granulite facies rocks (Vitanage, 1957; Murthy and Siddiquie, 1964) and

Table 2.20

Comparison between the most important mineralogical characteristics of the Highland Series metasediments, Ceylon, and the granulites found around Gosse Pile.

| Ceylon (Cooray, 1962)  | Gosse Pile Area  |
|--|--|
| <p>K-feldspar and sillimanite occur in pelitic rocks.</p>  | <p>Sillimanite is relatively rare but, where found, occurs in garnetiferous, K-feldspar bearing pelitic rocks.</p>   |
| <p>Hypersthene is the typical ferromagnesian mineral.</p>  | <p>Orthopyroxene is the dominant ferromagnesian mineral in the acid rocks.</p>   |
| <p>Pyroxenes occur in basic rocks of amphibolite composition.</p>  | <p>Pyroxenes always occur in amphibole-bearing granulites.</p>   |
| <p>Biotite is generally absent from basic rocks and both biotite and hornblende are absent in quartzo-feldspathic rocks.</p> | <p>Biotite is always absent from basic rocks and occurs in very small amounts in some pelitic rocks. The only amphibole in acid rocks is green hornblende which occurs as an alteration product.</p> |
| <p>Rutile is the characteristic titanium mineral; sphene is absent from all but calcareous rocks.</p>                        | <p>Rutile is a common accessory in the acid granulites, but ilmenite is the dominant titanium-bearing mineral. Sphene is not found at all.</p>   |
| <p>Forsterite occurs in marble, and diopside and scapolite in calc-silicate.</p>   | <p>The marble contains forsterite and chondrodite but lacks grossular. Scapolite is common in diopside-rich calc-silicate granulites.</p>  |

Fig. 2.48

Zircons in acid granulites from the Gosse Pile area.

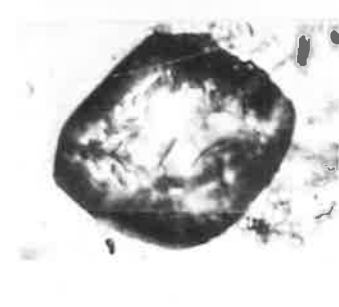
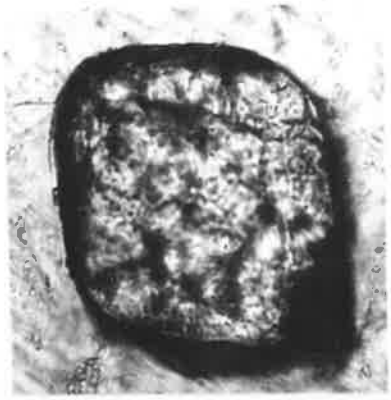
Top Row: Magnification x200

Second Row: Magnification x150

Third Row: Magnification x200

Bottom Row: Magnification x250

Photographs: A. Moore.





Marshall (1967), in a review article on zircon, pointed out that several authors have noted that rounded zircons often occur in granulite facies rocks but in amphibolite facies rocks signs of transformation (development of overgrowths and outgrowths, refaceting or possibly the formation of new crystals) are common. Murthy and Siddiquie (1964) considered this to be a function of the anhydrous nature of granulite facies metamorphism. The importance of the rôle of water in this respect has also been indicated by Wyatt (1954), Eckelmann and Poldervaart (1957) and Marshall (1969). Marshall (1969) has further demonstrated that transformation of zircon is restricted essentially to the pyroxene-hornfels facies (contact metamorphism at estimated conditions of about  $600^{\circ}$  -  $650^{\circ}\text{C}/1-2$  kb) and high amphibolite facies (regional metamorphism at estimated conditions of about  $680^{\circ}$  -  $800^{\circ}\text{C}/6-8$  kb) so that transformation appears to be dependent upon temperature rather than pressure. This information suggests that the acid granulites around Gosse Pile have passed through at least one sedimentary cycle and, if polymetamorphic, previous metamorphism has been at temperatures and pressures below those required for the transformation of zircon. It also suggests that the metamorphism is not progressive in the sense that an amphibolite facies assemblage preceded the present granulite facies assemblages.

Thus, from the evidence available, although slender, it appears that the majority of granulites have been formed by metamorphism of an original sedimentary sequence. During the granulite facies

metamorphism it has been shown that  $P_s \gg P_{H_2O}$ , a condition which can apply to sediments only after they have lost the greater part of their original water content (Winkler, 1967). This loss of water could take place during a long period of high-grade metamorphism or as a result of progressive dehydration during several metamorphic cycles. In view of the rounded zircons, lacking signs of transformation, the second alternative is favoured. This view has also been adopted by Scheumann (1961) for the Saxony granulites, and is consistent with the views of Yoder (1955) and Atherton (1965) concerning water and progressive metamorphism.

- (b) The marble, calc-silicate rocks and the basic, amphibole-bearing granulites.

The most plausible explanation for the origin of the marble is that it represents the high-grade metamorphic equivalent of an impure limestone horizon within a metasedimentary sequence. The diopside-scapolite rocks may represent simply metamorphic equivalents of original impure calcareous sediments, as has been suggested for similar rocks from Visakhapatnam, India (Krishna and Murthy, 1968), or they may have had a more complex origin, involving some metasomatism. This is discussed later.

In any discussion concerning the origin of the amphibole-bearing rocks, two factors should be borne in mind:

- (i) The rocks occur as relatively thin bands or lenses within large masses of acid rocks which are essentially free of hydroxyl-bearing minerals. Further, where good exposures
-

occur the basic rocks can be seen to be related to the axial plane regions of macroscopic folds, and are often well developed in the hinge zones (section 2.9.2).

- (ii) There is a common association between these basic granulites and the calc-silicate rocks, often in a zonal arrangement (e.g. A313/370A area, Fig. 1.3, B/2). Further, the calc-silicate rocks are themselves sometimes found in the axial plane regions of folds with amphibole-bearing rocks flanking them.

In the granulite facies, two subfacies have been generally recognised: the pyroxene granulite subfacies and the hornblende granulite subfacies (e.g. Turner and Verhoogen, 1960). An intimate intermingling of these two subfacies has been recorded from several areas throughout the world (e.g. the Adirondack Highlands area, de Waard, 1964). The rocks around Gosse Pile are no exception. This type of close association between the two subfacies, one "hydrous" and the other "anhydrous" has led to considerable discussion on the rôle of water in metamorphism (see section 2.11, p. 94). Winkler (1967) considered that under conditions where  $P_{H_2O} \ll P_s$  the intermingling of facies is a result of variations in  $P_{H_2O}$  and bulk composition. As de Waard (1964) states, "The separate status of the hornblende-granulite subfacies given to the univariant facies boundary, merely adds one more name to the number of intermingled subfacies." Water may thus be regarded essentially as a part of the bulk composition of the rocks in which amphibole crystallizes; a composition markedly different from the surrounding acid rocks. Scheumann (1961)

explains the amphibole-bearing bodies within the more acid gneisses of the Saxony granulite area as being remnants of basic igneous rocks which are part of a geosynclinal sequence. During "granulitization" they remained amphibolitic, presumably because each acted as a closed system with respect to water.

The occurrence of amphibole-bearing and calc-silicate granulites in the axial plane and hinge zones of folds is probably a function of their different response to deformation such that a greater strain rate develops locally. This, in turn, is dependent on the original composition of the rock. This would be analagous to the development of faults parallel to the axial planes of folds and to the formation of new minerals in the axial plane regions of kink bands in lower grade metamorphic terrains. Pressure gradients may thus be set up and any water present would migrate to the lower pressure zones where hydrous assemblages could develop. If sufficient water was available no orthopyroxene would be present, but as this mineral is common it implies that the amount of water was limited. Carpenter (1968) has recently discussed this structural control on metamorphic differentiation and has shown that the result of folding in the course of regional metamorphism causes the migration of components such as  $H_2O$ ,  $CO_2$  and hydrated cations to form relatively concentrated fluids in lower pressure zones. This results in the local formation of "lower grade" assemblages.

The occurrence of calc-silicate rocks in similar structural sites may be the result of similar mechanisms. Furthermore, the

---

local concentration of fluids would enhance diffusion processes (either intercrystalline or intracrystalline or both) and thus promote metasomatic exchanges between the calcareous rocks and the calcium-poor acid granulites. Orville (1969) has recently proposed a model for the metasomatic origin of such thin-layered amphibolite bodies which occur in association with calc-silicate rocks. He suggests that the amphibolites form by a redistribution of material by chemical reaction within a relatively restricted volume of rock. This model requires the fairly ready transfer of material (particularly  $K^+$ ,  $Ca^{2+}$  and  $H^+$  ions) through the rock, probably by means of an intergranular fluid, so reaction would be promoted by the concentration of such a fluid. The concentration of fluids, type of diffusion processes occurring and the area over which diffusion takes place in an effort to establish equilibrium, determine the size of the system. As the amphibole-bearing layer increases in size so the distance over which diffusion has to occur increases and, in the absence of thermal gradients, the reaction proceeds at a decreasing rate. As shown by Thompson (1959) and Orville (1969) this type of reaction tends to reduce the total number of phases, producing bimineralic, or even monomineralic, rocks. The mineralogy of the calc-silicate rocks is consistent with this: they consist essentially of diopside or diopside and scapolite, where the scapolite appears to be replacing plagioclase. This latter reaction is likely to represent a retrograde effect: as the temperature and pressure fall the anorthitic plagioclase would become unstable in the presence of a  $CO_2$ - and  $H_2O$ -rich fluid

phase and react to produce scapolite (Fig. 2.43). The presence of four phases in all but one of the basic rocks is probably a function of water content such that the amount of amphibole which can form is limited.

Some of the larger basic amphibole-bearing bands in the Gosse Pile area have no obvious association with calc-silicate rocks, nor do they appear to be in particular structural environments. Thus, if the metasomatic model (Orville, 1969) is applicable to some basic granulites it seems likely that similar rocks in this area have had more than one mode of formation. It is concluded that the presence of hornblende-granulite subfacies within the pyroxene-granulite subfacies is controlled by numerous factors, the most important of which are bulk composition, including variations in water content, the occurrences of favourable structural sites and, in some cases, by metasomatic reaction with calc-silicate rocks.

(c) The iron-rich granulites.

Two possible explanations can be proposed for the quartz + iron oxide associations. The first is to suppose that they represent original sedimentary sequences (either as laterites or as banded ironstone formations) which have undergone granulite facies metamorphism. The second is to suppose that they have formed entirely by metamorphism, as oxidized metamorphic differentiates. Although not conclusive, the little evidence at present available favours this latter alternative. It is unlikely that sedimentary bedding

has been preserved at all during the processes of deformation and metamorphism, although different original sediments probably are responsible for some of the major lithological differences still apparent (e.g. the marble). Yet, the iron-rich layers strike parallel to the regional layering ( $S_g$ ) for large distances (Fig. 1.3). This tends to suggest an origin linked with the origin of the metamorphic layering of the granulites.

Ramberg (1948) showed that, under conditions of granulite facies metamorphism, the stability relationships of some silicates (particularly sphene and amphibole) require the release of Fe and Ti from the lattice. He suggested that these liberated elements would diffuse away from the place of reaction and later consolidate in favourable sites, thus causing local concentrations of titanium-rich iron ores. Recently, Hagner and Collins (1967) have proposed a metamorphic origin for the magnetite ores of the Ausable district, U.S.A., where economic deposits occur in foliated gneisses which have mineralogies consistent with upper amphibolite to granulite facies. The source of iron in this case is thought to be from the breakdown of some silicate minerals and from the migration of iron from accessory magnetite. The released elements are thought to have migrated, probably as complexes, to zones of low pressure and high oxygen activity.

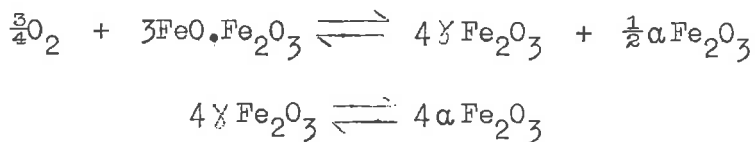
In the Gosse Pile area the iron-rich granulites are:

- (i) often associated with fracture zones and are themselves frequently strongly deformed;

- (ii) titanium-rich (Section 2.9.1);
- (iii) highly altered to haematite, indicating an oxidation stage.

Further, thin section studies of acid granulites show that the opaque minerals appear to be the most readily mobilized (Fig. 2.30). The above points tend to support the view that these rocks may have formed in a manner analogous to that proposed for the Ausable deposits.

The conversion from magnetite to haematite (martitization) is an oxidation effect and could have occurred under conditions of declining metamorphism (constant  $f_{O_2}$  and decreasing  $P_g/T$ ), or could be a relatively recent process occurring at a stage when the rocks now exposed at the surface were just above the water table. The process of martitization is best represented by the following equations, derived by Davis et. al. (1968):



- (d) Discussion of chemical changes involved during metamorphism

From the above discussion it is concluded that the Gosse Pile granulites probably started out as a sedimentary sequence and the question arises as to what chemical changes, if any, have taken place since these sediments were metamorphosed. In spite of the lack of large numbers of chemical analyses in this section, a brief discussion of this question is probably worthwhile in view of the



different opinions which have been expressed concerning the progressive metamorphism of rocks.

Engel and Engel (1958, 1960, 1962) studied a series of paragneisses along a profile from the Grenville Lowlands to the Adirondack Highlands, U.S.A. and found, with increasing metamorphic grade, considerable chemical changes both in major and trace elements. On a broad scale Heier (1965) considered that "regional metamorphism is potentially an active agent in chemical fractionation" and agreed with Barth (1962) in thinking that the transfer and transportation of both chemical elements and heat were essential parts of high grade metamorphism. Lambert and Heier (1968) showed that medium to high grade granulite facies terrains are generally dominated by rocks with  $\text{SiO}_2$  contents less than about 70% while upper amphibolite and low pressure granulite facies terrains are dominated by rocks with greater than about 70%  $\text{SiO}_2$ . They concluded that changes in the major and trace element contents of rocks from different metamorphic grades were the results of modifications of original (sedimentary) compositions by metamorphic processes, including melting. Arriens and Lambert (1969) discussed the distribution of Sr isotopes within rocks of different metamorphic grades. The high precision obtained by them for an isochron ( $1,325 \pm 12$  m.y.) for granulites from the Fraser Range indicates homogenisation of Sr isotope ratios on a regional scale followed by sudden "freezing" of this initial ratio after which no subsequent redistribution of Sr and Rb took place. They regard this

---

homogenisation of Sr as a product of the granulite facies metamorphism or, possibly, the result of the rocks being derived from contemporaneous volcanics.

On the other hand, numerous authors have concluded that, apart from the loss of volatiles and possibly  $K_2O$ , no significant chemical changes occur during progressive metamorphism (e.g. Shaw, 1956; Zwart, 1958; Chinner, 1960; Phinney, 1963). This is termed "conservative metamorphism" rather than "isochemical metamorphism" by Mehnert (1968). Blackburn (1968) studied the spatial extent of chemical equilibrium in high grade metamorphic rocks and concluded that, since the volumes within which equilibrium was achieved were very small (of the order of a few cubic centimetres) diffusion processes were very limited. Mueller (1967) had previously shown that lattice diffusion was ineffective as a means of large scale mass transport during metamorphism.

These apparently contradictory lines of evidence can possibly be reconciled if it is presumed that the granulites have undergone polymetamorphism. The progressive metamorphism of earlier cycles would cause gradual dehydration (Yoder, 1955; Atherton, 1965) and, with the movement of water and other volatiles, movement of elements could take place. The area studied by Engel and Engel (1958, 1960, 1962) could be considered as an hydrous environment (Buddington, 1963) so that changes in chemistry could be due to some metasomatic changes catalysed by volatiles. However, in rocks where the volatile content is low (as in rocks dehydrated by previous metamorphism)

there is no component to act as a carrier and reactions would involve little transfer of material, except for local areas where concentrations of fluid phases may accumulate. This implies that  $P_f$  is not equal throughout the area and is dependent upon the bulk composition of the rocks involved.

Thus, a model can be proposed whereby earlier metamorphic cycles cause dehydration, redistribution of certain elements and homogenization of isotopes (e.g. Sr). During such cycles the P-T conditions would have remained below those necessary for transformation of zircon. At a later state P-T conditions favourable for the formation of granulite facies assemblages prevailed and the conditions of very limited, structurally controlled diffusion, as outlined by Blackburn (1968) would apply. To account for features such as the precision outlined by Arriens and Lambert (1969) it would be necessary to assume that granulite facies metamorphism took place within a relatively short period of time after homogenization (approximately 300 m.y., see Arriens and Lambert, 1969) and thus cause "freezing in" of the homogeneous Sr isotopic ratios.

### 2.13 CONCLUSIONS

The granulites around Gosse Pile consist of a metasedimentary sequence which has undergone granulite facies metamorphism, probably as the final stage of a polymetamorphic cycle. It is thought unlikely that the rocks passed through a stage when minerals of the amphibolite facies were formed, either because the increase in pressure and temperature was too rapid to allow for the stable crystallization of amphibolite facies assemblages or, more likely, because insufficient water was present when the P-T conditions reached the appropriate level. Estimations (made with reservation) of the conditions of granulite facies metamorphism indicate temperatures and pressures of the order of  $1,000^{\circ}\text{C}$  at 10 kb, with  $P_{\text{H}_2\text{O}} \ll P_s$ .

Such conditions would require a geothermal gradient steeper than the possible average oceanic geotherm of about  $19^{\circ}\text{C}/\text{km}$  to 30 km, suggested by Ringwood (1966, Fig. 3). The minimum average gradient required is about  $25^{\circ}\text{C}/\text{km}$ . This value is, however, close to the "normal" gradient of Mehnert (1968) and Wyllie (1963) of about  $30^{\circ}\text{C}/\text{km}$ , and far less than some which have been proposed for other metamorphic regions. For example, Johnson (1963) suggested gradients of  $50^{\circ} - 150^{\circ}\text{C}/\text{km}$  in the Scottish Highlands, and Zwart (1962) suggests gradients of  $150^{\circ} - 180^{\circ}\text{C}/\text{km}$  were achieved during metamorphism in the central Pyrenees.

SECTION 3

LOCAL GEOLOGY.

THE GOSSE PILE ULTRAMAFIC BODY AND ASSOCIATED  
INTRUSIVES.

### 3.1 TERMINOLOGY

Jackson (1967) pointed out that many similarities between various mafic and ultramafic rocks in different intrusions are often obscured by differences in the terminology used by various authors. He proposed a two-fold system of nomenclature which, for rocks formed by crystal settling, takes into account both settled and interstitial material (originally suggested by Wager, Brown and Wadsworth, 1960), as well as the total modal composition. Although this scheme theoretically provides the clearest descriptive terminology available it is somewhat unwieldy and, except for ideal examples, it is difficult to apply the "cumulate" terminology of Wager, Brown and Wadsworth (1960) for want of adequate criteria for distinguishing the nature of post-accumulation crystallization (Abbot and Ferguson, 1965). For the rocks of Gosse Pile it is not entirely practical because post-crystallization deformation has affected the greater part of the layered sequence causing annealing and making the distinction between cumulus and intercumulus phases generally impossible. Cameron (1969) has also stated that a completely satisfactory terminology for cumulates (particularly adcumulates) is difficult to formulate because of the difficulties encountered in attempting to distinguish cumulus and adcumulus growth. For similar reasons McDonald (1967) included in situ overgrowths on settled grains in his definition of "cumulate". A further difficulty arises when considering the rocks which intrude the layered sequence of Gosse Pile because these rocks have a similar mineralogy, and often a similar texture, to the layered rocks but are themselves unlayered. For these reasons the names which have been

---

applied to the various rock types found in Gosse Pile are defined below so that, where possible, comparisons may be made with other igneous bodies. (A list of modal analyses is given in Appendix 1 and the rocks are more fully described in Section 3.5).

Orthopyroxenite: This name is applied to rocks consisting dominantly of orthopyroxene. In the relatively undeformed layered sequence the only cumulate phase is orthopyroxene, with interstitial clinopyroxene and plagioclase.

Olivine-orthopyroxenite: This name is given to any orthopyroxenite in which olivine occurs. Cumulate phases are orthopyroxene, olivine and oxides (spinel and chromite). In one small band on the north side of the Main Body clinopyroxene occurs as a cumulate phase and almost equals orthopyroxene in amount. Strictly speaking the rock should be termed an olivine-websterite but because of its very limited occurrence it is felt that a separate name is not justified.

Websterite: Where the rock is composed essentially of both pyroxenes it is given this name. The proportion of one pyroxene to another may be as low as 1:3, but it is never less than this and is usually nearer 1:1. Plagioclase sometimes occurs interstitially.

The names given to the plagioclase-rich rocks are slightly unconventional but this is done so that mineralogically similar rocks may be readily distinguished in the discussions.

Gabbro: This is a term applied only to the plagioclase-rich rock, in which both pyroxenes are essential, which occurs only in the Gabbro Band. In general, the amount of clinopyroxene exceeds that of orthopyroxene.

Olivine-gabbro: The rocks of the Mt. Davies intrusion (Fig. 1.3) consist essentially of plagioclase with a high proportion of olivine and clinopyroxene; orthopyroxene is relatively minor. Plagioclase and olivine are primary cumulus phases. A small plug, with identical mineralogy and similar texture, occurs on the south side of Gosse Pile. Both rock types are termed olivine-gabbro.

Norite: Plagioclase is the dominant mineral and both pyroxenes are essential, but in all cases orthopyroxene slightly exceeds clinopyroxene in amount. All norites of the layered sequence in Gosse Pile are deformed so that recognition of original cumulus and intercumulus phases is impossible.

Anorthosite: The rock is made up almost entirely of plagioclase, and other minerals, usually pyroxenes and oxide minerals, are present only in accessory amounts.

The later intrusive with noritic affinities: The mineralogy of this rock is simple: orthopyroxene, clinopyroxene and plagioclase. However, the proportions in which these minerals occur and the variability in grain-size are so great that no single name could cover all varieties present. For simplicity the rock is referred to as the "noritic intrusive".



Picrite: The picrite plugs, occurring in both the granulites and Giles Complex rocks (Section 1.3) have a characteristic texture: small, rounded olivine crystals poikilitically surrounded by large clinopyroxene crystals or, less commonly, by orthopyroxene and plagioclase. Plagioclase, orthopyroxene and oxides occur interstitially. The picrite in Gosse Pile has this texture in the central part ("central type" picrite) but towards the margins the poikilitic texture is no longer obvious, olivine is less abundant and biotite and hornblende are notable constituents ("marginal type" picrite).

Serpentinite: The highly weathered, friable rock consisting essentially of serpentine and associated magnesite veins is termed serpentinite. Magnetite is a common accessory. Because of its weathered nature it forms an area of low relief with few outcrops.

Dolerite: These are basaltic rocks, occurring as dykes, characterised by an ophitic texture. The dykes of the eastern Tomkinson Ranges have been classed by Nesbitt et. al. (1969) and by A.D.T. Goode (pers. comm.) into four types. In the Gosse Pile area only two distinct types occur and these are termed amphibole-dolerites and pyroxene-dolerites. The amphibole-dolerite dykes, which are older, are equivalent to the Type A (one pyroxene) dolerite dyke suite of Nesbitt et. al. (1969) and consist of plagioclase, clinopyroxene and green hornblende. They are commonly foliated but, where relatively undeformed, have an ophitic texture. The pyroxene-dolerite dykes are equivalent to types B and C of

Nesbitt et. al. (1969) and consist of plagioclase, orthopyroxene, clinopyroxene and abundant oxides while olivine may or may not be present. They are usually fine-grained and ophitic.

Silcretes (or chalcidonic horizons): These have been discussed on pp. 15-16.

### 3.2 GEOLOGY AND PETROGRAPHY

#### Introduction

Gosse Pile is an ultramafic portion of the Giles Complex and is separated from both the surrounding granulites and the rest of the complex by brittle faults, except for a short (1km) contact along the north-west margin of the main body (Fig. 1.3, C/2) where the later noritic intrusive forms an igneous contact against the granulites. The exposed strike length of Gosse Pile is 8km and the maximum width is 2km. The highest point is about 275m above the surrounding plains. Steele (1966) carried out a gravity survey (single traverse) across Gosse Pile (Fig. 3.1). He concluded that the southern contact was vertical, the northern dips at 65°S and the ultramafic rocks extend to a depth of 3,000 ft. (approximately 900m). He also deduced that the serpentized zone was asymmetric (the northern contact dips at about 35°S and the southern at about 60°S) with a depth of approximately 250 ft. (approximately 75m).

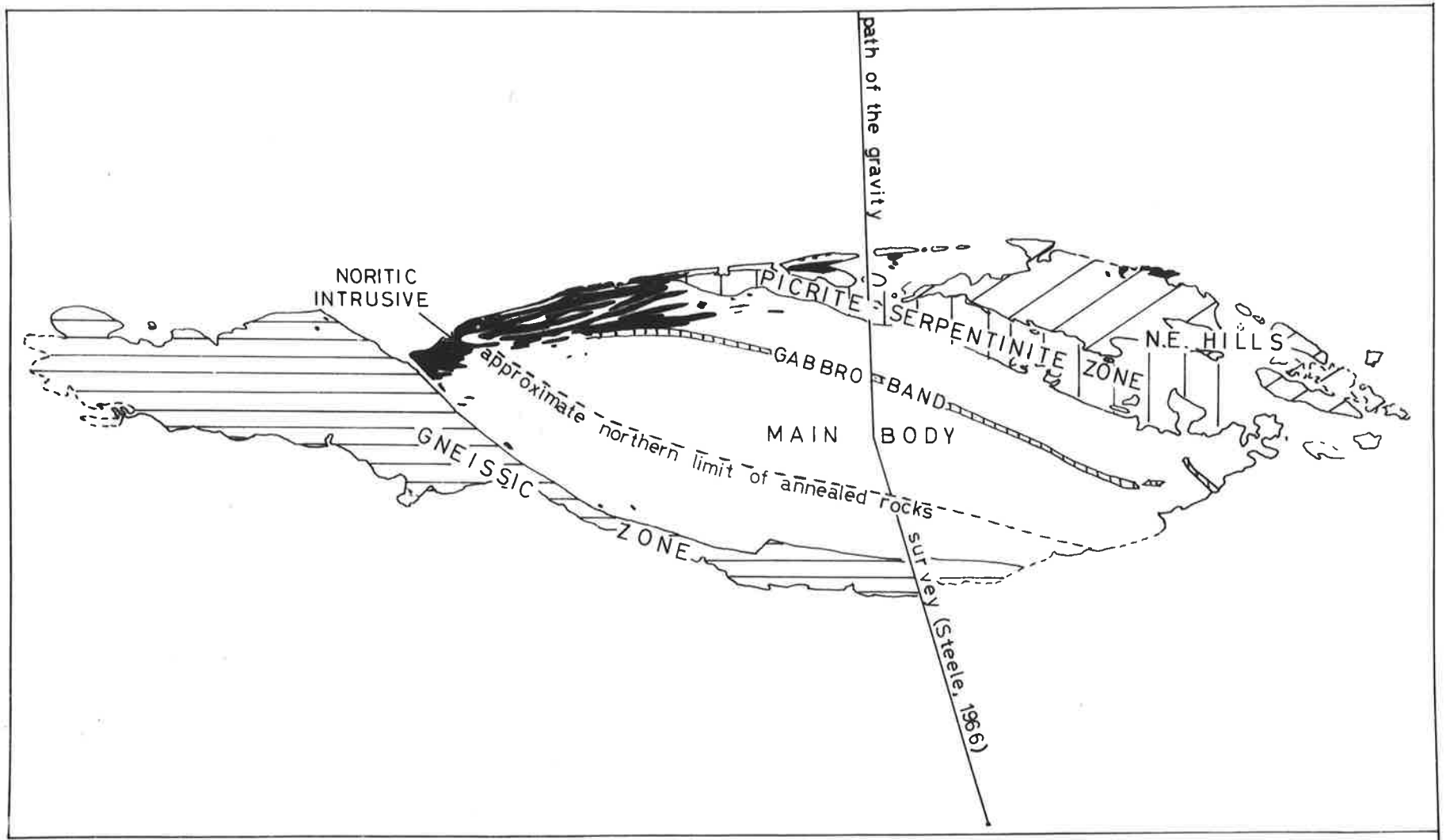
In general, the rocks are well exposed and apart from a thin (5-20mm) weathered "skin" they are unaltered. However, the olivine-

Fig. 3.1

Illustration of the subdivision of Gosse Pile into zones for descriptive purposes. The zones are chosen on the basis of geographical or petrological distinctions.

1. N.E. Hills (diagonal shading): part of the layered sequence.
2. Picrite-serpentinite Zone (vertical shading): post-Giles complex picrite to the west, and to the east serpentinite derived from the picrite.
3. Main Body (unshaded): the greater part of the layered sequence. It includes a small area of rocks north of the Picrite-serpentinite Zone.
4. Gabbro Band (close vertical shading): the steeply-dipping, east-west band of gabbro within the Main Body.
5. The Noritic Intrusive (black): irregular, post-Giles complex intrusives with noritic affinities. These are particularly well-developed in the northwest of the Main Body.
6. Gneissic Zone (horizontal shading): flow-layered deformed rocks of the layered sequence south and west of the Main Body.

Also marked are the path of Steele's (1966) gravity survey and the approximate northern limit to which the layered sequence rocks in the Main Body have been affected by annealing processes (Section 3.3).



rich rocks and coarse-grained varieties of the noritic intrusive are commonly very weathered and friable. Systematic traverses and the collection of orientated samples is made difficult by the steep topography (some northern slopes have a 1:1 gradient) and by the presence of extensive skree (float). This loose rubble also makes observations on the contact relationships between rock types difficult.

To aid description the area has been divided into a series of zones, each being either geographically or petrologically distinct. They are shown in Fig. 3.1. Furthermore, most, but not all, of the rocks can be placed into one of the following categories:

- (i) Giles Complex rocks, or layered sequence;
- (ii) The picrite-serpentinite intrusive;
- (iii) The noritic intrusive;
- (iv) The dolerites.

The overall distribution of rock types is best seen by reference to Fig. 1.3 and the relative abundances, measured directly from this map, are given in Table 3.1. From this it can be seen that orthopyroxenite is the most abundant rock type.

### 3.2.1 The Layered Sequence

These are the rocks making up the greater part of the N.E. Hills, the Main Body and the Gneissic Zone (Fig. 1.3) and they are considered to represent the oldest igneous rocks in the area. Four, possibly five, rock types can be distinguished: orthopyroxenite, olivine-

Table 3.1

The relative abundances of exposed rock types within Gosse Pile.

Areas are measured directly from Fig. 1.3.

|  | Area in km <sup>2</sup> | % rock type of total exposed |
|--|-------------------------|------------------------------|
| orthopyroxenite  | 2.3660                  | 51.27                        |
| olivine-orthopyroxenite  | 0.0957                  | 2.11                         |
| websterite   | 0.6585                  | 14.28                        |
| Gneissic Zone (undistinguished alternating bands of pyroxenite and norite)       | 1.1570                  | 25.06                        |
| Piorite (excluding minor exposures, usually as serpentinite, in alluvial valley) | 0.0742                  | 1.61                         |
| later noritic intrusive  | 0.1960                  | 4.25                         |
| Gabbro Band  | 0.0657                  | 1.42                         |
|  | 4.6131                  | 100.00                       |

orthopyroxenite, websterite and norite and, possibly, the gabbro of the Gabbro Band. At the time the geological map (Fig. 1.3) was drawn, the Gabbro Band was thought to form part of the layered sequence. Since then evidence has been found to suggest that it should be regarded rather as part of the later noritic intrusive phase. This evidence, discussed in Section 3.5, is not conclusive but, for the present, the Gabbro Band is considered not to be a part of the layered sequence. It has a mineralogy similar to the norite and hence probably should not be regarded as a distinct type but, because of its indeterminate relationship, it is given a distinguishing name.

On the northern side of Gosse Pile, where the effects of deformation are relatively slight, the three major rock types which have been developed can be recognised as having been formed by cumulates of orthopyroxene (orthopyroxenite), orthopyroxene and olivine (olivine-orthopyroxenite), and of orthopyroxene and clinopyroxene (websterite). On the southern side deformation and annealing have obliterated original igneous textures so that cumulus and intercumulus phases cannot be recognised. The only norites occur in this region so that, by comparison with the northern part of the body, the assumption is made that these rocks formed originally by settling of cumulus plagioclase and orthopyroxene and, possibly, clinopyroxene although this latter mineral may have been an intercumulus phase. Similarly, the southern websterite (Fig. 1.3) is thought to be a deformed equivalent of an orthopyroxene-

clinopyroxene cumulate.

Thus, the simple mineralogy of all rock types is as follows:

cumulus minerals: orthopyroxene (ubiquitous); clinopyroxene (common); olivine (fairly common); spinel and chromite (uncommon); sulphides (rare, found only in olivine-orthopyroxenites).

intercumulus minerals: clinopyroxene (very common); plagioclase (common); biotite and hornblende (rare, found mainly in olivine-orthopyroxenite).

In the field all rocks have a rust-red weathered surface and distinction between the types is difficult. On fresh surfaces the websterite has a slightly more greenish tinge than the grey-green orthopyroxenite. Olivine-bearing varieties are recognised by the fact that the more readily weathered olivine produces a slightly pitted surface (e.g. Fig. 3.34), but where the amount of olivine is small this feature can be easily overlooked. Plagioclase, because of its white weathered surface, stands out prominently to such an extent that there is a tendency to overestimate the amount present. Oxides are unusually scarce for an ultramafic sequence and the expected chromitite horizons are absent. Chromite, as euhedral crystals, and anhedral green and brown spinel are most abundant in the olivine-rich rocks, but even there never exceed about 3% of the total. The pyroxenites contain rare disseminated chromite euhedra (approximately 1 crystal per thin section of about  $9\text{ cm}^2$ ) which are commonly completely surrounded by a thin corona of plagioclase.



In the central and eastern parts of Gosse Pile, including the N.E. Hills, repetitive layering, which dies out westwards, can be recognised. Such layering is a characteristic feature of the major layered intrusions and distinguishes them from layered sills (Wager and Brown, 1968). Jackson (1961) called the repeated layers "cyclic units"; Wager and Brown (1968, p. 545) prefer the term "macro-rhythmic layering". Considering the Gosse Pile layered sequence as a whole, three complete cyclic units can be recognised (Table 3.2), all of which lack a feldspar-rich phase. However, the third complete cyclic unit grades southwards into a zone of alternating norite and pyroxenite layers which is a probable extension of the cyclic sequence to more feldspathic horizons. The Kalka intrusion (Fig. 1.3) is considered to represent a tectonically separated probable upper portion of Gosse Pile (Nesbitt *et. al.*, 1969) and has a lower ultramafic zone of orthopyroxenite and websterite, passing upward into feldspar-rich zones of norite and olivine-gabbro, repeated in a cyclic fashion, and finally anorthosite (A.D.T. Goode, pers. comm.).

This type of cyclic sequence (Table 3.2), with slight variations, has been recognised in the ultramafic parts of other layered intrusions: for example, Stillwater - Jackson, 1961, 1967; Muskox Intrusion - Irvine and Smith, 1967; Rhum - Wager and Brown, 1968; and it is probable that similar sequences will be recognised in the Bushveld Complex and the Great Dyke (see sections by Cameron, 1963, and Worst, 1958). In all cases the olivine cumulus crystals occur towards the base. For this reason, and because there is a marked

Table 3.2

Complete and partial cyclic units recognised in Gosse Pile.

| Complete cyclic unit number   | Rock type   | Comments  |
|---|---|---|
| <p>↑ SOUTH</p> <p>3 {</p> <p>2 {</p> <p>1 {</p> <p>↓ NORTH<br/>(Towards the base)</p> | <p>alternating pyroxenite and norite bands of Gneissic Zone</p>           | <p>pyroxenite may be either orthopyroxenite or, less commonly websterite; plagioclase assumed to be originally cumulate</p> |
|   | <p>websterite</p> <p>orthopyroxenite ←</p> <p>olivine-orthopyroxenite</p> | <p>approx. N limit of annealing →</p> <p>poorly developed layer</p>   |
|   | <p>-----</p>  | <p>probable fault</p>   |
|   | <p>orthopyroxenite</p>  | <p>"beheaded" unit between two fault zones</p>  |
|   | <p>-----</p>  | <p>possible fault</p>   |
|   | <p>Gabbro Band</p>  | <p>noritic intrusive or cumulate plagioclase ?</p>  |
|   | <p>websterite</p> <p>orthopyroxenite</p> <p>olivine-orthopyroxenite</p>   | <p>poorly developed layer, S of picrite</p>   |
|   | <p>websterite</p> <p>orthopyroxenite</p> <p>olivine-orthopyroxenite</p>   | <p>intruded by picrite - serpentinite body</p> <p>north N.E. Hills area</p>   |
|   | <p>orthopyroxenite</p>  | <p>"beheaded" horizon (i.e. no overlying websterite). Found only in eastern N.E. Hills area.</p>                            |

increase in the proportion of feldspathic rocks in Gosse Pile towards the south, it is considered that the base of the Gosse Pile ultramafic sequence was towards the north. Where dip measurements can be taken on primary igneous layering they give values ranging from vertical to  $50^{\circ}\text{N}$  and  $65^{\circ}\text{S}$ . Thus, assuming that the cyclic units represent, in part, gravity stratification (Buddington, 1939), Gosse Pile has been rotated from a near horizontal position, to a near vertical position with the base towards the north and the top towards the south.

In the western part of the Gneissic Zone occur irregular, elongate inclusions of fine-grained, purple, white-weathering anorthosite. This material is unlike any other found in the layered sequence but is very similar to the anorthosites found within the granulites along the northern contact of Gosse Pile. These inclusions are not thought to be a part of the layered sequence but most likely represent xenoliths of foreign material.

The area between Gosse Pile and Mt. Davies has been carefully mapped and shows that the two intrusions are separated by a fault zone approximately 10m wide (the Numbunja Creek fault). This fault zone consists of several, closely-spaced, parallel, brittle faults each about 1 to 2m wide and consisting of angular fragments of gneissic norite surrounded by grey or greenish-grey pseudotachylite veins, very similar in hand specimen to the fault breccia shown in Fig. 2.10. Most of the fault zone is covered by alluvium or silcrete but it is exposed in a few places by creek erosion. Immediately south of the fault zone is the slightly deformed olivine-gabbro of

the Mt. Davies layered intrusion (Fig. 1.3).

### 3.2.2 The picrite-serpentinite rocks

Between the Main Body and the N.E. Hills of Gosse Pile lies the Picrite-serpentinite Zone (Fig. 1.3 and Fig. 3.1). The western part is picrite, generally weathered and forming loose boulders, while the eastern part consists of friable serpentinite which is covered for the greater part by alluvium and rubble. In spite of the obscuring blanket of alluvium the indications are that there is no sharp contact between picrite and serpentinite but that the picrite becomes progressively more altered eastwards and eventually grades into serpentinite. Together these rocks produce a shallow valley (Fig. 3.2).

The contacts between the picrite and orthopyroxenite, or olivine-orthopyroxenite, are irregular but appear to be sharp, although considerable difficulty was encountered in following these contacts in the field. A small, rounded plug of picrite occurs within the orthopyroxenite at the southwestern end of, and isolated from, the main picrite mass (Fig. 1.3, D/2). Within the picrite occur xenoliths of orthopyroxenite, some of which exhibit well-developed igneous lamination. The contacts around such xenoliths are sharp, with no indication of reaction (Fig. 3.3 and Fig. 3.4).

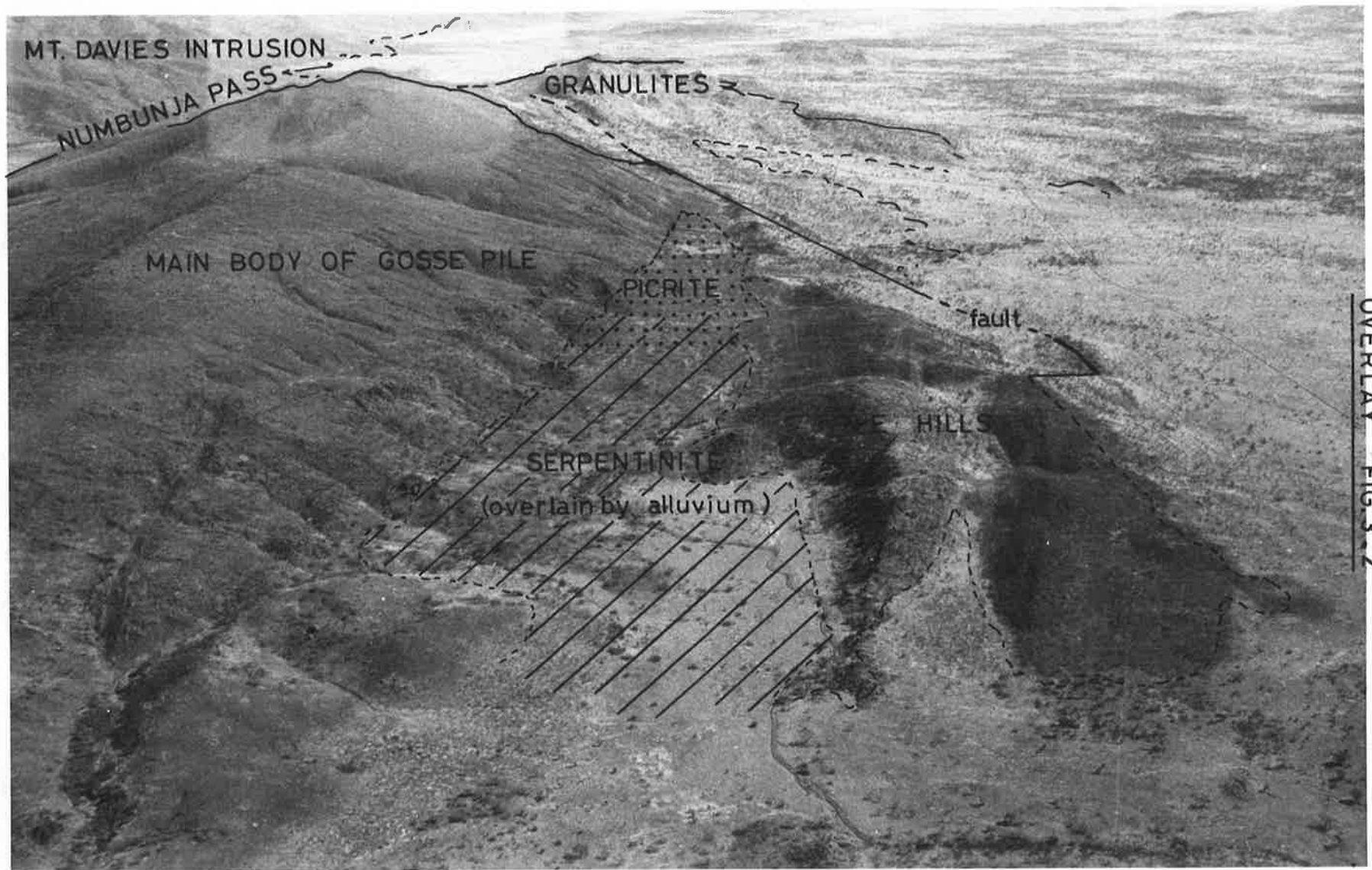
In the field the picrite can be seen to vary from a non-porphyrific, massive type which occurs near the margins of the

---

Fig. 3.2

Oblique aerial photograph looking west along the Picrite-serpentinite Zone (see Fig. 3.1).

Photograph: A. Moore.



OVERLAY FIG. 3.2

Fig. 3.3

Xenolith of orthopyroxenite (pxite) in central type picrite.

Location: A313/314E. Scale: 31 cm.

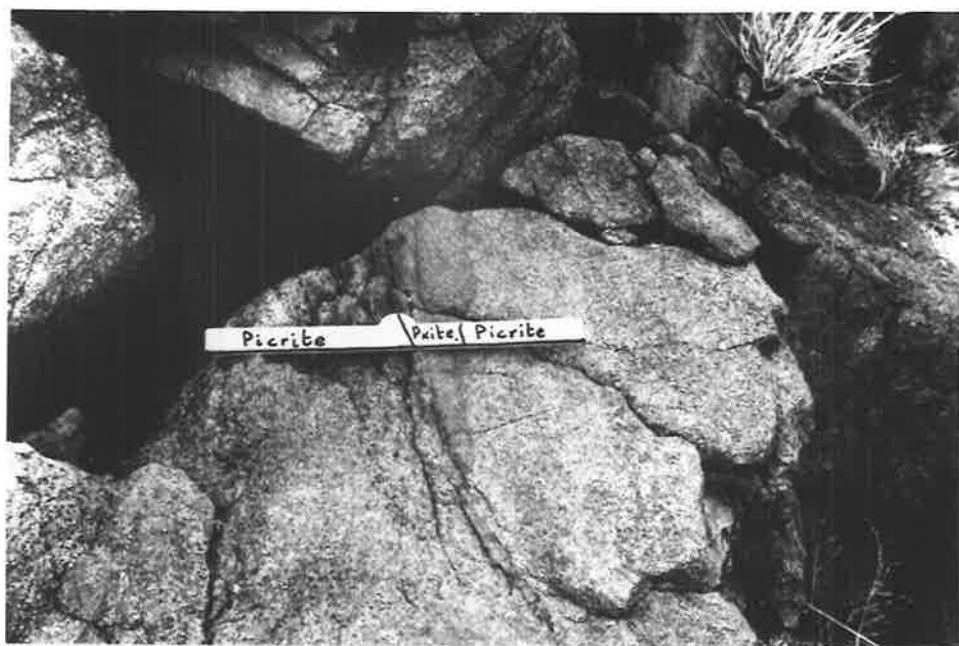
Photograph: A. Moore.

Fig. 3.4

Xenoliths of orthopyroxenite in central type picrite. The contact between the xenolith and the picrite in the foreground has been dotted in ink on the photograph. Location: A313/350.

Scale: 31 cm.

Photograph: A. Moore.





picrite body and which contains numerous orthopyroxenite xenoliths, to a porphyritic type which occurs towards the centre and contains few xenoliths. These types are informally termed "marginal type" and "central type" picrites. The central type is very similar to the numerous picrite bodies intrusive into both Giles Complex rocks and the granulites (Gray, 1967; Nesbitt et. al., 1969; R.W. Nesbitt and A.D.T. Goode, pers. comm.). In hand specimen it consists of large (up to 3cm) phenocrysts of clinopyroxene (sometimes orthopyroxene) which poikilitically enclose small (3-5mm), rounded olivine grains, while plagioclase occurs interstitially between olivine and pyroxene. The rock has a characteristic and easily recognisable weathered surface. The pyroxene forms knob-like protuberances because of the more rapid weathering of the olivine, while the white-weathering plagioclase gives a net-like appearance to the depressed areas. The marginal type picrite is far less distinctive and is often difficult to distinguish from olivine-orthopyroxenite in the field. It lacks phenocrysts and consists of numerous small (2-3mm) rounded olivine grains with abundant interstitial plagioclase and pyroxene. In hand specimen numerous biotite crystals can be seen - a useful distinguishing feature as this mineral is rare in the central type picrite and in the olivine-orthopyroxenites. The marginal type picrite is poorly exposed, and is generally covered by rubble or alluvium: this may explain why it has not so far been recognised elsewhere in the picrite bodies of the eastern Tomkinson Ranges.

Eastwards the picrite becomes increasingly weathered and exposures are less common. Further east the only exposures are those in creek banks where friable, green serpentinite occurs. This is cut by veins of magnesite and siliceous material, generally a white or brown chalcedonic rock but occasionally pale green. No chrysoprase of any quality has been found. Flanking the valley are massive outcrops of silcrete (brown, chalcedonic rock) beneath which is found serpentinite. In the contact zone between these two rock types veins of magnesite are more numerous, although they are found throughout the serpentinite.

Near the southern margin of the picrite several elongate outcrops of orthopyroxenite occur as "islands" in a "sea" of picrite. From field evidence there is little doubt that the picrite is intrusive into the layered rocks so that these orthopyroxene outcrops represent xenoliths or remnants around which the picrite has intruded. It is probable that the serpentinite represents the weathered eastward extension of the picrite. In numerous places veins of noritic material can be seen cutting the picrite, suggesting that intrusion of the picrite pre-dated that of the noritic intrusive (discussed in Section 3.2.3). However, to the west of Gosse Pile (Fig. 1.3, C/2) a small plug of picrite (central type - the margins are not exposed) occurs completely surrounded by the later noritic intrusive, suggesting that the reverse age relationships hold. Field observations make it seem unlikely that this picrite is a xenolith. The only reasonable explanation seems to be that the picrite was intruded over a period of time which straddled the time of intrusion

of the noritic rocks. The two types may even have petrographic affinities and form a single rock series.

### 3.2.3 The noritic intrusive

Along the northern margin of Gosse Pile are numerous outcrops of a transgressive norite which, in most areas, is faulted against the granulites. This rock type is difficult to map because of its variable mineralogical composition and because, in many places, of its similarity in appearance to plagioclase-bearing orthopyroxenites of the layered sequence. Because of the nature of the terrain it is not easy to recognise the transgressive nature of the noritic material but, in a few places, where creeks have cut deep channels, exposures are good and the transgressive nature is convincing (Fig. 3.5).

The noritic intrusive is dominantly developed in the northwest of Gosse Pile (Fig. 1.3, C/2) where it forms a sill-like body, dipping at about  $15^{\circ}$ SE. The contact with the granulites is gradational. Xenoliths (up to 40cm in diameter) of acid granulite occur within the norite and these, with increasing distance from the granulite, become more "ghost-like" suggesting reaction with, and assimilation by, the norite. Contact relationships further east are even more complex (e.g. at localities A313/299 and A313/361). There has been partial mobilization of the acid granulite by the norite so that rheomorphic veins of granulitic material (dominantly quartz with K-feldspar and some pyroxene) intrude both the norite and the

associated orthopyroxenite of the layered sequence (Fig. 3.6 and Fig. 3.7). In some areas (e.g. A313/364) the intrusive norite has been locally deformed, producing mylonitic (flow-layered) bands. Along strike these bands pass into areas in which angular blocks of orthopyroxenite (of the layered sequence) are surrounded by intrusive norite and quartz-feldspar-rich rocks, presumably derived from the acid granulites (Fig. 3.8). This is interpreted as being the result of local faulting soon after, or during, intrusion of the noritic material which produced flow-layering in the hot norites, brittle fracture in the layered rocks and enabled the mobilized granulite to intrude such fractures. All of these contact features extend for only a limited distance (5-10m) from the contact and, further east, where brittle faulting has occurred the boundary between granulites and igneous rocks is sharp. Here a fault breccia, about 2m wide, separates the rocks.

Apart from the sill and the irregular, ENE-trending bands of noritic intrusive there also occur related basic pegmatites. These may be either isolated plugs or veins within the layered sequence rocks or they may occur as coarse-grained lenses within one of the noritic bands. They are of two types: pyroxenite or norite. The pyroxenite types, because of their mineralogy, are difficult to detect in the field but a few have been found in the olivine-orthopyroxenite in the N.E. Hills (Fig. 3.9). They consist of large (3-5cm) orthopyroxene crystals with interstitial plagioclase and are usually very weathered. The norite basic pegmatites consist of very

Fig. 3.5

Transgressive nature of the later noritic intrusive near the NW contact of Gosse Pile. The pale material to the left and in the centre of the photograph is norite; the dark material, top and bottom, is strongly laminated orthopyroxenite. Location: A313/353. Scale: 31 cm.

Photograph: A. Moore.

Fig. 3.6

Irregular, transgressive norite, of the later noritic intrusive, occurs to the left of the scale (pale rock). To the right are rheomorphic veins of  $q + K-f + \text{plag} + \text{px}$  (white-weathered rock). The intruded rock (dark) is orthopyroxenite. Location: A313/361, very close to the contact between the granulites and later noritic intrusive rocks. Scale: 31 cm.

Photograph: A. Moore.



Fig. 3.7

Irregular, rheomorphic veins of  $q + K-f + plag + px$  (white) cutting orthopyroxenite (dark) near the contact between the granulites and later noritic intrusive. Location: A313/361. Scale: 31 cm.

Photograph: A. Moore.

Fig. 3.8

Flow-layered band of deformed later noritic intrusive (bottom right) which, along strike, can be traced through a zone of fractured orthopyroxenite and into a zone of angular blocks of orthopyroxenite surrounded by white, quartz + feldspar rock (left). Location: A313/364. Scale: 31 cm.

Photograph: A. Moore.





Fig. 3.9

Transgressive, coarse-grained, friable "pyroxenite-pegmatite" (right of scale). The host rock (olivine-orthopyroxenite) is to the left and the contact between the two rocks is almost vertical; on the photograph it can be traced down the centre and passes through the scale hinge. Location: A313/329. Scale: 31 cm.

Photograph: A. Moore.

Fig. 3.10

Mafic pegmatite, related to the later noritic intrusive. Note the large plagioclase laths with interstitial pyroxene. The white material above and right of the scale is surface magnesite. Location: A313/362. Scale: 31 cm.

Photograph: A. Moore.



Fig. 3.11

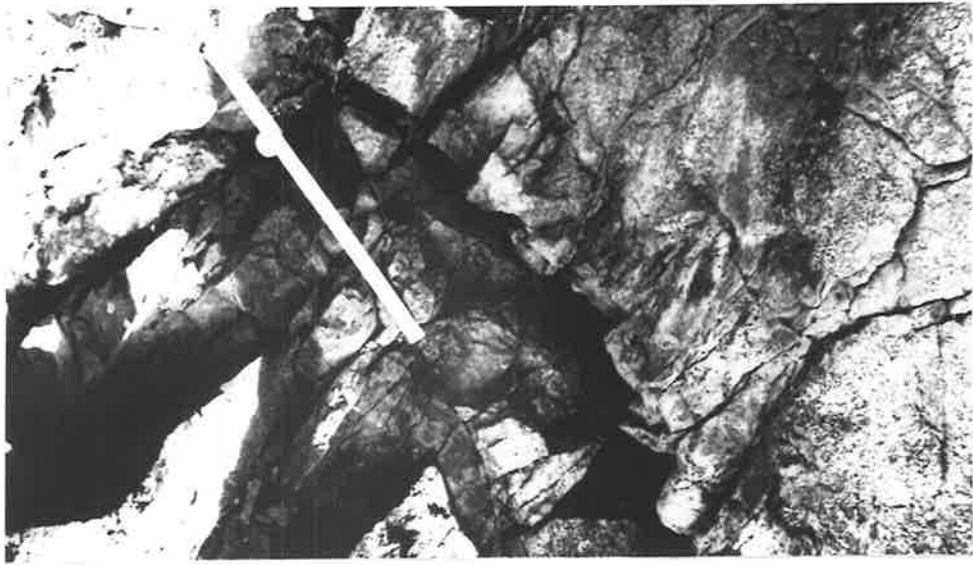
Fault contact between the Gabbro Band (right) and websterite (left). The approximate fault boundary is marked by the position of the scale. Location: A313/375. Scale: 62 cm.

Photograph: A. Moore.

Fig. 3.12

Irregular northern boundary of the Gabbro Band (top and centre) with orthopyroxenite (bottom and right). Note the lens-like nature of the gabbro above (south) of the scale. The white material (bottom right) is surface magnesite. Location: A313/380. Scale: 31 cm.

Photograph: A. Moore.



large plagioclase crystals (up to 40cm long) with coarse (5-6cm) orthopyroxene and some interstitial clinopyroxene, (Fig. 3.10). Undeformed transgressive norite plugs and veins are also found within the layered rocks of the Gneissic Zone and these are correlated with the later noritic intrusive.

The majority of rocks in the Gabbro Band (Fig. 3.1) consist of plagioclase laths with interstitial ortho- and clino-pyroxene. In the west they are very similar in appearance to the intrusive norite bands where subhedral orthopyroxene and interstitial anhedral clinopyroxene occur in a plagioclase matrix. The plagioclase may be lath-like or interstitial. Exposures along the Gabbro Band are poor because of a cover of rubble but, where observed, the southern contact is faulted, dipping  $47^{\circ}\text{S}$  (Fig. 3.11). The Gabbro Band itself contains numerous minor faults, many of which strike parallel to the length of the band and which dip between  $45^{\circ}\text{S}$  and  $50^{\circ}\text{S}$ . Some are closely spaced and give an initial appearance of layering. The northern contact of the band is even more poorly exposed than the southern and has been observed in only a few places. These indicate that the contact between the websterite and gabbro is irregular, with lens-like extensions of gabbro into the websterite (Fig. 3.12). In the central part of one section of the band (A313/2330) an irregular block of websterite, completely surrounded by gabbro, was found. The lens-like nature of the contact and the websterite inclusion could be interpreted as being caused by an "erosional" disconformity as a result of intermittent current action during

deposition of these rocks. However, because of the lack of any preferred orientation in the websterite and gabbro it is more likely that the northern contact is an irregular igneous contact, the Gabbro Band being a later intrusion, and the websterite inclusion is a xenolith. Thus, the field evidence, although not conclusive, suggests that the Gabbro Band is intrusive into, rather than part of, the layered sequence.

Near the southern contact of the Gabbro Band, often involved in the faulting, are occasionally found narrow (3m) elongate lenses of anorthosite.

#### 3.2.4 The dolerites

An approximately SE- to ESE-trending amphibole-dolerite dyke occurs between the Main Body and the Gneissic Zone to the west of Gosse Pile (Fig. 1.3). It is the largest dyke found in the area and has a strong foliation. This foliation (schistosity) is not parallel to either the strike of the dyke nor the foliation in the flanking deformed Gneissic Zone rocks. Several measurements show that this foliation strikes from  $250^{\circ}$  (near the northern contact) to  $260^{\circ}$  (centre) and  $279^{\circ}$  (near the southern contact). The dip is  $80^{\circ}$ S to vertical and, in the plane of the foliation, is a strongly developed lineation plunging  $80^{\circ}$ W. The foliation in the surrounding Gneissic Zone rocks strikes at  $300^{\circ}$ - $310^{\circ}$  and has dips of  $80^{\circ}$ N to vertical (i.e. the strike of the dyke and the foliation in the flanking

pyroxenites are parallel). The field evidence suggests that this dyke has been intruded along a fault zone which separated the rocks of the western Gneissic Zone from those of the Main Body. The discordance between the strike of the dyke and that of the foliation, however, indicate that the foliation is not due to fault movements. There is evidence elsewhere in the Tomkinson Ranges that dykes of this type pre-date the folding of the Giles Complex rocks ( $D_2$ ), (Nesbitt et. al., 1969; A.D.T. Goode, pers. comm.). The foliation in this dyke is therefore possibly related to this deformation and is equivalent to  $S_2$  in the granulites (Sections 2.2 and 2.3). Its development in the dyke and not in the rocks of the layered sequence is probably a function of rock type and temperature of the rocks at the time of deformation.

Elsewhere, throughout Gosse Pile there occur numerous smaller pyroxene-dolerite dykes, some of which are olivine-bearing. These are normally narrow (0.5-3 m) and seldom extend for more than 150m. They are fine- to very fine-grained, massive rocks which are commonly associated with pseudotachylite veins. It is often difficult to distinguish the dolerite and pseudotachylite veins in the field. These younger dykes are generally steeply dipping (vertical to  $70^\circ E$ ) and strike approximately NE or SW, and appear to be related to a NE-SW system of brittle faults.

### 3.2.5 Olivine-gabbro

Mt. Davies, southwest of Gosse Pile (Fig. 1.2), consists of cumulate olivine-gabbro in the area near the Numbunja Pass. No cumulate olivine-gabbro occurs within the Gosse Pile layered sequence but, in the Gneissic Zone, occurs a small (30 m x 15 m), elliptical, relatively undeformed plug of olivine-gabbro (Fig. 1.3, D/3) which, in hand specimen, is very similar to the material from Mt. Davies. Rounded or subhedral olivine occurs throughout and is enclosed by large plagioclase laths and clinopyroxene. Orthopyroxene and oxides are common interstitial phases, though minor in amount. Oxides occur as exsolution products in (as lamellae) and around (as granular particles) olivine, around pyroxene and as discrete grains surrounded by reddish biotite. Within the biotite are also found apatite laths. Most olivine is separated from the plagioclase by a narrow corona which consists of orthopyroxene and green spinel.

Plug-like olivine-gabbros and gabbros have been found elsewhere in the rocks of the Giles Complex and, on the basis of field data collected elsewhere (Ewarara and Kalka) they can be dated as having been intruded at a time intermediate between the intrusion of the dolerite types mentioned above (Nesbitt et. al., 1969). The olivine-gabbro plug in Gosse Pile certainly post-dates the deformation which produced the foliation in the rocks of the Gneissic Zone, and is most likely related to this period of igneous activity rather than to the olivine-gabbro cumulates of Mt. Davies. It is quite possible that a



relationship exists between the later noritic intrusive (which also post-dates the Gneissic Zone deformation), the olivine-gabbro and the picrite intrusions.

### 3.3 TEXTURES

All the rocks in Gosse Pile have been affected by directed stresses at least once in their history. Apart from the production of the tectonic layering (Gneissic Zone) and the later folding about an approximately east-west axis (Sections 2.3 and 2.5) there has been brittle faulting associated with the intrusion of the dolerite dykes, and Gosse Pile has probably also been affected to some extent by the deformation ( $D_3$ ) which folded Kalka, Mt. Davies and Michael Hills (Section 2.5 and Table 1.1). Any interpretation of textural features should take these facts into account.

A variety of textures can be identified, ranging from typically igneous to typically metamorphic, and no sharp boundary exists between these extremes.

#### 3.3.1 Igneous, or Primary, Textures

##### (a) The layered sequence

Wager, Brown and Wadsworth (1960) divided the types of cumulate textures found in layered complexes into several fairly easily recognisable groups. The majority of rocks on the northern side of

Gosse Pile would, according to their scheme, be classed as adcumulates and a few as mesocumulates. Both Hess (1960) and Jackson (1961, 1967) have stressed the importance of the sedimentary-type origin for such rocks, with the cumulus material being analogous to the settled grains and the intercumulus material being analogous to the cement. However, as has been pointed out by numerous authors, the most recent of whom is Cameron (1969), the distinction between primary precipitate and intercumulus material (both pore and reaction material) cannot be made in adcumulates. This problem has led to difficulties in terminology (see Section 3.1) and some authors (e.g. McDonald, 1967) use the term "cumulus" to designate minerals which crystallized above the floor of accumulation as well as the overgrowths on these grains. Since estimates of original porosity of cumulates, hence the volume of intercumulus liquid, range from 20% (Wager and Deer, 1939) to about 45% (Wager, Brown and Wadsworth, 1960), orthopyroxenites containing more than about 80% orthopyroxene indicate the removal of interstices by post-cumulus processes other than just simple crystallization of intercumulus liquid (Cameron, 1969).

The orthopyroxenites and olivine-orthopyroxenites on the north side of Gosse Pile have textures very similar to those of similar rocks from the Stillwater Complex, described and illustrated by Jackson, (1961; for example, Figs. 55, 61, 62, 66 and 68). In rocks with more than 90% orthopyroxene and lacking a preferred orientation the constituent crystals are approximately equidimensional with grain boundaries varying from straight, or gently curved, to serrated.


There is a marked tendency for orthopyroxene boundaries to meet in approximately  $120^\circ$  angles (Table 3.3). The general texture is very similar to that found in some high grade metamorphic rocks (compare Fig. 2.21 and Fig. 3.13) and could be described as equigranular polygonal. With an increase in the proportion of clinopyroxene the texture changes. The relationships between contiguous orthopyroxene crystals remain the same but clinopyroxene commonly occurs along the boundaries between such grains, extending from a position where it occupies space at a triple-point junction (Fig. 3.14). Where clinopyroxene is abundant (> approximately 8%) it often completely surrounds the orthopyroxene which is embayed and rounded (Fig. 3.15). Where this occurs in a laminated orthopyroxenite the enclosed orthopyroxene crystals retain their preferred orientation but they are much smaller than those not in contact with the large clinopyroxene areas.

Plagioclase in the orthopyroxenites and olivine-orthopyroxenites occurs interstitially but, even where large amounts are present (5-10%) it never completely surrounds other phases. Where it occurs in contact with orthopyroxene this latter mineral retains a subhedral shape (Fig. 3.16). Olivine is subhedral to anhedral and, even where the dominant phase (e.g. A313/250, ol = 46.2%) it never completely surrounds the other phases present. When it occurs in relatively small amounts (2-10%) it forms anhedral grains between the orthopyroxene such that the post-cumulus extensions of the olivine (a cumulus mineral) occur between opx-opx grain boundaries, and the

Table 3.3

Measurements of the dihedral angle (Vernon, 1968) in rocks from Gosse Pile.  $\theta$  = dihedral angle. Note: measurements were made using a flat stage so they do not represent true angles.

## IGNEOUS TEXTURES

| Spec. No.<br>A313/- | Phases<br>B-A/A |  | Number of<br>measurements | $\bar{x}$ | s   | Range     |
|---------------------|-----------------|---|---------------------------|-----------|-----|-----------|
| /112                | opx - opx/opx   |   | 99                        | 120°      | 26° | 90°-176°  |
| /112                | cpx - opx/opx   |   | 100                       | 155°      | 30° | 106°-180° |
| /457                | opx - opx/opx   |   | 99                        | 120°      | 12° | 98°-132°  |

## METAMORPHIC TEXTURES (matrix only)

|      |                  |  |     |      |     |           |
|------|------------------|--|-----|------|-----|-----------|
| /99  | opx - opx/opx    |  | 99  | 120° | 13° | 93°-157°  |
| /41  | plag - plag/plag |  | 99  | 120° | 8°  | 105°-142° |
| /100 | cpx - opx/opx    |  | 110 | 123° | 18° | 93°-160°  |
| /218 | plag - px/px     |  | 15  | 95°  | -   | 54°-121°  |

Fig. 3.13

Cumulus olivine and orthopyroxene. Note the approximately  $120^\circ$  triple-point junctions between the orthopyroxene grains and their regular grain boundaries compared with the rounded and indented boundaries against the olivine. A313/457. C.P.

Photograph: A. Moore.

Fig. 3.14

Intercumulus clinopyroxene surrounded by polygonal, cumulus orthopyroxene. Note the caries type texture of the clinopyroxene towards the orthopyroxene crystals surrounding it. A313/87. C.P.

Photograph: A. Moore.

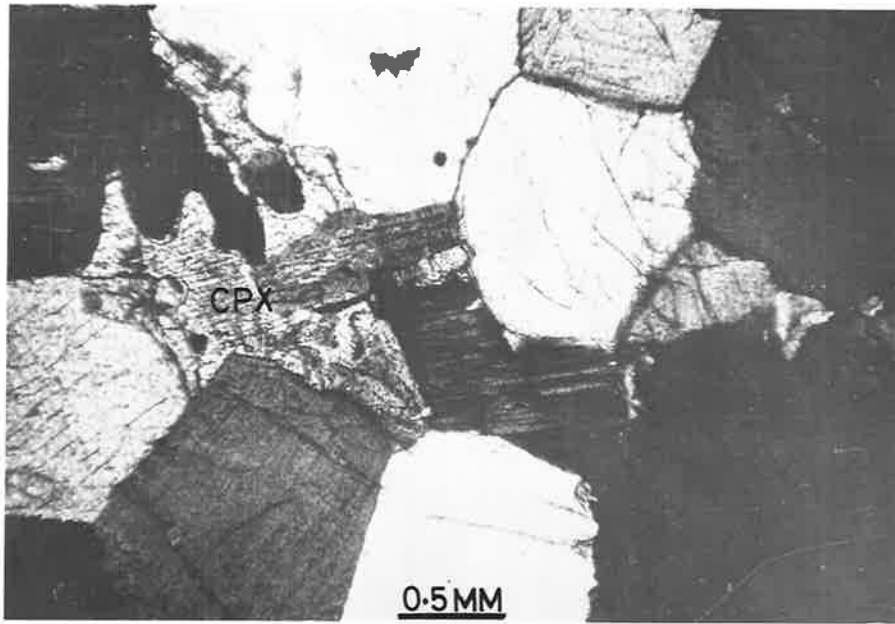
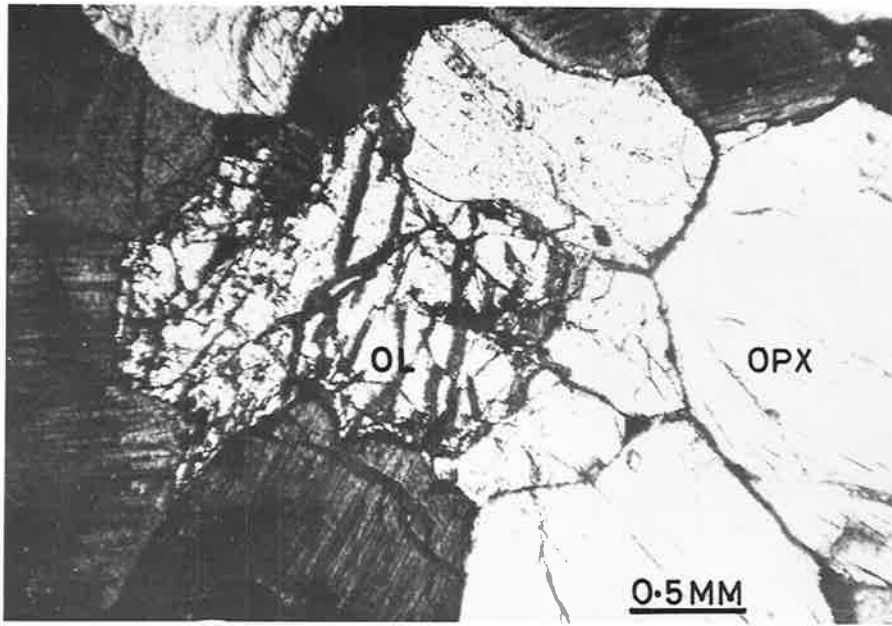


Fig. 3.15

Orthopyroxene completely surrounded and embayed by clinopyroxene, which forms optically continuous crystals, in places showing simple twinning. The distribution of one such crystal has been outlined in ink in the lower photograph; this photograph shows the same thin section but between crossed polars. The inset is a drawing (magnified) from a photomicrograph to illustrate the grain boundary relationships (lined-orthopyroxene; dotted-clinopyroxene) - "replacement" or caries textures.

A313/88. Upper photograph: P.P.L.

Lower photograph: C.P.

Photographs: A. Moore.

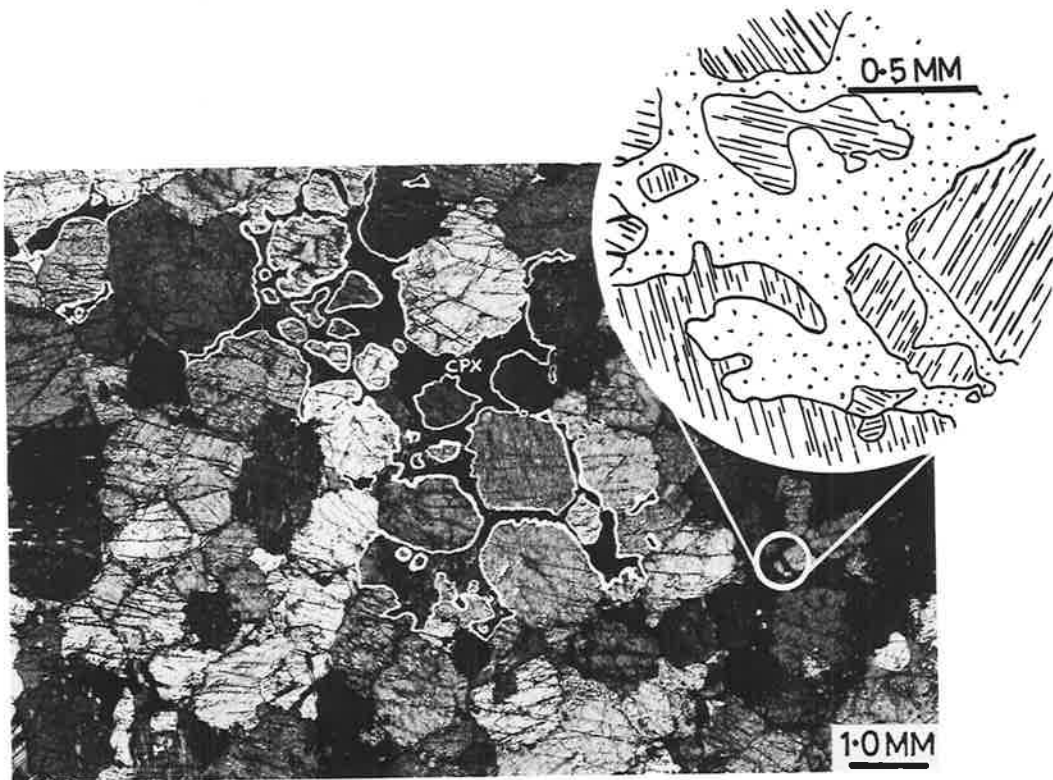
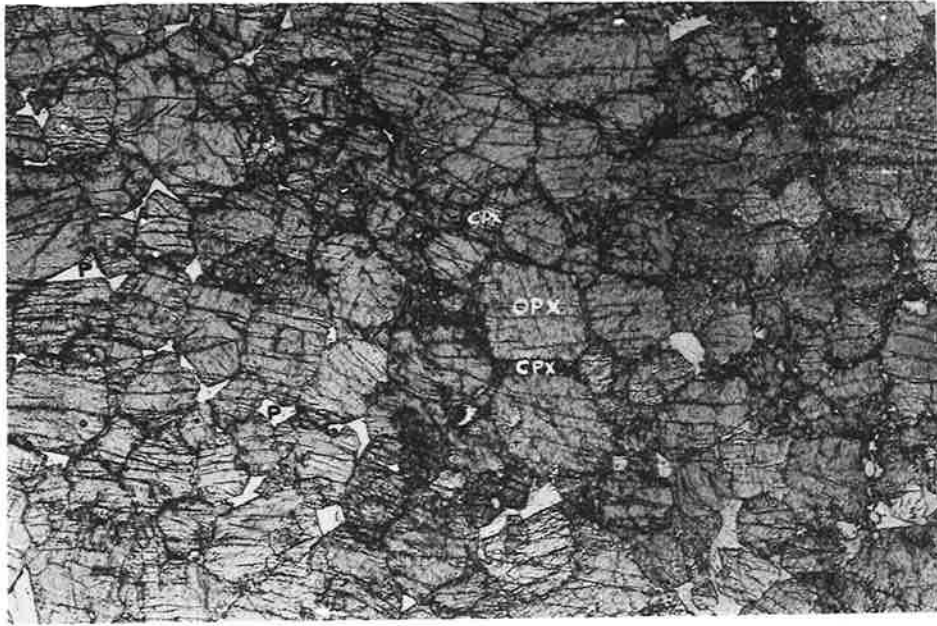




Fig. 3.16

Subhedral cumulus orthopyroxene crystal in contact with  
interstitial plagioclase. A313/60. C.P.

Photograph: A. Moore.

Fig. 3.17

Olivine-orthopyroxene grain boundary relationships. Note the  
extension of optically continuous olivine between orthopyroxene  
crystals. A313/133. C.P.

Photograph: A. Moore.

---

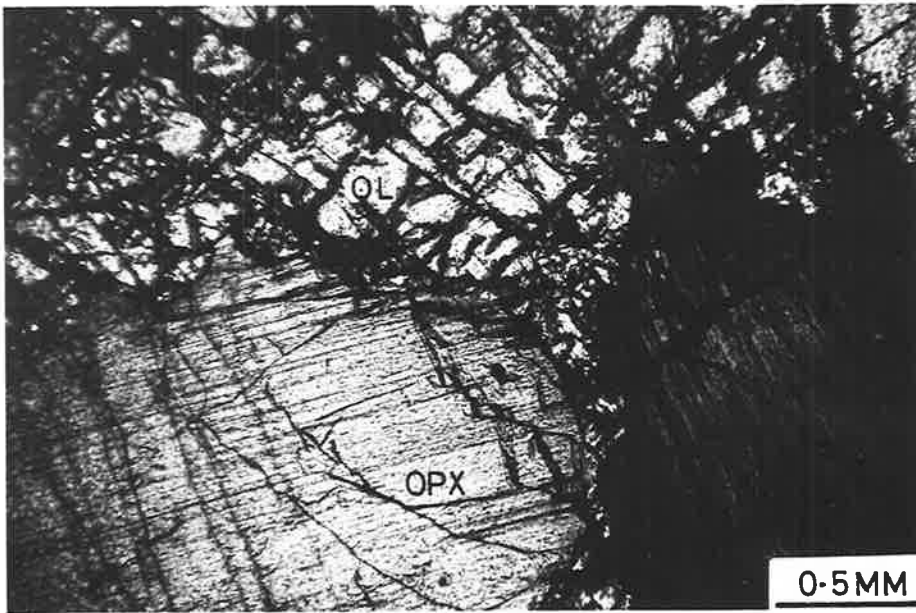
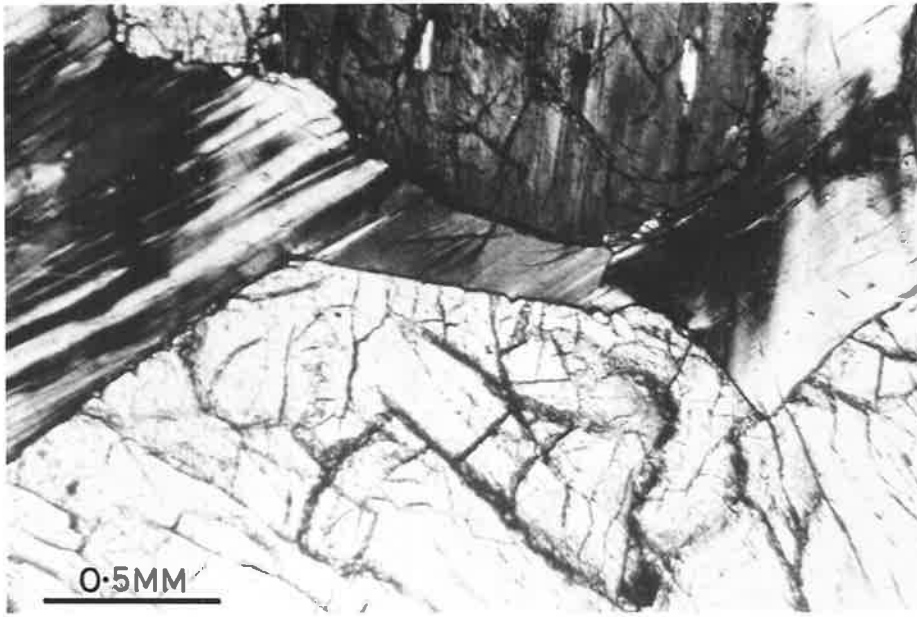


Fig. 3.18

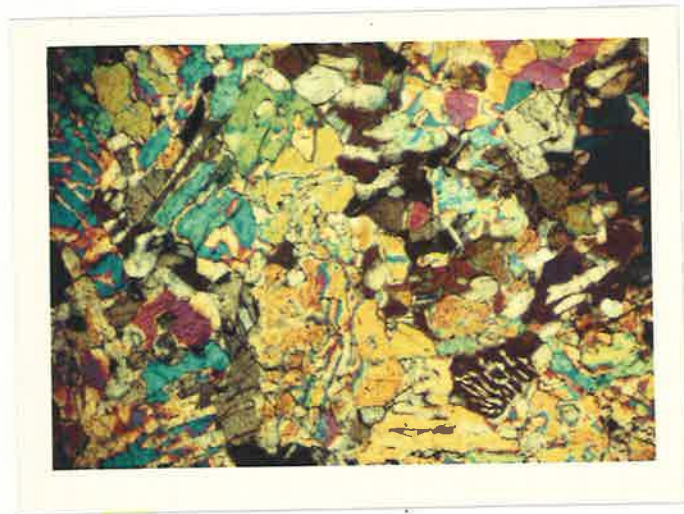
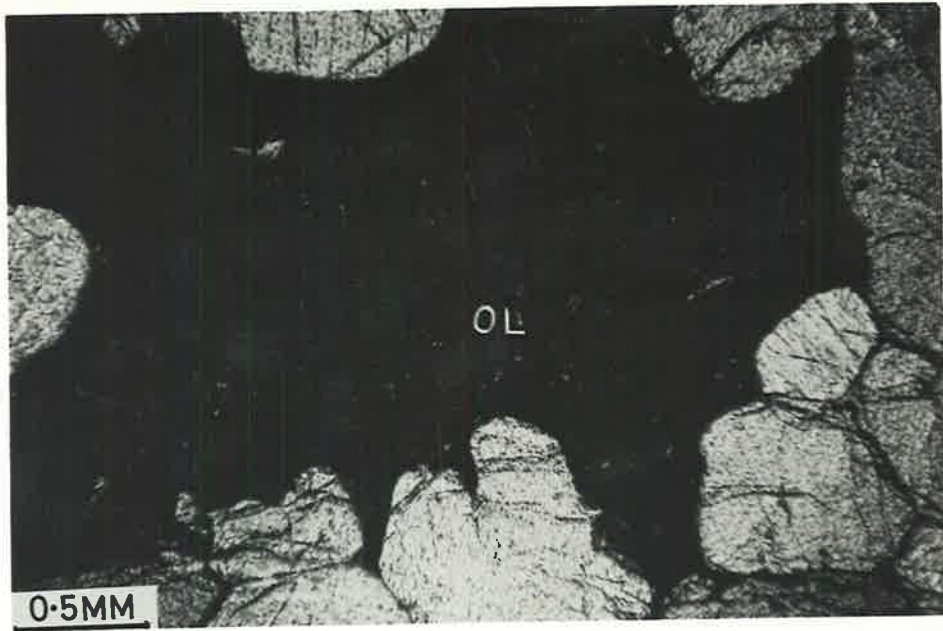
Cumulus olivine surrounded by cumulus orthopyroxene. The boundaries between olivine and orthopyroxene are irregular and concave toward the olivine, while those between orthopyroxenes are regular, straight and tend to terminate in  $120^\circ$  triple-point junctions. A313/32. C.P.

Photograph: A. Moore.

Fig. 3.19

Colour photograph of the complex texture of the northern websterite. The complexity is due to irregular grain boundaries and numerous exsolution features. The only two phases present are ortho- and clino-pyroxene. A313/53. C.P. Magnification: x4.

Photograph: A. Moore.



boundaries between olivine and orthopyroxene are generally concave toward the olivine (Fig. 3.17 and Fig. 3.18). It is only in the olivine-orthopyroxenites that oxide minerals become notable constituents. They occur as exsolution products (green spinel in the pyroxenes; magnetite in the olivine), as numerous crystals of spinel along grain boundaries, and as less abundant cumulus crystals of chromite.

Textures in the northern websterites are difficult to describe because of the large amount of coarse exsolution in both pyroxenes which tends to confuse individual grain boundary relationships. The complexity is best shown by a colour photograph (Fig. 3.19). In general, the rocks consist of equidimensional, anhedral ortho- and clino-pyroxene crystals with no preferred orientation. Other phases (plagioclase and chromite) are rare or absent.

The orthopyroxenites and olivine-orthopyroxenites are considered to represent primary precipitates of orthopyroxene or of orthopyroxene plus olivine. Secondary enlargement of both these phases has taken place which, in most cases must involve expulsion of nearly all of the interstitial liquid. This could take place:

- (i) by compaction;
- (ii) by continued growth of settled crystals as a result of diffusion of elements between intercumulus liquid and the overlying magma (Hess, 1960, p. 113);
- (iii) by enlargement of the crystals at the top of the pile by direct contact with the magma (Jackson, 1961, p. 61); or

(iv) by a combination of these processes.

The amount of intercumulus material now present is variable and this is probably a function both of the degree of secondary enlargement (efficacy of the above processes) and the original amount of interprecipitate liquid. Upton (1961) suggested that strongly laminated rocks would contain less original interprecipitate material than non-laminated rocks because of the closer packing of cumulate crystals as a result of modification by magma flow. This does not appear to be entirely true for the laminated orthopyroxenites in Gosse Pile, and there appears to be as great a variation in the proportion of intercumulus material in these rocks as in the non-laminated orthopyroxenites.

In spite of the existence of orthopyroxene grain boundaries meeting in approximately  $120^{\circ}$  junctions these rocks are thought to be igneous rather than metamorphic because of:

- (i) the interstitial nature of the clinopyroxene which, when present in sufficient amount, poikilitically encloses and "replaces" the orthopyroxene. Similarly, the olivine extends along grain boundaries and appears to be "replaced" by the secondary growth of the orthopyroxene; this is similar to textures in the Stillwater intrusion (Jackson, 1961).
- (ii) the high proportion of elongate orthopyroxene grains, especially in the laminated rocks, is atypical of metamorphic pyroxenes. This is particularly true of the crystals surrounded by clinopyroxene yet retaining their preferred orientation.

The polygonal textures can be explained as being produced by an igneous process whereby grains grew together after expulsion of most of the pore liquid. This growth would be under the influence of interfacial free energy and need not require post-crystallization deformation. It should thus be regarded as a process of static annealing, without prior deformation, the heat being residual from slow cooling of the whole intrusion. This process of grain boundary migration in strain-free aggregates to produce polygonal textures has been experimentally produced in metals (Beck, 1954, p. 270).

Textures such as those illustrated in Fig. 3.15 are not uncommon in cumulates and are generally termed resorption or reaction textures (van den Berg, 1946; Wells, 1952; Jackson, 1961). Since the orthopyroxenes have subhedral outlines where in contact with interstitial plagioclase (Fig. 3.16) but are irregularly embayed when in contact with clinopyroxene it seems reasonable to assume that the clinopyroxene formed as a result of reaction between orthopyroxene and intercumulus liquid whereas the plagioclase did not. There appears to be a similar reaction relationship between olivine and orthopyroxene (e.g. Fig. 3.18). Similar textures have been noted in other layered bodies (Wells, 1952; Jackson, 1961). Such textures are in harmony with the results of experimental work on the system Fo-Di-SiO<sub>2</sub>. These show that the Fo<sub>ss</sub>-En<sub>ss</sub> and the Di<sub>ss</sub>-En<sub>ss</sub> fields are both separated by reaction lines (Kushiro and Schairer, 1963; Boyd and Schairer, 1964) and the Di<sub>ss</sub>-En<sub>ss</sub> reaction line becomes even more noticeable with increase in pressure (Kushiro, 1964; Davis and Boyd,

1966) whereas the  $Fo_{ss}-En_{ss}$  reaction line disappears at very high pressures. Because of the apparent reaction between orthopyroxene and olivine (i.e.  $ol + liquid \rightarrow opx$ ) it suggests crystallization at pressures below those required for the elimination of the incongruent melting of the orthopyroxene. This pressure is estimated at about 6-15 kb for pure enstatite (Boyd, England and Davis, 1964).

Where olivine is poikilitically enclosed by clinopyroxene it forms rounded grains. This is not considered to represent a reaction relationship but is merely a function of grain boundary adjustment to an equilibrium shape. Kretz (1966) and Vernon (1968) have shown that inclusions of one phase within another are commonly rounded as this produces the most stable grain boundary relationship.

(b) The picrite.

The textures of the picrite are identical to those exhibited by olivine heteradcumulates although there is no layering developed which might be interpreted as having been caused by crystal settling. Both the small plugs and the central type picrite of the larger body consist of anhedral to rounded olivine crystals enclosed by large (3-5 cm) poikilitic clinopyroxene, or less commonly similarly sized orthopyroxene. Orthopyroxene and zoned plagioclase occur as interstitial phases (Fig. 3.20 and Fig. 3.21). The picrite is relatively rich in oxide minerals which occur along grain boundaries and as exsolution products. A narrow corona of orthopyroxene



Fig. 3.20

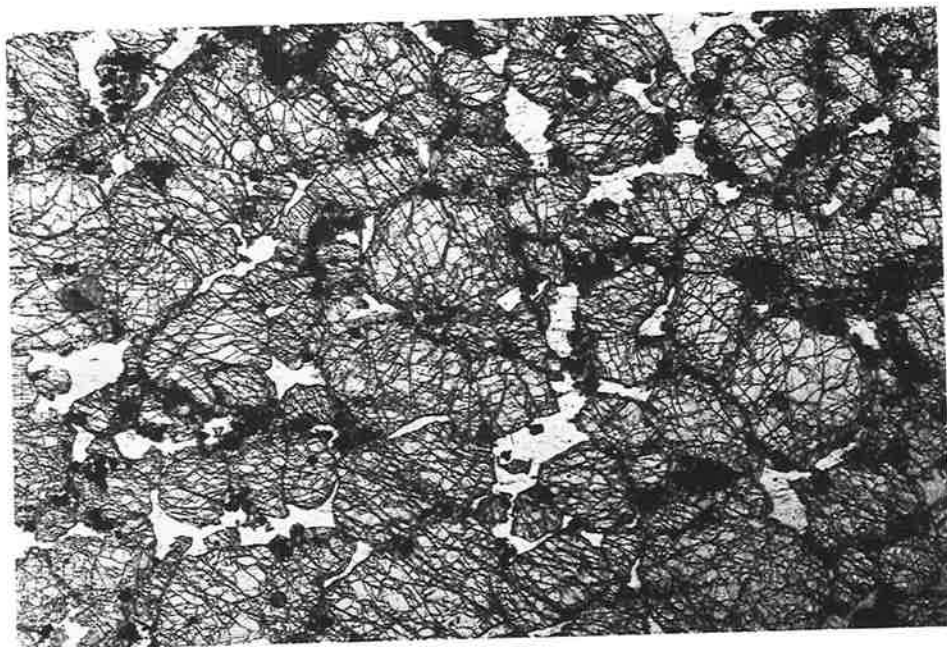
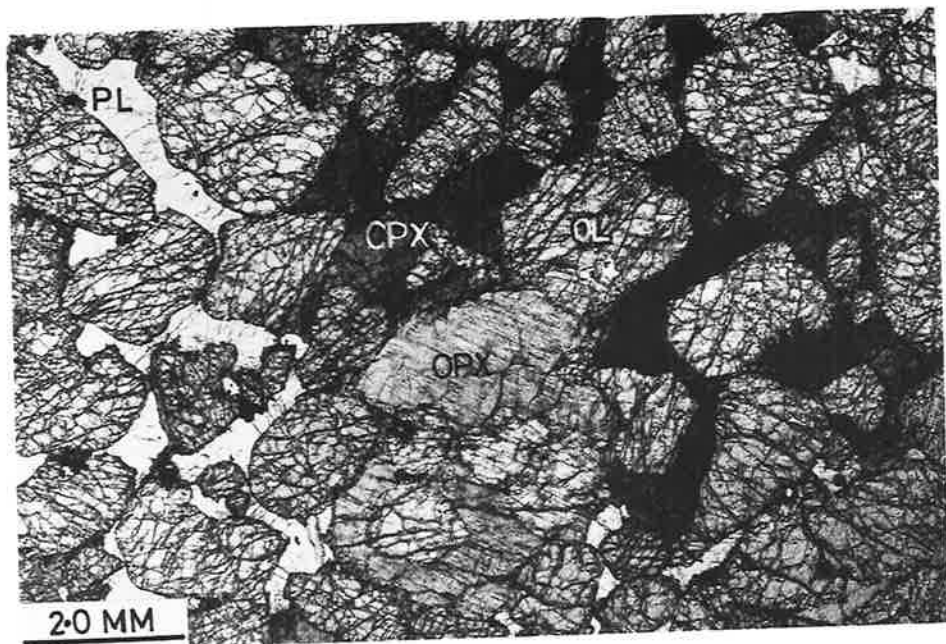
Photomicrograph of the central type picrite showing the rounded olivine grains surrounded by clinopyroxene which is extremely rich in exsolved spinel. A313/199(i). P.P.L.

Photograph: A. Moore.

Fig. 3.21

Photomicrograph of the central type picrite with rounded olivine surrounded by plagioclase. A313/199(ii). P.P.L.

Photograph: A. Moore.



sometimes separates olivine and plagioclase (Fig. 3.22) but in many areas of the same thin section these minerals are in direct contact and no corona has been developed (Fig. 3.23). The marginal type picrite lacks poikilitic crystals. It consists of anhedral or rounded olivine, anhedral to subhedral orthopyroxene and anhedral clinopyroxene in a cumulate-type texture, with interstitial plagioclase, brown hornblende and reddish biotite (Fig. 3.24).

(c) The serpentinite

Two types of texture have been recognised. The less common variety consists of olivine relicts, now completely converted to an unidentified, brown powdery mineral, within a complex network of magnesite veins. Opaque minerals occur scattered throughout. The more common texture consists of a matted network of serpentine veins ("mesh texture") the orientation of which is such that the approximate form of the olivine (and pyroxene ?) crystals which they pseudomorph can be seen. Magnetite octahedra are scattered irregularly throughout the rock.

(d) The noritic intrusive and Gabbro Band

Because of the variety of rock types produced by the noritic intrusive a variety of textures results. The commonest is that of the medium- to coarse-grained norites where subhedral orthopyroxene crystals are surrounded by plagioclase which, although apparently

Fig. 3.22

Corona of orthopyroxene separating olivine and plagioclase in a central type picrite. Similar coronas occur in olivine-orthopyroxenites of the layered sequence. A313/199. C.P.

Photograph: J.D. Kleeman.

Fig. 3.23

Sharp contacts between olivine and interstitial plagioclase with no evidence of corona development in a marginal type picrite. Similar textures occur in the central-type picrite. A313/312E. C.P.

Photograph: A. Moore.

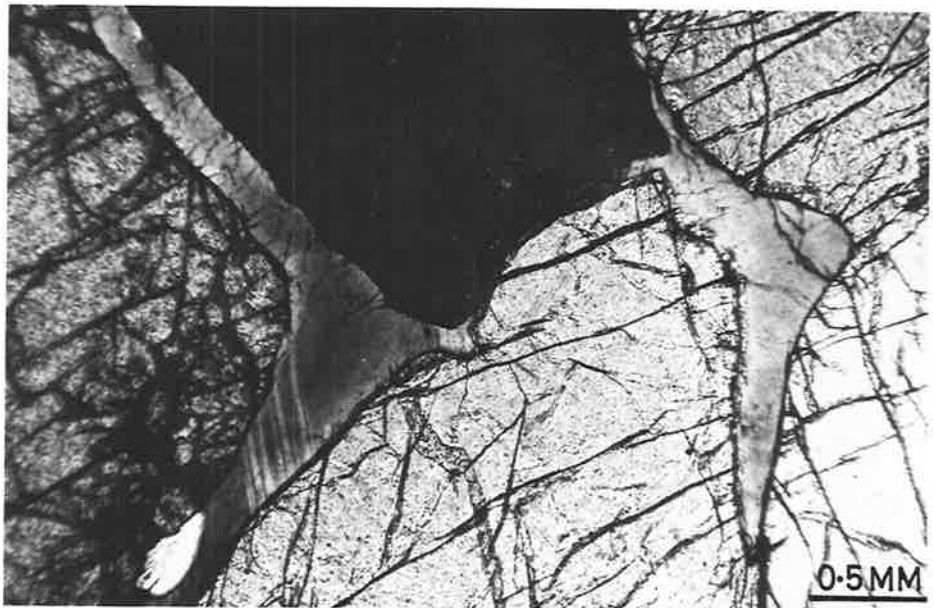
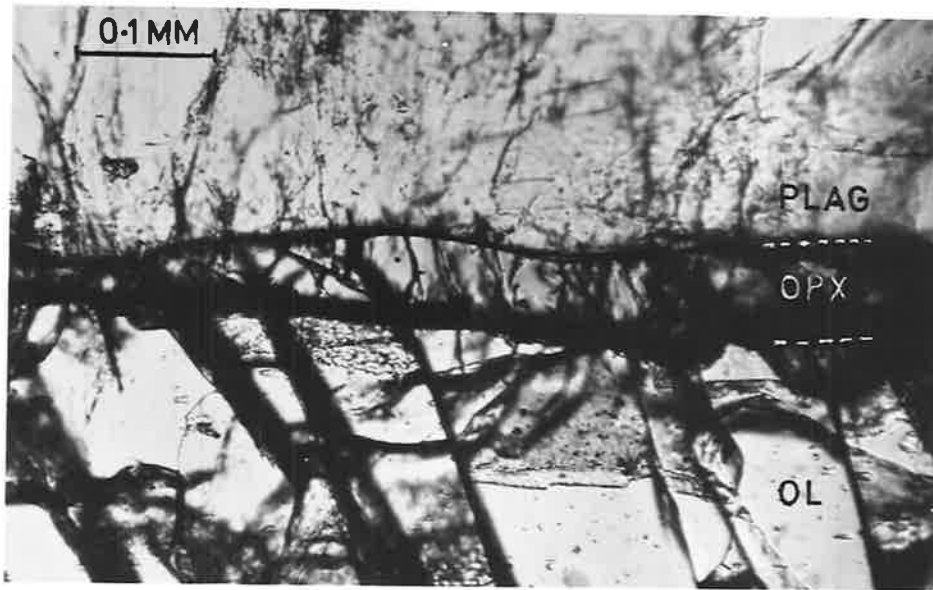


Fig. 3.24

Photomicrograph of the marginal type picrite. A313/312E.

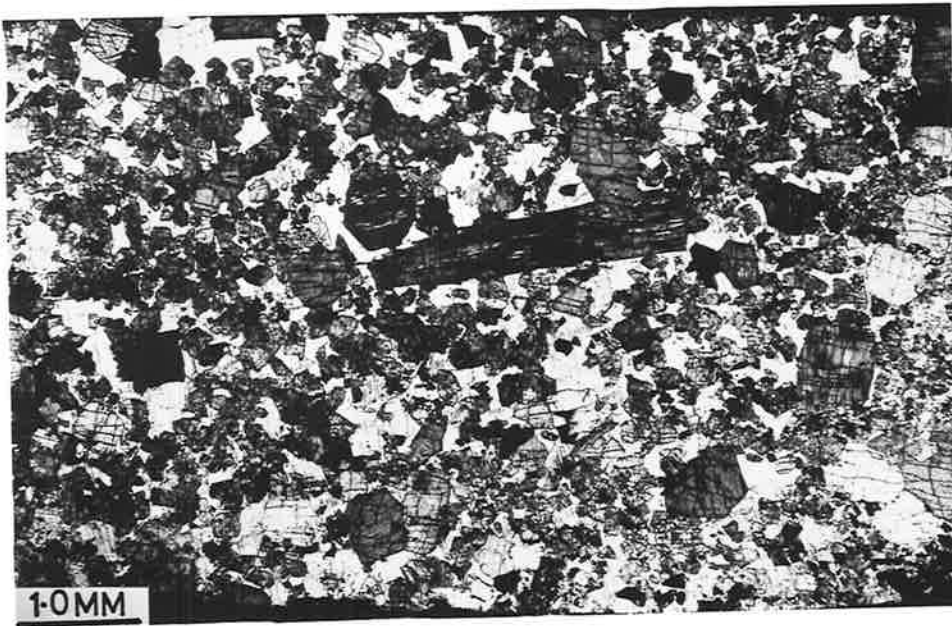
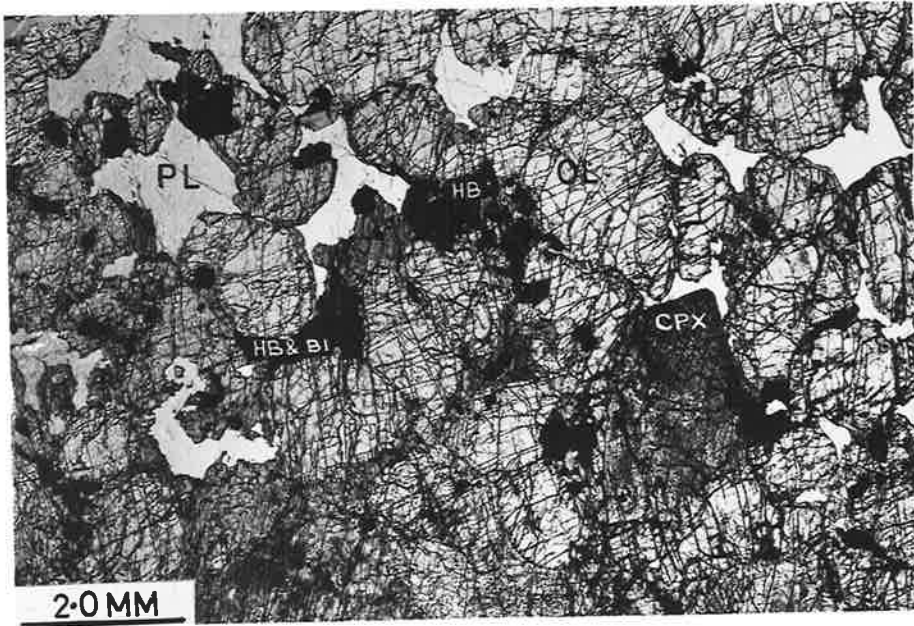
P.P.L.

Photograph: A. Moore.

Fig. 3.25

Photomicrograph of a typical specimen of norite from the later noritic intrusive. Note the subhedral and elongate orthopyroxene crystals surrounded by plagioclase, all of which is in optical continuity. A313/110. C.P.

Photograph: A. Moore.



interstitial, is optically continuous over large areas (Fig. 3.25). Anhedral, granular clinopyroxene occurs interstitially. In the basic pegmatites large (up to 40 cm long) laths of plagioclase are separated by interstitial orthopyroxene and clusters of clinopyroxene crystals. Where pyroxene is the dominant mineral, large anhedral orthopyroxene with interstitial clinopyroxene and some plagioclase form a texture similar to some adcumulates.

The texture of the Gabbro Band is often difficult to observe clearly because of the numerous brittle fracture zones and pseudotachylite veins which distort the original texture. However, in general, it consists of laths of plagioclase, frequently bent, with interstitial and granular pyroxenes (Fig. 3.26 and Fig. 3.27).

(e) The dolerites

The large amphibole-dolerite dyke separating the Main Body and western Gneissic Zone is highly deformed, thus has a metamorphic texture, tending to be mylonitic (Fig. 3.28). The smaller amphibole-dolerite dyke within the Gneissic Zone is far less deformed and has retained its ophitic texture (Fig. 3.29), with plagioclase laths and porphyritic and interstitial clinopyroxene and green hornblende. The younger pyroxene-dolerite dykes are very fine-grained, ophitic, with porphyritic ortho- and clino-pyroxene, plagioclase laths, abundant oxides and, rarely, olivine. Where olivine occurs it is always separated from the plagioclase by a double corona of



Fig. 3.26

Photomicrograph of a thin section from the Gabbro Band,  
showing the interstitial nature of the orthopyroxene.

A313/12. Partly crossed polars.

Photograph: A. Moore.

Fig. 3.27

Photomicrograph of a thin section from the Gabbro Band.

A313/233B. P.P.L.

Photograph: A. Moore.

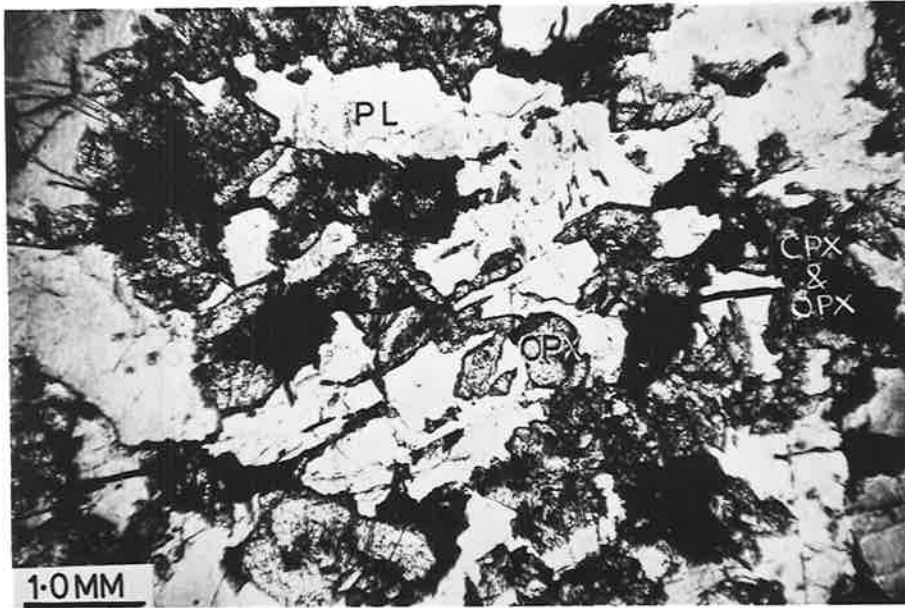
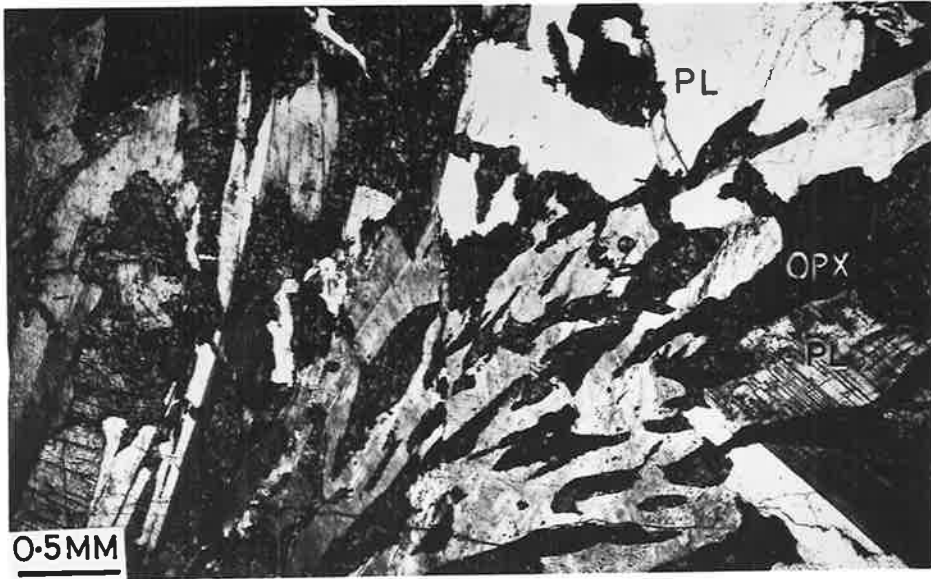


Fig. 3.28

Photomicrograph of a thin section from the large amphibole-dolerite dyke which occurs between the Main Body and Gneissic Zone.

A313/419. C.P.

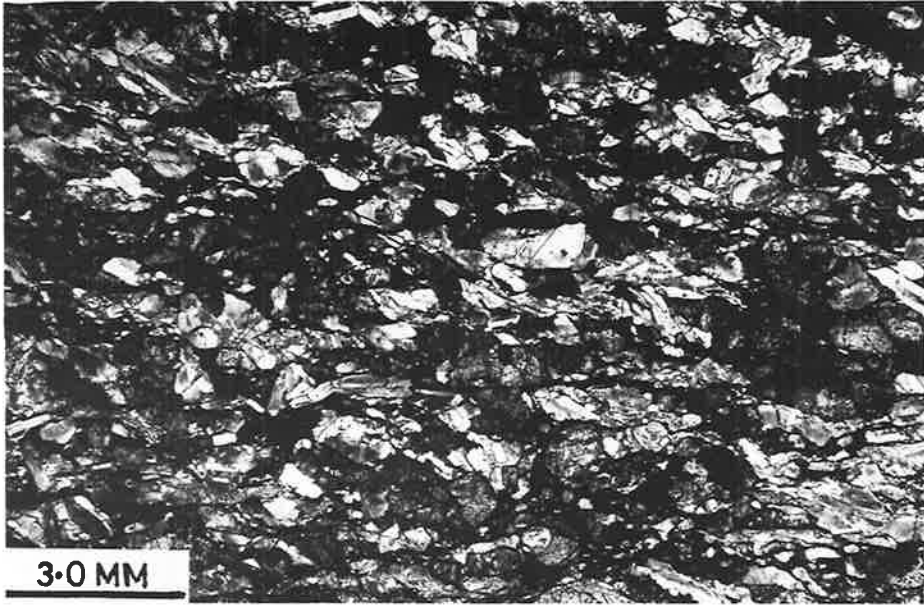
Photograph: A. Moore.

Fig. 3.29

Photomicrograph of a thin section from an amphibole-dolerite dyke which occurs within the Gneissic Zone. It is only slightly deformed and has largely retained its ophitic texture.

A313/470. C.P.

Photograph: A. Moore.



orthopyroxene plus spinel, similar to those described by Mason (1967).

(f) The olivine-gabbro

The single, elliptical plug of olivine-gabbro in the Gneissic Zone has a texture indistinguishable from the cumulate olivine-gabbros from south Mt. Davies. The texture tends to be xenomorphic granular, with large plagioclase laths enclosing rounded or subhedral olivine and separated from it by a narrow corona (of opx + sp?). Angular clinopyroxene tends to have an ophitic relationship towards the plagioclase and sometimes encloses small plagioclase laths. Orthopyroxene is subhedral, except where embayed by clinopyroxene.

### 3.3.2 Metamorphic, or Secondary, Textures

The rocks of the Gneissic Zone have textures which are characteristic of metamorphic rocks and, as such, could be classed as granoblastic polygonal inequigranular (Fig. 2.17). Pyroxenites consist of a fine-grained matrix (average grain size about 0.5 mm) of clino- and ortho-pyroxene, or of orthopyroxene alone, in which grain boundaries are straight and tend to meet in equilibrium angles of  $120^{\circ}$ . Within this matrix occur megacrysts which show strain shadows and are frequently kinked or bent. Finer grains have often developed internally along kinks or where the crystal is severely bent (Fig. 3.33). The megacrysts are always orthopyroxene, even in websterite. In the plagioclase-rich rocks the matrix consists of

equidimensional, polygonal plagioclase crystals which have a strong preferred orientation. The pyroxene forms either composite clusters (cpx + opx) (Fig. 3.30) or sliver-like, bent grains (opx), or augen which sometimes have "tails" of finer-grained pyroxene crystals (opx augen and tails of opx with minor cpx), see Fig. 3.44, Section 3.4.2. Even where plagioclase is a relatively minor constituent it forms lens-shaped clusters of polygonal grains which have a strong preferred orientation. The polygonal nature of the annealed matrix is shown in Fig. 3.31.

The change from igneous to metamorphic textures is gradational, with the proportion of matrix to relict megacrysts decreasing with increasing distance north of the Gneissic Zone. The approximate position where original igneous textures are first affected by the tectonic activity which has produced the Gneissic Zone textures is marked in Fig. 3.1 as the "approximate northern limit of annealed rocks". Rocks within the Gneissic Zone itself show the strongest development of metamorphic textures. The changes are most conveniently shown by a series of photomicrographs of orthopyroxenites collected at varying distances from the southern contact, Fig. 3.32 and Fig. 3.33. The first indication of the changes involved is the formation of strain-free, polygonal matrix grains between larger, slightly strained parent grains (megacrysts). In all cases the matrix grains are essentially strain-free and where they do show strain effects these can be correlated with later, local brittle faulting. In all cases the megacrysts show signs of strain, the effects of which are more

Fig. 3.30

Polygonal granoblastic texture of a norite from the Gneissic Zone. The pyroxenes form a composite cluster. A313/273. P.P.L.

Photograph: A. Moore.

Fig. 3.31

Polygonal nature of annealed matrix grains.  
A313/91. C.P.

Photograph: A. Moore.

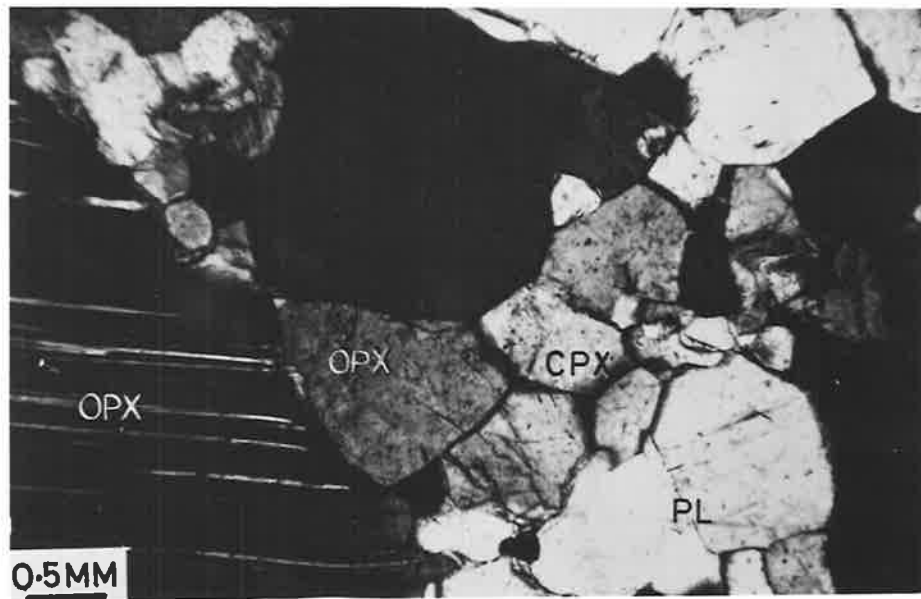
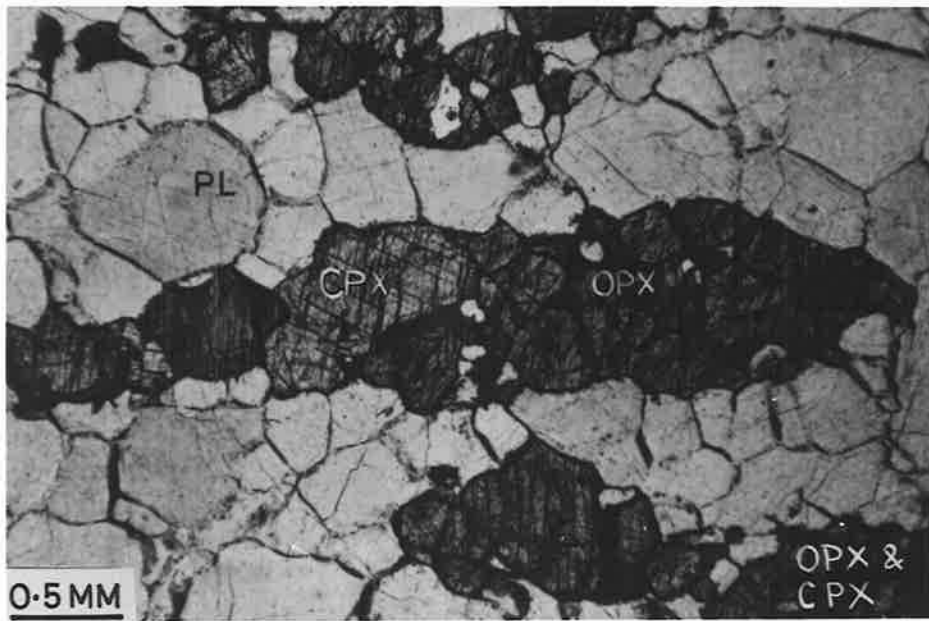




Fig. 3.32

A series of photomicrographs showing the change in texture of orthopyroxenites with increasing proximity to the southern contact. All photographs are the same scale; the upper part of each is in plane polarized light and the lower part is between crossed nicols. H = hole in slide.

A313/105

Approx. 0.95 km north of the southern contact. Typical adcumulate igneous texture. Brittle fracture has caused some deformation.

Approx. northern limit  
of annealed rocks.

A313/103

Approx. 0.7 km north of the southern contact. Subgrain growth (matrix) now apparent but of limited extent.

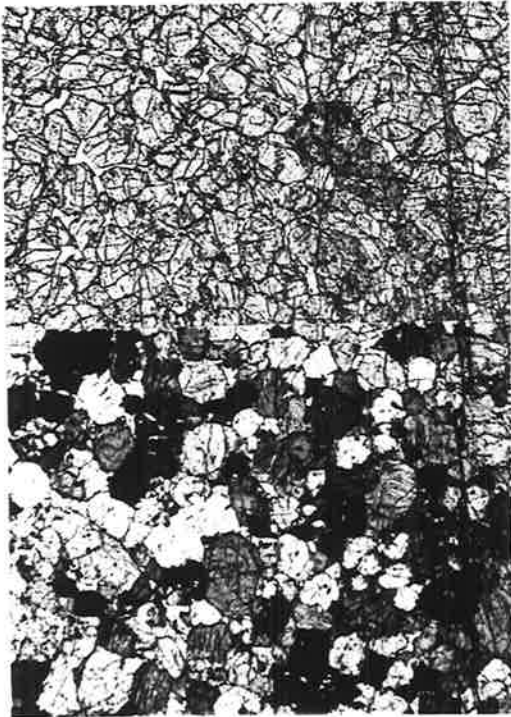
A313/101

Approx. 0.5 km north of the southern contact. Proportion of remnant megacrysts and annealed matrix approximately equal. Note preferred orientation of megacrysts.

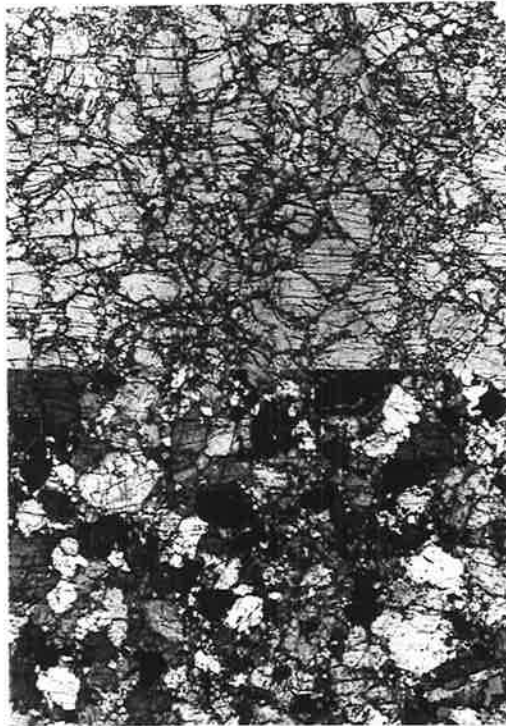
A313/99

Approx. 0.3 km north of the southern contact. More than half the rock consists of annealed matrix.

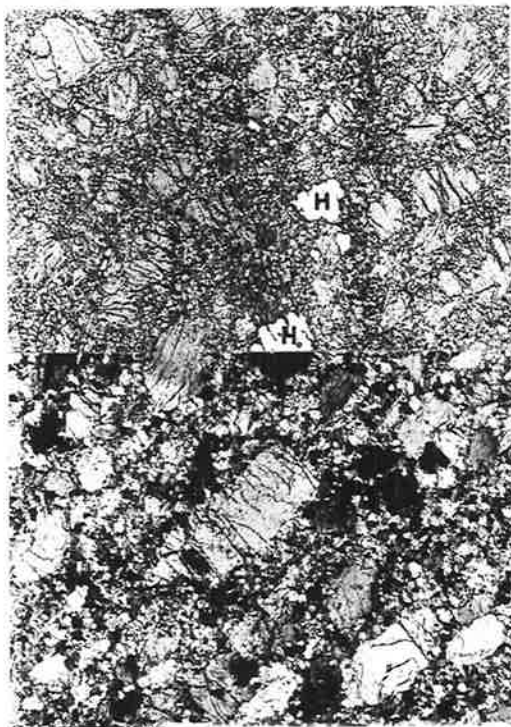
Photographs: A. Moore.



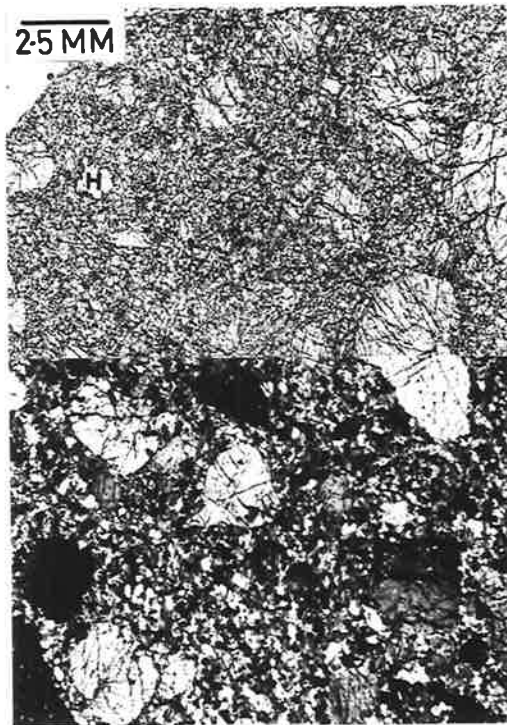
A313/105



A313/103



A313/101



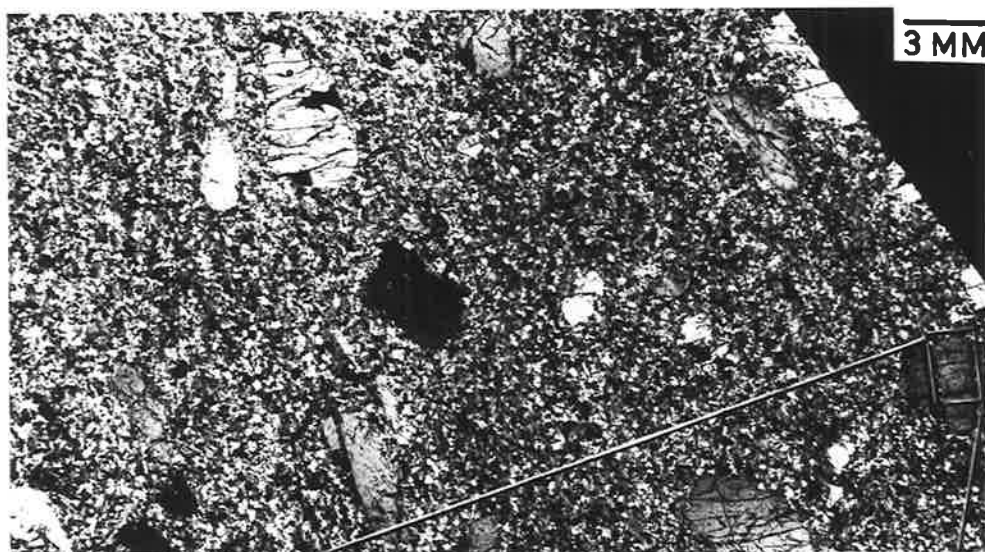
A313/99

Fig. 3.33

Photomicrograph of an orthopyroxenite approximately 0.1 km from the southern contact. More than 80% of the rock consists of annealed matrix.

Enlargement shows the development of subgrain growth along kink-band boundaries in a megacryst. C.P.

Photograph: A. Moore.



A 313/226



marked in the more southerly specimens. Within the matrix, flat-stage measurements indicate a very strong tendency for grains to meet in  $120^\circ$  angles (Table 3.3). All rocks have a mineralogy consistent with their igneous parentage and with the granulite facies of metamorphism (opx + cpx + plag), although the deformation which produced the Gneissic Zone post-dated the regional granulite facies metamorphism. There is no indication of the formation of hydrous phases. Temperatures were probably high as a result of residual heat from the partially cooled, but fully crystalline, igneous intrusion.

During the syntectonic annealing of metals and natural geological samples in the laboratory, textures similar to those illustrated in Fig. 3.31 and Fig. 3.33 have been produced (see pp. 39-42, this thesis). By comparison with experimentally deformed and annealed material it is thought that similar processes have operated in the Gosse Pile rocks. With increasing deformation an increasing number of dislocations are trapped at subgrain boundaries which are then converted into normal high angle boundaries (i.e. the degree of disorientation across the boundary exceeds  $10^\circ$ ). As the disorientation between subgrains (daughter grains) increases, the interfacial surface energy increases allowing the grain boundaries to adjust and meet in  $120^\circ$  triple-point junctions. Smith (1948) indicated that the  $120^\circ$  grain boundary angles (dihedral angle) result from static balance of three equal interfacial tensions. In rocks containing relatively high proportions of clinopyroxene (e.g. A313/64, 22% cpx) the clinopyroxene is commonly found as composite clusters of polygonal grains (about 5 mm in

diameter), each cluster containing only a few orthopyroxene crystals. These are likely to represent a previous poikilitic clinopyroxene which has annealed to a composite mass of crystals. If this is true then it indicates that there has been little transport of materials during the annealing processes.

The textures of the rocks on the southern side of Gosse Pile strongly suggest that annealing processes have occurred at least to the stage of primary recrystallization (see pp. 39-42, this thesis). This is recognised by the presence of the large, strained orthopyroxene megacrysts in an essentially strain-free matrix. Within the matrix some grain growth has probably occurred, resulting in equilibrium angles between grains (Fig. 3.30 and Fig. 3.31) but the stage of secondary recrystallization has not been reached, as indicated by the lack of strain-free porphyroblasts. Plagioclase and clinopyroxene are never found as megacrysts, hence it is concluded that these minerals underwent the process of annealing more readily.

In keeping with observations on experimentally annealed materials and metals which indicate that primary recrystallization is enhanced by an increasing amount of strain, and that new grains form preferentially in regions of local stress concentrations (grain boundaries, kink bands), it is concluded that the amount of stress in the rocks of south Gosse Pile decreased from south to north. The temperature across this relatively narrow zone is not expected to have varied much, so that differences in the degree of annealing (as

indicated by the proportion of matrix to megacrysts) are thought to be due to differences in the amount of strain. Because of the long times involved during geological deformation it is probable that primary recrystallization of strained grains could occur during the deformation (assuming a sufficiently high temperature) and, under such conditions, work-hardening is absent so that the deformation could take place under constant stress. By comparison with experimental work, textures such as those observed in the matrix can be produced either by deformation followed by a period of static annealing, or by syntectonic annealing (creep). Because of the development of a strong preferred orientation in the polygonal, equidimensional plagioclase grains, the latter alternative is favoured (see Sections 2.6 and 2.8 for discussion of this).

In the field the Gneissic Zone of Gosse Pile can be traced westwards through similarly deformed rocks cropping out in the Scarface Jasper Zone (Fig. 1.2) and along the "gabbro gneiss" on the south and N.E. side of Kalka (Dulgunja Hill, Fig. 1.2), (Nesbitt et. al., 1969; Goode and Nesbitt, 1969). It is thought likely that Gosse Pile and Kalka were once part of the same intrusion and have been tectonically separated. Part of this separation probably took place by faulting, now marked by gneissic zones, soon after crystallization. This faulting pre-dated the folding of the layered bodies into their present near-vertical positions (Nesbitt et. al., 1969) and so consisted of low-angle thrusts almost parallel to the igneous layering. The "gabbroic gneisses" of the layered bodies

have no obvious equivalent in the granulites but some of the flaser-mylonites (such as those found south of Gosse Pile, p. 28) may represent the manifestation of this deformation in the granulites. If the thrusting involved gradual movement (stable sliding) rather than sudden movement (stick slip) with constant stress and low strain rates under high confining pressure (Byerlee and Brace, 1968), then it is probable that the amount of strain within the igneous rocks would gradually diminish away from the locality of the fault plane(s). This is consistent with the development of the textures described above. The thrust was probably located very close to the present southern margin of Gosse Pile, though later deformations have produced faults (Hinckley mylonite zone, Numbunja Creek fault) which form the present boundary.

An interesting fact emerges from this textural study, concerning the behaviour of plagioclase, clino- and orthopyroxene under conditions of high confining pressure, high temperature and relatively low strain rate. Under these conditions it appears that plagioclase and clinopyroxene are the more ductile, deforming by "intracrystalline flow" (slip along glide lamellae, subgrain formation, dislocation climb and Nabarro-Herring diffusion), whereas orthopyroxene, although deforming in a similar way, appears to be more brittle and forms the relict megacrysts which are bent and kinked. Experimental work by Borg and Handin (1966) showed that under low confining pressures (1 kb) and temperatures (150°C) with high strain rates (1%/min) orthopyroxene showed no evidence of intracrystalline flow, while



clinopyroxene and plagioclase deform elastically or fracture. This confirms the observations of Prinz and Poldervaart (1964) on dolerite mylonites. They note that while plagioclase is brittle (i.e. elastic deformation followed by fracture) the pyroxenes are ductile. Experimental work by Riecker and Rooney (1966), with constant strain rates of  $10^{-1}$ /sec, under P-T conditions approximating those of the granulite facies (i.e. 900°C/10 kb) and greater (up to 900°C/39 kb), has shown that "intragranular flow" begins only at about 30 kb normal pressure. It would appear that, under the much lower strain rates assumed for the Gneissic Zone rocks, the minerals behave in a ductile manner at very much lower pressures. The reversal in behaviour of orthopyroxene and the other phases is probably also due to the difference in strain rate and also because other processes, other than strictly physical, may become important (e.g. chemical redistribution).

### 3.4 LAYERING

Within Gosse Pile two main types of layering have been recognised. The first is primary layering ( $S_i$ ) and results from various igneous processes. The second is secondary layering ( $S_t$ ) and has been produced as a result of tectonic processes.

### 3.4.1 Primary Layering (S<sub>1</sub>)

#### Phase layering and related features

The most obvious type of layering is that which produces the different rock types within the cyclic units (Table 3.2). In the north this can be seen to be caused by the appearance or disappearance of a cumulus phase, and a similar mechanism is presumed to have operated in the production of the major lithological boundaries in the deformed southern and western parts of Gosse Pile (Fig. 1.3). This type of layering is called phase layering (Hess, 1960), or isomodal layering (Jackson, 1967). Each layer is separated from the one below by a sharp contact, termed a phase contact (Jackson, 1967). With the exception of the olivine-orthopyroxenites in the N.E. Hills there appears to be little variation in either the mineral proportions or sizes in the field. However, modal analyses (Appendix 1) show that, in the websterite samples, the proportion of clino- to ortho-pyroxene can vary significantly. Thus, within each band (phase layer) there probably exists a subtle layering caused by variations in the proportions of cumulus minerals and variations in the proportions of cumulus to intercumulus phases. Because of the apparent uniform nature of the rocks in the field this variation cannot be readily detected and its exact nature has not been determined. However, it is probably the equivalent of Wager and Deer's (1939) rhythmic layering although it is not known whether the variations are regular, sharp or mineral graded. Mineral grading would not be expected because of the similar densities of the pyroxenes.

In the olivine-orthopyroxenite of the N.E. Hills there is a general tendency for the olivine content to decrease southwards, but rhythmic layering has not been observed. The phase contact between this rock type and the overlying orthopyroxenite is sharp and easily determined in the field. On weathered surfaces the olivine-orthopyroxenite shows an apparent layering (Fig. 3.34) which can be measured. Large thin sections of this rock reveal no obvious causes for the layering (mineral size and distribution is regular) and measurements show no obvious preferred orientation of the minerals (Fig. 3.35). The layering must be caused by subtle differences in the rock which the author is unable to detect. It may not be a primary feature but related to later tectonism.

On the south side of the N.E. Hills a series of minor parallel ridges (0.5 m high) give the impression of layering. Specimens collected from the "valleys" and the ridges show the only detectable difference to be that samples from the "valleys" contain more microscopic fracture zones along which weathering has been more active. This is probably the result of tectonism, such as may have accompanied the production of the east-west striking faults, rather than a feature resulting from primary deposition. Similar features have not been observed in other phase layers, although the apparent layering (Fig. 3.34) may have a similar origin.

Fig. 3.34

Apparent layering in an olivine-orthopyroxenite.

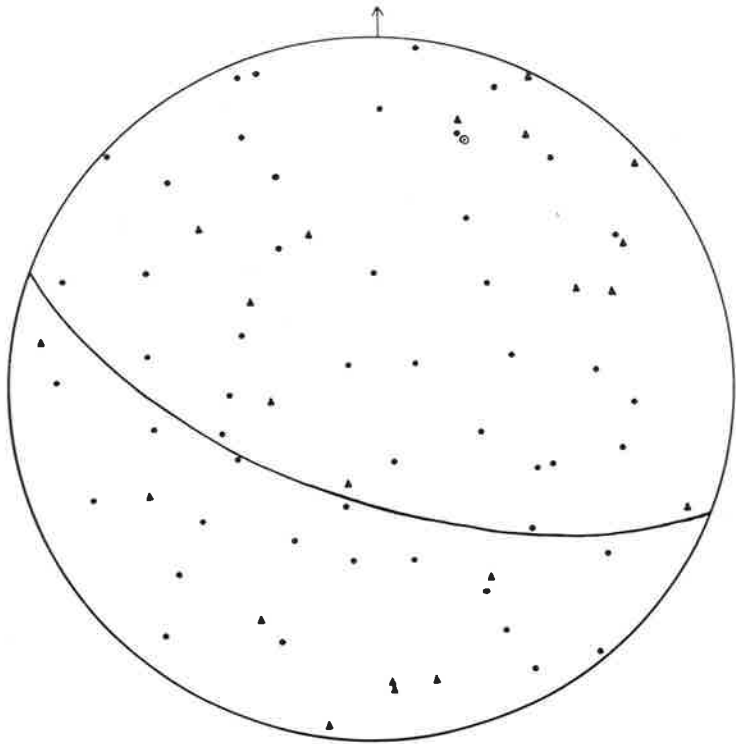
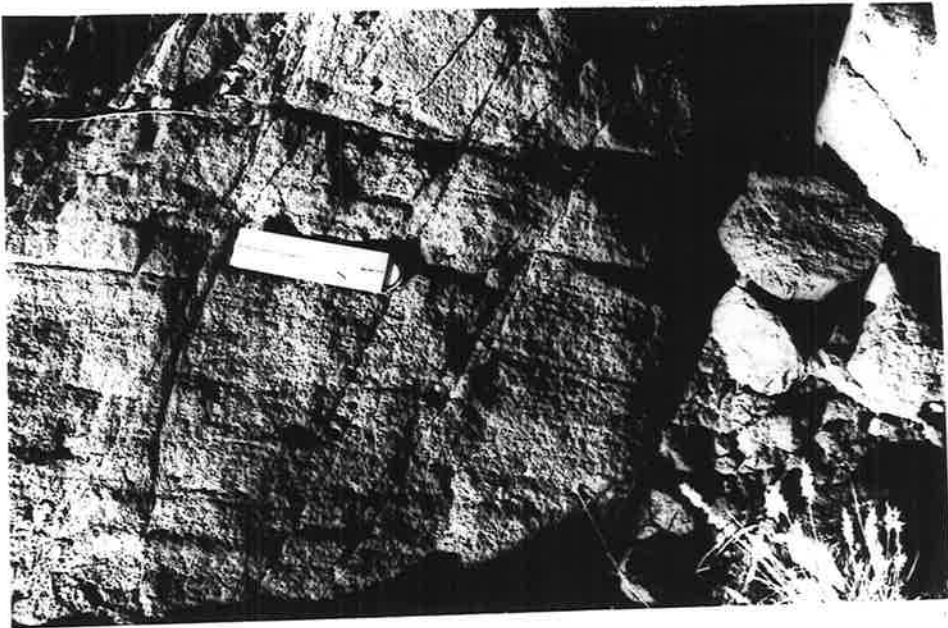
Location: A313/328A. Scale: 15.5 cm.

Photograph: A. Moore.

Fig. 3.35

Petrofabric diagram of the optic constants of 50 olivine grains from olivine-orthopyroxenite. A313/328A.

⊙ =  $\alpha$     $\blacktriangle$  =  $\gamma$  .   ⊙ = pole to the layering measured in the field (great circle) which has an orientation  $289^{\circ}/65^{\circ}\text{S}$ . The primitive is horizontal and the arrow indicates true north.



## Igneous lamination

This type of layering, named and described by Wager and Deer (1939) from Skaergaard, is caused by the arrangement of tabular crystals with their shortest axes perpendicular to the plane of the layering. Jackson (1967) terms this planar lamination and contrasts it with lineate lamination where there is a linear parallelism within the cumulate. Planar lamination is commonly well developed in layered intrusions and is generally best developed in the plagioclase-rich rocks (e.g. in Skaergaard - Wager and Deer, 1939; Stillwater - Hess, 1960, and Jackson, 1961; in the Gardar Province rocks - Ferguson and Pulvertaft, 1963; Rhum - Brothers, 1964; the Somerset Dam intrusion - Mathison, 1967). Planar preferred orientation of orthopyroxene in gabbro and in pyroxenite from the Bushveld Complex (van den Berg, 1946) and in bronzitites from the Stillwater Complex (Jackson, 1961) has been noted. Brothers (1964) has described a strong planar preferred orientation of olivine crystals from Rhum and Skaergaard. Lineate lamination, however, appears to be a relatively rare feature or, when it does occur, it is only weakly developed (e.g. Wager and Deer, 1939; van den Berg, 1946; Jackson, 1961).

The orthopyroxenites which crop out in the west of the Main Body (Fig. 1.3, C/2) show a very strong lamination, both in hand specimen and thin section (Fig. 3.36). It was hoped that a petrofabric study of these rocks would show several features (as suggested by Jackson, 1961):

Fig. 3.36

Photomicrographs of a thin section from an orthopyroxenite (A313/112) showing well developed lineate lamination and consisting of approximately 98% orthopyroxene. Note the elongate nature of most of the orthopyroxene crystals and, although grain boundaries are relatively irregular, for crystals to meet in approximately  $120^\circ$  triple-point junctions.

TOP: Thin section in  $45^\circ$  position.

BOTTOM: The same section in  $0^\circ$  position.

C.P.

Photograph: A. Moore.

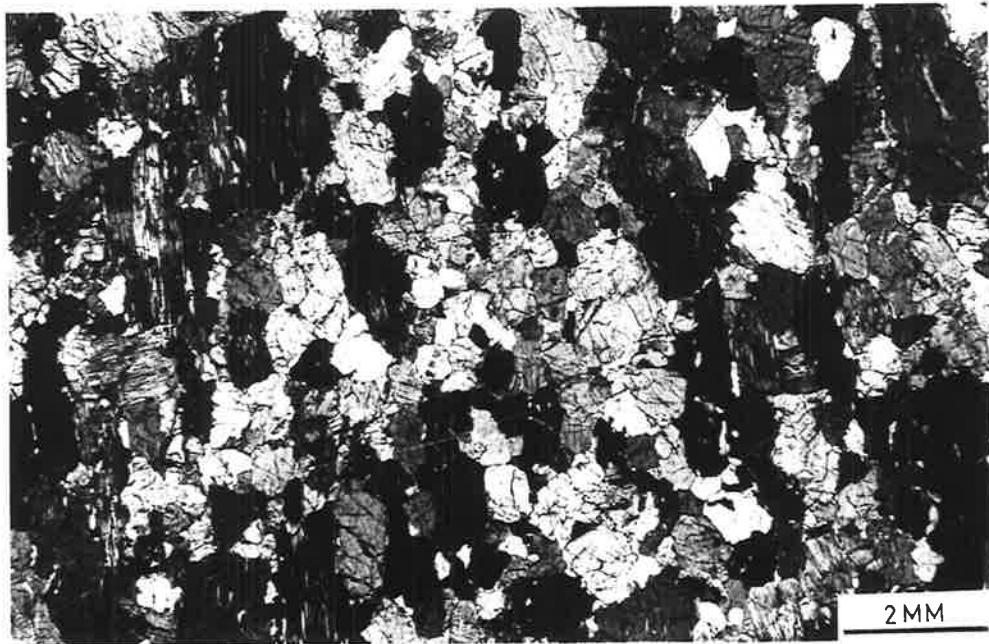
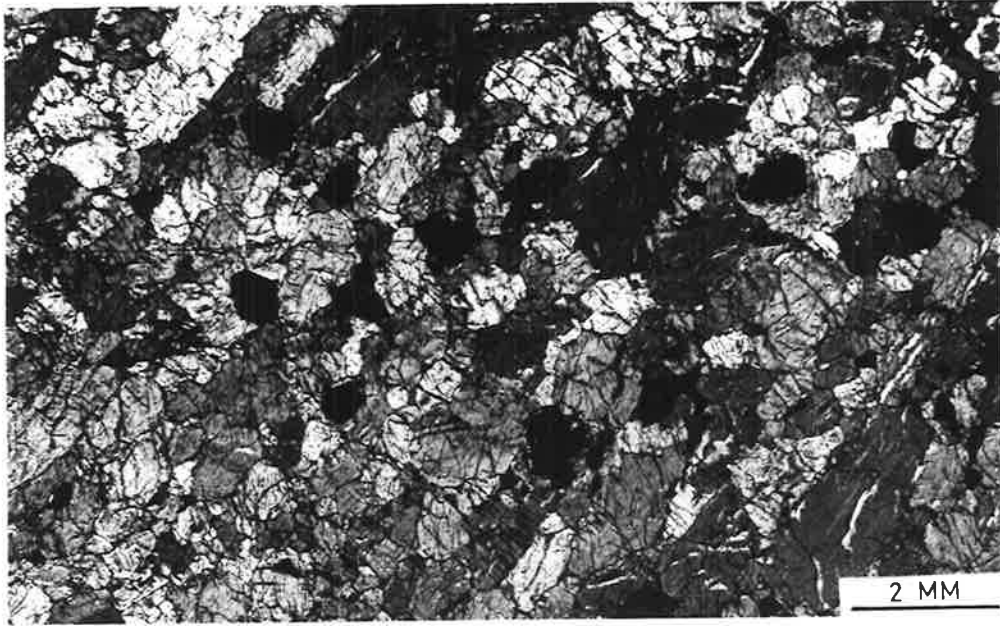




Fig. 3.37

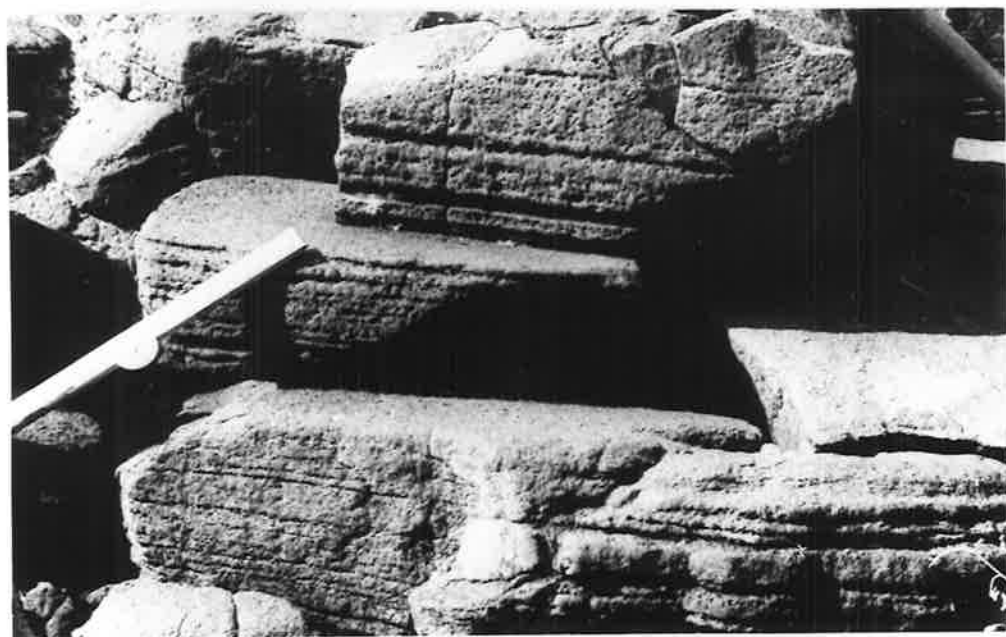
Primary igneous phase layering in olivine-orthopyroxenite showing well developed lineate lamination. The olivine-rich layers weather more readily, thus emphasising the layering. Note the tendency for the rocks to break into tabular slabs. Location: A313/387. Scale: 31 cm.

Photograph: A. Moore.

Fig. 3.38

Close-up of the above. Compare with Fig. 3.34. Scale: 31 cm.

Photograph: A. Moore.



- (i) the relationship between crystal habit and the lattice (optic) orientation;
- (ii) the degree of planar or linear lamination;
- (iii) whether the plane of layering could be fixed by petrofabric methods where it is not visible in the field;
- (iv) whether the flow directions of magma currents could be determined.

Of these features, (iii) was considered to be of the greatest value because, in this area, there is a general lack of phase layering and the rocks appear very uniform in the field. Also, it is in this area that the greatest volume of later noritic intrusive rocks occurs, giving an apparent ENE strike to the "layering" (Fig. 1.3, C/2).

Readily observable, small-scale phase layering is rare in Gosse Pile but, after an extensive search, a small area (extending only 20 m along strike and 10 m across) was found in the northwest where thin (1-10 cm wide) olivine-bearing layers alternate with olivine-free layers of orthopyroxenite in the laminated orthopyroxenite (A313/387). This is the only place so far found in the Main Body where the igneous layering can be measured with certainty in the field; it strikes WNW, and is cut, at a sharp angle, by the rocks of the noritic intrusive which have a general ENE strike. Because of the well-developed preferred orientation of the orthopyroxene within this rock, it tends to break into tabular slabs (Fig. 3.37 and Fig. 3.38). Measurements of the orthopyroxene within the rock allow for a correlation between the orientation of their optic constants and the orientation of the

---

small-scale phase layering. As shown in Fig. 3.39, there are strong  $\alpha$ ,  $\beta$  and  $\gamma$  maxima, corresponding respectively to the b, a and c crystallographic axes of orthopyroxene (orientation after Deer, Howie and Zussman, 1963). Thus, it can be seen that lineate lamination is extraordinarily well developed. Measurement of olivine is more difficult as, even in the richer olivine-bearing bands, there are relatively few olivine crystals accessible for U-Stage measurement. Measurements on 20 such olivines, from the same three sections as were used for the orthopyroxene measurements, are shown in Fig. 3.40. If a preferred orientation is present it is apparently much weaker than that developed in the orthopyroxene, although it is unwise to place too much interpretation of the fabric on the basis of only 20 measurements. A possible weak  $\beta$  maximum may occur within the plane of the layering.

In this rock (A313/387) the habit of the orthopyroxenes is such that they form tablets, flattened parallel to (010) and elongate parallel to c. Thus, in all three directions they present an elongate appearance in hand specimen. The approximate ratio of a:b:c is 0.45 : 0.38 : 1.0, (average of 50 measurements only). The average difference in area between the (010) and (100) faces is not considerable and is of the order of 0.07 units<sup>2\*</sup> compared with the

---

\* These figures were calculated from average ratios and hence the units are arbitrary. Actual orthopyroxene crystals range in length (c) from 2 cms to less than 1.0 mm.

Fig. 3.39

Contoured petrofabric diagrams of the optic constants of orthopyroxenes from an olivine-orthopyroxenite, A313/387 (See Fig. 3.37 and Fig. 3.38). 60 orthopyroxenes were measured in three mutually perpendicular thin sections. The primitive is horizontal and the arrow indicates true north.

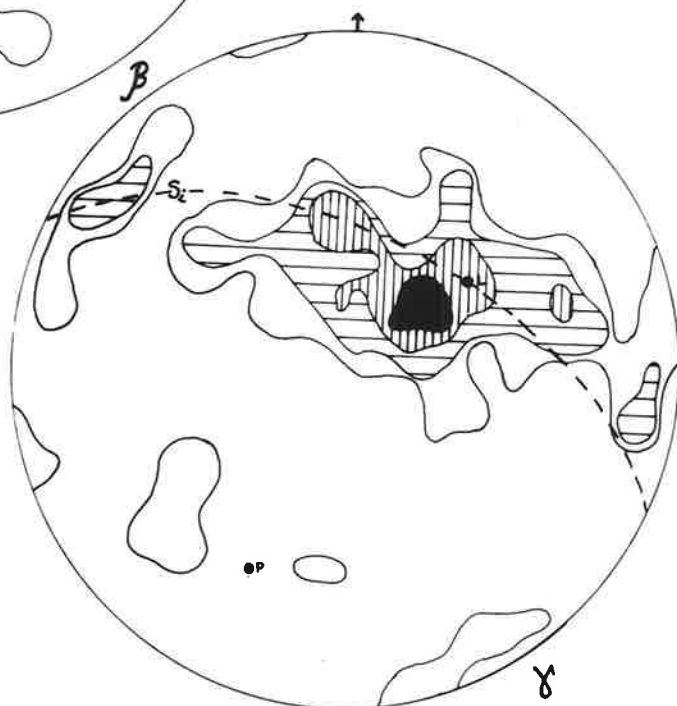
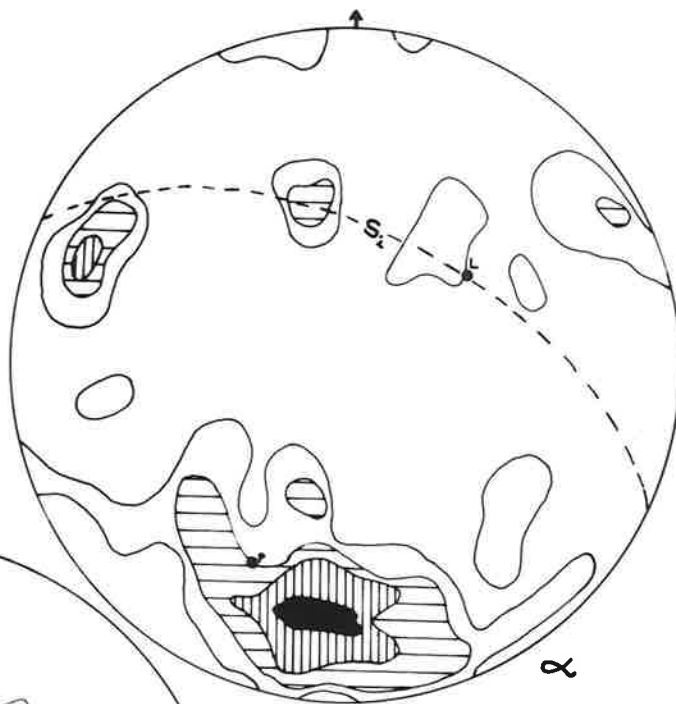
$S_i$ : (dashed great circle): layering, defined by the olivine-rich bands (Fig. 3.38) as measured in the field:  $293^\circ/55^\circ\text{N}$ .

L: weak lineation, defined by the elongate orthopyroxene crystals in the plane of the layering, as measured in the field.

P: pole to the layering,  $S_i$ .

Contour interval: 1%, 3%, 5%, 10% and > 10% per 1% area.

Maxima: for  $\alpha$  (top) : 14% per 1% area  
for  $\beta$  (middle) : 13% per 1% area  
for  $\gamma$  (bottom) : 13% per 1% area.



differences between (010) and (001) faces ( $0.38 \text{ units}^2$ ) and between (100) and (001) faces ( $0.21 \text{ units}^2$ ). Thus, under the influence of gravity alone the most stable orientation for the settled crystals would be such that the majority lie on (010) faces, a relatively high proportion on (100) faces and very few on (001) faces. This would produce an  $\alpha$ -maximum, while  $\beta$  and  $\chi$  would be spread out in a girdle parallel to the layering. A small concentration of  $\beta$  might be expected in the same position as the  $\alpha$ -maximum because of the small difference in size of the (100) and (010) faces. If magma currents played a rôle in determining the orientation of the orthopyroxene then one would expect the length of the crystals to function as the main factor in determining their orientation, such that they would tend to align themselves in a fixed position relative to the direction of flow. Cloos (1946) and Bhattacharyya (1966) have shown that the orientation of prismatic particles in a magmatic flow field (Newtonian viscosity) is such that the direction of elongation is parallel to the direction of flow currents. Although Turner (1948) has stated that the lineation in a flow plane cannot be taken as indisputable evidence of the flow direction because the movement may have been parallel to, or transverse to, the linear element, the author accepts the observational evidence of Cloos (1946) and the theoretical arguments of Bhattacharyya (1966). It is thus assumed that magma flow would produce a  $\chi$ -maximum in the orthopyroxene cumulates, the intensity of which would probably be related to current strength, and the magma flow would also emphasise any

tendency for crystals to settle on the (010) face (compare with Wager and Deer, 1939, p. 263).

A study of Fig. 3.39 shows that there are  $\alpha$ -,  $\beta$ - and  $\gamma$ -maxima, with the  $\alpha$ -maximum close to the pole of the layering as measured in the field, while the  $\beta$ - and  $\gamma$ -maxima lie in the plane of the layering, the  $\gamma$ -maximum close to the lineation as measured in the field. Furthermore,  $\beta$  forms a sub-maximum close to the position of the  $\alpha$ -maximum, and vice-versa, as predicted.  $\beta$  and  $\gamma$  tend to spread more to form a girdle in the plane of the layering. It is, therefore, concluded that the dominant factor in determining the preferred orientation in the orthopyroxenite is the tabular habit of the pyroxenes. The lineate lamination is probably caused by magma currents. This conclusion is in agreement with van den Berg (1946) who similarly found a strong  $\alpha$ -maximum perpendicular to the plane of the layering in a Bushveld Complex pyroxenite, while  $\gamma$  formed a girdle, with a weak maximum, in the plane of the layering. He concluded that the weak parallelism could be caused by convection currents or force of intrusion. Jackson (1961) concluded that the degree of preferred orientation of orthopyroxene crystals from the Ultramafic Zone of the Stillwater Complex was related to their habit such that an  $\alpha$ -maximum was produced at right angles to the layering, and  $\gamma$  lay within the plane of the layering, regardless of whether the crystals are flattened or not.

The olivine within A313/387 occurs in variable habits, and no dimensions are developed in preference to others. In most cases it

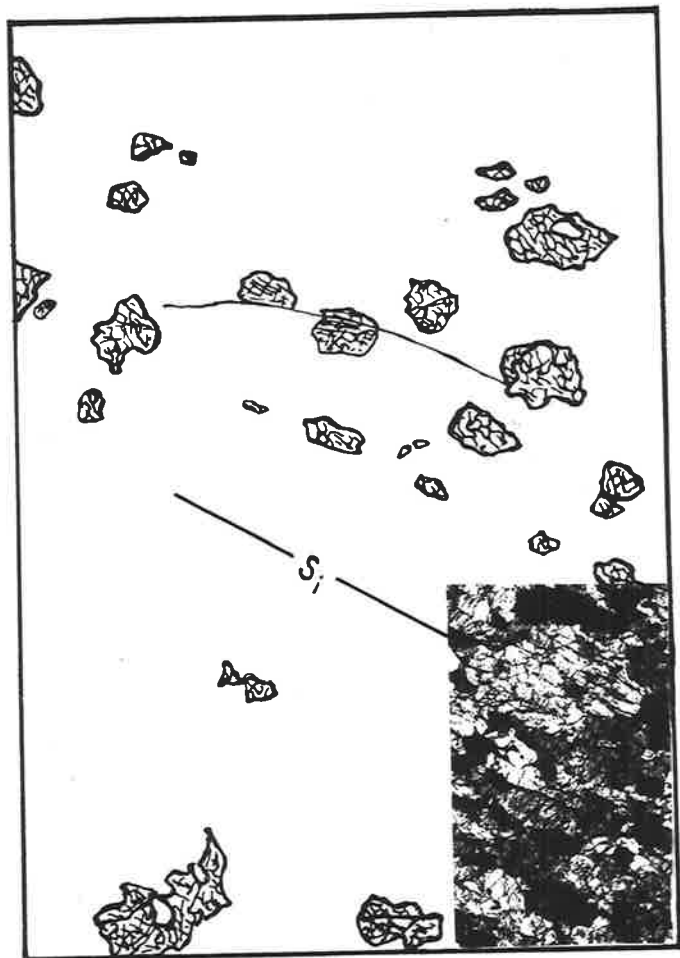


Fig. 3.40

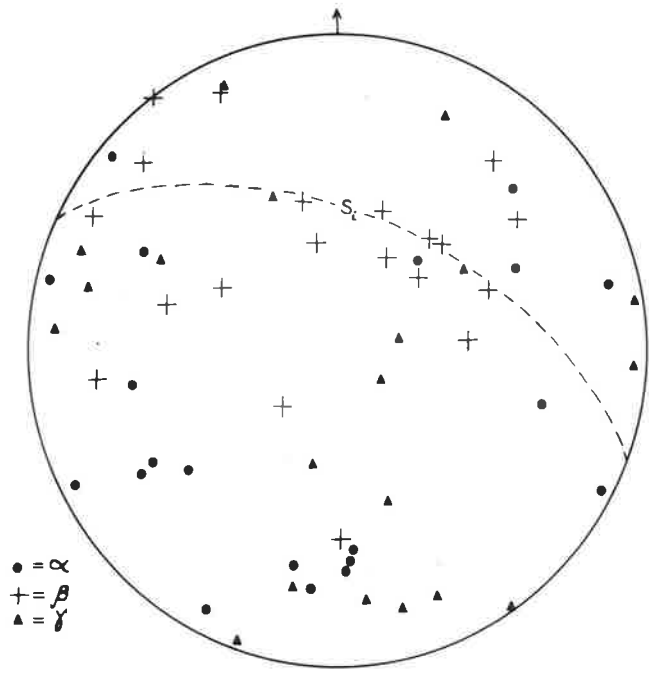
Distribution and petrofabric analysis of olivine in olivine-orthopyroxenite (A313/387).

Top figure illustrates the distribution, number and approximate size and shape of olivine grains in a single thin section of the rock taken from an olivine-rich band (Fig. 3.38).  $S_1$  marks the orientation of the phase layering. The inset illustrates the texture, which is almost identical to that in Fig. 3.36.

Lower figure is a petrofabric diagram of the optic constants for 20 olivine grains, from 3 mutually perpendicular thin sections. Orientation as in Fig. 3.39.



0.5 CM



● =  $\alpha$   
 + =  $\beta$   
 ▲ =  $\gamma$

has concave boundaries towards the surrounding orthopyroxene. Under these circumstances a preferred orientation, dependent upon shape, is not expected nor, apparently, achieved. Measurements on the interstitial clinopyroxenes showed a random distribution. This is to be expected as clinopyroxene occurs interstitially as an intercumulus precipitate. Van den Berg (1946) and Jackson (1961) found similar results.

Working on the assumption that, where phase layering was absent, the orientation of the primary layering ( $S_1$ ) could be determined from the position of the  $\alpha$ -maxima in laminated orthopyroxenites, 16 other specimens were measured (in each case between 60 - 100 grains measured in 3 mutually perpendicular thin sections cut from the same specimen). A selection of 6 of these contoured petrofabric diagrams is given in Fig. 3.41 and Fig. 3.42. From these it is apparent that while some give results consistent with the layering measured elsewhere (e.g. A313/75 and A313/112) such that the layering strikes approximately east-west with steep dips, others (e.g. A313/284, A313/126, A313/305E and A313/354) indicate an almost horizontal layering with strikes varying between north-south and east-west. Apart from A313/112 (Fig. 3.41) the relative orientations of the grains within each specimen are consistent. A313/112 is unusual in that the  $\beta$ - $\gamma$  girdle is more complete than in other specimens and each parameter appears to have developed two maxima. Jackson (1961, p. 41) noted a similar feature in some Stillwater rocks but could offer no explanation.

Fig. 3.41

Contoured petrofabric diagrams for 3 orthopyroxenites showing well developed lineate lamination. In all cases the primitive is horizontal and the arrow indicates true north.

Contour interval: 1%, 3%, 5%, 10% and > 10% per 1% area.

Maxima per 1% area:

A313/112  
(100 grains  
measured)

$\alpha$  : 8%

$\beta$  : 7%

$\gamma$  : 6%

A313/354  
(60 grains  
measured)

$\alpha$  : 15%

$\beta$  : 7%

$\gamma$  : 11%

A313/75  
(50 grains  
measured)

$\alpha$  : 14%

$\beta$  : 13%

$\gamma$  : 14%

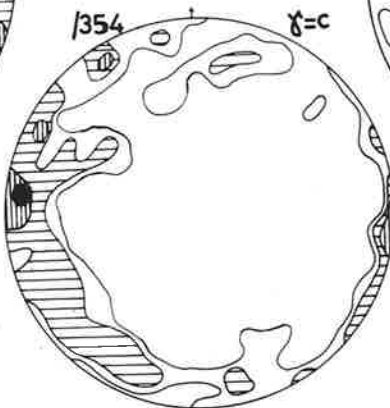
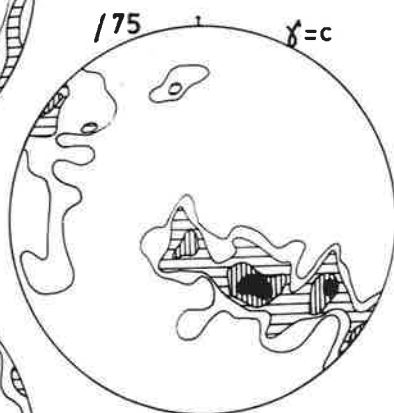
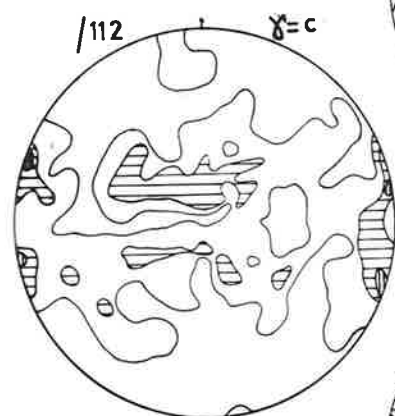
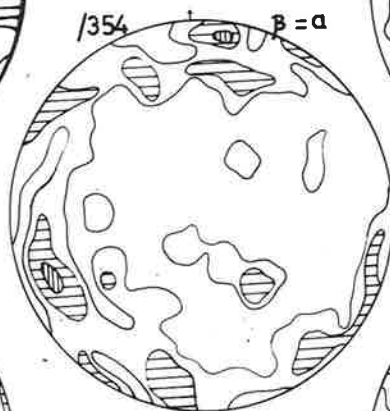
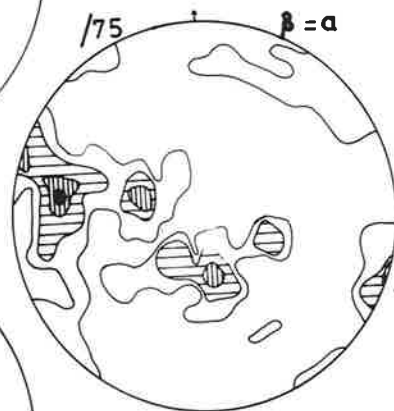
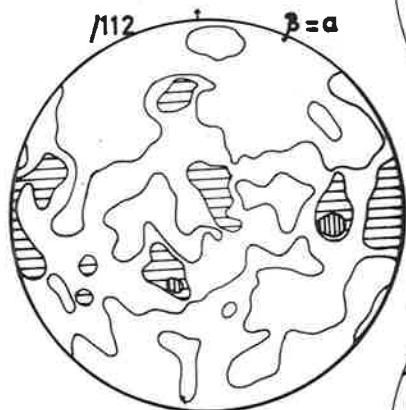
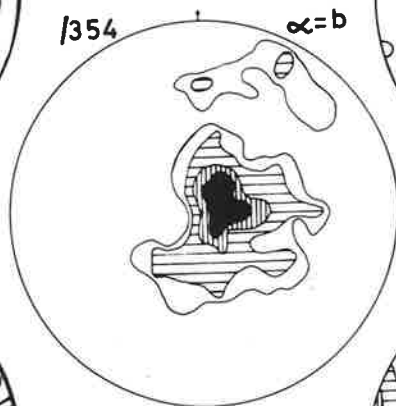
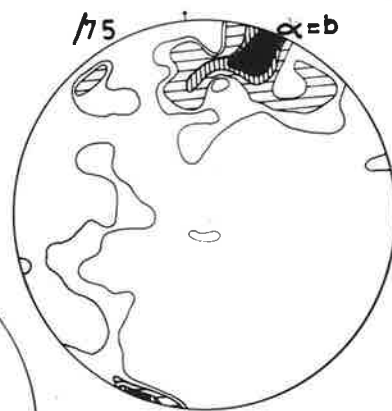
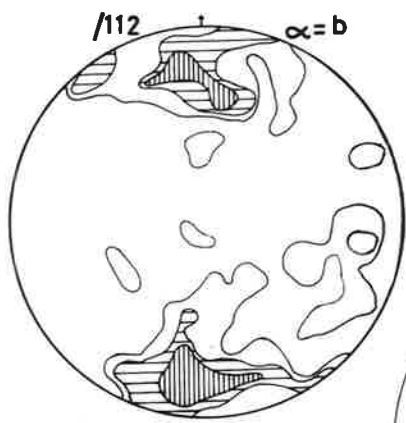


Fig. 3.42

Contoured petrofabric diagrams for three orthopyroxenites showing well developed lineate lamination. Details as for Fig. 3.41.

Maxima per 1% area:

A313/284  
(50 grains  
measured)

$\alpha$  : 14%

$\beta$  : 10%

$\delta$  : 14%

A313/126  
(100 grains  
measured)

$\alpha$  : 20%

$\beta$  : 11%

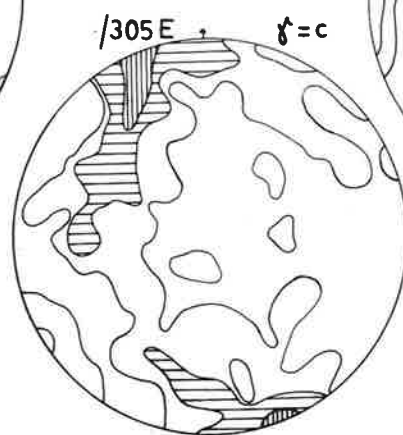
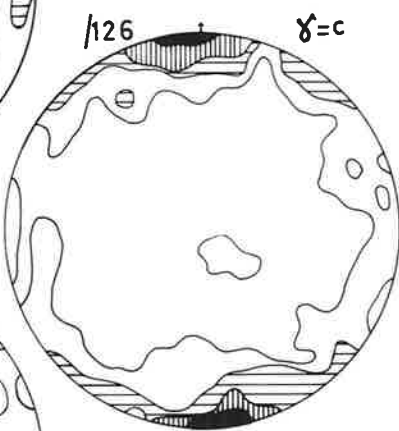
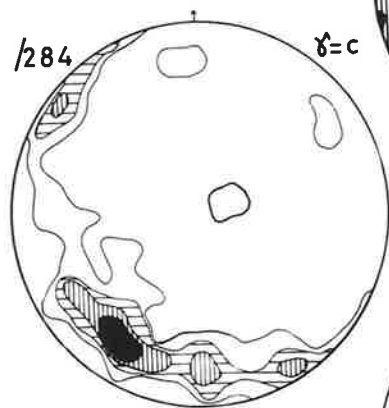
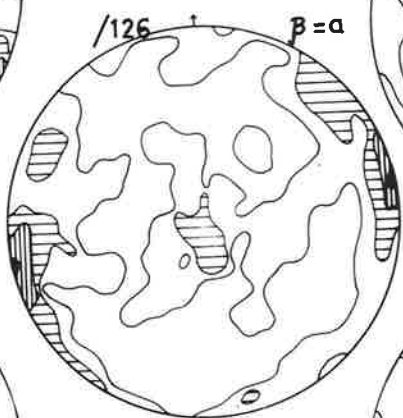
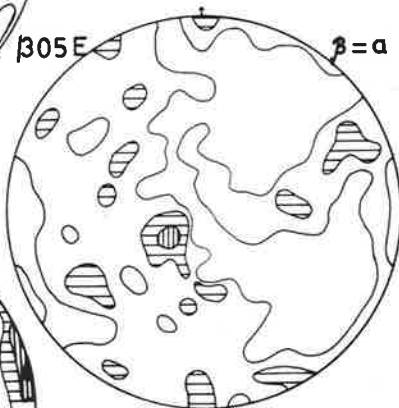
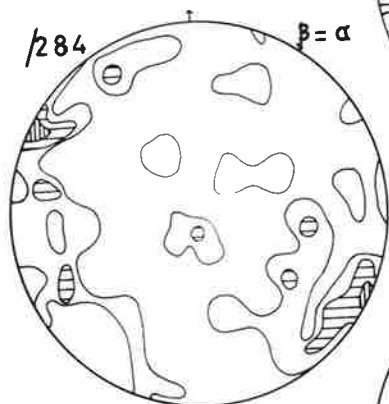
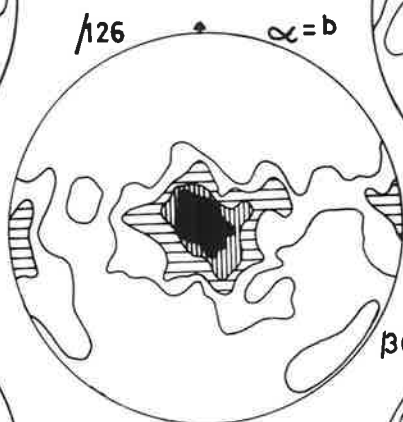
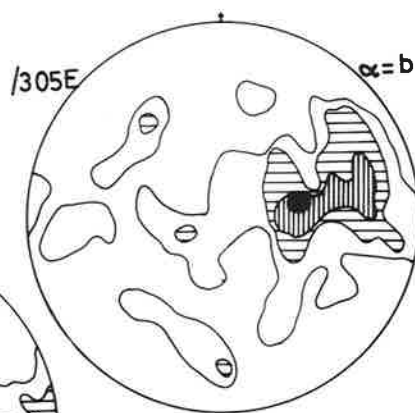
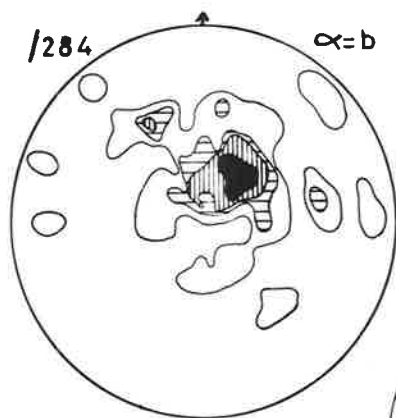
$\delta$  : 13%

A313/305E  
(100 grains  
measured)

$\alpha$  : 11%

$\beta$  : 7%

$\delta$  : 10%



The comparatively large variations in the orientation of the layering as determined by the positions of the  $\alpha$ -maxima, even over short distances, is difficult to explain and, because of it, the value of using the  $\alpha$ -maxima to orientate the layering becomes a questionable procedure. Three possible explanations may be suggested for the variability of the layering.

(i) The laminated orthopyroxenite is best developed in the northwest part of the Main Body and it is in this area that the volume of later noritic intrusive material is greatest. The noritic intrusive is transgressive and, during the process of intrusion, may have disrupted the original orientation of the layering. Whenever specimens of the laminated orthopyroxenite are found far from the noritic intrusive (as in the central part of the Main Body) they give consistent orientations for the layering (e.g. A313/75). This interpretation seems to be the most feasible, although the proportion of rocks with apparently almost horizontal layering (6 of the 16 measured) seems to be suspiciously high.

(ii) Undetected fold structures may have affected the western part of the Main Body producing the variations in the layering. This seems unlikely because a regular variation in the position of the  $\alpha$ -maxima has not been detected, and specimens collected within only 10 m of each other give completely different orientations for the  $\alpha$ -maxima (e.g. A313/383 and A313/383A).



(iii) The assumption that the  $\alpha$ -maximum always corresponds to the pole of the layering may be false. This is considered unlikely, not only because of the strong evidence given by specimen A313/387 (Fig. 3.39) and by the similar orientations deduced by van den Berg and Jackson, but also because of the consistent nature of the various maxima within each individual petrofabric diagram (Fig. 3.41 and Fig. 3.42).

#### Origin of the layering

The igneous layering produced in gabbroic rocks is generally explained in terms of density differences between the mafic minerals (pyroxene:  $3.2 \pm$  gm/cc) and plagioclase ( $2.7 \pm$  gm/cc) and their relative rates of settling under the influence of gravity. Various modifications have been suggested for producing rhythmic layering. Hess (1960) considers that magma currents with variable velocities could effectively produce the stratification observed in layered intrusions. Other explanations have involved flow of a partially consolidated heterogeneous magma. This hypothesis has been applied particularly to "alpine-type" intrusions (Thayer, 1963) but has also been suggested for some "stratiform" bodies (e.g. Bay of Islands Complex - Smith, 1958). Smith (1958) pointed out that in layered ultramafic sequences there was virtually no difference in density between the primary mineral components. Wager (1959) considered that the order of crystal nucleation may have been a controlling factor in the formation of the rhythmic units found in the Bushveld Complex and

possibly other layered bodies. Brown (1956) explained this type of layering in the ultramafic sequence of Rhum by proposing a successive series of magma pulses, in a modified version of the multiple injection hypothesis of Lombaard (1934) to explain the variations in the stratigraphy of the Bushveld Complex. Jackson (1961) explained the cyclic units of the Stillwater intrusion by suggesting that they are, "depositional products of periodically refreshed stagnant magma which became stabilized by bottom crystallization". He points out the similarity between Stillwater ultramafites and evaporite deposits (Jackson, 1961, p. 99) and shows that physico-chemical, rather than mechanical, processes best explain the composition and distribution of the rocks. Wager and Brown (1968, p. 340) have considered that Jackson's conclusions are not entirely justified and state that the origin of the layering in Stillwater ultramafic zone is an open question but, in their opinion, continuous convection is more likely than periods of local magma stagnation. Hawkes (1967), noting the absence of cryptic layering in the Freetown basic intrusion (a feature common in ultramafic layered sequences but rare in similar basic bodies), suggested that the ease of abundant crystal nucleation of the primary phases, during undercooling of the magma, causes the layering.

The origin of the layering in Gosse Pile must, like that of the Stillwater ultramafic zone, remain an open question and any hypotheses must be largely speculative without further work, particularly of the type outlined by Hawkes (1967). Unfortunately, this would be almost

impossible to carry out because of post-depositional processes (including deformation, solid-liquid reaction and static annealing of the cumulates) as well as the difficulty of distinguishing grain sizes in the relatively undeformed websterites (Fig. 3.19). However, it can be said that simple gravity sorting, even accompanied by "winnowing" effects (Wager and Deer, 1939) cannot be alone responsible for the layering within each cyclic unit, or for the repetition of the cyclic units themselves, because of the close similarity in the densities of the associated primary phases and the apparent lack of cryptic layering. In view of the development of strongly laminated orthopyroxenites it appears that magma currents have been active during crystallization, so the presence of stagnant magma (Jackson, 1961) seems to be unlikely, although such currents may have developed under conditions of convective overturn or during the periodic refreshment of stagnant magma. The author favours the views of Wager (1959) and Hawkes (1967). If these are correct then, with cooling of the magma, it appears that the order in which the minerals were precipitated was:

orthopyroxene and olivine (+ chromite  $\pm$  clinopyroxene)

orthopyroxene

orthopyroxene + clinopyroxene

orthopyroxene + clinopyroxene + plagioclase.

Olivine was never precipitated alone (there are no cumulate dunites or peridotites) and the amount of olivine is proportionately very small. In this respect Gosse Pile differs significantly from the ultramafic portions of most other layered bodies (Wager and Brown, 1968).

The origin of the cyclic units is possibly a function of influxes of fresh magma, each unit representing a new influx, as has been suggested for the Rhum ultramafic sequence (Brown, 1956; Wadsworth, 1961) and for the Muskox intrusion (Irvine and Smith, 1967). Such influxes would disturb any existing pattern of fractional crystallization and re-start the process from the beginning, and thus start a new cyclic unit.

### 3.4.2 Tectonic Layering ( $S_t$ )

If Gosse Pile is approached from the south one passes first over either olivine-gabbro (part of the Mt. Davies intrusion to the west) or acid granulites, then a brittle fault zone, about 5-20 m wide, before reaching the deformed rocks of the Gneissic Zone (Fig. 3.1). These rocks are typical metamorphic (secondary) S-tectonites (Sander, 1930) and consist of alternating pyroxenite and norite layers of varying thickness (a few centimetres to several hundred metres). On the map (Fig. 1.3) only the larger layers have been shown. Where the individual layers are thin (between a few centimetres to about 10 metres) they have not been mapped separately but as a single unit. On a small scale these form uniform, parallel-sided layers which are parallel to the foliation, or schistosity ( $S_t$ ), produced by the alignment of planar clusters of pyroxenes in the noritic horizons. However, if these layers are followed along strike it can be seen that they have the shape of very elongate lenses and eventually die out. This can also be seen on a large scale in the western part of the

Gneissic Zone (Fig. 1.3, AB/2). A vertical lineation, caused by streaking of single grains or clusters of pyroxene crystals, has been seen in only a few plagioclase-rich rocks where it is weakly developed. The contacts between norite and pyroxenite bands are sharp, even where individual bands are only a few millimetres thick (Fig. 3.43). This type of layering is typical of the flow-layering found in "alpine-type" complexes, as described by Thayer (1960, 1963). That illustrated in Fig. 3.43 is remarkably similar to interlayered anorthositic and peridotitic layers of the "alpine-type", Canyon Mountain intrusion (Thayer, 1963, Fig. 2).

The interlayered rocks, both in hand-specimen and in thin-section (Fig. 3.43, Fig. 3.44 and Fig. 3.45) closely resemble high-grade metamorphic gneisses and have a mineralogy consistent with the granulite facies (i.e.  $opx + cpx + plag$ ). No amphibole or biotite has been developed. In a few specimens a discordance between the schistosity ( $S_t$ ) and the lithological banding ( $S_i?$ ) has been observed (Fig. 3.47). On a large scale, it can be seen that a major norite band in the western part of the Gneissic Zone (Fig. 1.3, B/2) "vees" upstream, suggesting a significant dip to the north. However,  $S_t$  in this area is close to vertical ( $85^\circ N$  to vertical) and is consistent across the lithological boundary.

North of the Gneissic Zone no plagioclase-bearing rocks occur for some distance (Fig. 1.3) apart from the irregular veins and plugs of the undeformed later noritic intrusive. (This dates the intrusion of

Fig. 3.43

Flow layering ( $S_t$ ) in the Gneissic Zone showing the alternation of pyroxenite and gabbro bands of various thicknesses. Note the sharp boundaries between bands. Some late-stage brittle faulting has displaced some of the layers (e.g. top centre). The scale is graduated in inches and has a total length of approximately 5 inches (13 cm). Location: A313/218.

Photograph: A. Moore.

Fig. 3.44

Photomicrograph illustrating the contact between norite and pyroxenite bands in a rock (A313/218) from the Gneissic Zone. Note the elongate orthopyroxene augen, present in both rock types, and the "slivers" of orthopyroxene in the norite. Between partially crossed polars.

Photograph: A. Moore.

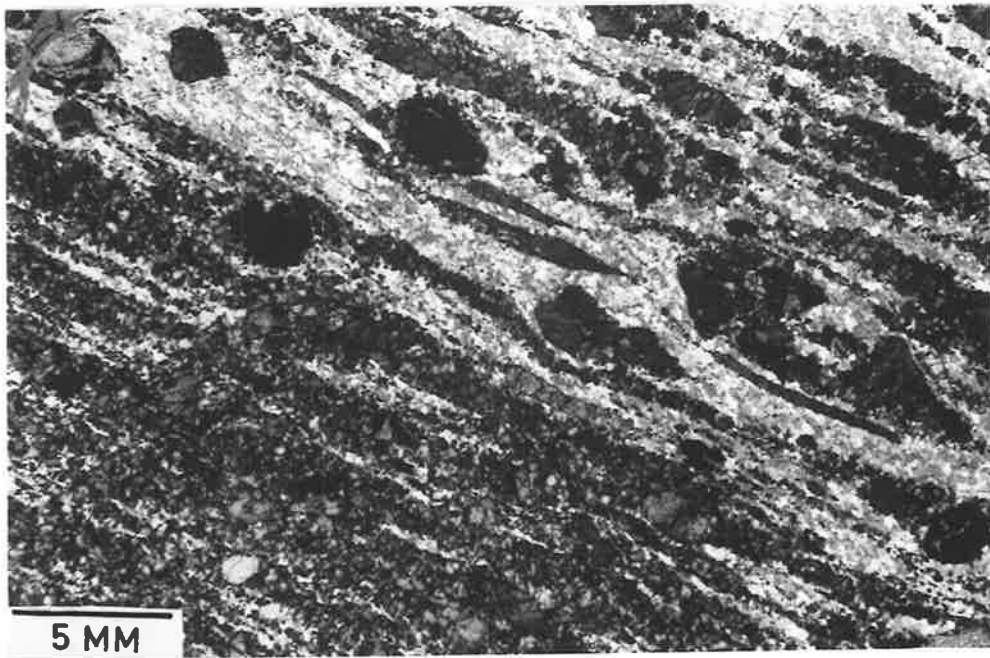
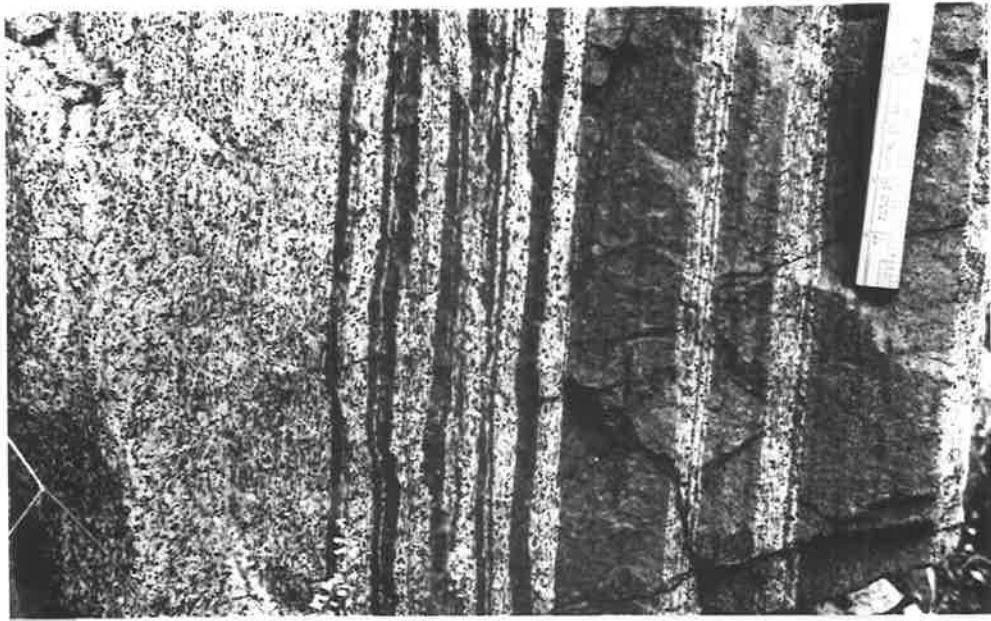


Fig. 3.45

Hand specimen showing well developed, fine-scale flow-layering producing pyroxenite-rich and feldspar-rich bands in a norite. Note the orthopyroxene augen around which the layering appears to flow.

Photograph: J. Probert.

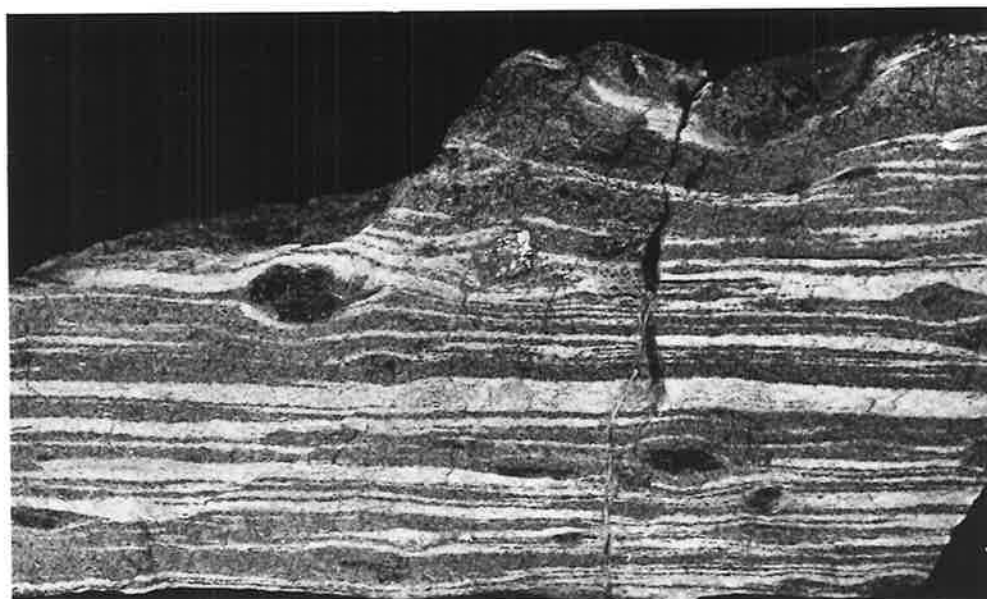
Fig. 3.46

Well developed tectonic layering in websterite.

Location: A313/95. Scale: 15.5 cm.

Photograph: A. Moore.





the noritic material as being after the deformation which produced the tectonites of the Gneissic Zone). However, within the southern websterite (Fig. 1.3) a tectonic layering has been developed which is made visible by differential weathering (Fig. 3.46). Jointing, approximately perpendicular to the layering, is well developed and thin-sections show microfractures, with a similar orientation, to be numerous. Thin-sections cut perpendicular to the layering show no obvious differences between the raised and depressed areas, although there is a possible tendency for the latter areas to be slightly richer in clinopyroxene and to contain slightly more microfractures. These depressed areas are centred about much narrower zones (2-5 mm) than the ridges (6-20 mm). The origin of this type of tectonic layering is not known, but it is possible that, during deformation, there was differential movement along discrete planes (weakly penetrative, Fig. 3.46) which have been exploited by weathering processes but which, in thin-section, cannot be readily detected.

Folding has not been observed in the rocks of the Gneissic Zone but in identical rocks, which occur in Kalka (10 km west of Gosse Pile, Fig. 1.2), there occur folds which, on the basis of fold style, are thought to have been produced during the deformation ( $D_2$ ) which was also responsible for folding the layered sequences into their present near-vertical position (Nesbitt et. al., 1969, Fig. 7).

As has been argued in Section 3.3, on the basis of the textures of these rocks, it is thought that the tectonic layering was produced during faulting at high temperatures and under relatively slow strain

rates. By analogy with flow in glaciers it can be suggested that the tectonic layering is equivalent to the "flow-layering" formed in active glaciers, parallel to the actual movement of the ice (Rigsby, 1960).

In Gosse Pile  $S_i$  and  $S_t$  are nearly parallel, and  $S_t$  predates the folding of the igneous body. Thus, at the time of formation, faulting must have been almost horizontal and would be regarded as low-angle thrusting, with the tectonic layering developing parallel to the fault plane.

#### Origin of the layering

The mode of formation of this type of layering is not known with certainty. Similar layering in other areas has been ascribed to cataclasis followed by static annealing (e.g. van Diver, 1967), "recrystallization under [granulite facies] metamorphic conditions" (e.g. the jotunites of Norway, Battey, 1965), or as flow in a mush form, while the gabbroic fractions were largely fluid, at the time of emplacement (Smith, 1958). Oosterom (1963), in proposing a tentative petrogenesis for the ultramafic and layered gabbro sequence on Stjernöy (Norway), in which an igneous layered sequence and gabbro gneiss are juxtapositioned in a similar way to the rocks of Gosse Pile, suggested that the appropriate P-T conditions were attained for dry anatexis within a metamorphic complex of mafic gneisses, resulting in a gabbroic magma. The degree of melting varied: in areas where complete melting was accomplished a rock with layering of truly igneous appearance was formed, and where only incipient differential

anatexis occurred a "gabbro gneiss" resulted, which contained remnants of rocks with high fusion temperatures (limestone and dolomite). Thayer (1963) considered that interlayered gabbro and peridotite in "alpine-type" intrusions was formed during emplacement, partly by remixing of pre-differentiated rocks and partly by processes akin to metamorphic differentiation. Bowes, Wright and Park (1964) concluded that the layered ultramafic rocks in parts of Scotland had retained original igneous layering in spite of a later granulite facies metamorphism.

The following model is suggested for the origin of the tectonic layering in the rocks of the Gneissic Zone and the southern part of the Main Body of Gosse Pile.

It is considered likely that the present distribution of rock types within the tectonic layered area reflects the original lithological distribution as caused by gravitational settling. This is because of the similarity in the distribution of rock types in the Gneissic Zone compared with that in sequences produced by igneous layering. For example, compare the similarity in the distribution of pyroxenite and norite (Fig. 3.43) and that of gabbro and melanogabbro (pyroxenite) produced by igneous layering (MacRae, 1969, Plate II). There is a striking similarity between rock distributions produced by igneous layering (Wager and Brown, 1968, Fig. XIIB) and that in rocks showing tectonic layering (Thayer, 1963, Fig. 2). In other parts of the Giles Complex a distribution of rock types, similar to that found in the Gneissic Zone, has been produced by

---

gravity settling (Nesbitt and Talbot, 1966).

The fact that the plagioclase in rocks of the Gneissic Zone is equidimensional yet has a strong preferred orientation (see later, p. 176) is regarded as strong evidence against an origin as a result of "mush flow" in a largely fluid body, particularly as plagioclase is relatively late in the crystallization sequence. Cataclastic deformation can produce well layered bodies from originally homogeneous rock, as shown by Prinz and Poldervaart (1964), but the resultant textures are very different from those described in Section 3.3. A later period of static annealing cannot be invoked to produce the present textures from a cataclastically deformed rock because this would not produce a strong preferred orientation in the plagioclase. Even in glaciers, which show the development of analogous flow-layering (Meier, Rigsby and Sharp, 1954) it has been shown that "recrystallization" of the ice crystals destroys to some extent the preferred orientation developed during flow of the glacier. Finally, in a few places, the schistosity ( $S_t$ ) is transgressive to what is considered to be remnant igneous layering ( $S_i$ ), thus indicating that the mineralogical distribution predated the development of the schistosity and tectonic layering.

Summarising then, it is thought that the tectonic layering forms as a result of thrust faulting approximately parallel to the igneous layering. This faulting took place soon after complete solidification of the intrusion and the distribution of strain through the igneous body decreased away from the fault plane. This strain caused

syntectonic annealing, to the stage of primary recrystallization, and a schistosity ( $S_t$ ) to be superimposed over the original igneous layering ( $S_i$ ), but with little change in the original distribution of minerals.

#### Preferred orientation studies

Studies of the preferred orientation of minerals within the deformed rocks south of Gosse Pile can be considered in two parts:

- (i) the development of a new preferred orientation;
- (ii) the destruction of any pre-existing preferred orientation.

(i) Measurement of the optic constants of the polygonal plagioclase grains was not carried out because of the time involved and because of the complex relationship between crystallographic directions and optic orientations in the triclinic system. However, using a  $\lambda$ -plate (gypsum) a strong preferred orientation has been observed in all plagioclase-bearing rocks from the Gneissic Zone. The orientations of the (010) twin planes were measured for 100 plagioclase grains in each of three specimens: two collected in place and the third from "float" found on the outwash plain south of Gosse Pile. This third specimen was used as it was the only hand specimen found in which there appeared to be an angular discordance between the schistosity ( $S_t$ ) and what is thought to represent primary layering ( $S_i$ ). See Fig. 3.47.

Fig. 3.47

Etched hand specimen of norite derived from the Gneissic Zone.  $S_t$  is considered to represent the orientation of the schistosity which is at an angle to the compositional layering,  $S_i(?)$ , thought to represent the original igneous layering. Late stage brittle faults (F), with associated pseudotachylite veins disrupt both layering and schistosity.

The diagram is a contoured petrofabric diagram of the poles to (010) of 100 plagioclase grains from the same rock. The orientations of  $S_i(?)$  and  $S_t$  are marked.

Contours at 1%, 3%, 5%, 10% and > 10% per 1% area.

Maximum: 8% per 1% area.

Photograph: J. Probert.

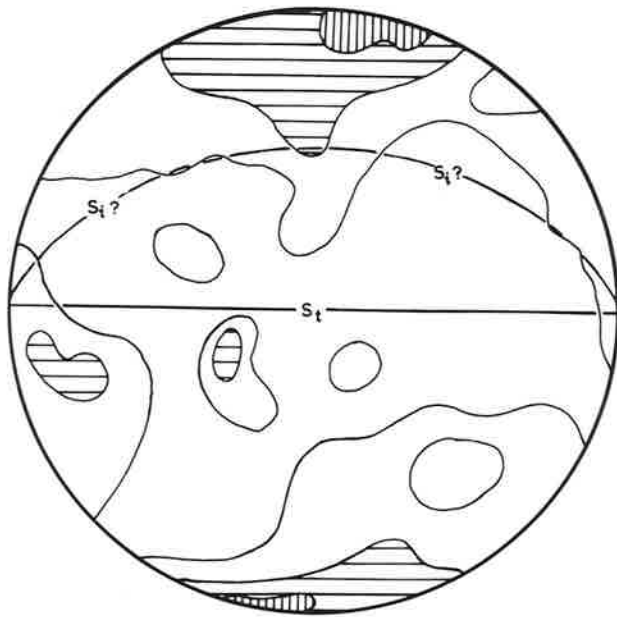
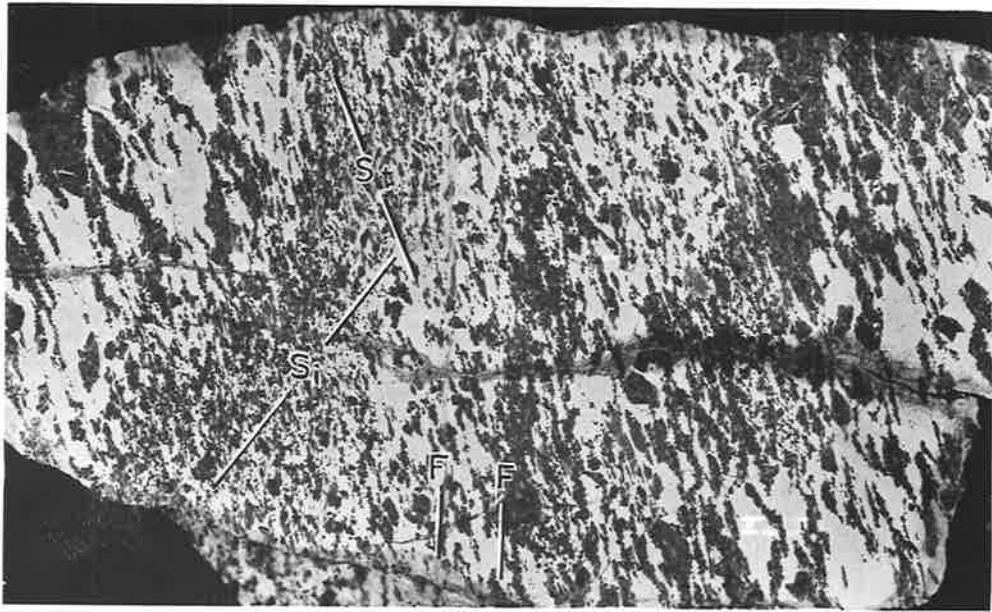




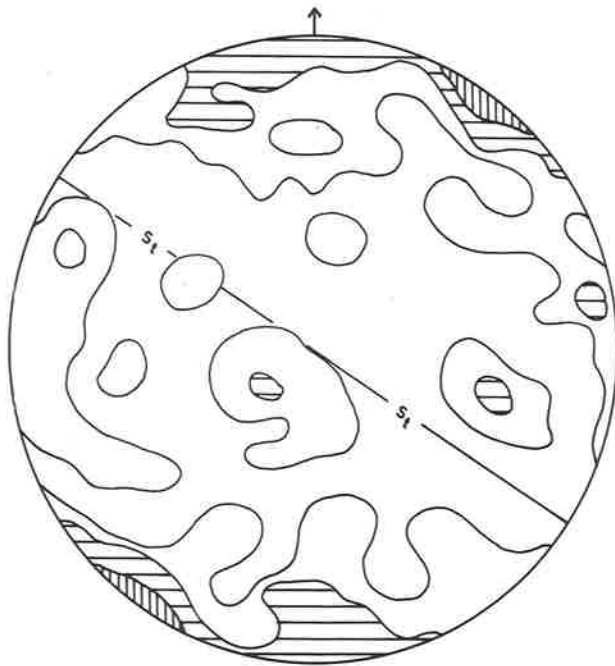
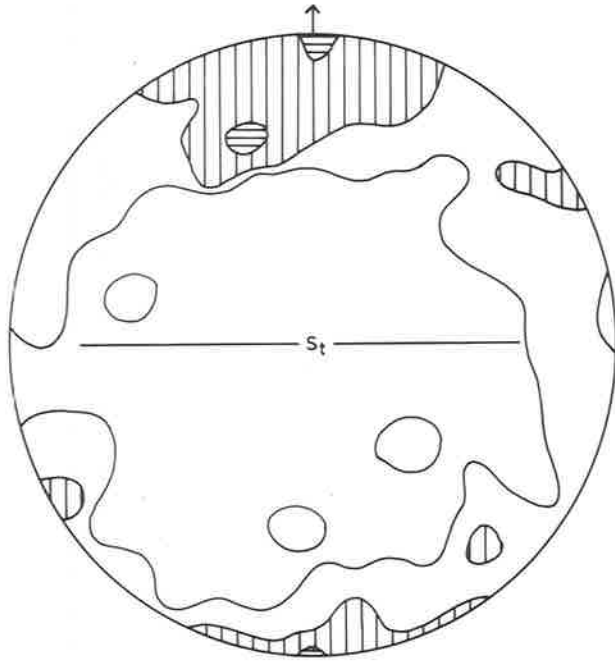
Fig. 3.48

Contoured petrofabric diagrams of the poles to (010) of plagioclase in norites from the Gneissic Zone. In both figures 100 grains were measured. The primitive is horizontal and the arrow indicates true north.  $S_t$  is the orientation of the tectonic layering (schistosity) as measured in the field.

Contours at 1%, 3%, 5%, 10% and > 10% per 1% area.

TOP: A313/38. Maximum: 7% per 1% area.

BOTTOM: A313/97. Maximum: 9% per 1% area.



The pole of the albite twin plane (010) was used by Brothers (1964) as one of three orthogonal orientations for defining the preferred orientation of plagioclase in Rhum and Skaergaard igneous layered rocks. This direction he termed  $\underline{C}$  and found that it was orientated at right angles to the plane of the layering. A similar result is found for the Gneissic Zone rocks (Fig. 3.48), where  $\underline{C}$  is perpendicular to the schistosity. Unfortunately no undeformed, laminated plagioclase-rich rocks, definitely part of the layered sequence, occur in Gosse Pile so that the contribution of an original igneous preferred orientation to the present one cannot be estimated. This is unfortunate because of the essentially parallel nature of  $S_i$  and  $S_t$  over the greater part of the Gneissic Zone. In the "float" specimen, however, measurements show that the orientation of the presumed remnant igneous layering bears no relationship to the preferred orientation of the plagioclase (Fig. 3.47) so that it seems likely that the development of the plagioclase orientation occurred during syntectonic annealing of the rocks.

(ii) Measurements of the pyroxenes in the plagioclase-rich rocks show only random orientation, as do measurements of both pyroxenes in the annealed southern websterite. However, measurements of orthopyroxene in some annealed orthopyroxenites have given more interesting results, although measurements of the associated clinopyroxene give random orientations. In some orthopyroxenites the megacrysts show a distinct preferred orientation, easily recognisable under the microscope. The orientations of 60 megacrysts from one

such rock (A313/101), in which the ratio of matrix to megacryst is estimated to be 60:40, show a distribution of optic constants comparable with those in rocks showing strong igneous lamination (Fig. 3.49). The matrix grains of A313/101 were measured separately and they revealed that, although the orientation of the megacryst preferred orientation is retained it is, in general, much weaker. However, the  $\beta$ -maximum which, in the igneous laminated rocks shows the weakest maximum and greatest scatter, shows a stronger maximum and also less scatter in the matrix grains than in the megacrysts. It is concluded that the syntectonic annealing of the laminated orthopyroxenites causes a general weakening of the pre-existing preferred orientation but, at the same time, may be in the process of developing a new orientation (reflected by the strength of the  $\beta$ -maximum). The process seems to occur only in rocks with a pre-existing preferred orientation, revealed by the present orientation of the megacrysts. In others a random orientation exists. In this respect the preferred orientations of orthopyroxenes from the garnet-peridotite (Ticino, Switzerland) described by Möckel (1969) and a high-temperature, "alpine-type" peridotite (Tinaquillo, Venezuela) described by MacKenzie (1960) are worth noting. In both cases they have strong  $\beta$ -maxima in contrast to the strong  $\alpha$ -, weak  $\beta$ -orientations in magmatic orthopyroxenes. Möckel (1969) considers this fabric type formed by deformation and metamorphism while MacKenzie (1960) ascribes it to "mush flow" with the orthopyroxenes elongate parallel to the direction of flow. It is worth noting that in the Gosse Pile rocks the deformation and annealing has caused no

Fig. 3.49

Contoured petrofabric diagrams of the optic constants of orthopyroxene grains from an annealed orthopyroxenite (A313/101).

See Fig. 3.32.

Contours at 1%, 3%, 5%, 10% and > 10% per 1% area.

Megacrysts (60 grains measured)

Matrix (100 grains measured)

Maxima:

Maxima:

$\alpha$  : 12% per 1% area

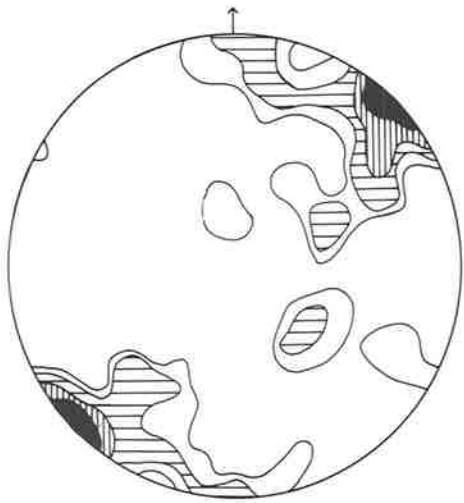
$\alpha$  : 8% per 1% area

$\beta$  : 8% per 1% area

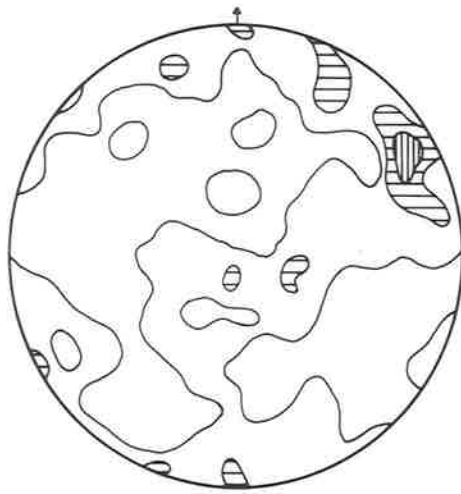
$\beta$  : 9% per 1% area

$\gamma$  : 8% per 1% area

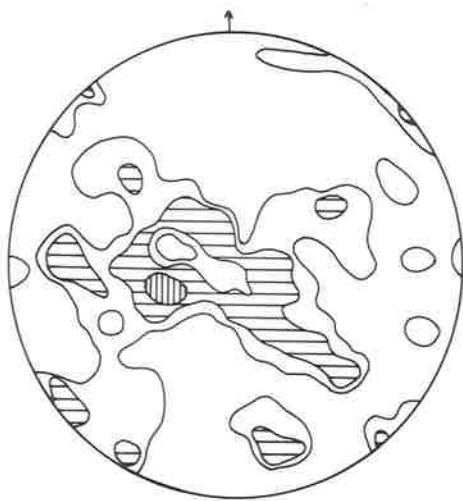
$\gamma$  : 8% per 1% area



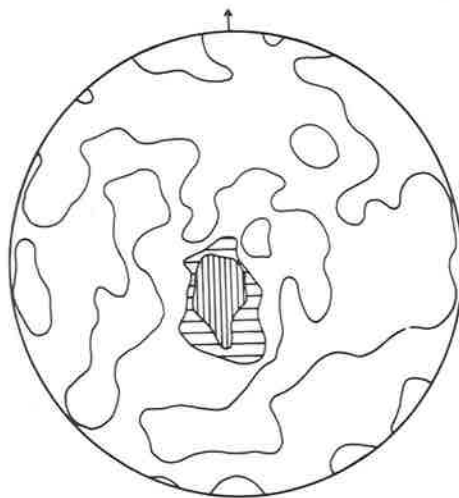
$\alpha$  : MEGACRYSTS (60)



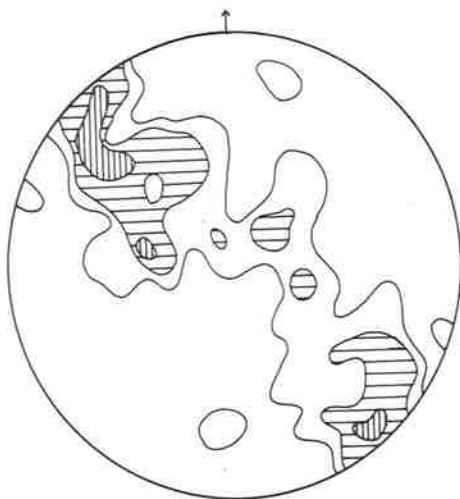
$\alpha$  : MATRIX (100)



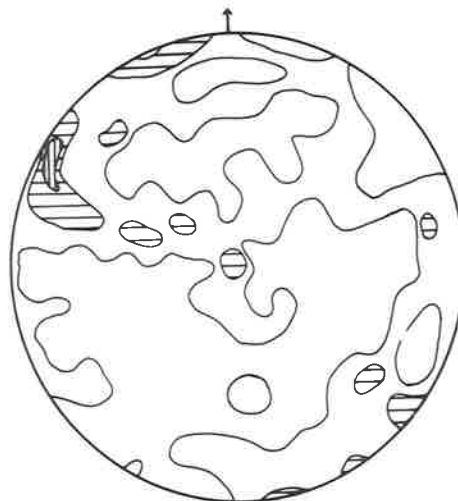
$\beta$  : MEGACRYSTS (60)



$\beta$  : MATRIX (100)



$\gamma$  : MEGACRYSTS (60)



$\gamma$  : MATRIX (100)

significant rotation or change in the orientation of the megacrysts. Not all specimens from the relatively undeformed northern part of Gosse Pile show igneous lamination so it would not be expected for all the annealed rocks to show a preferred orientation. Similarly, because of the great variation in grain-size between different unannealed rocks on the northern side of Gosse Pile, little heed should be paid to the variations in absolute grain-size measurements on megacrysts and matrix crystals.

Nearly all the plagioclase crystals and the majority of clinopyroxenes in the Gneissic Zone show twinning. In both cases it is considered to represent deformation (or glide, or secondary) twinning. For clinopyroxene the criteria for distinguishing the twinning are not as clear as in the case of plagioclase, because the numerous lamellae, parallel to (100), are similar to lamellae produced by exsolution of orthopyroxene, and they are so fine that the exact extinction positions of host and lamellae are difficult to locate using the U-Stage. However, they are considered to represent twin lamellae rather than exsolution because they commonly extend to the crystal boundaries and, in general, they appear to show inclined extinction. Orthopyroxene exsolution lamellae have also been recognised. An attempt was made at dynamic analysis using the technique described by Raleigh and Talbot (1967) and by Carter and Raleigh (1969) in which the optic direction  $\alpha(x)$  of the clinopyroxene is considered to be close to the maximum compression axes in twinned grains. The results were inconclusive as a random distribution of

points resulted.

Deformation twins in plagioclase were recognised on the basis of criteria listed by Vance (1961, p. 1103) and are predominantly albite twins, although pericline twins are well developed in some grains. In other crystals the two twin types are equally well developed and, in the absence of easily recognisable cleavage, some pericline twins may have been measured as albite twins in Fig. 3.48. However, this error is regarded as small. Growth twins have not been observed in any plagioclase grains and are rare in the clinopyroxenes. Since available evidence indicates that both minerals formed during syntectonic annealing the glide twinning must have formed during one or more of the later periods of deformation responsible for the brittle faulting in the area. In the case of the plagioclase this twinning would develop in such a way as to reflect their preferred orientation which had already been developed during the syntectonic annealing.

### 3.5 PETROLOGY

The layered sequence

The phase layers of Gosse Pile consist essentially of orthopyroxene, clinopyroxene and olivine, with relatively minor plagioclase, in different proportions. The rocks are characteristically deficient in oxide and sulphide minerals: these appear in limited



amounts in the olivine-bearing rocks. Within each phase layer there appears to be limited and irregular mineralogical variation, and cryptic layering is apparently absent.

Modal analyses of all rock types are plotted in Fig. 3.50 from data given in Appendix 1 (see also Table 3.4). Fig. 3.50 is similar to the diagram used by Irvine and Smith (1967, Fig. 2.6) but plagioclase has been included by projecting anorthite from the  $Al_2O_3$  corner of the  $CaO-(Mg,Fe)O-Al_2O_3-SiO_2$  tetrahedron so that plagioclase-rich rocks can be included. Olivine-bearing rocks may also contain plagioclase although this cannot be illustrated on the diagram: olivine-orthopyroxenites can contain up to about 7% plagioclase, and the picrites up to about 8% plagioclase (Table 3.4). This form of diagram is useful in that it allows for a rough comparison between the mineralogy of the rock sequences observed and the established, or possible, phase relations, as has been done by Irvine and Smith (1967).

Chemical analyses of mineralogically similar rocks from different cyclic units are essentially similar. Differences in the analyses (Table 3.5) reflect only differences in the mineralogy. This lack of chemical variation was expected from an ultramafic sequence. On the  $MgO-(FeO + Fe_2O_3)-(Na_2O + K_2O)$  diagram the rocks plot close to the iron-magnesium side of the triangle, close to the lower limit of the differentiation trend shown by the Mt. Davies rocks (Nesbitt *et. al.*, 1969, Fig. 9). The southern websterite, however, contains normative quartz (Table 3.5; Fig. 3.51) while the northern one contains normative

Table 3.4

Average modal analyses of Gosse Pile rocks. (See Appendix 1).

| Name  | Minerals  | $\bar{x}$<br>(Av. %) | Range |      | s    | Major cumulate<br>phase(s)  |
|---|-----------|----------------------|-------|------|------|---|
|   |           |                      | Min.  | Max. |      |   |
| olivine-<br>orthopyroxenite<br>(11 analyses)                                      | ol        | 19.6                 | 1.7   | 46.2 | 15.2 | orthopyroxene<br>olivine  |
|   | opx       | 64.3                 | 37.7  | 89.0 | 21.4 |   |
|   | cpx       | 11.6                 | 2.6   | 39.1 | 9.6  |   |
|   | plag      | 2.5                  | 0.0   | 6.8  | 2.1  |   |
|   | bi        | 0.6                  | 0.0   | 3.3  | 1.1  |   |
|   | oxides*   | 1.7                  | 0.5   | 2.8  | 0.7  |   |
| orthopyroxenite<br>(17 analyses)  | opx       | 90.5                 | 80.6  | 99.1 | 6.8  | orthopyroxene   |
|   | cpx       | 6.1                  | 0.7   | 14.3 | 4.5  |   |
|   | plag      | 3.2                  | 0.1   | 9.9  | 2.6  |   |
|   | bi        | < 0.1                | 0.0   | 0.2  | -    |   |
|   | oxides*   | 0.1                  | 0.0   | 0.5  | 0.5  |   |
| websterite<br>(6 analyses)  | opx       | 48.3                 | 22.1  | 76.0 | 22.7 | orthopyroxene<br>clinopyroxene  |
|   | cpx       | 49.8                 | 23.9  | 77.9 | 19.1 |   |
|   | plag      | 1.6                  | 0.0   | 10.0 | 3.4  |   |
|   | bi        | 0.0                  | 0.0   | 0.1  | 0.6  |   |
|   | oxides    | 0.3                  | 0.0   | 1.7  | -    |   |
| norite<br>(10 analyses)   | opx       | 32.5                 | 23.3  | 57.6 | 14.3 | presumed to be<br>plagioclase and<br>possibly<br>orthopyroxene<br>(in Gneissic<br>Zone only)                                      |
|   | cpx       | 14.6                 | 0.6   | 31.4 | 28.2 |   |
|   | plag      | 53.0                 | 28.5  | 71.2 | 43.1 |   |
|   | oxides    | 0.0                  | 0.0   | tr   | -    |   |
| Gabbro Band<br>(6 analyses)   | opx       | 23.8                 | 11.6  | 36.7 | 8.3  | possibly<br>plagioclase   |
|   | cpx       | 26.9                 | 17.8  | 38.1 | 6.5  |   |
|   | plag      | 49.4                 | 33.6  | 70.6 | 14.3 |   |
|   | oxides    | tr                   | 0.0   | tr   | -    |   |
| Later noritic<br>intrusive<br>(14 analyses)                                       | opx       | 47.4                 | 18.6  | 86.5 | 73.6 | -   |
|   | cpx       | 18.5                 | 1.6   | 38.2 | 11.7 |   |
|   | plag      | 33.9                 | 5.6   | 71.0 | 18.7 |   |
|   | oxides*   | 0.1                  | 0.0   | 0.4  | -    |   |
|   | bi & hb   | 0.1                  | 0.0   | 1.2  | -    |   |
| Picrites:<br>Central type;<br>(4 analyses).<br>Marginal<br>type;<br>(1 analysis). | ol        | 64.9 (55.6)          | 55.5  | 74.4 | -    | (Note: values<br>in parenthesis<br>are those of<br>the Marginal<br>type picrite<br>only. Averages<br>are from all 5<br>analyses.) |
|   | opx       | 12.7 (19.7)          | 6.4   | 20.5 | -    |   |
|   | cpx       | 12.7 (8.5)           | 5.9   | 24.9 | -    |   |
|   | plag      | 5.5 (6.4)            | 1.7   | 8.0  | -    |   |
|   | oxides*   | 3.5 (3.1)            | 2.5   | 5.4  | -    |   |
| bi & hb   | 0.7 (6.7) | 0.3                  | 1.2   | -    |      |   |

\* includes small amounts of sulphide minerals.

Fig. 3.50

Diagrammatic representation of the modal compositions of rocks from the layered sequence and the associated rocks of Gosse Pile.  
(See Appendix 1).

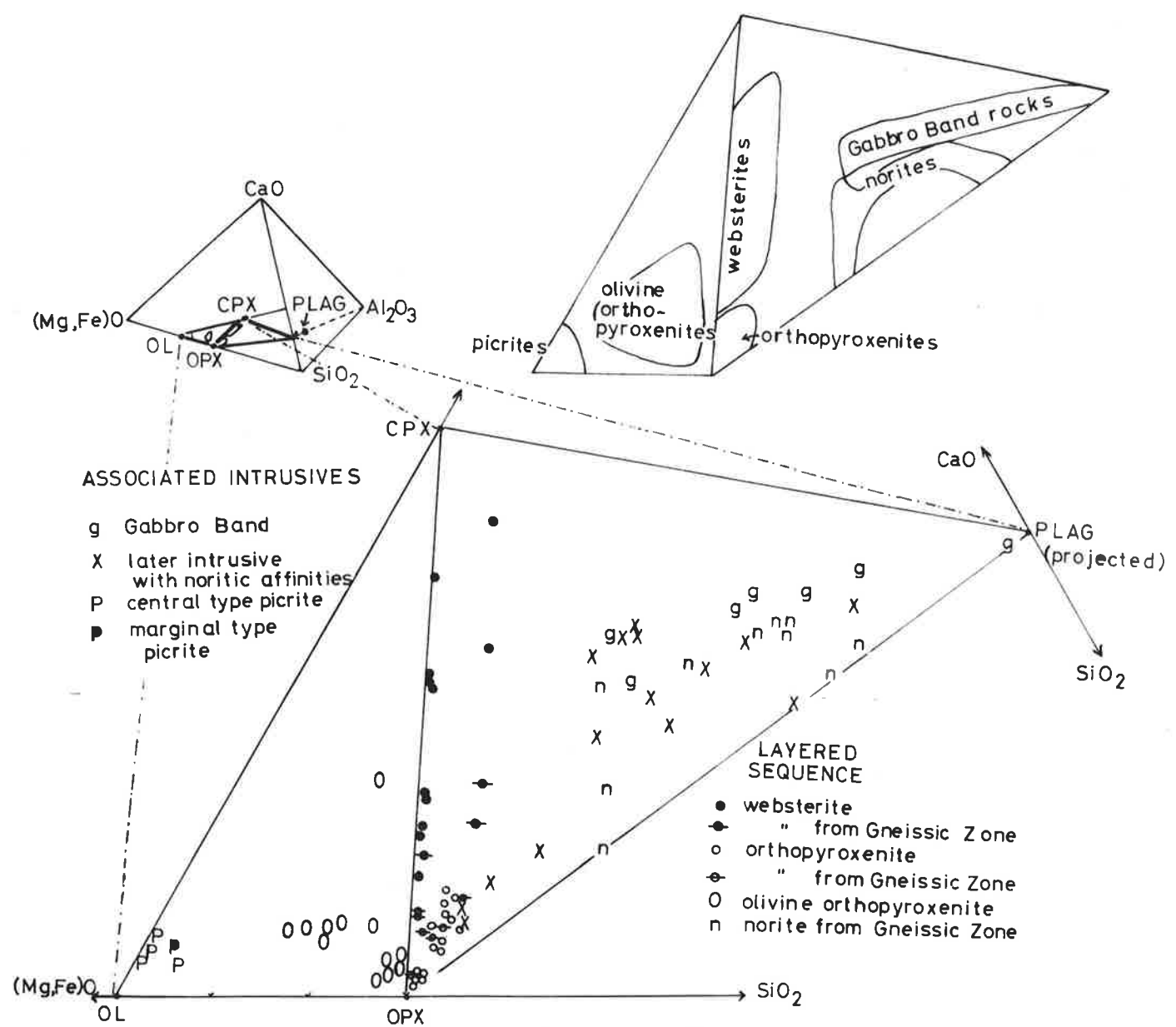


Table 3.5

Chemical analyses and norms of rocks from the Gosse Pile ultramafic layered sequence.

| Analysis No.                   | 1       | 2       | 3       | 4       | 5       | 6       | 7       | 8       |
|--------------------------------|---------|---------|---------|---------|---------|---------|---------|---------|
| Sample No.                     | A313/32 | A313/60 | A313/25 | A313/20 | A313/19 | A313/16 | A313/15 | A313/14 |
| SiO <sub>2</sub>               | 49.03   | 54.04   | 54.15   | 54.80   | 52.48   | 52.86   | 54.25   | 54.04   |
| Al <sub>2</sub> O <sub>3</sub> | 5.45    | 5.10    | 3.22    | 3.13    | 2.54    | 3.06    | 2.74    | 3.15    |
| Fe <sub>2</sub> O <sub>3</sub> | 2.44    | 0.59    | 0.63    | 1.08    | 0.94    | 1.23    | 2.14    | 1.10    |
| FeO                            | 8.47    | 8.48    | 6.07    | 7.66    | 8.85    | 8.00    | 7.47    | 6.38    |
| MgO                            | 30.00   | 27.00   | 22.48   | 29.30   | 31.68   | 30.69   | 29.65   | 21.84   |
| CaO                            | 3.38    | 3.35    | 12.62   | 2.36    | 1.98    | 2.33    | 2.42    | 11.31   |
| Na <sub>2</sub> O              | 0.34    | 0.35    | 0.14    | 0.15    | 0.14    | 0.17    | 0.13    | 0.33    |
| K <sub>2</sub> O               | 0.06    | 0.04    | 0.03    | 0.02    | 0.02    | 0.05    | 0.02    | 0.02    |
| TiO <sub>2</sub>               | 0.19    | 0.23    | 0.17    | 0.14    | 0.13    | 0.14    | 0.13    | 0.17    |
| MnO                            | 0.17    | 0.18    | 0.17    | 0.11    | 0.12    | 0.12    | 0.12    | 0.18    |
| P <sub>2</sub> O <sub>5</sub>  | n.a.    | 0.00    | 0.00    | n.a.    | 0.00    | 0.00    | 0.00    | 0.00    |
| H <sub>2</sub> O <sup>+</sup>  | 0.00    | n.a.    | 0.00    | 0.00    | 0.00    | n.a.    | 0.00    | n.a.    |
| H <sub>2</sub> O <sup>-</sup>  | 0.12    | 0.12    | 0.00    | 0.10    | 0.10    | 0.10    | 0.08    | 0.11    |
| Cr <sub>2</sub> O <sub>3</sub> | 0.25    | 0.50    | 0.24    | 0.65    | 0.50    | 0.61    | 0.50    | 0.54    |
| NiO                            | n.a.    | n.a.    | 0.09    | n.a.    | n.a.    | n.a.    | n.a.    | n.a.    |
| TOTAL                          | 99.90   | 99.98   | 100.01  | 99.50   | 99.48   | 99.36   | 99.65   | 99.17   |

continued

Table 3.5 (continued)

## C.I.P.W. Norms

| Analysis No. | 1       | 2       | 3       | 4       | 5       | 6       | 7       | 8       |       |
|--------------|---------|---------|---------|---------|---------|---------|---------|---------|-------|
| Sample No.   | A313/32 | A313/60 | A313/25 | A313/20 | A313/19 | A313/16 | A313/15 | A313/14 |       |
| q            | -       | -       | -       | 0.24    | -       | -       | -       | 1.12    |       |
| or           | 0.35    | 0.24    | 0.18    | 0.12    | 0.12    | 0.30    | 0.12    | 0.12    |       |
| ab           | 2.88    | 2.96    | 1.18    | 1.27    | 1.18    | 1.44    | 1.10    | 2.79    |       |
| an           | 13.17   | 12.23   | 8.07    | 7.81    | 6.24    | 7.44    | 6.83    | 7.06    |       |
| di           | { wo    | 1.50    | 1.83    | 22.77   | 1.63    | 1.49    | 1.72    | 2.16    | 20.48 |
|              | { en    | 1.14    | 1.36    | 17.23   | 1.24    | 1.13    | 1.32    | 1.67    | 15.46 |
|              | { fs    | 0.20    | 0.30    | 3.22    | 0.21    | 0.22    | 0.23    | 0.26    | 2.95  |
| hy           | { en    | 42.90   | 62.24   | 37.85   | 71.72   | 60.40   | 62.86   | 71.91   | 38.93 |
|              | { fs    | 7.65    | 13.52   | 7.07    | 12.37   | 11.52   | 10.81   | 11.22   | 7.44  |
| ol           | { fo    | 21.49   | 2.55    | 0.63    | -       | 12.17   | 8.58    | 0.19    | -     |
|              | { fa    | 4.22    | 0.61    | 0.13    | -       | 2.56    | 1.63    | 0.03    | -     |
| mt           | 3.54    | 0.86    | 0.91    | 1.57    | 1.36    | 1.78    | 3.10    | 1.59    |       |
| cm           | 0.37    | 0.74    | 0.35    | 0.96    | 0.74    | 0.90    | 0.74    | 0.80    |       |
| il           | 0.36    | 0.44    | 0.32    | 0.27    | 0.25    | 0.27    | 0.25    | 0.32    |       |
| TOTAL        | 99.78   | 99.86   | 99.92   | 99.40   | 99.38   | 99.26   | 99.57   | 99.06   |       |

continued

Table 3.5 (continued)

- 1: olivine-orthopyroxenite, N.E. Hills area.
- 2: plagioclase-bearing orthopyroxenite, N.E. Hills area.  
Originally collected and treated as part of the layered sequence, this rock has shown some peculiarities, discussed later, which throw some doubts on its kinship. It may be part of the later noritic intrusive.
- 3: northern websterite, Main Body.
- 4: orthopyroxenite, central Main Body.
- 5: olivine-orthopyroxenite, central Main Body.
- 6: orthopyroxenite, within annealed zone, Main Body.
- 7: orthopyroxenite, within annealed zone but further south than A313/16, Main Body.
- 8: southern websterite, Main Body.

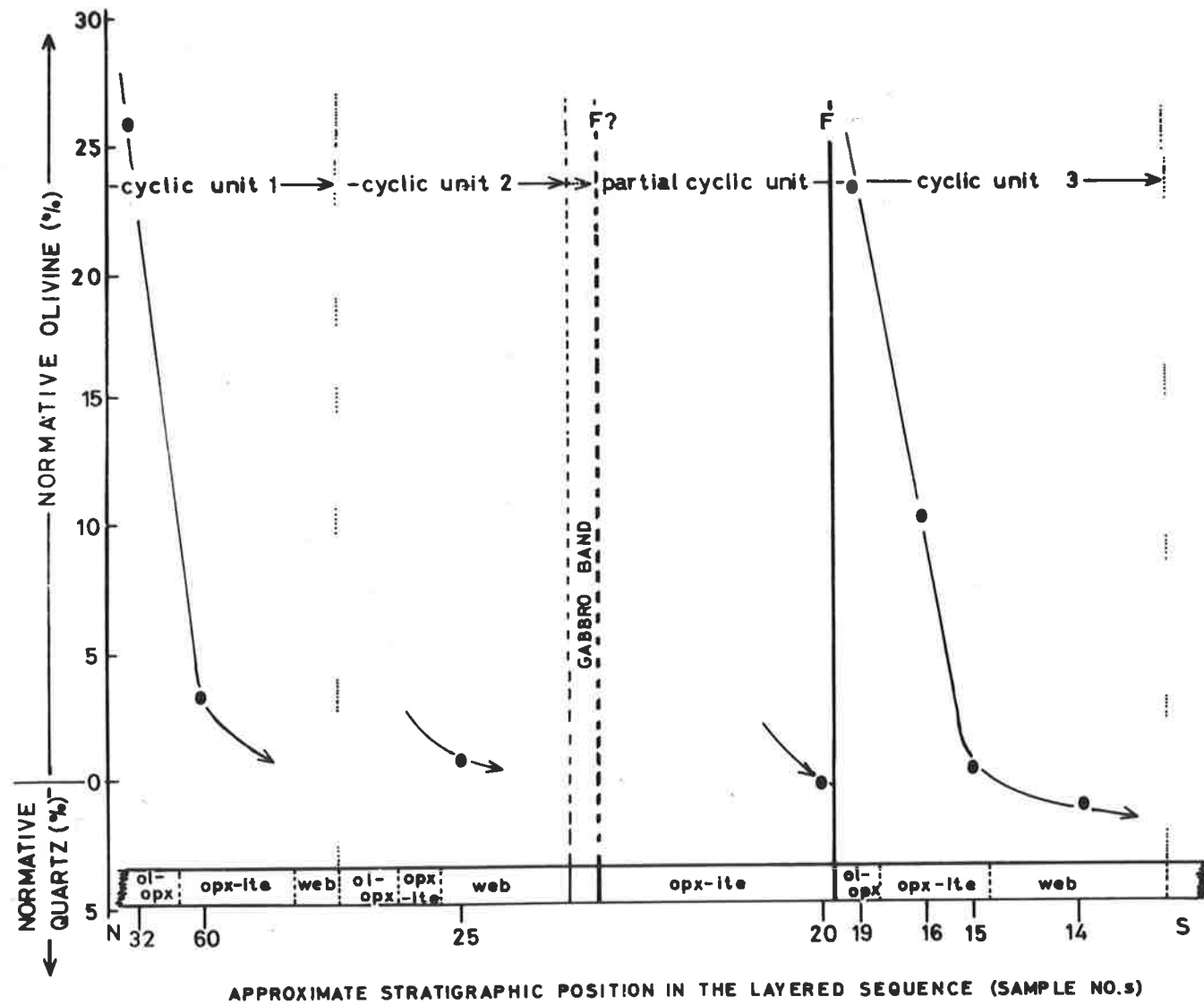
All analyses by A. Moore.

$\text{Cr}_2\text{O}_3$  and NiO were determined by atomic absorption spectroscopy (see Appendix 3A).

Fig. 3.51

Plot of normative quartz and normative olivine (representing silica enrichment or depletion) against the approximate stratigraphic position of the rocks in the layered sequence. See Table 3.5. There is a weak suggestion that, with progressively higher (more southerly) cyclic units, there is an increase in overall silica content.





olivine. This may indicate an overall slight silica enrichment of the magma. Such would be consistent with the argument that the cyclic units result from fresh influxes of parental magma. The fresh magma would mix with the partially fractionated magma to create a homogeneous magma which would then be somewhat richer in silica, because of the previous fractionation, than the initial magma. Silica enrichment of the residual magma is caused mainly by the precipitation of olivine. Since this is relatively minor in Gosse Pile the overall enrichment should also be only minor. Within each individual cyclic unit a more marked silica-enrichment is to be expected, caused first by the precipitation of olivine then pyroxene (as can be seen from the phase relations in the system diopside - forsterite - silica; e.g. see Turner and Verhoogen, 1960, pp. 128-129). This general trend is shown well by the cyclic unit 3 (Fig. 3.51) and rocks above this, in the plagioclase-bearing rocks of the Gneissic Zone, would probably be even more quartz normative. Similar possible trends in the other cyclic units are not so convincing, largely because of a lack of sufficient analyses.

#### The picrite-serpentinite body

Modal analyses (Table 3.4 and Appendix 1) show that the essential mineralogical difference between the marginal- and central-type picrite is in the content of biotite and hornblende. This is reflected in the partial chemical analyses which give:

|   | A313/312E (marginal type) | A313/310A (central type) |
|---|---------------------------|--------------------------|
| FeO:  | 10.41%                    | 8.59%                    |
| MgO:  | 28.71%                    | 32.68%                   |
| Na <sub>2</sub> O:                                    | 0.79%                     | 0.58%                    |
| K <sub>2</sub> O:                                     | 0.39%                     | 0.09%                    |
| SiO <sub>2</sub> (calculated from<br>modal analyses): | 43.7%                     | 42.5%                    |

This indicates an increase of about 36% Na<sub>2</sub>O and 330% K<sub>2</sub>O in the marginal type picrite relative to the central type, and a corresponding change in the MgO/FeO ratio from 2.76 to 3.80. According to the modal analyses and the calculated SiO<sub>2</sub> content the picrites are both ultramafic and ultrabasic (Wyllie, 1967a).

Seifert and Schreyer (1967) have discussed the origin of ultrabasic magmas, considering three ultramafic types:

- (i) those at the bases of layered intrusions;
- (ii) "alpine-type" peridotites;
- (iii) plug- or dyke-like intrusions in the craton.

The picrites of Gosse File (and the surrounding area in the east Tomkinson Ranges) correspond most nearly to the third type: they show no obvious metamorphic effects and their original igneous texture is largely undisturbed by tectonism (Seifert and Schreyer, 1967, p. 351). The intrusive nature of the picrites has been demonstrated by their field relationships.

The high temperatures required to produce a melt of picritic composition, particularly those with high MgO/FeO ratios, such as those now under discussion, has led to what Hess (1955) has termed a "magnificent argument": were such rocks intruded as magnas or as essentially solid masses? Field evidence generally favours the former view, while experimental petrologists favour the latter. However, Presnall (1966) showed experimentally that an original calcium-rich ultrabasic magma can precipitate the sequence of mineral assemblages similar to those observed in Alaskan ultramafic zoned complexes (Taylor, 1967) at high, but acceptable, temperatures (1,300° - 1,450°C) and low pressures. The crystallization path would require relatively high proportions of oxide minerals to be precipitated and, although the scheme may be applicable to some intrusions (e.g. Alaskan complexes - Taylor, 1967; Rainy Creek Complex - Boettcher, 1967) it seems unlikely to be representative of the mechanisms operating during the production of the post-Giles Complex picrite intrusions. This is because:

(i) these intrusions show similar mineralogical compositions over a wide area and are characteristically low in oxide minerals (about 4%);

(ii) the typical zoning (core of dunite passing into peridotite, olivine - pyroxenite, magnetite - pyroxenite and margin of hornblende - pyroxenite) is not found.

The most significant factor to be deduced from the work of Seifert and Schreyer (1967) was that the presence of only a few

percent  $K_2O$ , with water, can produce ultrabasic magmas at relatively low temperatures (Seifert and Schreyer, 1967, Fig. 4). One major problem is that there is now a general lack of  $K_2O$  and  $H_2O$  in ultramafic bodies. Seifert and Schreyer suggested that these magmas contained more alkalis and water during their emplacement than are at present found in the rocks. These elements are presumed to have migrated into the neighbouring rocks during, or after, solidification of the magma. There is no sign of alkali metasomatism in the rocks around the Gosse Pile picrite, but the very different mineralogy and alkali chemistry of the central- and marginal-types is significant.

It is suggested that the picrite was intruded as an ultrabasic (picritic) magma, the temperature of which was lowered considerably by the presence of alkalis and water, as suggested by the work of Seifert and Schreyer (1967). During, or following, intrusion the alkalis and water migrated to the margins of the intrusion, thus producing the marginal-type picrite. There is no field evidence in the Gosse Pile area to enable a relative time of intrusion to be given, apart from noting that it post-dates the formation of the layered sequence. The picrites are probably related, both genetically and in time, to the numerous picrites and olivine-bearing plug-like intrusions found throughout the eastern Tomkinson Ranges.

Serpentinization of the eastern part of the picrite intrusion is considered to be the result of weathering, caused by circulating ground water. No detailed work has been done on the serpentinite and the associated silcrete and magnesite deposits. This conclusion is

based on work by Thomson (1963, 1965) and Turner (1968 and pers. comm.), and by comparison of the Giles Complex laterite zones with similar zones, with magnesite deposits, as described by Illic (1968). The limitation of the extent of serpentinization to the eastern part of the picrite intrusion is not fully understood. A number of east-west fractures and faults occur in the exposed rocks, both in the Main Body and in the N.E. Hills area, so that the determining factor may be tectonic. If minor faulting occurred in the eastern part of the picrite - serpentinite zone, but died out westward it would possibly facilitate the circulation of ground waters in the eastern part, and so enable alteration to take place to a greater depth. Erosion has removed most of the serpentinite - magnesite - silcrete sequence in the picrite - serpentinite zone, leaving relatively unaltered picrite in the west, serpentinite in the east, overlain by remnants of silcrete.

#### The later noritic intrusive and Gabbro Band

Modal analyses of the rocks classed as being part of the later noritic intrusive are plotted in Fig. 3.50 and the scatter serves to emphasise the great variation in composition. Rocks from the Gabbro Band tend to plot within a relatively restricted range: most are gabbroic with a few anorthosites. These occur as small bands, or lenses, on the south side. In general, these rocks have modal compositions which differ from those of the norites in the Gneissic Zone (Fig. 3.50).

In an effort to establish the kinship of the Gabbro Band, samples from this, from the noritic intrusive and from Gneissic Zone norites (part of the layered sequence) were analysed to determine their respective strontium isotopic ratios. The results (Table 3.6) show a close similarity between the isotopic ratios of the Gabbro Band specimen and that from the later noritic intrusive, but a definite difference between the ratios of these rocks and those of the norites from different parts of the Gneissic Zone. Gray (pers. comm., by letter, 1969) considers that these results indicate a definite difference in isotopic ratios which are well outside the limits of experimental error.

The isotopic evidence may then be judged to suggest that the rocks of the Gabbro Band and those of the later noritic intrusive are closely related, but are not directly related to the norites of the layered sequence which contain a higher proportion of radiogenic strontium. This is in accordance with the opinions expressed, on the basis of inconclusive field evidence, in Section 3.2.3. However, noritic rocks, definitely part of the layered sequence, can be obtained only from the Gneissic Zone. Plagioclase-rich rocks are necessary to obtain workable quantities of Sr. Thus, there remains a possibility that, during the deformation of these rocks, a readjustment of Sr isotopic ratios took place and this may account for the differences now observed between the rocks of the Gabbro Band and those of the Gneissic Zone. All the rocks have low Rb contents (can be estimated at only 2 p.p.m. or less as the amount is below the detection limits

Table 3.6

Strontium isotopic ratios for some rocks from Gosse Pile.

$\text{Sr}^{88}/\text{Sr}^{86}$  normalised to 8.37520.

| Spec. No. | Classification                      | $\text{Sr}^{87}/\text{Sr}^{86}$ | s*     |
|-----------|-------------------------------------|---------------------------------|--------|
| A313/12   | Gabbro Band (gabbro)                | $0.7060 \pm 0.0005$             | 0.0002 |
| A313/111  | later noritic intrusive<br>(norite) | $0.7062 \pm 0.0004$             | 0.0002 |
| A313/218  | west Gneissic Zone (norite)         | $0.7075 \pm 0.0005$             | 0.0001 |
| A313/41   | central Gneissic Zone<br>(norite)   | $0.7078 \pm 0.0005$             | 0.0002 |

\* measure of internal precision, not precision of quoted isotopic ratio

Analyses and results by Mr. C.M. Gray, Australian National University, Canberra.



of the equipment available) so that, in the relatively short time between crystallization and deformation of the Gneissic Zone rocks, it seems unlikely that the ratio could have increased by about 0.0015.

A more serious weakness in the isotopic evidence is the recent discovery by Pankhurst (1969) that the  $\text{Sr}^{87}/\text{Sr}^{86}$  ratio can increase progressively with differentiation. For example, rocks of the Insch mass underwent a progressive increase of the Sr isotopic ratio from 0.703 to 0.712 during fractional crystallization. Pankhurst (1969) suggests that this may be due to addition of  $\text{Sr}^{87}$  from an external source — influxes of fresh magma, or possible equilibration over large distances with the country rock. Similar changes may have occurred within the Gosse Pile sequence so that the first-formed cumulate (?) plagioclase of the Gabbro Band would give a lower isotopic ratio than that of the later cumulate plagioclase of the Gneissic Zone norites.

Thus, the evidence of the isotopic ratios is inconclusive. However, closeness of the ratios of the Gabbro Band rocks and later noritic intrusive are perhaps significant. This, combined with the weak geological evidence tends to support the view that the Gabbro Band is not part of the layered sequence.

#### Anorthosites

Within Gosse Pile are found small anorthosite bodies which are of two types.

The first type of anorthosite is as bands, or lenses, approximately 2 m x 20 m in size at the eastern end of Gosse Pile, but generally much smaller. They are found associated with, and on the south side of, the Gabbro Band. A modal analysis of one such rock (A313/143) shows it to be 98.8% plagioclase (An<sub>75</sub>) and only 1.2% pyroxene. No other minerals were observed. These anorthosites are almost invariably cut by minor faults and associated pseudotachylite veins and it is, therefore, difficult to interpret their textures. It appears that, prior to the brittle deformation, they consisted of granular, anhedral plagioclase with neither shape nor lattice preferred orientation. In this respect the textures appear to have been the same as those now observed in some plagioclase adcumulates of layered intrusions (Wager and Brown, 1968) and in granular anorthosites found as inclusions in alkali-dolerite dykes of Greenland (Bridgwater, 1967). The pyroxene occurs interstitially.

If the Gabbro Band underwent some crystal fractionation either as part of the layered sequence or, as now seems more likely, as a later sill or dyke of gabbroic magma, then a concentration of feldspathic material near the top (south side) might be expected. It should be noted though, that within the Gabbro Band no other phase layering has been observed. Fractionation should lead to the late precipitation of plagioclase more sodic than those found elsewhere in the band, whereas the anorthosite plagioclase is more calcic (Fig. 3.54). Savolahti (1966) has described similar anorthosite lenses in gabbroic bodies from Finland. He explains these by assuming a sudden formation of an

abundance of plagioclase nuclei which took place at a time when the rate of generation of plagioclase nuclei in the magma was very high. The anorthosite lenses of the Finnish gabbroic bodies also occur in the marginal zones of the intrusions and so may have appeared even prior to intrusion as well as afterwards. A similar process may have operated in the Gabbro Band.

The second type of anorthosite occurrence is as irregular, massive, lens-like bodies in the western Gneissic Zone (Fig. 1.3, 2/B). These are unlike any rocks found elsewhere in Gosse Pile. They are fine-grained, purple rocks consisting of about 98% strongly antiperthitic plagioclase ( $An_{34}$ ) and about 2% of pyroxenes and magnetite. These anorthosites are very similar both in appearance and composition (including the plagioclase anorthite content) to the minor anorthosites in the granulites found along the northern contact of Gosse Pile (Section 2.9.2, p. 67). This similarity suggests a possible similar genesis.

Interaction between magma and the intruded granulites, resulting in rheomorphic veins and local contamination along the northern and western margins of the Main Body has already been noted. It is significant that the purple anorthosites in the granulites are similarly confined to these areas. It is suggested that these anorthosites represent the crystalline residuum produced by partial melting of the  $q + Kf + px$  granulites into which the magma of the later noritic intrusive was forced. Along the margins of the

intrusion no sign has been found, in the granulites, of the acid material which would necessarily have to be produced during the partial anatexis of the granulite. However, this may have gone to produce the acid rheomorphic veins and "contaminated rocks" such as are found at the northwest margin of Gosse Pile. These veins are rich in quartz and contain some antiperthite and mafic minerals. If the anorthosites in the western Gnoissic Zone similarly represent a residue from partially melted acid granulite, then it must be assumed that the magma was locally contaminated or the acid melt was removed, although there is no evidence for local contamination of the rocks around these anorthosite masses at present. However, any acid residuum produced could mix with the magma and need not necessarily produce any significant mineralogical changes in the immediate vicinity of the anorthosites. Such an origin for the anorthosites (i.e. residual material following partial anatexis of acid granulites, under high pressure) would explain their relatively high albite contents (Green, 1969).

---

### 3.6 MINERALOGY

#### 3.6.1 Plagioclase

##### Introduction

Gosse Pile, unlike the majority of other layered intrusions of the Giles Complex, is notably deficient in plagioclase: the first probably cumulus plagioclase is that found in the Gneissic Zone (Fig. 3.1), unless the Gabbro Band is considered to be part of the layered sequence. The plagioclase of the pyroxenites is always interstitial; it never exceeds 10% of the total rock and is generally present in much smaller amounts, a factor which causes difficulty in extracting sufficient material for study. Plagioclase is generally the major constituent of the later noritic intrusive rocks and of the Gabbro Band.

In all specimens some degree of strain is exhibited and, because of the strain shadows, it is often difficult to decide whether the crystals are zoned or not. In some interstitial plagioclase grains, changes in extinction are often more uniform than one would expect as a result of strain: the extinction shadow moves from the margin inwards, following the irregular crystal shape. Under such circumstances the plagioclase is thought to be normally and evenly zoned, the more calcic portion occurring at the centre. More commonly undulose extinction occurs unrelated to grain shape or twin positions.

---

Primary twins are rare and the majority of plagioclase crystals show secondary, or glide, twins developed according to the albite (very common), pericline (common) or albite - Carlsbad (uncommon) twin laws, Fig. 3.53. Distinctions between primary and secondary twins were based on the criteria given by Vance (1961).

The intercumulus plagioclase of the layered sequence is commonly antiperthitic (Fig. 3.52), as is that in the norites of the Gneissic Zone. The antiperthite takes the form of K-feldspar (recognised only on the basis of its lower refractive index and slight pinkish colour relative to the host plagioclase) occurring as very small blebs and stringers in the plagioclase. A slight concentration of K-feldspar has been observed at the boundaries of plagioclase grains in some orthopyroxenites. The later noritic intrusive may also contain antiperthite but it is not common. Antiperthite has not been found in any of the olivine-bearing rocks. Goode and Krieg (1967) reported antiperthite in transgressive mafic pegmatites of the Ewarara intrusion (Fig. 1.1), but the antiperthite occurring within the layered sequence of Gosse Pile appears to be the first reported from the layered intrusions. Its occurrence thus distinguishes Gosse Pile from other layered intrusions where antiperthite has not been described (Wager and Brown, 1968). Antiperthite has, however, been recognised in the Kalka intrusion (A.D.T. Goode, pers. comm.) and Gray (1967) has reported that it is found in the Teizi meta-anorthosite, which he regards as part of the Giles Complex.

Fig. 3.52

Two photomicrographs of antiperthite in rocks of the layered sequence. That on the left is interstitial feldspar in an orthopyroxenite (A313/60) near the base of the intrusion. That on the right is strongly antiperthitic, interstitial plagioclase from an orthopyroxenite (A313/116) from the Gneissic Zone.

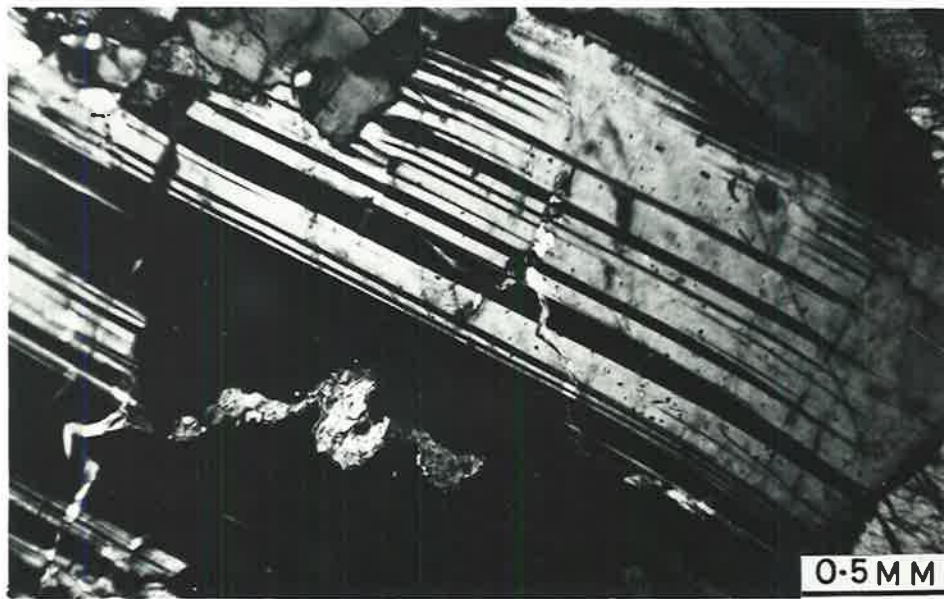
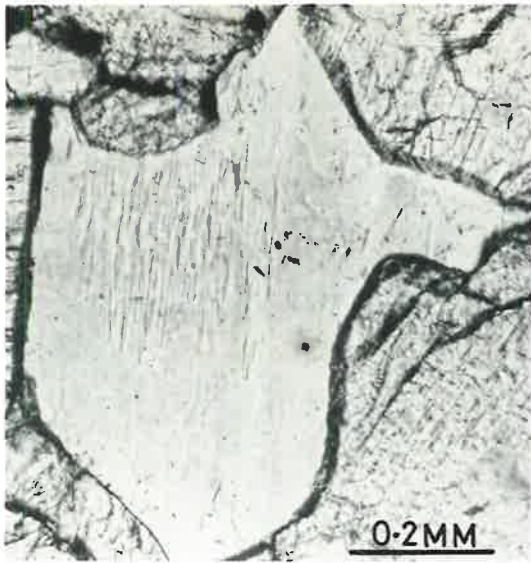
Both photographs: P.P.L.

Photographs: A. Moore.

Fig. 3.53

Photomicrograph illustrating the secondary, or glide, twinning according to the albite-Carlsbad twin law in plagioclase, and also the alteration to a colourless, highly birefringent mineral thought to be scapolite. A313/41. C.P.

Photograph: A. Moore.





In many plagioclase crystals of the later noritic intrusive are found numerous small (approximately  $15\mu$  in length) needles with a regular  $60^\circ$  orientation. These are thought to be either spinel or rutile. Plagioclase found elsewhere in Gosse Pile is generally very clear. No spectacular euhedral pyroxene crystals such as occur in the plagioclase from Ewarara (Goode and Krieg, 1967) were found. Some alteration has been observed, generally as fine veins of carbonate (calcite?) or sericite. In one crystal there occurs a colourless, high-relief alteration product which is thought to be scapolite (Fig. 3.53).

#### Composition and Structural State

The rapid, accurate measurement of plagioclase compositions posed a slight problem because:

- (a) Measurement of the maximum extinction angles of albite and albite - Carlsbad twins, and (010) - pericline twin lamellae (Chudoba and Kennedy, 1933), in thin sections orientated normal to (010) was difficult as most grains show undulose extinction. Further, the majority of twins are secondary with their twin planes meeting in a point. Measurements made on such twins commonly lie off the established migration curves and are of dubious value.
- (b) Most optical and X-ray parameters vary slightly with changes in the structural state of the plagioclase (e.g. Smith, 1958; Smith and Gay, 1958). It cannot be assumed that all the

plagioclases in Gosse Pile have had the same thermal history. Smith (1958) indicated that, for feldspars in the compositional range  $An_{20-60}$ , the refractive indices vary only slightly with changes in structural state. However, it is estimated that to obtain a precision of  $\pm 2\%$  An requires a precision in measurement of  $\pm 0.001$  (Brown, 1967). The estimated precision obtained for the measured refractive indices of Gosse Pile plagioclases was between  $\pm 0.001$  and  $\pm 0.003$ .

(c) The quantity of plagioclase in the pyroxenites is generally so small that large volumes of rock must be crushed to extract relatively small amounts of plagioclase for study.

Hall (1965) compared X-ray and optical measurements of plagioclases ( $An_{5-43}$ ) and concluded that the X-ray methods he used were generally superior to the optical methods. For this reason, and because the measurement of refractive indices (within  $\pm 0.001$ ) were so time-consuming, it was decided that measurements of the plagioclase compositions should be made using the parameter  $\Gamma$ , defined by Smith and Gay (1958) as  $2\theta(131) + 2\theta(220) - 4\theta(1\bar{3}1)$ . This parameter is dependent mainly on the reciprocal lattice angle  $\chi^*$ , which is sensitive to changes in composition and structural state. This should make possible estimations of the structural states of chemically analysed samples, as well as a comparison between plagioclases from Gosse Pile and other layered intrusions for which this data is available. During the measurement of the Sr contents of the plagioclases it was necessary to measure their mass absorption

coefficients. This led to the development of a further method for indirectly determining their compositions and this is described in Appendix 2. Table 3.7 lists the plagioclases mentioned in this section. Table 3.8 compares the compositions of several plagioclase samples determined using different methods.

Measurement of  $\Gamma$  using chemically analysed, unheated plagioclases from Gosse Pile showed that more than one structural state occurs (Fig. 3.54). Thus, the determinative curve for unheated Mt. Davies plagioclases after Kleeman (1965) and Kleeman and Nesbitt (1967) cannot be used. The scatter for unheated Gosse Pile plagioclases is considerable, even using samples from the same rock type. Plagioclases from the Bushveld Complex (Desborough and Cameron, 1968) also show some scatter, as do those from the Teizi meta-anorthosite (Gray, 1967). Apart from three samples, from the Gabbro Band, which lie on the Mt. Davies unheated plagioclase trend, the Gosse Pile plagioclases are more disordered than those from Mt. Davies and considerably more disordered than those from the Bushveld Complex (Fig. 3.54). The degree of disorder in igneous plagioclase feldspars is generally related to their rate of cooling: the more rapidly cooled the feldspar the more likely it is to preserve a disordered structural state (e.g. Hoffer, 1968).

The effect of dry heating (at  $1,050^{\circ}\text{C}$ ) for periods in excess of 6 weeks (1,000 hrs) was to produce a marked change in the value of  $\Gamma$ . Three samples (A313/12, /60 and /88) were measured after heating for

Table 3.7

List of rocks from which plagioclases, studied in detail, were obtained. See also the sample location map for exact location.

(a) plagioclases partially or completely analysed chemically:

| Sample No.<br>A313/- | Rock type and relationship                                   |
|----------------------|--|
| 11                   | orthopyroxenite; layered sequence. Main Body.                |
| 12                   | gabbro; Gabbro Band.   |
| 13                   | websterite (N); layered sequence. Main Body.                 |
| 60                   | orthopyroxenite; layered sequence (?). N.E. Hills.           |
| 88                   | orthopyroxenite; layered sequence. Main Body, N. of picrite. |
| 111                  | norite; noritic intrusive. Main Body (W).                    |
| 116                  | orthopyroxenite; layered sequence. Gneissic Zone.            |
| 143                  | anorthosite; Gabbro Band (S).                                |
| 176                  | norite; noritic intrusive. Main Body (W).                    |
| 204A                 | norite; noritic intrusive. Main Body, N. of picrite.         |
| 232                  | websterite (N); layered sequence. Main Body.                 |
| 233B                 | gabbro; Gabbro Band.   |
| 234                  | orthopyroxenite; layered sequence. Main Body, N. of picrite. |
| 243                  | orthopyroxenite; layered sequence. Main Body.                |
| 275                  | anorthosite; inclusion in Gneissic Zone.                     |
| 282B                 | mafic pegmatite; noritic intrusive. Main Body.               |

(b) plagioclases not chemically analysed:

|      |   |
|------|---|
| 47   | orthopyroxenite; layered sequence. Main Body.         |
| 50   | orthopyroxenite; layered sequence. Main Body.         |
| 52   | gabbro; Gabbro Band.                                  |
| 97   | orthopyroxenite; layered sequence. Gneissic Zone.     |
| 107  | orthopyroxenite; layered sequence. Main Body.         |
| 164A | norite; layered sequence. Gneissic Zone.              |
| 194  | orthopyroxenite; layered sequence. Main Body.         |
| 195  | olivine-orthopyroxenite; layered sequence. Main Body. |
| 273  | orthopyroxenite; layered sequence. Gneissic Zone.     |
| 285  | norite; noritic intrusive. Main Body.                 |
| 310A | picrite (central type); Picrite-serpentinite zone.    |
| 312E | picrite (marginal type); Picrite-serpentinite zone.   |

Table 3.8

Comparison of plagioclase compositional determinations using different methods. An value quoted is atomic ratio  $An\%$  = atomic ratio  $\frac{Ca + Sr \times 100}{Ca + Sr + Na + K}$ .

| Sample No.<br>A313/- | Chemical<br>analysis<br>(1) | Max. extinction<br>angle<br>(2) | Refractive<br>indices<br>(3) | $\Gamma$<br>(4) | $\mu$<br>(5) |
|----------------------|-----------------------------|---------------------------------|------------------------------|-----------------|--------------|
| 11                   | 62.30                       | 54 (a)                          | -                            | 63.02           | 61.76        |
| 12                   | 71.18                       | 72 (a-C)                        | 72                           | 70.82           | 70.10        |
| 13                   | 76.29                       | -                               | -                            | 76.53           | -            |
| 60                   | 36.65                       | 40 (a)                          | -                            | 49.83*          | -            |
| 88                   | 51.55                       | 50 (a)                          | -                            | 53.81           | 51.65        |
| 111                  | 54.06                       | 66 (a)                          | -                            | 54.65           | 53.93        |
| 116                  | 51.43                       | 47 (a)                          | -                            | 45.83           | 50.64        |
| 143                  | 75.44                       | 52 (a)                          | -                            | 74.88           | 75.41        |
| 176                  | 60.78                       | 70 (a)                          | -                            | 62.51           | 60.75        |
| 204A                 | 59.11                       | 62 (a-C)                        | 58                           | 57.25           | 58.98        |
| 232                  | 65.83                       | 48 (a)                          | -                            | 66.00           | 65.80        |
| 233B                 | 70.82                       | 74 (a-C)                        | 72                           | 70.19           | 70.86        |
| 234                  | 49.92                       | -                               | -                            | 49.07           | 49.88        |
| 243                  | 55.15                       | -                               | -                            | 57.31           | -            |
| 275                  | 33.96                       | 30 (a)                          | 32                           | 28.20*          | -            |
| 282B                 | 53.30                       | 49{(010) - PL}                  | 52                           | 56.68           | 50.34        |
|                      |                             | 54 (a)                          |                              |                 |              |

Notes: (1) In most cases analysed only for CaO, Na<sub>2</sub>O, K<sub>2</sub>O and Sr.

(2) Abbreviations: (a) = albite twins. (a-C) = albite - Carlsbad twins. {(010) - PL} = (010) to Pericline twin lamellae.

(3) See Appendix 3D. Values measured are:

12:  $\alpha = 1.5645$   
 204A:  $\alpha = 1.5582$ ;  $\beta = 1.5620$ ;  $\gamma = 1.5658$ .  
 233B:  $\alpha = 1.5642$ .  
 275:  $\alpha = 1.5450$ ;  $\beta = 1.5504$ ;  $\gamma = 1.5541$ .  
 282B:  $\alpha = 1.5555$ ;  $\beta = 1.5580$ ;  $\gamma = 1.5630$ .

continued

Table 3.8 (continued)

(4)  $\Gamma$  calculated from heated plagioclases.

$$\text{An}\% = 63.72\Gamma - 4.65 \quad (\text{see Appendix 3B}).$$

\* $\Gamma$  cannot be used for An values below about An<sub>45</sub> as there is little change in  $\Gamma$  with composition (Fig. 3.54). The equation is calculated only for compositions between An<sub>59-87</sub>, but probably is applicable to compositions as low as An<sub>45</sub>.

(5) See Appendix 2.  $\text{An}\% = 25.25 \mu \text{SrK}_a - 164.66$

Fig. 3.54

Plot of  $\Gamma$  (in  $^{\circ}2\theta$ ) against atomic ratio  $\%An$  for plagioclases from Gosse Pile, Teizi meta-anorthosite, the Bushveld, Stillwater and from Mt. Davies.

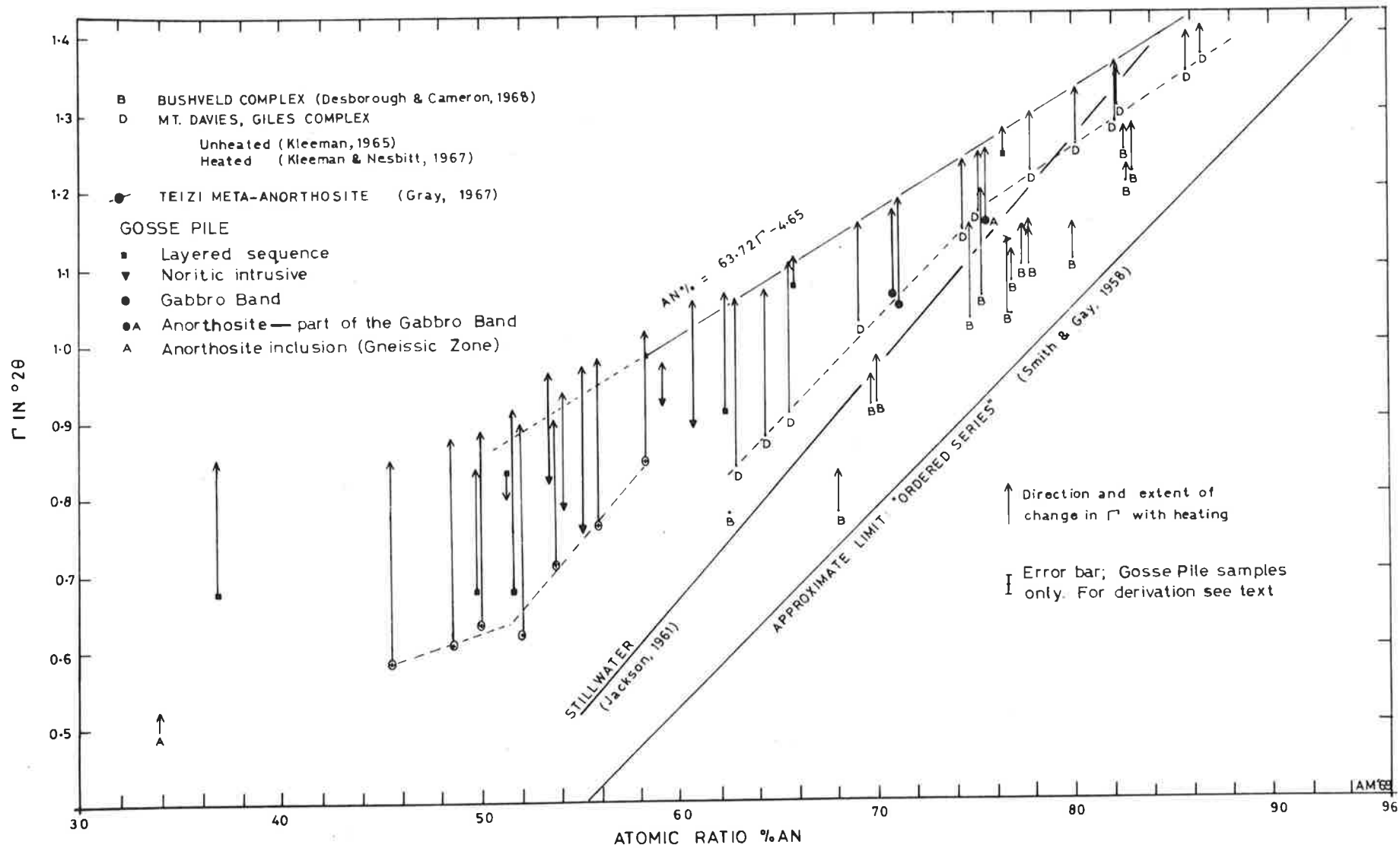




Table 3.12 Chemical analyses of clinopyroxenes and their structural formulae, (calculated on the basis of 6 Oxygens).

| Analysis   | 1a     | 2a     | 3a     | 4a     | 6a     | 7a     | 8a     | 12a    | 13b    | 14a    | 16a    | 18a    | 19a    | 22a    |
|--|--------|--------|--------|--------|--------|--------|--------|--------|--------|--------|--------|--------|--------|--------|
| Sample No.   | 11     | 12     | 13     | 14     | 25     | 39B    | 44     | 50     | 52     | 53*    | 55     | 60     | 116    | 273    |
| SiO <sub>2</sub>   | 52.33  | 52.70  | 51.77  | 51.51  | 51.82  | 52.87  | 52.24  | 51.10  | 51.12  | 51.42  | 52.56  | 52.98  | 51.57  | 53.52  |
| Al <sub>2</sub> O <sub>3</sub>                                     | 5.02   | 4.71   | 4.77   | 3.88   | 3.52   | 5.14   | 3.90   | 5.00   | 5.38   | 4.11   | 5.32   | 5.14   | 6.10   | 4.59   |
| Fe <sub>2</sub> O <sub>3</sub>                                     | 0.97   | 1.77   | 2.17   | 0.19   | 1.14   | 0.16   | 1.43   | 0.88   | 1.43   | 1.62   | 0.03   | 1.56   | 1.04   | 0.21   |
| Cr <sub>2</sub> O <sub>3</sub>                                     | 0.82   | 0.39   | 0.44   | 0.95   | 0.64   | 1.31   | 1.09   | 1.11   | 0.39   | 0.44   | 1.32   | 0.51   | 0.97   | 0.84   |
| FeO  | 4.00   | 4.25   | 4.02   | 4.48   | 4.50   | 3.97   | 2.71   | 3.69   | 4.50   | 4.09   | 3.90   | 3.47   | 3.12   | 5.15   |
| MgO  | 15.97  | 15.79  | 17.51  | 17.00  | 18.79  | 16.65  | 15.85  | 16.57  | 17.94  | 17.48  | 15.81  | 15.80  | 14.61  | 17.99  |
| CaO  | 18.91  | 18.62  | 18.19  | 21.12  | 18.69  | 18.46  | 22.21  | 20.43  | 17.92  | 19.86  | 19.67  | 19.41  | 20.45  | 16.46  |
| Na <sub>2</sub> O  | 0.69   | 0.40   | 0.44   | 0.53   | 0.37   | 1.06   | 0.57   | 0.89   | 0.54   | 0.39   | 1.06   | 0.16   | 1.14   | 0.50   |
| K <sub>2</sub> O   | 0.00   | 0.00   | 0.00   | 0.00   | 0.01   | 0.07   | 0.00   | 0.03   | 0.01   | 0.02   | 0.05   | 0.01   | 0.20   | 0.00   |
| TiO <sub>2</sub>   | 0.35   | 0.29   | 0.25   | 0.24   | 0.20   | 0.34   | 0.26   | 0.38   | 0.22   | 0.27   | 0.41   | 0.51   | 0.71   | 0.35   |
| MnO  | 0.13   | 0.15   | 0.16   | 0.13   | 0.16   | 0.11   | 0.13   | 0.13   | 0.16   | 0.16   | 0.12   | 0.13   | 0.11   | 0.14   |
| NiO  | 0.06   | 0.06   | 0.06   | 0.05   | 0.06   | 0.06   | 0.07   | 0.14   | 0.06   | 0.05   | 0.12   | n.a.   | 0.05   | 0.06   |
| TOTAL  | 99.25  | 99.13  | 99.78  | 100.08 | 99.90  | 100.20 | 100.46 | 100.35 | 99.67  | 99.91  | 100.37 | 99.68  | 100.07 | 99.81  |
| Trace elements (in p.p.m.)   |        |        |        |        |        |        |        |        |        |        |        |        |        |        |
| Cr   | 5616   | 2690   | 3012   | 6469   | 4383   | 8969   | 7454   | 7593   | 2699   | 2979   | 9025   | 5900   | 6621   | 5777   |
| Ni   | 466    | 491    | 496    | 398    | 458    | 450    | 557    | 1091   | 476    | 395    | 980    | n.a.   | 393    | 477    |
| Cu   | n.a.   | n.a.   | n.a.   | n.a.   | n.a.   | < 20   | n.a.   | n.a.   | n.a.   | < 20   | < 20   | n.a.   | < 20   | n.a.   |
| Sr   | n.a.   | 11.4   | 10.6   | 10.0   | 12.9   | 15.1   | 15.6   | 35.8   | 4.2    | 17.8   | n.a.   | 43.7   | 22.9   | 19.1   |
| Structural formulae of clinopyroxenes (on the basis of 6 Oxygens). |        |        |        |        |        |        |        |        |        |        |        |        |        |        |
| Si   | 1.9109 | 1.9258 | 1.8847 | 1.8854 | 1.8897 | 1.9089 | 1.8992 | 1.8619 | 1.8642 | 1.8797 | 1.9015 | 1.9188 | 1.8761 | 1.9310 |
| Al <sup>IV</sup>   | 0.0891 | 0.0742 | 0.1153 | 0.1146 | 0.1103 | 0.0911 | 0.1008 | 0.1381 | 0.1358 | 0.1203 | 0.0985 | 0.0812 | 0.1239 | 0.0690 |
| Al <sup>VI</sup>   | 0.1268 | 0.1287 | 0.0890 | 0.0525 | 0.0409 | 0.1276 | 0.0661 | 0.0764 | 0.0951 | 0.0567 | 0.1280 | 0.1382 | 0.1375 | 0.1261 |
| Fe <sup>3+</sup>   | 0.0263 | 0.0483 | 0.0590 | 0.0048 | 0.0311 | 0.0043 | 0.0388 | 0.0240 | 0.0390 | 0.0443 | 0.0004 | 0.0422 | 0.0284 | 0.0056 |
| Cr <sup>3+</sup>   | 0.0232 | 0.0109 | 0.0122 | 0.0272 | 0.0184 | 0.0373 | 0.0310 | 0.0319 | 0.0109 | 0.0123 | 0.0373 | 0.0143 | 0.0275 | 0.0238 |
| Fe <sup>2+</sup>   | 0.1220 | 0.1297 | 0.1222 | 0.1370 | 0.1371 | 0.1197 | 0.0823 | 0.1123 | 0.1371 | 0.1249 | 0.1178 | 0.1049 | 0.0948 | 0.1552 |
| Mg   | 0.8690 | 0.8599 | 0.9498 | 0.9273 | 1.0212 | 0.8958 | 0.8588 | 0.8997 | 0.9749 | 0.9522 | 0.8525 | 0.8527 | 0.7920 | 0.9672 |
| Ca   | 0.7397 | 0.7290 | 0.7094 | 0.8283 | 0.7302 | 0.7140 | 0.8651 | 0.7977 | 0.7001 | 0.7778 | 0.7624 | 0.7533 | 0.7970 | 0.6363 |
| Na   | 0.0487 | 0.0281 | 0.0306 | 0.0373 | 0.0258 | 0.0742 | 0.0397 | 0.0626 | 0.0381 | 0.0272 | 0.0743 | 0.0108 | 0.0800 | 0.0346 |
| K  | 0.0000 | 0.0000 | 0.0000 | 0.0000 | 0.0004 | 0.0030 | 0.0000 | 0.0013 | 0.0004 | 0.0008 | 0.0021 | 0.0004 | 0.0091 | 0.0000 |
| Ti   | 0.0094 | 0.0079 | 0.0067 | 0.0065 | 0.0054 | 0.0091 | 0.0069 | 0.0102 | 0.0059 | 0.0072 | 0.0110 | 0.0137 | 0.0192 | 0.0093 |
| Mn   | 0.0039 | 0.0046 | 0.0048 | 0.0039 | 0.0048 | 0.0032 | 0.0039 | 0.0039 | 0.0048 | 0.0048 | 0.0034 | 0.0039 | 0.0032 | 0.0041 |
| Ni   | 0.0017 | 0.0017 | 0.0017 | 0.0013 | 0.0017 | 0.0017 | 0.0019 | 0.0039 | 0.0017 | 0.0013 | 0.0034 | -      | 0.0013 | 0.0017 |
| Z  | 2.0000 | 2.0000 | 2.0000 | 2.0000 | 2.0000 | 2.0000 | 2.0000 | 2.0000 | 2.0000 | 2.0000 | 2.0000 | 2.0000 | 2.0000 | 2.0000 |
| WXY  | 1.9707 | 1.9488 | 1.9854 | 2.0261 | 2.0170 | 1.9899 | 1.9945 | 2.0239 | 2.0080 | 2.0095 | 1.9926 | 1.9344 | 1.9900 | 1.9639 |
| En   | 11.14  | 12.75  | 11.64  | 8.59   | 9.60   | 9.89   | 8.04   | 9.06   | 11.39  | 10.11  | 9.64   | 11.64  | 10.34  | 11.81  |
| Fs   | 48.26  | 48.05  | 50.73  | 47.99  | 52.44  | 49.58  | 45.83  | 47.56  | 51.52  | 49.45  | 47.37  | 48.47  | 44.66  | 53.50  |
| Wo   | 40.60  | 39.20  | 37.63  | 43.42  | 37.96  | 40.53  | 46.13  | 43.38  | 37.09  | 40.44  | 42.99  | 39.89  | 45.00  | 34.69  |
| Mg   | 49.46  | 48.67  | 51.61  | 48.87  | 53.20  | 51.67  | 46.55  | 49.07  | 52.67  | 50.14  | 49.19  | 48.64  | 46.26  | 54.82  |
| Σ Fe   | 8.44   | 10.07  | 9.85   | 7.47   | 8.76   | 7.15   | 6.56   | 7.43   | 9.51   | 8.91   | 6.82   | 8.39   | 7.20   | 9.11   |
| Ca   | 42.10  | 41.26  | 38.54  | 43.66  | 38.04  | 41.18  | 46.89  | 43.50  | 37.82  | 40.95  | 43.99  | 42.97  | 46.54  | 36.07  |
| Σ Fe as FeO  | 4.87   | 5.84   | 5.97   | 4.65   | 5.52   | 4.11   | 4.00   | 4.48   | 5.79   | 5.55   | 4.02   | 4.87   | 4.06   | 5.34   |
| MgO/Σ FeO  | 3.28   | 2.70   | 2.93   | 3.66   | 3.40   | 4.05   | 3.96   | 3.70   | 3.10   | 3.15   | 3.93   | 3.24   | 3.60   | 3.37   |
| %Al in Z   | 4.46   | 3.71   | 5.77   | 5.73   | 5.52   | 4.56   | 5.04   | 6.91   | 6.79   | 6.02   | 4.93   | 4.06   | 6.20   | 3.45   |
| %Al in WXY   | 6.43   | 6.60   | 4.48   | 2.59   | 2.03   | 6.41   | 3.31   | 3.78   | 4.74   | 2.82   | 6.42   | 7.14   | 6.91   | 6.42   |
| Mg   | 85.1   | 82.5   | 83.6   | 86.4   | 85.5   | 87.6   | 87.3   | 86.5   | 84.4   | 84.4   | 87.5   | 85.0   | 86.2   | 85.0   |

\* Poor analyses, probably due to incomplete separation of orthopyroxene and clinopyroxene. All are from rocks in which the two pyroxenes are intimately intergrown.

Z: The trivalent and quadrivalent cations in tetrahedral co-ordination (Si<sup>4+</sup>, Al<sup>3+</sup>).

WXY: The bi-, tri-, and quadri-valent cations in octahedral co-ordination (Al<sup>3+</sup>, Fe<sup>3+</sup>, Ti<sup>4+</sup>, Mg<sup>2+</sup>, Mn<sup>2+</sup>, Fe<sup>2+</sup>) and mono-, and bi-valent cations in hexahedral co-ordination (K<sup>+</sup>, Na<sup>+</sup> and Ca<sup>+</sup>).

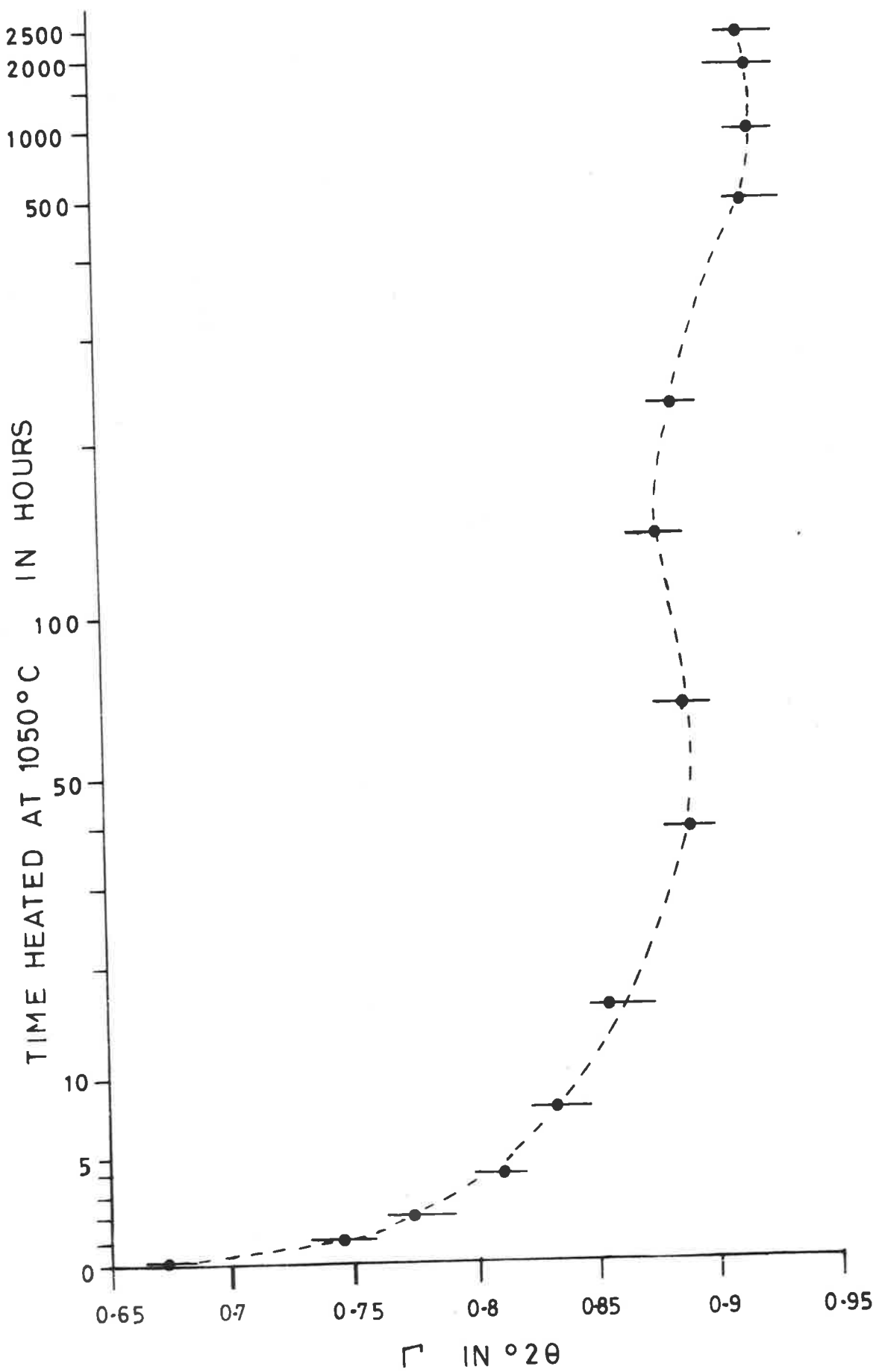
En: Molecular % enstatite = Mg + 1/2 Al<sup>IV</sup> + 1/2 Ti; Fs = molecular % ferrosilite = Fe<sup>2+</sup> + Fe<sup>3+</sup> + 1/2 Al<sup>IV</sup> + 1/2 Ti; Wo = molecular % wollastonite = Ca + Na.

Mg: Molecular % Mg<sup>2+</sup>. Σ Fe: molecular % (Fe<sup>2+</sup> + Fe<sup>3+</sup>). Ca = molecular % Ca<sup>2+</sup>.

mg: 100Mg/Mg + Fe<sup>2+</sup> + Fe<sup>3+</sup> + Mn.

Fig. 3.55

Graph showing the change of  $\Gamma$  (in  $^{\circ}2\theta$ ) as a function of time heated for a plagioclase from Gosse Pile (A313/88).



specific times. A graph of  $\Gamma$  vs heating time is given in Fig. 3.55 for A313/88, but the other samples showed similar patterns: a rapid increase in  $\Gamma$  at first, levelling off to a constant value after about 100-200 hrs, followed by an increase to the maximum  $\Gamma$  value achieved. Further heating causes no change. This indicates that heating for 500-1,000 hrs at 1,050°C should be adequate to obtain the maximum change in  $\Gamma$ . Heating at lower temperatures would require longer periods for the feldspars to achieve the equivalent disordered state. Thus some of the Bushveld plagioclases, heated at 975°C for periods of  $6\frac{1}{2}$  to  $36\frac{1}{2}$  days (156-876 hrs) by Desborough and Cameron (1968) are unlikely to have achieved the most disordered structural state and, with further heating, would probably attain values which would lie on the line marking the trend for heated plagioclases from Gosse Pile and Mt. Davies, Fig. 3.54.

The  $\Gamma$  values for heated plagioclases with compositions between  $An_{59-86}$  from Giles Complex and some Bushveld Complex rocks, lie on a straight line (Fig. 3.54). Kloeman and Nesbitt (1967) calculated the equation to the 12 heated Mt. Davies plagioclases as:  $An\% = 64.20\Gamma - 5.2$  (for  $An_{63-86}$ ). Using 20 heated plagioclases from both Gosse Pile and Mt. Davies, with compositions between  $An_{59-86}$ , the equation modifies to  $An\% = 63.72\Gamma - 4.65$  ( $s = 0.83 An$ ). The difference between the two equations is statistically not significant. The second equation has been used to determine the compositions of chemically unanalysed plagioclase from elsewhere in Gosse Pile.

The  $\Gamma$  values of heated plagioclases which are more sodic than about  $An_{59}$  lie close to the above line, but in some cases outside the limits of the associated error bars (see Appendix 3B), and the degree of scatter increases. The trend defined by both the Gosse Pile and Teizi heated plagioclases\* suggests a decrease in the slope of the line, as would be expected from the diagrams of Smith and Gay (1958). It should be noted that the  $\Gamma$  values of the heated natural plagioclase samples lie above the maximum "disordered series" line of Smith and Gay (1958) which was derived from synthetic samples. Desborough and Cameron (1968) found this for some of the heated Bushveld plagioclases, but offered no explanation.

One Gosse Pile plagioclase (A313/116) showed unexpected behaviour in that the  $\Gamma$  value of the unheated specimen was greater than that of the heated sample, indicating that, on heating, it achieves a more ordered structural state. The specimen was reheated, with no change in the  $\Gamma$  value and a second sample of the same material was also heated but gave the same result. Smith and Gay (1958, p. 757) found a similar anomaly in one of the samples studied by them: the  $\Gamma$  value for a plagioclase ( $An_{87}$ ) decreased by  $0.04^{020}$  following heat treatment. They offered no explanation. Specimen A313/116 is an antiperthite from the annealed rocks of the Gneissic Zone and is unusually rich in  $K_2O$  (1.13%). Bambauer *et. al.*, (1967) have shown that even low Or-contents

---

\* $\Gamma$  values from the Teizi heated plagioclases are from R.W. Nesbitt, pers. comm.

can exert noticeable influences on the values of  $\Gamma$ , but this does not explain the decrease of  $\Gamma$  on heating. Specimen A313/275 (from the anorthosite inclusion) is also annealed and contains more than 2%  $K_2O$ , yet it behaves normally on heating, although the increase in  $\Gamma$  is not as great as would be expected. Smith and Gay (1958) suggested that calcic specimens tended to reach the low entropy state more easily than sodic ones so that the small movement of  $\Gamma$  for A313/275 may be due to insufficient heating of this sample. The increased scatter of heated samples more sodic than  $An_{59}$  may be caused by the same effects. Desborough and Cameron (1968) found that one of the Bushveld plagioclase samples sustained no change in  $\Gamma$  after heating at  $975^\circ C$  for 14 days. It is perhaps significant that it was the most sodic plagioclase examined by them ( $An_{60.5} \pm 13.2$  wt.%). In the opinion of the author, hydrothermal rather than dry heating of plagioclase samples would probably provide a better method for achieving maximum disorder, particularly for sodic samples.

Assuming that  $\Gamma$  gives a measure of the structural state of the plagioclase, then it can be seen that plagioclases from different layered intrusions have different structural states. Fig. 3.54 shows that those from Gosse Pile are very variable but, in general, are more disordered than those from Mt. Davies. These, in turn, are more disordered than those from Stillwater and those from the Bushveld Complex are the most ordered of all. This shows, contrary to the views of Desborough and Cameron (1968, p. 116), that a determinative curve based on  $\Gamma$  vs  $An\%$  for unheated plagioclases which is calibrated

for any one layered intrusion is unlikely to be of value for other layered intrusions. Further, in some intrusions, such as Gosse Pile and Skaergaard (Gay and Muir, 1962) the structural states of the plagioclases are not the same throughout so that a simple determinative curve cannot be used. The structural states of cumulus and intercumulus plagioclases may also differ.

If the structural states of the plagioclases, measured by the  $\Gamma$  values, are determined essentially by the rate of cooling of the intrusions, it would suggest that Gosse Pile cooled more rapidly than the other layered bodies, with the rates of cooling decreasing in the order Mt. Davies, Stillwater and Bushveld. Values of  $\Gamma$  are not available for Skaergaard but optical and other data suggest that they will be generally low, with a range of values (Gay and Muir, 1962). It has been suggested elsewhere (Moore, 1968; Goode and Nesbitt, 1969; Nesbitt *et. al.*, 1969) that Gosse Pile crystallized under high pressure (at depth), while the Stillwater and Bushveld intrusions are generally considered to be relatively shallow bodies (e.g. Hess, 1960; Cousins, 1959). Under such circumstances it would seem more likely that the shallow bodies would cool more rapidly than the deep-seated ones. However, as pointed out by Smith and Gay (1958), factors such as pressure and volatile contents of the magmas have important effects on the degree of order of the plagioclase although their relative importance cannot be assessed. Romey (1969) has commented upon these difficulties and considers that there may be other unknown controls which may interfere with the inversion process. From the above it may

be suggested that the degree of disorder of the plagioclase crystallized from basaltic magma in layered intrusions tends to increase with pressure, assuming that the magmas cooled at approximately the same rate to the temperatures at which no further changes in plagioclase structural states may be expected (estimated at about 475°C by Leavitt and Slemmons, 1962).

### Chemistry

Chemical analyses (14 partial, 2 complete) of Gosse Pile plagioclases are given in Table 3.9.

The orthoclase content and antiperthite

Antiperthites are common in rocks of the granulite facies (including "charnockites" and associated anorthosites) and have also been found in volcanics (Sen, 1959) but they are unexpected in layered intrusions and, to the author's knowledge, have not been described from such rocks.

The K<sub>2</sub>O contents of Gosse Pile plagioclases are similar to values reported for plagioclases with similar An content from other layered intrusions (e.g. Smith, 1960, Table 52). The contents are considerably less than in plagioclase from norites of the Grenville Province of S. Quebec (Philpotts, 1966) where antiperthites always contain over 5% Or (approximately 8.5% K<sub>2</sub>O). Gray (1967) investigated the plagioclases of the Teizi meta-anorthosite, thought



Table 3.9

Partial chemical analyses of 16 plagioclases from Gosse Pile.

| Sample No.<br>A313/- | CaO<br>% | Na <sub>2</sub> O<br>% | K <sub>2</sub> O<br>% | Sr<br>ppm | Atomic Ratio |       |       | Γ values, °2θ |        |
|----------------------|----------|------------------------|-----------------------|-----------|--------------|-------|-------|---------------|--------|
|                      |          |                        |                       |           | An%          | Ab%   | Or%   | unheated      | heated |
| 11                   | 12.49    | 3.88                   | 0.36                  | 548       | 62.30        | 35.55 | 2.15  | 0.901         | 1.067  |
| 12                   | 14.24    | 3.10                   | 0.13                  | 466       | 71.18        | 28.06 | 0.76  | 1.047         | 1.190  |
| 13                   | 15.57    | 2.36                   | 0.47                  | n.a.*     | 76.29        | 20.98 | 2.73  | 1.245         | 1.280  |
| 60                   | 7.67     | 7.03                   | 0.42                  | n.a.      | 36.35        | 60.96 | 2.39  | 0.671         | 0.859  |
| 88                   | 10.23    | 5.01                   | 0.47                  | 588       | 51.55        | 45.66 | 2.79  | 0.672         | 0.917  |
| 111                  | 11.09    | 4.92                   | 0.43                  | 593       | 54.06        | 43.45 | 2.49  | 0.787         | 0.935  |
| 116                  | 9.98     | 4.47                   | 1.13                  | 516       | 51.43        | 41.67 | 6.90  | 0.829         | 0.796  |
| 143                  | 15.27    | 2.70                   | 0.07                  | 403       | 75.44        | 24.17 | 0.19  | 1.156         | 1.254  |
| 176                  | 12.35    | 4.25                   | 0.23                  | 498       | 60.78        | 37.85 | 1.35  | 0.895         | 1.059  |
| 204A                 | 11.79    | 4.13                   | 0.58                  | 529       | 59.11        | 37.47 | 3.43  | 0.922         | 0.976  |
| 232                  | 13.17    | 3.34                   | 0.67                  | 581       | 65.83        | 30.20 | 3.98  | 1.074         | 1.114  |
| 233B                 | 14.39    | 3.18                   | 0.14                  | 439       | 70.82        | 28.34 | 0.83  | 1.064         | 1.180  |
| 234                  | 10.02    | 5.31                   | 0.37                  | 598       | 49.92        | 47.85 | 2.23  | 0.678         | 0.847  |
| 243                  | 11.52    | 4.95                   | 0.33                  | n.a.*     | 55.15        | 42.99 | 1.86  | 0.760         | 0.977  |
| 275                  | 6.99     | 6.14                   | 2.06                  | 1337      | 33.96        | 54.14 | 11.90 | 0.498         | 0.518  |
| 282B                 | 10.40    | 4.77                   | 0.39                  | 431       | 53.30        | 44.34 | 2.36  | 0.824         | 0.967  |

\* insufficient material for Sr analysis.

continued

Table 3.9 (continued)

Complete analyses of 2 plagioclases      Calculated mineral formulae

| Sample No.                     | A313/176 | A313/204A |                  | A313/176 | A313/204A |
|--------------------------------|----------|-----------|------------------|----------|-----------|
| SiO <sub>2</sub>               | 52.36    | 52.40     | Si               | 9.5080   | 9.5974    |
| Al <sub>2</sub> O <sub>3</sub> | 30.21    | 29.50     | Al               | 6.4667   | 6.3704    |
| ΣFe as FeO                     | 0.11     | 0.20      | Fe <sup>2+</sup> | 0.0163   | 0.0297    |
| MgO                            | 0.32     | 0.34      | Mg               | 0.0862   | 0.0924    |
| CaO                            | 12.35    | 11.79     | Ca               | 2.4029   | 2.3135    |
| Na <sub>2</sub> O              | 4.25     | 4.13      | Na               | 1.4950   | 1.4660    |
| K <sub>2</sub> O               | 0.23     | 0.58      | K                | 0.0523   | 0.1342    |
| TiO <sub>2</sub>               | 0.02     | 0.05      | Ti               | 0.0021   | 0.0066    |
| MnO                            | 0.00     | 0.00      | Z                | 15.975   | 15.968    |
| TOTAL                          | 99.85    | 99.00     | X                | 4.055    | 4.042     |
|                                |          |           | An               | 60.83    | 59.11     |
|                                |          |           | Ab               | 37.85    | 37.46     |
|                                |          |           | Or               | 1.32     | 3.43      |

by him to be related to the Giles Complex, and suggests that, for a given An content, there exists a critical Or content above which the plagioclase would be antiperthitic. This critical value will be also dependent upon thermal conditions prevailing at the time. The critical Or value, marking the boundary between antiperthitic and "normal" (i.e. not antiperthitic) plagioclase from the Teizi rocks can be equally applied to the samples from Gosse Pile (Fig. 3.56) irrespective of the rock type from which the plagioclase is taken. This boundary is well below the 5% Or suggested by Philpotts (1966) for the Grenville Province rocks.

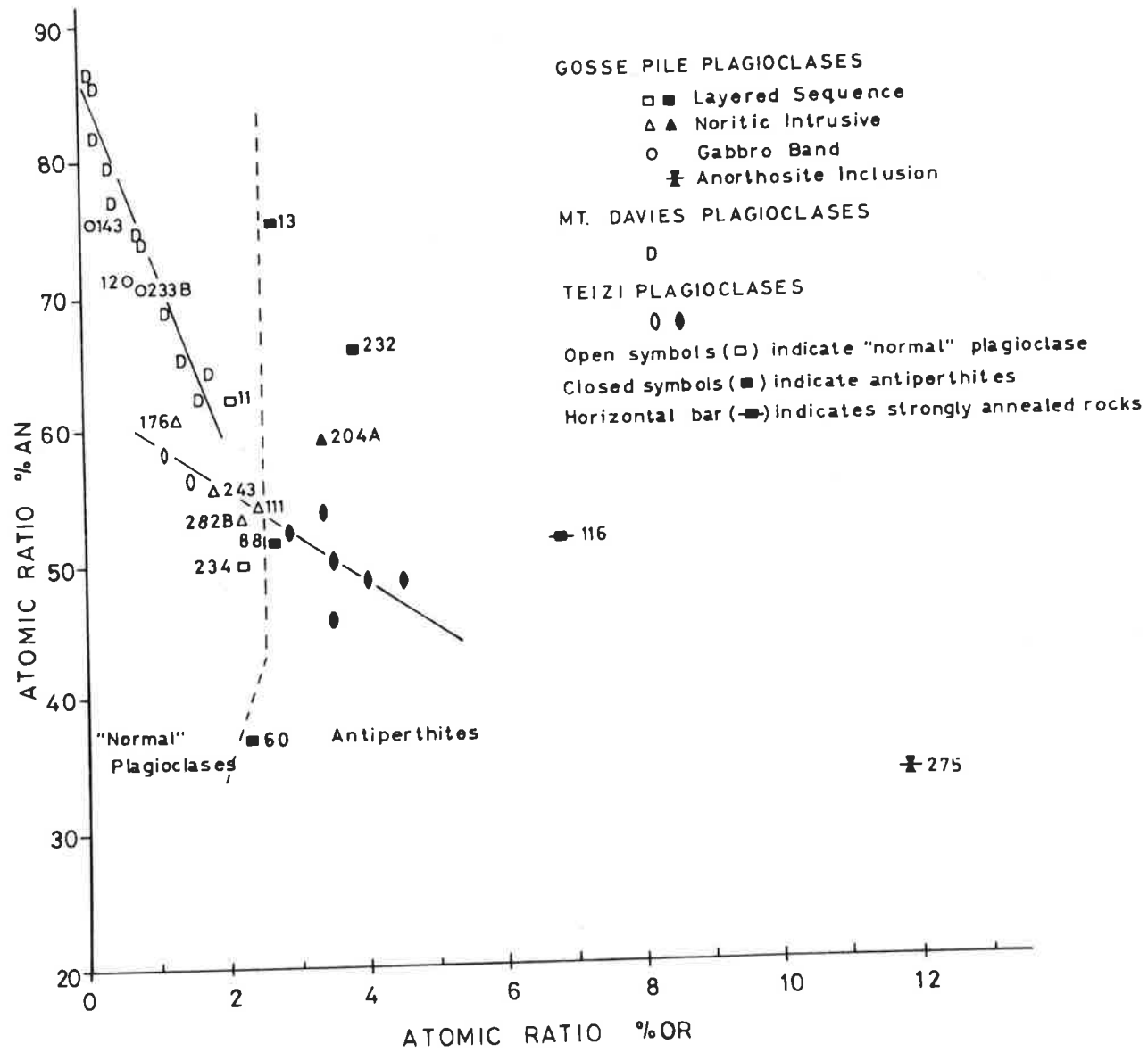
Smith (1956), Sen (1959), Vogel, Smith and Goodspeed (1968) have all noted a general increase in the Or content of plagioclase as the An content decreases. This relationship is clearly shown by the cumulus plagioclase samples ("normal") from Mt. Davies (Fig. 3.56). This trend is only very weakly detected for the Gosse Pile plagioclases, even considering those from only one rock type. In this respect they are similar to the samples examined by Philpotts (1966) where considerable scatter occurs.

It is generally considered that antiperthites of the type found in the Gosse Pile rocks originate by exsolution (Sen, 1959; Carstens, 1967). There are various kinetic difficulties involved in the exsolution process (Goldsmith, 1952) so that it is encouraged by processes which overcome the activation, or nucleation, energy barriers, such as slow cooling, metamorphism or deformation (Sen, 1959).

Fig. 3.56

Plot of atomic ratio  $\%An$  against atomic ratio  $\%Or$  for plagioclases from Mt. Davies, Teizi meta-anorthosite and Gosse Pile.

Data for Mt. Davies plagioclases from Kleeman (1965) and those for Teizi plagioclases from Gray (1967).



In his discussion of the effects of pressure and temperature on the development of antiperthites Sen (1959) suggested that enrichment in  $K_2O$  was favoured by an increase in temperature, but an increase in pressure ( $H_2O$ ) would probably retard the solubility of K-feldspar in plagioclase. Sen (1959, p. 488) considers that the availability of  $K_2O$  is not a very important determining factor. Examination of the plagioclases from Gosse Pile shows no apparent correlation between structural state and the development of antiperthite.

Because the Or contents of Gosse Pile plagioclases are, in general, not dissimilar from those of other layered intrusions and igneous rocks but do show the unexpected development of antiperthite, it is concluded that some unusual physical conditions prevailed and caused its formation. The temperature of crystallization (melting) of basaltic magma increases only slightly with increase in pressure (estimated at only  $50^{\circ}$ - $70^{\circ}C$  at depths of 30-40 km: Smith, 1963, p. 203), so that temperature differences are not likely to be significant factors in determining whether antiperthite will form. Most of the antiperthites are interstitial, and thus formed relatively late in the crystallization sequence. Some well-developed antiperthites occur in the norites of the Gneissic Zone where annealing crystallization has taken place at temperatures below the solidus.

Bearing in mind the influence of pressure, noted above (Sen, 1959), and the fact that it has been suggested that Gosse Pile probably crystallized, and was deformed, under high pressures (Moore, 1968; Nesbitt, et. al., 1969) it seems that pressure might be the significant

factor in determining the presence of antiperthite in some of the plagioclases from Gosse Pile. The lack of hydrous minerals suggests that  $P_{H_2O} \ll P_s$  for the magma, so that not only high  $P_{H_2O}$  (Sen, 1959) but also high  $P_s$  retards the solubility of K-feldspar in plagioclase and encourages its exsolution with falling temperature.

#### The Sr content

Turekian and Kulp (1956) noted the striking difference between the behaviour of Sr relative to Ca in granitic and in basaltic rocks. Even when applied to universal sampling there is an increase in the Sr content with an increase in the Ca content of granitic rocks, while the opposite appears to be true of basaltic rocks.

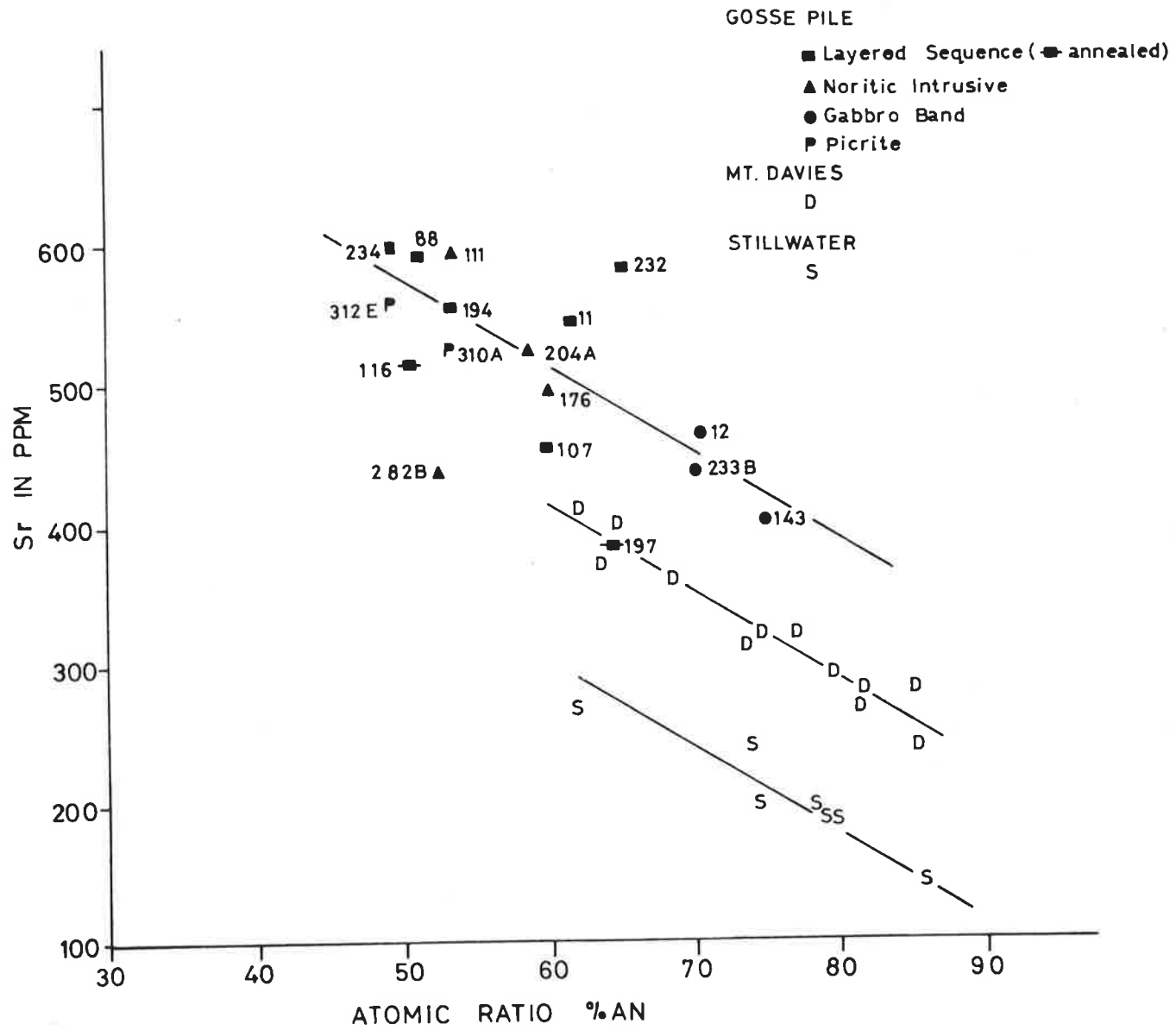
The relationship between the An and Sr contents of plagioclases from mafic intrusives is such that a decrease in Sr content accompanies an increase in An value (e.g. Skaergaard - Wager and Mitchell, 1951; Stillwater - Turekian and Kulp, 1956; Mt. Davies - Kleeman, 1965; the layered bodies of Somalia - Butler and Skiba, 1962). This trend is also weakly shown by the plagioclases from Gosse Pile, (Fig. 3.57).

In layered bodies this trend is usually explained by relating the presence of Sr in plagioclase to its diadochy with Ca. The larger  $Sr^{2+}$  ions are excluded from the plagioclase relative to the smaller  $Ca^{2+}$  ions, thus causing the liquid to become progressively enriched in Sr. The later, more sodic plagioclase, is thus enriched in Sr. Berlin and Henderson (1968) and Brooks (1968) independently concluded that this

Fig. 3.57

Change of Sr content of plagioclases with change in their composition. Data for Mt. Davies samples after Kleeman (1965) and those for Stillwater samples after Turekian and Kulp (1956).





explanation is unsatisfactory since the crystallizing calcium-rich clinopyroxene of the layered bodies is responsible for the increase in the Sr/Ca ratio of the magma, and this effect overshadows the effect of the plagioclase crystallization which, in fact, tends to decrease this ratio. Berlin and Henderson (1968) conclude that the increase in Sr content of the plagioclases from layered bodies, with decreasing Sr content of the liquid, is due to the Sr distribution factor increasing with decreasing An content of the plagioclase. The actual Sr content of the plagioclase is probably dependent on the Sr concentration of the magma during crystallization: plagioclases from the Somalia intrusions (Butler and Skiba, 1962) and Skaergaard (Wager and Mitchell, 1951; Hamilton, 1963) are far richer in Sr than those from Gosse Pile, Mt. Davies and Stillwater (Fig. 3.57). The granitic rocks are presumed to show the "correct" Sr-Ca relationship (i.e. a positive slope) because no other minerals have crystallized with the feldspar (alkali feldspar) to affect the Sr/Ca ratios of the residual liquid (Berlin and Henderson, 1968).

The plagioclases from Gosse Pile, plotted in Fig. 3.57, are from different rock types. There are intercumulus and cumulus (annealed) plagioclases from the layered sequence, laths from the Gabbro Band, interstitial material from the later noritic intrusive and samples from the picrites. Some are from rocks almost free of clinopyroxene (e.g. A313/143, with 1.2% total pyroxene) and others from websterites (e.g. A313/232, with 63.8% clinopyroxene). In spite of this, the characteristic trend in the Sr/An ratio can still be detected,

although it is less well developed than in other bodies. Because of this, it is suggested that this general trend reflects the relative ease of entry into the plagioclase lattice with change in composition, and the scatter is due to other effects. For example, intercumulus plagioclase from A313/232 has a higher Sr/An ratio than the other samples and this is probably a result of the secondary enlargement of clinopyroxene using large amounts of Ca and very little Sr from the interstitial liquid (cpx contains 18% CaO, 16 ppm Sr). Such a conclusion is in general agreement with the statement by Berlin and Henderson (1968, p. 82) that, "the increasing Sr of the basic rock plagioclases ... must ... be due to the Sr distribution factor increasing with decreasing An content of the plagioclase", although the concentration of Sr in residual liquid of Gosse Pile cumulates cannot be calculated because of the difficulty in distinguishing cumulus and adcumulus growth in many rocks. However, this conclusion, that the general negative trends of Fig. 3.57 reflect the relative ease of entry of Sr into the plagioclase lattice with compositional change, is not in harmony with the view that Sr enters more readily into the plagioclase structure than Ca (Brooks, 1968, p. 19).

The controlling factor in determining the Sr/An ratio in plagioclase is probably the plagioclase composition, which in turn determines the lattice structure (e.g. Smith and Ribbe, 1969). Wager and Mitchell (1951) found the maximum Sr content in a plagioclase of composition An<sub>37</sub>: a more sodic plagioclase had a smaller Sr content. This suggests that a composition of about An<sub>37</sub>

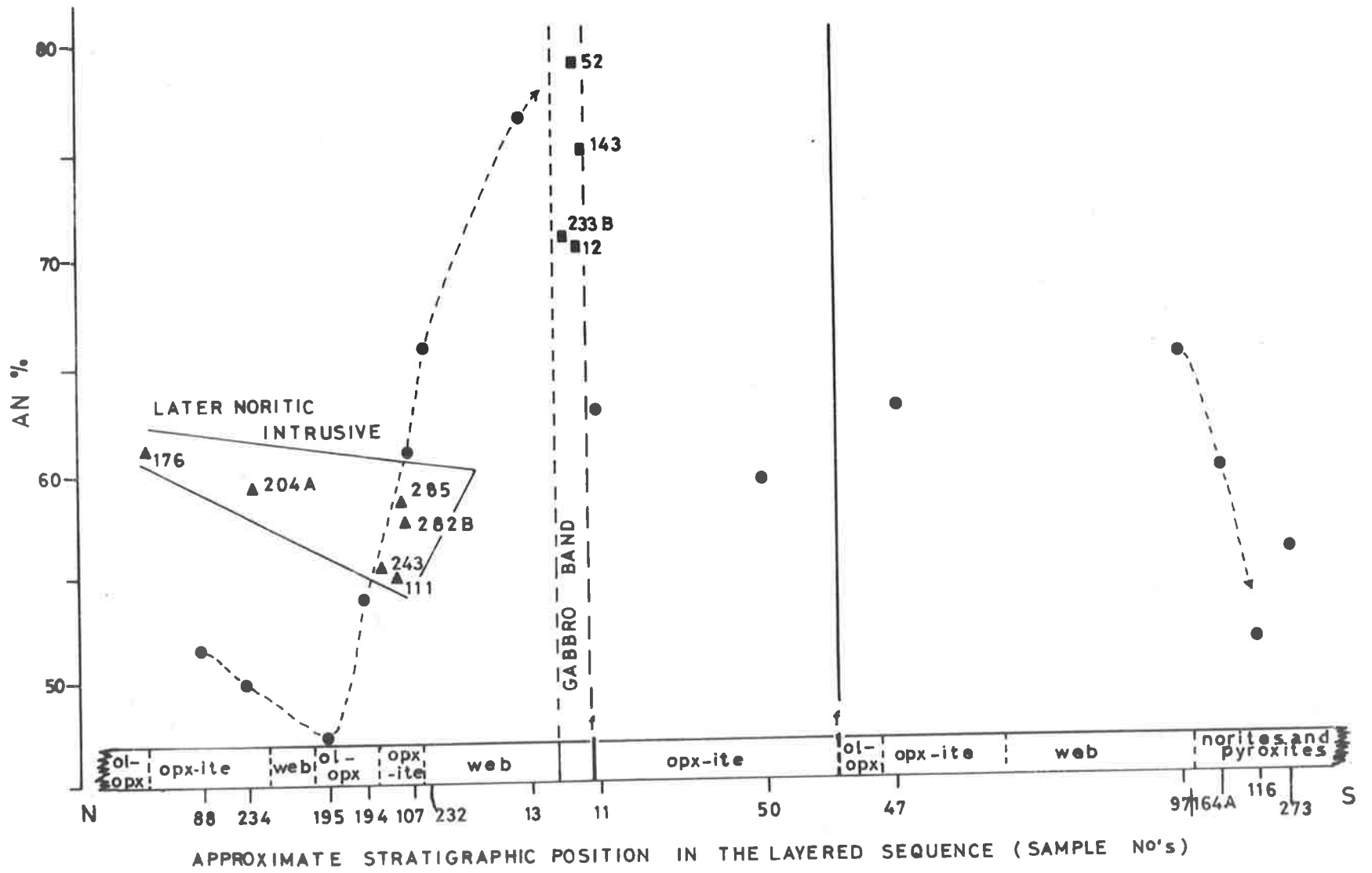
marks the limit for the maximum admittance of Sr. Ewart and Taylor (1969) showed that, in rhyolites, andesites and basalts, the Ca distribution factors are not consistently lower than the Sr factors (phenocryst: liquid) and, in plotting Sr/An values, noted a maximum Sr content at about An<sub>50</sub>. These data are in general agreement with the conclusions reached from the results from the Gosse Pile plagioclases.

#### Changes in composition with relative stratigraphic position

All of the plagioclase in the layered sequence of Gosse Pile, north of the Gneissic Zone, is interstitial. The compositions are therefore probably determined by factors such as the composition of the trapped liquid, other phases present and possible reactions between these phases and the liquid, the rate of growth of these phases and the rate of diffusion of elements within the unconsolidated cumulate. Thus, a variation trend, such as is shown for cumulus feldspars in other layered intrusions, is not expected for the intercumulus plagioclase. Fig. 3.58 shows the feldspar compositions plotted against the approximate stratigraphic position of the rock from which the plagioclase was separated. There is a possible trend present in the lower (N) rocks which is opposite to the trend usually produced by cumulus plagioclases in layered intrusions. There are some indications that the normal trend (i.e. decreasing An content with progressive crystallization) is starting in the presumed cumulus plagioclases of the Gneissic Zone: the first-formed cumulus

Fig. 3.58

Graph illustrating the change in the compositions of plagioclases with their approximate stratigraphic positions in the sequence. The compositions of plagioclases from the noritic intrusive are also shown.



plagioclase here is  $An_{60}$  (A313/164A). The reason for the apparent reverse trend shown by the intercumulus plagioclase near the base of the layered sequence is not known. It may be that, as olivine and orthopyroxene crystallize, the liquid is relatively enriched in CaO so that the interstitial plagioclase becomes progressively more anorthitic. Once clinopyroxene becomes a major phase this trend should end. In fact, the most anorthite-rich plagioclase is from the websterite; the reason for this is not known. This argument assumes closed system crystallization within each cyclic unit.

Fig. 3.58 also shows the compositional field occupied by plagioclases from rocks of the later noritic intrusive, ranging from approximately  $An_{54}$  to  $An_{61}$ . Cumulus (?) plagioclases from the Gabbro Band are the most anorthitic ( $An_{71-80}$ ). They lie on the trend defined by the plagioclases from the layered sequence rocks further north, and this might suggest they form part of the layered sequence. They have compositions very different from those recognised as belonging to the later noritic intrusive, which supports the idea that they may not be related. However, the Gabbro Band plagioclase laths are not interstitial and, if part of the layered sequence, should be regarded as the first cumulus feldspars.

### Summary

The information gained from the study of plagioclases from Gosse Pile is limited, largely because they are from different rock types of different generations and because those from the layered sequence are

predominantly interstitial. However, it has been shown that measurement of the  $\Gamma$  values of heated plagioclases can be used to determine indirectly compositions between about  $An_{45}$  and  $An_{86}$ , irrespective of their source. The method cannot be applied to unheated samples, even when the curve is calibrated for samples from the same intrusion.

For the first time to be recorded, the Gosse Pile rocks show the presence of antiperthite in a layered ultramafic sequence. Although the cause of this feature is not known, especially as the plagioclases have  $K_2O$  contents comparable with those from other layered intrusions, it is suggested that high pressure may be a significant factor in promoting the exsolution of K-feldspar.

In spite of the variety of rock types, with variable mineralogies, from which the plagioclases were extracted, a study of the Sr/An ratio has shown that a negative distribution curve is produced, similar to those derived from studies of plagioclases from other layered intrusions. It is thus concluded that, although cumulus clinopyroxene, where present, may strongly influence the Sr/An ratio, the overall negative distribution is rather a function of the change of relative ease of entry of Sr into the plagioclase lattice with change in composition.



### 3.6.2 The Pyroxenes

#### 1. ORTHOPYROXENE

##### Introduction

Orthopyroxene is the dominant mineral in Gosse Pile and is found in all rock types, orthopyroxenite being the most abundant.

##### Chemistry

Detailed studies of the chemistry of pyroxenes have been rewarding in the study of most layered intrusions as they show fractionation stages, both in terms of distinguishing magma types and in establishing the character and extent of fractionation (Poldervaart and Hess, 1951). For this reason chemical analyses of a number of pyroxenes, separated from rock samples taken across Gosse Pile, were carried out (Table 3.10 and Table 3.12). However, as in the case of the ultramafic portions of other layered intrusions (Wager and Brown, 1968), the results have shown little variation to be present. The only elements which give possible trends with position in the stratigraphic sequence are Cr and Ni, and even here the trends are irregular and poorly developed (Fig. 3.59). These trends show a generally rapid decrease in Cr and a tendency for a less rapid decrease in Ni with progressive crystallization (N to S) within the second and third cyclic units. This is similar to trends observed for pyroxenes elsewhere (e.g. Bushveld Complex - Atkins, 1969). Within the partial cyclic unit,

TABLE 3.10.

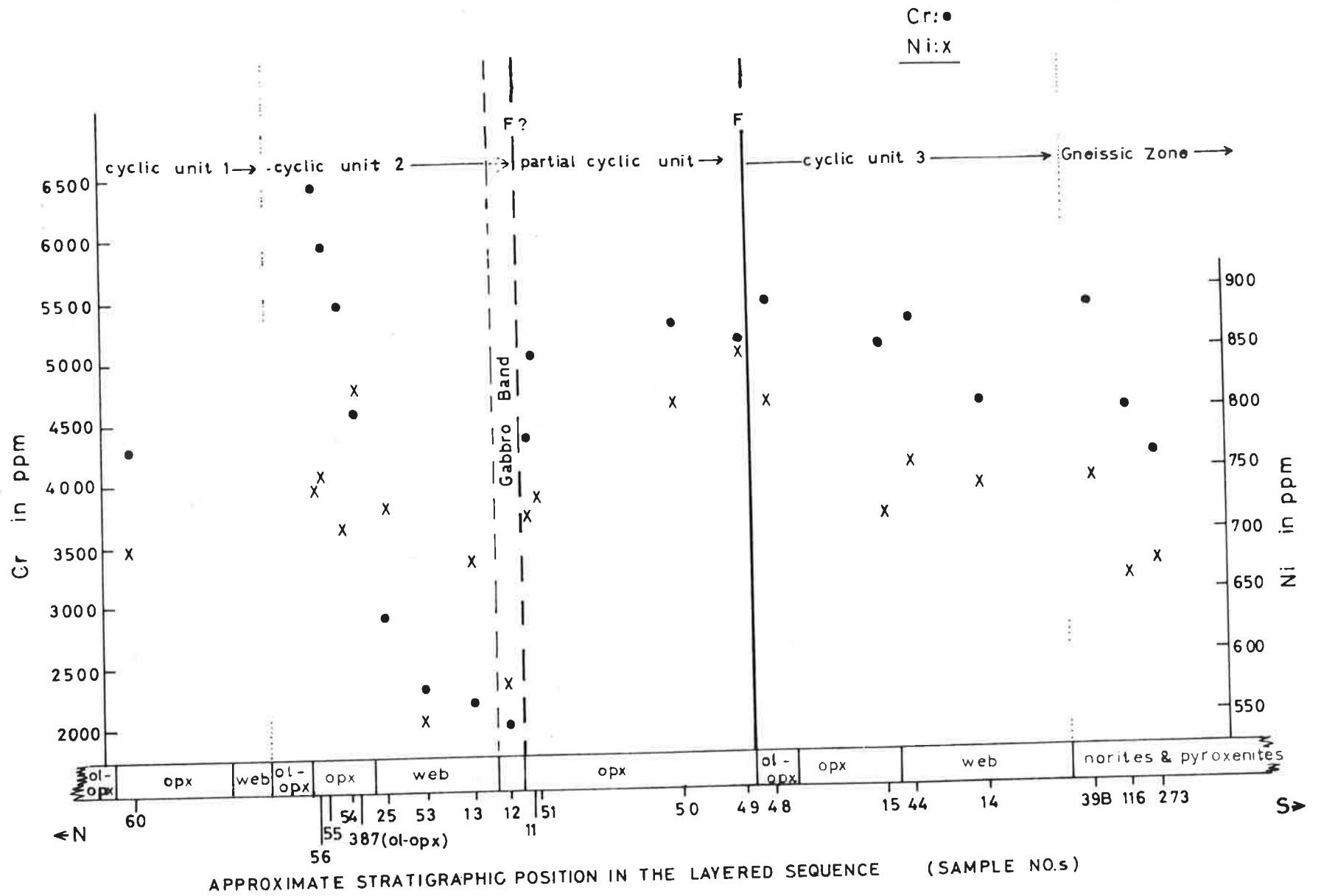
Chemical analyses of orthopyroxenes and their structural formulae.

This table is contained in the pocket at the back of this thesis.

---

Fig. 3.59

The Cr and Ni contents of orthopyroxenes as a function of their approximate stratigraphic position in the layered sequence.



bounded by the Gabbro Band and the central east-west fault, these trends are apparently reversed in the orthopyroxenite. Why this reversal occurs is not known, but it may be caused by fresh magma leaking into the system, on top of an already fractionated residue.

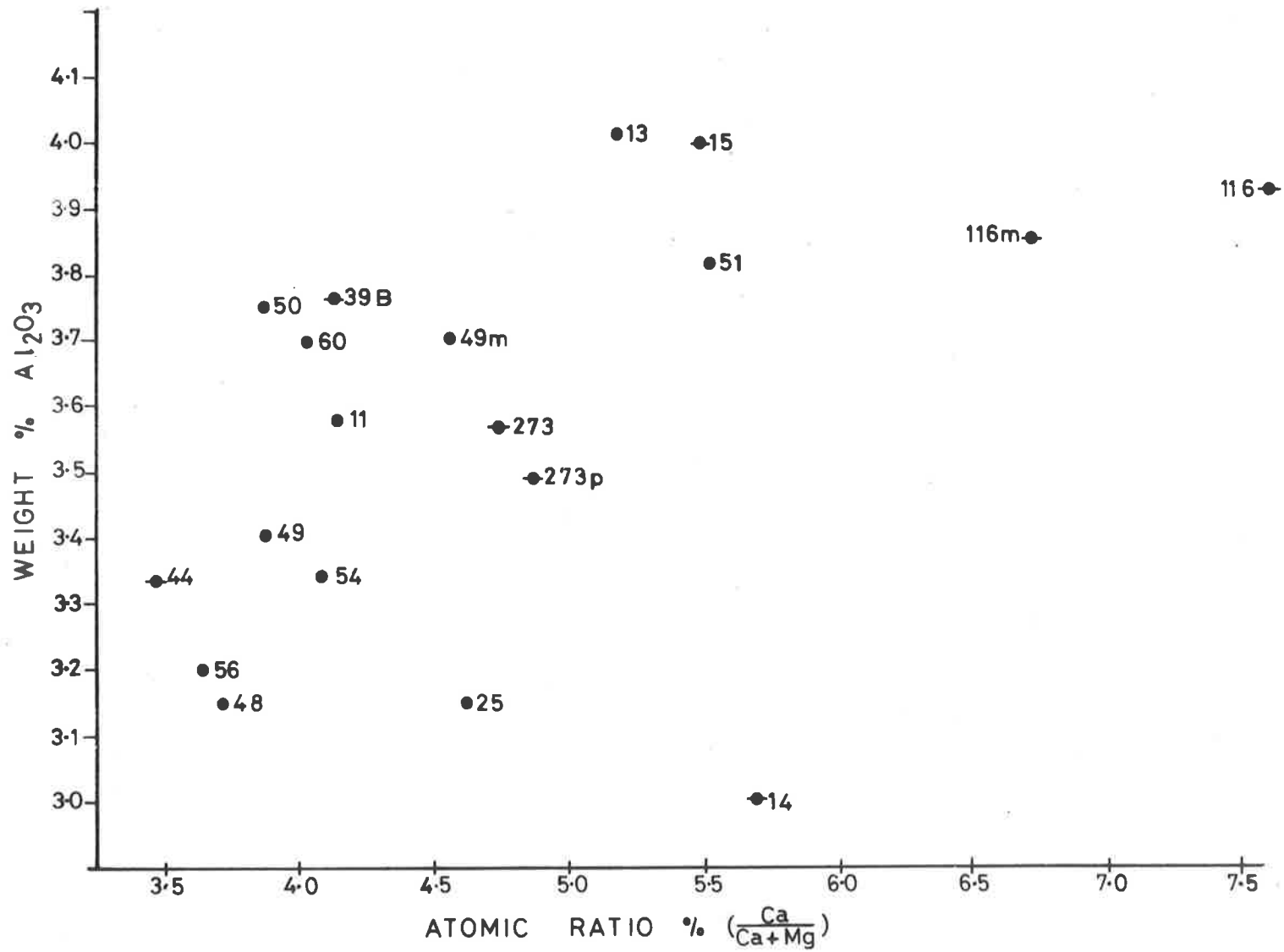
The  $R_2O_3$  content (particularly  $Al_2O_3$  and  $Cr_2O_3$ ) of the orthopyroxenes is high for igneous pyroxenes (Table 3.10). Boyd and England (1960) and Boyd (1966) have shown that the  $Al_2O_3$  content of orthopyroxene may be dependent on pressure, depending on the availability of  $Al_2O_3$  during crystallization. This general argument is probably applicable to the  $R_2O_3$  content of the pyroxenes. The  $R_2O_3$  values (average of 21 analyses [excluding analyses 2 and 14 of Table 3.10] give  $Al_2O_3 = 3.52\%$  and  $R_2O_3 = 5.47\%$ ) of Gosse Pile orthopyroxenes are well above those generally encountered in orthopyroxenes from plutonic igneous intrusions (e.g. Deer, Howie and Zussman, 1963) but are similar to the values for orthopyroxenes found in ultramafic nodules in basalts (Boyd and England, 1960). Garnet is absent from the Gosse Pile rocks so will not influence  $Al_2O_3$  distribution. This high  $R_2O_3$  content of the pyroxenes suggests that they have crystallized under high pressure, similar to those proposed for ultramafic nodules, i.e. near the base of the crust (e.g. Ross, Foster and Myers, 1954; Lovering and White, 1969).

O'Hara (1963) found evidence which suggested that the presence of  $Al_2O_3$  expanded the miscibility gap between diopside and enstatite. A relationship between the  $Al_2O_3$  contents and the atomic ratio  $Ca/Ca + Mg$  would therefore be expected for both orthopyroxene and

Fig. 3.60

Graphical relationship between the  $\text{Al}_2\text{O}_3$  content and the atomic ratio  $\% \text{Ca}/(\text{Ca}+\text{Mg})$  for orthopyroxenes from rocks of the layered sequence.

⊕ : indicates specimen is from an annealed rock.



clinopyroxene. Fig. 3.60 shows this relationship in the orthopyroxenes to be only poorly developed, with considerable scatter and a positive correlation. Boyd (1966), in attempting a similar correlation for clinopyroxenes from kimberlites found no relationship but this, as in the case of Gosse Pile, may be a function of the very limited chemical variation of the pyroxenes with which he was dealing.

### Exsolution

Three exsolution products have been recognised in the orthopyroxenes.

#### (i) Clinopyroxene

The fine lamellar structure in orthopyroxenes has been the subject of much discussion since it was first described (e.g. Bowen and Schairer, 1935; Scholtz, 1936; Hess and Phillips, 1938). Three interpretations have been given. The first, suggested by Bowen and Schairer (1935), was that it may be a form of polysynthetic twinning on (014). Henry (1942), using X-ray oscillation photographs concluded that it is best interpreted as translation of the orthopyroxene parallel to [001] on (100) with bending about [010]. The structure would thus not be a regular twin structure because a range of orientations can be observed. The third, and most commonly accepted, interpretation is that the lamellae represent exsolution of a calcium-rich, monoclinic pyroxene parallel to (100) of the orthopyroxene (e.g. Hess and Phillips, 1940).



Bruynzeel (1957) has been a strong advocate of the hypothesis that the lamellar structure in orthopyroxenes from the Insizwa dolerite sheet is due to polysynthetic twinning, and he considers that this is true of similar pyroxenes elsewhere (specifically in the Stillwater Complex). He states that the twinning cannot be on (014) but is polysynthetic twinning about the  $c$  axis, on (100). Deer, Howie and Zussman, (1963) also consider that twinning in orthopyroxene can occur parallel to (100). This would imply that the orthopyroxenes do not have true orthorhombic symmetry. Investigations by Ito (1950) and Ingham (1957) have given no indications that the structure is anything other than  $Pbca^*$ . That this structure can be derived from a twinned  $P2_1/c$  monoclinic cell (such as pigeonite) is well established, but this is only on a unit cell scale and could not be observed as optically distinct domains (Ingham, 1957, p. 56). The lamellae examined by Bruynzeel (1957) were less than 0.005 mm ( $5\mu$ ) thick. In the experience of the present author, accurate optic determinations on such fine lamellae are considerably hampered by interference effects of the host mineral. In the absence of electron microprobe data on the Insizwa orthopyroxenes the statement that the host material and lamellae are identical and, "the orthopyroxenes showing this

---

\* Similarly for the hypersthene investigated by Ghose (1965) but this is a metamorphic pyroxene and is not reported to contain the fine lamellar structure under consideration.

structure are homogeneous", (Bruynzeel, 1957, p. 502) should be treated with caution. Evidence is derived solely from optical properties: differences in extinction directions for lamellae and host of between  $3^{\circ}$  and  $6^{\circ}$  from (100) were recorded.

Hess (1960) examined 20 X-ray oscillation photographs of orthopyroxenes showing lamellar structure. He confirmed Henry's (1942) findings but disagreed with the interpretations. Hess pointed out that the observed disorientations are within the orthopyroxene host (observable under the microscope) and the amount of material in the fine lamellae is too small to give X-ray spots on the photographs. Bown and Gay (1959) could distinguish spots which could be assigned to "augite" in an oscillation photograph. The optical appearance of the crystal used by them is not described but is referred to as, "hypersthene with (100)augite lamellae" (from the Bushveld Complex). The clinopyroxene spots are only very weakly developed (see Fig. 5, their paper).

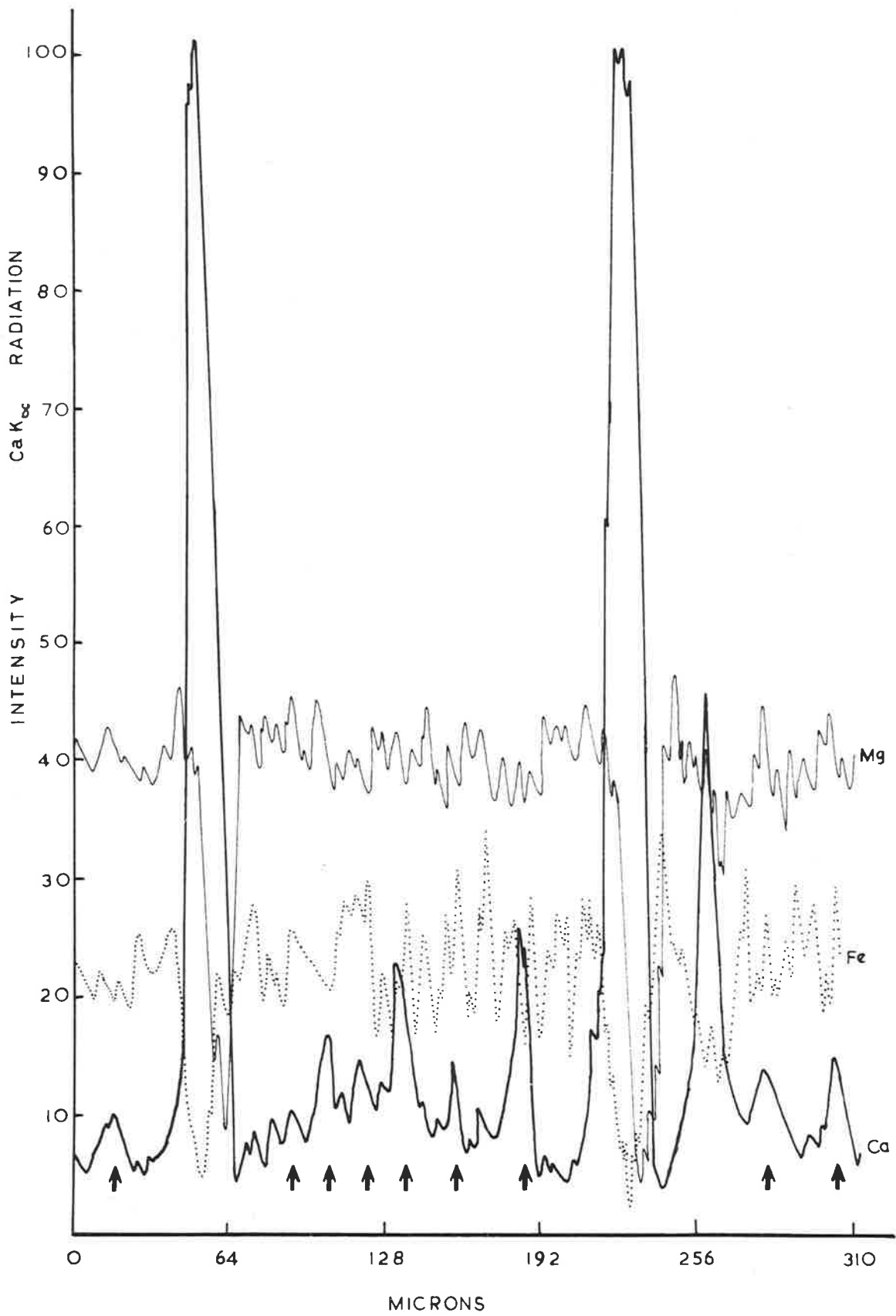
Boyd and Brown (1967) have presented the most convincing evidence that the lamellar structure is caused by exsolution. The bronzite they examined (from the Stillwater intrusion) has lamellae  $1-2\mu$  wide and is identical in appearance to bronzites from Gosse Pile (compare plate 1A, Boyd and Brown, 1967, with Fig. 3.63, this thesis). Two noteworthy points arise from the electron microprobe scan of this Stillwater bronzite. Although the lamellae are too fine for complete resolution (beam size is  $1.0$  to  $1.1\mu$ ) they are shown to be more calcic

than the host. Secondly, the proportion of lamellae to host is far too great for the lamellae to be augitic in composition because wet chemical analyses show the CaO content of host plus lamellae is only about 2%. Both points apply equally well to the orthopyroxenes from Gosse Pile. Bulk analyses (Table 3.10) of separated orthopyroxenes show the CaO content to be usually less than 2%. An electron microprobe scan across a single crystal (Fig. 3.61) shows the lamellae to be Ca-rich, and relatively poor in Mg and Fe. Boyd and Brown (1967) conclude that the bulk composition of the Stillwater pyroxene is such that it, "may lie to the (Mg,Fe)-rich side of the two pyroxene field, in which case we may be observing Ca-distribution between phases involved in the polymorphic inversion of Ca-poor pyroxenes". Such conclusions are equally applicable to the Gosse Pile orthopyroxenes. On the basis of the above discussion it is considered that the fine lamellar structure in these pyroxenes represents an exsolved Ca-rich, clinopyroxene phase.

This clinopyroxene is the commonest product of exsolution in the orthopyroxene and occurs both as the fine lamellae, described above, which thin towards the margins of the host crystals, and as elongate and irregular blebs. In all cases the orientation of the lamellae and the blebs is the same: they are exsolved parallel to (100) of the orthopyroxene. Contrary to observations by Hess and Phillips (1938, p. 452) on Stillwater orthopyroxenes, the lamellae in Gosse Pile orthopyroxenes are clearly visible in sections cut nearly parallel to (001) if such sections are orientated such that the (010) planes

Fig. 3.61

Electron microprobe scan across a single orthopyroxene crystal. The arrows at the base mark the positions of fine lamellae observed optically. The more intense peaks for Ca  $K_{\alpha}$  radiation occur over large blebs of clinopyroxene, also observed optically.



are within  $20^\circ$  of vertical. In several examples the fine lamellae can be traced into elongate blebs and both have the same extinction positions and thus apparently the same optic orientations (Fig. 3.62). This is useful because the lamellae ( $5-20\mu$  thick) are generally too small to be accurately measured on the U-Stage so that measurements made on the larger blebs probably can be applied to the lamellae. Measurements on larger lamellae and the elongate blebs indicate an optic orientation identical to that observed by Hess (1960) for similar lamellae and blebs in Stillwater orthopyroxenes; i.e. the  $\alpha_{(\text{opx})}$  and  $\beta_{(\text{cpx})}$  vibration directions are coincident, while  $\gamma_{(\text{cpx})}$  is inclined at  $47^\circ \pm 4^\circ$  (average of 10 measurements) to  $\gamma = \underline{c}_{(\text{opx})}$  in the (010) plane of the orthopyroxene.

The lamellae are not of uniform thickness, but generally thin towards the extremities, thus indicating an extensively flattened, lens-like shape. Although the fine lamellae sometimes pass into the larger blebs described above, they more commonly disappear in the immediate vicinity of the blebs, as at the margins of the host (Fig. 3.63). This suggests migration of material from the lamellae to the larger blebs within the crystal and, possibly, to the small interstitial clinopyroxene grains outside the crystal. The lamellae terminations commonly follow the irregular outline of the orthopyroxenes in the relatively undeformed rocks to the north (Fig. 3.63), suggesting that exsolution took place after any grain boundary adjustment occurred.

Fig. 3.62

Elongate blebs and fine lamellae in orthopyroxene.

A313/87. C.P.

Photograph: A. Moore.

Fig. 3.63

Fine lamellar structure in orthopyroxene. Note how the lamellae terminate near the margin of the crystal, and follow the outline, and near larger blebs of clinopyroxene within the crystal. A313/373I. C.P.

Photograph: A. Moore.

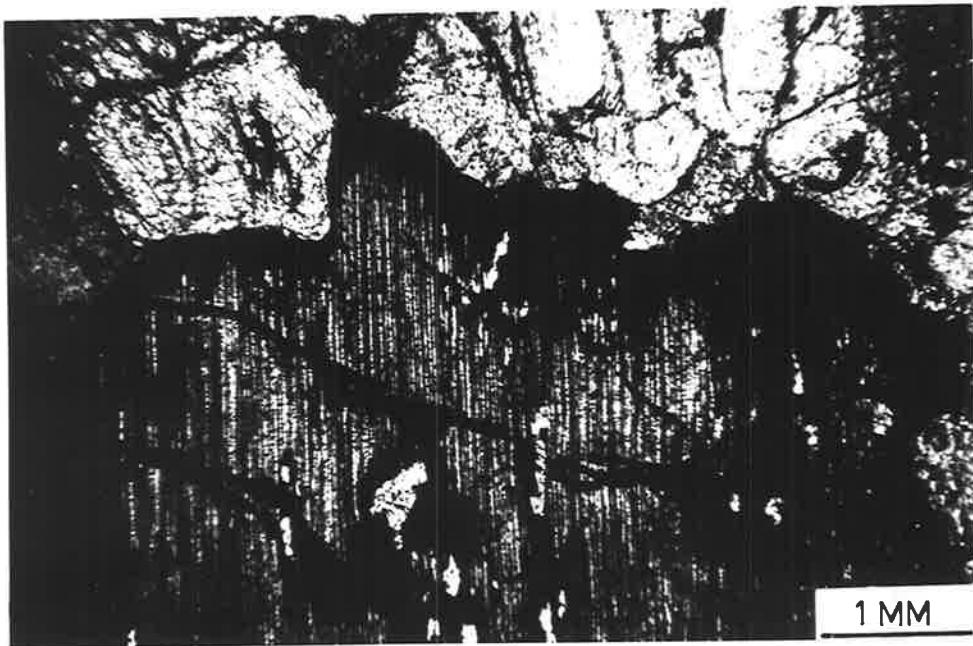
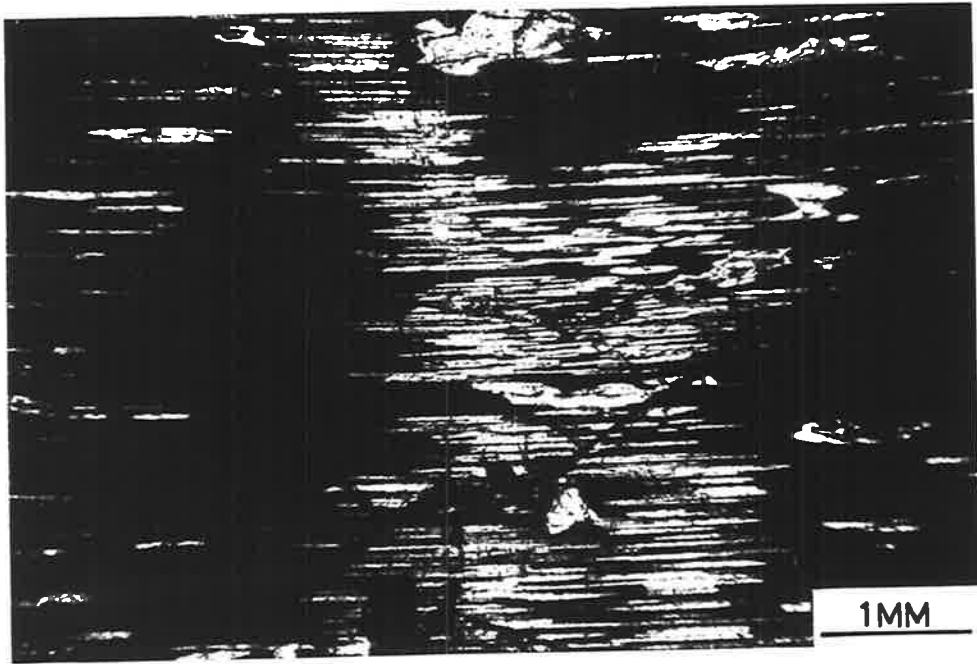




Fig. 3.64

Hour-glass structure in orthopyroxene.  $\Delta 313/245B$ . C.P.

Photograph: A. Moore.

Fig. 3.65

Zoning in orthopyroxene in a section cut almost parallel  
to c.  $\Delta 313/32$ .

Photograph: A. Moore.

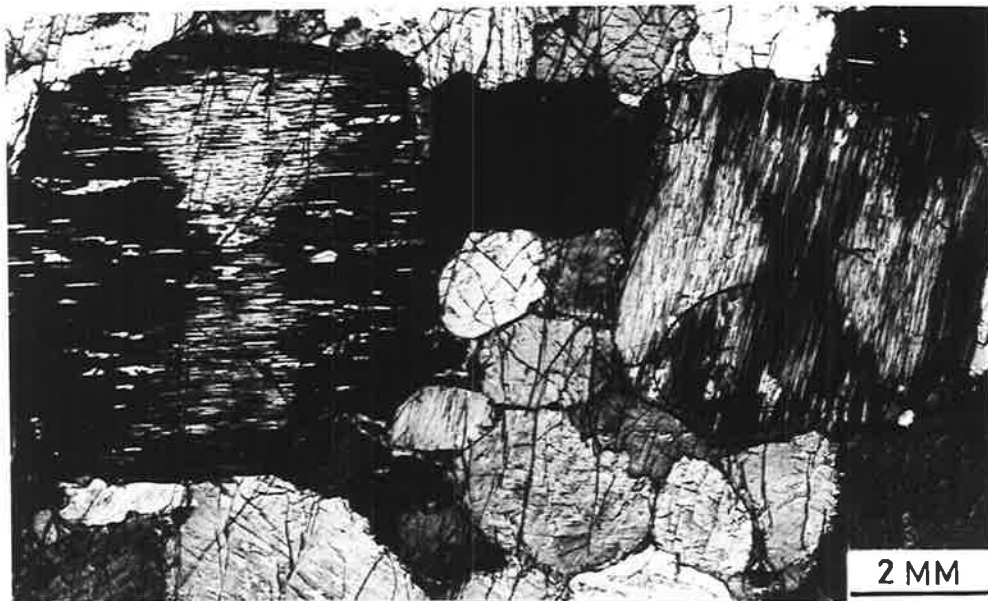


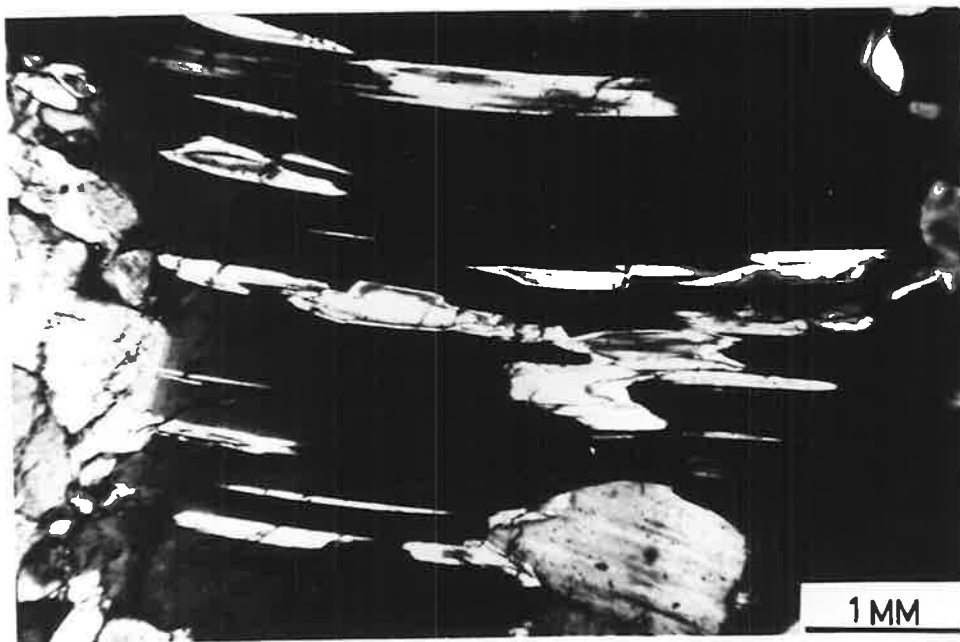
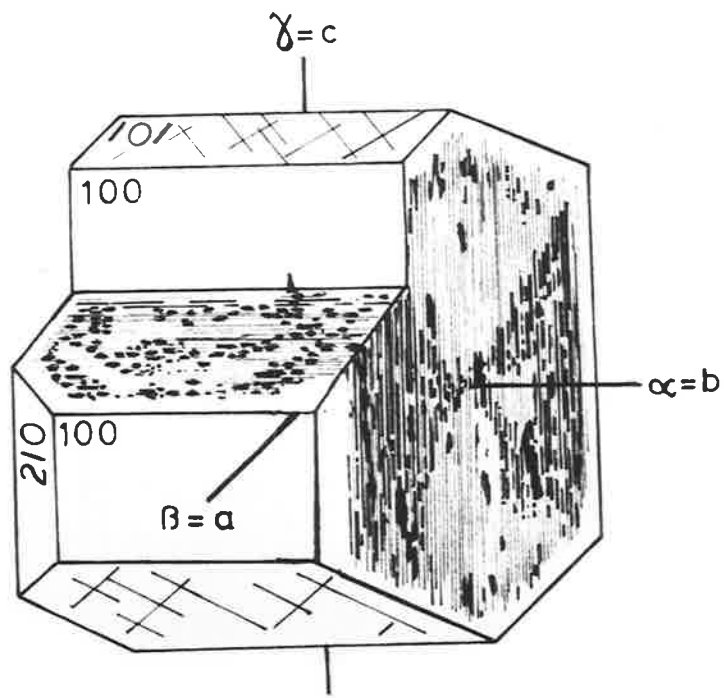
Fig. 3.66

Block diagram illustrating the form of the "hour-glass zoning" in orthopyroxenes from Gosse Pile.

Fig. 3.67

Clinopyroxene blebs within a deformed megacryst of orthopyroxene from orthopyroxenite of the Gneissic Zone. Note the lack of fine lamellar structure. A313/97. C.P.

Photograph: A. Moore.



Although the blebs and larger lamellae of exsolved clinopyroxene often occur irregularly throughout the orthopyroxene, an apparently unique feature of the Gosse Pile orthopyroxenes is that some display a type of "hour-glass zoning" caused by thickening of the lamellae in a regular fashion (Fig. 3.64, Fig. 3.65 and Fig. 3.66). The orientation is diagrammatically represented in Fig. 3.66. In sections nearly normal to c the thickened areas appear almost equidimensional (Fig. 3.65) and are arranged such that they indicate zoning parallel to crystal faces (Fig. 3.66).

Hour-glass zoning, revealed by pleochroic differences, is well known in titanaugites and Preston (1966) has described an hour-glass structure, defined by composition and exsolution features, in common augite from a dolerite pegmatite. However, to the author's knowledge, such structures have not been described from orthopyroxenes, apart from brief mention of "hour-glass zoning" in bronzite from Ewarara Intrusion, Giles Complex, by Goode and Krieg (1967). In the example described by them the zoning is defined by variations in the abundance of exsolved spinel needles within the bronzite (Goode and Krieg, 1967, Plate 9, Fig. 4). A.D.T. Goode (pers. comm.) has observed "hour-glass zoning" in orthopyroxenes from Ewarara and Kalka defined by both spinel and clinopyroxene exsolution. Those from Gosse Pile are spinel-free.

Why "hour-glass zoning", produced by exsolution, should occur only in orthopyroxenes from these Giles Complex intrusions but, apparently nowhere else, is not known. It is suggested that, during crystallization from the magma, growth in the a direction of the

Gosse Pile orthopyroxenes has shown a slight preference for  $\text{Ca}^{2+}$  ions compared with the b and c directions. When unmixing occurs the lamellae thicken near the areas where most Ca occurs within the crystal, thus producing the hour-glass structure when viewed normal to b (Fig. 3.66). The elongate nature of the thickened areas is probably a reflection of the greater ease of ionic migration along, rather than across, the Si-O chains (Poldervaart and Hess, 1951; Preston, 1966). The lack of hour-glass structures and generally finer scale of lamellae in orthopyroxenes from layered intrusions in other parts of the world suggests that there is a greater temperature interval between crystallization and exsolution in orthopyroxenes than in augites and pigeonites (Boyd and Brown, 1967). It also suggests ionic migration has not been as effective in these orthopyroxenes. Its increased effectiveness in the Gosse Pile orthopyroxenes suggests a smaller temperature interval between crystallization and exsolution has existed, and this may reflect the very different conditions under which the Gosse Pile pyroxenes crystallized (see later sections).

By comparison with the hour-glass structures (compositional and exsolution) of augite (Preston, 1966) and considering the basic similarity of the orthorhombic and monoclinic pyroxene structures (e.g. Appleman, 1966, Fig. 6), it might be expected that similar structures in orthopyroxene would also lie parallel to (001) instead of (010). Why this anticipated orientation is not achieved is not known.

Orthopyroxenes in the strongly annealed rocks (south Main Body and the Gneissic Zone) tend to lose the fine lamellar structure. Megacrysts within these deformed rocks still retain the lamellae but there is a tendency for thickening of the lamellae, particularly at the margins of the crystals. In others, the lamellae have completely disappeared, leaving only larger blebs (Fig. 3.67). In kink bands there is a noticeable increase in the proportion of clinopyroxene blebs. This implies renewed migration of the exsolved clinopyroxene under the influence of strain energy.

#### (ii) Spinel

Exsolution of spinel from orthopyroxene is a relatively rare, though not unique, phenomenon (e.g. Green, 1963; Le Maitre, 1965; White, 1966). Spinel, exsolved from Gosse Pile orthopyroxenes, occurs as elongate plates orientated parallel to  $c$  and flattened in (100). Le Maitre (1965) has shown that the spinel exsolved from hypersthene in gabbroic xenoliths from Gough Island has (111) of spinel parallel to (100) of hypersthene, and either [100] or  $[\bar{1}10]$  of spinel parallel to  $b$  of hypersthene.

Spinel exsolution in Gosse Pile orthopyroxenes is seldom dense and is quite often absent. It is most obvious in the olivine-rich rocks (both olivine-orthopyroxenites and picrite). Because of their very small size (estimated as  $5\mu$  wide and probably  $1\mu$  or less in thickness) analysis of these spinel inclusions is very difficult. However, in one rock (A313/250) they were found to be particularly

abundant and the platelets could be traced directly into larger blebs of spinel near the margins of crystals. One such bleb has been analysed by electron microprobe techniques (Table 3.11). This spinel has the composition of picotite (appreciable Cr;  $Al > Cr$ ;  $Fe:Mg::1:1$ ; Deer, Howie and Zussman, 1965, p. 426). It is assumed that the exsolved material within the crystal and that at grain boundaries is very similar in composition.

Le Maitre (1965) comments that the spinel exsolution in pyroxenes is, "undoubtedly due to reheating". For the Gosse Pile orthopyroxenes it is felt that the spinel is an exsolution product of aluminous pyroxenes, formed during cooling. As pointed out by Boyd (1966a), aluminous enstatite is stable at high temperatures and low pressures, but high pressures and low temperatures reduce the amount of Al which it may contain. Hence, it is considered probable that spinel exsolution, involving essentially Al, Cr, Fe and Mg, took place during cooling of the pyroxenes at constant (high) pressure. It is significant that, where spinel exsolution has been observed elsewhere, there is other evidence to suggest that the pyroxenes crystallized under high pressure. The most common occurrence is in nodules found within volcanics and such nodules are generally interpreted as being derived from areas within the mantle (Le Maitre, 1965, suggests depths of 40-50 km). White (1966) considers that exsolution of spinel from orthopyroxenes in nodules found in Hawaiian basaltic rocks most probably reflects a change in P,T conditions, and is unlikely to have occurred during cooling of the lavas at the surface.



Table 3.11

Analysis of green spinel exsolved from orthopyroxene in olivine-orthopyroxenite (A313/250).

| Analysis                       |      | Structural formula |      |
|--------------------------------|------|--------------------|------|
| SiO <sub>2</sub>               | 0.0  | Al                 | 12.2 |
| Al <sub>2</sub> O <sub>3</sub> | 45.2 | Cr                 | 2.8  |
| Cr <sub>2</sub> O <sub>3</sub> | 15.3 | Ti                 | 0.1  |
| ΣFe as FeO                     | 24.8 | Mg                 | 4.6  |
| MgO                            | 13.6 | Fe <sup>2+</sup>   | 4.7  |
| CaO                            | 0.0  |                    |      |
| TiO <sub>2</sub>               | 0.5  |                    |      |
| MnO                            | 0.0  |                    |      |
| TOTAL                          | 99.4 |                    | 24.4 |

Because of the apparent deficiency of cations in the B (6-fold co-ordination) positions, and the excess of cations in the A (4-fold co-ordination) positions as shown by the calculated structural formula, on the basis of 32 oxygens, it is probable that not all the iron is present as Fe<sup>2+</sup> but a high proportion is present as Fe<sup>3+</sup> in the A positions.

Analysis by A. Moore on A.R.L. electron microprobe at the Australian National University, Canberra (1966) through courtesy of Dr. J.F. Lovering. See Appendix 3C.

## (iii) Rutile

The first time that rutile was definitely recognised as an exsolution product in orthopyroxenes was from the rocks of Gosse Pile (Moore, 1968). Since then several workers have reported its occurrence in other bodies; e.g. Kalka intrusion by Goode and Nesbitt (1969); in the gabbro of the Gnama South Complex, western Fraser Ranges of Western Australia by Harley (1969); and in nodules from South African kimberlite pipes by W.L. Griffin (pers. comm. by letter, 1968). Dallwitz (1968) briefly stated that, in granulites from Antarctica, "the hypersthene invariably contains fine rutile needles . . .". However, in a written communication with Mr. Dallwitz (pers. comm., 1969) the author has established that these needles were not positively identified as rutile but they, "appeared similar to what were taken to be rutile needles in quartz", (quote from letter). It seems, in the author's view, that the black needles observed by Dallwitz are more likely to be haematite-magnetite, or ilmenite, inclusions which are relatively common in orthopyroxenes from granulite facies terrains, e.g. Bown and Gay, 1959; Howie, 1963. Unfortunately, Mr. Dallwitz was unable to supply a slide of the specimen under discussion for examination by the author.

The rutile needles in the Gosse Pile orthopyroxenes (Fig. 3.68 and Fig. 3.69) were originally identified on the basis of their optical properties (straight extinction, high relief and length show orientation). This identification was confirmed on the basis of the electron microprobe scans (Fig. 3.70). The needles have length to

Fig. 3.68

Rutile exsolved from orthopyroxene. A313/116. P.P.L.

Photograph: A. Moore.

Fig. 3.69

The same section. C.P.

Photograph: A. Moore.

---

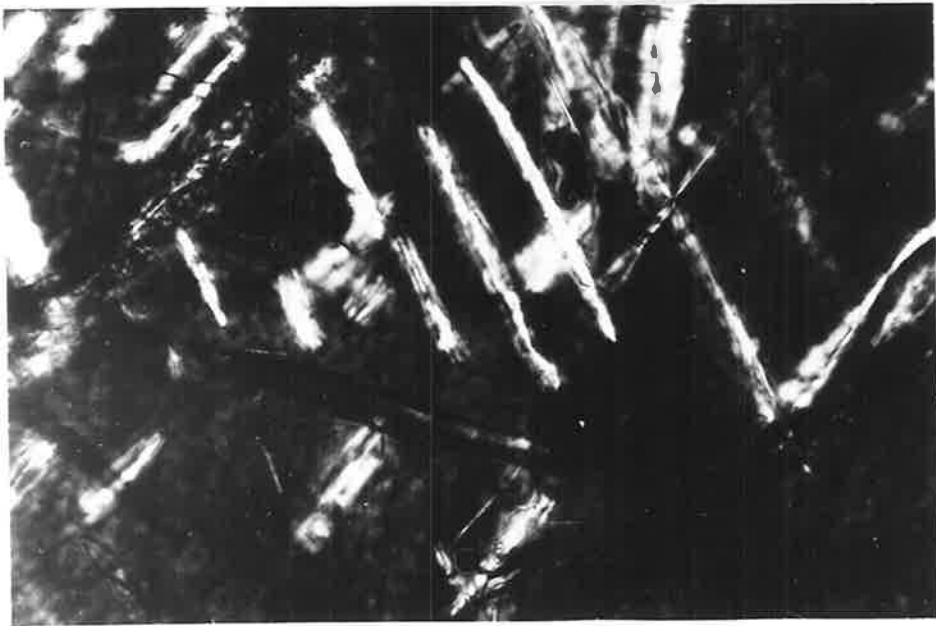
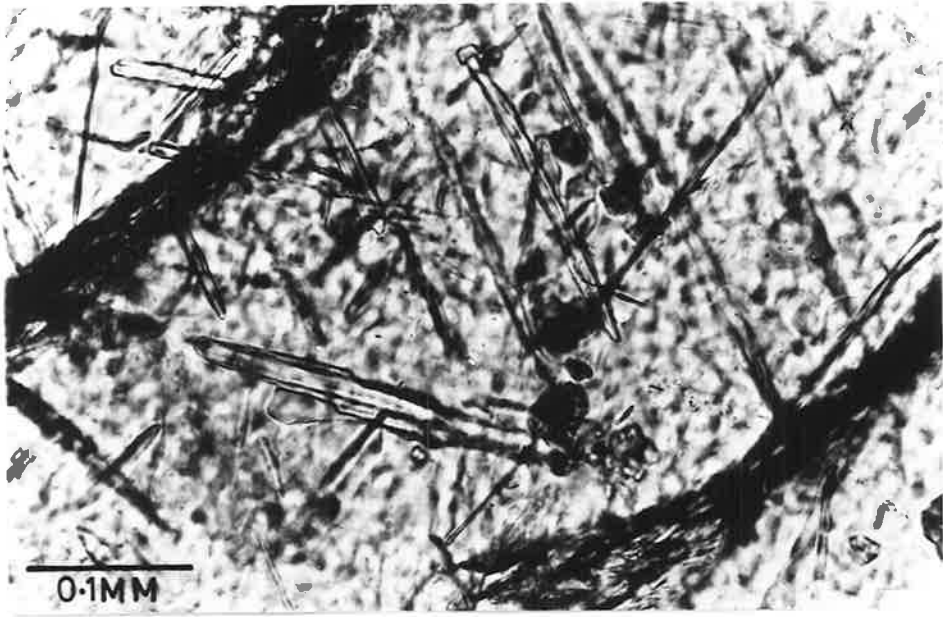


Fig. 3.70

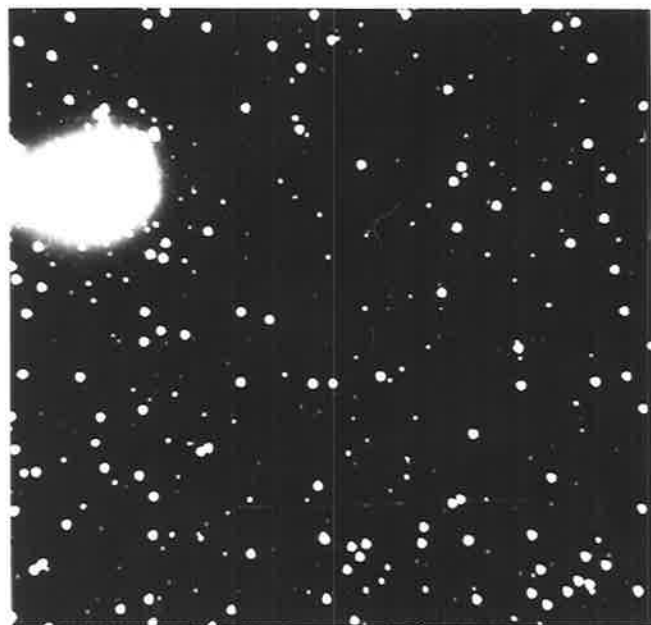
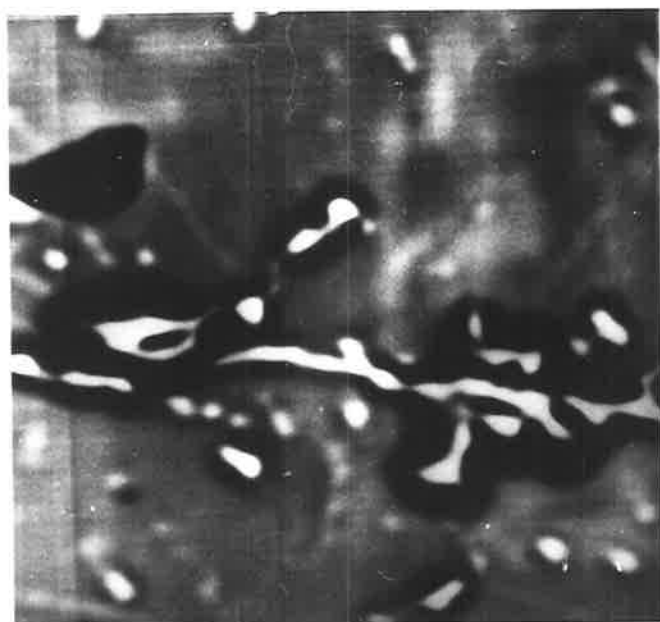
Electron microprobe studies on an orthopyroxene showing rutile exsolution (A313/116). Because of the small size of the rutile needles and the relatively random orientation of the thin section surface relative to the needles, it was extremely difficult to obtain a large area of rutile.

TOP: Image produced by specimen current. The rutile needle section is marked by the dark area (upper left). The east-west light area is a fracture.

BOTTOM:  $TiK_{\alpha}$  radiation (electron beam-scanning photograph).

Each photograph covers an area 0.2 mm x 0.2 mm.

Analysis and photographs: AMDEL



breadth ratios varying from 20:1 to 100:1 and vary in length from 0.1 mm to 1.0 mm. Occasionally they show slight curvature. They are contained in the (010) planes, and are elongate parallel to ( $\bar{6}01$ ), (601) and (001), of the orthopyroxene (Fig. 3.68). W.L. Griffin (1968, pers. comm.) noted that the rutile within the orthopyroxene, clinopyroxene and garnet from eclogite nodules in South African kimberlites is elongate parallel to (101) of the rutile and so gives apparent inclined extinction.

The rutile has probably formed by exsolution rather than by epitaxial growth because rutile does not occur as a primary phase elsewhere in the same rocks, and because  $\text{ilvospinel}$  or ilmenite would be more likely to form than rutile during the crystallization of orthopyroxene from the magma (Verhoogen, 1962).

The average  $\text{TiO}_2$  content for orthopyroxenes containing rutile exsolution is 0.13% (average of 11 analyses; range from 0.08% to 0.25%  $\text{TiO}_2$ ). This is a relatively small amount when compared with "high" values of 0.3% - 1.6%  $\text{TiO}_2$  for metamorphic pyroxenes which Howie (1963) thought might contain undetected rutile or ilmenite. Other igneous orthopyroxenes which do not show rutile exsolution have  $\text{TiO}_2$  contents which are similar or higher: 0.11% in enstatite from the Bushveld Complex; 0.22% in bronzite from the Stillwater Complex; 0.47% in hypersthene from Hakone volcano, Japan (values quoted from Deer, Howie and Zussman, 1963). This suggests that a chemical control only, such as exceptionally high  $\text{TiO}_2$  content, is not the deciding factor and that rutile exsolution may be caused by a combination of

chemical and physical conditions.

During crystallization from a magma orthopyroxene can accommodate titanium in small amounts, substituting for  $\text{Fe}^{2+}$  and  $\text{Mg}^{2+}$ , probably in  $M_2$  sites, and is unlikely to occur in tetrahedral sites (Hartman, 1969). If a significant amount of clinopyroxene is present then this probably takes up the greater part of the titanium present. Clinopyroxenes in Gosse Pile contain an average of 2.9 times as much  $\text{TiO}_2$  as the co-existing orthopyroxenes: this is in agreement with observations by de Vore (1957). Rutile exsolution has not been observed in any clinopyroxenes from Gosse Pile, nor in orthopyroxenes from the websterites. At temperatures below the magmatic range the solubility of Ti in pyroxene is small (Verhoogen, 1962, p. 217) but that which is in the pyroxene structure can normally be tolerated without giving any external evidence of its presence, although it does cause strain within the lattice. In general, the entry of Ti into silicate lattices is energetically unfavourable and is restricted to a high temperature range (Verhoogen, 1962). The amount of  $\text{R}_2\text{O}_3$  (particularly  $\text{Al}_2\text{O}_3$ ) in the pyroxene probably indirectly helps to determine the ease with which titanium can be taken into, and maintained within, the pyroxene lattice. Because Ti most likely replaces  $\text{Fe}^{2+}$  (and  $\text{Mg}^{2+}$ ) in  $M_2$  sites, charge balance requirements are such that di- or tri-valent ions must replace  $\text{Si}^{4+}$  in the tetrahedral sites. As  $\text{Al}^{3+}$  most commonly does this, the ease of emplacement of  $\text{Al}^{3+}$  in the tetrahedral sites indirectly assists the intake of titanium. However, while Al in 4-fold



co-ordination assists the intake of titanium into the pyroxene lattice, Al in 6-fold co-ordination tends to hinder it and decreases the stability of titanium already in the lattice. It should be noted that increased pressure tends to eliminate phases with Al in tetrahedral co-ordination in favour of those with Al in octahedral co-ordination. Orthopyroxenes showing rutile exsolution have an average  $R_2O_3$  content of 5.7% (range 5.0 - 6.3%, 11 analyses) and  $Al_2O_3$  content of 3.6% (range 3.3 - 4%, 11 analyses). All have a high proportion of Al in octahedral co-ordination.

If the pyroxenes crystallize under high pressure, then as the temperature falls, it is less likely that the lattice will be able to tolerate "foreign" elements such as titanium, especially if the stability of titanium within the lattice is further reduced by the presence of relatively large proportions of Al in 6-fold co-ordination. Thus, if Ti is present in amounts greater than some critical tolerance level for that pressure it will exsolve to form dense, close-packed rutile, the orientation of which is probably determined by the positions of the oxygen of the pyroxene lattice. If chromium is in the pyroxene in amounts greater than some critical tolerance level then it too will be exsolved as chrome-rich spinel.  $Ti^{4+}$  is likely to be removed from the lattice first because of its stabilization energy (zero) compared with that of  $Cr^{3+}$  (53.7 kcal/mole; Dunitz and Orgel, 1957)\*. Few pyroxenes show both

---

\* If titanium is present in the lattice as  $Ti^{3+}$ , as has been suggested by Chesnokov (1959) and by Burns and Fyfe (1967), then it has an unpaired 3d electron and a stabilization energy of about 20.9 kcal/mole in octahedral co-ordination. Otherwise the same arguments hold.

spinel and rutile exsolution, and where spinel exsolution is abundant no rutile is observed. This is probably because the Ti can be taken into the spinel lattice (Table 3.11). Rutile exsolution has not been observed in the annealed grains of the Gneissic Zone rocks although it is often abundant in the strained megacrysts.

Ringwood and Major (1966) have shown that, under very high pressures, pyroxene breaks down to spinel plus stishovite (rutile structure). In garnets, produced during high pressure (14 kbar) experimental runs, rutile has been observed as inclusions (Green and Ringwood, 1967, p. 777). Orientated inclusions of rutile in garnet (exsolution?) have also been observed in high pressure basic gneisses from Ghana (von Knorring and Kennedy, 1958). The occurrence of rutile exsolution in garnet and pyroxenes of eclogite nodules from kimberlites has already been noted (W.L. Griffin, pers. comm.). This supports the view that the common factor in the production of rutile exsolution is high pressure. However, in pyroxenes it is considered to be produced only by exsolution from igneous pyroxenes which cooled under high pressure, probably near the base of the crust. Rutile exsolution would not be expected in high-grade metamorphic pyroxenes as, during the elemental reorganization involved during such metamorphism, it is probable that there would be ample opportunity for the titanium to form ilmenite or rutile as distinct and separate phases. As pointed out by Verhoogen (1962, p. 217), "At temperatures below the magmatic range the solubility of  $TiO_2$  is very small: witness the co-existence of rutile and titanium-free pyroxenes in many metamorphic rocks".

The absence of rutile exsolution from the polygonal matrix grains of the annealed rocks south of Gosse Pile suggests that, during the syntectonic annealing processes, either the rutile was liberated and could form a discrete phase or that the Ti, liberated from the orthopyroxene, was able to enter the co-existing clinopyroxene. Neither rutile nor spinel has been observed as a discrete phase in the annealed rocks although either may be present as very fine grains.

#### Effects of deformation

Kink bands in orthopyroxene are common, particularly in rocks involved in the brittle faulting, although some are found in megacrysts of rocks in the Gneissic Zone. Numerous kink bands show apparent inclined extinction (Fig. 3.71) and so a detailed optical examination, using the U-Stage, of 100 kink bands was carried out in the expectation that clinoenstatite would be found. Trommsdorf and Wenk (1968) have identified this phase in the deformed bronzites of Giles Complex gabbros, near Wingellina (Fig. 1.1). However, even in the most optimistic-appearing areas no clinoenstatite could be positively identified in the Gosse Pile rocks. In all cases examined the material within the kink bands is optically negative. Commonly a concentration of clinopyroxene occurs along kink band boundaries, but this has been derived from the exsolution lamellae and forms discrete blebs unrelated to the material forming the kink band itself. More detailed and refined studies (single crystal X-ray work) may yet reveal clinobronzite within the kink bands.

Fig. 3.71

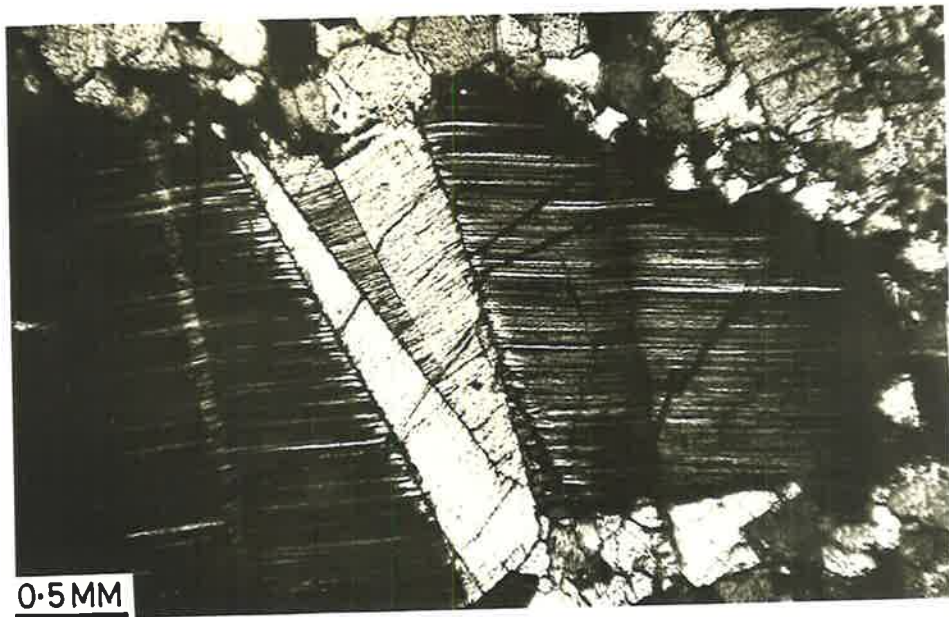
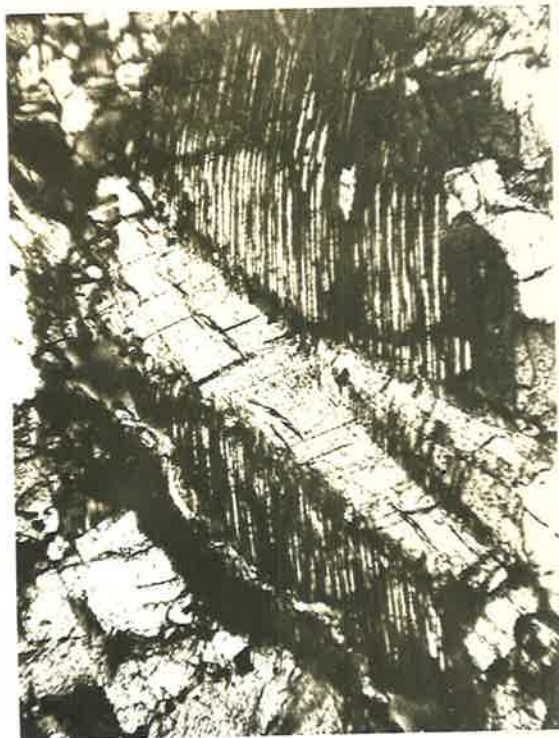
Kink bands (centre of crystal) with apparent inclined extinction in orthopyroxene in a deformed orthopyroxenite (A313/401). Angle of rotation from maximum brightness (right) to extinction (left) is  $27^{\circ}$ . U-Stage measurements on this band show it to be optically negative. C.P.

Photographs. A. Moore.

Fig. 3.72

Kink bands with straight extinction in orthopyroxene in a deformed orthopyroxenite (A313/287A). Slip system is  $T \approx (100)$ ,  $t = [001]$ . C.P.

Photograph: A. Moore.



The slip system of a typical multiple kink band (Fig. 3.72) is  $T \approx (100)$ ,  $t = [001]$ . This is consistent with the slip system found by Borg and Handin (1966) and by Riecker and Rooney (1966) for experimentally deformed enstatite.

## 2. CLINOPYROXENE

### Introduction

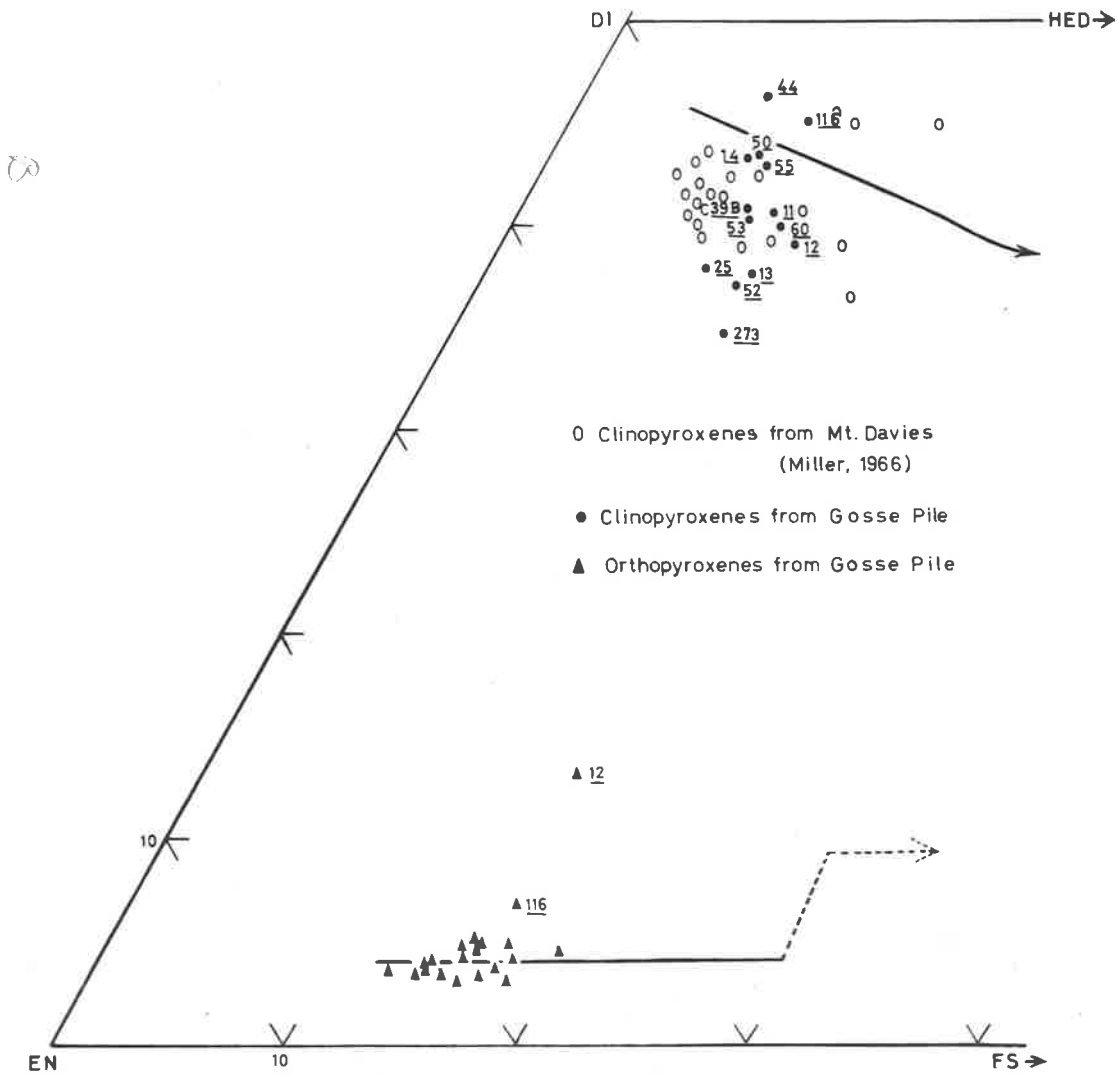
Although found in all rock types, clinopyroxene is seldom abundant. It most commonly occurs interstitially in the orthopyroxenites or as small grains in the noritic rocks. Only in some websterite samples is it the dominant mineral. Study of the clinopyroxenes has been particularly difficult, not only because it is usually present in such small quantities but also because intergrowths with orthopyroxene are so complex and on such a fine scale as to make clean separations for bulk chemical analyses almost impossible.

### Chemistry

Results of the chemical analyses (Table 3.12) were disappointing. They failed to define any differentiation trend when plotted on the classical En-Di-Wo diagram (Fig. 3.73) and also they showed considerable scatter. This scatter probably is caused largely by the presence of exsolved, unseparated orthopyroxene within the clinopyroxenes, particularly as the majority of clinopyroxenes analysed were from rocks in which it is a major mineral and it is in these rocks that intimate

Fig. 3.73

Part of the pyroxene quadrilateral showing the positions of pyroxenes from Gosse Pile and from Mt. Davies intrusion (after Miller, 1966). Orthopyroxenes A313/12 and A313/116 from Gosse Pile probably contain a relatively high proportion of unseparated Ca-pyroxene (See Table 3.10).





two-pyroxene intergrowths occur. Miller (1966) examined clinopyroxenes from Mt. Davies intrusion (Fig. 1.2) and, in spite of considerable care in separation, involving hours of hand-picking, she found a similar degree of scatter (Fig. 3.73). All analyses plot near the diopside end of the path marking the typical differentiation trend of clinopyroxenes from layered intrusions.

Various graphs, comparing the relative concentrations within the clinopyroxenes of one element with another, have been made. No obvious trends were observed. The plot of the atomic ratio  $\text{Ca}/\text{Ca} + \text{Mg}$  against  $\text{Al}_2\text{O}_3$  content does not reveal an obvious relationship, as was expected (see section on orthopyroxenes, p. 211). Le Bas (1962) showed that when wt.%  $\text{Al}_2\text{O}_3$  was plotted against wt.%  $\text{SiO}_2$  for selected soda-poor igneous clinopyroxenes there can be distinguished three distinct groups, each reflecting the parental magma type. Clinopyroxenes from Gosse Pile, when plotted on this diagram (Le Bas, 1962, Fig. 2) fall within the area occupied by high-alumina and tholeiitic magma types, but are more aluminous. Challis (1965) plotted the  $\text{Al}^{\text{IV}}$  content against the Si content of clinopyroxenes from intrusive ultramafic and basic rocks and nodules. The diagram indicates the approximate fields of pyroxenes from tholeiitic and alkaline igneous rocks. Clinopyroxenes from Gosse Pile, and from south Mt. Davies (Miller, 1966), all plot within the tholeiitic field.

An interesting comparison is that of  $\text{Al}^{\text{IV}}$  against  $\text{Al}^{\text{VI}}$ . Using the suggestion by Thompson (1947) that, in silicate structures, Al tends to enter into the tetrahedral site at higher temperatures and into the

octahedral site at higher pressures, Aoki and Kushiro (1968) compared the proportions of  $Al^{IV}$  and  $Al^{VI}$  in clinopyroxenes from various environments. They found that clinopyroxenes from igneous rocks have the Al mostly in tetrahedral sites, whereas those from eclogites have Al mostly in octahedral sites. Clinopyroxenes from granulites and from inclusions in basalts have Al in both sites and fall in a region between the other two. The clinopyroxenes from Gosse Pile fall within this zone (Fig. 3.74) and it is therefore likely that they formed under conditions similar to those prevailing during the crystallization of the ultramafic inclusions in basaltic rocks, i.e. near the base of the crust. A similar argument may be derived from the proportion of Ca-Tschermak's molecule in the clinopyroxene. This is a direct measure of the amount of Al in 4-fold co-ordination. In basaltic rocks the calculated proportion of Ca-Tschermak's molecule in the clinopyroxene is generally low (Aoki and Kushiro, 1968) but for the Gosse Pile clinopyroxenes it is relatively high (about 9%), again supporting the view that these pyroxenes crystallized under pressure. Hays (1966) showed that pure Ca-Tschermak's molecule ( $CaAl_2SiO_6$ ) becomes stable only above 12 kbars pressure.

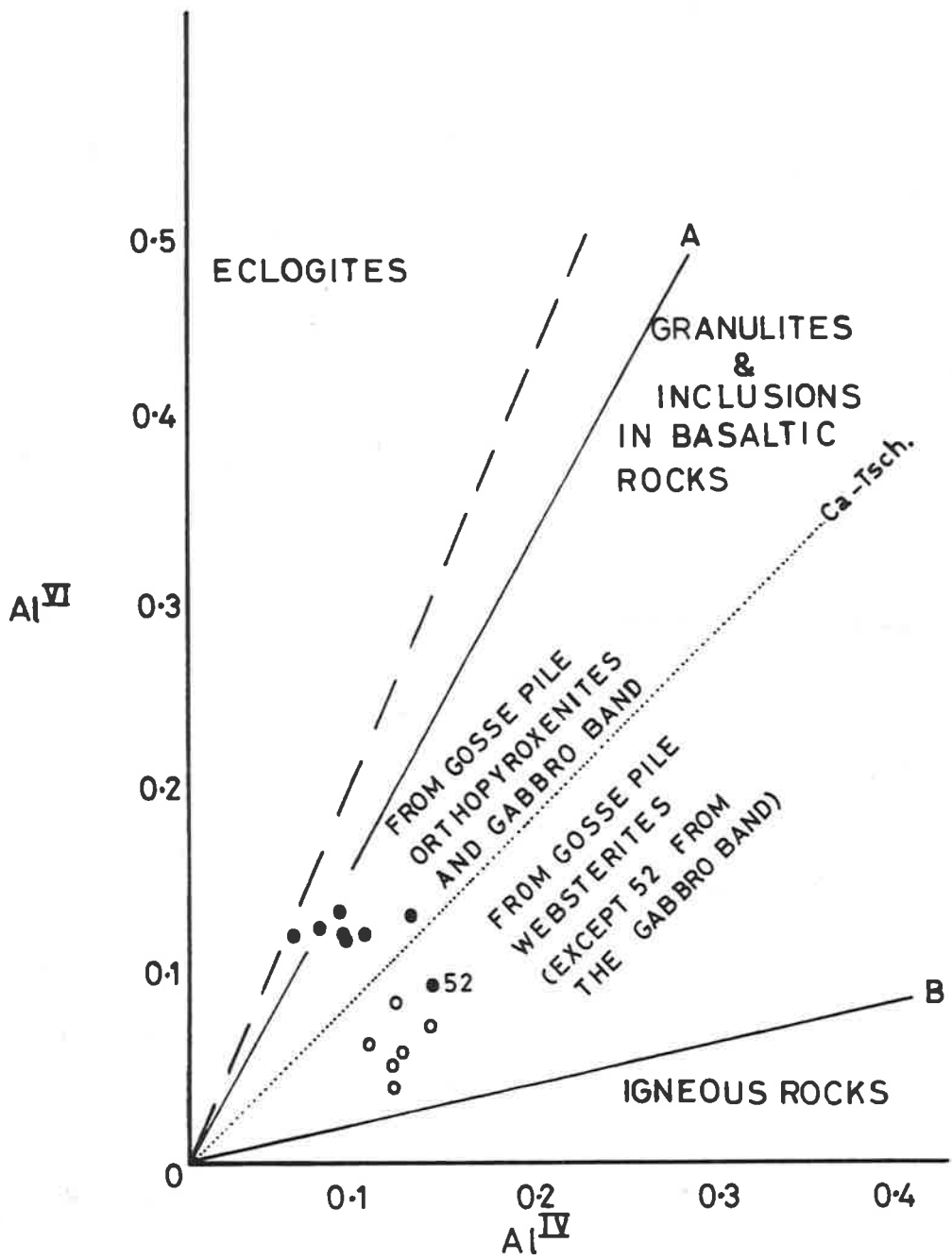
### Exsolution

#### (i) Orthopyroxene

All of the clinopyroxenes show exsolution of orthopyroxene. Where the clinopyroxene occurs interstitially the exsolved orthopyroxene takes the form of fine lamellae ( $50\mu - 100\mu$  wide) extending to the margins of

Fig. 3.74

Plot of  $Al^{VI}$  against  $Al^{IV}$  for clinopyroxenes separated from Gosse Pile rocks, after Aoki and Kushiro (1968). The line  $\Delta$  (separating the field of eclogites and that of granulites plus inclusions in basaltic rocks) of Aoki and Kushiro is poorly defined and, from their data, could equally include all the Gosse Pile samples (dashed line).



the crystals. These at first appear to be polysynthetic twinning but have been shown to be orthopyroxene by U-Stage measurements and by an electron microprobe traverse across a clinopyroxene of identical appearance from the Kalka intrusion (Fig. 1.2). The probe result (on sample A314/209, done by AMDEL; A.D.T. Goode, pers. comm.) shows that there are marked compositional changes across the pyroxene which can be correlated with the lamellae: they are poor in Ca and enriched in Mg and Fe. The U-Stage measurements (made on Gosse Pile clinopyroxenes) are difficult because there is considerable interference from the host, even at relatively low tilt angles, as a result of the fine nature of the lamellae. However, it has been shown that they have an orientation consistent with that determined by Poldervaart and Hess (1951) for lamellae in similar clinopyroxenes; i.e. the lamellae lie parallel to (100) of the host with  $\alpha_{\text{opx}}$  and  $\beta_{\text{opx}}$  coincident.

In relatively undeformed rocks rich in clinopyroxene, especially the northern websterite, the above-mentioned lamellar structure may still be observed, in addition to highly complex intergrowths. These take the form of blebs of one pyroxene regularly orientated within another, or myrmekite-like intergrowths (see Fig. 3.19). There also appear to be regular intergrowths between contiguous clinopyroxenes which, at first, appear to be twins. However, U-Stage measurements have so far failed to show any regular twin relationships. An example of this is given in Fig. 3.75. An apparently similar example is given in Fig. 3.76, but comparison of the stereographic projections shows the

Fig. 3.75

Three photomicrographs illustrating the complex intergrowths of pyroxenes within the northern websterite. Each photograph shows the section rotated to a different position so that different pyroxenes are in extinction. Top:  $143^{\circ}$ ; Middle:  $156^{\circ}$ ; Bottom:  $190^{\circ}$ . A313/24. C.P.

The stereographic projection illustrates the relationships of the optic constants of the pyroxenes: 1 & 2 are clinopyroxene and A & B are orthopyroxene.

$\odot = \alpha$      $+ = \beta$      $\triangle = \gamma$      $\diamond =$  pole to the plane separating individuals.

Photographs: A. Moore.

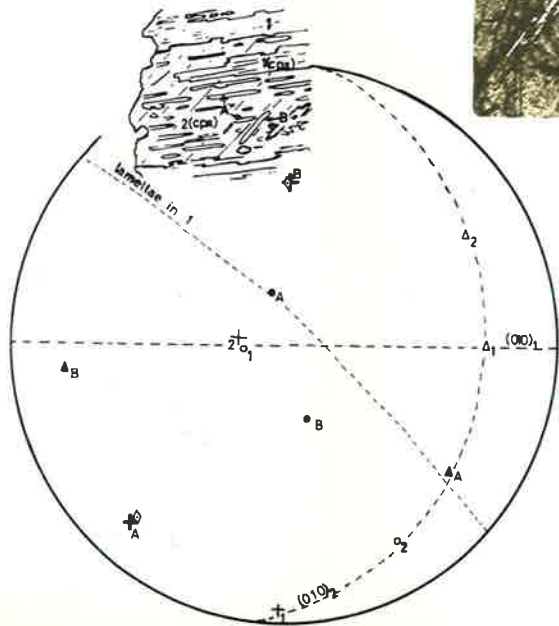
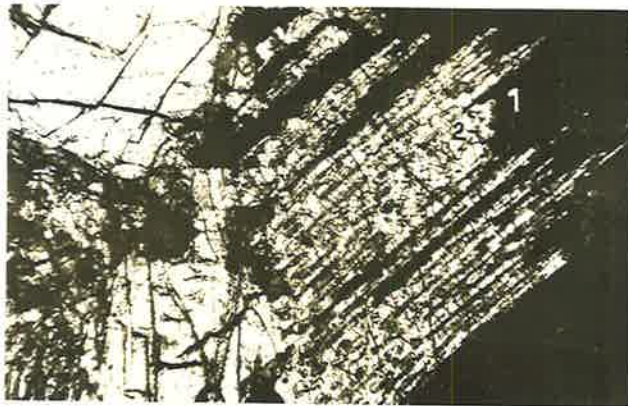
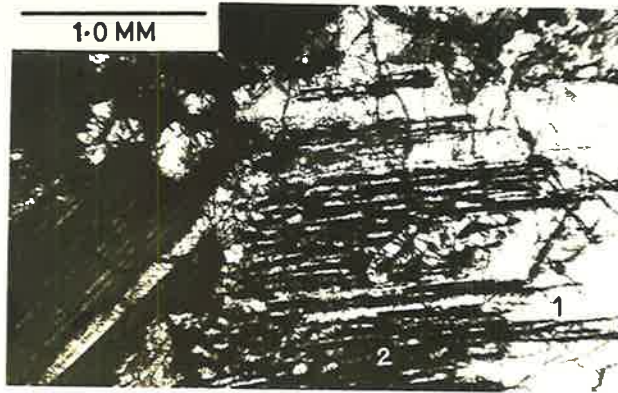


Fig. 3.76

TOP: Complex intergrowths of pyroxenes, similar in appearance to those in Fig. 3.75.

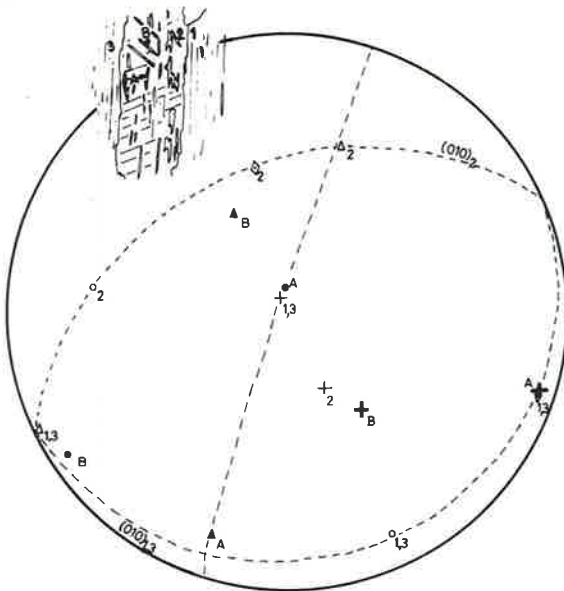
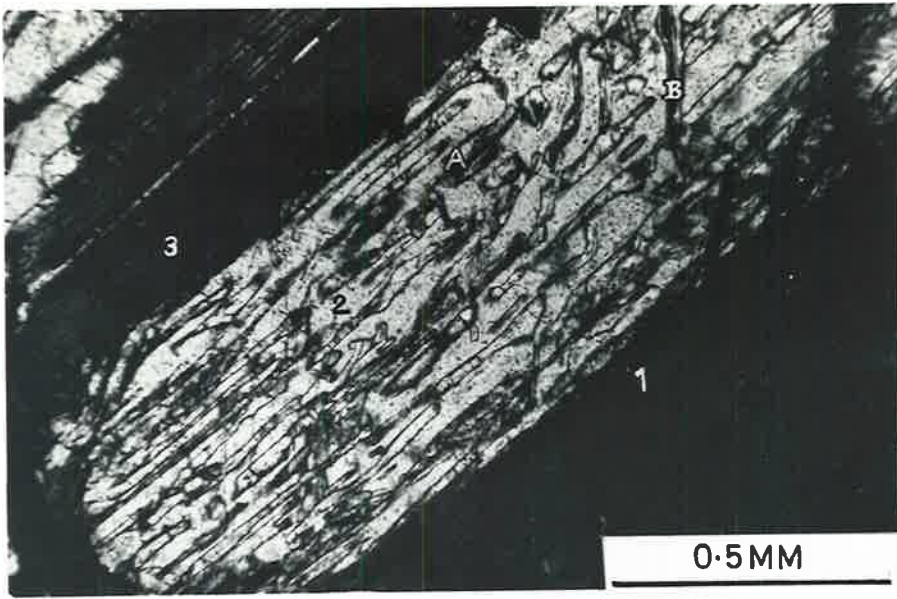
MIDDLE: Colour photograph of the same grains to illustrate the regular orientation in two directions (exsolution?) of orthopyroxene within the central part of the clinopyroxene, and also the fine lamellar structure within that grain, thought to be twinning.

BOTTOM: Stereographic projection of the optic constants of the various individuals shown in the above photographs. Note the lack of resemblance to the similar projection in Fig. 3.75.

A313/232. C.P.

Photographs: A. Moore.





pyroxenes to be quite differently orientated in each case, and in neither can any twin law be established. Similarly, the orthopyroxene intergrowths have different, although regular, orientations. These intergrowths may not be entirely due to exsolution features but may be caused by partial replacement of one pyroxene by another or by some, as yet undetermined, epitaxial relationship, (e.g. as has been found by Tarney, 1969, for pyroxene intergrowths in some Scottish picritic dykes)\*. The author is unaware of published descriptions of complex pyroxene relationships such as have been described here. Jackson (1970, in press) illustrated pyroxene textures of cumulate xenoliths in Hawaiian basalts and these appeared similar to the textures described here. Jackson commented on their unusual appearance and suggested that such peculiar intergrowths may be the result of partial melting. This suggestion is unlikely to be valid for the Gosse Pile examples, but it is significant that these relationships are found elsewhere in nodules from basalts.

A detailed study of these intergrowths, using X-ray analysis, electron microprobe analyses and optics would probably be a worthwhile project. It was not continued further here because of a shortage of

---

\* It is possible that, during settling of the pyroxenes, crystals may have drifted together and become attached. Overgrowths could then occur and the texture would be complicated by later exsolution features. Such mutual attachment of the crystals need not necessarily be in consistent crystallographic orientations.

time and a lack of readily accessible electron microprobe facilities.

(ii) Spinel

Green spinel is a very common exsolution phase in clinopyroxene, particularly in the olivine-rich rocks. It is always far denser than in the co-existing orthopyroxene and gives the clinopyroxene a deep green, almost translucent appearance in thin section (Fig. 3.77). The spinel forms rods rather than plates, which are elongate parallel to c. Such rods are very thin (estimated to be only  $1\mu$  in diameter). Spinel also occurs along grain boundaries (Fig. 3.78) and this material, which is elongate and plate-like within the boundaries, is thought to be derived from the spinel exsolved within the pyroxene by migration. Arguments concerning the origin and significance of spinel exsolution in orthopyroxene (p. 219) are probably equally applicable in the case of the clinopyroxene.

Rutile exsolution has not been observed in clinopyroxene from Gosse Pile.

Fig. 3.77

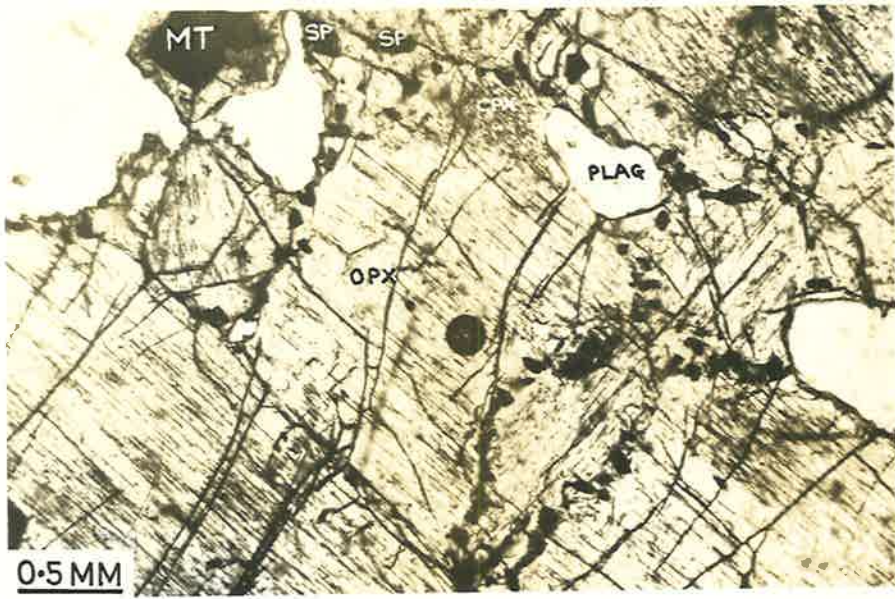
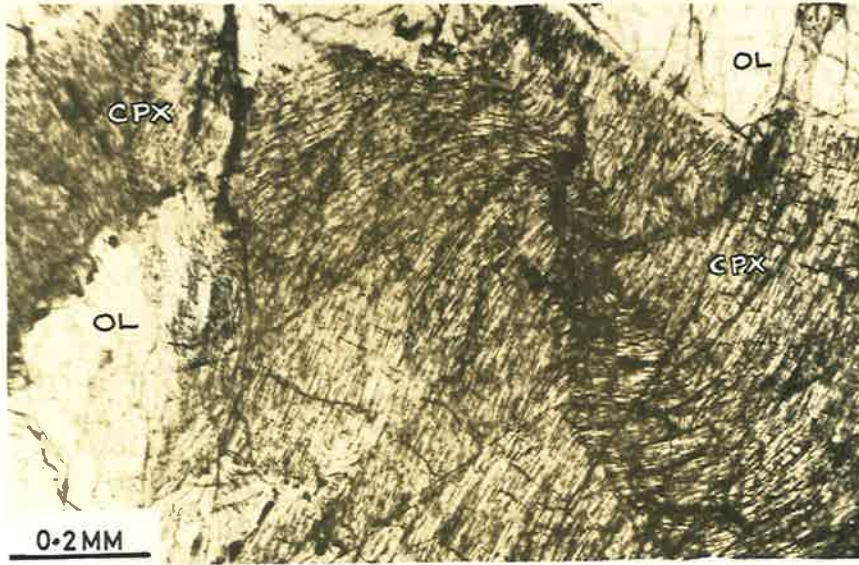
Spinel exsolved from clinopyroxene (now deformed). Note how much more dense it is in the clinopyroxene than in the orthopyroxene. A313/132. P.P.L.

Photograph: A. Moore.

Fig. 3.78

Spinel exsolved within pyroxene and spinel crystals concentrated along grain boundaries. A313/249. P.P.L.

Photograph: A. Moore.



## 3. DISTRIBUTION OF ELEMENTS BETWEEN CO-EXISTING PYROXENES

Iron and Magnesium

The distribution of Mg and Fe<sup>2+</sup> between orthopyroxene (Ca-poor) and clinopyroxene (Ca-rich), which are presumed to be in equilibrium, has been expressed most simply by Bartholomé (1961, 1962) as:

$$K_T = \left(\frac{\text{Fe}^{2+}}{\text{Mg}}\right)_{\text{opx}} \times \left(\frac{\text{Mg}}{\text{Fe}^{2+}}\right)_{\text{cpx}}$$

The more complex equation derived by Ramberg and de Vore (1951), termed  $K_D$ , is the reciprocal of  $K_T$ . Muir and Tilley (1958) and O'Hara (1960) concluded that the distribution of Fe<sup>2+</sup> and Mg between co-existing pyroxenes was the same for both metamorphic and for plutonic igneous rocks. However, Wilson (1960) made the suggestion that the distribution coefficient of such pyroxenes may be a useful guide to the temperature of formation. Kretz (1961) brought forward data to support this view, showing that  $K_D$  values for igneous rocks tend to be consistently higher than those for rocks which had supposedly equilibrated under metamorphic conditions (temperatures).

Ramberg and de Vore (1951) deduced the following equations to show the dependence of  $K_D$  on pressure and temperature:

$$K_{D_1} = (K_{D_2})^{T_2/T_1} \cdot e^{\Delta S(T_2 - T_1)/RT}$$

$$K_{D_1} = (K_{D_2}) \cdot e^{\Delta V(P_2 - P_1)/RT}$$

Table 3.13

Distribution coefficients for co-existing pyroxenes from Gosse Pile.

| Sample No.<br>A313/-       | (1)<br>$K_T$ | (2)<br>$K_T'$ | (3)<br>$K_D$ | (4)<br>$K_D'$ |
|----------------------------|--------------|---------------|--------------|---------------|
| 11                         | 1.10         | 1.09          | 0.91         | 0.92          |
| 12*                        | 1.19         | 0.90          | 0.84         | 1.11          |
| 13                         | 1.12         | 0.96          | 0.89         | 1.04          |
| 14                         | 1.10         | 1.22          | 0.91         | 0.82          |
| 25                         | 1.18         | 1.10          | 0.85         | 0.91          |
| 39B                        | 1.09         | 1.12          | 0.92         | 0.89          |
| 44**                       | 2.04         | 1.49          | 0.49         | 0.67          |
| 50                         | 1.37         | 1.27          | 0.73         | 0.79          |
| 53*                        | 1.45         | 1.12          | 0.69         | 0.89          |
| 55                         | 1.02         | 1.18          | 0.98         | 0.85          |
| 60                         | 1.45         | 1.16          | 0.69         | 0.86          |
| 116                        | 1.43         | 1.27          | 0.70         | 0.79          |
| 273                        | 1.04         | 1.10          | 0.96         | 0.91          |
| Average<br>(excluding /44) | 1.19         | 1.13          | 0.83         | 0.89          |

\* orthopyroxene analyses probably include much unseparated, exsolved clinopyroxene.

\*\* the very different  $K_T$  and  $K_D$  values here are probably caused by unseparated clinopyroxene in the orthopyroxene and poor analyses.

|  |   |  |
|--|---|--|
| <p>(1) <math>K_T = (Fe^{2+}/Mg)_{opx} \times (Mg/Fe^{2+})_{cpx}</math></p> <p>(2) <math>K_T' = (Fe^{2+} + Fe^{3+}/Mg)_{opx} \times (Mg/Fe^{2+} + Fe^{3+})_{cpx}</math></p> <p>(3) <math>K_D = 1/K_T</math></p> <p>(4) <math>K_D' = 1/K_T'</math></p> | } | <p>after<br/>Bartholomé (1961)<br/>and<br/>Oosterom (1963)</p> <p>after Ramberg<br/>and de Vore<br/>(1951)</p> |
|--|---|--|



where  $K_{D_1}$  and  $K_{D_2}$  are the distribution coefficients at the pressures  $P_1$  and  $P_2$ , or absolute temperatures  $T_1$  and  $T_2$ ;  $\Delta S$  is the entropy change involved in the partitioning reaction and  $\Delta V$  the change in partial molal volume. Calculations (for  $P_1 = 10$  kbars,  $P_2 = 0$  kbar) by Ramberg and de Vore (1951) for the olivine-pyroxene pair showed that pressure sensitivity of  $K_D$  is negligible, assuming ideal mixtures are involved and, "nothing serious happens to the molal volume under the increasing pressure". Eugster (1955) experimentally found that the distribution of K and Cs in the system sanidine-water gives an almost constant  $K_D$  at values between 1 kbar - 2 kbars  $P_{H_2O}$ , while it changed from 0.48 to 1.2 in the temperature range  $500^\circ - 800^\circ C$ . In natural systems  $K_D$  values have been correlated with temperature, (e.g. Kretz, 1961a; Bartholomé, 1962; McIntire, 1963; Binns, 1962; Moxham, 1965 and Saxena, 1968).

Following Oosterom (1963, p. 295) the distribution coefficients for the Gosse Pile pyroxene pairs have been calculated using ( $Fe^{2+} + Fe^{3+}$ ) since the relation Mg: total Fe gives a better approximation to the bulk chemical relations. However, for comparison with other published data, results of calculations involving only ferrous iron are also given in Table 3.13. The average  $K_{D_T}$  value is 1.19 ( $K_D$  equivalent is 0.83). Saxena (1968) showed that, for 41 metamorphic pyroxene pairs, the  $K_D$  value ranged between 0.501 to 0.647 (average, 0.556) while for 13 igneous ~~pyroxene~~ pairs it ranged between 0.536 to 0.857 (average, 0.717). This confirms the data of Kretz (1961, 1961a), who suggested a  $K_D$  value of 0.73 for igneous pyroxene pairs and 0.54



for metamorphic pyroxene pairs. Atkins (1969) has found an average  $K_D$  value of 0.67 for pyroxene pairs from the Bushveld igneous complex. He considers this somewhat lower  $K_D$  value (for igneous pyroxenes) to be a function of different P,T conditions. The average  $K_D$  value for the Gosse Pile pyroxene pairs is notably higher than the average value for igneous pyroxene pairs.

If variations in  $K_D$  are related essentially to the temperatures of crystallization of pyroxene pairs, provided that they are ideal mixtures of Mg and  $Fe^{2+}$ , then  $\ln K_D$  may be used as a crude temperature (and pressure) scale (Ramberg and de Vore, 1951). This has been done by Saxena (1968), who noted the close similarity in shape between the pyroxene solvus and the curves resulting from a plot of  $\ln K_D$  against  $(Mg,Fe) SiO_3$ . If the data of Table 3.13 is plotted on a diagram such as that given by Saxena (1968, Fig. 2) the Gosse Pile pyroxenes can be seen to plot well above the range of other plutonic igneous pyroxenes. The very different  $K_D$  and  $K_T$  (or  $K_D'$  and  $K_T'$ ) values of the Gosse Pile pyroxene pairs show that, if the temperature dependency of  $K_D$  is valid, these pyroxenes have crystallized well above the liquidus temperatures of other igneous intrusions, such as Skaergaard, Stillwater or Bushveld.

Kretz (1963), although expressing reservations about the P,T dependence of the  $K_D$  value, presented a tentative diagram correlating  $K_D$  and temperature. A linear extrapolation of the plot on this diagram suggests a temperature of crystallization of about  $1,400^\circ C$

for Gosse Pile pyroxenes. The average  $\text{Ca}/(\text{Ca}+\text{Mg})$  ratio for the clinopyroxenes is 45.4% (range from 39.7% to 50.2%) which is considerably greater than would be expected from the data of Davis and Boyd (1966, Fig. 3) if the pyroxenes did crystallize at  $1,400^{\circ}\text{C}$ . Peters (1968) found similar discrepancies when estimating the equilibrium temperature of pyroxenes from the Totalp serpentinite. He explained the discrepancy by showing that the high  $\text{Al}_2\text{O}_3$  contents of the pyroxenes tend to shift the  $\text{Ca}/(\text{Ca}+\text{Mg})$  ratios to higher values because  $\text{Al}_2\text{O}_3$  tends to increase the miscibility gap between enstatite and diopside. Similarly, the data of Davis and Boyd (1966) do not take into account the influence of other elements (e.g. Fe, Cr), and the influence of trivalent cations on the pyroxene field is not yet quantitatively known.

Brown (1967) considers that the distribution of Mg and  $\text{Fe}^{2+}$  between igneous pyroxenes in equilibrium is complicated by too many unknown factors to allow for precise evaluation at present. Similarly, both Kretz (1963) and O'Hara and Mercy (1963) have expressed doubts as to the dependence of  $K_D$ , for pyroxenes, solely on variations in P,T conditions. Binns (1962) found that the  $K_D$  values of pyroxene pairs in the high grade metamorphic terrain around Broken Hill did not follow the pattern predicted by Kretz (1961a, 1963), but that  $K_D$  was also composition dependent.

It has been long established that the distribution coefficient is dependent mainly upon temperature (Albee, 1965), less so on pressure and, in some cases, upon concentrations of other elements.

The strong dependency of  $K_D$  upon temperature is based on the assumption that the co-existing minerals form ideal solid solutions. Since it has been established that the orthopyroxene series is not an ideal mixed-crystal series (e.g. Ramberg and de Vore, 1951; Burns, 1968) the  $K_D$  values cannot be used directly as indicators of temperatures of crystallization (compare with Saxena, 1968). Moreover, the high  $R_2O_3$  content of Gosse Pile pyroxenes is likely to affect the Mg - Fe<sup>2+</sup> distribution (Brown, 1961). Davidson (1968) has emphasised the above points and has also shown that  $K_D$  values are dependent upon the changing absolute activities of Fe<sup>2+</sup> and Mg (presumably also of Ca and minor elements) in the equilibrium exchange. Thus, as shown by Binns (1962) the  $K_D$  values will vary with variations in the Fe<sup>2+</sup>/Mg ratios of the pyroxenes.

In spite of the above reservations on the applicability of  $K_D$  values to estimate temperatures of crystallization, it is felt that the generally higher  $K_D$  values for the pyroxene pairs from Gosse Pile are significant. They are comparable with  $K_D$  values from "alpine-type" ultramafic masses (Peters, 1968), and from nodules in basalt (Ross, Foster and Meyers, 1954, with  $K_D$  values recalculated by Oosterom, 1963), both thought to originate in the upper mantle. This is taken to indicate that the Gosse Pile pyroxenes probably crystallized at corresponding depths. Kretz (1963) considers such high  $K_D$  values to represent disequilibrium conditions as no reasonable temperature difference could account for values so much above those found for gabbros and basalts. The similarity in  $K_D$  values (0.83 for Gosse Pile

and nodules in basalt, and 0.85 for "alpine-type" ultramafic masses) would suggest that equilibrium has in fact been reached and that other factors, such as those outlined by Davidson (1968, pp. 256-257), and which are probably similar in all three environments, have been instrumental in determining the  $K_D$  values measured. Challis (1965), in attempting to explain the high  $K_D$  values of pyroxene pairs from New Zealand ultramafic intrusions (0.85 for harzburgite; 0.95 for dunite) which, on the basis of other evidence, are believed to show a close approach to equilibrium, made the suggestion that early separation of chromite, causing a depletion of  $Fe^{2+}$  in the magma, might produce abnormally high  $K_D$  values. Such an argument cannot be applied to the Gosse Pile pyroxenes as the intrusion is notably deficient in oxide minerals: they appear in only small amounts in the olivine-rich rocks, (maximum measured was 2.9%, see Appendix 1).

#### Minor elements

X-ray spectrographic determinations of copper were attempted for some pyroxenes and, in all cases, revealed quantities below the detection limit of the instrument at that time (i.e. < 20 ppm Cu).

Measurements were also made on the Sr content of some pyroxenes. This element was not found in the orthopyroxenes (detection limit 2 ppm Sr), but it is present in the clinopyroxenes in amounts ranging between 4.2 ppm and 43.7 ppm. (Table 3.12).

Kleeman (1969) measured the uranium contents of some Gosse Pile pyroxenes and found a generally low content. In clinopyroxenes it ranged from 0.005 ppm to 0.071 ppm and in the orthopyroxenes from 0.0002 ppm to 0.0054 ppm, (Kleeman, 1969, Table 41). The maximum values were recorded in pyroxenes from orthopyroxenite A313/60 (analysis 2, Table 3.5), and a 50-fold variation within one specimen was recorded by Kleeman. As has been noted elsewhere this rock shows somewhat unexpected features. The plagioclase is far more sodic than others from rocks of the layered sequence (Table 3.8 and Table 3.9), while the clinopyroxene has an unusually high Sr content (Table 3.12). Kleeman (1969) considers massive contamination of the rock may be a cause of the high U content. Alternatively, although this rock has been identified in the field as a part of the layered sequence it may be a part of the later noritic intrusive which has suffered local contamination.

The distribution of Ni, Cr, Mn and Ti between co-existing pyroxenes is similar to that observed for other igneous pyroxene pairs (Carstens, 1958; Atkins, 1969). In general, the clinopyroxene contains larger quantities of Cr and Ti, while the orthopyroxene is richer in Ni and Mn. This data is consistent with observations on the distribution of these elements in metamorphic pyroxene pairs (Howie, 1955; Engel, Engel and Havens, 1964; Leelanandam, 1967). The four elements under consideration are all transition metals and, with the exception of Mn and possibly Ti, they have a crystal field stabilization energy in an octahedral environment:

|                  |                   |   |                                       |
|------------------|-------------------|---|---------------------------------------|
| Ni <sup>2+</sup> | : 29.2 kcals/mole | } | Data from Dunitz and<br>Orgel (1957). |
| Cr <sup>3+</sup> | : 53.7 kcals/mole |   |                                       |
| Mn <sup>2+</sup> | : 0.0 kcals/mole  |   |                                       |
| Ti <sup>4+</sup> | : 0.0 kcals/mole  |   |                                       |
| Ti <sup>3+</sup> | : 20.9 kcals/mole |   |                                       |

The distribution of these elements in both igneous and metamorphic pyroxenes suggests that  $\Delta_o(\text{cpx}) > \Delta_o(\text{opx})$ , where  $\Delta_o$  is the energy between the t and e levels in octahedral co-ordination (Burns and Fyfe, 1967). This would also explain why the distribution of Cr is not proportional to the number of octahedral sites: orthopyroxene has twice as many such sites as clinopyroxene.

If it is assumed that members of the transition metals group are approximately favoured as is Fe<sup>2+</sup> in octahedral sites in the pyroxenes, and that crystal field stabilization energies cause only minor differences within the group, then the ratio of transition metal ion to Fe<sup>2+</sup> gives a corrected measure of the distribution of such transition metal ions for pyroxene pairs with very different Mg/Fe<sup>2+</sup> ratios. However, Curtis (1964) found that trends established using raw trace element concentrations give the same results for distribution of such elements with magmatic variation as do the trends established using corrected data (compare Fig. 5 and Fig. 6, Curtis, 1964). For Gosse Pile pyroxenes only the uncorrected concentrations of the trace elements are compared, (Fig. 3.79, Fig. 3.80, Fig. 3.81 and Fig. 3.82). Ti and Cr show strong and regular fractionation between the two

Fig. 3.79

Plot of the titanium content of orthopyroxene against that of the co-existing clinopyroxene.

- both pyroxenes cumulus phases.
- ⊗ pyroxenes from annealed rocks.
- cumulus orthopyroxene and intercumulus clinopyroxene

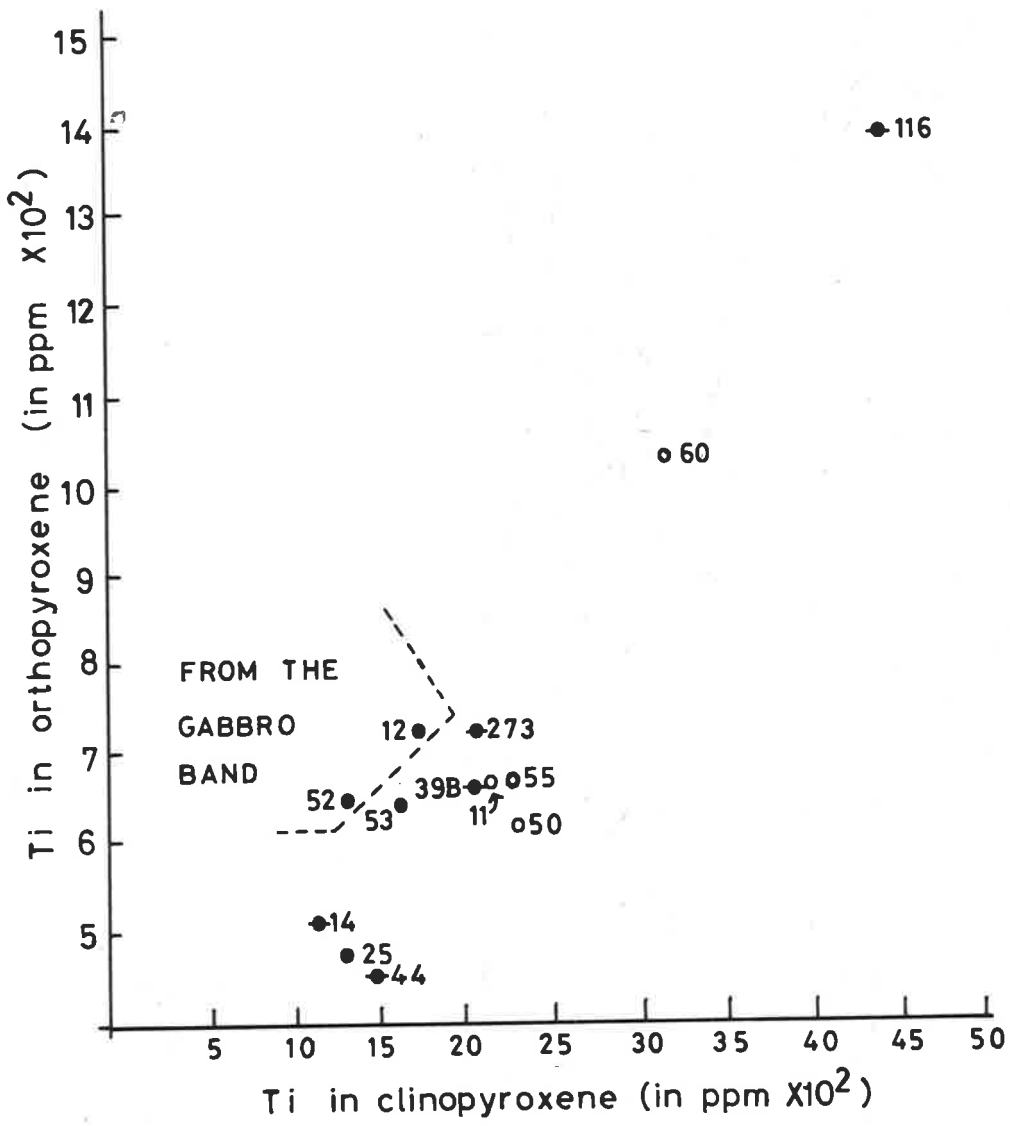




Fig. 3.80

Plot of the chromium content of orthopyroxene against  
that of the co-existing clinopyroxene.

Symbols as for Fig. 3.79.

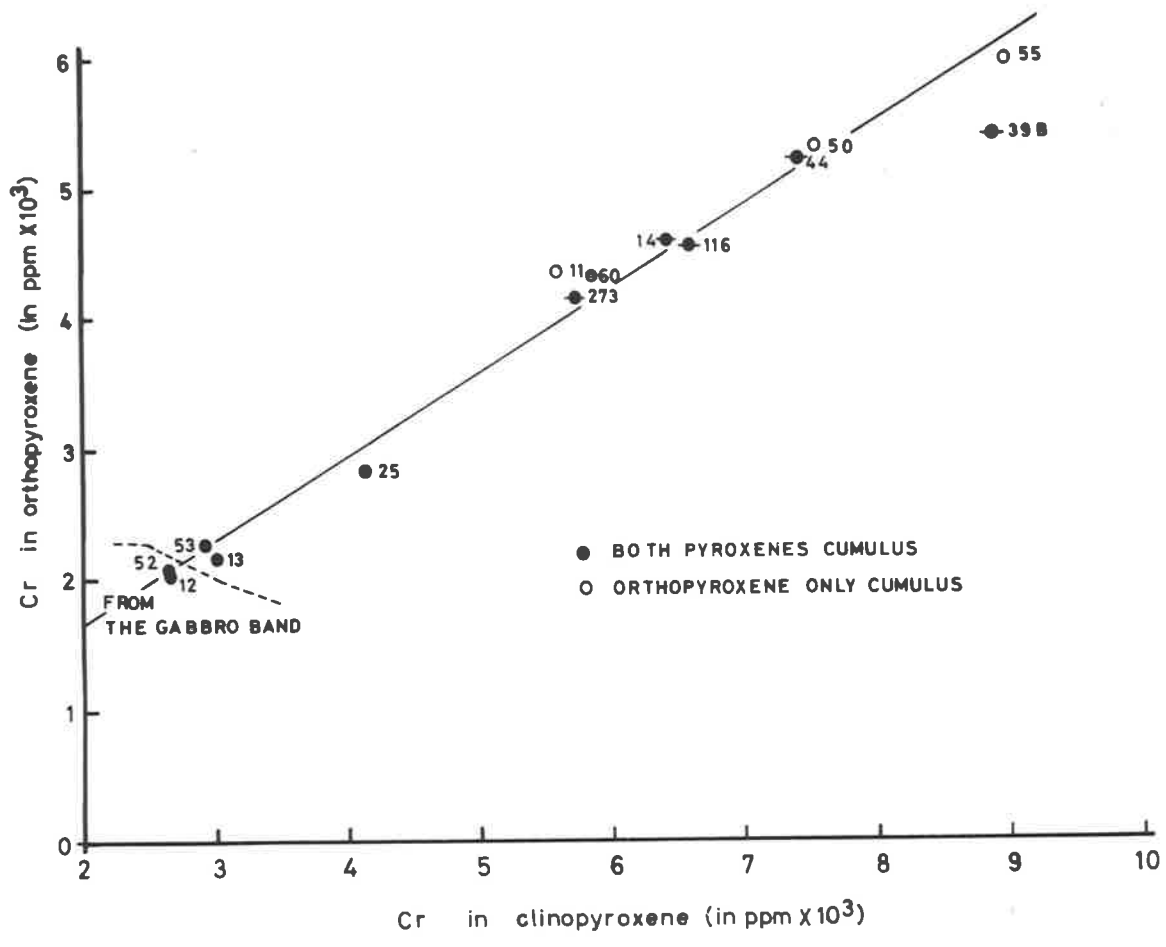


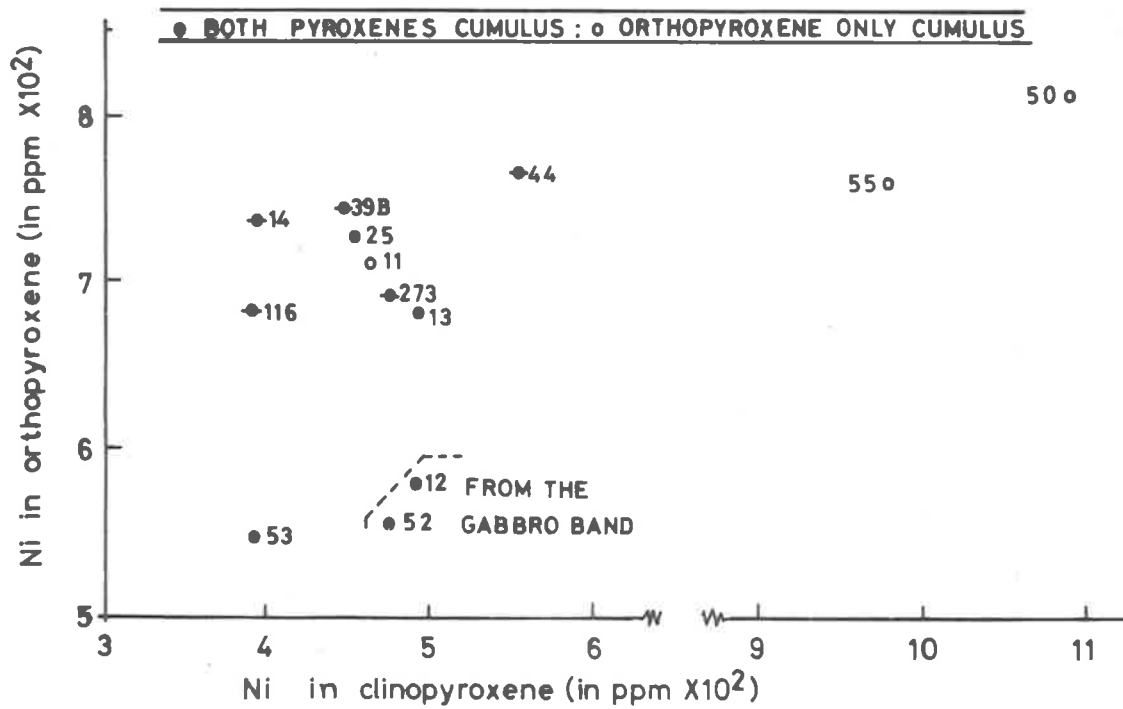
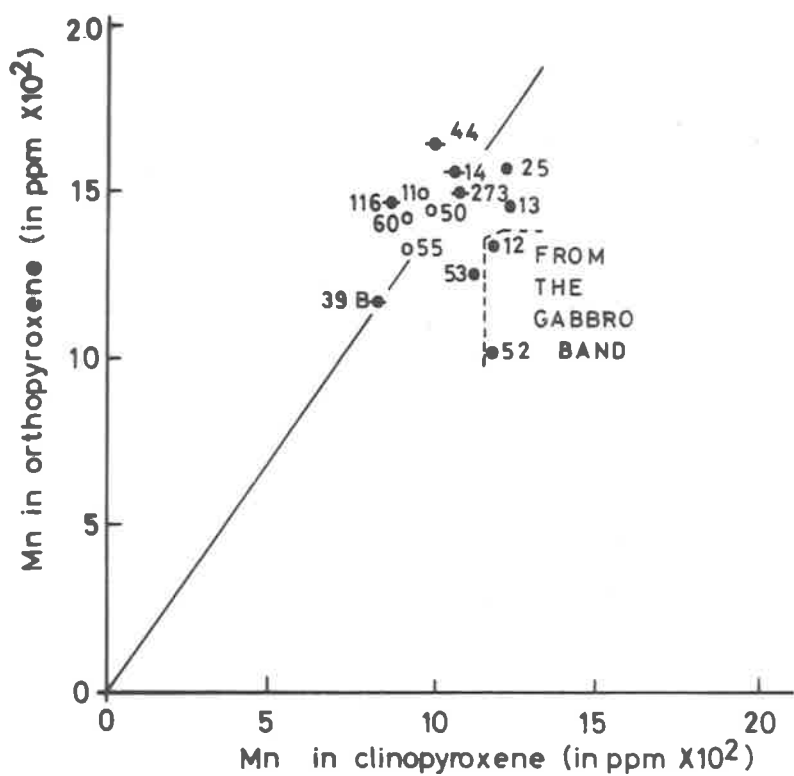
Fig. 3.81

Plot of the manganese content of orthopyroxene against that of the co-existing clinopyroxene.

Fig. 3.82

Plot of the nickel content of orthopyroxene against that of the co-existing clinopyroxene.

Symbols for both figures as in Fig. 3.79.



pyroxenes, while this is less obvious in the case of Mn and Ni.

Different rock types can be distinguished in some cases by their position on the diagrams. This is to be expected as an equilibrium established between two cumulus pyroxenes is likely to be different from that established between cumulus orthopyroxene and intercumulus clinopyroxene, which has crystallized from trapped magma. This is particularly noticeable in the case of Ni (Fig. 3.82). Equilibrium was probably established between the cumulus orthopyroxene and the magma, not between two pyroxenes. The Ni content of the liquid would be expected to be higher than that of the orthopyroxene as the  $\text{Ni}^{2+}$  ions can form distorted octahedra with  $(\text{SiO}_4)^{4-}$  ions in the magma, while in the orthopyroxene it must occupy pre-determined octahedral sites. In some rocks (e.g. A313/11), although the clinopyroxene is interstitial, there is good evidence for considerable reaction between orthopyroxene and trapped liquid to produce clinopyroxene (Fig. 3.15). In such instances there should be a change in the distribution of trace elements between cumulus orthopyroxene and intercumulus clinopyroxene. In Fig. 3.82 pyroxenes from A313/11 plot well within the group where both pyroxenes are cumulus phases. This effect is not as noticeable in the case of Mn, Cr and Ti.

### 3.6.3 Other Minerals

#### Olivine

This is not an abundant mineral in Gosse Pile, especially when one considers the olivine-rich basal zones of other major layered intrusions (Wager and Brown, 1968). Its general abundance can be seen from the modal analyses (Appendix 1). Where olivine occurs there is a noticeable increase in the proportion of oxide minerals within the rocks, and also an increase in the quantity of exsolved spinel in the pyroxenes. The olivines and pyroxenes thus attain very similar densities and magnetic susceptibilities so that large-scale separation by normal methods is almost impossible. For this reason, bulk chemical analyses of olivines were not carried out and the mineral has been studied mainly by optical and X-ray diffraction techniques, although some electron microprobe analyses (Table 3.14) were made possible through the courtesy of Dr. J.F. Lovering (Canberra).

The olivine almost invariably contains inclusions of dendritic plates, parallel to (100), which are thought to be exsolved magnetite (Le Maitre, 1962).

Both X-ray diffraction measurements and electron microprobe analyses indicate that the olivines from Gosse Pile are very magnesian (Table 3.14 and Table 3.15). Brown (1967) has listed the compositions of olivines from mafic and ultramafic rock types. Those from fractionated mafic layered intrusions have compositions, in general,

Table 3.14 Electron microprobe analyses of olivines.

| Analysis                       | 1     | 2a    | 2b    | 2c   | 3a    | 3b   | 4     | T1   | T2   |
|--------------------------------|-------|-------|-------|------|-------|------|-------|------|------|
| Sample No. A313/-              | 32    | 250   | 250   | 250  | 253   | 253  | 199   | -    | -    |
| SiO <sub>2</sub>               | 42.2  | 39.5  | 41.1  | 41.7 | 42.4  | 41.9 | 41.6  | 42.4 | 41.1 |
| ΣFe as FeO                     | 5.9   | 14.9  | 14.8  | 14.4 | 5.2   | 4.9  | 6.5   | 7.1  | 9.0  |
| MgO                            | 51.8  | 45.5  | 44.8  | 43.2 | 52.8  | 52.1 | 52.4  | 50.0 | 48.9 |
| NiO                            | 0.3   | 0.2   | 0.2   | n.a. | 0.3   | 0.3  | 0.2   | 0.28 | 0.39 |
| MnO                            | 0.0   | 0.0   | 0.0   | n.a. | 0.0   | 0.0  | 0.0   | 0.02 | 0.02 |
| Cr <sub>2</sub> O <sub>3</sub> | n.d.  | n.a.  | n.a.  | n.a. | n.a.  | n.a. | n.d.  | n.a. | n.a. |
| TOTAL                          | 100.2 | 100.1 | 100.9 | 99.3 | 100.7 | 99.2 | 100.7 | 99.8 | 99.4 |

Structural formulae on the basis of 4 oxygens.

|                  |       |       |       |          |       |       |       |       |       |
|------------------|-------|-------|-------|----------|-------|-------|-------|-------|-------|
| Si               | 1.012 | 0.991 | 1.019 | 1.044    | 1.009 | 1.011 | 0.997 | 1.025 | 1.009 |
| Fe <sup>2+</sup> | 0.118 | 0.313 | 0.306 | 0.301    | 0.103 | 0.099 | 0.130 | 0.144 | 0.185 |
| Mg               | 1.852 | 1.701 | 1.655 | 1.611    | 1.873 | 1.874 | 1.872 | 1.801 | 1.789 |
| Ni               | 0.006 | 0.004 | 0.004 | (0.004)* | 0.006 | 0.006 | 0.004 | 0.005 | 0.008 |
| Mn               | -     | -     | -     | -        | -     | -     | -     | 0.000 | 0.000 |
| Σ Y group        | 1.976 | 2.018 | 1.962 | 1.917    | 1.976 | 1.978 | 2.006 | 1.950 | 1.982 |

Atomic ratios

|                       |      |      |      |      |      |      |      |      |      |
|-----------------------|------|------|------|------|------|------|------|------|------|
| Mg (Fo)               | 94.0 | 84.5 | 84.4 | 84.2 | 94.8 | 95.0 | 93.5 | 92.6 | 90.6 |
| Fe <sup>2+</sup> (Fa) | 6.0  | 15.5 | 15.6 | 15.8 | 5.2  | 5.0  | 6.5  | 7.4  | 9.4  |

continued

Table 3.14 (continued)

- 1. cumulus olivine from olivine-orthopyroxenite, N.E. Hills area.
- 2a. } analyses of 3 different cumulus olivine grains within the same
- 2b. } thin section, cut from olivine-orthopyroxenite; N.E. Hills
- 2c. } area. \*Ni value derived from 2a and 2b.
- 3a. } analyses of 2 different cumulus olivine grains within the
- 3b. } same thin section, cut from olivine-orthopyroxenite; N.E.
- } Hills area.
- 4. cumulus (?) olivine in central type picrite.
- T1. olivine from "Scarface" (part of Kalka).
- T2. olivine from the "Greenwood Mesa", central Mt. Davies.

Analyses 1-4 by A. Moore, done at Canberra through courtesy of Dr. J.F. Lovering.

Analyses T1 and T2 by AMDEL and are quoted as a personal communication from Mr. A.R. Turner who presented them in an unpublished paper, "Nickel deposits in the north west of South Australia", read at an ordinary meeting of the South Australian branch of the Geological Society of Australia (1967).



Table 3.15

Olivine compositions determined from x-ray diffraction data by the method of Yoder and Sahama (1957), using ZnO as an internal standard.

| Sample    | Fo   | $d_{130}$ | rock type                           |
|-----------|------|-----------|-------------------------------------|
| A313/48   | 90.0 | 2.7725    | olivine-orthopyroxenite (Main Body) |
| A313/310A | 92.4 | 2.7703    | central type picrite                |
| A313/312E | 82.0 | 2.7780    | marginal type picrite               |
| A313/343B | 88.5 | 2.7735    | olivine-orthopyroxenite (Main Body) |
| A313/387  | 92.5 | 2.7706    | olivine-orthopyroxenite (Main Body) |
| A251/N8   | 88.0 | 2.7740    | olivine-orthopyroxenite (Main Body) |

of less than  $Fo_{88}$ . Those from rocks for which a primary ultramafic or fractionated basaltic origin is generally proposed have more magnesian compositions ( $Fo_{93-78}$ ), while olivines from rocks for which a primary ultramafic origin is generally proposed (e.g. nodules in basalts, peridotites and some "alpine-type" ultramafic complexes) are the most magnesian ( $Fo_{95-85}$ ). Olivines from Gosse Pile occur in olivine-orthopyroxenite (or picrite) yet appear to be more magnesian than those which generally crystallize in layered stratiform bodies, even those in dunite horizons. Brown (1967) pointed out that there is insufficient data at present to establish a difference in composition between the olivines separating from different basalt magma types, and those from nodules and massive peridotites. However, Il'vitskiy and Kolbantsev (1968) have attempted to do just this statistically and on a broad scale for magna-derived olivines. Using their data the olivines from the layered sequence of Gosse Pile can be seen to be more similar in composition to those from "alpine-type" ultramafic intrusions (average of 55 analyses,  $Fo_{91.5}$ ; range  $Fo_{90.5} - 92.6$ ) than to those from layered rocks (either: average of  $Fo_{89.1}$ , range  $Fo_{84.5} - 93.7$  for dunites in such bodies; or an average of  $Fo_{57.8}$ , range  $Fo_{47.2} - 68.4$  for olivines from basic rocks in layered plutons).

Where compositions of co-existing olivine and orthopyroxene are available the olivine is considerably more magnesian than the pyroxene:

A313/48 :  $Fo_{90}$  and  $En_{82.2}$

A313/387 :  $Fo_{92.5}$  and  $En_{81.5}$  .

Ramberg and de Vore (1951) showed that, in natural systems, the olivine co-exists with a more magnesian orthopyroxene, except for very Mg-rich compositions. In their diagram (Fig. 2) the change occurs at about 70 mol.% Mg-silicate. Bartholomé (1960)\* confirmed this general finding from the theoretical point of view by calculation, although only for compositions more magnesian than  $Fo_{90} - En_{90}$  is the orthopyroxene richer in magnesium than the co-existing olivine. From the discussion it would appear that, with increase in temperature of crystallization, the olivine is the more magnesium-rich mineral of the pair at increasingly low Fo-contents. The data from Gosse Pile would then suggest crystallization at very high temperatures.

Where plagioclase and olivine are in contact in rocks of the layered sequence (only in the N.E. Hills area) a narrow corona is produced between them. As far as can be determined, this corona consists of a single rim of orthopyroxene, very occasionally associated with a pale green, very fine, mineral thought to be spinel. In the picrite olivine and plagioclase commonly have a sharp contact between them with no evidence of reaction (Fig. 3.22) but in other places, even within the same thin section, the contact between these two minerals is marked by a narrow corona of orthopyroxene (Fig. 3.23). Multiple or double coronas have not been observed, although green spinel appears to be intergrown with the

---

\* original paper by Bartholomé was not consulted: the information was obtained from Oosterom (1963, p. 265).

orthopyroxene in some cases. In one rock (A313/329B) from the N.E. Hills area, which occurs as a transgressive feldspathic vein in olivine-orthopyroxenite and which was considered to be related to the later noritic intrusive in the field, a complex orthopyroxene-spinel intergrowth is found (Fig. 3.83). It is identical in appearance to that described by Hermes (1968) from the Mecklenburg complex, N. Carolina. He considers it may be either an exsolution or reaction phenomenon. No olivine can be recognised in A313/329B but there are patches, within the slide, of unidentified brownish material similar to that found in the weathered olivine-orthopyroxenites and which almost certainly represent weathered-out olivine. For this reason the spinel-orthopyroxene is considered to represent a reaction relationship between plagioclase and olivine:



The absence of a calcium-alkali phase, such as hornblende or clinopyroxene, implies a change in the plagioclase composition during reaction.

Goode and Krieg (1967) considered that coronas (opx + cpx + sp) between plagioclase and olivine in Ewarara intrusion were produced by an autometamorphic reaction, and that they indicated crystallization and reaction of these minerals at high pressures. Their conclusions were based on the data gained from the experimental work of Green and Ringwood (1967). Nesbitt (1966), on the other hand, favoured intrusion of the Giles Complex at relatively shallow depths (9 km)

Fig. 3.83

Myrmekitic intergrowth of spinel and orthopyroxene.

A313/329B. P.P.L.

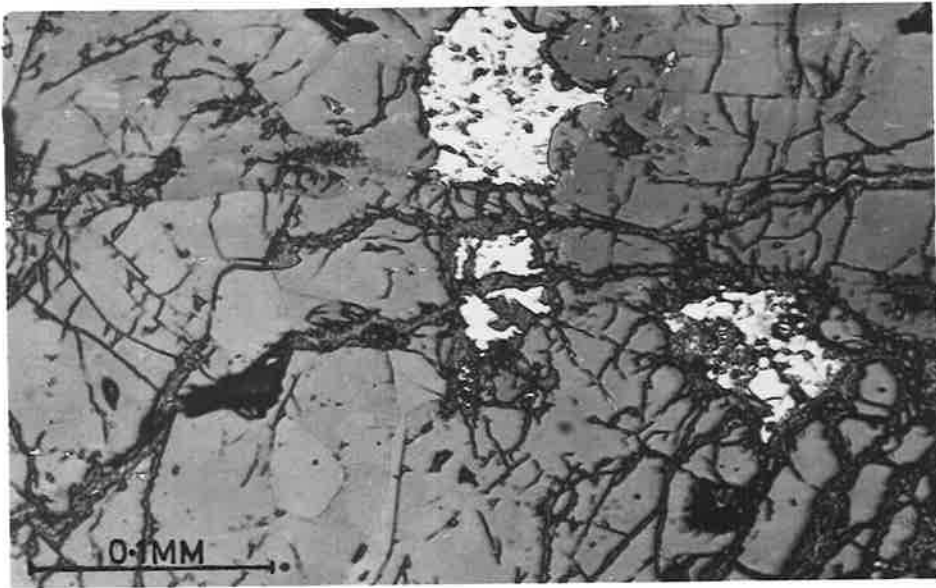
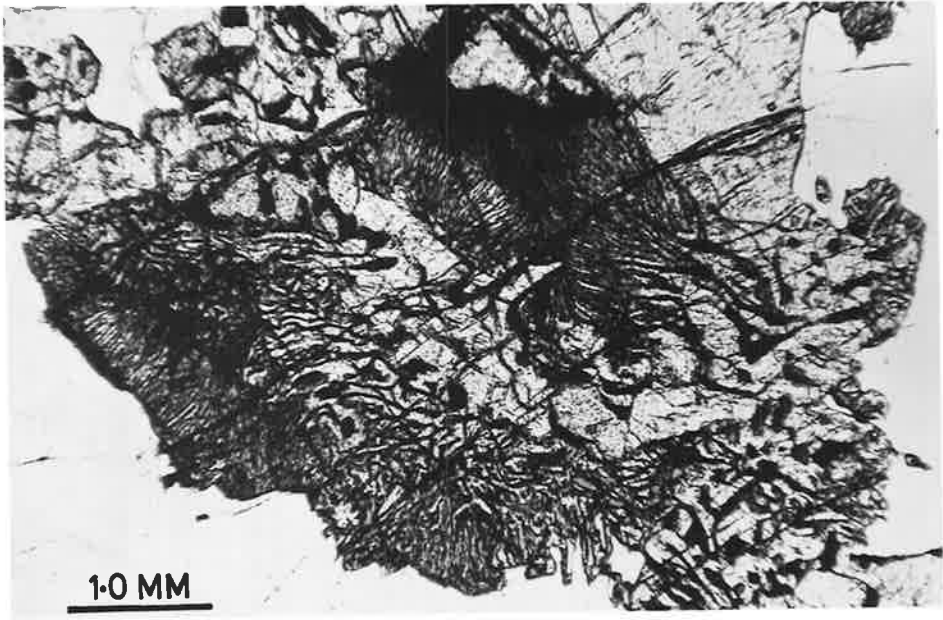
Photograph: A. Moore.

Fig. 3.84

Pyrite in olivine-orthopyroxenite. A313/32.

P.P.L. (reflected).

Photograph: J.D. Kleeman.



because he considered that the coronas could be produced only at pressures of less than 2.3 kbars, basing this conclusion on the experimental work of Boyd, England and Davis (1964). Similar arguments were used by Weedon (1965) for coronas in gabbro, east Aberdeenshire. However, as pointed out by O'Hara and Stewart (1966) this argument assumes that the coronas were produced as a result of solid-liquid reaction and that the reaction relationship, which is suppressed by increase in pressure in the system  $MgO - SiO_2$ , accurately reflects the reaction relationship in a magma. Both assumptions have been criticized by O'Hara and Stewart (1966) and by Moore (1968). In the Gosse Pile picrites and olivine-orthopyroxenites the coronas occur between plagioclase and olivine only (and even here they are sometimes absent) and never between olivine and other late phases (e.g. cpx). Thus, they are considered more likely to represent solid-solid reaction during cooling. However, because similar corona structures are commonly found between plagioclase and olivine in numerous rock types which have crystallized under various conditions, especially of pressure and temperature, (e.g. Shand, 1945; Friedman, 1955; Murthy, 1958; Oosterom, 1963; Mason, 1967; Frodesen, 1968), it is felt that their existence, or absence, can give little information as to the conditions of pressure and temperature under which the rock crystallized.

#### Opaque minerals

Gosse Pile is unusually deficient in opaque minerals, especially considering the economic concentrations of magnetite, chromite and

sulphides in the basal, mafic-ultramafic zones of layered intrusions elsewhere in the world (Wager and Brown, 1968). It is only in the olivine-bearing rocks (both olivine-orthopyroxenites and picrites) that they occur in significant proportions and, even there, they are relatively minor in amount (see Appendix 1).

Spinel, which is usually green or occasionally brown, occurs as an exsolved phase within the pyroxenes and along the grain boundaries (Fig. 3.78). The composition is close to picotite (Table 3.11).

Polished sections of olivine-orthopyroxenites show the presence of small crystals of magnetite, usually as orientated stringers in olivine, which have a slight brownish colour in reflected light, possibly indicating that they are titaniferous. Chromite, as euhedral grains, has also been recognised. Chromite, separated from one olivine-orthopyroxenite (A313/387) was found to have a cell dimension  $a = 8.254\text{\AA}$ , indicating considerable substitution for  $\text{Cr}^{3+}$  by smaller cations (probably  $\text{Al}^{3+}$  and  $\text{Mg}^{2+}$ ). Pyrite occurs in small quantities along grain boundaries. Both magnetite and pyrite occur as small crystals, (between  $1-15\mu$  diameter). Other sulphide phases recognised (in A313/32) included pyrrhotite\*, intergrown with marcasite\* ( $1-5\mu$ ) and very rare traces of chalcopyrite ( $2-5\mu$ ). Because of the interest in the nickeliferous laterites in the area an electron microprobe<sup>+</sup> scan at the  $\text{NiK}_{\alpha}$  wavelength was made across several

---

\* First identified for the author by Dr. A.W.G. Whittle.

<sup>+</sup> Done at A.N.U., Canberra, through the courtesy of Dr. J.F. Lovering.



grains optically identified as pyrite and pyrrhotite. No Ni was detected.

The oxides and sulphides appear to be either concentrations of material exsolved from the silicate phases (e.g. spinel) or interstitial material. The sulphides commonly have convex boundaries towards the silicates (Fig. 3.84). Pyrite also occurs as veins, some of which appear to infill minor cracks within silicate phases.

Polished sections of the picrite show that the opaque minerals are identical, both in type and size, to those found in the olivine-orthopyroxenites of the layered sequence, although there is a slight tendency for sulphide phases to be slightly more abundant.

#### Serpentine minerals

No detailed work has been done on the serpentinite of Gosse Pile. A sample of the rock was crushed and the oxide minerals removed. The majority of these were magnetite but some chromite was identified. A smear mount was then used to produce an X-ray diffraction trace. Using the methods outlined by Whittaker and Zussman (1956), lizardite was identified as the predominant serpentine group mineral present, and a tentative recognition of some chrysotile was made. Magnesite and chalcedony veins occur throughout the rock.

### 3.7 CONCLUSIONS

On the basis of what has been established in the preceding sections, the essential features of Gosse Pile can be summarised.

(i) The greater part of Gosse Pile consists of an ultramafic sequence of repeated cyclic units which pass upward (south) into a mafic sequence of alternating pyroxenites and norites. The present orientation of these units is close to vertical.

(ii) Both typical igneous and typical metamorphic textures and fabrics are found within the rocks of the layered sequence.

(iii) There is a dominance of orthopyroxene over olivine as an early cumulus phase.

(iv) Certain features of the mineralogy (e.g. the presence of antiperthites; exsolution phenomena in the pyroxenes; rarity of oxide minerals; high  $K_D$  values for co-existing pyroxenes) suggest conditions of crystallization significantly different from those prevailing during the crystallization of ultramafic sequences described elsewhere (e.g. Rhum, lower Bushveld complex, lower Stillwater complex).

(v) Later, transgressive noritic and picritic rocks occur within the layered sequence.

## Proposed origin of Gosse Pile

The above features must be considered when discussing a possible origin of Gosse Pile. It is suggested, on the basis of the fabric and textures as well as mineralogy of the rocks from the north side of Gosse Pile, that the layered sequence represents the ultramafic part of a layered intrusion, and has been formed by fractional crystallization and gravity settling. The similarity between the rocks of this body and those of other layered intrusions (e.g. Rhum; Muskox) is striking. The cyclic units found in Gosse Pile are probably caused by influxes of fresh magma (either from the initial source or through convective overturn within the chamber) which mix with the residual, partly differentiated magma already present and the process of fractional crystallization starts once more. From the evidence of the clinopyroxenes and the bulk rock analyses (hypersthene-normative), as well as by comparison with rocks elsewhere in the Giles complex (Nesbitt, et. al., 1969) the source magma is thought to have been tholeiitic in composition.

Many of the unusual mineralogical features of Gosse Pile are thought to result from crystallization under high pressure (the notable lack of hydrous minerals, even in the Gneissic Zone, suggests the  $P_s \gg P_{H_2O}$  during crystallization). Crystallization under high pressure is thought to explain not only features such as spinel and rutile exsolution in the orthopyroxenes, the unusually high  $K_D$  values of co-existing pyroxenes and their high  $R_2O_3$  contents, but also the

dominance of orthopyroxene over olivine as an early cumulus phase. Boyd, England and Davis (1964) noted the increase in size of the primary orthopyroxene field at high pressures. Green and Ringwood (1967a) have shown experimentally that, at about 11 kb, orthopyroxene replaces olivine as the most important mineral in the early stages of fractionation of basaltic magmas (olivine tholeiite; olivine basalt; alkali olivine basalt and picrite). Thus, the dominance of orthopyroxene may be correlated with high pressures during the crystallization.

There is a significant absence of chromite horizons in the ultramafic sequence when compared with similar sequences elsewhere in the world. However, the pyroxenes are unusually rich in  $\text{Cr}_2\text{O}_3$  and it seems likely that this is a pressure-induced effect (note the common occurrence of chrome-rich pyroxenes in nodules). This is of economic significance because, elsewhere (e.g. Bushveld complex, Great Dyke) ultramafic intrusions are important sources of chrome. Since early-formed pyroxenes have taken up the greater part of the Cr present in the Giles complex magma there is little likelihood that economic chromite deposits will be found associated with these layered intrusions. Chromite may, however, form relatively rich deposits in the later picrites, but this is unlikely as the picrites are unlayered.

It is difficult to fix the absolute P,T conditions for the crystallization of the Gosse Pile sequence because of the uncertainties

involved when comparing results derived from synthetic, or natural, systems in the laboratory with actual rocks. However, on the basis of what has been discussed in Section 3.6 it is apparent that the rocks crystallized under lower crustal conditions, probably similar to those prevailing at the time of crystallization of many ultramafic nodules found in basalts. Although the rocks of Gosse Pile layered sequence are not ultrabasic, a crude estimation of the P,T conditions can be made using the techniques outlined by O'Hara (1967) for clinopyroxenes from ultrabasic sequences. From O'Hara's (1967) P,T projection for ultrabasic mineral facies the Gosse Pile clinopyroxenes plot in the spinel-lherzolite facies (Seiland subfacies) close to 10-14 kb and 1,200° - 1,300°C.

The metamorphic textures and fabrics of the rocks from south Gosse Pile, mainly in the Gneissic Zone, are interpreted as having been produced by deformation soon after complete crystallization of the layered sequence. This deformation, in the form of low angle thrusting, is partly responsible for the removal of the upper layers of the layered sequence, now probably represented, in part at least, by the rocks forming the Kalka intrusion (Fig. 1.2). This thrusting has produced distinctive fabrics and textures in the igneous rocks but is not readily recognized in the surrounding granulites. The reason for this is thought to be that it occurred while the igneous rocks were still hot (deformation under granulite facies conditions, the temperature being residual from the igneous body) so that syntectonic annealing could take place. The granulites, being

---

relatively cold, were more likely to deform by brittle fracture, so that the "flaser mylonites" may be correlated with the Gneissic Zone deformation. To further complicate the issue there have been at least two periods of brittle faulting post-dating the low angle thrusting. One such fault (the near vertical Numbunja Creek Fault) now separates Gosse Pile from Mt. Davies intrusion and the granulites to the south, and has produced a fault breccia ("trapschotten gneiss") within the norites of the southern Gneissic Zone.

The bridging characteristics of rocks of the Giles complex between "stratiform-type" and "alpine-type" intrusions, as distinguished by Thayer (1960, 1967) have already been noted (Nesbitt and Talbot, 1966; Nesbitt et. al., 1969). The Gneissic Zone deformation serves to illustrate how some "alpine-type" characteristics may be derived from an original "stratiform-type" intrusion and, combined with the characteristics of crystallization under high pressure, illustrates the possible genetic link between the two types of intrusion. However, it is felt that if a label for classification is to be attached to Gosse Pile at all, it is definitely of the "stratiform-type" and the later deformation is irrelevant to its description as such.

The question of the ultimate origin of the tholeiitic magma which gave rise to the Gosse Pile ultramafic sequence cannot be answered on the basis of the limited study carried out here. It is assumed that it was derived from partial melting of mantle material. Work on the Giles complex as a whole (Nesbitt et. al., 1969) has

shown it to consist of a number of isolated intrusions which show a depth stratification: those in the west have been emplaced at a higher structural level than those in the east. A broad correlation also exists between structural height and degree of fractionation (the higher level gabbros are, in general, more highly fractionated). This has led to the conclusion that fractionation of the source magma took place at an early stage so that liquids of varying bulk composition were intruded at different levels, each forming a separate layered intrusion, some of which have been dismembered by later deformation. All the major ultramafic zones of the Giles complex, including Gosse Pile, are found in bodies with high pressure characteristics. This further supports the correlation between depth of emplacement and degree of fractionation (Nesbitt et. al., 1969).

SECTION 4

SUMMARY OF THE GEOLOGICAL HISTORY OF THE  
AREA AROUND GOSSE PILE.



4.1 SUMMARY OF THE GEOLOGICAL HISTORY

The rocks around Gosse Pile are thought to represent an original sedimentary sequence subjected to polymetamorphic cycles. This culminated in granulite facies metamorphism (between 1,300 - 1,600 m.y. ago). After a considerable period (Nesbitt *et. al.*, 1969, estimate it to be at least 200 m.y.) large-scale intrusions of tholeiitic magma occurred over a large area, probably greater than the present exposed area of intrusions which covers some 2,500 km<sup>2</sup> in the Musgrave Block. The intrusion which fractionated to give ultimately the Gosse Pile ultramafic sequence was intruded into the granulite facies rocks at depths estimated to be of the order of 30 km. Fractional crystallization of this magma, with occasional influxes of fresh magma, produced the layered sequence of ultramafic rocks, grading upwards into more felsic units. When crystallization was complete, but prior to complete cooling of the body, low angle thrusting separated the more felsic upper layers and produced the Gneissic Zone. At some later stage amphibole-dolerite dykes were intruded, cutting both the layered intrusion and the granulites.

Rocks of the later noritic intrusive suite were intruded, forming a sill-like body at the western end of Gosse Pile, and interrupting the layering. Mafic pegmatites and, possibly, the olivine-gabbro plug and picrites are related to this period of igneous activity which is thought to have continued over an extended period. On the basis of field evidence available in the Gosse Pile

area it is not known whether these intrusions preceded or post-dated the deformation which folded the ultramafic sequence about an approximately east-west axis into a near-vertical position ( $D_2$ ). A third deformation ( $D_3$ ) which has produced gentle folding elsewhere in the Giles complex is not recorded in the rocks around Gosse Pile. The most recent tectonic event has been brittle faulting, associated with the intrusion of numerous, small, oxide-rich dolerite dykes.

Weathering processes produced the serpentinite and associated silcrete and magnesite from the picrite. Weathering and erosion have produced the present profile of Gosse Pile and of the surrounding granulites.

APPENDIX 1

MODAL ANALYSES OF ROCKS FROM GOSSE PILE.

MODAL ANALYSES OF ROCKS FROM GOSSE PILE

All modal analyses involved counting at least 2,000 points and more often this total exceeded 3,500 points. Where relatively coarse-grained rocks were counted, in which the mineral content varied markedly even within a single thin section (e.g. the picrite) several thin sections, cut from the same specimen, were counted and the average value used as representative of the modal analysis. The letters (a), (b) and (c) after a specimen number refer to replicate analyses on different slides cut from the same specimen. The letters A, B ... Z after a specimen number refer to different samples collected from different localities in the field.

Rocks of the layered sequence, excluding those of the Gneissic Zone.

| Rock Type                | Specimen No. A313/- | ol   | opx  | cpx  | plag | opaques | others |
|--------------------------|---------------------|------|------|------|------|---------|--------|
| olivine-orthopyroxenites | 32                  | 38.5 | 42.6 | 12.4 | 6.8  | 1.6     | 1.1 bi |
|                          | 48                  | 2.4  | 89.8 | 6.8  | 0.3  | 0.7     |        |
|                          | 133                 | 11.8 | 85.1 | 2.6  | tr   | 0.5     |        |
|                          | 195                 | 14.6 | 64.9 | 14.4 | 2.9  | 2.0     | 1.2 bi |
|                          | 249                 | 2.5  | 91.0 | 5.0  | 1.0  | 0.5     |        |
|                          | 250                 | 46.2 | 37.7 | 12.6 | 2.3  | 1.2     | tr bi  |
|                          | 253                 | 25.7 | 52.3 | 13.7 | 3.1  | 1.9     | 3.3 bi |
|                          | 290                 | 32.2 | 45.0 | 12.4 | 5.0  | 2.8     | 2.6 bi |
|                          | 312D                | 13.3 | 42.1 | 39.1 | 3.3  | 1.7     | 0.5 bi |
|                          | 314E                | 34.6 | 50.4 | 9.0  | 2.5  | 2.9     | 0.6 bi |
|                          | 387A                | 1.7  | 89.0 | 7.0  | 0.4  | 1.9     | tr bi  |
|                          | 387B (a)            | 6.7  | 87.1 | 4.0  | 0.3  | 1.8     |        |
|                          | 387B (b)            | 6.9  | 84.0 | 6.8  | 0.3  | 2.0     | tr bi  |
|                          | orthopyroxenites    | 1    |      | 98.0 | 1.5  | 0.5     | tr     |
| 33                       |                     |      | 85.7 | 4.3  | 9.9  | 0.1     |        |
| 59 (a)                   |                     |      | 92.8 | 4.7  | 2.5  | -       |        |
| 59 (b)                   |                     |      | 92.5 | 4.6  | 2.9  | -       |        |
| 60 (a)                   |                     |      | 81.9 | 11.8 | 6.2  | tr      | 0.1 bi |
| 60 (b)                   |                     |      | 80.6 | 12.6 | 6.7  | tr      | 0.1 bi |
| 60 (c)                   |                     |      | 83.8 | 9.4  | 6.2  | 0.4     | 0.2 bi |
| 88                       |                     |      | 83.9 | 11.3 | 4.3  | 0.5     |        |
| 112                      |                     |      | 97.6 | 2.3  | tr   | 0.1     |        |
| 131                      |                     |      | 93.7 | 4.4  | 1.9  | -       |        |
| 134A                     |                     |      | 91.4 | 4.7  | 3.7  | 0.2     |        |
| 135 (a)                  |                     |      | 96.9 | 2.7  | 0.4  | -       |        |
| 135 (b)                  |                     |      | 97.1 | 2.6  | 0.3  | -       |        |
| 135A (a)                 |                     |      | 99.1 | 0.7  | 0.2  | tr      |        |
| 135A (b)                 |                     |      | 98.0 | 1.8  | 0.2  | -       |        |
| 136                      |                     |      | 98.6 | 1.3  | 0.1  | -       |        |
| 194                      |                     |      | 83.0 | 11.7 | 5.2  | 0.1     | tr bi  |
| 312A                     |                     | 80.8 | 14.3 | 4.3  | 0.4  | 0.2     |        |
| websterites              | 13                  |      | 76.0 | 23.9 | 0.1  | -       |        |
|                          | 14                  |      | 55.8 | 44.2 | -    | -       |        |
|                          | 24                  |      | 27.8 | 72.2 | -    | -       |        |
|                          | 25                  |      | 56.0 | 44.0 | tr   | tr      |        |
|                          | 53                  |      | 34.9 | 65.1 | -    | -       |        |
|                          | 86                  |      | 57.0 | 43.0 | -    | -       |        |
|                          | 139                 |      | 22.1 | 77.9 | -    | tr      |        |
|                          | 232                 |      | 35.8 | 63.8 | 0.4  | -       |        |
|                          | 241                 |      | 28.2 | 71.8 | -    | -       |        |
| 312C                     |                     | 52.2 | 36.7 | 9.3  | 1.7  | 0.1 bi  |        |

## Rocks from the Gneissic Zone.

| Rock Type       | Specimen No. A313/- | opx  | cpx  | plag | opaques |
|-----------------|---------------------|------|------|------|---------|
| norite          | 38                  | 34.6 | 23.2 | 42.2 | -       |
| norite          | 39A                 | 40.1 | 31.4 | 28.5 | tr      |
| norite          | 40                  | 27.7 | 14.1 | 58.2 | -       |
| norite          | 41                  | 25.7 | 17.3 | 57.0 | -       |
| websterite      | 64                  | 68.3 | 22.0 | 9.7  | -       |
| orthopyroxenite | 68                  | 91.1 | 7.7  | 1.2  | -       |
| orthopyroxenite | 70                  | 97.8 | 2.2  | tr   | -       |
| websterite      | 91A                 | 75.8 | 23.4 | 0.8  | -       |
| orthopyroxenite | 95                  | 86.5 | 13.5 | -    | -       |
| norite          | 97                  | 57.6 | 11.4 | 31.0 | tr      |
| norite          | 169                 | 29.6 | 8.3  | 62.1 | -       |
| orthopyroxenite | 170                 | 75.6 | 24.3 | 0.1  | -       |
| norite          | 218                 | 32.4 | 0.6  | 67.0 | -       |
| websterite      | 218A                | 62.3 | 27.7 | 10.0 | -       |
| norite          | 270                 | 27.0 | 19.9 | 53.1 | -       |
| norite          | 270A                | 26.7 | 12.1 | 61.2 | -       |
| norite          | 273p                | 23.3 | 17.3 | 59.4 | -       |
| orthopyroxenite | 280                 | 87.4 | 8.1  | 4.5  | -       |

## Rocks from the Gabbro Band.

| Rock Type   | Specimen No. A313/- | opx  | cpx  | plag | opaques |
|-------------|---------------------|------|------|------|---------|
| "gabbro"    | 12                  | 23.5 | 27.4 | 49.1 | -       |
| "gabbro"    | 52                  | 31.5 | 38.1 | 30.4 | -       |
| "gabbro"    | 106                 | 21.3 | 27.3 | 51.4 | -       |
| "gabbro"    | 127                 | 11.6 | 17.8 | 70.6 | -       |
| anorthosite | 143                 | 1.0  | 0.2  | 98.8 | -       |
| "gabbro"    | 233                 | 18.0 | 20.8 | 61.2 | -       |
| "gabbro"    | 374                 | 36.7 | 29.7 | 33.6 | -       |

Rocks considered part of the later noritic intrusive.

| Rock Type       | Specimen No. A313/- | opx  | cpx  | plag | opaques | others       |
|-----------------|---------------------|------|------|------|---------|--------------|
| gabbro          | 109                 | 26.9 | 37.9 | 35.2 | tr      | tr bi        |
| gabbro          | 110                 | 31.4 | 37.3 | 32.3 | -       | -            |
| norite          | 111                 | 45.2 | 14.5 | 40.0 | 0.1     | 0.1bi, 0.1hb |
| gabbro          | 205                 | 34.9 | 38.2 | 26.9 | -       | -            |
| norite          | 206                 | 41.1 | 21.8 | 37.1 | tr      | -            |
| norite          | 210                 | 30.5 | 23.3 | 46.2 | -       | tr bi        |
| norite          | 251A                | 78.6 | 9.1  | 12.2 | 0.1     | tr bi, hb    |
| norite          | 251B                | 71.1 | 8.9  | 20.0 | tr      | tr bi, hb    |
| orthopyroxenite | 251C                | 86.5 | 7.7  | 5.6  | 0.2     | tr bi, hb    |
| norite          | 252                 | 49.4 | 21.5 | 28.8 | 0.3     | -            |
| norite          | 263A                | 28.0 | 19.0 | 51.4 | 0.4     | 1.0bi, 0.2hb |
| norite          | 282C                | 37.3 | 1.6  | 6.1  | -       | -            |
| norite          | 285                 | 18.6 | 10.1 | 71.0 | 0.1     | 0.2bi        |
| orthopyroxenite | 373D                | 84.4 | 8.5  | 7.1  | tr      | tr bi        |

The picrites.

| Type                    | Specimen No. A313/- | ol   | opx  | cpx  | plag | opaques | others       |
|-------------------------|---------------------|------|------|------|------|---------|--------------|
| "central type" picrites | 199                 | 68.1 | 8.9  | 10.5 | 6.0  | 5.4     | 0.9bi+hb     |
|                         | 310A                | 55.5 | 15.1 | 24.9 | 1.7  | 2.5     | 0.3bi+hb     |
|                         | 312F                | 61.6 | 20.5 | 5.9  | 8.0  | 3.4     | 0.6bi+hb     |
|                         | 312G                | 74.4 | 6.4  | 9.5  | 6.2  | 2.6     | 1.2bi+hb     |
| "marginal type" picrite | 312E                | 55.6 | 19.7 | 8.5  | 6.4  | 3.1     | 4.1bi, 2.6hb |

APPENDIX 2

A METHOD FOR DETERMINING MINERAL COMPOSITIONS BY  
MEASUREMENT OF THE MASS ABSORPTION COEFFICIENT.

Reprinted from

American Mineralogist, 54, 1180-1189 (1969).



A METHOD FOR DETERMINING MINERAL  
COMPOSITIONS BY MEASUREMENT OF  
THE MASS ABSORPTION COEFFICIENT

---

BY  
ALAN C. MOORE

*Reprinted from American Mineralogist*  
54: 1180-1189 (1969)

---

A METHOD FOR DETERMINING MINERAL COMPOSITIONS BY MEASUREMENT OF THE MASS ABSORPTION COEFFICIENT

ALAN C. MOORE, *Department of Geology & Mineralogy, The University of Adelaide, Australia.*

ABSTRACT

A technique is described whereby measurement of the mass absorption coefficients of minerals can be used to give an estimation of the mineral composition. Direct measurements of  $\mu_{Sr,K\alpha}$  on chemically analyzed plagioclases demonstrates the applicability of the method. The straight line regression so derived from 41 plagioclase samples gives the following equation:  $An\% = 25.27 \mu_{Sr,K\alpha} - 164.66$ , with a standard deviation of 1.61  $\%$  An.

The method can be extended to other solid solution series, such as olivine, orthopyroxene and zinblendite series, and calculated values of  $\mu_{Sr,K\alpha}$  for different members of these series are presented. By judicious selection of the wavelengths of the absorbed X-ray beam the effects of interfering elements can be reduced to a minimum.

Although the experimental work reported in this paper was done using an X-ray spectrophotograph, measurements of  $\mu$  can be made using a diffractometer.

The advantage of this method over other indirect methods for determining mineral compositions is that the measured values of  $\mu$  are directly related to the chemical compositions of the samples.

INTRODUCTION

When X-rays are passed through matter they are both scattered and absorbed and, in general, absorption is the dominant process. If a beam of parallel, monochromatic X-rays of intensity  $I_0$  is passed through material of thickness  $t$  and density  $\rho$  then the intensity of the emergent radiation,  $I$ , can be related to  $I_0$  by the equation:

$$I = I_0 e^{-\mu \cdot \rho t} \dots \text{(Beer's Law)} \dots$$

where  $\mu$  is the mass absorption coefficient of the absorbing material. Both  $I$  and  $I_0$  are corrected for any counting losses.

Mass absorption coefficients (hereafter termed  $\mu$ ) have a fixed value for a given element for a particular wavelength of X rays. Furthermore, since  $\mu$  is an additive property it is directly related to the bulk chemical composition of the compound, or mixture.

In mineral groups displaying solid solution the progressive compositional change is matched by a change in  $\mu$ . Provided that there is sufficient contrast in  $\mu$  between the dominant cations making up the mineral (*e.g.* Ca and Na in plagioclases) the change in  $\mu$  of the total specimen can readily be detected. In this sense the application is restricted essentially to simple two component systems since the assumption is made that differences in  $\mu$  are directly related to changes in one of the cations. If more than two dominant cations are present (as in garnets) and these

contribute significantly to the total  $\mu$  then the method breaks down. However, in practice certain contributing cations can be ignored, either because they are present in such small amounts that their contribution to the total  $\mu$  is insignificant or because their  $\mu$  is low compared with that of the major cation. By measuring the total  $\mu$  at different wavelengths the influence of minor cations may, in some cases, be emphasised. Thus, by a combination of measurements, at different wavelengths, a better estimation of the mineral composition may be made.

#### METHOD

The method is dependent on the experimental determination of  $\mu$  and much of its usefulness depends on the rapidity with which  $\mu$  can be determined. The most rapid determinations are made by direct measurements of an attenuated and unattenuated X-ray beam passed through a finely-powdered sample of known mass per unit area. This technique has been described by Norrish and Taylor (1962), Sweatman *et al.* (1963), Sweatman *et al.* (1967) and by Norrish and Chappell (1967).

High intensity fluorescent  $\text{SrK}_\alpha$  radiation ( $I_0$ ) is obtained from a  $\text{SrCO}_3$  pressed mount in the sample position of the spectrograph and excited using primary molybdenum radiation. A powdered sample is pressed into a perspex holder of known area ( $1.27 \text{ cm}^2$ ) using a piston-type die. The minimum weight which will be self-supporting in mounts of this type is about 200 mg. If only small amounts of sample are available, or if the radiation to be used is of a relatively long wavelength (*e.g.*,  $\text{CoK}_\alpha$ ,  $1.790 \text{ \AA}$ ) then it is necessary to mix the sample with a known amount of some substance of low absorption, such as boracic acid or filter paper pulp (*e.g.* Whatman's ashless cellulose powder, Standard Grade). The measured  $\mu_{\text{total}}$  must then be corrected for the presence of the diluent:

$$\mu_{\text{sample}} = \frac{\mu_{\text{total}} - (1 - p)\mu_{\text{diluent}}}{p}$$

where  $p$  is the proportion of sample in the mixture. This pressed sample is placed in front of the scintillation counter and the intensity of the attenuated beam ( $I$ ) measured. In all measurements reported in this paper the ratio  $I_0/I$  ranged between 15 and 25, and count rates were corrected for dead time. Pulse height selection is used to eliminate possible higher order harmonics in the attenuated beam.

This method of direct measurement of  $\mu$ , devised by Dr. K. Norrish, shows good reproducibility with respect to variations in the intensity of the incident beam (35,000 c.p.s. to 70,000 c.p.s.) and for different mounts and sample weights (Table 1).

An alternative procedure for determining  $\mu$  is the Compton scatter method which has been fully described by Reynolds (1963, 1967). He has shown that  $\mu$  "is inversely and closely related to the intensity of the Compton scattered portion of a primary X-ray beam," and has presented a method for measuring  $\mu$ , with an error of less than 3 percent, for materials of high mean atomic number. The mass absorption coefficient can then be computed for regions on the long wavelength series of major element absorption edges by the use of a series of simultaneous equations, Reynolds (1967). This method may be used for long wavelength radiation or for heavily absorbing samples if the operator wishes to avoid mixing the sample with a diluent.

#### EQUIPMENT

Measurements in this department have been made using a Phillips All-Vacuum Spectrograph. However, the method may readily be applied in laboratories where a diffractom-

TABLE 1. REPLICATE DETERMINATIONS OF THE MASS ABSORPTION COEFFICIENT USING DIFFERENT SAMPLE WEIGHTS AND DIFFERENT MOUNTS FOR SrK<sub>α</sub> RADIATION. DATA FROM VIRGO (1966)

| Sample              | μ <sub>SrK<sub>α</sub></sub> |      |      |
|---------------------|------------------------------|------|------|
|                     |                              |      |      |
| 221/35 plagioclase  | 7.66                         | 7.64 | 7.67 |
| 152/79 plagioclase  | 7.24                         | 7.25 | —    |
| OL/181 plagioclase  | 7.24                         | 7.28 | —    |
| 30829 plagioclase   | 7.69                         | 7.67 | 7.67 |
| 34611 plagioclase   | 6.96                         | 6.92 | 6.95 |
| S28 plagioclase     | 8.91                         | 8.88 | 8.90 |
| GI standard granite | 8.64                         | 8.67 | 8.65 |
| 30829 K-feldspar    | 9.27                         | 9.24 | —    |
| 34611 K-feldspar    | 9.48                         | 9.46 | —    |

eter is available, as shown by Norrish and Taylor (1962). Drawings of the necessary attachments for measuring  $\mu$  directly are available from Dr. K. Norrish.<sup>1</sup>

### RESULTS

*Plagioclase feldspar series.* The mass absorption coefficients of 41 plagioclase samples, analyzed for CaO, Na<sub>2</sub>O, K<sub>2</sub>O and, in some cases, for SrO and BaO, were measured directly for SrK<sub>α</sub> radiation using the pressed mount method. The data are presented in Figure 1, where  $\mu_{\text{SrK}_\alpha}$  is plotted against

$$\text{An}\% = \text{atomic ratio} \frac{\text{Ca}(+\text{Sr}) \times 100}{\text{Ca}(+\text{Sr}) + \text{Na} + \text{K}}$$

Although Sr is included in this equation its effect on the measured  $\mu$  is considered negligible since it is present in such small amounts. K<sub>2</sub>O, because of the closeness of the mass absorption coefficients of CaO and K<sub>2</sub>O (24.80 and 24.93 respectively), is potentially a more important source of error. However, most plagioclases have K<sub>2</sub>O contents within approximately the same range. The 41 samples measured had K<sub>2</sub>O contents ranging between 0.04 to 1.13 percent with an average of 0.36 percent. The 87 plagioclase analyses quoted in Deer, Howie and Zussman (1963) have an average K<sub>2</sub>O content of 0.42 percent. Most of the scatter on the measured graph (Fig. 1) is probably due to the presence of K<sub>2</sub>O and the standard deviation of the fitted line, giving a measure of the precision of the method, takes into account the presence of K<sub>2</sub>O. However, significant amounts of K<sub>2</sub>O in a plagioclase (*i.e.* > 1.0% K<sub>2</sub>O) would lead to greater errors in the determination. As a general approxi-

<sup>1</sup> Dr. K. Norrish, C.S.I.R.O., Division of Soils, Adelaide, 5063, South Australia.

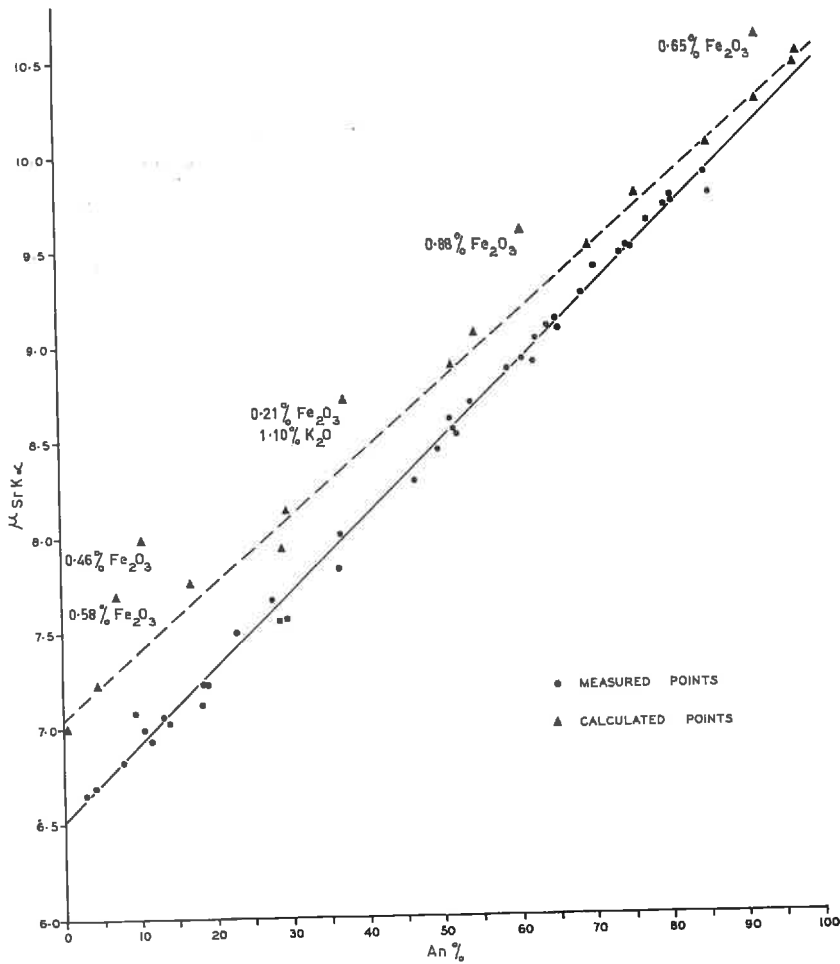


FIG. 1. Plot of

$$\text{An}\% \left( = \frac{\text{Ca}(+\text{Sr}) \times 100}{\text{Ca}(+\text{Sr}) + \text{Na} + \text{K}} \right), \text{ against } \mu_{\text{SrK}\alpha}$$

which is calculated and measured directly. Plagioclase compositions determined from chemical analyses. Measured values of  $\text{SrK}\alpha$  (41 samples) from Kleeman (1965), Virgo (1966), Oliver (unpublished) and Moore (unpublished). Calculated values of  $\mu_{\text{SrK}\alpha}$  from published analyses, Deer, Howie and Zussman (1963).

mation, for every 0.5 percent  $\text{K}_2\text{O}$  present in plagioclase sample the measured anorthite content increases by about 2 percent anorthite.

A least squares fit of the measured data in Figure 1 gave a straight line fit with an equation:

$$\text{An}\% = 25.27\mu_{\text{SrK}\alpha} - 164.66 \quad (s = 1.61\% \text{ An}).$$

No improvement resulted from a second order curve.

On the same graph (Fig. 1) are plotted 16 points for which  $\mu_{\text{SrK}\alpha}$  values were calculated (using tables published by Heinrich, 1966) from analyses published in Deer, Howie and Zussman (1963). The degree of scatter for the calculated points is much greater than for the measured points, and the line not only has a different slope but is displaced upwards, particularly at the albite end. The reason for the difference in slope and position of the two lines is not known, although it may be due to uncertainties in the published mass absorption coefficients of the elements. Similar discrepancies may be found between measured and calculated mass absorption coefficients at longer wavelengths. The high degree of scatter is in large part due to the fact that those analyses displaced significantly upwards from the line are unusually rich in iron, an element which contributes strongly to the total  $\mu_{\text{SrK}\alpha}$ . It appears then that the plagioclases for which  $\mu_{\text{SrK}\alpha}$  was measured are essentially free of iron. If an operator suspects high iron ( $>0.1\%$   $\text{Fe}_2\text{O}_3$ ) in plagioclase it would be better to use a radiation for which the mass absorption contribution by iron is low. For example, at the  $\text{SrK}\alpha$  wavelength the mass absorption contributions by  $\text{CaO}$ ,  $\text{Na}_2\text{O}$ ,  $\text{FeO}$  and  $\text{Fe}_2\text{O}_3$  are 24.80, 5.34, 52.55 and 47.54 respectively while at  $\text{CoK}\alpha$  wavelength they are 176, 39.1, 49.2 and 46.2 respectively. Figure 2 shows 25 plagioclase analyses (from Deer, Howie and Zussman, 1963) plotted against their calculated mass absorption coefficients for  $\text{CoK}\alpha$  radiation (Heinrich, 1966). A least squares regression analysis gave the following result, with only slight improvement for the second order fit:

$$\text{An}\% = 4.07\mu_{\text{CoK}\alpha} - 211.85 \quad (s = 2.34\% \text{ An})$$

The advantages of this indirect method for determining the composition of plagioclases over other indirect methods is that it is independent of the structural state of the plagioclase. The most promising X-ray method has been the determination of  $\Gamma = \text{angular separation } 2\theta (131) + 2\theta (220) - 4\theta (1\bar{3}1)$  of Smith and Gay (1958). However, this parameter is dependent on (1) the  $\text{K}_2\text{O}$  content and (2) on the structural state of the plagioclase (Kleeman and Nesbitt, 1967; Bambauer *et al.*, 1967; Smith and Gay, 1958).  $\Gamma$  cannot readily be used to determine the compositions of plagioclases from different environments. The mass absorption method is applicable to all plagioclases, irrespective of their history. There are two disadvantages. The first, which applies to all mineral groups, is the necessity to have a pure specimen. The second, peculiar to the plagioclases, is that  $\text{SrK}\alpha$  radiation cannot be used for iron-bearing

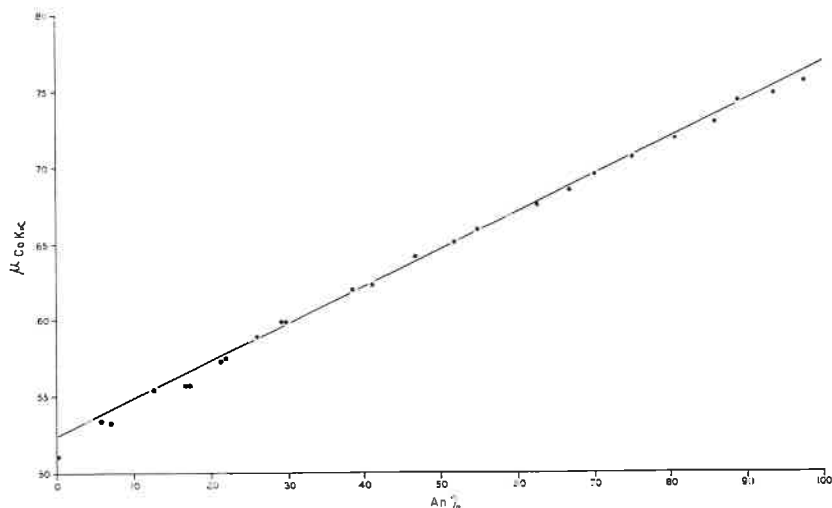


FIG. 2. Plot of plagioclase composition as

$$\text{An}\% \left( = \frac{\text{Ca}(+\text{Sr}) \times 100}{\text{Ca}(+\text{Sr}) + \text{Na} + \text{K}} \right), \text{ against } \mu_{\text{CoK}\alpha},$$

which is calculated from published analyses, Deer, Howie and Zussman (1963).

samples and it is necessary to use  $\text{CoK}\alpha$  radiation. This increases the time needed for making measurements since the samples must either be mixed with some substance of low absorption or else the mass absorption coefficients must be measured by the Compton scatter method.

*Olivine and orthopyroxene series.* The mass absorption method is applicable to both the olivine and orthopyroxene series. Figure 3 shows a plot of olivine compositions against their calculated  $\mu_{\text{SrK}\alpha}$  values (analyses from Deer, Howie and Zussman, 1963). In this case the relationship is non-linear. For the olivine series the method has little application because X-ray diffraction methods (*e.g.* Yoder and Sahama [1957]) have been shown to be very suitable and have the added advantage that the olivines need not be completely separated from associated minerals.

In the case of the orthopyroxenes this method has decided advantages over other indirect methods, such as optics and cell size variation, in that it is independent of changes in cell size and the presence of minor elements (*e.g.* Al and Cr), which have negligible effect on the total  $\mu_{\text{SrK}\alpha}$ . Figure 4 presents the data for orthopyroxenes (analyses from Deer, Howie and Zussman, 1963 and  $\mu_{\text{SrK}\alpha}$  calculated from Heinrich, 1966).

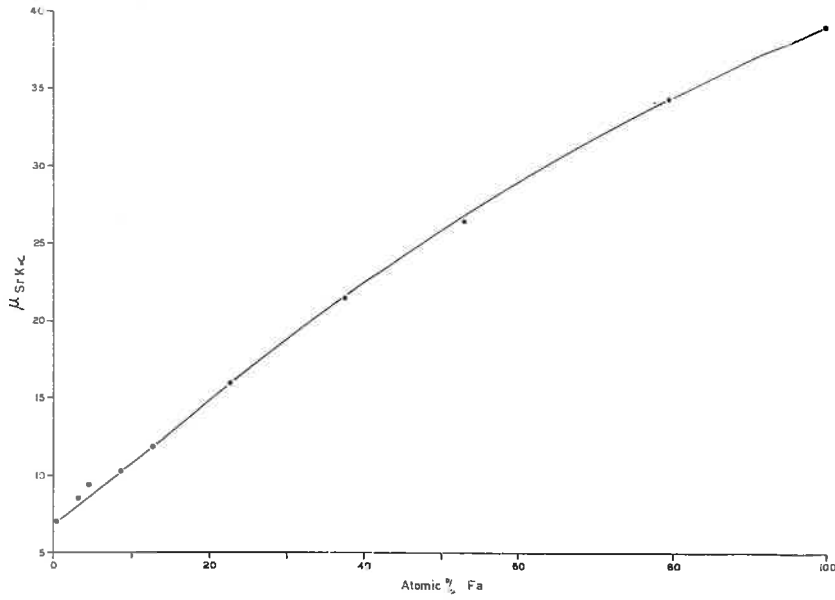


FIG. 3. Plot of olivine composition, as atomic percentage fayalite, against  $\mu_{SrK\alpha}$ , which is calculated from published analyses, Deer, Howie and Zussman (1963).

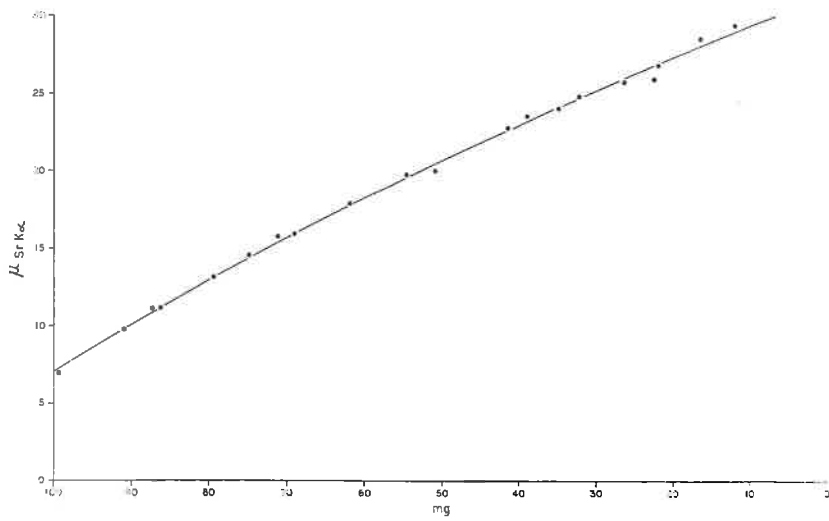


FIG. 4. Plot of orthopyroxene composition, as  $mg \left( = \frac{100 \text{ Mg}}{\text{Mg} + \text{Fe}^{2+} + \text{Fe}^{3+} + \text{Mn}} \right)$ , against  $\mu_{SrK\alpha}$ , which is calculated from published analyses, Deer, Howie and Zussman (1963).



Least-squares regression analysis of the data shows the second order fit is better with the following equation:

$$\text{mg} = 119.90 - 2.54\mu_{\text{SrK}\alpha} - 0.041\mu_{\text{SrK}\alpha}^2 \quad (s = 1.38\% \text{ mg})$$

where

$$\text{mg} = \left( \frac{\text{Mg} \times 100}{\text{Mg} + \text{Fe}^{2+} + \text{Fe}^{3+} + \text{Mn}} \right).$$

A straight line fit of the same gives a standard deviation of 2.11 percent mg.

*Zinblendes series.* The composition of opaque minerals is particularly difficult to determine indirectly because of the limitations imposed on optical methods. X-ray diffraction techniques are also difficult because such small changes are caused in cell size by relatively large differences in composition. The method of mass absorption coefficient measurement appears to be well suited, although there are problems caused by the increased degree of absorption for most opaque minerals. The ZnS-(Fe, Mn)S system has been chosen to show the applicability of the technique described in this paper. The data, shown in Figure 5, are taken from Skinner (1961). The relationship between  $\mu_{\text{SrK}\alpha}$  and the weight percent ZnS-(Fe, Mn)S is linear. In this case the system has three components and the mass absorption coefficients for FeS and MnS, at the SrK $\alpha$  wavelength, are very close (49.1 and 45.1 respectively). Thus, the minerals can be treated as a simple binary mixture. A line drawn for a theoretical, pure ZnS-FeS mixture has almost the same position and slope as that shown in Figure 5, showing the effect of MnS is negligible. By using a different radiation (*e.g.* CoK $\alpha$ ) the effect of MnS on the total  $\mu$

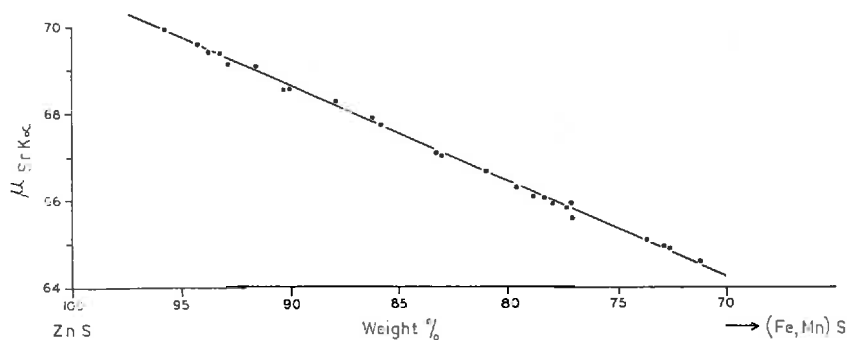


FIG. 5. Plot of zinblendes composition, as wt % ZnS-(Fe, Mn)S, against  $\mu_{\text{SrK}\alpha}$ , which is calculated from published analyses, Skinner (1961).

can be made appreciable and the method may thus be extended to give information about the amount of MnS in the zincblendes.

#### CONCLUSIONS

A method of indirectly determining the composition of minerals by measuring their mass absorption coefficients has been described. The method seems to have much potential with a wide field of applicability. By judicious selection of the wavelength of the absorbed X-ray beam the effects of interfering elements (*e.g.* iron in plagioclase) can be reduced to a minimum. Direct measurements on the plagioclase series demonstrates the applicability of the method. Calculations based on published analyses of olivines, orthopyroxenes and zincblendes indicate that the method may be applied to other solid solution series. It should be noted, however, that values of  $\mu$  measured directly will probably not be the same as those calculated from published tables (such as Heinrich, 1966), as has been shown for the plagioclase series for  $\text{SrK}_\alpha$  radiation.

#### ACKNOWLEDGMENTS

I appreciate permission from Drs. R. L. Oliver and D. Virgo, and Mr. J. D. Kleeman to use unpublished data. Dr. R. W. Nesbitt and Dr. K. Norrish critically read the manuscript. The work has been financed in part by a grant to Dr. R. W. Nesbitt by the Australian Research Grants Committee No. 66/16362.

*Note added in proof.* Since the completion of this work it has been pointed out to the author that Overkott (1958) had proposed a similar method for the determination of plagioclase compositions after noting the linear dependence of the calculated  $\mu$  values of plagioclases and their An contents. He further pointed out that the method has a possible application in determining the proportions of different mineral phases in a mixture.

#### REFERENCES

- BAMBAUER, H. U., M. CORLETT, E. EBERHARD, AND K. VISWANATHAN (1967) Diagrams for the determination of plagioclases using X-ray powder methods. *Schweiz. Mineral. Petrog. Mitt.*, **47**, 333–364.
- DEER, W. A., R. A. HOWIE, AND J. ZUSSMAN (1963) *Rock Forming Minerals*, vols. 1, 2, 4 and 5. Longmans, London.
- HEINRICH, K. F. J. (1966). X-ray absorption uncertainty. *In*, T. D. MCKINLEY, K. F. J. HEINRICH AND D. B. WITTRY (Eds.), *The Electron Microprobe*, John Wiley and Sons, Inc., New York.
- KLEEMAN, J. D. (1965) *Studies on the X-ray Diffraction, Analysis and Geochemistry of Plagioclase from the Mt. Davies Igneous Intrusion*, Honors Thesis, University of Adelaide.
- , AND R. W. NESBITT (1967) X-ray measurements on some plagioclases from the Mt. Davies intrusion, South Australia. *J. Geol. Soc. Aust.*, **14**, 39–42.
- NORRISH, K., AND B. W. CHAPPELL (1967) X-ray fluorescence spectrography. *In* J. Zussman (ed.) *Physical Methods in Determinative Mineralogy*, Academic Press, London—New York.
- OVERKOTT, E. (1958) Eine röntgenographische Methode zur Bestimmung der An-Gehalte von Plagioklasen. *N. Jahrb. Mineral., Monatsh.*, **1958** 113–120.

- , AND R. M. TAYLOR (1962) Quantitative analysis by X-ray diffraction. *Clay Minerals. Bull.*, **5**, 98–109.
- REYNOLDS, R. C. (1963) Matrix corrections in trace element analysis by X-ray fluorescence: estimation of the mass absorption coefficient by Compton scattering. *Amer. Mineral.*, **48**, 1133–1143.
- (1967) Estimation of mass absorption coefficients by Compton scattering: improvements and extensions of the method. *Amer. Mineral.*, **52**, 1493–1502.
- SKINNER, B. J. (1961) Unit-cell edges of natural and synthetic sphalerites. *Amer. Mineral.*, **46**, 1399–1411.
- SMITH, J. V., AND P. GAY (1958) Powder patterns and lattice parameters of plagioclase feldspars II. *Mineral. Mag.*, **31**, 744–762.
- SWEATMAN, T. R., K. NORRISH AND R. A. DURIE (1963) An assessment of X-ray spectrometry for the determination of inorganic constituents in brown coals. *Misc. Rep. Div. Coal Res., C.S.I.R.O.*, **177**.
- , Y. C. WONG, AND K. S. TOONG (1967) Application of X-ray fluorescence analysis to the determination of tin in ores and concentrates. *Inst. Mining Met. Trans.*, **76 B**, 149–154.
- VIRGO, D. (1966) *Some Elemental Distributions Between Co-existing Feldspars in Metamorphic Rocks*. Ph.D. Thesis, University of Adelaide.
- YODER, H. S., AND TH. C. SAHAMA (1957). Olivine X-ray determinative curve. *Amer. Mineral.*, **42**, 475–491.

*Manuscript received December 9, 1968; accepted for publication, April 29, 1969.*

APPENDIX 3

METHODS AND TECHNIQUES.

METHODS OF ANALYSIS AND OPERATING CONDITIONS.A. Chemical analysis.

## General

Standard Philips equipment was used throughout for X-ray fluorescence work:

|            |                               |            |                                    |
|------------|-------------------------------|------------|------------------------------------|
| PW 1010    | X-ray generator               | PW 4032    | electronic counter                 |
| PW 4029/01 | power supply                  | PW 4062    | electronic liner                   |
| PW 4072/01 | linear amplifier              | PW 1965/10 | proportional counter               |
| PW 4082    | discriminator                 | PW 1964/10 | scintillation counter              |
| PW 1540    | Universal vacuum spectrograph | PW 4025/10 | high voltage supply (for counters) |

## Major elements

Unless otherwise stated all major elements, except FeO, Mg and alkalis, were analysed using X-ray fluorescence (X.R.F.) operating under the conditions listed below. Rock samples were fused with a lithium borate-lanthanum oxide mixture to produce a glass, as specified by Norrish and Chappell (1967), and analysed against several natural and artificial standard rocks similarly fused. The analytical technique is that devised by Norrish and Chappell (1967). As a check on the precision an analysed rock was re-analysed several times, the results of which are listed below.

Alkalies ( $\text{Na}_2\text{O}$  and  $\text{K}_2\text{O}$ ) were determined using an EEL flame photometer. The samples were dissolved with hydrofluoric and perchloric acid in platinum crucibles according to the scheme of Riley and Williams (1959).

## Operating conditions for X.R.F.

| Element sought                           | Primary radiation | Analysing crystal  | Counter       |
|--|-------------------|--------------------|---------------|
| Si (as SiO <sub>2</sub> )                | Cr                | P.E.T.             | Proportional  |
| Al (as Al <sub>2</sub> O <sub>3</sub> )  | Cr                | P.E.T.             | "             |
| Ca (as CaO)                              | Cr                | LiF <sub>200</sub> | "             |
| Ti (as TiO <sub>2</sub> )                | Cr                | LiF <sub>200</sub> | "             |
| ΣFe (as Fe <sub>2</sub> O <sub>3</sub> ) | Cr                | LiF <sub>200</sub> | "             |
| Mn (as MnO)                              | Mo                | LiF <sub>200</sub> | "             |
| Cr                                       | Mo                | LiF <sub>200</sub> | "             |
| Ni                                       | Mo                | LiF <sub>200</sub> | "             |
| Sr                                       | Mo                | LiF <sub>200</sub> | Scintillation |
| Cu                                       | Mo                | LiF <sub>200</sub> | Proportional  |

Replicate analyses of A251/N118C (gabbro from Mt. Davies).

|  | 1     | 2     | 3     | 4     | 5     | 6     | 7     | 8     |
|--|-------|-------|-------|-------|-------|-------|-------|-------|
| SiO <sub>2</sub>                             | 49.5  | 49.56 | 48.38 | 49.15 | 49.34 | 48.61 | 48.34 | 49.45 |
| Al <sub>2</sub> O <sub>3</sub>               | 5.50  | 5.79  | 5.70  | 5.68  | 5.19  | 5.54  | 5.83  | 5.44  |
| Fe <sub>2</sub> O <sub>3</sub><br>(total Fe) | 5.48  | 5.66  | 5.79  | 5.59  | 5.42  | 5.59  | 5.54  | 5.23  |
| CaO  | 17.30 | 16.76 | 16.85 | 16.95 | 16.54 | 16.29 | 16.75 | 17.13 |
| TiO <sub>2</sub>                             | 0.13  | 0.17  | 0.16  | 0.14  | 0.14  | 0.13  | 0.16  | 0.16  |
| MnO  | 0.03  | 0.11  | 0.12  | 0.10  | 0.11  | 0.11  | 0.11  | 0.12  |

1. Analysis by AMDEL.
2. Analysis by Miller (1966).
3. Analysis by A. Moore in 1966 (October).
4. Analysis by A. Moore in 1967 (February).
5. Analysis by A. Moore in 1967 (February).
6. Analysis by A. Moore in 1967 (May).
7. Analysis by A. Moore in 1967 (November).
8. Analysis by A. Moore in 1968 (March).

Standard solutions of  $K_2O$  and  $Na_2O$  were used to calibrate the flame photometer and a blank was run with each batch of samples.

MgO was determined by TECHTRON atomic absorption spectrophotometer (A.A.S.). The same solutions as used for the determination of the alkalis were used, although in some cases they were diluted because of the high MgO content. The scheme used was that of Nesbitt (1966a). Conditions were as follows:

Slit width: 100  $\mu$   
 Lamp filament current: 6mA  
 Wavelength: 2853 $\overset{\circ}{A}$   
 Flame: rich  $N_2O/C_2H_2$

Because very high MgO values were measured in some cases (up to 30% MgO) there were some doubts as to the accuracy of the A.A.S. method for high MgO values. As a check a duplicate gravimetric analysis was carried out on one sample (A251/118C). Agreement between the MgO content determined by A.A.S. and that determined gravimetrically was very close, thus confirming the usefulness of the more rapid A.A.S. analysis.

A251/118C: %MgO (AMDEL) : 21.7 (method unknown)  
 %MgO (A. Moore) : 22.1 (A.A.S.)  
 %MgO (A. Moore) : 21.5 (gravimetric 1)  
 %MgO (A. Moore) : 21.1 (gravimetric 2)

FeO was determined by titration against a standard  $\text{KMnO}_4$  solution (standardized against sodium oxalate). The total iron determined by X-ray fluorescence spectrography is corrected for the FeO content and the difference regarded as  $\text{Fe}_2\text{O}_3$ . Replicate FeO analyses are shown below to give an indication of the precision, and the value of FeO for W1 gives a measure of the accuracy attained.

A251/118C: %FeO : . 4.15 (AMDEL, method unknown).

|            |      |   |
|------------|------|---|
| %FeO : (i) | 4.18 | } (A. Moore, titration against $\text{KMnO}_4$ .<br>Each value quoted is the average of<br>three titrations which differed by less<br>than $\pm 0.05\%$ FeO from each other). |
| : (ii)     | 3.89 |   |
| : (iii)    | 4.09 |   |

W1: recommended value: 8.74%FeO

determined by A. Moore: 8.69%FeO (average of three titrations which differed by less than  $\pm 0.05\%$  from each other).

Water content was determined by heating a previously weighed sample (2 gm  $\pm$ ) at  $110^\circ\text{C}$  to constant weight ( $\text{H}_2\text{O}^-$ ).  $\text{H}_2\text{O}^+$  was determined according to the method described by Washington (1930) using an oxy-acetylene flame for the final heating. In some cases "loss on ignition" is quoted. This involved heating a previously weighed rock powder (2 gm  $\pm$ ) at  $1,000^\circ\text{C}$  to constant weight. In some cases this led to an increase in weight due to oxidation of ferrous iron.

Carbon dioxide was determined using the technique of Fahey (1946).



## Trace elements

All trace elements were measured by X-ray fluorescence spectrography using finely powdered, pelletized rock or mineral samples with a boracic acid backing (Norrish and Chappell, 1967). Standard rocks were used for calibration and mass absorption corrections applied. The mass absorption values were measured directly.

The standards used were (with recommended values in parenthesis).

|       |   |
|-------|---|
| G1    | (Sr = 257 p.p.m.)                                   |
| W1    | (Cr = 120 p.p.m.; Ni = 78 p.p.m.; Cu = 110 p.p.m.)  |
| PCC-1 | (Cr = 2593 p.p.m.; Ni = 2138 p.p.m.; Cu = 9 p.p.m.) |
| DTS-1 | (Cr = 3713 p.p.m.; Ni = 2111 p.p.m.; Cu = 5 p.p.m.) |

Atomic absorption spectroscopy was used to determine the Cr and Ni contents of the whole rocks and, in some cases, those of pyroxenes. In the case of the pyroxenes, although the results were generally within 10% of the values determined by X-ray fluorescence spectrography it was found that they were not as reproducible and for relatively high concentrations (> 5,000 p.p.m. Cr; > 2,000 p.p.m. Ni) the A.A.S. measurements were as much as 30% greater than the X.R.F. results.

B. X-ray diffraction (X.R.D.)

## General

A Philips X-ray diffractometer was used throughout with a "10/9" generator and "1050" goniometer. Pulses from the scintillation counter were discriminated and amplified using ECKO N606A ratemeter equipment. Chart recordings were obtained on a HONEYWELL chart recorder. Samples were finely powdered, in some cases mixed with a suitable standard, then spread by hand as an acetone-powder slurry on a suitably orientated quartz plate.

## Plagioclase

Measurements of  $\Gamma = 2\theta (131) + 2\theta (220) - 4\theta (1\bar{3}1)$ , were made by measuring the angular separations of the three peaks directly from the chart. Operating conditions were as follows:

Generator: 44kv/18mA, Cu target. Diffracted X-rays were passed through a Ni-filter and a 0.1 mm receiving slit ( $1^\circ$  divergent slit,  $0.5^\circ$  scatter slit). Goniometer drive rate:  $\frac{1}{4}^\circ/\text{min}$ . Chart scale calibrated as 401.32 mm/ $^\circ 2\theta$ .

An even number of oscillations, varying between 8 and 20 per sample were made to counter possible inaccuracy in the geometry. Peaks were measured at  $\frac{2}{3}$  peak height. The average difference between the maximum and the minimum value of  $\Gamma$  obtained from single oscillations was  $0.045^\circ 2\theta$  (30 samples). The average difference between  $\Gamma$  values derived for the same sample from different charts

(i.e. new slurry mounts) was  $0.018^{020}$  (8 samples). This value is used in Fig. 3.54 to give the size of the error bar. The same techniques were used by Kleeman (1965) and Kleeman and Nesbitt (1967) who found the standard deviation of  $\Gamma$  from 8 oscillations was  $0.01^{020}$ .

As a check on the accuracy of the method the  $\Gamma$  value of plagioclase 55BE-1, from Stillwater, was measured. This gave a value of  $1.330^{020}$  compared with Jackson's (1961a) value of  $1.331^{020}$  and Kleeman and Nesbitt's (1967) value of  $1.336^{020}$ .

To change the structural state of the plagioclases, powdered samples ( $0.2 \text{ gm} \pm$ ) were placed in platinum foil envelopes and suspended in air in a furnace at  $1,050^{\circ}\text{C}$ . On removal from the furnace they were rapidly cooled in air but not quenched. Before measuring, the heated samples were hand-ground in a mortar.

#### Olivine

Mounts were made in the same way as those for plagioclase but the olivine powder (usually severely contaminated by pyroxenes) was mixed with a ZnO powder to act as an internal standard.

#### Powder photographs

These were taken using the Straumanis setting with a 114.6 mm diameter camera. Powdered samples were mounted with a gum tragacanth mixture.

### C. Electron microprobe analyses.

The majority of work involving the use of an electron microprobe was done commercially through AMDEL. Some work was done personally at The Australian National University, Canberra, through the courtesy of Dr. J. Lovering. The machine used was an Applied Research Laboratories electron microprobe X-ray analyser. Polished thin sections, coated with a layer of vaporized carbon, were analysed by comparing the intensities of the emitted characteristic X-rays with those of standards. Sample current was used as a drift check, and drift was also corrected linearly between readings on standards. Other corrections made were background, dead-time and absorption (after Philibert, 1963). No corrections were made for secondary fluorescence (negligible in the silicates) and for atomic number (standards used were of similar mean atomic number).

### D. Optical methods and petrofabric analysis.

The determination of refractive indices was made using a single variation technique with immersion oils of known dispersion. Mineral grains were mounted in oil of known refractive index on a Universal stage and suitably orientated. A match between the oil and the mineral was achieved using a monochromator. The refractive index of the oil was determined to 0.0001 using an Abbe refractometer. However, replicate measurements of the same minerals, plotted on Hartmann graphs, indicated that the actual refractive index

determinations were only  $\pm 0.003$  or, less often,  $\pm 0.001$ .

Both crystallographic orientations and preferred orientation studies were done using a 4-axis Universal stage. For the former an equal-angle (Wulff) net was used, and for the latter an equal-area (Schmidt) net. In all cases plots were made on the lower hemisphere. In fabric diagrams at least two, and generally three, mutually perpendicular thin sections were used and contouring was done according to the scheme outlined by Strand (1944) and slightly modified by Dr. A.W. Kleeman (pers. comm.).

#### E. Measurement of area.

Areas occupied by each rock type were measured directly from the map (Fig. 1.3) and no corrections were made for topography. A Coradi compensating planimeter was used.

APPENDIX 4

SUMMARY OF THE PAPER BY NESBITT, R.W., GOODE, A.D.T.,  
MOORE, A.C. AND HOPWOOD, T.P. (1969), (IN PRESS).

THE GILES COMPLEX, CENTRAL AUSTRALIA: A STRATIFIED SEQUENCE OF BASIC  
AND ULTRABASIC INTRUSIONS

The Giles complex is a series of deformed mafic-ultramafic sheets, now found as isolated intrusions, scattered over an area of 2,500 km<sup>2</sup> in the Musgrave Block of central Australia. The sheets which are late Precambrian in age were emplaced into a granulite facies terrain, the metamorphism of which has been variously dated from 1,300 to 1,600 m.y.

The intrusions display many characteristics of stratiform bodies, including prominent large and small scale mineralogical layering of the ratio type. There is also a depth stratification developed between intrusions, those in the western portion of the complex being emplaced at a higher level than those of the central zone which were intruded into the lower crust. The evidence for the high pressure development of some of the central zone intrusions can be summarised as follows:

- 1) sub-solidus reaction relationships between olivine + plagioclase  $\rightleftharpoons$  orthopyroxene + clinopyroxene + spinel, and orthopyroxene + plagioclase  $\rightleftharpoons$  garnet;
- 2) spinel and rutile exsolution in pyroxenes;
- 3) high R<sub>2</sub>O<sub>3</sub> contents in the pyroxenes;
- 4) unusually high K<sub>D</sub> values for co-existing pyroxenes (requiring

high liquidus temperatures and hence high pressures);

- 5) dominance of orthopyroxene rather than olivine in the early crystallization sequence;
- 6) where observed, chilled zones are very thin (e.g. south Mt. Davies is 4,200 m thick and has a chilled zone of a few centimetres).

There is a broad correlation between structural height and degree of fractionation. In general the higher level gabbros are more highly fractionated, although no overall marked iron enrichment has been observed. At least two of the sheets have different bulk compositions which may be the result of progressive movement of liquids away from the partially crystalline lower sheets into higher zones. Final differentiates of the fractionation series may be represented by the Tollu volcanics, a group of acid and basic volcanics found in close association with the high level gabbros at the western end of the Musgrave Block. The volcanics and gabbros have the same initial Sr 87/86 ratios and therefore can be considered to be comagmatic. The best age estimate for both rock suites is 1,100 m.y.

High temperature deformation of the sheets, particularly in the central zone, resulted in the formation of localised gabbro-gneiss zones approximately parallel to the main igneous layering. In many respects this resembles the flow layering, described by Thayer (1963) as being characteristic of alpine ultramafic bodies. This feature, together with rotation of the intrusions into a near vertical position



by later deformations, illustrates the possible relationship between flat-lying stratiform intrusions and those of the alpine ultramafic association.

In the central zone, numerous suites of minor basic intrusions were emplaced after the crystallization of the Giles complex. The major deformation phases of the Giles complex and the injection of many of the minor bodies occurred before major uplift of the central zone.

Economically, the Giles complex has proved disappointing since major chromite and nickel deposits are absent from the ultramafic zones. Low grade lateritic nickel deposits are known, these being due to the weathering of transgressive picrites. Vanadiferous magnetites occur in a high level gabbro in the western zone, but this and the nickel deposits are too far removed from industrial centres to have been exploited. However, it should be possible to locate stratigraphically favourable portions of the complex where there may be areas of potential economic interest.

#### CONCLUSIONS

1. The intrusions of the complex were emplaced at varying heights within the crust.
2. They are all of stratiform type, showing mineralogical and chemical layering.

3. There is a broad correlation between depth of emplacement and degree of fractionation, and the sheets can be stratigraphically located.
4. The basaltic and rhyolitic volcanics represent the extrusive differentiates of the complex.
5. The deformation has resulted in the development of features normally referred to as being characteristic of alpine ultramafic associations.

To be published as a Special Publication of the Geological Society of South Africa and may appear during 1970 rather than 1969.

APPENDIX 5

BRIEF DESCRIPTIONS OF ROCKS MENTIONED IN THE TEXT.

BRIEF DESCRIPTIONS OF ROCKS MENTIONED IN THE TEXT.

All specimens referred to in this thesis are catalogued in the museum of the Department of Geology and Mineralogy, The University of Adelaide. Specimen numbers prefixed A313/- were collected by Alan Moore; those prefixed A253/R were collected by Dr. R.L. Oliver, and those prefixed A253/N by Dr. R.W. Nesbitt. Other numbers are linked with the name of the collector in the text. The catalogued information includes rock name, catalogue number and the location, which is also marked on an outline map of the area (see back pocket, this thesis).

A. Granulites

\* = chemically analysed.

A313/A25\*: Quartz + feldspar + pyroxene granulite (acid granulite).

Modal analysis: Table 2.3. Inequigranular interlobate granoblastic texture. Dominantly quartz, perthite and antiperthite with green clinopyroxene, strongly pleochroic orthopyroxene and oxide minerals (ilmenite + magnetite) present in relatively small amounts.

Accessories include rounded zircon and subhedral apatite laths.

A313/297: Plagioclase + pyroxene + amphibole granulite (basic granulite). Modal analysis: Table 2.10. Seriate polygonal granoblastic texture. Approximately equal amounts of plagioclase and mafic minerals (strongly pleochroic orthopyroxene; brown hornblende, and green clinopyroxene) with accessory oxide minerals (magnetite + ilmenite?), traces of reddish biotite and euhedral apatite.

A313/297A: Diopside + scapolite rock (calc-silicate). Modal analysis: Table 2.12. Equigranular polygonal granoblastic texture. Consists almost entirely of grey-green, twinned diopside with traces of scapolite, pargasite and very rare bright green spinel. Calcite occurs interstitially.

A313/302: Quartz + feldspar + pyroxene granulite (acid granulite). Modal analysis: Table 2.3. Seriate, platy interlobate granoblastic texture with quartz and perthite stringers in a matrix of these minerals plus antiperthite and both pyroxenes. Oxide minerals (magnetite + ilmenite) occur in only very small quantities.

A313/370A\*: Quartz + feldspar + garnet granulite (acid granulite). Leucocratic, with seriate interlobate granoblastic texture. Consists dominantly of quartz and antiperthite, with smaller amounts of perthite and mafic minerals. The garnet forms granular clusters associated with biotite and oxide minerals (magnetite, ilmenite and traces of green spinel), which enclose laths of corundum. Rare rounded zircon grains are found throughout.

A313/370B\*: Diopside + scapolite rock (calc-silicate). Modal analysis: Table 2.12. Inequigranular polygonal granoblastic texture: the diopside tends to be equigranular but has a generally coarser grain-size than the scapolite. Large, but rare, crystals of pargasite occur enclosing diopside and scapolite. Pale, very weakly pleochroic phlogopite occurs in trace amounts, as does highly altered plagioclase.

A313/372: Quartz + feldspar + pyroxene granulite (acid granulite).  
Modal analysis: Table 2.3. Seriate, amoeboid granoblastic texture.  
The rock consists almost entirely of antiperthite, quartz and perthite with only a small amount of both pyroxenes (the orthopyroxene is only weakly pleochroic). Accessories include oxide minerals, large subhedral apatite and rare rounded zircon.

A313/381A: Quartz + feldspar granulite (acid granulite). Modal analysis: Table 2.3. Flaser amoeboid texture. The rock consists almost entirely of quartz (stringers and matrix) and perthite. No plagioclase has been identified. Small amounts of altered orthopyroxene and oxide minerals form the only mafic minerals. Traces of rounded zircon occur.

A313/381D: Quartz + feldspar granulite (acid granulite). Essentially the same as A313/381A, except that apatite has also been recognised as an accessory mineral. The rock has also been affected by brittle fracture and contains numerous pseudotachylite veins.

A313/398: Flaggy mylonite. Grey-green rock which breaks into slate-like fragments. Extremely fine-grained, with individual minerals unrecognisable under the microscope. Megacrysts, around which the layering bends, of plagioclase contain needles of sillimanite (?) and euhedral garnet. Pale green chlorite and magnetite have been recognised.

A313/404: Quartz + feldspar + garnet granulite (acid granulite).

Seriate amoeboid granoblastic texture. Quartz and perthite are the dominant minerals, both containing rod-like inclusions of rutile (?). Anhedral garnet is the chief mafic mineral and is commonly associated with weakly pleochroic biotite. Strongly pleochroic, reddish biotite occurs in small amounts throughout the rock. Accessories include oxide minerals (magnetite, ilmenite and rare green spinel found only within the garnet), rutile and corundum (?) laths within the ilmenite.

A313/407: Quartz + feldspar + garnet granulite (acid granulite).

Seriate amoeboid granoblastic texture. Quartz is the dominant mineral and feldspar is very rare. Garnet, as anhedral crystals, occurs in bands and is associated with sillimanite laths. Magnetite (and ilmenite?) is abundant in the garnet-rich bands. Accessories include green spinel and apatite laths.

A313/413: Quartz + feldspar granulite (acid granulite). Seriate amoeboid granoblastic texture. Quartz and perthite are the dominant minerals with small amounts of plagioclase, magnetite (which occurs as discrete grains and along fractures), some highly altered pyroxene (?) and apatite laths, which contain numerous inclusions.

A313/415: Quartz + feldspar + pyroxene granulite (acid granulite).

Modal analysis: Table 2.3. Inequigranular amoeboid granoblastic texture. Consists essentially of quartz and perthite with smaller amounts of plagioclase, twinned, green clinopyroxene and magnetite. Green, weakly pleochroic hornblende occurs as an alteration product

of the pyroxene. Accessories include rounded zircon (one zircon crystal as a square cross-section) and numerous apatite laths.

A313/417: Quartz + magnetite rock (iron-rich granulite). Modal analysis: Table 2.9. Equigranular amoeboid granoblastic texture, with considerable replacement of original magnetite by haematite and limonite veins. Quartz is the only felsic mineral which occurs both as original grains and as spherulitic, cavity fillings.

A313/418: Plagioclase + pyroxene + amphibole granulite (basic granulite). Modal analysis: Table 2.10. Equigranular polygonal granoblastic. Plagioclase-rich bands and mafic-rich bands occur. Brown, strongly pleochroic hornblende occurs in only relatively small quantities, with strongly pleochroic orthopyroxene and green clinopyroxene being the dominant mafic minerals.

A313/424A: Quartz + feldspar + garnet granulite (acid granulite). Seriate amoeboid granoblastic texture. Felsic bands consist essentially of quartz (with rutile? inclusions) and perthite with some plagioclase. Mafic-rich bands consist of these minerals with abundant anhedral garnet. Associated with the garnet are rims of K-feldspar within which are "mats" of fibrolite (sillimanite). Accessories include pale, weakly pleochroic biotite (or phlogopite), rutile and green spinel.



A313/428: Clinopyroxene + hornblende granulite (basic granulite).

Modal analysis: Table 2.10. Equigranular polygonal granoblastic texture. Dominantly green clinopyroxene and pleochroic brown hornblende; plagioclase occurs in only small amounts. Accessories include oxide minerals (magnetite, ilmenite and green spinel) and some apatite, as rounded laths.

A313/429: Quartz + feldspar + pyroxene granulite (acid granulite).

Modal analysis: Table 2.3. Equigranular amoeboid granoblastic texture. Dominantly quartz, perthite and antiperthite with small amounts of green, twinned clinopyroxene, sometimes altered at the margins to green amphibole. Accessories include oxide minerals and some rounded apatite. Rare rounded zircon is found.

A313/437: Quartz + feldspar + pyroxene granulite (acid granulite).

Seriate interlobate granoblastic texture. Mineralogy as in A313/429.

A313/446A: Quartz + feldspar granulite (acid granulite). Flaser mylonite. Elongate quartz ribbons in a quartz-rich matrix. Augen of K-feldspar are common. Rounded zircon is the only accessory.

A313/447: Quartz + feldspar + hornblende granulite (acid granulite).

Seriate amoeboid granoblastic texture. Deformed quartz and perthite are dominant, with considerable antiperthite. The main mafic is pleochroic green hornblende and some orthopyroxene. Accessories include oxide minerals, zircon and apatite. The rock is cut by numerous brittle fracture zones.

A313/455: Iron-rich granulite. Modal analysis: Table 2.9. Flaser texture, with elongate quartz and magnetite, much altered to haematite, and rare pyroxene?

A313/456: Iron-rich granulite. Modal analysis: Table 2.9.  
Same as A313/455.

A313/460: Quartz + feldspar granulite (acid granulite). Seriate interlobate granoblastic texture. Dominantly quartz, perthite and some antiperthite with green clinopyroxene, weakly pleochroic orthopyroxene and oxide minerals as accessories. Small amounts of apatite and zircon are found.

A313/M\*: Marble (calc-silicate rock). Inequigranular interlobate granoblastic texture where calcite-rich, and polygonal where diopside-rich. Modal analysis: Table 2.15. Dominantly calcite with rounded forsterite, diopside and twinned chondrodite as the main silicate phases. Other common minerals are phlogopite and green spinel. Pargasite has been recognised in places.

A253/R2B\*: Plagioclase + pyroxene + amphibole granulite (basic granulite). Modal analysis: Table 2.10. Very similar to A313/418 in mineralogy and texture, but contains a significant amount of garnet, which forms rims around other mafic phases.

A253/R3: Plagioclase + pyroxene + amphibole granulite (basic granulite). Almost identical to A313/297.

A253/R16A: Diopside + scapolite rock (calc-silicate rock). Modal analysis: Table 2.12. Equigranular polygonal granoblastic texture. Consists almost entirely of green-grey diopside. Pale phlogopite and traces of scapolite, pargasite and calcite are the only other minerals.

A253/R16B\*: Quartz + feldspar + garnet granulite (acid granulite). Modal analysis: Table 2.7. Essentially seriate interlobate granoblastic texture, but corona textures are well developed. The rock is mineralogically banded. The dominant phases are quartz, perthite and plagioclase, with smaller amounts of garnet, sillimanite, brown mica and oxide minerals (including spinel). Accessories include rutile, apatite and zircon.

A253/R16C: Diopside + scapolite rock (calc-silicate rock). Modal analysis: Table 2.12. Apart from mineral proportions, the rock is the same as A313/370B.

A253/R41: Diopside + scapolite rock (calc-silicate rock). Modal analysis: Table 2.12. Identical to A313/297A.

A253/R45A and A253/R45B: Plagioclase + pyroxene + amphibole rocks (basic granulites). Modal analysis (R45B): Table 2.10. Apart from slight variations in the proportions of minerals present these are the same as A313/297. A253/R45A is unusual in that no magnetite has been observed: the only oxide mineral is green spinel containing laths identified as corundum.

A253/R49A: Same as A253/R45B, but with less amphibole and more oxide minerals (both magnetite and spinel). Modal analysis: Table 2.10.

A253/R52B: Diopside + scapolite rock (calc-silicate granulite). Modal analysis: Table 2.12. Essentially the same as A313/370B.

### B. Gosse Pile Rocks

Many of the rocks from Gosse Pile which are referred to in the text are very similar. For this reason only selected representative specimens are briefly described below.

1. Those referred to in Tables 3.10 and 3.12.

A313/11: Orthopyroxenite. Subhedral and anhedral cumulus orthopyroxene (average size: 1.5 mm) with interstitial clinopyroxene and plagioclase. Trace of picotite.

A313/12: Gabbro (from the Gabbro Band). Large laths of plagioclase (average length: 3 mm) with multiple albite, albite-Carlsbad and pericline deformation twinning. Both pyroxenes occur interstitially; orthopyroxene as anhedral or subhedral grains and clinopyroxene as numerous, granular crystals.

A313/13: Websterite. Seriate grain-size (average: 2 mm) with anhedral orthopyroxene and clinopyroxene showing complex intergrowths and grain boundary relationships (Fig. 3.19). Orthopyroxene tends to be slightly larger than clinopyroxene and, where these orthopyroxene grains are in contact, they meet in  $120^\circ$  triple-point junctions. Plagioclase occurs interstitially in very small amounts.

A313/14\*: Websterite. Anhedral orthopyroxene and clinopyroxene, with the clinopyroxene occurring mainly as interstitial grains. The rock is partly annealed and cut by late-stage brittle fractures. No plagioclase was identified.

A313/15\*: Orthopyroxenite. Anhedral orthopyroxene (average size: 2 mm) with interstitial clinopyroxene. The rock has been extensively deformed by late-stage fractures, and micro-breccia veins traverse the rock. This deformation has also produced numerous kink bands in the orthopyroxene.

A313/25\*: Websterite. Identical to A313/13, but no plagioclase has been observed. In a similar rock further south (A313/24) a single chromite crystal, surrounded by plagioclase has been noted.

A313/39B: Orthopyroxenite. Seriate and coarse-grained (average: 3.5 mm) rock consisting of orthopyroxene and interstitial clinopyroxene and plagioclase in small amounts. The rock has been extensively deformed and contains numerous micro-fractures, pseudotachylite and micro-breccia veins. Kink-bands in orthopyroxene are numerous.

A313/44: Websterite. Inequigranular with megacrysts (60%) of orthopyroxene and, rarely, clinopyroxene (up to 2 mm) in a fine-grained (average: 0.5 mm) matrix of ortho- and clino-pyroxene. These were the only minerals identified.

A313/48: Olivine-orthopyroxenite. Equigranular rock consisting essentially of anhedral cumulus orthopyroxene (average: 1 mm). These have irregular boundaries but tend to meet in  $120^{\circ}$  triple-point junctions. Small amounts of large (up to 3 mm), anhedral and irregular cumulus olivine occur. Clinopyroxene occurs interstitially. The rock is cut by numerous micro-fractures and pseudotachylite veins.

A313/49: Orthopyroxenite. Equigranular, anhedral cumulus orthopyroxene crystals, meeting in  $120^{\circ}$  triple-point junctions, are dominant (average size: 1.5 mm). Plagioclase and clinopyroxene are common, but not abundant, as interstitial phases. Numerous small crystals of chromite occur along grain boundaries. In Table 3.10, "49 m" refers to the slightly more magnetic orthopyroxene separated from the same crushed specimen.

A313/50: Orthopyroxenite. Very similar to A313/49, but it contains less chromite and very little interstitial clinopyroxene.

A313/51: Orthopyroxenite. Identical to A313/39B. Along one border of a vein of micro-breccia is a narrow zone consisting of crystals of orthopyroxene which have grown at  $90^{\circ}$  to the vein.

A313/52: Gabbro (from the Gabbro Band). Very similar to A313/12, except that the clinopyroxenes contain numerous complex intergrowths and exsolution lamellae of orthopyroxene, and that the rock contains many micro-fractures.

A313/53: Websterite. This has the same appearance as A313/25.

A313/54: Orthopyroxenite. Seriate, with anhedral cumulus orthopyroxene (average size: 2.5 mm) and intercumulus clinopyroxene and plagioclase. Large areas of intercumulus clinopyroxene (4-5 mm) have the same optical orientation and have a "replacement" texture towards the orthopyroxene which, in places, it poikilophitically encloses. Oxide minerals are rare.

A313/55: Orthopyroxenite. Anhedral cumulus orthopyroxene (average size: 1 mm) with interstitial clinopyroxene and plagioclase. The rock is similar to A313/54 but has been deformed by brittle fracture and contains micro-breccia veins and numerous micro-fractures.

A313/56: Orthopyroxenite. Indistinguishable from A313/55.

A313/60\*: Orthopyroxenite. Equigranular, anhedral and subhedral cumulus orthopyroxene (average size: 2 mm) with considerable interstitial clinopyroxene (sometimes poikilophitically enclosing and "replacing" orthopyroxene) and plagioclase (antiperthitic). Traces of oxide minerals (chromite, magnetite and picotite) occur along grain boundaries, and rare, strongly pleochroic red-brown biotite occurs interstitially.

A313/116: Orthopyroxenite. Seriate, with anhedral pyroxenes in a highly deformed partly annealed, rock. Plagioclase occurs interstitially and traces of red-brown biotite and opaques are found along grain boundaries. The plagioclase is very strongly antiperthitic. The rock occurs within the Gneissic Zone, but has also been affected by brittle faulting which has produced microfractures, micro-breccia veins and well developed kinking in the orthopyroxenes. In Table 3.10, "116 m" refers to the slightly more magnetic orthopyroxene separated from the same crushed specimen.

A313/273: Orthopyroxenite. A313/273p: Norite. Both occur within a single hand specimen and refer to plagioclase-rich and plagioclase-poor bands of a banded, flow-layered rock within the Gneissic Zone. The rocks are strongly annealed. In both occur orthopyroxene megacrysts, strained and bent, within a matrix of polygonal plagioclase or pyroxene grains.

A313/387: Olivine-orthopyroxenite. Laths of cumulus anhedral and subhedral orthopyroxene with a strong preferred orientation dominate, with less common bands of anhedral cumulus olivine. Clinopyroxene is a fairly common intercumulus phase, but plagioclase is found only rarely. Oxide minerals (cumulus) occur scattered throughout, particularly along grain boundaries (separated opaque minerals indicate that they consist of chromite, or picotite, and some ilmenite-magnetite grains).



## 2. Others.

A313/16\*: Orthopyroxenite. Seriate, consisting of anhedral orthopyroxene (average size: 2 mm) and interstitial clinopyroxene. No other minerals have been identified. It is partly annealed, but also contains numerous micro-fractures and micro-breccia veins.

A313/19\*: Olivine-orthopyroxenite. Identical to A313/48.

A313/20\*: Orthopyroxenite. Equigranular, anhedral orthopyroxene crystals (average size: 1.5 mm) are dominant, with interstitial clinopyroxene and a trace of plagioclase. Rare oxide minerals occur. The rock contains abundant micro-fractures, pseudotachylite and micro-breccia veins.

A313/32: Olivine-orthopyroxenite. Rounded, anhedral cumulus olivine (average size: 2 mm) and anhedral, laths or equidimensional crystals of cumulus orthopyroxene (average size: 1 mm) are dominant. Some anhedral or subhedral cumulus oxide minerals occur. These are predominantly titaniferous magnetite and chromite. Olivine is also rich in exsolved magnetite. Intercumulus phases include abundant clinopyroxene and plagioclase. Opaque minerals occur along grain boundaries; they include pyrite, with haematite, pyrrhotite, marcasite and chalcopyrite. Pale green spinel is common, both as an exsolution product in the pyroxenes and along grain boundaries. Traces of brown, pleochroic biotite or hornblende have been observed, closely associated with the orthopyroxene. Olivine is generally,

---

but not always, separated from the plagioclase by a narrow corona of orthopyroxene.

A313/143: Anorthosite (from the Gabbro Band). Seriate, consisting almost entirely of plagioclase (range from 0.1 mm to 10 mm in size). The rock has been extensively deformed, making recognition of grain shapes difficult. Interstitial orthopyroxene and, possibly, some clinopyroxene, is the only other mineral.

A313/275: Anorthosite (inclusion in the Gneissic Zone).

Inequigranular, with a fine-grained, polygonal equigranular matrix (average size: 0.05 mm) of plagioclase which contains megacrysts (up to 3 mm) of plagioclase crystals. Clusters of orthopyroxene and magnetite (2-4 mm in size) are relatively common. The orthopyroxene is very strongly pleochroic. Accessories include clinopyroxene and oxide minerals (magnetite and ilmenite) scattered evenly throughout. All of the plagioclase megacrysts are strongly antiperthitic; a few of the plagioclase crystals in the matrix are antiperthitic.

A313/310A: Central type picrite. Rounded, irregular olivine crystals (average size: 2 mm) occur within large subhedral to anhedral clinopyroxenes (some as large as 5 cm). In some specimens they are surrounded by plagioclase or orthopyroxene. The plagioclase usually occurs interstitially. Other minerals include oxide and sulphide minerals (magnetite, chromite, pyrite) and small amounts of red-brown biotite and brown hornblende. Both are commonly intergrown

with orthopyroxene. Spinel is a common phase, both as an exsolution product from the pyroxenes and as a separate phase along grain boundaries.

A313/312E: Marginal type picrite. Anhedral slightly rounded olivines (average size: 2 mm) are surrounded by interstitial clinopyroxene, orthopyroxene, plagioclase, brown hornblende and, to a lesser extent, biotite. Oxide minerals are common and are usually surrounded by hornblende or biotite. The pyroxenes are rich in spinel exsolution. Biotite and orthopyroxene are commonly intergrown in a regular fashion.

#### REFERENCES

- ABBOTT, D. and FERGUSON, J., 1965. The Losberg intrusion, Fochville, Transvaal. *Trans. geol. Soc. S. Afr.*, 68, 31-52.
- ALBEE, A.L., 1965. Phase equilibria in three assemblages of kyanite-zone pelitic schists, Lincoln Mountain Quadrangle, central Vermont. *J. Petrology*, 6, 246-301.
- ALLING, H.L., 1936. Interpretative petrology of the igneous rocks, (1st Ed.). McGraw-Hill, N.Y. 353 p.
- ALTHAUS, E., 1967. The triple point andalusite - sillimanite - kyanite. *Contr. Miner. Petrology*, 16, 29-44.
- ALTHAUS, E., 1969. Experimental evidence that the reaction of kyanite to form sillimanite is at least bivariant. *Am. J. Sci.*, 267, 273-277.
- ANDERSON, E.M., 1948. On lineation and petrographic structure and the shearing movement by which they have been produced. *Q. Jl geol. Soc. Lond.*, 104, 99-132.
- AOKI, K. and KUSHIRO, I., 1968. Some clinopyroxenes from ultramafic inclusions in Dreiser Weiher, Eifel. *Contr. Miner. Petrology*, 18, 326-337.
- APPLEMAN, D.E., 1966. Crystal chemistry of the pyroxenes, in Short course lecture notes: chain silicates. (Am. Geol. Inst.) Introduction. 24 p.
- ARRIENS, P.A. and LAMBERT, I.B., 1969. On the age and strontium isotope geochemistry of granulite facies rocks from the Fraser Range, Western Australia, and Musgrave Ranges, central Australia. Paper read at Granulite Facies Symposium, Canberra. Now published in *Spec. Publs geol. Soc. Aust.*, 2, 377-388.

- ATHERTON, M.P., 1965. The chemical significance of isograds, in Controls of metamorphism. Pitcher, W.S. and Flinn, G.W. (Ed.). Oliver and Boyd. 368 p.
- ATKINS, F.B., 1969. Pyroxenes of the Bushveld Intrusion, South Africa. *J. Petrology*, 10, 222-249.
- BAMBAUER, H.U., CORLETT, M., EBERHARD, E. and VISWANATHAN, K., 1967. Diagrams for the determination of plagioclases using X-ray powder methods. *Schweiz. Miner. Petrographische Mitt.*, 41, 333-364.
- BARNES, L., 1968. The petrography and geochemistry of some high grade metamorphic rocks from the Mt. Davies - Giles region, central Australia. Unpublished Hons. thesis. Univ. Adelaide.
- BARTH, T.F.W., 1959. Theoretical petrology, (2nd Ed.), John Wiley & Sons, Inc., N.Y. 387 p.
- BARTH, T.F.W., 1962. Theoretical petrology, (3rd Ed.), John Wiley & Sons, Inc., N.Y. 416 p.
- BARTHOLOMÉ, P., 1960. L'interprétation pétrogénétique des associations d'olivine et d'orthopyroxène. *Ann. Soc. Géol. Belg.*, 83, 319-345.
- BARTHOLOMÉ, P., 1961. Coexisting pyroxenes in igneous and metamorphic rocks. *Geol. Mag.*, 98, 346-348.
- BARTHOLOMÉ, P., 1962. Iron-magnesium ratio in associated pyroxenes and olivines, in Engel, A.E.J., James, H. and Leonard, B.F. (Eds.) pp. 1-20. *Petrologic studies (Buddington Volume)*, Geol. Soc. Am., 660 p.
- BASEDOW, H., 1905. Geological report on the country traversed by the South Australian government north-west prospecting expedition, 1903. *Trans. R. Soc. S. Aust.*, 29, 57-102.

- BATTEY, M.H., 1965. Layered structure in rocks of the Jotunheim complex, Norway. *Mineralog. Mag.*, 34, 35-51.
- BECK, P.A., 1954. Annealing of cold worked metals. *Adv. Phys.*, 3, 245-324.
- BERLIN, R. and HENDERSON, C.M.B., 1968. A reinterpretation of Sr and Ca fractionation trends in plagioclase from basic rocks. *Earth Plan. Sci. Lett.*, 4, 79-83.
- BERTHELSEN, A., 1960. Structural studies in the Precambrian of west Greenland, geology of Tovqussap Nuna. *Meddr Grønland*, 123, 1-223.
- BHATTACHARYYA, D.S., 1966. Orientation of mineral lineation along the flow direction in rocks. *Tectonophysics*, 3, 29-33.
- BINNS, R.A., 1962. Metamorphic pyroxenes from the Broken Hill district, New South Wales. *Mineralog. Mag.*, 33, 320-338.
- BINNS, R.A., 1964. Zones of progressive regional metamorphism in the Willyama Complex, Broken Hill district, New South Wales. *J. geol. Soc. Aust.*, 11, 283-330.
- BLACKBURN, W.H., 1968. The spatial extent of chemical equilibrium in some high grade metamorphic rocks from the Grenville of southeastern Ontario. *Contr. Miner. Petrology*, 19, 72-92.
- BOETTCHER, A.L., 1967. The Rainy Creek alkaline-ultramafic igneous complex near Libby, Montana. I. Ultramafic rocks and fenite. *J. Geol.*, 75, 526-553.
- BOONE, G.M. and WHEELER, E.P., 1968. Staining for cordierite and feldspars in thin section. *Am. Miner.*, 53, 327-331.
- BORG, I. and HANDIN, J., 1966. Experimental deformation of crystalline rocks. *Tectonophysics*, 3, 249-368.

- BOWEN, N.L. and SCHAIRER, J.F., 1935. The system  $MgO-FeO-SiO_2$ .  
Am. J. Sci., 29, 151-217.
- BOWEN, N.L. and TUTTLE, O.F., 1950. The system  $NaAlSi_3O_8-KAlSi_3O_8-H_2O$ .  
J. Geol., 58, 489-511.
- BOWES, D.R., WRIGHT, A.E. and PARK, R.G., 1964. Layered intrusive rocks in the Lewisian of the north-west Highlands of Scotland.  
Q. Jl geol. Soc. Lond., 120, 153-192.
- BOWN, M.G. and GAY, P., 1959. The identification of oriented inclusions in pyroxene crystals. Am. Miner., 44, 592-602.
- BOYD, F.R., 1966. Electron probe study of diopsidic pyroxenes from kimberlites, in P.H. Abelson, Ann. Rept. Director Geophys. Lab., Carnegie Inst. Washington, Yearbook 65, 252-260.
- BOYD, F.R., 1966a. Phase relations of sodic and aluminous pyroxenes with some applications to pyroxenes from kimberlites. Lecture 9, Short course lecture notes; chain silicates. (Am. Geol. Inst.), 14 p.
- BOYD, F.R. and BROWN, G.M., 1967. Electron-probe study of exsolution in pyroxenes, in P.H. Abelson, Ann. Rept. Director Geophys. Lab., Carnegie Inst. Washington, Yearbook 66, 353-359.
- BOYD, F.R. and ENGLAND, J.C., 1960. Minerals of the mantle, in P.H. Abelson, Ann. Rept. Director Geophys. Lab., Carnegie Inst. Washington, Yearbook 59, 47-52.
- BOYD, F.R. ENGLAND, J.L. and DAVIS, B.T.C., 1964. Effects of pressure on the melting and polymorphism of enstatite. J. geophys. Res., 69, 2101-2109.
- BOYD, F.R. and SCHAIRER, J.F., 1964. The system  $MgSiO_3-CaMgSi_2O_6$ .  
J. Petrology, 5, 275-309.



- BRIDGWATER, D., 1967. Feldspathic inclusions in the Gardar igneous rocks of south Greenland and their relevance to the formation of major anorthosites in the Canadian Shield. *Can. J. Earth Sci.*, 4, 995-1014.
- BROOKS, C.K., 1968. On the interpretation of trends in element ratios in differentiated igneous rocks, with particular reference to strontium and calcium. *Chemical geol.*, 3, 15-20.
- BROTHERS, R.N., 1964. Petrofabric analyses of Rhum and Skaergaard layered rocks. *J. Petrology*, 5, 255-274.
- BROWN, G.M., 1956. The layered ultrabasic rocks of Rhum, Inner Hebrides. *Trans. R. phil. Soc. Lond.*, (B), 240, 1-53.
- BROWN, G.M., 1961. Co-existing pyroxenes in igneous assemblages: a re-evaluation of the existing data on tie-line orientations. *Geol. Mag.*, 98, 333-343.
- BROWN, G.M., 1967. Mineralogy of basaltic rocks, in *Basalts*, Vol. 1, H.H. Hess and A. Poldervaart, (Eds.). Interscience Publishers, N.Y. 482 p.
- BRUYNZEEL, D., 1957. A petrographic study of the Waterfall Gorge profile at Insizwa. *Annals Univ. Stellenbosch*, 33, A, 484-535.
- BUDDINGTON, A.F., 1936. Gravity stratification as a criterion in the interpretation of the structure of certain intrusives of the northwestern Adirondacks. *Rept. 16th Internat. geol. Congr.*, Washington.
- BUDDINGTON, A.F., 1939. Adirondack igneous rocks and their metamorphism. *Mem. geol. Soc. Am.*, 7, 354 p.
- BUDDINGTON, A.F., 1963. Isograds and the role of H<sub>2</sub>O in metamorphic facies of orthogneisses of the northwest Adirondack area, New York. *Bull. geol. Soc. Am.*, 74, 1155-1182.
-

- BURKE, J.E. and TURNBULL, D., 1952. Recrystallization and grain growth. *Prog. Metal Phys.*, 3, 220-292.
- BURLEY, B.J., FREEMAN, E.B. and SHAW, D.M., 1961. Studies on scapolite. *Can. Miner.*, 6, 670-679.
- BURNS, R.G., 1966. Origin of optical pleochroism in orthopyroxenes. *Mineralog. Mag.*, 35, 715-719.
- BURNS, R.G., 1968. Crystal field phenomena and iron enrichments in pyroxenes and amphiboles, in 5th General mtg., *Int. Mineralog. Assoc.* (1966) pp. 170-183.
- BURNS, R.G. and FYFE, W.S., 1967. Crystal-field theory and the geochemistry of transition elements, in *Researches in geochemistry*, 2, P.H. Abelson (Ed.). John Wiley and Sons, Inc., N.Y., 259-285.
- BUTLER, J.R. and SKIBA, W., 1962. Strontium in plagioclase feldspars from four layered basic masses in Somalia. *Mineralog. Mag.*, 33, 213-225.
- BYERLEE, J.D. and BRACE, W.F., 1968. Stick slip, stable sliding, and earthquakes - effect of rock type, pressure, strain rate and stiffness. *J. geophys. Res.*, 73, 6031-6037.
- CAMERON, E.N., 1963. Structure and rock sequences of the Critical Zone of the eastern Bushveld Complex. *Spec. Pap., Miner. Soc. Am.*, 1, 93-107.
- CAMERON, E.N., 1969. Postcumulus changes in the eastern Bushveld complex. *Am. Miner.*, 54, 754-779.
- CARMICHAEL, D.M., 1968. On the mechanism of prograde metamorphic reactions in quartz-bearing pelitic rocks. *Contr. Miner. Petrology*, 20, 244-267.
- CARMICHAEL, I.S.E., 1963. The crystallization of feldspar in volcanic acid liquids. *Q. Jl geol. Soc. Lond.*, 119, 95-131.
-

- CARPENTER, J.R., 1968. Apparent retrograde metamorphism. Another example of the influence of structural deformation on metamorphic differentiation. *Contr. Miner. Petrology*, 17, 173-186.
- CARR, R.M., 1968. The problem of quartz - corundum stability. *Am. Miner.*, 53, 2092-2095.
- CARSTENS, H., 1958. Note on the distribution of some minor elements in co-existing ortho- and clino-pyroxene. *Norsk geol. Tidsskr.*, 38, 257-260.
- CARSTENS, H., 1967. Exsolution in ternary feldspars. I. On the formation of antiperthites. *Contr. Miner. Petrology*, 14, 27-35.
- CARTER, N.L., CHRISTIE, J.M. and GRIGGS, D.T., 1964. Experimental deformation and recrystallization of quartz. *J. Geol.*, 72, 687-733.
- CARTER, N.L. and RALEIGH, C.B., 1969. Principle stress directions from plastic flow in crystals. *Bull. geol. Soc. Am.*, 80, 1231-1264.
- CHALLIS, G.A., 1965. The origin of New Zealand ultramafic intrusions. *J. Petrology*, 6, 322-364.
- CHESNOKOV, B.V., 1959. Spectral absorption curves of certain minerals coloured by titanium. *Doklady, Akad. Nauk SSSR (English translation)*, 129, 1162-1163.
- CHINNER, G.A., 1960. Pelitic gneisses with varying ferrous/ferric ratios from Glen Cova, Angus, Scotland. *J. Petrology*, 1, 178-217.
- CHINNER, G.A., 1966. The distribution of pressure and temperature during Dalradian metamorphism. *Q. Jl Geol. Soc. Lond.*, 122, 159-186.
-

- CHINNER, G.A., SMITH, J.V. and KNOWLES, C.R., 1969. Transition metal contents of  $Al_2SiO_5$  polymorphs. *Am. J. Sci.*, 267-A, Schairer Vol., 96-113.
- CHRISTIE, J.M., 1960. Mylonitic rocks of the Moine thrust-zone in the Assynt region, north-west Scotland. *Trans. Edin. geol. Soc.*, 18, 79-93.
- CHRISTIE, J.M., 1963. The Moine thrust zone in the Assynt region northwest Scotland. *Univ. California Pub. Geological Sciences*, 40, 345-440.
- CHUDOBA, K. and KENNEDY, W.Q., 1933. The determination of the feldspars in thin section. Thomas Murby, London. 61 p.
- CLOOS, H., 1946. Lineation. *Mem. geol. Soc. Am.*, 18, 122 p.
- COATES, R.P., 1963. Geology of the Alberga 4-mile military sheet. *Geol. Surv. S. Aust. Rep. Invest.*, 22.
- COMPSTON, W. and ARRIENS, P.A., 1968. The Precambrian geochronology of Australia. *Can. J. Earth Sci.*, 5, 561-583.
- COMPSTON, W. and NESBITT, R.W., 1967. Isotopic age of the Tollu volcanics, W.A. *J. geol. Soc. Aust.*, 14, 235-238.
- COORAY, P.G., 1962. Charnockites and their associated gneisses in the pre-Cambrian of Ceylon. *Q. Jl geol. Soc. Lond.*, 118, 239-273.
- COORAY, P.G. and KUMARAPALI, P.S., 1960. Corundum in biotite-sillimanite gneiss from near Polgahawela, Ceylon. *Geol. Mag.*, 97, 480-487.
- COUSINS, C.A., 1959. The structure of the mafic portion of the Bushveld igneous complex. *Trans. geol. Soc. S. Afr.*, 62, 179-189.

- CURTIS, C.D., 1964. Applications of the crystal-field theory to the inclusion of trace transition elements in minerals during magnetic differentiation. *Geochim. cosmochim. Acta*, 28, 389-403.
- DALLWITZ, W.B., 1968. Co-existing sapphirine and quartz in granulite from Enderby Land, Antarctica. *Nature*, 219, 476-477.
- DANIELS, J.L., 1967. Subdivision of the Giles Complex, Central Australia. *Ann. Rep. geol. Surv. West. Aust. for 1966*, 58-62.
- DAVIDSON, L.R., 1968. Variation in ferrous iron-magnesium distribution coefficients of metamorphic pyroxenes from Quairading, Western Australia. *Contr. Miner. Petrology*, 19, 239-259.
- DAVIS, B.T.C. and BOYD, F.R., 1966. The join  $Mg_2Si_2O_6 - CaMg_2Si_2O_6$  at 30 kilobars pressure and its application to pyroxenes from kimberlites. *J. geophys. Res.*, 71, 3567-3576.
- DAVIS, B.L., RAPP, G. and WALAWENDER, M.J., 1968. Fabric and structural characteristics of the martitization process. *Am. J. Sci.*, 266, 482-496.
- DEER, W.A., HOWIE, R.A. and ZUSSMAN, J., 1963. Rock forming minerals, V. 1-5. Longmans, London.
- DEER, W.A., HOWIE, R.A. and ZUSSMAN, J., 1965. An introduction to the rock forming minerals. Longmans, London, 528 p.
- DEN TEX, E., 1965. Metamorphic lineages of orogenic plutonism. *Geol. Mijnbouw*, 44, 105-132.
- DESBOROUGH, G.A. and CAMERON, E.N., 1968. Composition and structural state of plagioclases from the lower part of the eastern Bushveld complex, South Africa. *Am. Miner.*, 53, 116-122.

- DE VORE, G.W., 1957. The association of strongly polarizing cations with weakly polarizing cations as a major influence in element distribution, mineral composition and crystal growth. *J. Geol.*, 65, 178-195.
- DE VORE, G.W., 1966. Elastic strain energy and mineral recrystallization: a commentary on rock deformation. *Contr. Geol.*, 5, 19-43.
- DE WAARD, D., 1964. Mineral assemblages and metamorphic subfacies in the granulite-facies terrane of the Little Moose Mountain syncline, south-central Adirondack highlands. *Proc. K. ned. Akad. Wet.*, B, 67, 344-362.
- DE WAARD, D., 1965. A proposed subdivision of the granulite facies. *Am. J. Sci.*, 263, 455-461.
- DE WAARD, D., 1965a. The occurrence of garnet in the granulite-facies terrane of the Adirondack highlands. *J. Petrology*, 6, 165-191.
- DE WAARD, D., 1967a. Absolute P-T conditions of granulite facies metamorphism in the Adirondacks. *Proc. K. ned. Akad. Wet.*, B, 70, 400-410.
- DE WAARD, D., 1967b. The occurrence of garnet in the granulite-facies terrane of the Adirondack highlands and elsewhere, an amplification and a reply. *J. Petrology*, 8, 210-232.
- DOBRETISOV, N.L., 1968. Paragenetic types and compositions of metamorphic pyroxenes. *J. Petrology*, 9, 358-377.
- DUNITZ, J.D. and ORGEL, L.E., 1957. Electronic properties of transition metal oxides - II. *J. Phys. Chem. Solids*, 3, 317-323.

- ECKELMANN, F.D. and POLDERVAART, A., 1957. Geologic evolution of the Beartooth Mountains, Montana and Wyoming. Bull. geol. Soc. Am., 68, 1225-1261.
- ENGEL, A.E.J. and ENGEL, C.G., 1958. Progressive metamorphism and granitization of the major paragneiss, northwest Adirondack Mountains, New York. Part I. Total rock. Bull. geol. Soc. Am., 69, 1369-1414.
- ENGEL, A.E.J. and ENGEL, C.G., 1960. Migration of elements during metamorphism in the northwest Adirondack Mountains, New York. U.S. Geol. Surv., Prof. Pap. 400-B, 465-470.
- ENGEL, A.E.J. and ENGEL, C.G., 1962. Progressive metamorphism of amphibolite, northwest Adirondack Mountains, New York, in Petrologic studies, Engel, A.E.J., James, H.L. and Leonard, B.F. (Ed.). Geol. Soc. Am., Buddington Volume, 37-82.
- ENGEL, A.E.J., ENGEL, C.G. and HAVENS, R.G., 1964. Mineralogy of amphibolite interlayers in the gneiss complex, northwest Adirondack Mountains, New York. J. Geol., 72, 131-156.
- ENGELS, J.P. and VOGEL, D.E., 1966. Garnet reaction-rims between plagioclase and hypersthene in a metanorite from Cabo Ortegal (N.W. Spain). Neues Jb. Miner. Mh., 13-18.
- ESKOLA, P., 1952. On the granulites of Lapland. Am. J. Sci., Bowen Volume, 133-171.
- ESKOLA, P., 1954. On the granulites of Lapland. Am. J. Sci., Bowen Volume, 136-146.
- EUGSTER, H.P., 1955. The cesium-potassium equilibrium in the system sanidine-water. Carnegie Inst. Washington, Yearbook 54, 112-113.
-

- EUGSTER, H.P. and WONES, D.R., 1962. Stability relations of the ferruginous biotite, annite. *J. Petrology*, 3, 82-125.
- EWART, A. and TAYLOR, S.R., 1969. Trace element geochemistry of the rhyolitic volcanic rocks, central North Island, New Zealand. Phenocryst data. *Contr. Miner. Petrology*, 22, 127-146.
- FACER, R.A., 1967. A preliminary study of the magnetic properties of rocks from the Giles Complex, Central Australia. *Aust. J. Sci.*, 30, 237-238.
- FAHEY, J.J., 1946. A volumetric method for the determination of carbon dioxide, *in* Contributions to geochemistry, 1942-45, *Bull. geol. Surv. Am.*, 950, 139-141.
- FERGUSON, J. and PULVERTAFT, T.C.R., 1963. Contrasted styles of igneous layering in the Gardar Province of south Greenland. *Miner. Soc. Am., Spec. Pap.* 1, 10-21.
- FLINN, D., 1965. Deformation in metamorphism, *in* Controls of metamorphism, Pitcher, W.S. and Flinn, G.W. (Ed.). Oliver and Boyd, Edinburgh and London, 368 p.
- FORBES, B.G., 1966. Features of Palaeozoic tectonism in South Australia. *Trans. R. Soc. S. Aust.*, 90, 45-56.
- FORMAN, D.J., 1966. The geology of the south western margin of the Amadeus Basin, central Australia. *Rept. Bur. Miner. Res., Geol. Geophys. Aust.*, 87.
- FOSTER, R.J., 1962. Precambrian corundum-bearing rocks, Madison Range, southwestern Montana. *Bull. geol. Soc. Am.*, 73, 131-138.
- FRANKEL, J.J. and KENT, L.E., 1937. Grahamstown surface quartzites (silcretes). *Trans. geol. Soc. S. Afr.*, 40, 1-42.
-



- FRIEDMAN, G.M., 1955. Petrology of the Memesagamesing Lake norite mass, Ontario, Canada. *Am. J. Sci.*, 253, 590-608.
- FRODESEN, S., 1968. Coronas around olivine in a small gabbro intrusion, Bamble area, south Norway. *Norsk geol. Tidsskr.*, 48, 201-206.
- GAY, P. and MUIR, I.D., 1962. Investigation of the feldspars of the Skaergaard intrusion, east Greenland. *J. Geol.*, 70, 565-581.
- GHOSE, S., 1965.  $Mg^{2+} - Fe^{2+}$  order in an orthopyroxene,  $Mg_{0.93}Fe_{1.07}Si_2O_6$ . *Z. Kristallogr.*, 122, 81-99.
- GILES, E., 1874. Parl. Paper S. Aust., Paper 215, 1-67 (with map). "Mr. E. Gile's explorations, 1873".
- GLAESSNER, M.F. and PARKIN, L.W., 1958. The geology of South Australia. *J. geol. Soc. S. Aust.*, 5, 1-163.
- GLAESSNER, M.F., PREISS, W.V. and WALTER, M.R., 1969. Precambrian columnar stromatolites in Australia: morphological and stratigraphic analysis. *Science*, 164, 1056-1058.
- GOLDSMITH, J.R., 1952. Diffusion in plagioclase feldspar. *J. Geol.*, 60, 288-291.
- GOODE, A.D.T. and KRIEG, G.W., 1965. The geology of Ewarara intrusion, Giles Complex, central Australia. Unpublished Honours thesis, Univ. Adelaide.
- GOODE, A.D.T. and KRIEG, G.W., 1967. The geology of the Ewarara intrusion, Giles Complex, central Australia. *J. geol. Soc. Aust.*, 14, 185-194.
- GOODE, A.D.T. and NESBITT, R.W., 1969. Granulites and basic intrusions of part of the eastern Tomkinson Ranges, central Australia. Paper read at Granulite Facies Symposium, Canberra. Now published in *Spec. Publs geol. Soc. Aust.*, 2, 279-281.

- GOSSE, W.C., 1874. Parl. Paper S. Aust., Paper 48, 1-69.  
"W.C. Gosse's explorations, 1873".
- GRAY, C.M., 1967. The geology, petrology and geochemistry of the Teizi metanorthite<sup>os</sup>. Unpublished Honours thesis, Univ. Adelaide.
- GREEN, D.H., 1963. Alumina content of enstatite in a Venezuelan high-temperature peridotite. Bull. geol. Soc. Am., 74, 1397-1402.
- GREEN, D.H. and LAMBERT, I.B., 1965. Experimental crystallization of anhydrous granite at high pressures and temperatures. J. geophys. Res., 70, 5259-5267.
- GREEN, D.H. and RINGWOOD, A.E., 1967. An experimental investigation of the gabbro to eclogite transformation and its petrological implications. Geochim. cosmochim. Acta, 31, 767-833.
- GREEN, D.H. and RINGWOOD, A.E., 1967a. The genesis of basaltic magmas. Contr. Miner. Petrology, 15, 103-190.
- GREEN, T.H., 1967. An experimental investigation of sub-solidus assemblages formed at high pressure in high alumina basalt, kyanite eclogite and grosspydrite compositions. Contr. Miner. Petrology, 16, 84-116.
- GREEN, T.H., 1969. High pressure experimental studies on the origin of anorthosite. Can. J. Earth Sci., 6, 427-440.
- GREENWOOD, H.J., 1961. The system  $\text{NaAlSi}_2\text{O}_6 - \text{H}_2\text{O} - \text{argon}$ : total pressure and water pressure in metamorphism. J. geophys. Res., 66, 3923-3946.
- GRIGGS, D.T., PATERSON, M.S., HEARD, H.C. and TURNER, F.J., 1960. Annealing recrystallization in calcite crystals and aggregates. Mem. geol. Soc. Am., 79, 21-37.

- GUIDOTTI, C.V., 1963. Metamorphism of the pelitic schists in the Bryant Pond quadrangle, Maine. *Am. Miner.*, 48, 772-791.
- HAGNER, A.F. and COLLINS, L.G., 1967. Magnetite ore formed during regional metamorphism, Ausable magnetite district, New York. *Econ. Geol.*, 62, 1034-1071.
- HALL, A., 1965. Determination of the composition of zoned plagioclases from granitic rocks. *Am. Miner.*, 50, 427-435.
- HAMILTON, E.I., 1963. The isotopic composition of strontium in the Skaergaard intrusion, E. Greenland. *J. Petrology*, 4, 383-391.
- HARKER, A., 1895. *Petrology for students*, 1st Ed. (8th Ed., 1954). Cambridge University Press, Cambridge. 283 p.
- HARLEY, D.N., 1969. The mafic and ultramafic intrusives of the Fraser Range, Western Australia. Unpublished Honours thesis, Univ. Adelaide.
- HARTMAN, P., 1969. Can  $Ti^{4+}$  replace  $Si^{4+}$  in silicates? *Mineralog. Mag.*, 37, 366-369.
- HAWKES, D.D., 1967. Order of abundant crystal nucleation in a natural magma. *Geol. Mag.*, 104, 473-486.
- HAYS, J.F., 1966. Stability and properties of the synthetic pyroxene  $CaAl_2SiO_6$ . *Am. Miner.*, 51, 1524-1529.
- HEARD, H.C., 1963. Effect of large changes in strain rate in the experimental deformation of Yule marble. *J. Geol.*, 71, 162-195.
- HEIER, K.S., 1957. Phase relations of potash feldspar in metamorphism. *J. Geol.*, 65, 468-479.

- HEIER, K.S., 1961. The amphibolite-granulite facies transition reflected in the mineralogy of potassium feldspars. Cursillos Conf., Inst. "Lucas Malada", VIII, 131-137.
- HEIER, K.S., 1965. Metamorphism and the chemical differentiation of the crust. Geol. Fören. Stockh. Förhandl., 87, 249-256.
- HENRY, N.M.F., 1942. Lamellar structure of orthopyroxenes. Mineralog. Mag., 26, 179-188.
- HENSEN, B.J., 1969. Experimental data on the stability of cordierite and garnet in high-grade metamorphic rocks. Paper read at Granulite Facies Symposium, Canberra. Now published by Hensen, B.J. and Green, D.H., Spec. Publs geol. Soc. Aust., 2, 345-347.
- HERMES, O.D., 1968. Petrology of the Mecklenburg gabbro-metagabbro complex, north Carolina. Contr. Miner. Petrology, 18, 270-294.
- HESS, H.H., 1955. Serpentinities, orogeny and epeirogeny. Geol. Soc. Am., Spec. Pap., 62, 391-408.
- HESS, H.H., 1960. Stillwater igneous complex, Montana. Mem. geol. Soc. Am., 80, 230 p.
- HESS, H.H. and PHILLIPS, A.H., 1938. Orthopyroxenes of the Bushveld type. Am. Miner., 23, 450-456.
- HESS, H.H. and PHILLIPS, A.H., 1940. Optical properties and chemical composition of magnesian orthopyroxenes. Am. Miner., 25, 271-285.
- HIETANEN, A., 1967. On the facies series in various types of metamorphism. J. Geol., 75, 187-214.
- HOBBS, B.E., 1968. Recrystallization of single crystals of quartz. Tectonophysics, 6, 353-401.

- HOFFER, J.M., 1968. Order-disorder relationships of plagioclase in a porphyritic basalt flow. *Am. Miner.*, 53, 908-916.
- HOLLAND, Th.H., 1900. The charnockite series, a group of Archaean hypersthenic rocks in Peninsular India. *Mem. geol. Surv. India*, 28, 119-249.
- HORWITZ, R.C., 1967. Provisional subdivisions of the Precambrian in Western Australia, 1966. *Geol. Surv. West. Aust. a. Rep. (1966)*, 58.
- HORWITZ, R.C. and DANIELS, J.L., 1967. A late Precambrian belt of vulcanicity in central Australia. *Ann. Rep. geol. Surv. West. Aust. for 1966*, 50-53.
- HORWITZ, R.C., DANIELS, J.L. and KRIEVALDT, M.J.B., 1967. Structural layering in the Precambrian of the Musgrave block, Western Australia. *Ann. Rep. geol. Surv. West. Aust. for 1966*, 56-58.
- HOSSFELD, P.S., 1954. Stratigraphy and structure of the Northern Territory of Australia. *Trans. R. Soc. S. Aust.*, 77, 103-161.
- HOWIE, R.A., 1955. The geochemistry of the charnockite series of Madras, India. *Trans. roy. Soc. Edinburgh*, 62, 725-768.
- HOWIE, R.A., 1963. Cell parameters of orthopyroxenes. *Spec. Pap. Min. Soc. Am.*, 1, 213-222.
- HUBBARD, F.H., 1965. Antiperthite and mantled feldspar textures in charnockite (enderbite) from south-west Nigeria. *Am. Miner.*, 50, 2040-2051.
- HUBBARD, F.H., 1966. Myrmekite in charnockite from south-west Nigeria. *Am. Miner.*, 51, 762-773.

- ILIC, M., 1968. Genesis of magnesite deposits. Geol. Zborník - geol. Carpathica, 19, 149-160.
- IL'VITSKIY, M.I. and KOLBANTSEV, R.V., 1968. Paragenetic types of olivine and statistical analysis of their chemistry. Doklady Akad. Nauk, SSSR, 179, 1428-1432. (Translated by A.G.I., 179, 135-138).
- INGHAM, K.W., 1957. X-ray investigation of a hypersthene. Unpublished M.Sc. thesis, Univ. Manchester.
- IRVINE, T.N. and SMITH, C.H., 1967. The ultramafic rocks of the Muskox Intrusion, Northwest Territories, Canada, in Ultramafic and related rocks, P.J. Wyllie (Ed.). John Wiley and Sons, Inc., N.Y. 464 p.
- ITO, T., 1950. X-ray studies on polymorphism, Maruzen Co. Ltd., Tokyo, 30-41.
- JACKSON, E.D., 1961. Primary textures and mineral associations in the ultramafic zone of the Stillwater Complex, Montana. U.S. Geol. Surv. Prof. Pap. 358, 106 p.
- JACKSON, E.D., 1961a. X-ray determinative curve for some natural plagioclases of composition  $An_{60-85}$ . U.S. geol. Surv. Prof. Pap. 424C, 286-288.
- JACKSON, E.D., 1967. Ultramafic cumulates in the Stillwater, Great Dyke, and Bushveld intrusions, in Ultramafic and related rocks, P.J. Wyllie (Ed.). John Wiley and Sons, Inc., N.Y. 464 p.
- JACKSON, E.D., 1970. Xenoliths in Hawaiian basalts - fragments of the lower crust and upper mantle. Abstract only. Paper presented at Int. Symp. on Phase transformations and the earth's interior, Canberra, Australia. Jan., 1969.
-

- JOHNSON, J.E., 1963. Basal sediments of the north side of the Officer Basin. Q. geol. Notes, Geol. Surv. S. Aust., 7.
- JOHNSON, M.R.W., 1963. Some time relations of movement and metamorphism in the Scottish Highlands. Geologie Mijnb., 42, 121-142.
- JOHNSON, M.R.W., 1967. Mylonite zones and mylonite banding. Nature, 213, (5073), 246-247.
- JONES, J.B., NESBITT, R.W. and SLADE, P.G., 1969. The determination of the orthoclase content of homogenised alkali feldspars using the  $\bar{201}$  X-ray method. Miner. Mag., 37, 489-496.
- JONES, N.W., RIBBE, P.H. and GIBBS, G.V., 1969. Crystal chemistry of humite. Am. Miner., 54, 391-411.
- KATZ, M., 1968. The fabric of the granulites of Mont Tremblant Park, Quebec. Can. J. Earth Sci., 5, 801-812.
- KING, W. and FOOTE, R.B., 1864. On the geological structure of portions of Madras. Mem. geol. Surv. India, 4, 223-379.
- KLEEMAN, A.W., 1965. The origin of granitic magmas. J. geol. Soc. Aust., 12, 35-52.
- KLEEMAN, J.D., 1965. Studies on the X-ray diffraction, analysis and geochemistry of plagioclase from the Mount Davies intrusion. Unpublished Honours thesis, Univ. Adelaide.
- KLEEMAN, J.D., 1969. Fission track studies and the geochemistry of uranium in rocks from the crust and upper mantle. Unpublished Ph.D. thesis, Australian National University, Canberra. 198 p.
- KLEEMAN, J.D. and NESBITT, R.W., 1967. X-ray measurements on some plagioclases from the Mt. Davies Intrusion, South Australia. J. geol. Soc. Aust., 14, 39-42.

- KRETZ, R., 1959. Chemical study of garnet, biotite and hornblende from gneisses of southwestern Quebec, with emphasis on the distribution of elements in co-existing minerals. *J. Geol.*, 67, 371-402.
- KRETZ, R., 1961. Co-existing pyroxenes. *Geol. Mag.*, 98, 344-345.
- KRETZ, R., 1961a. Some applications of thermodynamics to co-existing minerals of variable composition. Examples: orthopyroxene-clinopyroxene and orthopyroxene-garnet. *J. Geol.*, 69, 361-387.
- KRETZ, R., 1963. Distribution of magnesium and iron between orthopyroxene and calcic pyroxene in natural mineral assemblages. *J. Geol.*, 69, 361-387.
- KRETZ, R., 1966. Interpretation of the shape of mineral grains in metamorphic rocks. *J. Petrology*, 7, 68-94.
- KRISHNA, R.J.S.R. and MURTHY, R.T., 1968. Occurrence and paragenesis of diopside-scapolite gneisses from Visakhapatnam. *Bull. geol. Soc. India*, 5, 19-21.
- KULLBACH, S., 1959. Information theory and statistics, John Wiley and Sons, Inc., N.Y. 359 p.
- KUSHIRO, I., 1964. The system diopside-forsterite-enstatite at 20 kilobars, *in* P.H. Abelson, Ann. Rept. Director Geophys. Lab., Carnegie Inst. Washington, Yearbook 63, 101-108.
- KUSHIRO, I. and SCHAIRER, J.F., 1963. New data on the system diopside-forsterite-silica, *in* P.H. Abelson, Ann. Rept. Director Geophys. Lab., Carnegie Inst. Washington, Yearbook 62, 95-103.
- KUSHIRO, I. and YODER, H.S., 1966. Anorthite-forsterite and anorthite-enstatite reactions and their bearing on the basalt-eclogite transformation. *J. Petrology*, 7, 337-362.



- KVALE, A., 1953. Linear structures and their relation to movement in the Caledonides of Scandinavia and Scotland. *Q. Jl geol. Soc. Lond.*, 109, 51-73.
- KWESTROO, W., 1959. Spinel phase in the system  $MgO-Fe_2O_3-Al_2O_3$ . *J. Inorg. Nucl. Chem.*, 9, 65-70.
- LAMBERT, I.B. and HEIER, K.S., 1968. Geochemical investigations of deep-seated rocks in the Australian shield. *Lithos*, 1, 30-53.
- LAMPLUGH, G.W., 1902. Calcrete. *Geol. Mag.*, 9, 575.
- LAMPLUGH, G.W., 1907. The geology of the Zambesi basin. *Q. Jl geol. Soc. Lond.*, 63, 198.
- LAPWORTH, C., 1885. The highland controversy in British geology: its causes, course and consequences. *Nature*, 32, 558-559.
- LAVES, F. and SOLDATOS, K., 1963. Die Albit-Mikroklin-Orientierungs-Beziehungen in Mikroklinperthiten und deren genetische Deutung. *Z. Kristallogr.*, 118, 69-102.
- LEAKE, B., 1968. Optical properties and composition in the orthopyroxene series. *Mineralog. Mag.*, 36, 745-746.
- LEAVITT, F.G. and SLEMMONS, D.B., 1962. Observations on order-disorder relations of natural plagioclase, IV. Order-disorder relations in plagioclase of the White Mountain and New Hampshire magma series. *Norsk geol. Tidsskr.*, 42 (Feldspar vol.), 578-585.
- LEELANANDAM, C., 1967. Chemical study of pyroxenes from the charnockitic rocks of Kondapalli (Andhra Pradesh), India, with emphasis on the distribution of elements in co-existing pyroxenes. *Mineralog. Mag.*, 36, 153-179.
- LEITH, C.K., 1905. Rock cleavage. *Bull. U.S. geol. Surv.*, 239, 216 p.

- LE BAS, M.J., 1962. The role of aluminium in igneous clinopyroxenes with relation to their parentage. *Am. J. Sci.*, 260, 267-288.
- LE MAITRE, R.W., 1962. Petrology of volcanic rocks, Gough Island, south Atlantic. *Bull. geol. Soc. Am.*, 73, 1309-1340.
- LE MAITRE, R.W., 1965. The significance of the gabbroic xenoliths from Gough Island, south Atlantic. *Mineralog. Mag.*, 34 (Tilley Vol.), 303-317.
- LINDSLEY, D.H., 1966. Melting relations of plagioclase at high pressures, *in* P.H. Abelson, *Ann. Rept. Director Geophys. Lab., Carnegie Inst. Washington, Yearbook* 65, 204-205.
- LOMBAARD, B.V., 1934. On the differentiation and relationships of the rocks of the Bushveld igneous complex. *Trans. geol. Soc. S. Afr.*, 37, 5-52.
- LOVERING, J.F. and WHITE, A.J.R., 1964. The significance of primary scapolite in granulitic inclusions from deep-seated pipes. *J. Petrology*, 5, 195-218.
- LOVERING, J.F. and WHITE, A.J.R., 1969. Granulitic and eclogitic inclusions from basic pipes at Delegate, Australia. *Contr. Miner. Petrology*, 21, 9-52.
- LUTH, W.C. and TUTTLE, O.F., 1966. The alkali feldspar solvus in the system  $\text{Na}_2\text{O}-\text{K}_2\text{O}-\text{Al}_2\text{O}_3-\text{H}_2\text{O}$ . *Am. Miner.*, 51, 1359-1373.
- MACKENZIE, D.B., 1960. High-temperature alpine-type peridotite from Venezuela. *Bull. geol. Soc. Am.*, 71, 303-318.
- MACRAE, N.D., 1969. Ultramafic intrusions of the Abitibi area, Ontario. *Can. J. Earth Sci.*, 6, 281-303.

- MAJOR, R.B., 1966. Preliminary notes on the geology of the Woodroffe 1:250,000 sheet area. S. Aust. Dept. Mines, Rept. 639/66.
- MAJOR, R.B., JOHNSON, J.E., LEESON, B. and MIRAMS, R.C., 1967. Geological atlas of South Australia, Sheet Woodroffe, 1:250,000 series.
- MAJOR, R.B. and TELUK, J.A., 1967. The Kulyong volcanics. Quart. notes Geol. Surv. S. Aust., 22, 8-11.
- MARSHALL, B., 1967. The present status of zircon. Sedimentology, 2, 119-136.
- MARSHALL, B., 1969. Zircon and ultrametamorphism. Paper read at Granulite Facies Symposium, Canberra. Now published as Zircon behaviour during extreme metamorphism, Spec. Publs geol. Soc. Aust., 2, 349-351.
- MASON, R., 1967. Electron probe microanalysis of coronas in a troctolite from Sulitjehna, Norway. Mineralog. Mag., 36, 504-514.
- MATHISON, C.I., 1967. The Somerset Dam layered basic intrusion, southeastern Queensland. J. geol. Soc. Aust., 14, 57-86.
- MCCARTHY, W.R., 1964. Petrography of granulites and associated rocks, in "The geology of the Mann 4-mile sheet". Rept. Invest. Dept. Mines S. Aust., 25, 21-30.
- MCDONALD, J.A., 1967. Evolution of a part of the lower Critical Zone, Farm Ruighoek, western Bushveld. J. Petrology, 8, 165-209.
- McINTIRE, W.L., 1963. Trace element partition coefficients - a review of theory and applications to geology. Geochim. cosmochim. Acta, 27, 267-296.

- McKIE, D., 1959. Yoderite, a new hydrous magnesium iron aluminosilicate from Mautia Hill, Tanganyika. *Mineralog. Mag.*, 32, 282-307.
- McKIE, D., 1963. The hōgbomite polytypes. *Mineralog. Mag.*, 33, 563-580.
- MEHNERT, K.R., 1968. *Migmatites*. Elsevier, Amsterdam. 393 p.
- MEIER, M.M., RIGSBY, G.P. and SHARP, R.P., 1954. Preliminary data from Saskatchewan Glacier, Alberta, Canada. *Arctic*, 7, 3-26.
- MICHOT, P., 1951. Essai sur la geologie de la catazone. *Bull. Acad. R. de Belgique, classe des sciences*, 37, 5 ser., 271-272.
- MILLER, C., 1966. A geochemical study of clinopyroxenes from the igneous intrusion, south Davies, N.W. South Australia. Unpublished Honours thesis, Univ. Adelaide.
- MIRAMS, R.C., 1964. "The geology of the Mann 4-mile sheet" with appendix by McCARTHY, W.R., "Petrography of granulites & associated rocks". Dept. Mines S. Aust., Rept. Invest., 25, 1-30.
- MÖCKEL, J.R., 1969. Structural petrology of the garnet-peridotite of Alpe Arami (Ticino, Switzerland). *Leid. geol. Meded.*, 42, 61-130.
- MOORE, A.C., 1968. Rutile exsolution in orthopyroxene. *Contr. Miner. Petrology*, 17, 233-236.
- MOORE, A.C., 1969. Corona textures in granulites from the Tomkinson Ranges, central Australia. Paper read at Granulite Facies Symposium, Canberra. Now published in *Spec. Publs geol. Soc. Aust.*, 2, 361-366.

- MOXHAM, R.L., 1965. Distribution of minor elements in co-existing hornblendes and biotites. *Can. Miner.*, 8, 204-240.
- MUELLER, R.F., 1967. Mobility of elements in metamorphism. *J. Geol.*, 75, 565-582.
- MUIR, I.D. and TILLEY, C.E., 1958. Contributions to the petrology of Hawaiian basalts, I. The picrite basalts of Kilauea. *Am. J. Sci.*, 255, 241-253.
- MURTHY, M.V.N., 1958. Coronites from India and their bearing on the origin of coronas. *Bull. geol. Soc. Am.*, 69, 23-38.
- MURTHY, M.V.N. and SIDDIQUIE, H.N., 1964. Studies of some zircons from some garnetiferous sillimanite gneisses (Khondalites) from Orissa and Andhra Pradesh, India. *J. Geol.*, 72, 123-128.
- NESBITT, R.W., 1966. The Giles igneous province, Central Australia. An example of an eroded volcanic zone. *Bull. volcan.*, 29, 271-282.
- NESBITT, R.W., 1966a. The determination of magnesium in silicates by atomic absorption spectroscopy. *Anal. Chim. Acta*, 35, 413-420.
- NESBITT, R.W. and KLEEMAN, A.W., 1964. Layered intrusions of the Giles Complex, Central Australia. *Nature*, 203, 391-393.
- NESBITT, R.W. and TALBOT, J.L., 1966. The layered basic and ultrabasic intrusives of the Giles Complex, Central Australia. *Contr. Miner. Petrology*, 13, 1-11.
- NESBITT, R.W., GOODE, A.D.T., MOORE, A.C. and HOPWOOD, T.P., (1969). The Giles complex, central Australia: a stratified sequence of basic and ultrabasic intrusions. *Spec. Publs geol. Soc. S. Afr.*, 1. (IN PRESS. May appear in 1970, not 1969).

- NEWTON, R.C., 1966a. Kyanite-sillimanite equilibrium at 750°C.  
Science, 151, 1222-1225.
- NEWTON, R.C., 1966b. Kyanite-andalusite equilibrium from 700° to  
800°C. Science, 153, 170-172.
- NEWTON, R.C., 1969. Some high-pressure hydrothermal experiments  
on severely ground kyanite and sillimanite. Am. J. Sci., 267,  
278-284.
- NORRISH, K. and CHAPPELL, B.W., 1967. X-ray fluorescence spectrography,  
in Physical methods in determinative mineralogy, Zussman, J.  
(Ed.). Academic Press, London. 514 p.
- O'HARA, M.J., 1960. Coexisting pyroxenes in metamorphic rocks.  
Geol. Mag., 96, 498-503.
- O'HARA, M.J., 1963. Melting of garnet peridotite at 30 kb, in  
P.H. Abelson, Ann. Rept. Director Geophys. Lab., Carnegie Inst.  
Washington, Yearbook 62, 71-76.
- O'HARA, M.J., 1967. Mineral parageneses in ultrabasic rocks, in  
Ultramafic and related rocks, Wyllie, P.J. (Ed.). John Wiley  
and Sons, Inc., N.Y. 464 p.
- O'HARA, M.J. and MERCY, E.L.P., 1963. Petrology and petrogenesis  
of some garnetiferous peridotites. Trans. roy. Soc. Edinburgh,  
65, 251-314.
- O'HARA, M.J. and STEWART, F.H., 1966. Olivine-liquid reaction and  
the depth of crystallization of the east Aberdeenshire gabbros.  
Nature, 210, 830-831.
- OOSTEROM, M.G., 1963. The ultramafites and layered gabbro sequences  
in granulite facies rocks on Stjernøy (Finnmark, Norway).  
Leid. geol. Meded., 28, 177-296.

- ORVILLE, P.M., 1963. Alkali ion exchange between vapor and feldspar phases. *Am. J. Sci.*, 261, 201-237.
- ORVILLE, P.M., 1969. A model for metamorphic differentiation origin of thin-layered amphibolites. *Am. J. Sci.*, 267, 64-86.
- PANKHURST, R.J., 1969. Strontium isotope studies related to petrogenesis in the Caledonian basic igneous province of NE. Scotland. *J. Petrology*, 10, 115-143.
- PARRAS, K., 1958. On the charnockites in the light of a highly metamorphic rock complex in southwestern Finland. *Bull. Commn géol. Finl.*, 181, 1-37.
- PATERSON, M.S. and WEISS, L.E., 1961. Symmetry concepts in the structural analysis of deformed rocks. *Bull. geol. Soc. Am.*, 72, 841-882.
- PETERS, T.J., 1968. Distribution of Mg, Fe, Al, Ca and Na in coexisting olivine, orthopyroxene and clinopyroxene in the Totalp serpentinite (Davos, Switzerland) and in the Alpine metamorphosed Malenco serpentinite (N. Italy). *Contr. Miner. Petrology*, 18, 65-75.
- PHILIBERT, J., 1963. A method of calculating the absorption correction in electron-probe microanalysis, in X-ray optics and X-ray microanalysis - 3rd Symposium. Patee, H.H., Cosslett, V.E. and Engström, A. (Eds.). Academic Press, N.Y. 380 p.
- PHILLIPS, E.R. and RANSOM, D.M., 1968. The proportionality of quartz in myrmekite. *Am. Miner.*, 53, 1411-1413.
- PHILPOTTS, A.R., 1964. Origin of pseudotachylites. *Am. J. Sci.*, 262, 1008-1035.

- PHILPOTTS, A.R., 1966. Origin of the anorthosite-mangerite rocks in southern Quebec. *J. Petrology*, 7, 1-64.
- PHINNEY, W.C., 1963. Phase equilibria in the metamorphic rocks of St. Paul Island and Cape North, Nova Scotia. *J. Petrology*, 4, 90-130.
- POLDERVAART, A. and HESS, H.H., 1951. Pyroxenes in the crystallization of basaltic magma. *J. Geol.*, 59, 472-489.
- PRESNALL, D.D., 1966. The join forsterite-diopside-iron oxide and its bearing on the crystallization of basic and ultramafic magmas. *Am. J. Sci.*, 264, 753-809.
- PRESTON, J., 1966. An unusual hourglass structure in augite. *Am. Miner.*, 51, 1227-1233.
- PRINZ, M. and POLDERVAART, A., 1964. Layered mylonite from Beartooth Mountains, Montana. *Bull. geol. Soc. Am.*, 75, 741-744.
- QUENSEL, P., 1916. Zur Kenntnis der Mylonitbildung, erläutert an material aus dem Kebnekaisegebiet. *Bull. geol. Inst. Univ. Uppsala*, 15, 91-116.
- RALEIGH, C.B. and TALBOT, J.L., 1967. Mechanical twinning in naturally and experimentally deformed diopside. *Am. J. Sci.*, 265, 151-165.
- RAMBERG, H., 1948. Titanic iron ore formed by dissociation of silicates in granulite facies. *Econ. Geol.*, 43, 553-570.
- RAMBERG, H. and DEVORE, G., 1951. The distribution of  $Fe^{++}$  and  $Mg^{++}$  in coexisting olivines and pyroxenes. *J. Geol.*, 59, 193-210.
- RAMDOHR, P., 1960. Die Erzminerale und ihre Verwachsungen. Akademie-Verlag, Berlin, 1089 p.



- RAST, N., 1965. Nucleation and growth of metamorphic minerals, in Controls of metamorphism, Pitcher, W.S. and Flinn, G.W. (Ed.). Oliver & Boyd, Edinburgh & London. 368 p.
- READ, R.A., 1965. The interpretation of deformation and annealing textures in metamorphic rocks. Unpublished M.Sc. thesis, Univ. Sydney.
- RICHARDSON, S.W., BELL, P.M. and GILBERT, M.C., 1968. Kyanite-sillimanite equilibrium between 700° and 1500°C. Am. J. Sci., 266, 513-541.
- RICHARDSON, S.W., GILBERT, M.C. and BELL, P.M., 1969. Experimental determination of kyanite-andalusite and andalusite-sillimanite equilibria; the aluminium silicate triple point. Am. J. Sci., 267, 259-272.
- RIECKER, R.E. and ROONEY, T.P., 1966. Shear strength, polymorphism, and mechanical behaviour of olivine, enstatite, diopside, labradorite and pyrope garnet: tests to 920°C and 60 kb. U.S. Air Force Camb. Res. Lab., Environmental Res. Pap. 216, 68 p.
- RIGSBY, G.P., 1960. Crystal orientation in glacier and experimentally deformed ice. J. Glaciology, 3, 589-606.
- RILEY, J.P. and WILLIAMS, H.P., 1959. The microanalysis of silicate and carbonate minerals, III. Mikrochim. Acta, 6, 804-824.
- RINGWOOD, A.E., 1966. Mineralogy of the mantle, in Advances in earth science, P.M. Hurley (Ed.). M.I.T. Press, 357-399.
- RINGWOOD, A.E. and GREEN, D.H., 1966. An experimental investigation of the gabbro-eclogite transformation and some geophysical implications. Tectonophysics, 3, 383-427.
-

- RINGWOOD, A.E. and MAJOR, A., 1966. High pressure transformations in pyroxenes. *Earth Plan. Sci. Lett.*, 1, 351-357.
- ROBINSON, E.G., 1949. The petrological nature of some rocks from the Mann, Tompkinson and Eyre ranges of Central Australia. *Trans. R. Soc. S. Aust.*, 73, 29-39.
- ROMEY, W.D., 1969. Anorthite content and structural state of plagioclases in anorthosites. *Lithos*, 2, 83-108.
- ROSENFELD, J.L., 1969. Stress effects around quartz inclusions in almandine and the piezothermometry of co-existing aluminium silicates. *Am. J. Sci.*, 267, 317-351.
- ROSS, C.S., FOSTER, M.D. and MYERS, A.T., 1954. Origin of dunites and of olivine-rich inclusions in basaltic rocks. *Am. Miner.*, 39, 693-737.
- RUTLAND, R.W.R., 1964. Tectonic overpressures, in Controls of metamorphism, Pitcher, W.S. and Flinn, G.W. (Ed.). Oliver & Boyd, Edinburgh & London. 368 p.
- SANDER, B., 1930. *Gefügekunde der Gesteine*. Springer-Verlag, Vienna.
- SAVOLAHTI, A., 1966. The differentiation of gabbro-anorthosite intrusions and the formation of anorthosite. *Bull. Commn géol. Finl.*, 38 (222), 173-197.
- SAXENA, S.K., 1968. Crystal-chemical aspects of distribution of elements among certain co-existing rock-forming silicates. *Neues Jb. Miner. Abh.*, 108, 292-323.
- SCHEUMANN, K.H., 1961. Über die Genesis des sächsischen Granulits. *Neues Jb. Miner. Abh.*, 96, 162-171.
-

- SCHOLTZ, D.L., 1936. The magmatic nickeliferous ore deposits of East Griqualand and Pondoland. Trans. geol. Soc. S. Afr., 39, 81-210.
- SCHREYER, W. and YODER, H.S., 1964. The system Mg-cordierite-H<sub>2</sub>O and related rocks. Neues Jb. Miner. Abh., 101, 271-342.
- SEIFERT, Von F., and SCHREYER, W., 1967. Die Möglichkeit der Entstehung ultrabasischer Magmen bei Gegenwart geringer Alkalimengen. Geol. Rdsch., 57, 349-362.
- SEN, S.K., 1959. Potassium content of natural plagioclases and the origin of antiperthites. J. Geol., 67, 479-495.
- SHAND, S.J., 1916. The pseudotachylyte of Parijs (Orange Free State). Q. Jl geol. Soc. Lond., 72, 198-221.
- SHAND, S.J., 1945. Coronas and coronites. Bull. geol. Soc. Am., 56, 247-266.
- SHAW, D.M., 1956. Geochemistry of pelitic rocks. Part III. Major elements and general geochemistry. Bull. geol. Soc. Am., 67, 919-934.
- SHAW, D.M., 1960. The geochemistry of scapolite. J. Petrology, 1, 218-285.
- SMITH, C.H., 1958. Bay of Islands igneous complex, western Newfoundland. Mem. geol. Surv. Can., 290, 132 p.
- SMITH, C.S., 1948. Grains, phases and interfaces: an interpretation of microstructure. Trans. Am. Inst. Min. metall. Engrs., 175, 15-51.
- SMITH, F.G., 1963. Physical geochemistry. Addison-Wesley Publishing Co., Inc., Reading. 624 p.

- SMITH, J.R., 1958. The optical properties of heated plagioclases. *Am. Miner.*, 43, 1179-1194.
- SMITH, J.R., 1960. Optical properties of low-temperature plagioclase, in Stillwater igneous complex, Montana (by H.H. Hess), *Mem. geol. Soc. Am.*, 80, 230 p.
- SMITH, J.V., 1956. The powder patterns and lattice parameters of plagioclase feldspars. I. The soda-rich plagioclases. *Mineralog. Mag.*, 31, 47-68.
- SMITH, J.V. and GAY, P., 1958. The powder patterns and lattice parameters of plagioclase feldspars. II. *Mineralog. Mag.*, 31, 744-762.
- SMITH, J.V. and RIBBE, P.H., 1969. Atomic movements in plagioclase feldspars: kinetic interpretation. *Contr. Miner. Petrology*, 21, 157-202.
- SPRIGG, R.C., WILSON, B. and COATES, R.P., 1959. Geological atlas of South Australia, Sheet Alberga, 1:250,000 series.
- SPRIGG, R.C. and WILSON, R.B., 1959. The Musgrave mountain belt in South Australia. *Geol. Rdsch.*, 47, 531-542.
- STEELE, R.J., 1966. Gravimetric investigation of the Mt. Davies and Gosse Pile intrusions of the Giles Complex. Unpublished Honours thesis, Univ. Adelaide.
- STRAND, T., 1944. A method of counting out petrofabric diagrams. *Norsk geol. Tidsskr.*, 24, 112-115.
- STREICH, V., 1893. Geology-Scientific results of the Elder exploring expedition. *Trans. R. Soc. Aust.*, 16, 74-115.
-

- STURT, B.A., 1962. The composition of garnets from pelitic schists in relation to the grade of regional metamorphism. *J. Petrology*, 3, 181-191.
- TALBOT, H.W.B. and CLARKE, E de C., 1917. Geological reconnaissance of country between Laverton and the South Australian border. *W. Aust. geol. Surv., Bull.* 75.
- TARNEY, J., 1969. Epitaxial relations between co-existing pyroxenes. *Mineralog. Mag.*, 37, 115-122.
- TAYLOR, H.P., 1967. The zoned ultramafic complexes of southeastern Alaska, in *Ultramafic and related rocks*, Wyllie, P.J. (Ed.). John Wiley and Sons, Inc., N.Y. 464 p.
- TERRY, M., 1928. *Untold Miles*. Selwyn and Blount, London. 288 p. with 2 maps.
- THAYER, T.P., 1960. Some critical differences between Alpine-type and stratiform peridotite-gabbro complexes. *Repts. 21st. Intern. geol. Congr., Copenhagen*, 13, 247-259.
- THAYER, T.P., 1963. Flow layering in alpine peridotite-gabbro complexes. *Mineralog. Soc. Am., Spec. Pap.* 1, 55-61.
- THAYER, T.P., 1967. Chemical and structural relations of ultramafic and feldspathic rocks in alpine intrusive complexes, in *Ultramafic and related rocks*, Wyllie, P.J. (Ed.). John Wiley and Sons, Inc., N.Y. 464 p.
- THOMPSON, J.B., 1947. Rôle of aluminium in rock forming silicates. *Bull. geol. Soc. Am.*, 58, 1232. (Abstract only).
- THOMPSON, J.B., 1959. Local equilibrium in metasomatic processes, in *Researches in geochemistry*, Abelson, P.H. (Ed.), John Wiley and Sons, Inc., N.Y. 511 p.
-

- THOMSON, B.P., 1963. Nickel mineralization and the Giles Complex in the Tomkinson Ranges, South Australia. Q. Notes Geol. Surv. S. Aust., 8, 2-3
- THOMSON, B.P., 1964. Geological atlas of South Australia, Sheet Davies, 1:63,360 series.
- THOMSON, B.P., 1965. Weathering and related nickel mineralization, Mt. Davies area. Q. Notes Geol. Surv. S. Aust., 16, 6-8.
- THOMSON, B.P., MIRAMS, R.C. and JOHNSON, J., 1962. Geological atlas of South Australia, Sheet Mann, 1:250,000 series.
- TILLEY, C.E., 1924. Contact metamorphism in the Cowrie Area, Perthshire Highlands. Q. Jl geol. Soc. Lond., 80, 22-71.
- TILLEY, C.E., 1936. Enderbite: a new member of the charnockite series. Geol. Mag., 73, 312-316.
- TROMMSDORF, V. and WENK, H.R., 1968. Terrestrial metamorphic clinoenstatite in kinks of bronzite crystals. Contr. Miner. Petrology, 19, 158-168.
- TUREKIAN, K.K. and KULP, J.L., 1956. The geochemistry of strontium. Geochim. cosmochim. Acta, 10, 245-296.
- TURNER, A.R., 1968. The distribution and association of nickel in the ferruginous zones of the laterites of the Giles Complex. AMDEL Bulletin, 5, 76-93.
- TURNER, F.J., 1948. Mineralogical and structural evolution of the metamorphic rocks. Mem. geol. Soc. Am., 30, 342 p.
- TURNER, F.J., 1968. Metamorphic petrology. McGraw-Hill, N.Y. 403 p.

- TURNER, F.J. and VERHOOGEN, J., 1960. Igneous and metamorphic petrology, 2nd Ed. McGraw-Hill, N.Y. 694 p.
- TURNER, F.J. and WEISS, L.E., 1963. Structural analysis of metamorphic tectonites. McGraw-Hill Co. Inc., N.Y. 545 p.
- TURNOCK, A.C., 1959. Spinels, *in* P.H. Abelson, Ann. Rept. Director Geophys. Lab., Carnegie Inst. Washington, Yearbook 58, 134-137.
- TURNOCK, A.C. and EUGSTER, H.P., 1962. Fe-Al oxides: phase relationships below 1000°C. *J. Petrology*, 3, 553-565.
- TUTTLE, O.F. and BOWEN, N.L., 1958. Origin of granite in the light of experimental studies in the system  $\text{NaAlSi}_3\text{O}_8$ - $\text{KAlSi}_3\text{O}_8$ - $\text{SiO}_2$ - $\text{H}_2\text{O}$ . *Mem. geol. Soc. Am.*, 74, 153 p.
- TYRRELL, G.W., 1926. The principles of petrology, 1st Ed., (2nd Ed., 1929). Methuen, London. 349 p.
- UPTON, B.G.J., 1961. Textural features of some contrasted igneous cumulates from south Greenland. *Meddr Grønland*, 123, 6, 6-32.
- VANCE, J.A., 1961. Polysynthetic twinning in plagioclase. *Am. Miner.*, 46, 1097-1119.
- VAN DEN BERG, J.J., 1946. Petrofabric analysis of the Bushveld gabbro from Bon Accord. *Trans. geol. Soc. S. Afr.*, 49, 155-204.
- VAN DIVER, B.B., 1967. Contemporaneous faulting-metamorphism in Wenatchee Ridge area, northern Cascades, Washington. *Am. J. Sci.*, 265, 132-150.
- VERHOOGEN, J., 1962. Distribution of titanium between silicates and oxides in igneous rocks. *Am. J. Sci.*, 260, 211-220.

- VERNON, R.H., 1968. Microstructures of high-grade metamorphic rocks at Broken Hill, Australia. *J. Petrology*, 9, 1-22
- VITANAGE, P.W., 1957. Studies of zircon types in the Ceylon Precambrian complex. *J. Geol.*, 65, 117-128.
- VOGEL, D.E., 1967. Petrology of an eclogite- and pyrigarnite-bearing polymetamorphic rock complex at Cabo Ortegal, NW Spain. *Leid. geol. Meded.*, 40, 121-213.
- VOGEL, T.A., SMITH, B.L. and GOODSPEED, R.M., 1968. The origin of antiperthites from some charnockitic rocks in the New Jersey Precambrian. *Am. Miner.*, 53, 1696-1708.
- VOLL, G., 1960. New work on petrofabrics. *Lpool Manchr geol. J.*, 2, 503-567.
- VON KNORRING, O. and KENNEDY, W.Q., 1958. The mineral paragenesis and metamorphic status of garnet-hornblende-pyroxene-scapolite gneiss from Ghana (Gold Coast). *Mineralog. Mag.*, 31, 846-859.
- WADSWORTH, W.J., 1961. The ultrabasic rocks of southwest Rhum. *Trans. R. phil. Soc. Lond.*, (B), 244, 21-64.
- WAGER, L.R., 1959. Differing powers of crystal nucleation as a factor producing diversity in layered igneous intrusions. *Geol. Mag.*, 96, 75-80.
- WAGER, L.R. and BROWN, G.M., 1968. Layered igneous rocks. Oliver & Boyd, Edinburgh. 588 p.
- WAGER, L.R., BROWN, G.M. and WADSWORTH, W.J., 1960. Types of igneous cumulates. *J. Petrology*, 1, 73-85.
-



- WAGER, L.R. and DEER, W.A., 1939. Geological investigations in east Greenland. Part III. Petrology of the Skaergaard intrusion, Kangerdlugssuaq, east Greenland. Meddr Grønland, 105, 335 p.
- WAGER, L.R. and MITCHELL, R.L., 1951. The distribution of trace elements during strong fractionation of basic magma - a further study of the Skaergaard intrusion, east Greenland. Geochim. cosmochim. Acta, 1, 129-208.
- WASHINGTON, H.S., 1930. The chemical analysis of rocks, 4th Ed. John Wiley and Sons, N.Y. 296 p.
- WATERS, A.C. and CAMPBELL, C.D., 1935. Mylonites of the San Andreas fault zone. Am. J. Sci., 229, 473-503.
- WEEDON, D.S., 1965. Corona structures in the basic igneous masses of east Aberdeenshire. Nature, 208, 885.
- WELLS, A.K., 1952. Textural features of some Bushveld norites. Mineralog. Mag., 29, 913-924.
- WELLS, A.T., STEWART, A.J. and SKWARKO, S.K., 1966. Geology of the south-eastern part of the Amadeus Basin, Northern Territory. Rept. Bur. Miner. Res., Geol. Geophys. Aust., 88.
- WHITE, R.W., 1966. Ultramafic inclusions in basaltic rocks from Hawaii. Contr. Miner. Petrology, 12, 245-314.
- WHITTAKER, E.S.W. and ZUSSMAN, J., 1956. The characterization of serpentine minerals by X-ray diffraction. Min. Mag., 31, 107-126.
- WILCOX, R.E. and POLDERVAART, A., 1958. Metadolerite dyke swarm in Bakersville-Roan mountains area, North Carolina. Bull. geol. Soc. Am., 69, 1323-1368.
-

- WILSON, A.F., 1947. Charnockitic and associated rocks of north-western South Australia - I. The Musgrave Ranges - an introductory account. *Trans. R. Soc. S. Aust.*, 71, 195-211.
- WILSON, A.F., 1948. Charnockitic and associated rocks of north-western South Australia - II. Dolerites from the Musgrave and Everard Ranges. *Trans. R. Soc. S. Aust.*, 72, 178-200.
- WILSON, A.F., 1952. Precambrian tillites east of the Everard Ranges, northwestern South Australia. *Trans. R. Soc. S. Aust.*, 75, 160-163.
- WILSON, A.F., 1954. Studies on Australian charnockitic rocks and related problems. Unpublished D.Sc. thesis, Univ. Western Australia.
- WILSON, A.F., 1958. The charnockitic rocks of Australia. *Geol. Rdsch.*, 47, 491-510.
- WILSON, A.F., 1960. Co-existing pyroxenes: some causes of variation and anomalies in the optically derived compositional tie-lines, with particular reference to charnockitic rocks. *Geol. Mag.*, 97, 1-17.
- WINKLER, H.G.F., 1967. *Petrogenesis of metamorphic rocks*, 2nd Ed. Springer-Verlag, N.Y. Inc., 237 p.
- WONES, D.R. and EUGSTER, H.P., 1965. Stability of biotite: experiment, theory, and application. *Am. Miner.*, 50, 1228-1272.
- WORST, B.G., 1958. The differentiation and structure of the Great Dyke of Southern Rhodesia. *Trans. geol. Soc. S. Afr.*, 61, 283-354.

- WRIGHT, T.L., 1968. X-ray and optical study of alkali feldspar: II. An X-ray method for determining the composition and structural state from measurement of  $2\theta$  values for three reflections. *Am. Miner.*, 53, 88-104.
- WRIGHT, T.L. and STEWART, D.B., 1968. X-ray and optical study of alkali feldspar: I. Determination of composition and structural state from refined unit-cell parameters and  $2V$ . *Am. Miner.*, 53, 38-87.
- WYATT, M., 1954. Zircon as provenance indicators. *Am. Miner.*, 39, 983-990.
- WYLLIE, P.J., 1963. Applications of high pressure studies to the earth sciences, in *High pressure physics and chemistry*, Bradley, R.S. (Ed.). Academic Press, London. 361 p.
- WYLLIE, P.J., 1967. The application of experimental data to metamorphic reactions, in *Chemistry of the earth's crust*, V2, Vinogradov, A.P. (Ed.). (Translated by the Israel Program for Scientific Translations, from *Khimiya Zemnon Kory*). Jerusalem.
- WYLLIE, P.J., 1967a. Ultramafic and ultrabasic rocks. 1. Petrography and petrology, in *Ultramafic and related rocks*, P.J. Wyllie (Ed.). John Wiley and Sons, Inc., N.Y. 464 p.
- WYNNE-EDWARDS, H.R., GREGORY, A.F., HAY, P.W., GIOVANELLA, C.A. and REINHARDT, E.W., 1966. Mont Laurier and Kempt lake map-areas. *Geol. Surv. Can.*, Pap. 66-32.
- YODER, H.S., 1952. The  $MgO-Al_2O_3-SiO_2-H_2O$  system and the related metamorphic facies. *Am. J. Sci.*, Bowen Volume, 569-627.

- YODER, H.S., 1955. Rôle of water in metamorphism, in Crust of the earth, A. Poldervaart, (Ed.). Geol. Soc. Am. Spec. Pap. 62, 505-524.
- YODER, H.S. and EUGSTER, H.P., 1954. Phlogopite synthesis and stability range. Geochim. cosmochim. Acta, 6, 157-187.
- YODER, H.S. and SAHAMA, Th.G., 1957. Olivine X-ray determinative curve. Am. Miner., 42, 475-491.
- YODER, H.S., STEWART, D.B. and SMITH, J.R., 1956. Ternary feldspars, in P.H. Abelson, (Ed.). Ann. Rept. Director Geophys. Lab., Carnegie Inst. Washington, Yearbook 55, 190-194.
- YODER, H.S., STEWART, D.B. and SMITH, J.R., 1957. Ternary feldspars, in P.H. Abelson, (Ed.). Ann. Rept. Director Geophys. Lab., Carnegie Inst. Washington, Yearbook 56, 206-214.
- YONG, S.K., 1964. The distribution of trace elements nickel, copper, strontium, chromium and manganese in the Mt. Davies basic intrusion of South Australia. Unpublished Honours thesis, Univ. Adelaide.
- ZEN, E-AN, 1969. The stability relations of the polymorphs of aluminium silicate: a survey and some comments. Am. J. Sci., 267, 297-309.
- ZWART, H.J., 1958. Regional metamorphism and related granitization in the Valle de Arán (central Pyrenees). Geol. Mijnbouw, 20, 18-30.
- ZWART, H.J., 1962. On the determination of polymetamorphic mineral associations, and its application to the Bosost area (central Pyrenees). Geol. Rdsch., 52, 38-65.

Publications which are relevant to this thesis but which became available after typing had been completed.

- HOLLAND, J.G. and LAMBERT, R.St.J., 1969. Structural regimes and metamorphic facies. *Tectonophysics*, 7, 197-217.
- KATZ, M.B., 1969. The nature and origin of the granulites of Mont Tremblant Park, Quebec. *Bull. geol. Soc. Am.*, 80, 2019-2038.
- MILLER, P.G., 1969. Final report on nickel investigation, northwest province 1953-1967. Rept. Bk. No. 68/95; G.S. No. 4244. Vol. I, II & III. D.M. 777/69. Dept. Mines, S. Aust. Geol. Surv., Mineral Res. Div.
- PARK, R.C., 1969. Structural correlation in metamorphic belts. *Tectonophysics*, 7, 323-338.
- SPRY, A.H., 1969. *Metamorphic textures*. Pergamon Press, Oxford, 350 p.
- STRONG, D.F., 1969. Formation of the hour-glass structure in augite. *Mineralog. Mag.*, 37, 472-479.